

The University Of Sheffield.

Analysis of *Staphylococcus aureus* virulence

By:

Dr Emma Boldock

A thesis submitted in partial fulfilment of the requirements for the degree of Doctor of Philosophy

The University of Sheffield
Faculty of Science
Department of Molecular Biology and Biotechnology

Submission Date: April 2016

Summary

Staphylococcus aureus continues to cause significant clinical burden globally and therapeutic approaches must adapt swiftly to meet the emerging challenges of multi-drug resistant strains. Detailed understanding of host:pathogen dynamics is paramount in developing optimal control strategies.

The first aim of this project was to identify novel virulence traits of *S. aureus* by screening genetically related isolates from a dominant MRSA clade, ST 239, through the zebrafish embryo systemic model of infection. Virulence differences between strains and bioinformatic analysis of whole genome sequence data revealed single nucleotide polymorphisms in both characterised and putative genes however technical errors in sequencing data prevented further interrogation of *S. aureus* pathogenomics.

The second aim sought to characterise the role of genes required for growth on human blood. A library of transposon mutated non-essential *S. aureus* genes was screened for growth phenotype on human blood and strains of interest were prioritised by virulence assessment in the zebrafish infection model. Genes involved in purine and folate synthesis were found to be important for growth on human blood. Growth of a folate deficient mutant (*pabA*) was re-established if exogenous pyrimidines were added to human blood and a key gene in the pyrimidine salvage pathway, *tdk*, is implicated in this process. Lysis products of RBCs are currently speculated to either inhibit Tdk directly or cause toxicity thereby increasing the need for dTTP against a pyrimidine poor background. Further understanding of the requirements for growth in human blood may highlight novel areas of therapeutic target development.

Finally, the need for a large bacterial inoculum to establish *S. aureus* infection in both zebrafish and mammalian models of infection was interrogated. It was found that other Gram-positive, nonpathogenic bacteria (and even their components) enable *S. aureus* to initiate infection. The other bacteria themselves cannot cause disease but augment infection by the pathogen. Either live bacteria or purified, particulate cell wall peptidoglycan of *Micrococcus luteus* or *Staphylococcus epidermidis* increased host mortality when co-injected with low dose *S. aureus*. Inert latex beads and solubilised peptidoglycan did not. These findings have important ramifications for human disease as it may begin to explain how initiation of *S. aureus* infection occurs.

Acknowledgements

Firstly, I would like to thank Professor Simon Foster for encouraging and supporting a medic to undertake basic science research. It has been a privilege to work in his laboratory and be continually spurred on to learn about the intricate details of host pathogen interactions, by asking difficult questions. I am eager to continue along this roller coaster that is academia, heavily inspired by his exceptional leadership and passion for furthering knowledge.

I would also like to thank my co-supervisor, Professor Steve Renshaw, my Wellcome Trust sponsor and mentor, Professor David Dockrell and my external mentor Professor Sharon Peacock. Forging a path in academic microbiology has been made far easier with their help, guidance and willingness to discuss both my science and career plans whenever needed. Having successful, approachable clinical academics to look up to during and hopefully after my PhD has been a lifeline and I've benefitted greatly from our meetings.

I have worked with so many fantastic people throughout my PhD that there are too many to name. I will always be grateful for being warmly welcomed and supported by everyone I have had the pleasure of working with in F18, F25 and the Renshaw lab. These three years have been intellectually stimulating and incredibly fun - I thank you all very much indeed.

I also would like to thank the technical support provided by the University, the Department of Immunity and Infection for taking me under their wing and providing biological samples and also our collaborators in Sweden and Canada for adding valuable data to the project.

Finally, I would like to thank my amazing family – my parents, Nana, Uncle Ralph, my sister, Michaela, brother-in-law, Drew and beautiful nephew, Isaac. Sorry for all the times I haven't answered my phone but I love you very much. Last but certainly not least, thank you to my (newly acquired!) husband for looking after me when I need it most and for always making me smile.

This project was funded by a Wellcome Trust Clinical Research Training Fellowship.

Abbreviations

°C	Degree Celsius
aa	amino acid
ADC	4-amino-4-deoxychorismate
AFS	Ammonium ferrous sulphate
AG	Adenine and guanine
AICAIR	5-amino-1-(5-phospho-D-ribosyl)imidazole-4-carboxamide
AIP	Autoinducing peptide
AIR	5-amino-1-(5-phospho-β-D-ribosyl)imidazole
Amp	Ampicillin
AMPs	Antimicrobial peptides
APC	Antigen presenting cell
ATP	Adenosine triphosphate
attB	Attachment site in the bacterial genome
attP	Attachment site in the phage genome
BALB/c	Inbred mouse strain
BCIP	5-bromo-5-chloro-3-indolyl phosphate
BHI	Brain heart infusion
BLAST	Basic local alignment search tool
bp	Base pair
BSA	Bovine serum albumin
C3H/HeN	Inbred mouse strain
CA	Community acquired
Cd	Cadmium
CAIR	5-amino-1-(5-phospho-D-ribosyl)imidazole-4-carboxylate
CC	Clonal complex
CCL2	Chemokine (C-C motif) ligand 2
CCL4	Chemokine (C-C motif) ligand 4
CDM	Chemically defined media
CFU	Colony forming units
CGD	Chronic granulomatous disease
CHIPs	Chemotaxis inhibitory protein of staphylococci
Cm	Chloramphenicol
CNS	Coagulase negative staphylococci
CXCL1	Chemokine (C-X-C motif) ligand 1
dH_2O	Distilled water
DHF	Dihydrofolate
DIC	Differential interference contrast
DMF	Dimethylformamide
DMSO	Dimethyl sulphoxide
DNA	Deoxyribonucleic acid
dNTPs	Deoxyribonucleoside-5'-phosphate
dpf	days post fertilisation
dpi	days post infection
dTMP	Deoxythymidine monophosphate
dTTP	Deoxythymidine triphosphate
DTT	Dithiothreitol
dUMP	Deoxyuracil monophosphate
EB	Elution buffer
EDTA	Ethylenediamine tetra-acetic acid

ExPEC	Extraintestinal Pathogenic *Escherichia coli*
Ery	Erythromycin
FA	Folic acid
FAICAIR	5-formamido-1-(5-phospho-D-ribosyl)-imidazole-4-carboxamide
FBS	Foetal bovine serum
FGAM	2-(formamido)-N1-(5-phospho-β-D-ribosyl)acetamidine
FGAR	N2-formyl-N1-(5-phospho-β-D-ribosyl)glycinamide scatter
g	Grams
GAR	N1-(5-phospho-β-D-ribosyl)glycinamide
gDNA	Genomic DNA
GFP	Green fluorescent protein
GlcNAc	*N*-acetyl glucosamine
Gly	Glycine
GMP	Guanosine monophosphate
GTP	Guanosine triphosphate
GWAS	Genome-wide association studies
h	hours
HA	Hospital acquired
HF	Hydrofluoric acid
hpf	hours post fertilisation
hpi	hours post infection
HU	Haemolysin unit
Kan	Kanamycin
kb	Kilobase pairs
KCs	Kupffer cells
ICU	Intensive Care Unit
IL-1β	Interleukin 1 beta
IL-6	Interleukin 6
IL-8	Interleukin 8
IL-10	Interleukin 8
IL-12	Interleukin 12
IL-17A	Interleukin 17A
IFN-δ	Interferon gamma
IMP	Inosine monophosphate
l	Litre
LB	Luria-Bertani medium
Lin	Lincomycin
LPS	Lipopolysaccharide
LTA	Lipoteichoic acid
LWT	London Wildtype
M	Molar
MAC	Membrane attack complex
Mb	Megabase
MCS	Multiple cloning site
MDP	Muramyl dipeptide
Met	Methionine
mg	Milligrams
MGE	Mobile genetic element
MHC	Major histocompatibility complex
min	Minutes
MIC	Minimum inhibitory concentration
ml	Millilitres

mM	Millimolar
MO	Morpholino oligonucleotide
MOI	Multiplicity of infection
MRSA	Methicillin resistant *Staphylococcus aureus*
MSCRAMM	Microbial surface components recognising adhesive matrix molecules
MurNAc	*N*-acetyl muramic acid
MyD88	Myeloid differentiation primary response gene 88
N5-CAIR	N5-carboxyaminoimidazole ribonucleotide
NA	Numerical aperture
NARSA	Network on Antimicrobial Resistance in *Staphylococcus aureus*
NCBI	National Centre for Biotechnology Information
NETs	Neutrophil extracellular traps
NF-κB	Nuclear Factor
NITU	Neonatal Intensive Therapy Unit
NTML	Nebraska transposon mutagenesis library
NCBI	National Center for Biotechnology Information
Neo	Neomycin
NGS	Next generation sequencing
nl	nanolitre
nm	nanometre
nM	Nanomolar
Nod	Nucleotide oligomerisation domain
NLR	Nucleotide oligomerisation domain like receptor
OCT	Optimum cutting temperature compound
OD_x	Optical density at indicated wavelength x (nm)
OM	Outer membrane
ORF	Open reading frame
PAMP	Pathogen-associated molecular pattern
PBS	Phosphate buffered saline
PBPs	Penicillin binding proteins
PCR	Polymerase chain reaction
pfu	Plaque forming units
PG	Peptidoglycan
PGRP	Peptidoglycan recognition protein
PMSF	Phenylmethanesulfonylfluoride
pPGN	Polymeric peptidoglycan
PPP	Platelet poor plasma
PRA	5-phospho-β-D-ribosylamine
PRP	Platelet rich plasma
PRPP	5-phospho-β-D-ribose 1-diphosphate
PRR	Pattern recognition receptors
psi	Pounds per square inch
PSM	Phenol-soluble modulin
PVL	Panton-Valentine leukocidin
RNA	Ribonucleic acid
RBC	Red blood cell
RIP2	Receptor interacting protein 2
RM	Restriction modification
ROS	Reactive oxygen species
rpm	Revolutions per min
RT	Room temperature
SAICAIR	5'-phosphoribosyl-4-(N-succinocarboxamide)-5-aminoimidazole

SCBU	Special Care Baby Unit
SCC	Staphylococcal chromosomal cassette
SCIN	Staphylococcal complement inhibitor
SCVs	Small colony variants
Ser	Serine
SNPs	Single nucleotide polymorphism
Spc	Spectinomycin
sPGN	Soluble peptidoglycan
Spp.	Species
ST	Sequence type
STM	Signature tagged mutagensis
t	Time
TA	Teichoic acid
TAE	Tris-acetate EDTA (buffer)
TES	Tris-EDTA NaCl
Tet	Tetracycline
THF	Tetrahydrofolate
TLR	Toll like receptor
TMP	Trimethoprim
Tn	Transposon
TNFα	Tumour necrosis factor alpha
TraDIS	Transposon directed insertion site sequencing
Tris	Tris (hydroxymethyl) aminomethane
TSS	Toxic shock syndrome
TSST-1	Toxic shock syndrome toxin-1
µg	Microgram
µl	Microlitre
µm	Micrometre
µM	Micromolar
UV	Ultraviolet
V	Volts
Van	Vancomycin
VRE	Vancomycin resistant enterococci
VISA	Vancomycin intermediate *Staphylococcus aureus*
VitB5	Vitamin B5
VRSA	Vancomycin resistant *Staphylococcus aureus*
v/v	Volume for volume
WITS	Wildtype isogenic tagged strains
WT	Wild-type
WTA	Wall teichoic acid
w/v	Weight for volume
×	Times
X-Gal	5-bromo-4-chloro-3-indolyl-β-D-galactoside
σ	Sigma factor
Ω	Ohms
Φ	Phage
~	Approximately
<	Less than

Table of Contents

	Title page	i
	Summary	iii
	Acknowledgements	iv
	Abbreviations	v
	Table of Contents	ix
	List of Figures	xvi
	List of Tables	xx
	Chapter 1. Introduction	**1**
1.1	*Staphylococcus aureus*	1
1.2	Metabolism of *S. aureus*	1
1.2.1	Role of purine biosynthesis	2
1.2.2	Role of folate production	2
1.2.3	Linking metabolism and virulence	3
1.3	Requirements for growth	3
1.3.1	Bypassing 'nutritional immunity'	4
1.4	Clinical significance of *S. aureus*	5
1.5	Antibiotic resistance of *S. aureus*	9
1.6	Prevention of *S. aureus* infection	12
1.7	Current strategies for treatment	13
1.8	Immune protection against *S. aureus*	14
1.8.1	Innate immune system	14
1.8.1.1	Phagocytosis	15
1.8.1.2	Cellular components of the innate immune system and their role in *S. aureus* killing	15
1.8.1.3	Pathogen ligand and host receptor associations	17
1.8.2	Adaptive immune system	21
1.9	The bacterial cell wall	22
1.9.1	Peptidoglycan	23
1.9.2	Peptidoglycan modification	23
1.9.3	Peptidoglycan immune recognition and response	24
1.9.3.1	Identifying the TLR2 *S. aureus* ligand	26
1.9.3.2	Non-TLR *S. aureus* peptidoglycan receptors	27
1.9.3.3	Immune response to *M. luteus* and *S. epidermidis*	29
1.9.4	Role of phagocytosis and the inflammasome in immune signalling	30
1.10	Virulence Determinants of *S. aureus*	31
1.10.1	Tissue adhesion	31
1.10.2	Tissue invasion and spread	32
1.10.3	Immune evasion	33
1.10.4	Regulation of *S. aureus* virulence factors	34
1.11	Whole genome sequence of *S. aureus*	38
1.11.1	Bacteriophages	38
1.11.2	*S. aureus* pathogenicity islands	39
1.11.3	Staphylococcal chromosome cassettes	39

1.11.4	Plasmids	39
1.11.5	Transposons	40
1.11.6	Restriction-modification systems of *S. aureus*	40
1.11.7	Next generation sequencing technology	41
1.12	Model organisms to study *S. aureus* disease	42
1.12.1	Invertebrate models	43
1.12.1.1	*Caenorhabditis elegans*	43
1.12.1.2	*Drosophila melanogaster*	43
1.12.2	Vertebrate models	46
1.12.2.1	Zebrafish	46
1.12.2.1.1	Zebrafish innate immune system	47
1.12.2.2	Mammalian	50
1.12.2.2.1	Murine	50
1.12.2.2.2	Other rodents	51
1.12.2.2.3	Rabbits	52
1.12.2.2.4	Larger mammals	52
1.13	Hypothesis and aims of the project	53
	Chapter 2. Materials and methods	**54**
2.1	Media	54
2.1.1	Brain Heart Infusion (BHI) broth	54
2.1.2	Luria-Bertani (LB) broth	54
2.1.3	LK broth	54
2.1.4	Mueller-Hinton broth	55
2.1.5	Chemically defined minimal media (CDM)	55
2.1.6	Blood and blood component media	56
2.1.6.1	Human blood collection	56
2.1.6.2	Human plasma preparation	56
2.1.6.3	Serum or plasma agar (50% v/v)	56
2.1.6.4	Human or animal blood agar (30% v/v)	56
2.1.6.5	Rabbit blood agar (10% v/v)	57
2.1.6.6	Horse blood agar (5% v/v)	57
2.1.6.7	Sheep blood agar (5-30% v/v)	57
2.2	Plate photography	57
2.3	Measuring haemolysis	57
2.3.1	Qualitative analysis of haemolysis on rabbit blood agar	57
2.3.2	Quantitative haemolysis assay	58
2.4	Antibiotics	59
2.4.1	Antibiotic susceptibility testing of *S. aureus* isolates	59
2.4.1.1	Antibiotic breakpoint determination	59
2.4.1.2	Gradient strips for MIC determination	60
2.5	Bacterial strains	60
2.5.1	*S. aureus* strains	60
2.5.2	Other Gram-positive strains	65
2.5.3	*E. coli* strains	65
2.6	Plasmids	66
2.7	Buffers and solutions	67
2.7.1	Phage buffer	67
2.7.2	Phosphate buffered saline (PBS)	67
2.7.3	Haemolysin salts solution	67
2.7.4	50 mM Tris-HCl pH 7.5	67
2.7.5	TAE (x 50)	67

2.7.6	Tris/EDTA/NaCl buffer (TES)	68
2.7.7	0.1 M Sodium phosphate buffer (pH 5.5)	68
2.7.8	Promega Buffers	68
2.7.8.1	Membrane Binding Solution	68
2.7.8.2	Membrane Wash Solution	68
2.7.9	QIAGEN buffers	68
2.7.9.1	QIAGEN Buffer P1	68
2.7.9.2	QIAGEN Buffer P2	69
2.7.9.3	QIAGEN Buffer P3	69
2.7.9.4	QIAGEN Buffer EB	69
2.7.9.5	QIAGEN Buffer TE	69
2.7.9.6	QIAGEN Buffer QBT	69
2.7.9.7	QIAGEN Buffer QC	69
2.7.9.8	QIAGEN Buffer QF	70
2.7.9.9	QIAGEN Buffer N3, PB, PE	70
2.8	Chemicals, compounds and enzymes	71
2.9	Centrifugation	71
2.10	Growth curves	72
2.11	Determining bacterial density	72
2.11.1	Spectrophotometric measurement (OD_{600})	72
2.11.2	Direct cell counts (CFU ml^{-1})	72
2.12	DNA purification techniques	73
2.12.1	Small scale plasmid purification	73
2.12.2	Large scale plasmid purification	73
2.12.3	Gel extraction of DNA	74
2.12.4	PCR purification	75
2.12.5	Pellet paint precipitation of DNA	75
2.13	*In vitro* DNA manipulation techniques	75
2.13.1	Polymerase Chain Reaction (PCR) techniques	75
2.13.1.1	Primer design	75
2.13.1.2	DNA amplification	78
2.13.1.3	Colony PCR screening of *E. coli*	79
2.13.1.4	Colony PCR screening of *S. aureus*	79
2.13.2	Restriction endonuclease digestion	79
2.13.3	Gibson Assembly™ Method	80
2.13.4	Agarose Gel Electrophoresis	80
2.13.5	DNA sequencing	83
2.14	Transformation techniques	83
2.14.1	Transformation of *E. coli*	83
2.14.1.1	Preparing electrocompetent *E. coli* cells	83
2.14.1.2	Electroporation of DNA into electro-competent *E. coli* cells	83
2.14.2	Transformation of *S. aureus*	84
2.14.2.1	Preparing electro-competent *S. aureus* cells	84
2.14.2.2	Electroporation of DNA into competent *S. aureus* cells	84
2.15	Phage techniques	85
2.15.1	Bacteriophage techniques	85
2.15.2	Preparation of phage lysate	85
2.15.3	Determination of phage titre	85
2.15.4	Phage transduction	85
2.16	Construction of *S. aureus* mutants	86
2.17	Genetic complementation of the *pab* operon	87

2.18	Screening the Nebraska transposon mutagenesis library (NTML) on solid media	87
2.19	Zebrafish techniques	87
2.19.1	Zebrafish strains	87
2.19.2	Zebrafish husbandry	87
2.19.3	Zebrafish E3 medium (x10)	88
2.19.4	Methylcellulose	88
2.19.5	Zebrafish anaesthesia	88
2.19.6	Microinjections of *S. aureus* into zebrafish embryos	88
2.19.7	Addition of compounds to zebrafish by immersion	89
2.19.8	Determination of zebrafish embryo mortality following infection	90
2.19.9	Determination of growth of *S. aureus in vivo*	90
2.19.10	Microinjection of morpholino oligonucleotide into zebrafish embryos	90
2.19.10.1	Morpholinos	90
2.19.10.2	Injection of morpholino into zebrafish eggs	90
2.19.11	Microscopic observations	91
2.19.11.1	Mounting of zebrafish	91
2.19.11.2	Imaging of zebrafish	91
2.19.11.3	pHrodo^{TM} and Fluorescein succinimidyl ester staining of *S. aureus*	91
2.20	Latex fluorescent beads for *in vivo* experiments	92
2.21	Murine sepsis model	92
2.22	Histological preparation of murine organs	93
2.23	Murine serum cytokine sampling	93
2.24	Peptidoglycan purification	94
2.24.1	Breakage of cell walls	94
2.24.2	Extraction of cell wall and removal of proteins	94
2.24.3	Hydrolysis of peptidoglycan	95
2.24.4	Quantification of peptidoglycan for *in vivo* experiments	95
2.25	Ethical Permissions	96
2.26	Data and statistical analysis	96
2.27	Collaborative work	97
	Chapter 3. Identifying novel virulence determinants of *S. aureus* by phenotypic:genotypic analysis	**98**
3.1	Introduction	98
3.2	Aims of this chapter	100
3.3	Results	101
3.3.1	Selection of whole genome sequenced clinical strain collections	101
3.3.2	Annotation of the whole genome sequence data	102
3.3.3	Determining relative pathogenicity of clinical strains	105
3.3.4	Bioinformatic analysis of whole genome sequence data	113
3.3.5	Candidate genes	123
3.3.5.1	SATW20_13140	123
3.3.5.2	*isaB*	123
3.3.5.3	*saeS*	123
3.3.5.4	*htrA2*	124
3.3.6	Antibiotic susceptibility of ST239 clinical strains	124
3.3.7	Phenotypic analysis of *S. aureus* strains	128
3.3.8	Construction of *S. aureus* mutants	131
3.3.8.1	Construction of *S. aureus saeS* mutant	131
3.3.8.1.1	Phenotypic analysis of SH1000 *saeS*$^{A->T}$ *in vitro* and *in vivo*	143
3.3.8.2	Construction of *S. aureus htrA2* mutant	147

3.3.8.3	Construction of *S. aureus isaB* mutant	149
3.3.8.4	Construction of *S. aureus* SATW20_13140 mutant	152
3.3.9	Virulence screen of additional clinical strain collections	154
3.3.9.1	MRSA outbreak collection from a Neonatal Intensive Care Unit	154
3.3.9.2	MRSA outbreak collection from a Special Care Baby Unit	155
3.4	Discussion	161
	Chapter 4. Identification of *S. aureus* genes required for growth on human blood	**167**
4.1	Introduction	167
4.2	Aims of this chapter	170
4.3	Results	170
4.3.1	Phenotypic screen of the NTML *in vitro*	170
4.3.2	Initial analysis of strains of interest both *in vitro* and *in vivo*	172
4.3.2.1	Analysis of purine biosynthesis mutants *in vitro*	177
4.3.2.1.1	Growth in nutrient variable liquid media	177
4.3.2.1.2	Biochemical complementation of purine biosynthesis mutants *in vitro*	181
4.3.2.2	Analysis of the role of purine biosynthesis *in vivo*	181
4.3.2.2.1	Virulence phenotype in the zebrafish assay	181
4.3.2.2.2	Biochemical complementation of purine biosynthesis mutants *in vivo*	184
4.3.2.3	Further analysis of the haemolytic strains from the NTML screen	186
4.3.2.4	Analysis of *pabA in vitro*	186
4.3.2.4.1	Unusual growth phenotype of *pabA* on blood vs. blood components	186
4.3.2.4.2	Biochemical complementation of *pabA in vitro*	191
4.3.2.5	Analysis of *pabA in vivo*	197
4.3.2.5.1	Virulence phenotype in the zebrafish assay	197
4.3.2.5.2	Virulence of *pabA* in the murine sepsis model of infection	199
4.3.2.5.3	Biochemical complementation of *pabA* in the zebrafish model	199
4.3.3	Role of other genes in the *pab* operon during pathogenesis	206
4.3.4	Confirmation of the role of *pabA*, *glyA* and PABA in *S. aureus* virulence in the zebrafish embryo model	208
4.3.4.1	Genetic complementation of the *pab* operon	208
4.3.4.2	Serine-glycine inter-conversion and pathogenesis *in vivo*	208
4.3.4.3	Specificity of PABA to rescue virulence of folate deficient mutants	208
4.3.5	Investigating the mechanism underlying the *pabA* growth phenotype	211
4.3.5.1	Analysis of the role of red blood cells	211
4.3.5.2	Analysis of the role of white blood cells and platelets	215
4.3.5.3	Use of chemically defined media to assess the importance of pyrimidines	219
4.3.5.4	Investigation of the role of pyrimidine salvage pathways in growth on human blood	221
4.3.5.4.1	Construction of multiple mutant strains	221
4.3.5.4.2	Investigating the effect of Tdk inhibitors on *pabA* growth	227
4.3.5.4.3	Metal ion chelation and Tdk activity	231
4.3.5.5	Investigation of antibiotics targeting folate metabolism	234
4.3.5.6	Comparison of *pabA* with *thyA*	240
4.3.5.6.1	Growth of *pabA* and *thyA* on Mueller-Hinton agar	240
4.3.5.6.2	Growth of *pabA* and *thyA* on sheep and horse blood	241
4.3.5.6.3	Comparison of *pabA* and *thyA* growth on human blood agar	243
4.3.5.6.4	Effect of lysed human RBCS on *thyA* growth	246
4.3.5.7	Investigating cellular stress caused by heme toxicity	248
4.4	Discussion	249

4.4.1	Purine biosynthesis mutants	249
4.4.2	Analysis of *pabA*	251
4.4.2.1	Attempting to identify the mechanism for the distinctive *in vitro pabA* growth phenotype	251
4.4.2.2	Further considerations and future work	254
	Chapter 5. Augmentation of *S. aureus* pathogenesis	**257**
5.1	Introduction	257
5.2	Aims	260
5.3	Results	261
5.3.1	Identification of an augmentation phenomenon during *S. aureus* infection	261
5.3.1.1	Co-injection of antibiotic sensitive and resistant strains	261
5.3.1.2	Co-injection of attenuated and parent *S. aureus* strains	265
5.3.2	Host pathogen dynamics during pathogenesis augmentation with attenuated mutant mixed inocula	271
5.3.2.1	Bacterial growth kinetics of mixed inocula *in vivo*	271
5.3.2.2	The role of phagocytes in mediating augmentation of pathogenesis in the zebrafish embryo model of infection	273
5.3.2.2.1	Investigation of *phePsaeR* growth in the absence of phagocytes	273
5.3.2.2.2	*In vivo* zebrafish imaging of phagocytosis of *S. aureus* mixed strains during pathogenesis	275
5.3.3	Population dynamics of mixed inocula that do not augment pathogenesis	277
5.3.4	Determining the breadth of the augmentation phenomenon in zebrafish embryos	279
5.3.4.1	Using latex fluorescent beads	279
5.3.4.2	Investigation of the effect of commensal skin bacteria on *S. aureus* pathogenesis in the zebrafish infection model	284
5.3.4.3	Is there a common mechanism underlying the augmentation phenomenon?	290
5.3.4.3.1	The cell wall component, peptidoglycan, can augment *S. aureus* pathogenesis	290
5.3.4.3.2	Microscopy imaging of the fate of fluorescently labelled peptidoglycan with and without live bacteria in the zebrafish infection model	298
5.3.4.3.3	Is the structural integrity of peptidoglycan important in augmentation of pathogenesis?	301
5.3.5	Investigation of the pathogenesis augmentation phenomenon in the murine sepsis model	303
5.3.5.1	Co-injection of attenuated mutant *phePsaeR* and low dose *S. aureus*	303
5.3.5.2	Establishing the augmentation phenomenon in the murine host using purified peptidoglycan	308
5.3.5.2.1	Investigating murine host response to purified peptidoglycan alone	308
5.3.5.2.2	Co-injection of *M. luteus* peptidoglycan and low dose *S. aureus* in the murine sepsis model	310
5.3.5.2.3	Co-injection of *S. aureus* peptidoglycan and *S. aureus* bacteria in a murine sepsis model	314
5.3.5.3	Examining the extent of the augmentation phenomenon in the murine sepsis model	317
5.3.5.3.1	Is the composition of peptidoglycan important?	317
5.3.5.3.2	Can any particulate material augment pathogenesis in the murine sepsis model?	322

5.3.5.3.3 Macroscopic images and histopathological analysis of murine livers 325
5.3.5.3.4 Titration of bacteria or peptidoglycan dose in pathogenesis augmentation in the murine sepsis model 327
5.3.5.3.5 Is the augmentation phenomenon bacterial strain specific? 331
5.3.5.3.6 Investigating if the augmentation phenomenon is mouse strain specific 333
5.3.5.3.7 Effect of live commensal bacteria on *S. aureus* pathogenesis in the murine sepsis model 338
5.3.5.4 Interrogating the mechanism of pathogenesis augmentation 344
5.3.5.4.1 Population dynamics following mixed inocula administration 344
5.3.5.4.2 Cytokine analysis of mouse serum 353
5.4 Discussion 356
5.4.1 Potential mechanisms of augmentation of *S. aureus* infection 357
5.4.2 Clinical importance of infection potentiation 360
5.4.3 Further work 362

Chapter 6. General discussion 365
6.1 Defining the ‘players’ 366
6.2 Understanding the requirements for disease 367
6.3 Understanding the effects of disease 370
6.4 Further considerations 371

References 373

List of Figures

Figure 1.1 Waves of *S. aureus* antibiotic resistance associated with antibiotic introduction 11
Figure 1.2 The innate and adaptive arms of the vertebrate immune system 19
Figure 1.3 Mammalian Toll-like receptors and their signaling pathways 20
Figure 1.4 Structure of *S. aureus* peptidoglycan 25
Figure 1.5 The currently known virulence regulatory network of *S. aureus* 37
Figure 1.6 Evolution of the immune system 45
Figure 1.7 Anatomy of a zebrafish embryo at 2 dpi 49
Figure 3.1 Maximum likelihood phylogenetic tree of MRSA 'global ST239 strains' based on core genome SNPs 103
Figure 3.2 Maximum likelihood phylogenetic tree of MRSA 'local ST239 strains', based on core genome SNPs 104
Figure 3.3 MRSA 'global ST239 strains' show variable virulence phenotypes when injected into the zebrafish circulation valley 106
Figure 3.4 MRSA 'local ST239 strains' show variable virulence phenotypes when injected into the zebrafish circulation valley 107
Figure 3.5 MRSA 'local ST239 strains' show similar virulence phenotypes when injected into the zebrafish circulation valley 108
Figure 3.6 Representation of SNP designation compared to the reference strain 115
Figure 3.7 Distinguishing SNPs between neighbouring strains 116
Figure 3.8 Antibiotic susceptibility of (A) SH1000, (B) GRE18 and (C) R35 as tested by disc diffusion on BHI media 126
Figure 3.9 Extent of RBC haemolysis between strains on defibrinated horse blood agar 129
Figure 3.10 Extent of RBC haemolysis between (A) GRE18, (B) R35 and (C) SH1000 (positive control) strains on defibrinated rabbit blood agar 130
Figure 3.11 Construction of the *S. aureus saeS*$^{\Delta A \rightarrow T}$ plasmid, pEJ1 136
Figure 3.12 PCR products of *S. aureus saeS*$^{\Delta A \rightarrow T}$ mutant recreation in pIMAY-Z. 137
Figure 3.13 Construction of the *S. aureus saeS*$^{\Delta A \rightarrow T}$ plasmid, pEJ2 138
Figure 3.14 PCR products of *S. aureus saeS*$^{\Delta A \rightarrow T}$ mutant recreation using pIMAY 139
Figure 3.15 Diagrammatic representation of the likely outcomes of a single cross over recombination event of pEJ2 into the *S. aureus* R35 chromosome 140
Figure 3.16 Diagrammatic representation of the outcomes of the double cross over excision event after upstream integration 141
Figure 3.17 Final steps of recreating mutant SH1000 *saeS*$^{\Delta A \rightarrow T}$ 142
Figure 3.18 Haemolysis caused by BHI culture supernatants of SH1000 (wildtype) and two mutants of *saeS* at various dilutions on rabbit blood agar 145
Figure 3.19 Zebrafish embryo survival rates upon bacterial circulation injection of SH1000 (wildtype) and two mutants of *saeS* 146
Figure 3.20 Construction of the *S. aureus htrA2*$^{\Delta G \rightarrow A}$ plasmid, pEJ3 148
Figure 3.21 Construction of the *S. aureus isaB* plasmid, pEJ4 150
Figure 3.22 PCR products of various *S. aureus* mutants 151
Figure 3.23 Construction of the *S. aureus* SATW20_13140$^{\Delta Gdel}$ plasmid, pEJ5 153
Figure 3.24 Maximum likelihood phylogenetic tree of MRSA ST22 NITU strains, based on core genome SNPs 157
Figure 3.25 Results from the phenotypic assay from the small ST22 MRSA outbreak 158

Figure 3.26 Maximum likelihood phylogenetic tree of MRSA ST2173 SCBU strains, based on core genome SNPs 159
Figure 3.27 Survival rate of zebrafish embryos injected with various strains from the SCBU ST 2371 MRSA outbreak 160
Figure 4.1 Workflow chart displaying NTML phenotypic screen to identify strains of interest 173
Figure 4.2 Purine biosynthesis mutant growth is prevented in mammalian serum 178
Figure 4.3 The purine *de novo* biosynthesis pathway 180
Figure 4.4 Role of adenine and guanine in the growth, on solid media, of purine biosynthesis mutants 182
Figure 4.5 *In vivo* attributes of purine biosynthesis mutants in the zebrafish infection model 183
Figure 4.6 *In vivo* complementation of purine biosynthesis mutants in the zebrafish embryo model of infection 185
Figure 4.7 Virulence of haemolytic NTML strains in the zebrafish infection model 187
Figure 4.8 The *de novo* folate biosynthesis pathway in *S. aureus* 188
Figure 4.9 Growth of parent and *pabA* strains on human blood/components or mammalian whole blood agar 190
Figure 4.10 Analysis of the JE2-*pabA* phenotype in liquid CDM 195
Figure 4.11 Growth of JE2 and JE2-*pabA* on 30% (v/v) human blood agar plates with or without pyrimidines 196
Figure 4.12 *In vivo* attributes of *pabA* in the zebrafish infection model 198
Figure 4.13 Virulence of SH-*pabA* in the murine sepsis model of infection 200
Figure 4.14 Survival curves demonstrating biochemical complementation of SH-*pabA* in the zebrafish embryo infection model 204
Figure 4.15 Biochemical complementation of SH-*pabA* with pyrimidines in the zebrafish model of infection 205
Figure 4.16 Virulence of *pabB* and *pabC* in the zebrafish infection model 207
Figure 4.17 Investigation of the role of the *pab* operon, *glyA* and PABA in *S. aureus* pathogenesis in the zebrafish embryo infection model 210
Figure 4.18 Growth of parent or mutant on plasma agar with increasing amounts of vortexed red plasma 213
Figure 4.19 Analysis of the effect of human haemoglobin on JE2-*pabA* growth 214
Figure 4.20 Metabolic pathways associated with dTTP production 217
Figure 4.21 Analysis of the effect of non-RBC components on JE2-*pabA* growth 218
Figure 4.22 Role of serine, glycine and thymidine on growth of JE2 (top half) and JE2-*pabA* (bottom half) 220
Figure 4.23 Resistance cassette replacement in Tn mutants 223
Figure 4.24 Role of PABA and other components in growth on human blood with or without pyrimidine supplementation 226
Figure 4.25 Effect of Tdk inhibitors on parent and *pabA* growth on human blood 230
Figure 4.26 Effect of zinc chloride on bacterial growth on human blood 233
Figure 4.27 Strain susceptibility to trimethoprim with or without exogenous thymidine on BHI media 236
Figure 4.28 Strain susceptibility to trimethoprim with or without exogenous thymidine on 30% (v/v) human blood agar 237
Figure 4.29 Strain susceptibility to trimethoprim with or without exogenous thymidine on 30% (v/v) sheep blood agar 238
Figure 4.30 Strain susceptibility to trimethoprim with or without exogenous thymidine on 30% (v/v) horse blood agar 239
Figure 4.32 Strain susceptibility to trimethoprim with or without exogenous thymidine on Mueller-Hinton agar 242

Figure 4.32 Growth of parent and mutants on whole or lysed animal blood agar 244
Figure 4.33 Growth of parent and mutants on whole human blood agar with varying levels of thymidine 245
Figure 4.34 Growth of parent or *pabA* on Mueller-Hinton agar supplemented with thymidine with addition of discs impregnated with blood components 247
Figure 4.35 Summary of data on potential mechanisms of the *pabA* growth phenotype 253
Figure 5.1 Co-injection of tetracycline resistant and sensitive strains in a 1:9 ratio followed by the administration of tetracycline 264
Figure 5.2 The effect of attenuated strains on *S. aureus* SH1000 pathogenesis in the zebrafish infection model 268
Figure 5.3 Combining *purB* or *pheP* with *sae*Δ did not permit augmentation of pathogenesis in the zebrafish infection model 269
Figure 5.4 Non-viable *phePsaeR* was unable to augment host death in the zebrafish infection model 270
Figure 5.5 Population dynamics of bacterial strains in single and mixed infections in the zebrafish infection model 272
Figure 5.6 Myeloid depleted zebrafish embryos show susceptibility to both the parent and *phePsaeR* mutant 274
Figure 5.7 Parental GFP-labelled *S. aureus* and red fluorescent *phePsaeR* were internalised by zebrafish phagocytes 276
Figure 5.8 Population dynamics of *purB* and *sagB* in single and mixed infections in the zebrafish infection model 278
Figure 5.9 Microscopy of 1 μm latex beads injected into the zebrafish embryo circulation valley 281
Figure 5.10 Microscopy of 'low dose' *S. aureus* and 1 μm latex beads co-injected into the zebrafish embryo circulation valley 282
Figure 5.11 Effect of beads on *S. aureus* pathogenesis in the zebrafish infection model 283
Figure 5.12 Gram-positive nonpathogenic bacteria are able to augment pathogenesis with low dose *S. aureus* in the zebrafish infection model 287
Figure 5.13 Microscopy of low dose *S. aureus* SH1000 coinjected with other Gram-positive bacteria 289
Figure 5.14 Peptidoglycan alone was unable to kill the zebrafish embryo host 293
Figure 5.15 Effect of co-injection of peptidoglycan from various species with low dose *S. aureus* bacteria 295
Figure 5.16 Composition of peptidoglycan from various Gram-positive bacteria 296
Figure 5.17 Bacterial kinetics when low dose *S. aureus* was co-injected with peptidoglycan in the zebrafish pathogenesis model 297
Figure 5.18 Microscopy of phagocytosed labelled *M. luteus* peptidoglycan in live zebrafish 299
Figure 5.19 Microscopy of phagocytosed labelled *M. luteus* peptidoglycan and live *S. aureus* within live zebrafish 300
Figure 5.20 Disruption of the peptidoglycan backbone may be important during augmentation of zebrafish infection 302
Figure 5.21 Mixed inocula with *phePsaeR* does not elicit an augmentation phenomenon in the murine sepsis model 307
Figure 5.22 Mouse health in response to different doses and types of peptidoglycan 309
Figure 5.23 Co-inoculation of *M. luteus* peptidoglycan with a low dose of *S. aureus* promotes recovery of high bacterial numbers from the murine liver 313
Figure 5.24 Co-inoculation of *S. aureus* peptidoglycan and low dose of *S. aureus* promotes recovery of high bacterial numbers from the murine liver 315

Figure 5.25 Lipoproteins are not responsible for augmentation of pathogenesis by peptidoglycan 316
Figure 5.26 *C. flaccumfaciens* or *B. subtilis* peptidoglycan can enhance *S. aureus* pathogenesis 320
Figure 5.27 *S. epidermidis* peptidoglycan can enhance *S. aureus* pathogenesis 321
Figure 5.28 Polystyrene latex beads cannot augment pathogenesis of *S. aureus* in the murine sepsis model 324
Figure 5.29 Macroscopic images and histopathology of murine livers 326
Figure 5.30 Titration of *S. aureus* dose in mixed inocula during *S. aureus* pathogenesis in the murine sepsis model 328
Figure 5.31 Titration of *M. luteus* peptidoglycan dose in mixed inocula during *S. aureus* pathogenesis 330
Figure 5.32 *S. aureus* strain specific effects may play a role in augmentation of murine infection 332
Figure 5.33 Use of the C57BL/6 mouse strain to demonstrate the pathogenesis augmentation phenomenon 337
Figure 5.34 Co-injection of live *S. epidermidis* and low dose *S. aureus* pathogenesis in the murine sepsis model 340
Figure 5.35 Co-injection of live *S. epidermidis* augments low dose *S. aureus* pathogenesis in the murine sepsis model 341
Figure 5.36 Co-injection of live *M. luteus* augments low dose *S. aureus* pathogenesis in the murine sepsis model 343
Figure 5.37 Distribution of bacterial load in mouse organs at various time points during infection 345
Figure 5.38 The pattern of *S. aureus* clonal expansion observed with and without peptidoglycan during murine infection 350
Figure 5.39 Assessment of the degree of clonality in murine liver abscesses 352
Figure 5.40 Cytokine measurements from mouse serum at baseline, 6 and 48 hours post intravenous injection with *S. aureus* and/or peptidoglycan 355

List of Tables

Table 1.1 Comparison of CA-MRSA and HA-MRSA characteristics 8
Table 1.2 Immune evasion mechanisms of *S. aureus* 35
Table 2.1 Composition of chemically defined minimal media 55
Table 2.2 Antibiotic stock solutions and concentrations 59
Table 2.3 *S. aureus* strains used in this study 64
Table 2.4 Other Gram-positive strains used in this study 65
Table 2.5 *E. coli* strains used in this study 65
Table 2.6 List of plasmids used in this study 66
Table 2.7 Stock solutions and concentrations 71
Table 2.8 List of primers used in this study 77
Table 2.9 DNA fragments used for DNA sizing and approximate quantification for agarose gel electrophoresis. 82
Table 2.10 Morpholino used in this study 90
Table 2.11 Peptidoglycan digest conditions 95
Table 3.1 Pairwise comparisons across the MRSA 'global ST239 strain' collection 110
Table 3.2 Pairwise comparisons of the MRSA 'local ST239 strain' collection 111
Table 3.3 Pairwise comparisons of the strains from the MRSA 'local ST239 strain' collection which showed minimal virulence differences 112
Table 3.4 Bioinformatic analysis of core genome SNP differences and indels between nodes and/or isolates in the 'global ST239 strain' and 'local ST239 strain' collection compared to the reference genome, TW20 118
Table 3.5 Potential functional impact of identified mutations on candidate genes 122
Table 3.6 Table of antibiotic and heavy metal susceptibility of *S. aureus* strains 127
Table 4.1 Strains identified as having an altered phenotype on human blood agar 175
Table 4.2 Summary of JE2 strains with altered phenotype changes than remained post-transduction 176
Table 4.3 Growth analysis on solid media of JE2-*purA* and JE2-*purB* in the presence or absence of adenine and guanine 182
Table 4.4 A summary of the roles of folate in *S. aureus* metabolism 189
Table 4.5 Growth of wildtype and mutant on solid CDM base agar with various nutrient combinations 194
Table 4.6 Pyrimidine contribution to growth of *pabA* in nutrient poor media 220
Table 4.7 Concentrations of thymidine measured in the serum of various mammals 229
Table 5.1 Description of attenuated mutant strains 267

Chapter 1. Introduction

1.1 *Staphylococcus aureus*

Staphylococcus aureus is a Gram-positive coccus, approximately 0.5-1.5 μm in diameter, belonging to the Firmicute phylum and of the order Bacillales. Staphylococcal cell division occurs in multiple planes (Tzagoloff and Novick, 1977), producing a 'bunch of grapes' formation, after which this bacterial genus was named, from the Greek, *staphyle* (bunch of grapes) and *kokkos* (berry), in 1880 by Sir Alexander Ogston. *S. aureus* is a non-motile and non-sporing-forming bacterium able to colonise all mammalian species and also some species of bird. In humans, it has a niche preference for the anterior nares, from where the bacteria can be shed to the skin and other mucosa. Although *S. aureus* is a commensal organism, causing no harm to many carriers, it is also a successful pathogen, able to employ a plethora of virulence determinants, regulated by sophisticated networks. The golden colour of *S. aureus* colonies is caused by the carotenoid, staphyloxanthin, which not only provides its distinctive appearance but importantly, a mechanism of resisting oxidative stress (Clauditz et al., 2006).

The colony colour and marked virulence potential is in contrast to many other members of the staphylococcal genus, for example, *Staphylococcus epidermidis*. Coagulase negative staphylococci including *S. epidermidis* generally produce white colonies and are some of the most abundant human skin colonising bacteria. Clinical sequelae of *S. epidermidis* are most often associated with prosthetic devices and of a more indolent nature, compared to the pyogenic, rapidly progressive spectrum of infections caused by *S. aureus* (Rogers et al., 2009).

1.2 Metabolism of *S. aureus*

S. aureus is a facultative anaerobe, which defines its ability to generate adenosine tri-phosphate (ATP) by fermentation in oxygen-poor environments. As with many other bacteria, highly conserved metabolic pathways exist which are unique to prokaryotes, allowing a more 'self-sufficient' existence compared to that of higher eukaryotic cells

(Bermingham and Derrick, 2002). Furthermore, such pathways can be exploited as pathogen specific therapeutic targets (Darrell et al., 1968).

1.2.1 Role of purine biosynthesis

The role of purine biosynthesis in bacterial pathogenesis has been studied across various pathogens including *S. aureus*. A signature tagged mutagenesis approach was conducted using Tn917 in *S. aureus*. After screening 1248 mutants through a murine model of intraperitoneal infection, several attenuated mutants were identified including an enzyme involved in *de novo* purine biosynthesis, phosphoribosylformylglycinadmidine synthetase, PurL (Mei et al., 1997). A similar approach was used in *S. pneumoniae* and by screening for virulence through a mouse pneumonia model, *purE*, *purK*, *purC* and *purL* were all identified as genes necessary for host persistence and proliferation (Polissi et al., 1998). During attempts to develop more defined and efficacious vaccines against *Salmonella typhi*, strains with stable mutations in *purA*, were significantly attenuated when administered orally or intravenously into BALB/c mice (O'Callaghan et al., 1988). *purA* and *purB* are also known to be attenuated *in vivo* in *Listeria monocytogenes* (Faith et al., 2012). Finally, adenine dependent *Bacillus anthracis* strains administered orally were unable to cause mortality in a mouse model, unlike their prototypic counterparts (Ivánovics et al., 1968).

1.2.2 Role of folate production

Unlike in humans, bacteria *de novo* synthesise folate via the *pab* operon which contains three genes, *pabA, pabB* and *pabC*, converting chorismate to para-aminobenzoic acid (PABA). The active forms of folate, dihydrofolate (DHF) and tetrahydrofolate (THF), are synthesized further downstream. The effector molecule, THF, functions as a cofactor in many essential biosynthetic pathways and has wide ranging involvement in purine, pyrimidine and amino acid synthesis (Sonenshein et al., 1993). Humans ingest dietary folate in fortified foods or supplements and cannot synthesise it *de novo*. This provides unique antibiotic targets specific to bacteria and several anti-microbial drugs against *S. aureus* target key components of the *de novo* bacterial folate biosynthesis pathway. Sulphonamides antagonise the FolP enzyme which converts PABA and pteridine to 7,8 dihydropteroate (Hampele et al., 1997). However, prolonged treatment

with folate antagonist antibiotics can lead to antibiotic resistant subpopulations and treatment failure (Zander et al., 2010a).

1.2.3 Linking metabolism and virulence

Common to many bacteria, pathogenesis and metabolism are inextricably linked, as *S. aureus* must be able to make use of the available resources across different *in vivo* habitats. From colonisation to distant dissemination, the environmental conditions of *S. aureus* can alter dynamically. Transcriptomic analysis of *S. aureus* gene expression during early adaptation to the murine lung revealed that gluconeogenesis and the citric acid cycle are down regulated within thirty minutes of entering the lung environment yet amino acid synthesis and protein translation are up regulated (Chaffin et al., 2012). The metabolic activity of *S. aureus* during nasal colonisation was recently studied both *in vitro* and *in vivo* using a cotton rat nasal colonisation model. RNA from *S. aureus* grown in a media designed to replicate the nasal environment was analysed using microarrays. Major differences in the transcriptome during colonisation were found in genes for central metabolic functions with the majority of up regulated genes belonging to amino acid transport and synthesis (Krismer et al., 2014). Finally, signature tagged mutagenesis (STM) was applied to multiple *S. aureus* infection models (mouse abscess, bacteraemia, wound and rabbit endocarditis) to identify genes involved in growth *in vivo*. Genes involved in amino acid transport and biosynthesis were heavily represented in the mutant pool found to be associated with attenuation in the murine models (Coulter et al., 1998). These studies highlight that metabolic determinants of pathogenesis require ongoing investigation as it may identify factors universally required for pathogenesis and expose novel therapeutic strategies not previously considered.

1.3 Requirements for growth

Growing optimally between 30°C and 37°C, *S. aureus* remains able to grow throughout a wide range of temperatures from 7°C to 48.5°C (Schmitt et al., 1990). A range of pH can also be tolerated (4.0 and 10.0) with the optimum between 6.0 and 7.0 (Valero et al., 2009). *S. aureus*, when grown in complex media, is extremely tolerant to sodium chloride, withstanding solutions up to 25% (w/v) NaCl (Parfentjev and Catelli, 1964). As many other organisms cannot withstand such concentrations, halotolerance of *S.*

aureus is used as a selective marker to isolate *S. aureus* from clinical specimens. Resistance to desiccation is also marked as *S. aureus* is able to survive on dry plastic surfaces for up to three years (Chaibenjawong and Foster, 2011).

S. aureus are chemoheterotrophs as they use organic carbon as their energy source. As such they grow well in undefined complex media. The exact biochemical requirements of *S. aureus* are not well studied nor defined. Due to advances in sequencing technologies, transposon mutant library screens can now be combined with high-throughput genome sequencing data to study genes necessary for growth under defined conditions (Valentino et al., 2014). Using this technique, *S. aureus* genes contributing to fitness in *ex vivo* fluids such as whole blood or a murine subcutaneous abscess model were compared to those required for growth in synthetic rich media. Many of the 426 genes identified as important in these infection models were involved in metabolic pathways such as nucleotide biosynthesis and amino acid interconversion. Whilst some of these were already known, many were novel with unclear functional roles that require further exploration.

1.3.1 Bypassing 'nutritional immunity'

Understanding the exact requirements for energy, growth factors including vitamins, macro and micro nutrients, is essential for the development of novel therapeutic strategies as limiting essential requirements *in vivo*, a concept known as 'nutritional immunity', is a viable and under-explored strategy for *S. aureus* control.

Iron sequestration is one of the best known examples of nutritional immunity in *S. aureus* host:pathogen interactions (Trivier and Courcol, 1996). In order to be able to use haemoglobin as an iron source, *S. aureus* employ an elegant system known as the iron regulated surface determinant system (Isd). The negative regulator of this system is the iron dependent ferric uptake regulator (Fur). In iron poor conditions, Fur no longer binds the *fur* box (upstream of *fur*-regulated genes) and the *isd* system is transcribed (Baichoo et al., 2002). IsdA, IsdB and IsdH are attached to the cell surface by sortase A (SrtA). IsdB and IsdH recognise haemoglobin and other complexes whilst IsdA removes heme from the bound hemoproteins and transfers it to another surface attached protein, IsdC. Ultimately, IsdC aids in the transfer of heme across the cell wall using the IsdDEF transport and once inside, heme is degraded by the heme oxygenases IsdG and

IsdI (Pishchany et al., 2013) and iron is liberated for use in diverse bacterial biochemical reactions.

Other examples of 'nutritional immunity' can also be found and phagocytes, cells able to ingest and destroy foreign particles such as bacteria, may play a role. It has been previously noted that activated macrophages have functional folate receptors (Xia et al., 2009). Upon inflammatory signal stimulation, folate receptors are up regulated on the macrophage surface and capable of internalisation of folate. As activated macrophages are terminally differentiated, it is not fully understood why up regulation of folate receptors should occur during infection. One hypothesis is that macrophages scavenge folate from the environment to help prevent bacterial growth, as is seen for iron (Theurl et al., 2005). However, for bacteria with intracellular survival capability, such as *S. aureus*, this presents an intriguing situation which has not been explored and there may be an interesting link between folate acquisition and pathogenesis. Another pathogen that survives well in phagocytes is *Francisella tularensis* which is able to escape the hostile internal compartment within the phagocyte, the phagosome, and replicate in the cytoplasm. In an attempt to identify genes associated with live vaccine strain virulence, a mutation in a enzyme involved in folate metabolism, 5-formyltetrahydrofolate cycloligase, led to reduced virulence *in vivo* (Ulland et al., 2013). The mechanism was attributed to folate deficiency affecting bacterial membrane stability which in turn led to an enhanced inflammatory cascade leading to increased macrophage, and therefore, bacterial death.

1.4 Clinical significance of *S. aureus*

For nearly 150 years, *S. aureus* has been known to cause purulent disease, spanning from uncomplicated skin and soft tissue infections to life-threatening bacteraemia leading to sepsis and death (Lowy, 1998). Recognition of the asymptomatic or 'healthy' carrier state became possible with the introduction of the coagulase test, allowing coagulase positive and negative staphylococci to be distinguished (Chapman et al., 1934). Epidemiological studies have consistently recorded *S. aureus* colonisation rates of around 30%, predominately in the nose (Williams, 1963). Individuals colonised with *S. aureus* are at an increased risk of subsequent disease and *S. aureus* bacteraemia was three times more frequent in carriers compared to non-carriers. Furthermore, 80% of

disease strains isolated from carriers were found to be endogenous (Wertheim et al., 2004).

S. aureus is a leading cause of skin, joint, bone and endovascular infections. Establishing niches in both the community (Miller et al., 2014) and nosocomial environment, there is a high incidence of this versatile pathogen globally and over 10,000 *S. aureus* bacteraemias reported per year in England, Wales and Northern Ireland alone (Public Health England, 2015). With current treatment options, the case fatality rate from *S. aureus* bacteraemia is approximately 25-35% (Laupland et al., 2008). In the 1960s, the first methicillin-resistant *S. aureus* (MRSA) isolate was identified and twenty years on, these strains are a predominant cause of health-care associated infections (HA-MRSA), particularly in areas of high antibiotic usage such as intensive care units (Boucher and Corey, 2008). MRSA is associated with a significantly higher likelihood of death compared to its less antibiotic resistant counterpart, methicillin-sensitive *S. aureus* (MSSA) (Cosgrove et al., 2003).

Since the 1990s, new community-acquired (CA-MRSA) strains have emerged, particularly in the United States but also worldwide (Buckingham et al., 2004). Of concern, healthy individuals with no health care contact or identifiable risk factors are increasingly infected with CA-MRSA (Table 1.1) (David and Daum, 2010). Aside from clinical information, a distinguishing marker between HA-MRSA and CA-MRSA is the genomic staphylococcal chromosomal cassettes (SCC) containing the gene responsible for methicillin resistance, *mecA*. As seen in Figure 1.1 and discussed further in Section 1.11.3, the SCC mec elements within strains have changed in tandem with the type of infection i.e. HA vs CA-MRSA. In the United States, CA-MRSA disease burden now represents a public health crisis which requires novel control strategies and adapted antibiotic prescribing regimes (David et al., 2014).

At least in the United Kingdom, MRSA bacteraemia rates have declined in recent years from around 4,500 cases per year in 2007/8 to 800 in 2014/2015. There has not been a similar decline in MSSA bacteraemia rates with approximately 9000 bacteraemias being reported each year since recording started in 2010 (Public Health England, 2015). There are several hypotheses as to why the epidemiology of MRSA and MSSA infection varies so widely. *S. aureus* is a clonal organism, allowing for small groups of successful, genetically similar organisms to predominate at different times (Feil et al.,

2003). Once new clones emerge causing clinical consequences, control strategies are implemented (e.g. patient admission MRSA screening and decolonisation, clean hand campaigns, government target initiatives) such as occurred when epidemic MRSA strains caused large numbers of nosocomial infections in the mid-2000s (Wyllie et al., 2011). However, measuring isolation rates of epidemic MRSA strains over time, Wyllie and colleagues noted a decrease in MRSA from 2006 onwards, which is before the more intensive infection control strategies were actually implemented. This suggests biological or environmental factors may play more of a role in clone success, than previously anticipated and further research is required in this area.

IMAGE REMOVED

Table 1.1 Comparison of CA-MRSA and HA-MRSA characteristics

[a] based on Clinical Laboratory and Standards Institute (CLSI) breakpoints

[b] inducible resistance may occur

SCC – Staphylococcal chromosomal cassette

TMP-SMZ – trimethoprim + sulphamethoxazole

Reproduced from (Weber, 2005)

1.5 Antibiotic resistance of *S. aureus*

Prior to the mass introduction of benzylpenicillin in 1944, the mortality rate of *S. aureus* bacteraemia was in excess of 80% and a sinusoidal relationship between mortality rate and antibiotic effectiveness has since continued (Dancer, 2008). 'Waves' of antibiotic resistance have followed introduction of new antibiotics (Figure 1.1).

Gram-positive bacteria possess thick cell walls composed of a large polymer, peptidoglycan. Penicillin based antibiotics inhibit cell wall synthesis by preventing polymerisation of peptidoglycan subunits. The molecular structure of penicillins include a beta-lactam ring (a four-membered lactam or cyclic amide) which inhibits the bacterial transpeptidases that are required to attach new peptidoglycan to the pre-existing cell wall (Neu and Gootz, 1996). Not long after the introduction of penicillin, resistant *S. aureus* isolates were found (Wilson and Cockcroft, 1952) due to bacterially produced beta-lactamase enzymes capable of hydrolysing the beta-lactam ring (Abraham and Chain, 1988). Therefore, further modifications to the standard beta-lactam ring were necessary to overcome these adaptive mechanisms. Methicillin, oxacillin and flucloxacillin, introduced in the 1960s, are semi-synthetic beta-lactam antibiotics stable to the beta-lactamases produced by *S. aureus*. Flucloxacillin is now used worldwide to treat infections due to MSSA whereas methicillin and oxacillin are no longer used clinically but are often employed in antibiotic susceptiblity testing (de Lencastre et al., 1991).

Penicillin binding proteins (PBPs), including transpeptidases, are enzymes required in the terminal stages of peptidoglycan production. Beta-lactam antibiotics resemble the D-alanine-D-alanine end of the peptidoglycan pentapeptide required for cross-linking of the peptidoglycan in Gram-positive bacteria by PBPs. Inhibition of these enzymes leads to bacterial death (Sauvage et al., 2008). However, MRSA strains possess a novel PBP, classified as PBP2a, which has low-affinity for beta-lactam antibiotics and continues to catalyse peptidoglycan biosynthesis (Brown and Reynolds, 1980).

Fortunately, other antibiotics have been developed with different mechanisms of action to penicillins. One of the most effective against MRSA is a class of antibiotics known as glycopeptides, which includes vancomycin and teicoplanin. These large molecules act by binding with high affinity to the D-alanine-D-alanine terminus of the pentapeptide,

thus blocking the addition of peptidoglycan precursors to the nascent peptidoglycan chain (Reynolds, 1989). As this mechanism is unaffected by the novel PBP found in MRSA, these antibiotics are the mainstay for treatment of MRSA infections. Unsurprisingly, since their accelerated usage in the 1980s, when MRSA was becoming an increasing problem, resistance to these agents has also emerged.

The first vancomycin-insensitive *S. aureus* (VISA) was detected in a sternotomy incision site of a Japanese infant (Hiramatsu et al., 1997). A VISA is characterised by a vancomycin minimum inhibitory concentration (MIC) between 4-8 μg ml^{-1} due to a thickened and incompletely cross-linked cell wall (Cui et al., 2003). Since then many more VISA strains have been reported (Liu and Chambers, 2003). Importantly, vancomycin-resistant *S. aureus* (VRSA) has also now appeared (MIC > 16 μg ml^{-1}), first in the USA and later reported from South Asia (Saha et al., 2008; Sievert et al., 2008). VRSA is mediated by the acquisition of the *vanA* operon from an *Enterococcus* species, resulting in minimum inhibitory concentrations (MIC) to vancomycin of over 256 μg ml^{-1} (Périchon and Courvalin, 2009). Acquisition of the transposon mediated *vanA* operon, affords the bacteria an enzyme which replaces the D-Alanine-D-Alanine terminus with D-Alanine-D-Lactate, the latter of which has markedly reduced affinity for vancomycin. As such strains were recorded, two new classes of antibiotics have been employed against multiply resistant *S. aureus*, namely linezolid and daptomycin. However, resistance towards these novel classes of antibiotics is already reported (Sánchez García et al., 2010; Thwaites et al., 2011). With limited capacity to treat multi-drug resistant strains and bacterial antibiotic resistance evolving rapidly, novel approaches to therapeutics and preventative measures are needed.

Between 1935 and 1968, 14 new classes of antibiotics were introduced yet from 1968 to date, only 5 have been developed (Powers, 2004). Accelerated antibiotic discovery from the 1930-60's allowed multiple antibiotic choices to be available to treat infections. Vancomycin was originally developed in the 1950s but it was not widely used for another 30 years, when it was required to help control the increasing number of MRSA infections. It is no longer possible to wait for emergence of antibiotic resistance, then revisit antibiotic options and choose one that can overcome the particular resistance mechanism. With decreased investment in novel antimicrobials and increased sophistication and complexity of bacterial resistance mechanisms, the 'post-antibiotic era' is a real threat to the population.

IMAGE REMOVED

Figure 1.1 Waves of *S. aureus* antibiotic resistance associated with antibiotic introduction

Waves are indicated above the graph:
1 the first pandemic antibiotic-resistant strains (phage type 80/81)
2 the first MRSA strain (MRSA-I containing SCC*mec*I)
3 new MRSA strains and (MRSA-II containing SCC*mec*II and MRSA-III containing SCC*mec*III) mainly affecting health care facilities.
4 emergence of VISA and CA-MRSA strains (containing smaller *mec* elements such as SCC*mec*IV) (MRSA-IV). VRSA strains were first identified in 2002.

A - accelerated use of vancomycin (Kirst et al., 1998)
B - introduction of linezolid and daptomycin

Adapted from (Chambers and DeLeo, 2009).

1.6 Prevention of *S. aureus* infection

The significant heterogeneity of the global *S. aureus* bacterial population makes a unifying prevention strategy particularly challenging. Both MRSA and MSSA bacterial populations are diverse, with further sub-populations predominating in specific niches. Whilst there are multiple circulating clonal complexes of MSSA in the UK (Feil et al., 2003), strain replacement has allowed two epidemic MRSA (E-MRSA) strains to predominate in UK hospitals since the early 1990s, E-MRSA 15 (ST 22) and E-MRSA 16 (ST 36) (Johnson et al., 2001). Furthermore, mobile genetic elements (MGEs) that carry genes encoding virulence factors and antibiotic resistance are unstable between different sequence types of *S. aureus* (Lindsay and Holden, 2004).

The UK government mandated identification and decolonisation of asymptomatic carriers of MRSA admitted to healthcare environments, may have contributed to the decline in MRSA prevalence, as measured by episodes of MRSA bacteraemia (Pearson et al., 2009). However, a similar decline has not been observed in rates of MSSA bacteraemia, highlighting the differences in epidemiology and acquisition risk factors, of these infections (Wyllie et al., 2011). As such, preventative approaches such as pre-operative decolonisation of known MSSA carriers in at-risk groups is increasingly attempted, with varying success (Simor, 2011). In addition, numerous attempts to produce an efficacious vaccine have been undertaken. A vaccine providing protection from *S. aureus* autoinfection in colonised patients would be of significant use, particularly in high-risk groups.

Development of a successful vaccine requires a multi-faceted approach able to interrupt the myriad of temporally expressed virulence factors and sophisticated adaptations that *S. aureus* has developed to establish infection within the host (Scully et al., 2014). Unsurprisingly, vaccines targeting single elements of this complex system e.g. IsdB (Kuklin et al., 2006) or capsular polysaccharide vaccines (Matalon et al., 2012) have failed in clinical trials. Multi-antigen vaccines are currently in development and testing phase, with antigen selection including toxins, nutrient acquisition genes and adhesion molecules (Spaulding et al., 2013).

Passive immunization has also been studied with data supporting a favourable outcome in a mouse pneumonia model (Foletti et al., 2013). Mice infected with *S. aureus* strain

USA300 LAC and then given human derived alpha-haemolysin antibodies, showed increased survival. Moreover, when administered in addition to linezolid, there was additional benefit. This has important clinical translation, as antibodies used in treatment are unlikely to be used in isolation.

Recently, mini-antibodies have been developed against the extracellular fibrinogen binding (Efb) protein, a complement inhibitor (Georgoutsou-Spyridonos et al., 2015). Mini-antibodies lack the fragment crystallisable region (Fc) and consist of dimeric fragment antigen binding (Fab) fragments only. In a mouse renal abscess model, mice injected prior to infection, with the blocking mini-antibodies, had significantly less bacteria recovered compared to control group animals. Novel antibody based therapies targeting *S. aureus* virulence factors are promising additions to current strategies.

1.7 Current strategies for treatment

Clinical guidelines on treatment of *S. aureus* disease are well established (Thwaites et al., 2011). For invasive infection such as bacteraemia, upon presumption or confirmation of MSSA and in the absence of beta-lactam allergy, high dose flucloxacillin is recommended. For MRSA bacteraemia, glycopeptides such as vancomycin is the antibiotic of choice. However, antibiotic choice varies depending on site of infection and additional agents inhibiting bacterial protein synthesis such as clindamycin or linezolid are added when *S. aureus* toxin production is likely to be playing a major role. Toxic shock syndrome, mediated by the toxic shock syndrome toxin (TSST-1) or infections caused by Panton Valentine Leukocidin (PVL) positive strains are examples of this.

More generally, however, patients presenting to hospital with signs of severe infection are often initially treated with broad anti-microbial cover. This is because at the onset of any infection, it is unlikely that the causative pathogen will be known. Investigations such as blood cultures may take up to 24 hours to flag positive and then the organism has to be identified. Even if there are indicators of *S. aureus* being the causative agent, sepsis guidelines recommend broad-spectrum anti-microbials in severely ill patients (www.survivingsepsis.org). An important implication of this is the effect of broad-spectrum antibiotics on the host microbiome. Currently, there is no detailed understanding of these effects and it is likely that disruption of colonising flora may

pre-dispose to other infections (Brown et al., 2013). Antibiotic-associated *Clostridium difficile* infection is an example of this occurring in the gut. Therefore, patients being treated for sepsis are likely to have markedly altered microbiomes compared to healthy individuals (Grice and Segre, 2011). As *S. aureus* is a significant cause of cannula-associated infections, routine insertion of cannulas to deliver drugs and take blood from patients leaves the host susceptible because of this potential portal of entry for *S. aureus*. In addition, further investigation into the role of surrounding skin flora on the likelihood of *S. aureus* infection is required as factors predisposing to infection are not fully elucidated (Chiller et al., 2001).

1.8 Immune protection against *S. aureus*

1.8.1 Innate immune system

Host immunological competence, influenced by both genetic and environmental factors, plays a vital role in preventing infections as demonstrated by the increased frequency and severity of infection in immuno-compromised patients (Jacobson et al., 1988). Physical innate defenses such as the skin and other epithelial layers provide a barrier to bacterial penetration. The mucus layer of the human intestine contains antimicrobial peptides (Ostaff et al., 2013) which are secreted into the lumen whilst the skin contains a range of peptides with antimicrobial activity such as cathelicidins and beta-defensins (Schauber and Gallo, 2008). Other skin components such as human skin fatty acid *cis*-6-hexadecenoic (C6H) have bacteriocidal effects on *S. aureus* (Cartron et al., 2014).

However, when pathogens breach these innate defences, the mainstay of protection against bacteria such as *S. aureus* is the immune system. Unlike invertebrates, vertebrates have both the immediate, danger sensing, response elements of the innate system but also the slower, highly specific and memory based adaptive immune system (Cooper and Alder, 2006). Both cellular and soluble components of the innate immune system are described. Soluble components include proteins from the complement system. Synthesised primarily in the liver, three distinct pathways can be triggered by microbial presence: the classical pathway which recognises antibody opsonised bacteria; the lectin pathway which recognises mannose in bacterial cell walls and the alternative pathway, all of which converge to allow formation of the membrane attack complex (MAC) in the bacterial outer surface, causing lysis (Janeway et al., 2001). *S. aureus* has been shown to activate all three arms of the complement system (Neth et al.,

2002; Verbrugh et al., 1979). The common link between all three pathways is the C3 protein that can be cleaved into C3a and C3b. Given the ability of *S. aureus* to cause persistent infections, it is not surprising that a secreted protein, extracellular fibrinogen-binding protein (Efb), has been identified allowing the pathogen to subvert immune responses (Lee et al., 2004).

1.8.1.1 Phagocytosis

Cellular components of the innate immune system, including neutrophils, macrophages and dendritic cells (DCs), are capable of phagocytosis. These phagocytes are able to destroy *S. aureus* but subversion of such processes is possible by the pathogen as discussed below in Section 1.10 and shown in Table 1.2.

Phagocytosis is an actin dependent process relying on cytoskeletal rearrangements to traffic particles intracellularly into a membrane bound vacuole (Kaplan, 1977). Most of the detailed work on phagocytosis has centered on macrophages. It has been shown that microparticles (particles with μm diameters) can be captured by specialised liver macrophages known as Kupffer cells whereas smaller, nanoparticles (less than 100 nm) leave the blood vasculature through holes in the endothelial lining (Mitragotri and Lahann, 2009). Therefore, phagocytosis is often defined as 'the cellular engulfment of large particles, usually those over 0.5 μm in diameter' (May and Machesky, 2001). However, other forms of engulfment exist including macropinocytosis and clarithin dependent and independent endocytosis, the latter of which may be involved in uptake of smaller particles, particularly in non-phagocytic cells (Rejman et al., 2004). Many factors are known to influence phagocytic capability including degree of opsonisation (Tuazon et al., 1981), size (Champion et al., 2008) and shape of the cargo (Champion et al., 2007). Using rat macrophage lines, particles between 2 and 3 μm displayed maximal phagocytosis (Champion et al., 2008), whereas using mouse peritoneal macrophages, 1.7 μm was optimal (Tabata and Ikada, 1988).

1.8.1.2 Cellular components of the innate immune system and their role in *S. aureus* killing

After engulfment, *S. aureus* reside in phagosomes, the vesicle that forms around ingested material. The phagosome maturation pathway differs between neutrophils and

macrophages but both ensure *S. aureus* is exposed to multiple degradative antimicrobial agents, which are released from specific cellular organelles after fusion events (Weiss and Schaible, 2015). The most abundant granulocyte, neutrophils, contain three types of granules with primary, azurophilic granules (containing myeloperoxidase, MPO) being the most important for bacterial killing *in vitro* (Klebanoff et al., 2013). Interestingly, whilst myeloperioxidase deficiency can occur in humans, this autosomal recessive disorder leads to increased risk of disseminated candidiasis more than increased rates of *S. aureus* infection (Lanza, 1998).

Neutrophil killing of *S. aureus* is not restricted to the intracellular environment. Neutrophil extracellular traps (NETs) are a chromatin structure, containing AMPs, histones and proteases that can trap and kill *S. aureus* (von Köckritz-Blickwede and Nizet, 2009). However, the key killing mechanism of *S. aureus* by both neutrophils and macrophages is via neutrophil NADPH-oxidase. This multicomponent enzyme complex transfers electrons between NADPH and molecular oxygen which generates the extremely toxic reaction oxygen species (ROS), superoxide anion (van Kessel et al., 2014). Further reactions can then occur to form several other ROS including hydrogen peroxide. In the absence of an intact oxidative burst, recurrent *S. aureus* (and other bacterial/fungal) infections occur as seen in the primary immunodeficiency, chronic granulomatous disease (CGD). Other rare genetic conditions highlight the most important parts of *S. aureus* killing pathways. Chediak Higashi syndrome (CHS) is associated with defective phagolysosome formation and impaired lysosome degranulation. Amongst other pathologies, patients affected by this syndrome are particularly susceptible to *S. aureus* infection (Lozano et al., 2014).

Whilst both neutrophils and macrophages are important for host defence against *S. aureus*, neutrophils are the most numerous phagocyte population and the first to arrive at the site of infection (Rooijakkers et al., 2005). In addition, they exhibit more rapid rates of phagocytosis and a higher intensity of oxidative respiratory response than do macrophages (Nordenfelt and Tapper, 2011).

Kupffer cells (KCs) are tissue resident macrophages in the liver and represent the largest innate immune system cell subset in this organ. They are the first barriers to pathogens entering the liver from the bloodstream, which occurs within seconds of intravenous injection into peripheral veins (Benacerraf et al., 1959). They are excellent

phagocytic cells with a relatively high basal level of reactive oxygen species production (Movita et al., 2012). Whilst there is no doubt that such cells can 'catch' *S. aureus*, it has been shown that eradication is incomplete with a subset of KCs harboring large clusters of *S. aureus* post intravenous murine injections (Surewaard et al., 2016). Moreover, the same study demonstrated that *S. aureus* clearance is dependent on ROS generation, whereas MPO and nitrosative stress play a limited role.

1.8.1.3 Pathogen ligand and host receptor associations

Microbial molecules (pathogen-recognition molecular patterns, PAMPs) common to bacteria but not eukaryotes are recognised by the cellular arm of the innate immune system. Recognition occurs via binding to pattern recognition receptors (PRRs), which mediates inflammatory signaling, and/or engulfment of the bacteria i.e. phagocytosis. Upon microbial engulfment, phagocytes are activated causing cytokine and chemokine production which enables cross-talk between the innate and adaptive arms of the immune response (Mogensen, 2009) (Figure 1.2).

The first cell surface PRR to be discovered was the Drosphila Toll, a transmembrane receptor with a large extracellular domain (Nüsslein-Volhard and Wieschaus, 1980). After being shown to be important in resistance of the fly to fungal infection, downstream signaling pathways via NF-κB were fully elucidated (Hetru and Hoffmann, 2009). Mammals are now known to possess ten Toll-like receptor (TLR) genes and as shown in Figure 1.3, many signal in a myeloid differentiation primary response protein-88 (MyD88), dependent manner, leading ultimately to inflammatory cytokine release and immune cell recruitment (O'Neill et al., 2013). Specific PAMPs recognised by the TLRs have been extensively studied and include peptidoglycan cell wall as well as surface associated molecules, lipopolysaccharide (LPS) on Gram-negative bacteria or teichoic acids on Gram-positive bacteria. TLR4 was first identified as the signaling receptor of LPS (Hoshino et al., 1999). Thereafter, TLR2 was found to recognise several bacteria lipoproteins (Hashimoto et al., 2006). By heterodimerising with TLR1 triacylated lipoproteins are sensed, yet if heterodimerisation occurs with TLR6 diacylated forms are bound (O'Neill et al., 2013).

Macrophages have a vast array of PRRs, as do neutrophils and these are well characterised (Hayashi et al., 2003). However, less is known about PRRs on KCs. PRRs

present on macrophages such as TLRs have been described on KCs in addition to the more general scavenger receptors (Reid et al., 2004). Human KCs are known to express TLR2 and are capable of cytokine production but perhaps at a lower level that other macrophage subsets (Visvanathan et al., 2007; Movita et al., 2012). KCs secrete the anti-inflammatory cytokine IL-10 in response to LPS challenge (Knolle et al., 1995). The lower overall cytokine production ability of KCs has been proposed to be due to their 'tolerogenic' function whereby bombardment with bacterial components of gut commensals, for example, may require such cells to be less reactive.

IMAGE REMOVED

Figure 1.2 The innate and adaptive arms of the vertebrate immune system

a) Innate immunity - macrophages and neutrophils ingest microbes and secrete cytokines that co-ordinate the immune response.
b) Dendritic cells (DCs) present antigens to lymphocytes to initiate adaptive immunity.

PRR – pathogen recognition receptor

PAMP – pathogen-associated molecular pattern

NLR – Nod like receptor

IL – interleukin

TNF – tumour necrosis factor

MHC – major histocompatibility complex

TCR – T-call receptors

$T_H1/2$ – T helper cells

Reproduced from (Buer and Balling, 2003)

IMAGE REMOVED

Figure 1.3 Mammalian Toll-like receptors and their signaling pathways

Signalling commences by ligand-induced receptor dimerisation. The TLR Toll–IL-1-resistance (TIR) domains then interact with adaptor proteins such as MyD88 or MyD88-adaptor-like protein (MAL).

TIR domain-containing adaptor protein inducing IFNβ (TRIF)
TRIF-related adaptor molecule (TRAM)
IL-1R-associated kinases (IRAKs)
TNF receptor-associated factors (TRAFs)
Mitogen-activated protein kinases (MAPKs)
JUN N-terminal kinase (JNK)
Interferon-regulatory factors (IRFs)
Cyclic AMP-responsive element-binding protein (CREB)
Activator protein 1 (AP1)
IKK inhibitor of NF-κB kinase
MKK MAP kinase kinase
RIP1 receptor-interacting protein 1
TAB TAK1-binding protein
TAK TGFβ-activated kinase
TBK1 TANK-binding kinase 1

Reproduced from (O'Neill et al., 2013)

1.8.2 Adaptive immune system

The adaptive immune system is divided into humoral, antibody mediated and cell mediated components. The initiation of an adaptive response occurs after dendritic cells phagocytose the invading microbe before migrating to the local lymph nodes whereby interaction with lymphocytes occurs (Figure 1.2). Dendritic cells are specialised antigen presenting cells and the presented antigen is recognised by mature naïve lymphocytes carrying a corresponding receptor to that specific antigen. Thereafter, the hallmark of adaptive immunity occurs – clonal selection of lymphocytes leading to a specific and long lasting immune response. Once activated, T lymphocytes differentiate into either cytotoxic T cells (CD8+) or T helper (CD4+) cells and B cells secrete antibody. Both humoral and cell mediated immunity are thereby focused onto the presenting pathogen (Alberts et al., 2002). Antibodies that bind the pathogen rendering them more recognisable by phagocytes, a process called opsonisation, provide an important synergy between the innate and adaptive immune system.

$CD4^+$ T helper (T_H) cells are further subdivided into either T_H1 or T_H2 cells, the difference being the secreted cytokines that are released. T_H1 preferentially secrete interferon-gamma (IFN-ϒ) whilst T_H2 secrete interleukins IL-4, IL-5 and IL-10. These cytokines feed back to activate phagocytes (IFN-ϒ) and differentiate B cells (interleukins) (Kaiko et al., 2008). In addition to these classical T helper cells, around 10 years ago, a novel class of helper cell was described, the T_H17 cell, capable of IL-17 production (Harrington et al., 2005). After an infection, the majority of T cells undergo apoptosis but some remain as memory T-cells, primed to re-proliferate upon repeat stimulation (MacLeod et al., 2010).

Based on sera from colonised or non-colonised young children, antibody responses to *S. aureus* show wide inter-individual variation (Verkaik et al., 2010a). Recurrent *S. aureus* infections encountered by many individuals suggest that antibody responses are not protective in the longer term and following bacteraemia patients over time with repeated serum sampling confirmed significant heterogeneity in antibody responses between individuals (Verkaik et al., 2010b). In addition, generally speaking, patients with humoral deficiencies e.g. hereditary X-linked agammaglobulinaemia, do not show increased susceptibility to *S. aureus* infection (Karauzum and Datta, 2016). However, as for the innate immune components, rare human genetic deficiencies can highlight key

pathways involved in adaptive immunity to *S. aureus*. Hyper IgE syndrome (HIES) causes multi-organ dysfunction and patients are at particular risk of deep abscesses secondary to *S. aureus*. Elevated levels of IgE and eosinophilia are found and autosomal dominant forms are known to be due to STAT3 (a transcription factor) deficiency (Freeman and Holland, 2008). Defective STAT3 protein signalling results in a lack of T_H17 cell development. The importance of T_H17 cells and IL-17 in protection against *S. aureus* has recently been described (Miller and Cho, 2011).

Therefore, it is increasingly thought that cell mediated responses are important for protection against recurrent infection (Montgomery et al., 2014) but also vaccine efficacy. Vaccination induced CD4+ T cells to release IFN- ϒ and IL-17A, which upon later exposure to *S. aureus* caused enhanced phagocytic killing by the innate immune system (Lin et al., 2009). Understanding of the contribution of the adaptive immune system and the interplay with the innate components is in its infancy and may be context and site of infection specific (Karauzum and Datta, 2016).

In summary, despite robust innate and adaptive immune responses to *S. aureus*, antibiotic therapy is still required to improve outcome in the majority of infections. However, the extent to which the immune system is tackling sub-clinical challenges with *S. aureus* is unknown.

1.9 The bacterial cell wall

The bacteria cell envelope consists of the cell membrane and other structures that serve to protect the cytoplasm from the hostile external environment. In Gram-negative bacteria, the envelope consists of the outer membrane (OM), a thin peptidoglycan cell wall and the inner membrane (IM). Gram-positive bacteria however lack the OM and instead have a far thicker peptidoglycan cell wall (Silhavy et al., 2010). The marked rigidity of peptidoglycan determines the cell shape and maintains cell integrity by providing protection against the internal osmotic pressure. It also acts as a scaffold for other cell envelope components. In *S. aureus*, covalently attached to the peptidoglycan are wall teichoic acids (WTAs) whereas lipoteichoic acids (LTAs) are anchored to membrane lipids. *S. aureus* peptidoglycan is also decorated with a large and responsive array of proteins (Scott and Barnett, 2006).

1.9.1 Peptidoglycan

Peptidoglycan contains a disaccharide backbone of alternating N-acetylglucosamine (GlcNAc) and N-acetylmuramic acid (MurNAc) residues, joined through glycosidic bonds forming long glycan chains. This glycan backbone is highly conserved but secondary modifications are frequently found as discussed in Section 1.9.2 below. A peptide stem is found on each MurNAc composed, in *S. aureus*, of L-alanine, D-iso-glutamic acid, L-lysine and D-alanine, when in a macromolecular form. The cross-linking interpeptide bridge is the site of most variation between peptidoglycans from different species. *S. aureus* contains a pentaglycine bridge (Vollmer et al., 2008a). During cell growth and division, peptidoglycan is continually remodelled by the action of hydrolases and re-synthesised by PBPs. Several hydrolases exist in *S. aureus* including *N*-acetylmuramyl-L-alanine amidases, which cleave the amide bond between the MurNAc and L-alanine of the peptide stems. This separates the peptide from the glycan chain. Glycosidases cleave the glycosidic bonds within the glycan chains, and either cleave between the MurNAc and GlcNAc, known as N-acetyl-β-D-muramidases, or between the GlcNAc and MurNAc, known as N-acetyl-β-D-glucosaminidases (Figure 1.4). The major autolysin in *S. aureus* is Atl which has both glucosaminidase and amidase activity (Foster, 1995). Separation of daughter cells is required for ongoing proliferation yet tight control of autolysins is required to prevent autolysis of the cell (Sugai et al., 1995). Endopeptidases cleave amide bonds between amino acids in the stem peptides (Vollmer et al., 2008b). Lysostaphin is a glycylglycine endopeptidase isolated from *Staphylococcus simulans* (Schindler and Schuhardt, 1964). This enzyme specifically cleaves the *S. aureus* pentaglycine bridge (Figure 1.4).

1.9.2 Peptidoglycan modification

Peptidoglycan modification is a bacterial defense strategy to protect against host antimicrobial products. Hydrolytic enzymes such as lysozyme, an N-acetyl-β-D-muramidase, are secreted by host cell epithelium and also contained within professional phagocyte granules (Borregaard and Cowland, 1997). Such enzymes degrade peptidoglycan and cause bacterial cell lysis (Ibrahim et al., 2001).

In Gram-negative organisms, the OM affords some protection from the direct effect of host enzymes on peptidoglycan. Yet Gram-positive bacteria rely mainly on modifications to peptidoglycan to prevent cell lysis by host enzymes. For example, a large proportion of the GlcNAc residues in *S. pneumoniae* are N-deacetylated, contributing to lysozyme resistance in this organism (Ohno et al., 1982).

S. aureus uses O-acetyltransferase A (OatA) which acetylates the MurNAc at the C-6 position to confer lysozyme resistance. Mutanolysin (produced from *Streptomyces globisporus*) is a muramidase that is able to hydrolyse O-acetylated peptidoglycan. OatA homologs are found in *Streptococcus pneumoniae* (Crisóstomo et al., 2006), *Enterococcus faecalis* (Hébert et al., 2007) and *Lactococcus lactis* (Veiga et al., 2007). Interestingly, OatA is only found in pathogenic staphylococci highlighting its role as an important virulence determinant (Bera et al., 2006). In *S. aureus*, it has been suggested that lysozyme resistance acts as a broad immune evasion tool as release of bacterial fragments at the site of infection is reduced which, in turn, reduces the host cytokine response (Shimada et al., 2010).

1.9.3 Peptidoglycan immune recognition and response

Peptidoglycan has been implicated as an important pathogenicity factor in Gram-positive sepsis with studies noting that heat-killed Gram-positive bacteria can initiate similar cytokine responses *in vivo* to that seen with *E. coli* (Wakabayashi et al., 1991). The primary response of the host to *S. aureus* is predominantly pro-inflammatory, mediated by TLR (recognising lipoproteins) and nucleotide-binding-oligomerisation domain (Nod) like receptors (NLRs) (recognising peptidoglycan fragments). Via the adaptor protein MyD88, TLR2 activates the canonical nuclear factor (NF-κB) pathway, and other mitogen activated protein kinases. The Nod2 receptor signals by the same NF-κB pathway but in a RIP2 dependent manner as is discussed in Section 1.9.3.2 (Kobayashi et al., 2002). Nuclear accumulation of NF-κB causes transcription of genes involved in the expression of cytokines, chemokines, and other inflammatory mediators. Identifying specific *S. aureus* ligands and host receptor interactions is complex as the type of immune activation study, the design of experiments including type of cell lines and animal models and nature of preparations used are vastly different between studies, making direct comparisons within the extensive literature challenging.

IMAGE REMOVED

Figure 1.4 Structure of *S. aureus* peptidoglycan

Digestion sites by various enzymes (glucosaminidase, muramidase, amidase, and endopeptidase) is indicated by the dashed arrows. Muramyl dipeptide (MDP) structure is highlighted in the dashed square.

* indicates action of lysostaphin.

Adapted from (Fournier and Philpott, 2005)

1.9.3.1 Identifying the TLR2 *S. aureus* ligand

There is controversy in the literature regarding which *S. aureus* ligands are most important for immune system recognition. TLR2 is the most likely PRR as TLR2 deficient mice readily succumb to *S. aureus* infection (Takeuchi et al., 2000). However, over the years, the critical bacterial factor for activation of this PRR has been proposed to be either the *S. aureus* peptidoglycan polymer itself (Dziarski and Gupta, 2005), other ligands such as lipoteichoic acid (LTA) or lipoproteins or a combination of these.

LTA is a macroamphiphilic glucoconjugate that is covalently attached to the peptidoglycan cell wall and shed during growth in culture (Wicken and Knox, 1975). Studies investigating TLR2 ligands often use commercially available *S. aureus* peptidoglycan and its components, which may not address the issue surrounding contamination of preparations (Takeda and Akira, 2003). Contamination of LTA or peptidoglycan with lipoproteins may have a confounding role in some studies and chemical removal of lipoproteins or other biologically active compounds is challenging.

Lipoproteins are lipid-protein complexes involved in a variety of dynamic processes and have been shown to be necessary for host immune stimulation by *S. aureus*, both *in vitro* (Stoll et al., 2005) and *in vivo* (Bubeck Wardenburg et al., 2006). They are synthesised initially as preproteins containing an N-terminal signal peptide including a lipobox (Kovacs-Simon et al., 2011). A diacylglyceryl group is transferred to the cysteine residue within the lipobox by diacyl-glyceryl transferase (*lgt*), which then acts as a membrane anchor. Whilst WTA can be removed chemically by deacylation using hydrofluoric acid (Seo and Nahm, 2009), the only definitive way to assess lipoprotein contribution is to use a lipoprotein deficient mutant. After removal of lipoproteins or LTA, peritoneal murine macrophages did not produce cytokines when challenged with purified peptidoglycan (Travassos et al., 2004). This was refuted however by another group who argued that only digestion of the purified polymer glycan backbone can abolish signaling indicating that the intact polymer itself is immunostimulatory, though the extraction processes differ between manuscripts (Dziarski and Gupta, 2005). In house purified staphylococcal peptidoglycan was shown to induce the pro-inflammatory cytokine, TNFα, in human monocytes which is now presumed to be lipoprotein mediated (Timmerman et al., 1993).

Peptidoglycan from wildtype *S. aureus* activated NF-κB through TLR2 whereas peptidoglycan from the *S. aureus lgt* mutant failed to do so, suggesting that lipoproteins contained in the preparation, but not peptidoglycan itself, activates TLR2 (Volz et al., 2010). Using LTA from an *S. aureus lgt* mutant, lacking palmitate-labelled lipoproteins, TLR2 stimulation was markedly reduced in the mutant compared to the wildtype (Hashimoto et al., 2006). However, LTA from the mutant retained a small amount of TLR2 activity, which eluted out separately to the LTA peak, suggesting that unknown TLR2 active compounds may also be contaminating LTA preparations.

Therefore, unless derived from a genetically deficient lipoprotein mutant, it should be assumed that peptidoglycan preparations, regardless of purification processes, are contaminated with immunostimulatory lipoproteins.

1.9.3.2 Non-TLR *S. aureus* peptidoglycan receptors

Peptidoglycan is recognised by the innate immune system and stimulates cellular responses through receptors other than TLRs. As *S. aureus* is now understood to be not only an extracellular pathogen, phagolysosomal escape to the cytoplasm may allow peptidoglycan fragments to be sensed by the intracellular Nod receptors (Grosz et al., 2014). Nod1 receptors are expressed in all adult tissues, whereas Nod2 are predominantly expressed in immune cells and Nod2 caspase recruitment domain-containing protein (CARD) mutations were the first susceptibility genes discovered in Crohn's disease (Girardin et al., 2003a). Nod2 has been shown to detect peptidoglycan from both Gram-positive and Gram-negative organisms (Girardin et al., 2003a). This receptor specifically recognises MDP intracellularly and is independent of TLR2 (Travassos et al., 2004).

In 2003, a specific moiety of peptidoglycan, muramyl-dipeptide (GluNAc-MurNAc-l-alanine-d-isoglutamine fragment, MDP) was shown to be directly sensed by Nod2 (Girardin et al., 2003a) (Figure 1.4). Whilst many studies commercially purchase this product, it has been shown that MDP is a naturally occurring degradation product released during bacterial growth (Girardin et al., 2003b). The question then arose as to how a monomeric, water-soluble peptidoglycan component can access the intracellular environment. Too small to be phagocytosed, other methods of intracellular entry could play a role (Rejman et al., 2004). For example, as yet undefined transporters may allow

direct MDP uptake into phagocytes, as has been shown to be true for human colonic cells (Vavricka et al., 2004). Evidence for direct stimulation of human embryonic kidney (HEK) cells overexpressing Nod2, by MDP or products of peptidoglycan degradation may be misleading as some studies prime cells with LPS or indeed directly transfect cells with MDP which would not occur naturally (Coulombe et al., 2009).

The polymeric three-dimensional structure of peptidoglycan has been repeatedly shown to be essential for eliciting a host immune response both *in vitro* and *in vivo*. The most plausible explanation would be phagocytosis of whole bacteria surrounded by polymeric peptidoglycan and digestion by host enzymes leading to unmasking of cryptic ligands (Iyer and Coggeshall, 2011). Fragments such as MDP from *S. pneumoniae* were not sufficient to cause pro-inflammatory cytokine release from bone marrow derived macrophages as whole cell uptake was required (Davis et al., 2011). *B. anthracis* peptidoglycan monomers, e.g. MDP or solublised peptidoglycan, do not elicit cytokine production from peripheral naïve human blood monocytes yet polymeric peptidoglycan was a potent stimulator for cytokine release from these phagocytic cells. After engulfment, lysosomal digestion products activated Nod2 proteins suggesting that internalisation, trafficking and degradation permits exposure of Nod2 ligands. In a previous publication by the same group, *B. anthracis* was shown to bind to the surface of immune cells prior to phagocytosis but the mediating receptor was not identified (Iyer et al., 2010).

Integrity of the glycan backbone was important in triggering inflammatory responses for a range of Gram-positive bacterial peptidoglycans *in vivo* including *S. aureus*, *B. subtilis* and *C. flaccumfaciens* (Myhre et al., 2004). Furthermore, organ disruption was minimised in a rat intravenous infection model when mutanolysin was used to digest the *S. aureus* peptidoglycan to a soluble form. The pentaglycine bridge connecting the peptide stems have also been targeted and induction of arthritis in murine knee joints injected directly with peptidoglycan was decreased if prior digestion was carried out, disrupting this glycine bridge (Liu et al., 2001). In a mouse arthritis model, digestion of intracellular digestion of *S. aureus* peptidoglycan by PGLYRP-2 (possessing amidase activity) was necessary to cause arthritis induced by peptidoglycan but the effect was abolished in Nod2 knockout mice (Saha et al., 2009). The authors suggest that peptidoglycan is first phagocytosed and processed to release MDP, which is sensed by Nod2, which then activates local PG-LYRP2 expression, leading to arthritis. This

sequence of events highlights the multiple receptors and effectors that can be at play simultaneously or sequentially to cause pathological processes.

Many studies have focused on identifying the exact motif of peptidoglycan that can activate immune cells but these vary in the use of synthesised vs. biological ligands and often do not seek to disentangle phagocytosis, which is likely to be required in order to release peptidoglycan fragments including MDP, from extracellular TLR signalling via lipoproteins. *In vivo,* it is likely that dual signaling occurs by both TLRs and NLRs as *S. aureus* exists both extra and intracellularly. A naturally occurring peptidoglycan monomer released by bacterial cell wall turnover (achieved *in vitro* by dual lysostaphin and mutanolysin digestion) or MDP were unable to elicit a TLR2 response as detected using a NF-κB assay in HEK cells or TNFα release from human monocytic cell lines (Volz et al., 2010). However, in the presence of TLR2 stimulants, peptidoglycan monomer acted as a co-stimulant for the release of pro-inflammatory cytokines, via the intracellular Nod2 receptor. Addition of polymeric peptidoglycan to murine macrophages produced more cytokine production than polymeric peptidoglycan from the *S. aureus lgt* mutant indicating that dual TLR2 and Nod2 ligands enhanced the inflammatory response (Schäffler et al., 2014).

1.9.3.3 Immune response to *M. luteus* and *S. epidermidis*

Certain PAMPs are specific to *S. epidermidis* including exopolymers such as polysaccharide intercellular adhesion (PIA) (Otto, 2012) which is purported to be a ligand for TLR2 (Stevens et al., 2009) though this is not confirmed. This bacterium has an unusual type of lipoteichoic acid but again the immunostimulatory potential of this has not been fully characterised (Lambert et al., 2000).

There is a paucity of information on potential *M. luteus* PAMPs that might be recognised by the immune system. *M. luteus* cell wall preparations have been shown to cause anaphylactic like reactions and death within 1 hour of systemic injection into C3H/HeN mice (MoNodane et al., 1997). Another study suggested *M. luteus* teichuronic acids are recognised by human monocytes in a CD14 and TLR4 dependent manner (Yang et al., 2001).

1.9.4 Role of phagocytosis and the inflammasome in immune signalling

TLRs are not canonical phagocytic receptors in that they do not participate in the actin cytoskeleton dynamics that enables pathogen engulfment. Their main role therefore is pathogen sensing and downstream inflammatory cascade initiation. The links between *S. aureus* PAMP extracellular recognition, phagocytic engulfment, intracellular recognition and downstream signalling are not fully understood.

Inhibition of phagocytosis completely blocked production of pro-inflammatory cytokines in response to heat-killed *S. aureus* but not *E. coli*, suggesting that interplay between internalisation and downstream signalling is intimately coupled with Gram-positive bacteria (Ip et al., 2010). Preventing internalisation by the addition of cytochalasin D, abolished all cytokine production suggesting that surface signalling only is not enough for the full immune response. Interestingly, if zymosan, a yeast cell wall derived particle that also signals through TLR2 was used instead of *S. aureus*, inhibition of phagocytosis actually increased cytokine signalling, due to prolonged surface signalling. This highlights that recognition of the specific cargo, and not necessarily phagocytosis itself, is important to tailor appropriate immune signals. TLR2 signalling remains important after phagocytosis and has been shown to sample the phagolysosome contents in order to adjust the immune response appropriate to the pathogen involved (Underhill et al., 1999).

The concept of extra and intracellular signalling has also been investigated by measuring IL-1β production. Unlike most cytokine production cascades, which require a single signal only, two signals are required for IL-1β production. Inflammasome activation and IL-1β release are important coordinators of local inflammation and key in the immune control of *S. aureus*. The first signal, such as that from TLR2, causes production of pro-IL-1β and a second signal e.g. phagocytosis and acid related product degradation, stimulates assembly of the inflammasome (consisting of NLRP3, ACS and caspase) allowing pro-IL-1β to be digested by caspase producing the mature form IL-1β (Shimada et al., 2010). *S. aureus* peptidoglycan was able to elicit IL-1β release from murine bone marrow derived macrophages (BMDMs) whereas MDP produced pro-IL-1β only. Solubilised peptidoglycan was unable to produce IL-1β. The authors concluded that once the pathogen is phagocytosed, digested products are sensed either in phagosome or the cytosol that trigger inflammasome activation, thus providing the

second signal necessary for IL-1β production. This coupling between PAMP recognition, phagocytosis and appropriate immune signalling is likely to be key for effective *S. aureus* control by the host.

Non-bacterial particles can also activate the inflammasome including silica crystals (Hornung et al., 2008) and asbestos (Dostert et al., 2008) yet the model particle, zymosan can only cause activation in the presence of ATP, which provides the additional signal required (Lamkanfi et al., 2009). Due to the diverse nature of these particles, a single unifying theory as to how the inflammasome is activated may not exist but hypotheses include particulate induced reactive oxygen species production (Dostert et al., 2008); destabilisation of the phagolysosome due to swelling and subsequent lysis (Hornung et al., 2008) or direct sensing of degradation products by NLRs (Faustin et al., 2007).

1.10 Virulence Determinants of *S. aureus*

Bacterial determinants, including genetic, biochemical or structural, influence the pathogenicity of *S. aureus* and virulence determinants are ascribed if such determinants are removed or blocked, and virulence is attenuated (Casadevall and Pirofski, 1999). Table 1.2 summarises some of the immune evasion mechanisms employed by *S. aureus*. Temporal expression of virulence factors is important and virulence determinants can be broadly divided into those affecting tissue adhesion (exponential phase), immune evasion (both exponential and post-exponential) or tissue invasion and spread (predominantly post-exponential phase). *S. aureus* expresses a broad spectrum of both secreted and cell surface associated virulence determinants. Some virulence determinants serve multiple purposes, for example, Protein A (*spa*) binds the Fc portion of immunoglobulin, preventing opsonisation and phagocytosis (Uhlén et al., 1984) and release of Protein A from the cell wall can cross-link B cells and act as a superantigen (Becker et al., 2014).

1.10.1 Tissue adhesion

Bacterial survival *in vivo* is dependent upon tissue adhesion, through surface proteins such as ‘microbial surface components recognizing adhesive matrix molecules’ (MSCRAMMs) (Foster and Höök, 1998). Effective colonisation of the nares plays a

crucial role in the success of *S. aureus* as a human pathogen and many MSCRAMMs are involved. Clumping factor B (ClfB) which binds to both cytokeratin and fibrinogen, is a major determinant of nasal colonisation in both mice and human studies (Wertheim et al., 2008). *S. aureus* mutants lacking fibronectin-binding protein (FnBP) bind less well to human endothelial cells *in vitro* suggesting that FnBP promotes adherence. The same mutants also show a loss of internalization of *S. aureus* (Massey et al., 2001). Desquamated nasal epithelial cells were used to demonstrate that multiple *S. aureus* components are involved in adhesive processes. In addition to ClfB, iron regulated surface determinant protein A, IsdB, serine-aspartic acid repeat proteins, SdrC and SdrD, all contributed to host cell adherence and a quadruple deletion mutant was unable to adhere to squamous epithelial cells (Corrigan et al., 2009).

1.10.2 Tissue invasion and spread

S. aureus secretes a large number of enzymes such as proteases, lipases and nucleases that enable destruction and invasion into host tissue, assisting dissemination (Gordon and Lowy, 2008). For example, secreted proteases degrade host collagen and fibrinogen but also affect the stability of bacterial surface proteins which is thought to allow the 'adhesive' phase of the pathogen to transition to the 'invasive' phase (Kolar et al., 2013). Interestingly, in a strain lacking all 10 exo-proteases, excess mortality was noted in a murine infection model due to overproduction of toxins. This highlights the complex role of virulence determinants in regulating host:pathogen interactions. Another degrative enzyme, hyaluronidase, HysA, cleaves the extracellular matrix component, hyaluronidic acid. In a neutropenic, pulmonary murine infection model, *hysA* mutants were significantly attenuated, producing far less lung damage compared to parent strains (Ibberson et al., 2014).

In addition, *S. aureus* produces a range of toxins including exfoliative toxins, enterotoxins such as TSST-1, the haemolysins (α toxin, β toxin and δ toxin) and two-component leukotoxins (Foster, 1996). The haemolysins play an important role in iron acquisition by their ability to lyse RBCs. The best characterised of these is α-toxin which binds to a broad range of cell types via the ADAM-10 receptor causing membrane damage and pore formation (Berube and Bubeck Wardenburg, 2013). β toxin is a sphingomyelinase which cleaves the phospholipid, sphingomyelin, in cell membranes of RBCs and monocytes (Walev et al., 1996). Two-component leukotoxins

gained much notoriety with the discovery of Panton-Valenine leucocidin (PVL) which induces rapid neutrophil death in rabbit and human derived, but not murine, cells (Loffler et al., 2010). LukAB/GH is another bicomponent leucocidin that was recently shown to target human neutrophils via the cellular receptor CD11b (DuMont et al., 2013). Phenol soluble modulins (PSMs) were recently discovered as a novel *S. aureus* virulence factor in 2007 and reported to have significant cytolytic and pro-inflammatory activity thus enhancing bacterial pathogenesis (Cheung et al., 2014). However, contradictory work has demonstrated that functionality of these cytotoxins can be nulled by the presence of human serum, with lipoproteins being identified as the neutralisation factor (Surewaard et al., 2012).

1.10.3 Immune evasion

Immune evasion by *S. aureus* is dynamic and complex and allows the bacteria to resist killing by the professional phagocytes. In order to prevent initial recognition by phagocytes, *S. aureus* synthesises a protein, TirS, that interferes with the adaptor proteins required for TLR2 signalling (Toll/interleukin-1 receptor) (Askarian et al., 2014). In addition, superantigen-like staphylococcal protein 3 (SSL3) interferes with *S. aureus* ligand binding to TLR2 (Koymans et al., 2015). Another strategy employed to promote growth and survival *in vivo* is the production of complement inhibitory proteins. One such protein, the staphylococcal complement inhibitor (SCIN) binds to C3 convertase preventing the onward cascades that would lead to formation of the MAC (Rooijakkers and van Strijp, 2007).

As discussed above, as neutrophils are well adapted to killing *S. aureus,* preventing effective chemotaxis to the site of infection is crucial for pathogen survival. Extracellular adherence protein A (EapA) is a secreted immune evasion molecule that prevents neutrophil adhesion and trans-endothelial migration (Haggar et al., 2004). Chemotaxis inhibitory molecule (CHIPs) is an exoprotein that inhibits phagocyte chemotaxis by preventing C5a and formylated peptides from binding on the neutrophil surface (Postma et al., 2004). If *S. aureus* is ingested, carotenoid pigments such as staphyloxanthin confer resistance to superoxide killing by functioning as an anti-oxidant (Liu et al., 2005). Peptidoglycan modification by O-acetylation of the glycan backbone renders lysozyme unable to damage the structural integrity of the bacterial cell wall (Bera et al., 2005).

Even if engulfed by professional phagocytes, *S. aureus* can escape the phagolysosome and proliferate in the cell cytoplasm (Kubica et al., 2008). Intracellular survival was shown to be dependent on the dose of bacteria administered to human monocyte derived macrophages and at high dose, sudden release of extracellular bacteria was seen, indicating cell lysis. Survival and growth within professional phagocytes allows dissemination of *S. aureus* to distant sites and niche formation in sites less amenable to antibiotic penetrations (Thwaites and Gant, 2011)

1.10.4 Regulation of *S. aureus* virulence factors

Co-ordination of virulence factor expression is required for pathogenesis. Figure 1.5 shows how inter-related regulatory pathways are used and the diversity of functions that are regulated. Though the majority of the data used to generate this image is reported to be qualitative, it gives a clear impression of the elaborate and complicated systems involved (Priest et al., 2012).

To take a few examples, the accessory gene regulator (*agr*) system functions during the post-exponential phase, activating exotoxins and repressing surface proteins according to cell density (Novick et al., 1993). The effector molecule, RNAIII, exerts effects at the transcriptional and translational level of virulence factors such as haemolysins α, β, γ, δ, TSST-1, enterotoxins and PVL (Bronner et al., 2004). Autoinducing peptide (AIP) provides a positive feedback mechanism to mediate quorum sensing which ensures energy expensive virulence factor expression occurs only when necessary. Inhibiting this system may provide alternative therapeutic strategies as *S. aureus agr* mutants are attenuated in the mouse septic arthritis model (Abdelnour et al., 1993; Nielsen et al., 2014).

The *agr* system is a two-component regulatory system, comprised of a sensor histidine kinase and a response regulator. The majority of regulatory systems in *S. aureus* are composed of two-component systems, including the *S. aureus* exoprotein expression (*saeRS*) locus (Giraudo et al., 1994). This locus is essential for transcription of genes including haemolysin α and β, coagulase, extracellular fibrinogen binding protein (*efb*) and an *sae* mutant is attenuated in multiple animal models including the murine model of haematogenous pyelonephritis (Liang et al., 2006).

Strategy	Immunomodulatory molecules	References
Inhibit chemotaxis of immune cells	Chemotaxis inhibitory protein (CHIPs), Extracellular adherence protein (Eap), Staphylococcal superantigen like (SSLs)	(Haas et al., 2005) (Haggar et al., 2004) (Zecconi and Scali, 2013)
Prevents opsonisation mediated phagocytosis	Protein A, ClfA, Capsule (SpA), Staphylococcal complement inhibitor (SCIN)	(Falugi et al., 2013) (Rooijakkers and van Strijp, 2007)
Evades killing by phagocytes	Lysozyme resistance, superoxide dismutase, staphyloxanthin	(Herbert et al., 2007) (Liu et al., 2005)
Causes phagocyte and other cellular damage	Leukocidins, PVL, PSMs	(Loffler et al., 2010) (Wang et al., 2007)
Phagocyte persistence/ escape	PSMs, stringent response	(Kubica et al., 2008) (Geiger et al., 2012)
Overzealous immune stimulation	Enterotoxins, TSST-1	(Alber et al., 1990) (Chesney et al., 1984)

Table 1.2 Immune evasion mechanisms of *S. aureus*

Responding to external stimuli is important *in vivo*, as factors essential for bacterial survival may be limited. The staphylococcal respiratory response (*srrAB*) system responds to environmental conditions such as the presence of nitric oxide (NO) and oxygen limitation and activates expression of genes involved in NO detoxification and anaerobic metabolism (Kinkel et al., 2013).

The staphylococcal accessory regulator (*sarA*) is not a two-component system. SarA binds to DNA in the promotor region of target genes and multiple homologs exist in the genome (*sarR, sarS, sarT, sarU, rot* etc). Depending on the phase of growth, *sarA* upregulates expression of many genes including *agr*, capsular polysaccharide (*cap8*), TSST-1 and α haemolyin (Morrison et al., 2012). In a rabbit endocarditis model, *sarA* mutants showed lower protein levels of haemolysin and fibronectin binding proteins (Cheung et al., 1994).

Regulatory networks do not work in isolation and complex inter-network signaling has been shown (Priest et al., 2012). Constitutive activation of the *sae* locus reverses the attenuation of *sarA* mutants in an implant-associated biofilm formation murine model, possibly due to the fine balance between protein production and degradation (Beenken et al., 2014). Alpha haemolysin is regulated by *sae* yet the *sarA* homologs, *rot* and *sarT*, are known repressors. By constructing a triple mutant of *rot sae sarT*, it has been shown that repression of alpha haemolysin by *rot* is *sae*-dependent (Li and Cheung, 2008).

Figure 1.5 The currently known virulence regulatory network of *S. aureus*

Outside the circle are the effects of the regulatory genes on adhesiveness (A), toxicity (T) and immune evasiveness (E). A question mark indicates no information about direct activity of the regulator or that the available information is opposing.

Adapted from (Priest et al., 2012)

1.11 Whole genome sequence of *S. aureus*

MRSA strains N315 and Mu50 were the first *S. aureus* genomes to be fully sequenced (Kuroda et al., 2001). Currently, sequence data for thousands of *S. aureus* strains exist which are approximately 2.6 – 2.9 Mb in size. The core genome constitutes around 75% of the genome and is highly conserved between strains, including gene order and 98-100% amino-acid composition similarity of individual genes (Lindsay and Holden, 2004). The core genome mutation rate is calculated to be approximately 1 SNP per 6 weeks which allows dating of clade emergence to be estimated (Harris et al., 2010).

Constituting approximately 25% of the *S. aureus* genome, the accessory genome can, however, vary significantly from strain to strain. It is comprised of MGEs including transposons, pathogenicity islands, bacteriophages, plasmids and chromosomal cassettes. The presence or absence of these elements may explain why certain strains are adept at becoming epidemic strains in either the community (Jiménez et al., 2012) or hospital environment (Holden et al., 2013). Virulence factors e.g. TSST-1 and antibiotic resistance genes are commonly found as MGEs enabling genetic transfer of advantageous traits throughout a bacterial population (Gillet et al., 2002). Worryingly, MGEs can transfer between bacterial genera and species. As discussed in Section 1.5, transposon, Tn1546, containing the *vanA* gene, was previously only found in enterococci but horizontal transfer has led to the emergence of VRSA isolates.

1.11.1 Bacteriophages

As *S. aureus* is not naturally competent, bacteriophages are thought to aid bacterial diversification. Most *S. aureus* strains carry at least one bacteriophage and these are classified according to the site at which they insert into the chromosome (Xia and Wolz, 2014). However, horizontal gene transfer is still limited by bacterial restriction-modification systems which explains why MGEs from one strain will more likely move to a strain in the same lineage rather than a different one (Waldron and Lindsay, 2006). Phages can package up to 45 Kb of bacterial host DNA and transfer that DNA to a new *S. aureus* cell, often integrating into the chromosome. If that DNA encodes for a virulence factor, successful clones can emerge which are able to disseminate and cause disease when previously, the prevalence of that virulence factor was low. An example

of this was when the toxin PVL, encoded by the *lukSF-PV* gene was transferred by phage into the successful MRSA USA300 strain (Shallcross et al., 2013).

1.11.2 *S. aureus* pathogenicity islands

Pathogenicity islands are stretches of DNA that contain one or more virulence genes. In *S. aureus* pathogenicity islands (SaPIs), superantigen genes for toxins such as TSST-1 and enterotoxins B and C are nearly always carried and phages are employed to facilitate transfer between strains. SaPIs are highly mobile but transfer is often limited to a small set of clonal complexes (Peacock et al., 2002).

1.11.3 Staphylococcal chromosome cassettes

SCCs have gained much notoriety since the SCC*mec* element was characterised. This particular SCC introduced a methicillin resistance gene, *mec*, into the *S. aureus* genome, giving rise to MRSA. These cassettes are too large to be packaged by bacteriophages and the exact mechanisms of excision and integration are under investigation (Stojanov et al., 2012). An interesting feature of the SCC cassettes is that each type is associated with different niches in which they are successful. For example, the original pandemic HA-MRSA strains carried the large SCC*mec* I,II or III but more recently emerged CA-MRSA strains carry smaller cassettes (SCCmec IV or V). The smaller cassettes are more easily transferred between strains (Monecke et al., 2011).

1.11.4 Plasmids

S. aureus often carries one or more plasmids, encoding a variety of resistance and virulence genes. Like pathogenicity islands, they are likely transferred by phage. They have important clinical consequences but, once again, appear to be lineage specific which limits the spread (Lacey, 1975; McCarthy and Lindsay, 2010). Most worryingly, plasmids from other genera can transfer into *S. aureus* bringing dire consequences for antibiotic resistance (Chang et al., 2003).

1.11.5 Transposons

Transposons are DNA segments that can undergo transposition by encoding their own transposase which catalyses movement of the DNA. In *S. aureus*, these are often not site specific and can be as large as 60 Kb (Lindsay, 2008). Due to the potential for random chromosomal insertion, transposons e.g. Tn551, Tn917 have been used to generate *S. aureus* mutant libraries (Bae et al., 2004). Natural transposon transfer between strains often occurs via other MGEs such as plasmids and most strains contain multiple transposons, usually encoding for antibiotic resistance genes.

1.11.6 Restriction-modification systems of *S. aureus*

Aside from a small number of clonal complexes, the majority of *S. aureus* isolates are genetically recalcitrant. To undertake molecular biology techniques, in general, after synthesis of the plasmid construct, electro-competent *E. coli*, which are restriction deficient but able to modify DNA (R^-M^+), are transformed. Following plasmid isolation, an intermediary strain of *S. aureus*, RN4220 (R^-M^+), is then transformed. The plasmid is extracted and transduced or transformed, under selective pressure, into a standard laboratory strain of choice such as SH1000. The intermediary strain *S. aureus* RN4220 was created by extensive chemical mutagenesis of *S. aureus* 8325-4 (Kreiswirth et al., 1983) and was later found to have a premature stop codon in the type I restriction gene (*hsdR*) permitting it to accept DNA from wild-type *E. coli* (Waldron and Lindsay, 2006). However, onward transduction or electroporation from RN4220 remains limited to a small number of closely related strains, including SH1000.

The restriction-modification (RM) systems of clinical strains are variable and poorly understood (Monk et al., 2012; Chua et al., 2013). Four RM systems are thought to exist amongst *S. aureus* strains and the type 1 system, mediated by the type I restriction gene *hsdR*, is well-described (Murray, 2000). However, more recently, the role of the type IV RM system in *S. aureus* has been studied (Corvaglia et al., 2010). The modification dependent, restriction endonuclease, SauUSI, recognises DNA cytosine methylation and when this, in addition to *hsdR*, is inactivated, the *S. aureus* strain is able to be transformed by *E. coli* and parental *S. aureus* strains (Xu et al., 2011). Subsequently, the cytosine methylation gene (*dcm*) of the high efficiency cloning strain of *E. coli*, DH10B, was knocked out, creating strain DC10B. Using these tools, clinical strains of

S. aureus from a wide range of clonal complexes are now able to be transformed with DNA isolated from *E. coli* DC10B, bypassing the use of *S. aureus* RN4220 and vastly expanding the number of clonal complexes of *S. aureus* that can be genetically manipulated (Monk et al., 2012).

1.11.7 Next generation sequencing technology

Such detailed information about the core and accessory *S. aureus* genome has been possible for some time using whole genome sequencing technology. However, complete genome sequencing including genome assembly is time consuming, computationally costly and impractical for large population samples (Harris et al., 2010).

However, next generation sequencing (NGS) technology, e.g. the Illumina Miseq desktop analyser, has revolutionised the accessibility and practical uses of this powerful tool (www.illumina.com/systems/miseq.html). In NGS, bacterial DNA to be sequenced is first sheared into small fragments (100-300 bp). DNA libraries from each strain are individually 'tagged' which increases throughput as multiple strains can be sequenced on a single sequence run. Each short fragment, termed a 'read' is amplified by PCR, separated into single strands before fluorescently labelled nucleotides and DNA polymerase are added (Metzker, 2010). To sequence large collections, it is only necessary to fully sequence a reference isolate to which the short reads (see below) are then compared or 'mapped'.

Mapping reads from the strain of interest to the reference strain will begin to compile a database of single nucleotide polymorphisms (SNPs) that differentiate the two strains. These variable sites can then be used to construct a phylogenetic tree constructed by several statistical methods including maximum likelihood. The tree is then evaluated by a method called 'bootstrapping', which gives an indication of the consistency and reliability of the data (Douady et al., 2003). Whilst previously in the realm only of expert bioinformaticians, user-friendly software for NGS data analysis is beginning to emerge. This is not just for research purposes as there is a drive to introduce routine NGS technology into clinical microbiology laboratories (Fricke and Rasko, 2014). This would mean that bacteria isolated from patients could be rapidly and comprehensively examined for specific and even novel virulence and resistance gene carriage. Such

information may open avenues for patient specific therapies if for example, certain toxin or antibiotic resistance genes are identified earlier than would routinely be available.

1.12 Model organisms to study *S. aureus* disease

In vitro and *ex vivo* methods for studying *S. aureus* disease, including cell based assays, are extensively used (Pohlmann-Dietze et al., 2000; Koziel et al., 2009; Filkins et al., 2015) yet transcriptional profiling studies have shown that *in vitro* bacterial gene expression during pathogenesis is not always replicated *in vivo* (Pragman and Schlievert, 2004). Of course, ethical constraints and feasibility prevent direct investigation of host-pathogen interactions in humans and information can be extrapolated from model organisms of *S. aureus* disease. Model organisms are non-human species used to study a variety of disease or phenomena with the ultimate goal of translating the insight gained to other, often higher, species.

Use of model organisms to further understand *S. aureus* range from studies on basic biology through to drug screening (Lambein, 2015) and pre-clinical vaccine testing (Fattom et al., 1996). Whilst the mouse is considered the mainstay of model organisms in this field, non-mammalian organisms are also employed. There is a large degree of functional conservation in basic cellular processes between mammals and invertebrates. However, as shown in Figure 1.6. the adaptive immune system is a relatively recent evolutionary gain to vertebrates including zebrafish, mice and humans.

Genetic manipulation of invertebrate models is generally achieved more quickly and simply than in vertebrates. Reverse genetic approaches including transposon library creations exist but targeted, highly efficient methods for specific mutation have been an important development in recent years. The CRISPR/Cas9 system (clustered regularly interspaced palindromic repeats) is now widely used across many organisms (Bassett et al., 2013; Shen et al., 2014).

Invertebrate models possessing mainly innate immune defenses are best used in conjunction with other models to grasp a wider understanding of host:pathogen interactions. However, their affordability, high throughput capabilities and ease of use make them an attractive option for researchers.

1.12.1 Invertebrate models

1.12.1.1 *Caenorhabditis elegans*

C. elegans is a small (approximately 1 mm long) non-parasitic, soil dwelling, nematode. With a short life cycle, it can be cultivated in high numbers in the laboratory and is safe to work with. It is transparent with a constant number of somatic cells which allows cell tracking and the study of how each cell contributes to the living organism, to be carried out with relative ease (Wood, 1988). In its natural habitat, *C. elegans* feeds on soil bacteria and thus nematode killing assays can be conducted after pathogen ingestion (Garsin et al., 2001). Feeding wildtype *S. aureus* to *C. elegans* caused them to succumb with high numbers of bacteria in the digestive tract yet bacterial mutants with defective virulence traits, e.g. *agr*, *sarA*, *hla,* were less able to kill (Sifri et al., 2003). Immune components can also be studied as the whole genome sequence is available and a vast repertoire of well characterised mutants are accessible (Ewbank, 2002). Whole animal automated platforms for anti-staphylococcal drug discovery is ongoing (Rajamuthiah et al., 2014). A disadvantage of this model however is the nematode cultivation temperature of 25°C which is lower than the optimum growth temperature for *S. aureus*.

1.12.1.2 *Drosophila melanogaster*

Slightly larger than *C. elegans* at 3 mm in length, *D. melanogaster* is commonly known as a fruit fly, so named due to its development occurring on decaying organic matter such as rotten fruit. This model organism is well characterised, genetically tractable, easy to breed and maintain and was established as a model organism for *S. aureus* infection over ten years ago (Needham et al., 2004). The dorsal thorax of the fly is pricked with a needle dipped in *S. aureus* culture. As with *C. elegans*, *S. aureus* is not a natural host yet conserved innate immune pathways are activated upon exposure to the pathogen, which can be interrogated to ascertain relative importance (Tzou et al., 2002).

Ultimately, invertebrate models of pathogenesis lack the complex organization of organ systems and full immune repertoire pertinent to human infectious disease progression and therefore are limited.

IMAGE REMOVED

Figure 1.6 Evolution of the immune system

Pink – immune system components restricted to invertebrates
Green – immune system components restricted to jawless vertebrates
Blue – immune system components restricted to jawed vertebrates
1R, 2R and 3R refer to the occurrence of 'rounds' whole genome duplication

VCBP V-region containing chitin-binding protein
TLR Toll-like receptor
NLR Nod-like receptor
SR scavenger receptor
VLR variable lymphocyte receptor
NICIR novel immunoreceptor tyrosine-based activation motif-containing immunoglobulin superfamily receptor
APAR Agnathan paired receptors resembling antigen receptors
Rag – recombination activating gene
TCR T cell receptor
BCR B cell receptor
MHC major histocompatibility complex
Mya – millions of years ago

Adapted from (Flajnik and Kasahara, 2010).

1.12.2 Vertebrate models

1.12.2.1 Zebrafish

Initially used for embryological and developmental studies, zebrafish are now widely used for infection studies as this model has many orthologs of the human immune system including phagocytic cells, cytokines and signalling molecules (van der Vaart et al., 2012) and later in development, an adaptive immune repertoire (Trede et al., 2001). The development of a zebrafish model of infectious disease and a rapid expansion in available tools for interrogation of host:pathogen interactions has enabled integrated, real-time pathogenesis studies of many bacteria including mycobacteria (Swaim et al., 2006); *S. aureus* (Prajsnar et al., 2008) and *S. pneumoniae* (Saralahti et al., 2013). A systemic *S. aureus* infection can be achieved by injection of bacteria into the circulation valley of the embryo (Figure 1.7).

Zebrafish are easy to breed and once infrastructure is in place to maintain the fish in aquaria, generated mutants can be housed and readily accessed. Wildtype embryos are transparent enough to allow *in vivo* imaging on day 1 and 2 post fertilisation. The pigmentation that develops subsequently can be prevented if transgenic fish with a lack of melanocytes are used (Lister et al., 1999). Transient knockdown methods such as morpholino-modified antisense oligonucleotides (morpholinos) have been developed (Summerton and Weller, 1997). Complementary to the transcription factor, the *pu.1* morpholino depletes myeloid cells such that macrophages do not appear until 48 hours post fertilization (hpf) and neutrophils at 36 hpf (Klemsz et al., 1990). The *gata 1* morpholino subverts erythroid cell production to that of myelopoesis, thereby increasing the myeloid cell components in the zebrafish (Rhodes et al., 2005). However, there has been concern recently that morpholino knock down approaches do not always correlate well with mutant phenotypes (Kok et al., 2015).

Therefore, one of the most significant advances in zebrafish pathogenesis research has been the development of high throughput, efficient, targeted mutagenesis approaches. The CRISPR/cas9 system depends on two short pieces of RNA, one that recognises the DNA target of interest and another that binds Cas9, a cleaving protein. Once a double stranded DNA break is achieved, the cellular Non-homologous End Joining pathway is activated which has low fidelity, resulting in disruption of the target DNA (Varshney et al., 2015). Targeted genetic manipulation of zebrafish has allowed an enormous bank of

mutants to be generated from which complex transgenic lines have been created (Kimura et al., 2014).

Limitations of the zebrafish model include the necessary maintenance temperature of 28°C, at which, some pathogen virulence factors may not be expressed. In addition, as zebrafish and humans diverged 450 million years ago, compared to mouse and humans at 112 million years ago, there is greater genetic conservation between the latter (Woods et al., 2000). Most zebrafish stocks are kept as outbred but even those designated as inbred have significant genetic heterogeneity unlike occurs in other vertebrate animal models such as inbred mouse strains (Guryev et al., 2006). There is little doubt however, that the zebrafish model of infection is an important complement to murine models.

1.12.2.1.1 Zebrafish innate immune system

Zebrafish innate immunity develops at one day post fertilisation (dpf), with functional macrophages emerging at 25 hpf (Herbomel et al., 1999) and primitive neutrophils may develop as early as 18 hpf, as detected by presence of myeloperoxidase in the intermediate cell mass (ICM) (Crowhurst et al., 2002). Mature neutrophils have been detected at 2 dpf by electron microscopy (Lieschke et al., 2001). The zebrafish neutrophil shares many functional features with those of the mammalian species including the ability to migrate to the site of injury/infection. They are morphologically and biochemically similar possessing a multi-lobed nucleus, primary azurophilic and secondary granules and a myeloperoxidase homologue (Lieschke et al., 2001). Importantly for the study of *S. aureus* infection, using respiratory burst assays and morpholino knock-down approaches, a functional NADPH oxidase has been described (Brothers et al., 2011). Zebrafish neutrophils effectively phagocytose and clear bacteria yet in contrast to macrophages, zebrafish neutrophils were unable to engulf bacteria in fluid environments (Colucci-Guyon et al., 2011). In addition, they have also been shown to produce extracellular traps (NETs) (Palić et al., 2007).

Using transgenic reporter lines with fluorophore-labelled macrophages, zebrafish macrophages are also seen to exhibit chemotaxis towards infection (Ellett et al., 2011). PAMPs binding to scavenger or C-type lectin receptors induces phagocytosis and mammalian receptor orthologs of both families are found in the zebrafish genome

(Jackson et al., 2007; van der Sar et al., 2009). Bacterial killing is achieved through generation of ROS and other degradative processes (Bilan et al., 2013) however selective ablation of macrophages demonstrated that neutrophils are more likely to be required for disseminated *S. aureus* infection in the zebrafish host (Prajsnar et ., 2012).

The zebrafish adaptive immune system is not constituted until 4-6 weeks post fertilisation, at which time immunoglobulins are detected (Lam et al., 2004). Both B and T lymphocytes have been identified, the latter with the characteristic pathogen recognising TLRs (Trede et al., 2004). However, genome duplication during fish evolution explains why many mammalian TLR genes have two orthologs in the zebrafish e.g. *tlr4ba/tlr4bb* for TLR4. The specificity of ligands against TLR 2, 3 and 5 are conserved between fish and mammals and many downstream adaptor proteins including MyD88 have been identified (Stein et al., 2007). However, TLR4 cannot be stimulated by lipoprotein highlighting that different ligand:receptor associations occur (Sepulcre et al., 2009). Canonical NLRs are conserved in the zebrafish and have a role in antimicrobial innate immunity (Oehlers et al., 2011). In humans, a total of 23 NLRs are known yet aside from Nod1 and Nod2, the function of zebrafish NLR orthologs have not been investigated. Furthermore, some unique NLR subgroups have been identified (Laing et al., 2008). Using zebrafish gene knockdown, the role of Nod1 and Nod2 in controlling infection by *Salmonella enterica* was demonstrated with a decreased ability to produce ROS and higher bacterial burdens observed in Nod-deficient embryos (Oehlers et al., 2011).

Regarding effector molecules of the innate immune system, whilst many cytokine subgroups can be found in the zebrafish, diversification of the roles of these compounds is described compared to that of the mammalian system. IL-1β, IL 6, IL 10, IL 8 and TNF are conserved in the zebrafish yet functionally, differences are described between the two species (van der Vaart et al., 2012). Extensive research into zebrafish immune profiling is ongoing and functional studies in infection models will yield further insight.

Dendritic cells were the most elusive hematopoietic lineage but evidence of their presence now exists (Lugo-Villarino et al., 2010). Lymph nodes do not exist in zebrafish and surrogate lymphoid organs include the liver and kidney with secondary lymphoid organs e.g. spleen, being the site of antigen presentation (Renshaw and Trede, 2012).

Figure 1.7 Anatomy of a zebrafish embryo at 2 dpi

A Yolksac/circulation section with erythroblasts (pink circles) and macrophages (blue cells).

B Lateral view of the embryo, demonstrating the pericardial cavity (light blue) and heart (red). The site of systemic injection into the circulation valley is shown with a green arrow. Blood flow across the yolksac is indicated by the red arrows.

Adapted from (Herbomel et al., 2001).

1.12.2.2 Mammalian

Attempts to recapitulate human *S. aureus* disease *in vivo* has predominately involved a variety of small mammals. In addition to the most commonly used mouse model, rabbits, rats and guinea pigs have been used. Divergence of such mammals and humans occurred approximately 100 millions years ago, compared to that of flies and nematodes approximately 600 million years ago. This alongside their small size, ease of breeding with short generation time, large numbers of offspring, ease of handling, low cost to maintain and ability to inbreed, make them an attractive *in vivo* infection model with many advantages.

1.12.2.2.1 Murine

When recombinant DNA cloning techniques became mainstream around 30 years ago, it was confirmed that many mouse genes have human orthologs. Since the publication of the high quality sequence of a mouse genome in 2002, just one year after the first human genome sequence became available, comparisons between the two have yielded novel information (Mouse Genome Sequencing Consortium et al., 2002). Similarly sized between 2.5-3 billion base pairs, more than 90% of the mouse genome aligns with regions in the human genome. Not surprisingly though, delving deeper, there is far less exact alignment of specific genes and DNA sequence as variation has occurred through evolutionary processes. An insightful study compared the molecular basis of inflammation between mouse and human using gene expression profiling and temporal changes (Seok et al., 2013). During acute inflammation, from a variety of causes, changes in genes in humans were vastly different to those in the mouse (R^2 between 0.0 and 0.1). Therefore, it is clear that complex disease processes such as infection and inflammation affecting humans is overwhelmingly difficult to exactly mimic in any non-human mammalian model. Notwithstanding, many types of murine infection model have been established, involving different modes of bacterial administration i.e. intravenous (Clarke et al., 2006), subcutaneous (Bunce et al., 1992), intra-peritoneal (Rauch et al., 2012) and intra-nasal (Wardenburg and Schneewind, 2008). Using a variety of routes, the wide spectrum of disease caused by *S. aureus* infection in humans can be imitated such as sepsis, septic arthritis, skin and soft tissue infection including wound/surgical infections, peritonitis, pneumonia and many more.

S. aureus is a natural pathogen of mice (although human clinical isolates differ from common mouse strains) and inbred mouse strains are readily available. Furthermore, measured data on each strain is available in large databases that compare and contrast characteristics between strains (Maddatu et al., 2012). Disadvantages, however, are that a high inoculum is required to initiate infection and effective doses can vary between 10-100 fold between strains and routes of administration (von Kockritz-Blickwede et al., 2008). As some *S. aureus* secreted virulence factors are human specific, humanised mouse strains are being developed to improve the sensitivity of this model host (Spaan et al., 2013; Knop et al., 2015). Despite these limitations, the murine model of *S. aureus* disease has been and will continue to be, extensively used, including in pre-clinical vaccine testing.

1.12.2.2.2 Other rodents

Nasal colonisation of *S. aureus* is an important precursor to invasive disease (von Eiff et al., 2001). Nasal histology of the cotton rat *(Sigmodon hispidus)* is remarkably similar to that of humans, more so than when compared with the mouse, for example. Therefore, this model has been successfully used for *S. aureus* nasal colonisation studies and demonstrated bacterial surface molecules (glycosylated wall teichoic acids) that are necessary for colonisation (Kokai-Kun, 2008; Winstel et al., 2015). Therapies for decolonisation have also been tested (Kokai-Kun et al., 2003).

The Wistar strain of rat has also been used in *S. aureus* host:pathogen interaction studies. One of their advantages is that due to their larger size compared to the mouse, cannulation of major blood vessels is more amenable which enables haemodynamic tracking during conditions such as sepsis (Kimpe et al., 1995; Hanses et al., 2014).

Many *S. aureus* infection protocols have been established in guinea pigs with the most common being the burn, surgical wound and prosthetic device implantation models. By applying a burn and infecting the area with *S. aureus*, studies have shown striking similarities between colonisation rates and complement system consumption in the human and guinea pig (Bjornson et al., 1984). Staphylococcal contaminated prosthetic devices also appear to form biofilms and testing of anti-biofilm agents was possible (Menzies et al., 2002). The main limitation of guinea pig experimentation is the lack of

study of immune function in this animal. However, this is now improving as the model is currently being used for vaccine research (Kim et al., 2015).

1.12.2.2.3 Rabbits

Rabbits are commonly used to model bone and joint infections by *S. aureus*. Although larger than the mouse or other rodents, they remain easy to handle and do not require vast space for housing. Practically, their bones are large enough to allow surgical manipulation including the addition of prosthetics, with materials that are used in human clinical practice (Reizner et al., 2014). In addition, rabbit models of *S. aureus* endocarditis are also common as vegetations that arise on the heart valves are shown to contain similar numbers of bacteria and resemble those found in patients (Garrison and Freedman, 1970).

1.12.2.2.4 Larger mammals

Mammals of larger size are not often used to imitate *S. aureus* infection but *S. aureus* is a common cause of cattle mastitis, a condition with significant financial implications for dairy herds. Therefore, carriage and control studies have been undertaken (Sommerhäuser et al., 2003). Exploring within-host evolution of *S. aureus* strains in a sheep colonisation model is currently in progress (personal communication, Professor Ross Fitzgerald, Roslin Institute).

Livestock associated MRSA (LA-MRSA) is an emerging concern as multiply antibiotic resistant strains can potentially transmit to humans. The pig associated clonal complex, CC398, was studied in gnotobiotic piglets, in co-colonisation with human isolates to monitor the transfer of genetic material (McCarthy et al., 2014). A high frequency of horizontal gene transfer was found *in vivo*, in excess of that which would be predicted from *in vitro* data, highlighting the need for further investigation of the zoonotic potential threat of livestock associated strains.

At the present time, there is no substitute for animal models to interrogate complex host: pathogen interactions. But it is also the case than no single animal model is sufficient and translation to human disease is ambitious. Ultimately, it is important that models of *S. aureus* infection are used in conjunction with one another and the advantages and

disadvantages of each are understood at the outset. Depending on the choice of model used, different *S. aureus* mutants are identified as attenuated, highlighting the challenges in comparing results across experimental models (Coulter et al., 1998). Finally, the principals of the '3Rs' (replacement, reduction and refinement) when conducting animal research must be considered in all experimental planning (www.nc3rs.org.uk/the-3rs).

1.13 Hypothesis and aims of the project

It was hypothesised that novel virulence traits of *S. aureus* account for differences in comparative virulence studies, may govern survival and/or growth of *S. aureus* in hostile but clinically relevant environments such as human blood, and that immunological bottlenecks may be perturbed by the presence of nonpathogenic bacteria or their components.

The specific aims of the work presented in this thesis are as follows:

i. To use a phenotypic zebrafish virulence assay and whole genome sequence data analysis for novel virulence factor identification
ii. To identify genes required for growth on human blood and pathogenesis *in vivo*
iii. To investigate how mixed inocula impact on pathogen success.

Chapter 2. Materials and methods

2.1 Media

Media were prepared using distilled water (dH_2O) and were sterilised by autoclaving for 20 minutes at 121°C and 15 psi.

2.1.1 Brain Heart Infusion (BHI) broth

Brain Heart Infusion	(Oxoid)	37 g l^{-1}

1.5% (w/v) Oxoid No. 1 agar was added to make BHI agar.
This is a highly nutritious general purpose growth media.

2.1.2 Luria-Bertani (LB) broth

Tryptone (Oxoid)	10 g l^{-1}
Yeast extract (Oxoid)	5 g l^{-1}
NaCl	5 g l^{-1}

1.5% (w/v) Oxoid No. 1 agar was added to make LB agar.
This is a rich media often used for the cultivation of *E. coli*.

2.1.3 LK broth

Tryptone (Oxoid)	10 g l^{-1}
Yeast extract (Oxoid)	5 g l^{-1}
KCl	7 g l^{-1}

1.5% (w/v) Oxoid No. 1 agar was added to make LK bottom agar.
0.5% (w/v) Oxoid No. 1 agar was added to make LK top agar.
This is a rich media mainly used for bacteriophage transduction experiments.

2.1.4 Mueller-Hinton broth

Mueller-Hinton (Oxoid) 21 g l^{-1}

1.5% (w/v) Oxoid No. 1 agar was added to make BHI agar.
This is a thymidine poor media reducing interference with antimicrobial susceptibility testing.

2.1.5 Chemically defined minimal media (CDM)

Chemical	Weight (g)	Chemical	Weight (g)
Solution 1			
$Na_2HPO_4.2H_2O$	7	L-Lysine	0.1
KH_2PO_4	3	L-Leucine	0.15
L-Aspartic Acid	0.15	L-Methionine	0.1
L-Alanine	0.1	L-Phenylalanine	0.1
L-Arginine	0.1	L-Proline	0.15
L-Cysteine	0.05	L-Serine	0.1
Glycine	0.1	L-Threonine	0.15
L-Glutamic Acid	0.15	L-Tryptophan	0.1
L-Histidine	0.1	L-Tyrosine	0.1
L-Isoleucine	0.15	L-Valine	0.15
Solution 2			
Biotin	0.02	Pyridoxal HCl	0.8
Nicotinic Acid	0.4	Pyridoxamine di-HCl	0.8
D-Pantothenic Acid	0.4	Riboflavin	0.4
Thiamine HCl	0.4		
Solution 3			
Adenine Sulphate	0.02	Guanine HCl	0.02
Solution 4			
$CaCl_2.6H_2O$	0.01	$(NH_4)_2Fe(SO_4)_2.6H_2O$	0.006
Solution 5			
Glucose	10	$MgSO_4.7H_2O$	0.5

Table 2.1 Composition of chemically defined minimal media

Solution 1 chemicals were dissolved in 700 ml of dH_20 and pH adjusted to 7.2. Solution 2 chemicals were dissolved in 140 ml of dH_20 to produce a 1000 fold concentrated solution. Solution 3 chemicals were dissolved in 50 ml of 0.1 M HCl and solution 4 was dissolved in 10ml of 0.1 M HCl. Finally, solution 5 was dissolved in 100 ml of dH_20 (Table 2.1).

To make 1 L of CDM broth, 700 ml of solution 1 was combined with 100 ml of 1 x solution 2, 50 ml of solution 3, 10 ml of solution 4 and 100 ml of solution 5.

1.5 % (w/v) Oxoid No. 1 agar was added to make CDM agar.

2.1.6 Blood and blood component media

2.1.6.1 Human blood collection

After informed consent, venous blood was taken from healthy volunteers at the Royal Hallamshire Hospital. Blood was collected in 50 ml Falcon tubes containing the anticoagulant sodium citrate, to give a final concentration of 0.4% (w/v) and gently rotated. Blood was stored at 4°C and used the same day.

2.1.6.2 Human plasma preparation

Blood samples collected as in section 2.1.6.1 were centrifuged at 270 g for 20 min in 50 ml Falcon tubes. The upper platelet rich phase was collected and used directly as platelet rich plasma (PRP), or centrifuged again at 1155 g for 40 min to give platelet poor plasma (PPP). Plasma was stored at -20°C.

2.1.6.3 Serum or plasma agar (50% v/v)

3% (w/v) agar No. 1 (Oxoid) 30 g l^{-1}

The agar was cooled to 55°C and the serum or plasma was warmed to 37°C before mixing to give 50% (v/v) serum or 50% (v/v) plasma agar.

2.1.6.4 Human or animal blood agar (30% v/v)

2% (w/v) agar No. 1 (Oxoid) 20 g l^{-1}

The agar was cooled to 55°C and the blood was warmed to 37°C before mixing to give 30% (v/v) blood agar.

2.1.6.5 Rabbit blood agar (10% v/v)

1.5% (w/v) agar No. 1 (Oxoid) 15 g l^{-1}

Agar was cooled to 55°C and sterile defibrinated rabbit blood (TCS Biosciences Ltd) was warmed to 37°C before mixing to produce a final concentration of 10% (v/v) rabbit blood agar. 10 ml was used to overlay a pre-made base agar plate (20 ml) and kept at room temperature to solidify.

2.1.6.6 Horse blood agar (5% v/v)

1.5% (w/v) agar No. 1 (Oxoid) 15 g l^{-1}

Agar was cooled to 55°C and horse blood (Thermoscientific) was warmed to 37°C before mixing to produce a final concentration of 5% (v/v) horse blood agar.

2.1.6.7 Sheep blood agar (5-30% v/v)

Columbia agar (Sigma Aldrich) 42 g l^{-1}

Agar was cooled to 55°C and sheep blood (Thermoscientific) was warmed to 37°C before mixing to produce a final concentration of 5-30% (v/v) sheep blood agar. Columbia agar is a highly nutritious base agar.

2.2 Plate photography

Agar plates were photographed using a Canon DS126191 and processed using Microsoft Office®, Powerpoint® for Mac (2011).

2.3 Measuring haemolysis

2.3.1 Qualitative analysis of haemolysis on rabbit blood agar

Rabbit blood agar plates were prepared as described in Section 2.1.6.5 onto which *S. aureus* strains were patched. After overnight incubation at 37°C, alpha-haemolysin

activity was visualised by observing a zone of clearing (lysis) around the patch of bacteria.

2.3.2 Quantitative haemolysis assay

A colony of *S. aureus* was inoculated into 5 ml BHI and grown overnight at 37°C on a rotary shaker at 250 rpm. The OD_{600} was measured and 600 µl of culture was removed to a microcentrifuge tube and centrifuged (13,000 rpm, 1 minute, RT). 500 µl was removed and 5 µl of PMSF was added before 100 µl aliquots were made.

100 µl was added to 900 µl haemolysin salts solutions and 25 µl of defibrinated rabbit blood was added before mixing. A spectrophotometer blank was made using 1 ml haemolysin salts solution and 25 µl rabbit blood. Samples were incubated at 37°C for 15 minutes before centrifuging as before. The OD_{543} of the supernatant was then measured. Haemolysin units (HU) were calculated by the equation:

$$HU = (OD_{543} \times 1000)/(V \times T \times OD_{600} \times 0.5)$$

V = volume of supernatant (0.1 ml); T = incubation time at 37°C (15 minutes)

Therefore, one haemolysin unit was defined as the amount that caused an increase in OD_{543} of 0.5 per minute due to erythrocyte lysis per OD_{600} of original culture.

2.4 Antibiotics

All antibiotics used in this study are listed in Table 2.2. The antibiotic stock solutions were prepared by dissolving antibiotics in the appropriate solvent before filter-sterilising (0.22 μm pore size) and storing at -20°C. For use in liquid media, antibiotic stock solutions were added prior to usage. For use in agar plates, molten agar was cooled to 55°C before the addition of antibiotics.

Antibiotic	**Stock concentration (mg ml^{-1})**	**Solvent**	***E. coli* working concentration (μg ml^{-1})**	***S. aureus* working concentration (μg ml^{-1})**
Ampicillin (Amp)	100	dH_2O	100	-
Chloramphenicol (Cat)	10	100% v/v ethanol	15	10
Erythromycin (Ery)	5	100% v/v ethanol	-	5
Kanamycin (Kan)	50	dH_2O	-	50
Lincomycin (Lin)	25	50% v/v ethanol	-	25
Neomycin (Neo)	50	dH_2O	-	50
Tetracycline (Tet)	5	100% v/v ethanol	-	5
Trimethoprim (Trim)	5	100% v/v DMSO	-	0.05-32
Spectinomycin (Spc)	50	dH_2O	-	150-1000
Anhydrotetracycline (ATc)	1	100% v/v ethanol	-	1

Table 2.2 Antibiotic stock solutions and concentrations

2.4.1 Antibiotic susceptibility testing of *S. aureus* isolates

2.4.1.1 Antibiotic breakpoint determination

BHI agar plates were made containing the appropriate antibiotic at the standard laboratory breakpoints (Table 2.2). A single *S. aureus* colony was spread using a sterile inoculation loop onto the antibiotic agar and incubated overnight at 37°C. A positive control was set up concurrently using the standard laboratory strain, *S. aureus* SH1000.

Growth of the test colony was compared to the positive control and interpreted as either sensitive (no growth observed on test plate) or resistant (growth observed on test plate).

2.4.1.2 Gradient strips for MIC determination

A bacterial colony was inoculated into 2 ml sterile dH_2O and spread onto an agar plate using sterile swabs (Oxoid). The gradient strip was applied to the surface using tweezers and allowed to dry before plate inversion and incubation over night at 37°C.

2.5 Bacterial strains

2.5.1 *S. aureus* strains

The *S. aureus* strains used in this study are listed in Table 2.3. Strains were grown from -80°C Microbank beads (Pro Lab Diagnostics) and cultured onto BHI agar plates with antibiotics incorporated where necessary, to maintain resistance markers. For short-term storage, strains were kept on BHI agar plates, wrapped in Parafilm® at 4°C. For long-term storage, a single colony was inoculated into Microbank bead stocks and kept at -80°C.

For bacterial growth in liquid media, strains were grown aerobically at 37°C. Strains containing temperature sensitive plasmids were grown between 25-28°C. For standard experiments, a single colony was used to inoculate 5 ml BHI broth and incubated overnight at 37°C on a rotary shaker at 250 rpm. 0.5 ml of overnight culture was used to inoculate 50 ml BHI broth in a 250 ml conical flask and re-incubated at 37°C and 250 rpm on a rotary shaker until exponential phase growth was reached.

Strain	Description	Reference
RN4220	Restriction deficient, transformation recipient	(Kreiswirth et al., 1983)
SH1000	Functional *rsbU*$^{+}$ derivative of 8325-4	(Horsburgh et al., 2002)
USA300 JE2	Plasmid cured USA300_FPR3757, Met^{R}	(Fey et al., 2013)
Newman	High level of clumping factor	(Duthie and Lorenz, 1952)
NewHG	Newman, repaired *saeS*	(Mainiero et al., 2010)
LS1	Murine arthritis isolate	(Bremell et al., 1991)
COL	Met^{R}	(Shafer and Iandolo, 1979)
NE108 (JE2)	USA300 *pabC* Ery^{R}	This study
NE108 (SH)	SH1000 *pabC* Ery^{R}	This study
NE277 (JE2)	USA300 *tdk* Ery^{R}	This study
NE277 (SH)	SH1000 *tdk* Ery^{R}	This study
NE 441 (JE2)	USA300 *nrfp* Ery^{R}	This study
NE 424 (JE2)	USA300 *pdp* Ery^{R}	This study
NE 424 (SH)	SH1000 *pdp* Ery^{R}	This study
NE 460 (JE2)	USA300 *atl* Ery^{R}	This study
NE 522 (JE2)	USA300 *purB* Ery^{R}	This study
NE 522 (SH)	SH1000 *purB* Ery^{R}	This study
NE 529 (JE2)	USA300 *purA* Ery^{R}	This study
NE 529 (SH)	SH1000 *purA* Ery^{R}	This study
NE 544 (JE2)	USA300 *nupC* Ery^{R}	This study
NE 544 (SH)	SH1000 *nupC* Ery^{R}	This study
NE 557 (JE2)	USA300 *isdC* Ery^{R}	This study
NE 557 (SH)	SH1000 *isdC* Ery^{R}	This study
NE 821 (JE2)	USA300 *pabA* Ery^{R}	This study
NE 821 (SH)	SH1000 *pabA* Ery^{R}	This study
NE 821 (SH)	SH1000 *pabA* Spc^{R}	This study
NE1063 (JE2)	USA300 *pabB* Ery^{R}	This study
NE1063 (SH)	SH1000 *pabB* Ery^{R}	This study
NE1253 (JE2)	USA300 *murQ* Ery^{R}	This study
NE1253 (SH)	SH1000 *murQ* Ery^{R}	This study
NE1304 (JE2)	USA300 *araC* Ery^{R}	This study
NE1304 (SH)	SH1000 *araC* Ery^{R}	This study
NE1315 (JE2)	USA300 *mecA* Ery^{R}	This study
NE1315 (SH)	SH1000 *mecA* Ery^{R}	This study
NE1391 (JE2)	USA300 *odhB* Ery^{R}	This study
NE1391 (SH)	SH1000 *odhB* Ery^{R}	This study
NE1775 (JE2)	USA300 *lipA* Ery^{R}	This study
NE1775 (SH)	SH1000 *lipA* Ery^{R}	This study
NE 1856 (JE2)	USA300 JE2 *epiD* Ery^{R}	This study
NE 1856 (SH)	SH1000 JE2 *epiD* Ery^{R}	This study
SJF 2685	Newman *sae* Kan^{R}	(Geiger et al., 2008)
SJF 1293	SH1000 *saeS::Tn551* Ery^{R}	(Needham et al., 2004)
SJF 3673	SH1000 *lysA::*Ery^{R} *lysA+*	(McVicker et al., 2014)
SJF 3674	SH1000 *lysA::*Kan^{R} *lysA+*	(McVicker et al., 2014)
SJF 3675	SH1000 *lysA::*Tet^{R} *lysA+*	(McVicker et al., 2014)
SJF 3676	Newman *lysA::*Ery^{R} *lysA+*	(McVicker et al., 2014)
SJF 3677	Newman *lysA::*Kan^{R} *lysA+*	(McVicker et al., 2014)

SJF 3678	Newman *lysA::*Tet^R *lysA+*	(McVicker et al., 2014)
SJF 3679	NewHG *lysA::*Ery^R *lysA+*	(McVicker et al., 2014)
SJF 3680	NewHG *lysA::*Kan^R *lysA+*	(McVicker et al., 2014)
SJF 3681	NewHG *lysA::*Tet^R *lysA+*	(McVicker et al., 2014)
SJF 4290	SH1000 *saeR* Ery^R *pheP* Tet^R	This study
SJF 4391	NewHG *saeR* Ery^R *pheP* Tet^R	This study
SJF 4308	SH1000 carrying pMV158-*mCherry*	Constructed by T. Prajsnar (University of Sheffield)
SJF 4405	SH1000 carrying pMV158-*gfp*	Constructed by T. Prajsnar (University of Sheffield)
SJF 4582	SA113 *lgt* Ery^R	(Stoll et al., 2005)
SJF 4591	SH1000 *lgt* Ery^R	This study
SJF 4669	SH1000 *pabA* Spc^R *pdp* Ery^R	This study
SJF 4670	SH1000 *pabA* Spc^R *nupC* Ery^R	This study
SJF 4671	SH1000 *thyA* Ery^R	(Kriegeskorte et al., 2014)
SJF 4675	LS1Δ*htsA*Δ*isdE*	(Wright and Nair, 2012)
SJF 4677	SH1000 *saeS*$^{\Delta A->T}$	This study
SJF 4678	SH1000 *pabA* Spc^R *tdk* Ery^R	This study
SJF 4679	SH1000 *sae* Kan^R *purB* Ery^R	This study
SJF 4681	SH1000 *pheP* Tet^R *purB* Ery^R	This study
SJF 4683	NewHG *pabA* Ery^R	This study
SJF 4685	LS1Δ*htsA*Δ*isdE pabA* Ery^R	This study
JC010	SH-*pabA*, pJC002 inserted at lipase – *pabA*$^+$ Ery^R Lin^R Tet^R	This study
JC011	SH-*pabA*, pKasbar inserted at lipase Ery^R Lin^R Tet^R	This study
GRE4	ST239, Met^R	(Harris et al., 2010)
GRE18	ST239, Met^R	(Harris et al., 2010)
GRE317	ST239, Met^R	(Harris et al., 2010)
R35	ST239, Met^R	(Harris et al., 2010)
ANS46	ST239, Met^R	(Harris et al., 2010)
BK2421	ST239, Met^R	(Harris et al., 2010)
LHH1	ST239, Met^R	(Harris et al., 2010)
TW20	ST239, reference genome, Met^R	(Holden et al., 2009); (Harris et al., 2010)
DEN907	ST239, Met^R	(Harris et al., 2010)
S26	ST239, Met^R	(Harris et al., 2010)
S25	ST239, Met^R	(Harris et al., 2010)
S97	ST239, Met^R	(Harris et al., 2010)
S2	ST239, Met^R	(Harris et al., 2010)
S106	ST239, Met^R	(Harris et al., 2010)
S78	ST239, Met^R	(Harris et al., 2010)
S39	ST239, Met^R	(Harris et al., 2010)
S24	ST239, Met^R	(Harris et al., 2010)
S81	ST239, Met^R	(Harris et al., 2010)
S40	ST239, Met^R	(Harris et al., 2010)
S102	ST239, Met^R	(Harris et al., 2010)
S85	ST239, Met^R	(Harris et al., 2010)
S130	ST239, Met^R	(Harris et al., 2010)
S87	ST239, Met^R	(Harris et al., 2010)

CHI59	ST239, Met^R	(Harris et al., 2010)
CHI61	ST239, Met^R	(Harris et al., 2010)
ICP5011	ST239, Met^R	(Harris et al., 2010)
ICP5014	ST239, Met^R	(Harris et al., 2010)
ICP5062	ST239, Met^R	(Harris et al., 2010)
FFP103	ST239, Met^R	(Harris et al., 2010)
HSA10	ST239, Met^R	(Harris et al., 2010)
StTom 38	ST239, Met^R	(Harris et al., 2010)
StTom 3	ST239, Met^R	(Edgeworth et al., 2007)
StTom 64	ST239, Met^R	(Edgeworth et al., 2007)
StTom 65	ST239, Met^R	(Edgeworth et al., 2007)
StTom 26	ST239, Met^R	(Edgeworth et al., 2007)
StTom 14	ST239, Met^R	(Edgeworth et al., 2007)
StTom 46	ST239, Met^R	(Edgeworth et al., 2007)
StTom 13	ST239, Met^R	(Edgeworth et al., 2007)
StTom 73	ST239, Met^R	(Edgeworth et al., 2007)
StTom 96	ST239, Met^R	(Edgeworth et al., 2007)
StTom 7	ST239, Met^R	(Edgeworth et al., 2007)
StTom 6	ST239, Met^R	(Edgeworth et al., 2007)
StTom 97	ST239, Met^R	(Edgeworth et al., 2007)
StTom 17	ST239, Met^R	(Edgeworth et al., 2007)
StTom 41	ST239, Met^R	(Edgeworth et al., 2007)
StTom 115	ST239, Met^R	(Edgeworth et al., 2007)
StTom 128	ST239, Met^R	(Edgeworth et al., 2007)
StTom 105	ST239, Met^R	(Edgeworth et al., 2007)
StTom 83	ST239, Met^R	(Edgeworth et al., 2007)
StTom 118	ST239, Met^R	(Edgeworth et al., 2007)
StTom 77	ST239, Met^R	(Edgeworth et al., 2007)
StTom 125	ST239, Met^R	(Edgeworth et al., 2007)
StTom 94	ST239, Met^R	(Edgeworth et al., 2007)
StTom 126	ST239, Met^R	(Edgeworth et al., 2007)
StTom 116	ST239, Met^R	(Edgeworth et al., 2007)
StTom 57	ST239, Met^R	(Edgeworth et al., 2007)
StTom 53	ST239, Met^R	(Edgeworth et al., 2007)
StTom 74	ST239, Met^R	(Edgeworth et al., 2007)
StTom 23	ST239, Met^R	(Edgeworth et al., 2007)
StTom 58	ST239, Met^R	(Edgeworth et al., 2007)
StTom 71	ST239, Met^R	(Edgeworth et al., 2007)
StTom 86	ST239, Met^R	(Edgeworth et al., 2007)
StTom 15	ST239, Met^R	(Edgeworth et al., 2007)
StTom 28	ST239, Met^R	(Edgeworth et al., 2007)
StTom 78	ST239, Met^R	(Edgeworth et al., 2007)
1 B	ST22, Met^R	(Köser et al., 2012)
7 C	ST22, Met^R	(Köser et al., 2012)
8 C	ST22, Met^R	(Köser et al., 2012)
10 C	ST22, Met^R	(Köser et al., 2012)
11 C	ST22, Met^R	(Köser et al., 2012)
12 C	ST22, Met^R	(Köser et al., 2012)
P 1	ST2371, Met^R	(Harris et al., 2013)
P 2	ST2371, Met^R	(Harris et al., 2013)

P 5	ST2371, Met^R	(Harris et al., 2013)
P 6	ST2371, Met^R	(Harris et al., 2013)
P 7	ST2371, Met^R	(Harris et al., 2013)
P 10	ST2371, Met^R	(Harris et al., 2013)
P 13	ST2371, Met^R	(Harris et al., 2013)
P 14	ST2371, Met^R	(Harris et al., 2013)
P 15	ST2371, Met^R	(Harris et al., 2013)
P 17	ST2371, Met^R	(Harris et al., 2013)
P 19	ST2371, Met^R	(Harris et al., 2013)
P 24	ST2371, Met^R	(Harris et al., 2013)
44 C	ST2371, Met^R	(Harris et al., 2013)
44 E	ST2371, Met^R	(Harris et al., 2013)
44 F	ST2371, Met^R	(Harris et al., 2013)
44 G	ST2371, Met^R	(Harris et al., 2013)
44 H	ST2371, Met^R	(Harris et al., 2013)
44 L	ST2371, Met^R	(Harris et al., 2013)
44 M	ST2371, Met^R	(Harris et al., 2013)
44 K	ST2371, Met^R	(Harris et al., 2013)
44 O	ST2371, Met^R	(Harris et al., 2013)
44 P	ST2371, Met^R	(Harris et al., 2013)
44 R	ST2371, Met^R	(Harris et al., 2013)
44 S	ST2371, Met^R	(Harris et al., 2013)

Table 2.3 *S. aureus* strains used in this study

Met^R – methicillin resistant, Ery^R – erythromycin resistant; Lin^R – lincomycin resistant; Tet^R – tetracycline resistant; Spc^R – spectinomycin resistant

All NE strains contain Tn *bursa aurealis*.

2.5.2 Other Gram-positive strains

Other non-staphylococcal Gram-positive strains used in this study are listed in Table 2.4. *M. luteus* and *Curtobacterium flaccumfaciens* were grown aerobically at 30°C in BHI broth. *S. epidermidis* was grown aerobically at 37°C in BHI broth. The same storage conditions were used as for *S. aureus* (Section 2.5.1).

Strain	Description	Source
SJF 256	*M. luteus*	ATCC4698, Sigma Lysophilised cells
SJF 4393	*M. luteus*, rif^R	This study
SJF 449	*C. flaccumfaciens*	This study
SJF 229	*S. epidermidis* (strain 138)	(Modun et al., 1998)
SJF 4381	*S. epidermidis* (strain 138), rif^R	This study
SJF 1	*Bacillus subtilis* 168	This study

Table 2.4 Other Gram-positive strains used in this study

2.5.3 *E. coli* strains

The *E. coli* strains used in this study are listed in Table 2.5. All strains were grown at 37°C, with the same culture and storage conditions as used for *S. aureus* (Section 2.5.1) except LB broth and agar were used as optimal media.

Strain	Description	Reference
TOP10	F- *mcrA* Δ(*mrr-hsd*RMS-*mcr*BC) Φ80*lac*ZΔM15 Δ *lac*X74 *rec*A1 *ara*D139 Δ(*araleu*)7697 *gal*U *gal*K *rps*L (StrR) *end*A1 *nup*G	Invitrogen
DC10B	*dcm* mutation in high efficiency cloning strain DH10B	(Monk et al., 2012)

Table 2.5 *E. coli* strains used in this study

2.6 Plasmids

The plasmids used in this study are listed in Table 2.6. Purification of plasmid DNA was carried out as described in Section 2.12 below. Plasmid DNA was eluted into dH_20 or elution buffer and stored at 20°C.

Plasmid	Genotype/markers	Source
pIMAY	Low copy shuttle vector with temperature sensitive replication of origin in *S. aureus* and an inducible *secY* antisense RNA; Cat^R	(Monk et al., 2012)
pIMAY-Z	Low copy shuttle vector with temperature sensitive replication origin in *S. aureus*; an inducible *secY* antisense RNA and beta-D-galactosidase *lacZ*; Cat^R	(Monk et al., 2012)
pEJ1	pIMAY-Z containing a 2001 bp insert of *S. aureus saeS*$^{A->T}$; Cat^R	This study
pEJ2	pIMAY containing a 2001 bp insert of *S. aureus saeS*$^{A->T}$; Cat^R	This study
pEJ3	pIMAY-Z containing a 2001 bp insert of *S. aureus htrA2*$^{G->A}$; Cat^R	This study
pEJ4	pIMAY-Z containing a 2001 bp insert of *S. aureus isaB*^{Adel}; Cat^R	This study
pEJ5	pIMAY-Z containing a 2001 bp insert of *S. aureus* SATW20_13140$^{\Delta Gdel}$; Cat^R	This study
pJC002	pGM073 containing the *pab* operon, *pabA*, *pabB* and *pabC* and upstream control elements; Tet^R	This study

Table 2.6 List of plasmids used in this study

Cat^R – chloramphenicol resistance; Tet^R – tetracycline resistance

2.7 Buffers and solutions

All buffers and solutions were prepared using dH_2O, sterilised by autoclaving and stored at room temperature or 4°C as necessary.

2.7.1 Phage buffer

$MgSO_4$	1 mM
$CaCl_2$	4 mM
Tris-HCl pH 7.8	50 mM
NaCl	100 mM
Gelatin	0.1 % (w/v)

2.7.2 Phosphate buffered saline (PBS)

NaCl	8 g l^{-1}
Na_2HPO_4	1.4 g l^{-1}
KCl	0.2 g l^{-1}
KH_2PO_4	0.2 g l^{-1}

2.7.3 Haemolysin salts solution

NaCl	0.145 M
$CaCl_2$	20 mM

2.7.4 50 mM Tris-HCl pH 7.5

Tris base	6.05 g l^{-1}

The pH was adjusted to 7.5 with HCl before autoclaving.

2.7.5 TAE (x 50)

Tris base	242 g l^{-1}
Glacial acetic acid	0.57 % (v/v)
EDTA, pH 8.0	0.05 mM

The stock solution was diluted 1:50 with dH_2O prior to use.

2.7.6 Tris/EDTA/NaCl buffer (TES)

Tris base	2.42 g l^{-1}
EDTA	1.86 g l^{-1}
NaCl	5.84 g l^{-1}

The pH was adjusted to 8.0 before autoclaving.

2.7.7 0.1 M Sodium phosphate buffer (pH 5.5)

Na_2HPO_4 (1.0 M)	93 ml
NaH_2PO_4 (1.0 M)	7 ml

The volume was adjusted to 1 L with dH_2O before autoclaving.

2.7.8 Promega Buffers

2.7.8.1 Membrane Binding Solution

Guanidine isothiocyanate	4.5 M
Potassium acetate, pH 5.0	0.5 M

2.7.8.2 Membrane Wash Solution

Potassium acetate, pH 5.0	10 mM
Ethanol	80 % (v/v)
EDTA, pH 8.0	16.7 µM

2.7.9 QIAGEN buffers

2.7.9.1 QIAGEN Buffer P1

Tris-HCl, pH 8.0	50 mM

EDTA	10 mM
RNase A	100 µg ml^{-1}

2.7.9.2 QIAGEN Buffer P2

NaOH	200 mM
SDS	1 % (w/v)

2.7.9.3 QIAGEN Buffer P3

Potassium acetate, pH 5.5	3.0 M

2.7.9.4 QIAGEN Buffer EB

Tris-HCl, pH 8.5	10 mM

2.7.9.5 QIAGEN Buffer TE

Tris-HCl, pH 8.0	10 mM
EDTA	1 mM

2.7.9.6 QIAGEN Buffer QBT

NaCl	750 mM
MOPS	50 mM, adjusted to pH 7.0 with NaOH
Isopropanol	15 % (v/v)
Triton X-100	0.15 % (v/v)

2.7.9.7 QIAGEN Buffer QC

NaCl	1.0 M
MOPS	50 mM, adjusted to pH 7.0 with NaOH
Isopropanol	15 % (v/v)

2.7.9.8 QIAGEN Buffer QF

NaCl	1.25 M
Tris-HCl pH 8.5	50 mM
Isopropanol	15 % (v/v)

2.7.9.9 QIAGEN Buffer N3, PB, PE

Supplied in QIAprep™ Spin Miniprep Kits, details not provided by manufacturer.

2.8 Chemicals, compounds and enzymes

Concentrations, storage and solvents of stock solutions are shown in Table 2.7. All chemicals and enzymes used in this study were of analytical grade and purchased from Fisher Scientific, Roche, Life Technologies or Sigma-Aldrich.

Stock solution	Stock concentration	Solvent	Storage
pHrodo™ Red	10 mM	DMSO	-20 °C in dark
Fluorescein-5-EX	16.95 mM	DMSO	-20 °C in dark
Mutanolysin	10 mg ml^{-1}	100 mM sodium phosphate buffer	-20 °C
Lysostaphin	5 mg ml^{-1}	20 mM sodium acetate	-20 °C
Bovine Serum Albumin (BSA)	10% (w/v)	PBS	4 °C
5-bromo-4-chloro-3-indolyl-β-D-galactopyranoside (X-gal)	40 mg ml^{-1}	DMF	-20 °C in dark
Cadmium chloride ($CdCl_{2)}$	100 mg ml^{-1}	dH_2O	-20 °C
Inosine	10 mg ml^{-1}	dH_2O	RT
Adenine hemisulphate	10 mg ml^{-1}	0.5 M HCl	RT
Guanine	25 mg ml^{-1}	5M HCl	RT
Serine	50 mg ml^{-1}	dH_2O	RT
Glycine	100 mg ml^{-1}	dH_2O	RT
Thymine	50 mg ml^{-1}	1M NaOH	RT
Thymidine	20 mg ml^{-1}	dH_2O	RT
Para-aminobenzoic acid (PABA)	50 mg ml^{-1}	100% v/v ethanol	4 °C in dark
EDTA	1 M	dH_2O	4 °C
EGTA	1 M	0.2 M Na OH	4 °C
Dipyridyl	1 M	100% v/v ethanol	4 °C
Zinc chloride	1 M	dH_2O	4 °C

Table 2.7 Stock solutions and concentrations

2.9 Centrifugation

The centrifuges used in this study are listed below.

- Eppendorf microfuge 5415D; maximum volume of 2 ml, maximum speed of 13,200 rpm (10,000 x g)

- Sigma centrifuge 4K15C; maximum volume of 50 ml, maximum speed of 5,100 rpm (5525 x g)
- Avanti™ J-25I (Beckman); JA-25,50; maximum load of 6 × 50 ml; maximum speed of 25,000 rpm (75, 600 x g
- Avanti™ J-26XP (Beckman); JLA 8.1000; maximum load of 6 x 1000 ml; maximum speed of 8,000 rpm (15, 970 x g).

2.10 Growth curves

After streaking out strains from Microbank bead frozen stocks onto BHI plates containing antibiotics where necessary (Section 2.4), a single colony was used to inoculate 5 ml BHI in a sterile 25 ml Universal tube. This was incubated overnight at 37°C with shaking at 250 rpm and used to inoculate 50 ml of pre-warmed BHI to an OD_{600} of 0.01. In triplicate, cultures were incubated at 37°C in a Grant OLS 200 water-bath with shaking (250 rpm) and growth was monitored by serial OD_{600} measurements (section 2.11.1) or direct cell counts (section 2.11.2) until stationary phase was reached.

2.11 Determining bacterial density

2.11.1 Spectrophotometric measurement (OD_{600})

To quantify bacterial yield in liquid broth, spectrophotometric measurements were taken at OD_{600} using a Jenway 6100 spectrophotometer. Samples were diluted 1:10 in appropriate sterile culture medium where necessary.

2.11.2 Direct cell counts (CFU ml^{-1})

To quantify viable bacterial numbers, direct cell counts were performed. Bacterial suspensions were serially diluted 1:10 in PBS in duplicate and 10 µl of each dilution was spotted onto BHI agar, allowed to dry and incubated at 37°C overnight. The number of colony forming units (CFU) was counted directly the following day.

2.12 DNA purification techniques

2.12.1 Small scale plasmid purification

Small-scale plasmid purification from *E. coli* or *S. aureus* was carried out using the QIAGEN QIAprep™ Spin miniprep kit. An overnight culture of 5 ml *E. coli* or *S. aureus* was centrifuged at 4°C, 5100 rpm, for 10 min before the pellet was re-suspended in 250 µl of buffer P1 containing RNase A (100 µg ml^{-1}). For *S. aureus* plasmid isolation, 10 µl of 5 mg ml^{-1} lysostaphin was added and the sample was incubated for 1 h at 37°C. To lyse the cells, 250 µl of buffer P2 was added and the sample was mixed gently by inverting the tube 4-6 times. The lysis buffer was prevented from proceeding for more than 5 minutes by the addition of 350 µl of neutralising buffer N3 to halt cell lysis and the tube was inverted 4-6 times as before. The mixture was then centrifuged at 13,000 rpm, room temperature, for 10 min to remove cell debris. The supernatant was transferred to a QIAprep spin column and centrifuged for 1 min at 13,000 rpm, room temperature, before the flow-through was discarded. Subsequently, 500 µl of buffer PB was added to wash the column and the column was centrifuged for 30 seconds at 13,000 rpm, room temperature. The flow-through was discarded again before adding 750 µl of buffer PE to the column and the column was centrifuged again. To remove residual buffer that may inhibit further reactions, the flow-through was discarded and the column was centrifuged for an additional 1 min. The column was then placed into a clean microcentrifuge tube and the DNA was eluted by the addition of 50 µl of buffer EB or nuclease-free water to the centre of the column. After a 1 min incubation the microcentrifuge tube, together with column, was centrifuged for 1 min as before and the collected sample was stored at −20°C.

2.12.2 Large scale plasmid purification

Large scale plasmid purification from *E. coli* and *S. aureus* was carried out using a Hispeed® Plasmid Midi-kit. A single colony from a freshly streaked plate was inoculated into 50 ml (high-copy plasmid) or 150 ml (low-copy plasmid) appropriate liquid culture medium and grown overnight. The culture was recovered by centrifugation at 5100 rpm for 15 minutes at 4°C. The pellet was re-suspended homogenously in 6 ml Buffer P1 with RNase A (100 µg ml^{-1}). For *S. aureus*, 20 µl of 5 mg ml^{-1} lysostaphin was added and the sample was incubated for 60 minutes at 37°C on a rotatory shaker. 6 ml Buffer P2 was then added and the sample thoroughly mixed by

inverting 4-6 times before incubating at room temperature for 5 minutes. Next, 6 ml pre-chilled Buffer P3 was added and the sample mixed as before. The lysate was then poured into the barrel of the QIAfilter cartridge which has a screw cap on the outlet nozzle. During a 10 minute incubation at room temperature, a HiSpeed Tip was equilibrated with 4 ml Buffer QBT. The screw cap was removed and the plunger inserted to filter the cell lysate into the HiSpeed Tip. Once the lysate had entered, the HiSpeed Tip was washed with 20 ml Buffer QC. The DNA was eluted from the filter membrane by the addition of 5 ml Buffer QF. DNA was precipitated by adding 3.5 ml isopropanol, mixing, and incubating at room temperature for 5 minutes. The eluate-isopropanol mixture was poured into a 20 ml syringe from which the plunger has been removed and the outlet nozzle inserted into a QIAprecipitator Module. By inserting the plunger, the mixture was filtered through the Module under constant pressure. The Module was then washed with 2 ml 70 % (v/v) ethanol and the membrane dried by forcibly pressing air through the Module several times, using the plunger. The QIAprecipitator Module was then attached to the outlet nozzle of a syringe with the plunger removed and 1 ml of Buffer TE added. Holding the Module-syringe over a clean 1.5 ml microcentrifuge tube, the plunger was inserted and the DNA eluted into the collection tube under pressure. The eluate was poured back into the same syringe and the plunger re-inserted into the same collection tube to ensure maximal elution. DNA was stored at -20°C.

2.12.3 Gel extraction of DNA

DNA was separated in a 1% (w/v) TAE agarose gel, stained with Ethidium Bromide. Following electrophoresis, DNA of interest was excised using x-tracta™ Gel Extractor (Promega) under ultraviolet (UV) light and DNA was purified using the Wizard® SV Gel and PCR Clean-Up System. The gel slice was placed in a 1.5 ml microcentrifuge tube and Membrane Binding Solution was added. The tube was vortexed and incubated in a water bath at 55°C until the gel slice was completely dissolved. The SV Minicolumn was placed in a Collection Tube and the dissolved gel mixture was transferred into the Minicolumn assembly and incubated at room temperature for 1 minute. The sample was then centrifuged at 13 000 rpm for 1 minute and the flow-through discarded. 700 µl of Membrane Wash Solution (containing ethanol) was added to the column and re-centrifuged as above. The flow-through was discarded and 500 µl of Membrane Wash Solution added before centrifuging at 13 000 rpm for 5 minutes. To

allow evaporation of any residual ethanol, the collection tube was emptied and the column assembly re-centrifuged for 1 minute. The Minicolumn was transferred to a clean 1.5 ml microcentrifuge tube and 50 µl of nuclease-free water or Buffer TE was added to the centre of the column. The sample was incubated at room temperature for 1 minute and finally centrifuged for 1 min at 13 000 rpm. DNA was stored at -20°C.

2.12.4 PCR purification

To purify DNA products for PCR reactions, the Wizard® SV Gel and PCR Clean-Up System was used. An equal volume of Membrane Binding Solution was added to the PCR amplification and the prepared PCR product was transferred to the Minicolumn assembly and further processed as described above in Section 2.12.3. DNA was stored at -20°C.

2.12.5 Pellet paint precipitation of DNA

Pellet Paint NF Co-Precipitant (Novagen) was used to precipitate DNA. 2 µl of Pellet Paint NF Co-Precipitant was added to the sample, followed by 0.1 volume of 3 M Sodium Acetate, pH 5.2. Next, 2 volumes of 100 % (v/v) ethanol was added and the sample was briefly vortexed before incubating at room temperature for 2 minutes. The sample was then centrifuged at 13 000 rpm for 5 minutes. A dark blue pellet was visible in the bottom of the tube and the supernatant was removed. The pellet was washed with 70% (v/v) ethanol, vortexed and re-centrifuged as above. The pellet was then washed with 100% (v/v) ethanol, vortexed and re-centrifuged again. The supernatant was removed and the pellet dried on a 90°C heat block before being re-suspended in an appropriate volume of dH_2O and stored at -20°C.

2.13 *In vitro* DNA manipulation techniques

2.13.1 Polymerase Chain Reaction (PCR) techniques

2.13.1.1 Primer design

The primers used in this study are shown below in Table 2.8. Designed as short oligonucleotides (20-60 bases in length), the primers were used for DNA amplification, according to the DNA sequence of *S. aureus*. For use within the Gibson assembly® (see section 2.13.3), primers were designed within New England Biolabs software,

NEbuilder™ (www.nebuilder.neb.com). This software predicted the optimal annealing temperature. Primers not being used for Gibson assembly® reactions, were designed using the National Centre for Biotechnology Information Primer-BLAST (NCBI) software (www.ncbi.nlm.nih.gov/tools/primer-blast). Predicted annealing temperatures were calculated within New England Biolabs Tm Calculator (www.neb.com/tools-and-resources/interactive-tools/tm-calculator). Primers were received lysophilised and reconstituted in dH_2O at a stock concentration of 100 µM and diluted to 10 µM for working concentration before being stored at -20°C.

Primer	Sequence 5'-3'	Source
MCS FWD	TACATGTCAAGAATAAACTGCCAAAGC	(Monk et al., 2012)
MCS REV	AATACCTGTGACGGAAGATCACTTCG	(Monk et al., 2012)
EJ1 F	CTCCACCGCGGTGGCTTAACTTCAACTATTTTAGCAATTG	This study
EJ2 R	AGGGAACAAAAGCTGGACATCAACAATTAACTGAAATACTTTC	This study
EJ3 F	GGGGATATGACTATTACGAAGATGC	This study
EJ4 R	GGGGAAGTCATTACACAAACACA	This study
EJ5 F	CTCCACCGCGGTGGCTCATTATGATGAATCTGGTGAAG	This study
EJ6 R	AGGGAACAAAAGCTGGGTTCACATTATTAAAAATGGCATTC	This study
EJ7 F	CTCCACCGCGGTGGCTGATTGATTTGAATTTGATTGATTC	This study
EJ8 R	AGGGAACAAAAGCTGGTATTTTCTTTGATAACGTCATCTTG	This study
EJ9 F	CTCCACCGCGGTGGCAACCGAATTATTATTTAACAGTAAACC	This study
EJ10 R	AGGGAACAAAAGCTGGGCAAAAAATAGCACCGCTTTC	This study
EJ3 OUT	GGGGATATGACTATTACGAAGATGC	This study
EJ4 OUT	GGGGAAGTCATTACACAAACACA	This study
Upstream	CTCGATTCTATTAACAAGGG	(Fey et al., 2013)
Buster	GCTTTTTCTAAATGTTTTTTAAGTAAATCAAGTACC	(Fey et al., 2013)
repA_F	TTCAAAATCTGCGGTTGCGG	This study
repA_R	AACCCCCTTCGACTTTCGTC	This study
MALF1	TAGATGGGAGACTAAATATGG	This study
MALR1	GAATGGTAACATGGTAATAAT	This study
saeR_F	GCTGCTAGTTTCTTTGGAGCC	This study
saeR_R	GTCATATGGCCGTTAAACCACA	This study
pabA F	ATGGCATTGATAAGCCCGTT	This study
pabA R	TGCTGTAATCTTTAAGCAATTTGG	This study
Tdk F	ACGACTGTGTTCAAAGAAGTGAC	This study
Tdk R	ATCGATCATCAATCGCCGGT	This study
Pdp F	TGGCGGCTATGTTAAAGGGG	This study
Pdp R	CGCCATCGTATTACGTCCCA	This study
NupC F	GCGTTTCTATTTAGCTCAGACAGG	This study
NupC R	TGCGCCTACAATGACAGCTA	This study
htsA F	CATCAAATAAATGAAGTAGCAGAAG	(Wright et al., 2012)
htsA R	TTCCCTTAATAGCATCAATCG	(Wright et al., 2012)
isdE F	GACCATCATTACAACATTACATATAA	(Wright et al., 2012)
isdE R	TTAGCATTGGACCACCGAC	(Wright et al., 2012)

Table 2.8 List of primers used in this study
The 15-20 bp overlap region to the linearized vector is shown as underlined.

2.13.1.2 DNA amplification

Phusion® High Fidelity PCR Master Mix with HF buffer (New England Biolabs) was used for DNA amplification. Supplied at 2 x concentration, the Master Mix was used at a final reaction volume of 50 µl and contained the following:

DNA polymerase	1 U
$MgCl_2$	1.5 mM
dNTPs	0.2 mM (each)

The following components were added to either 0.2 ml or 0.5 ml thin walled PCR tubes, on ice:

Phusion® High Fidelity PCR Master Mix with HF buffer	25 µl
Forward primer	0.2 µM
Reverse primer	0.2 µM
Template DNA	100 ng

To give a 1 x concentration of Master Mix, an appropriate volume of sterile water was added. Reactions were carried out in a TC-3000 (Techne) PCR machine. The lid was pre-heated to 105°C for 4 minutes, hot start was de-activated and the following thermal cycling conditions were set:

1 cycle	Initial denaturation	98°C	30 s
30 cycles	Denaturation	98°C	30 s
	Annealing	40-65°C	30 s
	Extension	72°C	30s per Kb
1 cycle	Final extension	72°C	7 min

Reaction products were stored at -20°C.

2.13.1.3 Colony PCR screening of *E. coli*

One colony of *E. coli* was patched onto a BHI agar plate containing appropriate antibiotics where necessary and then emulsified into 20 µl dH_20 within a 0.5 ml thin walled PCR tube. Primers and Master Mix were added as described in section 2.13.1.2 and the PCR reaction was carried out as above.

2.13.1.4 Colony PCR screening of *S. aureus*

One colony of *S. aureus* was patched onto a BHI agar plate containing appropriate antibiotics where necessary and then emulsified into 20 µl dH_20 within a 0.5 ml thin walled PCR tube. An additional cell lysis step was performed:

37°C	15 min
99°C	20 min
4°C	1 min
99°C	2 min
4°C	1 min

Primers and Master Mix were added to the PCR tube as described in section 2.13.1.2 and the PCR reaction was carried out as above.

2.13.2 Restriction endonuclease digestion

Restriction enzymes were used as per the manufacturers instructions (New England Biolabs or Promega). Supplied buffers, temperature and duration of incubation were all employed as recommended. For digested products that were used in further cloning reactions, the enzymes were de-activated by incubation in a water bath at 65°C for 15 minutes. The Wizard® SV Gel and PCR Clean-Up System was used to remove unwanted reaction components as described in 2.12.4.

2.13.3 Gibson Assembly™ Method

Gibson Assembly™ (Synthetic Genomic, Inc) joins overlapping DNA fragments in a single-tube isothermal reaction (Gibson et al., 2009). The vector of choice was linearized by restriction enzyme digested as above and gel extracted as described in section 2.13.2. The insert was PCR-generated using primers designed specifically for use in the Gibson Assembly™ reaction. PCR product purification was not necessary if the product was 90% pure as seen by agarose gel electrophoresis. Concentration of both vector and insert was determined using a Nanodrop™ (ND-1000 Spectrophotometer, Peqlab Ltd) and the following reaction was set-up on ice, in 0.5 ml thin walled PCR tubes:

Insert	150-300 ng
Vector	50-100 ng
Gibson Assembly™ Master Mix (x2)	10 µl

An appropriate volume of dH_20 was added to give a 1 x concentration of Gibson Assembly™ Master Mix in a total volume of 20 µl. As a negative control, the reaction mixture above was prepared as above but without insert DNA. 10 µl of the positive control reagents provided was added to 10 µl of the Gibson Assembly™ Master Mix (x 2) to provide a positive control. Samples were incubated in a TC-3000 (Techne) PCR machine at 50°C for 60 minutes. Following incubation, samples were stored on ice or at -20°C for subsequent transformation.

2.13.4 Agarose Gel Electrophoresis

DNA samples were separated by electrophoresis in 1% (w/v) agarose gels in 1 x TAE buffer. Horizontal electrophoresis tanks (Life Technologies) of various sizes were used and pre-poured agarose gels were submerged horizontally. Before the gels became solid, 5-10 µl of Ethidium Bromide (10 mg ml^{-1}, BioRad) was added to allow visualization of DNA under UV light.

DNA samples were mixed, in 1.5 ml microcentrifuge tubes, with one-fifth their volume of 6 x loading buffer (ThermoScientific) and pipetted into the wells of the gel. DNA

was electrophoresed at 120 V for 30 min – 1 hour and visualised by a UV transilluminator at 260 nm. Photographs were taken using UVi Tec Digital Camera and UVi Doc Gel documentation system. The size and approximate concentration of DNA fragments was estimated using GeneRuler™ 1 Kb DNA ladder (ThermoScientific) as shown in Table 2.9.

Size (bp)
10000
8000
6000
5000
4000
3500
3000
2500
2000
1500
1000
750
500
250

Table 2.9 DNA fragments used for DNA sizing and approximate quantification for agarose gel electrophoresis.

Fragments in bold are bright reference bands.

2.13.5 DNA sequencing

Plasmid and PCR products used in this study were sequenced by GATC Biotech, Germany. 10-100 ng μl^{-1} of DNA dissolved in dH_20 was sent in a 1.5 ml microcentrifuge tube. Sequencing results were analysed using Geneious® 6 software (Biomatters Ltd) and SnapGene® Viewer (GSL Biotech LLC).

2.14 Transformation techniques

2.14.1 Transformation of *E. coli*

2.14.1.1 Preparing electrocompetent *E. coli* cells

E. coli TOP10 or DC10B were streaked from freezer stock onto LB agar and incubated at 37°C to obtain single colonies. One colony was inoculated into 5 ml LB broth and grown at 37°C, 250 rpm overnight. This culture was used to inoculate 500 ml of LB broth and was grown until the OD_{600} reached 0.5-0.7. After incubating on an ice slurry for 20 minutes, 4 x 50 ml aliquots of culture were centrifuged at 4°C, 5000 rpm for 10 minutes. The supernatant was removed and a further 50 ml of culture was added to each 50 ml Falcon tube. The samples were centrifuged as before and the supernatant was removed. The pellets were then washed three times with 30 ml ice-cold dH_20 by resuspension and centrifugation as above. Next, each pellet was re-suspended in 10 ml ice-cold, 10% (v/v) glycerol and all four samples were combined into a single 50 ml Falcon tube. After a further centrifugation step, the supernatant was removed before re-suspension in 1 ml ice-cold, 10% (v/v) glycerol. 50 µl of sample was aliquotted into pre-cooled 1.5 ml microcentrifuge tubes and stored at -80°C.

2.14.1.2 Electroporation of DNA into electro-competent *E. coli* cells

Aliquots containing 50 µl of competent cells were defrosted on ice and 2 µl of Gibson assembled product was added. The mixture was transferred into pre-chilled electroporation cuvettes (1 mm, Bio-Rad) and electroporated using a Gene Pulser system set at 200 Ω, 1.75 kV and 25 µF. The cells were thoroughly mixed in the cuvettes with 500 µl of LB medium and immediately recovered. The mixture was incubated for 1 hour at 37°C, 250 rpm and 100 µl aliquots were plated onto LB selective agar before overnight incubation at 37°C.

2.14.2 Transformation of *S. aureus*

2.14.2.1 Preparing electro-competent *S. aureus* cells

An abbreviated preparation protocol was used (Monk, 2012). *S. aureus* was streaked from freezer stock onto BHI agar and incubated at 37°C, to obtain single colonies. One colony was inoculated into 10 ml BHI media and grown overnight at 37°C, 250 rpm. The overnight culture was diluted to OD_{600} of 0.5 in a flask containing 50 ml pre-warmed BHI before incubation for 30 minutes, to achieve an OD_{600} of 0.8-0.9. The culture was immediately cooled in an ice-water slurry for 10 minutes before cells were harvested by centrifugation at 3900 rpm, 4°C for 10 minutes. After discarding the supernatant, the cells were washed twice in 50 ml ice-cold dH_20 and harvested as before. The pellet was suspended in 10 ml of sterile ice-cold 10% (v/v) glycerol, centrifuged and the supernatant discarded. The pellet was suspended in 2 ml sterile ice-cold 10% (v/v) glycerol, centrifuged for a final time before discarding the supernatant and re-suspending in 250 µl of sterile ice-cold 10% (v/v) glycerol. 50 µl aliquots were made and either immediately used for transformation or stored at -80°C.

2.14.2.2 Electroporation of DNA into competent *S. aureus* cells

Aliquots containing 50 µl of competent cells were thawed on ice for 5 minutes and left at room temperature for 5 minutes. The cells were then centrifuged at 5000 g for 1 minute and the supernatant discarded before re-suspending in 50 µl of sterile 10% (v/v) glycerol + 500 mM sucrose. Up to 5 µg of purified plasmid was added to cells, gently mixed and the mixture added to 1 mm electroporation cuvettes. Electroporation was carried out using a Gene Pulser system set at 100 Ω, 2.1 kV and 25 µF. The cells were thoroughly mixed in the cuvettes with 1 ml BHI + 500 mM sucrose and immediately recovered. The mixture was incubated for 1-2 hours at 28°C, 250 rpm (for temperature sensitive vectors) or 37°C as standard and subsequently, 200 µl aliquots were plated onto BHI selective agar before overnight incubation at either 28°C or 37°C, depending on the vector for 48 hours.

2.15 Phage techniques

2.15.1 Bacteriophage techniques

The bacteriophage ϕ11 was used for the phage transduction of *S. aureus*. This is a temperate, transducing, 45 Kb phage, specific to *S. aureus* and requires Ca^{2+} ions to maintain infectivity (Novick, 1991).

2.15.2 Preparation of phage lysate

The donor *S. aureus* strain was inoculated into 5 ml BHI medium preparation and grown overnight at 37°C with appropriate antibiotics where necessary. In a Universal container, 5 ml phage buffer, 5 ml BHI, 100 µl of stock SH1000 ϕ11 phage lysate were mixed together with 150-300 µl of overnight culture. The sample was incubated stationary, overnight at 25°C until the mixture had cleared before the lysate was filter sterilised (0.2 µm pore size) and stored at 4°C.

2.15.3 Determination of phage titre

S. aureus SH1000 was grown in 5 ml BHI to OD_{600} of approximately 0.5. Using phage buffer, serial dilutions of the phage lysate were made (10^{-4} – 10^{-7} range) and 100 µl of each dilution was added to a 400 µl aliquot of SH1000 culture with 50 µl 1 M $CaCl_2$. After static incubation for 10 minutes at room temperature, the aliquots were gently combined with 5 ml phage top agar and overlaid onto a pre-heated phage bottom agar plate. Plates were incubated at 37°C for 48 h before quantification of plaque forming units. Optimal phage lysates had titres in the range of 10^7 to 10^{10} pfu ml^{-1}.

2.15.4 Phage transduction

The recipient *S. aureus* strain was inoculated into 50 ml LK and grown overnight at 37°C, 250 rpm and then harvested at 5000 rpm for 10 minutes at room temperature. The pellet was re-suspended in 3 ml LK. Next, 500 µl of recipient cells were added to 1 ml LK, 10 µl 1M $CaCl_2$ and 500 µl pre-prepared phage lysate. A negative control was made containing the same except without the addition of phage lysate. Samples were

incubated at 37°C for 25 minutes, without shaking and a further 15 minutes at 37°C at 250 rpm. 1 ml of ice-cold sterile 0.02 M sodium citrate was added and the samples were incubated on ice for 5 minutes. The samples were then centrifuged at 5000 rpm for 10 minutes at 4°C and then all the supernatant was removed. Finally, the pellets were re-suspended in 1 ml ice cold 0.02 M and incubated on ice for 45 minutes. 100 µl aliquots were spread onto LK plates containing the appropriate antibiotic and 0.05% (w/v) sodium citrate. Plates were incubated at 37°C for 48 hours.

2.16 Construction of *S. aureus* mutants

A temperature sensitive plasmid was used which enables a homologous recombination event between the gene of interest in the chromosome and a homologous region of DNA within the plasmid. Incubation at a low temperature under antibiotic selective pressure allows plasmid replication whereas a higher, non-permissive, temperature in the presence of antibiotics selects for integrants of the plasmid into the chromosome. A second cross-over event allowing excision of the plasmid from the chromosome occurs when clones are grown at the permissive temperature, in the absence of selective pressure. Either the wild-type or mutant allele will remain in the chromosome whilst the allelic counterpart will be lost on the excised plasmid. Clone screening is achieved by either colometric or alternative positive discrimination i.e. loss of haemolysis.

The vector pIMAY is a low-copy number shuttle vector, designed for allelic exchange in *S. aureus*, via *E. coli* (Monk et al., 2012). A sister vector, pIMAY-lacZ (pIMAY-Z) is identical except for the addition of the β-galactosidase (*lacZ*) gene which allows colometric screening for successful mutants on X-Gal (5-bromo-4chloro-3indoyl-β-D-galactopyranoside) plates.

pIMAY+/-Z contains the *p15a E. coli* origin of replication allowing plasmid replication at 37°C. It also contains a highly temperature sensitive origin for *S. aureus* ($repA^{TS}$) which permits replication only at the permissive temperature (28°C), allowing integration of the plasmid into the chromosome at a non-permissive, higher temperature (37°C) (Maguin et al., 1992). The vector contains a chloramphenicol acetyl transferase (*cat*) gene for plasmid selection in both *E. coli* and *S. aureus* and an antisense *secY* (*anti-secY*) inducible by anhydrotetracycline. The latter prevents growth of clones that

contain the plasmid after the first recombination single crossover event, allowing selection of clones that no longer contain the plasmid and have undergone the second recombination event (Bae and Schneewind, 2006).

2.17 Genetic complementation of the *pab* operon

In brief, the *pab* operon was amplified and ligated into pKASBAR, a plasmid encoding an *attP* site. Using this *attP* site, bacteriophage DNA can integrate into the *S. aureus* genome at the *attB* site, in the presence of an integrase (Lee and Iandolo, 1986). The *attB* site is located at the glycerol ester hydrolase (*geh*) gene so integration can be verified by loss of lipase activity. For such genetic manipulation, the integrase is provided by an additional helper plasmid, pYL112Δ19, propagated in the *S. aureus* recipient strain, RN4220. Integration was confirmed before the complemented strain was transduced into the relevant genetic background (Connolly, 2016).

2.18 Screening the Nebraska transposon mutagenesis library (NTML) on solid media

The NTML containing *S. aureus* JE2 strains with transposon-disrupted genes was stored at -80°C in twenty 96 well microtiter plates. Plates were thawed on ice and a 96-pin replicator (Boekel Industries) was used to inoculate solid media with the well contents of each microtiter plate. Plates were incubated at 37°C for 24-48 hours, depending on the media employed.

2.19 Zebrafish techniques

2.19.1 Zebrafish strains

London Wild Type (LWT) strains were used for the zebrafish experiments.

2.19.2 Zebrafish husbandry

Adult zebrafish were maintained at 28°C in a continuous re-circulating closed system aquarium with a light/dark cycle of 14/10 hours. LWT zebrafish embryos were kept in E3 medium at 28.5°C.

2.19.3 Zebrafish E3 medium (x10)

NaCl	50 mM
KCl	1.7 mM
$CaCl_2$	3.3 mM
$MgSO_4$	3.3 mM

A 10 x stock was diluted to 1 x concentration of medium using distilled water. To prevent fungal growth, methylene blue was added to a final concentration of 0.00005% (Nusslein-Volhard and Dahm, 2002). The 1 x E3 medium was sterilised by autoclaving for 20 minutes at 121°C and 15 psi.

2.19.4 Methylcellulose

A 3.0% (w/v) solution of methylcellulose was prepared in E3 medium. In order for full solubilisation to occur, the solution was repeatedly stirred, frozen and defrosted (Nusslein-Volhard and Dahm, 2002). The solution was then aliquotted into 20 ml syringes and frozen for long-term storage. Each aliquot was thawed at 28.5°C for use or short-term storage.

2.19.5 Zebrafish anaesthesia

A stock solution of 0.4% (w/v) 3-amino benzoic acid ester (tricaine or MS322, Sigma) was prepared in 20 mM tris-HCl (pH adjusted to 7) and stored at -20°C. A working stock was kept at -4°C in the dark. Prior to bacterial injections, zebrafish embryos were anaesthetised in 0.02% (w/v) tricaine.

2.19.6 Microinjections of *S. aureus* into zebrafish embryos

Bacteria used for injection into zebrafish embryos were grown from an overnight culture in a 50 ml flask of BHI medium, until the OD_{600} reached approximately 1. Next, 40 ml of culture was centrifuged at 5100 rpm, 4°C for 10 minutes before the supernatant was discarded and the cells were re-suspended in sterile PBS to a known concentration. The volume of PBS was adjusted for the OD_{600} of each culture and bacterial

quantification was performed before and after each microinjection experiment. To do this, bacteria were diluted 1:4 in sterile PBS and 10 µl was spotted, in duplicate, onto BHI agar, allowed to dry and incubated at 37°C overnight. The number of colony forming units (CFU) was counted directly the next day.

Manual dechorionation of 30 hpf zebrafish embryos was performed 2 hours prior to injection with 1 nl of bacterial suspension. Immediately before injections, zebrafish embryos were briefly immersed in 0.02% (w/v) buffered tricaine anaesthetic solution before being immobilised onto 3.0% (w/v) methylcellulose. By heating non-filament glass capillary tubes (World Precision Instruments, WPI), microinjection needles were made by an electrode puller to produce a fine bore needle. Bacterial suspension, prepared as above, was loaded into microinjection needles using microcapillary pipettes (Fisher Scientific Ltd.) and the volume injected was calibrated using a graticule slide (approximately 1 nl) before embryos were injected in the circulation valley. To perform the injections, a pneumatic micropump (WPI, PV820), a micromanipulator (WPI) and a dissecting light microscope (Leica) were employed.

Post injections, embryos were removed from the methylcellulose into Petri dishes containing 30 ml sterile E3 medium and returned to a controlled temperature of 28.5°C. After 1-2 hours, any remaining methylcellulose had dissolved and embryos were washed with E3 medium and placed individually into 96-well plates.

2.19.7 Addition of compounds to zebrafish by immersion

For *in vivo* complementation experiments, compounds were dissolved in E3 medium and buffered to a pH of 6.5-7.5. Immediately following injections, embryos were placed in compound solutions and further compound solution was added in the embryo washing step. To maintain the initial concentration of the compound, 96-well microtitre plates were incubated in a plastic box, with damp paper, to reduce evaporation during incubation.

2.19.8 Determination of zebrafish embryo mortality following infection

Based on the sensitivity of this virulence assay, each strain of *S. aureus* was injected into 20-30 embryos. Visual inspection of the zebrafish using a dissecting light microscope (Leica) was carried out twice daily to assess embryo mortality as evidenced by cessation of heartbeat.

2.19.9 Determination of growth of *S. aureus in vivo*

To quantify growth *in vivo*, bacteria were recovered from embryos by collecting single fish, with the surrounding 100 µl E3 medium, into ceramic bead-containing 2 ml cap containers (Peqlab). Embryos were individually homogenised in a PreCellys 24-dual (Peqlab) and homogenates were serially diluted in sterile PBS and plated onto BHI agar. Colonies were counted after overnight incubation at 37°C. During a standard experiment, embryos were collected for bacterial recovery every 12 hours.

2.19.10 Microinjection of morpholino oligonucleotide into zebrafish embryos

2.19.10.1 Morpholinos

Morpholino modified antisense oligonucleotides were purchased from Gene Tools. Morpholine rings replace the ribose or deoxyribose sugar motieties on DNA thus allowing specific binding to complementary bases. The translational start site (ATG) of genes were knocked down by the presence of morpholino oligonucleotides.

Morpholino target	Sequence 5'-3'	Quantity per embryo	Reference
pu.1	GATATACTGATACTCCATTGGTGGT	0.5 pmole	(Rhodes et al., 2005)

Table 2.10 Morpholino used in this study

2.19.10.2 Injection of morpholino into zebrafish eggs

2 mM stock solutions of morpholino oligonucleotides were made in dH_20. A working concentration of 1 mM was injected into the yolk sac of 1-4 cell stage embryos, using microinjection needles and the same equipment as described in section 2.19.6.

2.19.11 Microscopic observations

2.19.11.1 Mounting of zebrafish

Anaesthetised embryos were placed in 27 mm glass base dishes (Nunc™, Thermo Scientific™) and surrounded by 1% (w/v) low melting point agarose (Sigma) in solution with methylene-blue omitted E3 medium. Agarose was allowed to solidify before microscopy was performed.

2.19.11.2 Imaging of zebrafish

Depending on availability, one of two microscopes were used for *in vivo* zebrafish imaging:

1. Nikon TE-2000 U microscope with Hamamatsu Orca-AG camera and Volocity™ (Image Processing and Vision Company Ltd. UK) was used for image acquisition and processing. The following objectives were used: 4 x Nikon Plan Fluor NA 0.13; 60 x Nikon Plan Apo oil objective NA 1.4. GFP and mCherry fluorophores were excited with 488 nm and 543 nm, respectively. Images were captured with 1 µm z-spacing. For imaging of cells *in vivo* focal depth limits were defined for each embryo and exposure times kept to a minimum.

2. UltraVIEW VoX spinning disk confocal microscope (Perkin Elmer) and Volocity™ (Image Processing and Vision Company Ltd. UK) was used for image acquisition and processing. GFP, mCherry and Alexa Fluor® 647 were excited by the 457-514nm argon laser, 561nm sapphire laser and 642nm diode laser respectively.

2.19.11.3 pHrodo™ and Fluorescein succinimidyl ester staining of *S. aureus*

A working concentration of 2.5 mM pHrodo™ Red was used whereas Fluorescein-5-EX was used at stock concentration (16.95 mM). From an overnight liquid culture of *S. aureus* in BHI broth at 37 °C, 250 rpm shaker, 0.5 ml was diluted in 50 ml of fresh BHI broth and incubated to the OD_{600} 1. 40 ml of this liquid culture was centrifuged (5100

rpm, 15 min, 4 °C), the supernatant discarded and pellet retained on ice. The pellet was re-suspended in an appropriate volume of PBS pH 9 and 200 µl of the suspension was mixed in a microcentrifuge tube with 0.5 µl working concentration pHrodo or 1.5 µl of stock concentration Fluorescein. The mixture was pipetted up and down to thoroughly mix and then the microcentrifuge tube was incubated at 37 °C on a 100 rpm rotatory shaker for 30 min. To remove excess dye, 1 ml PBS pH 8 was added to the tube, vortexed and centrifuged (13,400 rpm, 3 min, RT). The supernatant was removed and 1 ml 25 mM Tris pH 8.5 added, vortexed and centrifuged as before. The supernatant was removed again and 1 ml of PBS pH 8 added, vortexed and centrifuged for a final time. After supernatant removal, the bacterial cells were finally re-suspended in 200 µl of PBS pH 7.4 and kept on ice until used. The same protocol was followed for peptidoglycan labelling.

2.20 Latex fluorescent beads for *in vivo* experiments

Polystyrene latex beads of similar diameter to *S. aureus*, 1 µm, were purchased from Sigma at a concentration of 1.828×10^{11} per ml (or 1.828×10^{5} per nl). Dilution to the desired concentrations was carried out after the beads were sonicated (Soniprep 150, MSE, UK). Several type of beads were used including fluorescent amine or carboxylate modified beads and non fluorescent unmodified beads. Amine modified beads were received suspended in a buffer containing 0.05% (w/v) sodium azide so washing steps involving centrifugation and re-suspension in PBS were carried out prior to injection into infection models.

2.21 Murine sepsis model

Female BALB/c or C57BL/6J mice aged 7 weeks were purchased from Charles River (Margate, UK) or Envigo (Cambridgeshire, UK) respectively and maintained at the University of Sheffield (Biological Services) using standard husbandry techniques. Bacterial strains were grown in BHI to stationary phase, washed in endotoxin free sterile PBS and resuspended in a mixture of PBS and 10% (w/v) bovine serum albumin. Depending on the dose required, dilutions were made prior to intravenous injection into the tail vein of 6 - 7 week old mice. Bacterial doses ranging from $1 \times 10^{2} – 1 \times 10^{8}$ CFU per mouse in 100 µl were used. For experiments involving purified peptidoglycan,

doses in the range of 50 μg – 1 mg were centrifuged at 14,000 rpm for 2 minutes before being re-suspended in endotoxin free PBS. The sample was then sonicated thrice (Sanyo Soniprep 150) for 30 s with 1 min chilling on ice between each sonication.

Viable bacteria in the inoculum were quantified by serial dilutions and plating onto solid BHI medium with antibiotics added where necessary. Mice were checked for wellbeing twice daily and weighed daily throughout the 72-hour experiment. At the end of the procedure or if culling limits were reached prior to that time, mice were sacrificed under Schedule 1 via anaesthetic overdose (intra-peritoneal) followed by cervical dislocation. Organs were harvested and bacterial CFUs were enumerated.

The organs were assessed for staphylococcal persistence aseptically by individual homogenisation in a suitable volume of sterile PBS (2 ml for kidneys, 3 ml for livers). Serial dilutions were plated onto BHI agar and colony counts per organ were performed after overnight incubation at 37°C.

2.22 Histological preparation of murine organs

Each organ was placed in an embedding cube pre-filled with 5 mm of optimal cutting temperature (OCT) medium. Ensuring correct positioning for optimal sectioning, the organ was stabilised whilst the cube was filled with more OCT medium. This was carried out within a liquid nitrogen dewar and once organs were fully frozen, they were stored at -80°C. Pre-sectioning, organs were placed at -20°C and sectioning was kindly performed by technicians in the Histology Core Facility (University of Sheffield). For each organ, sections of 200 μm were cut and stained with hematoxylin and eosin (H&E) stain based on previously established methods (Cheng et al., 2009).

2.23 Murine serum cytokine sampling

For serum cytokine measurements, a small blood sample was taken from a superficial vessel (e.g. tail vein) by venesection. The volume of blood removed did not exceed 15% of total blood volume over any four-week period. Blood was collected in microcentrifuge tubes and left to clot by standing at room temperature for 2 hours before centrifugation for 10 minutes at 5000 g to separate the blood clot from serum.

Serum was stored at -20°C until analysis. Cytokine/chemokine concentrations were measured by cytometric bead array (CBA) flex sets on a FACSArray bioanalyzer (BD Biosciences, USA), by technical staff at the University of Sheffield Core Flow Cytometry Unit, in accordance with the manufacturer′s protocols.

2.24 Peptidoglycan purification

2.24.1 Breakage of cell walls

To obtain sufficient peptidoglycan for *in vivo* experiments, a mid-exponential phase BHI culture (10 litres of OD_{600} 1) of the required strain was harvested (11000 g, 10 min, 4 °C) and the cell pellet resuspended in a minimal volume of ice-cold 50 mM Tris-HCl (pH 7.5). The suspension was then boiled, to kill the cells, for 7 minutes in a water bath (100 °C) before being disrupted using the Braun homogenizer (Braun, Germany). In brief, 50 g of sterile glass beads were placed into each Braun Homogeniser bottle and the thick re-suspended cells (custard consistency) were added and placed on ice. Each bottle was homogenized for 6 x 1 min with intermittent cooling using liquid withdrawal CO_2. The beads were separated from the broken cells using a vacuum sintered glass filter and the suspension was centrifuged (18,000 rpm, 10 min, 18 °C) before the supernatant was discarded.

2.24.2 Extraction of cell wall and removal of proteins

The pellet was resuspended in 30 ml 50 mM Tris-HCl (pH 7.5) plus 2% (w/v) SDS. After incubation at 50°C for 15 min and centrifugation as before, the pellet was washed twice in water by resuspension and centrifugation. Covalently attached proteins were removed by treatment with 2 mg ml^{-1} pronase in TES for 1 h at 60°C. After centrifugation as previously, the pellet was resuspended in 30 ml of 50 mM Tris-HCl (pH 7.5) plus 3% (w/v) SDS, 50 mM dithiothreitol (DTT) and 1 mM EDTA. The suspension was boiled for 10 min, centrifuged as before and the pellet resuspended and the process repeated for a second time. The sample was then centrifuged again and washed five times in dH_2O. The pellet was then suspended in hydrofluoric acid (10 ml of 48% v/v) and the mixture was incubated at 2°C for 24 h. The insoluble material was collected by centrifugation (18,000 rpm, 5 min, 18°C) and washed repeatedly by

centrifugation and resuspension with alternating Tris-HCl buffer (50 mM, pH 7) and cold dH_2O until the pH was neutral. The peptidoglycan was finally resuspended in PBS to the required concentration, autoclaved and stored at -20^oC.

2.24.3 Hydrolysis of peptidoglycan

Peptidoglycan hydrolases were used throughout this study. Enzymes and reaction conditions are provided in Table 2.11.

Enzyme	Concentration (μg ml^{-1})	Buffer
Lysostaphin	250	50 mM Tris-HCl, pH 7.0
Mutanolysin	250	50 mM sodium phosphate buffer, pH 5.5

Table 2.11 Peptidoglycan digest conditions

2.24.4 Quantification of peptidoglycan for *in vivo* experiments

There is no literature available on injecting peptidoglycan into zebrafish embryos so dose calculations were based on attempting to match the equivalent amount of peptidoglycan that is injected via whole bacteria. It has been reported that 10^7 *S. aureus* cells correspond to 0.1 μg peptidoglycan (Timmerman et al., 1993). In order to calculate the amount of peptidoglycan per bacterium in these experiments, an overnight culture *S. aureus* was sub-cultured into 10 ml BHI broth and incubated for two hours at 37°C, with shaking at 250 rpm. At OD_{600} 1, a micro-centrifuge tube was first weighed before 1 ml of culture was added. This was centrifuged at 13 000 rpm for 2 mins before the supernatant was removed. A further 1 ml of culture was added on top of the existing pellet and the process was repeated until 10 ml was pelleted into the microcentrifuge tube. The sample was then snap frozen by immersion in liquid nitrogen and placed in a freeze-drier (ScanVac Cool Safe 55-4 Pro 3800) overnight allowing sublimation to occur. The following day, the microcentrifuge tube was re-weighed and the mass of peptidoglycan per ml of culture was calculated (0.26 mg ml^{-1}). As the OD_{600} was 1 (exponential phase) at the time of harvest, it can be estimated from data previously collected in the laboratory, that 2 x 10^8 CFU/ml were present. It was also estimated that peptidoglycan constitutes up to 10% of the cell mass (personal communication, Dr

Stephane Mesnage, University of Sheffield), hence peptidoglycan from 2 x 10^8 CFU weighed approximately 26 μg.

2.25 Ethical Permissions

Murine work was carried out according to UK law in the Animals (Scientific Procedures) Act 1986, under Project License PPL 40/3699 (*Staphylococcus aureus*, pathogenesis to therapy). On 12.02.16, an amendment was granted to include other Gram-positive species as detailed in the amended version. Personal license PIL IC40C2E16 (Categories A & B).

Zebrafish embryos less than 5 days post fertilization (dpf) are not protected under the Animals (Scientific Procedures) Act 1986 as they are not capable of independent feeding but all zebrafish work was carried out according to the details set out in Project License PPL 40/3574.

The South Sheffield Ethics Committee (reference number STH13927) approved the protocol for phlebotomy used in Chapter 4.

2.26 Data and statistical analysis

In zebrafish embryo survival experiments, the Kaplan-Meier method was employed. Comparison between survival curves was made using the log-rank (Mantel Cox) test.

For bacterial count comparison in murine experiments the Mann-Whitney U test or chi-square test with Yates correction was used. For comparison of two or more independent samples (non-parametric), the Kruskal Wallis test was applied with Dunn's multiple comparison test e.g. Figure 5.22 and 5.40. For clonality experiments, species evenness was derived from the Shannon diversity index.

Per strain, 30 zebrafish were injected to detect a 40% survival difference (power 80%, significance level 0.05). Based on typical values from previous *S. aureus* murine experiments, 10 mice per group are required (power of 80%, significance level 0.05).

Statistical analysis was performed using Prism version 6.0 (GraphPad). All zebrafish experiments are representative of at least n=2 unless otherwise stated. Representative data are shown from replicate experiments. Experimental zebrafish data was not combined due to embryo batch variation.

Mouse experiments were conducted as described in individual experiments. The following p value cut offs were used: * $p < 0.05$; ** $p < 0.01$; *** $p < 0.001$; **** $p < 0.0001$; NS – non significant.

2.27 Collaborative work

Chapter 3 – whole gene sequencing data analysis was carried out in collaboration with Dr Matthew Holden (University of St. Andrews). The initial zebrafish screening experiments were conducted in collaboration with Mr Alexander Williams (University of Sheffield).

Chapter 4 – initial screen of the Nebraska transposon library, liquid growth curve assays and genetic complementation of the *pab* operon were carried out by Dr John Connolly (University of Sheffield).

Chapter 5 – all murine experiements were conducted in collaboration with Ms Daria Shamarina (University of Sheffield). For the majority of experiments, I wrote the Individual Study Plans (ISPs), prepared the inocula, managed the experimental procedures and performed data analysis. We both equally contributed to animal injection, sacrifice/tissue harvesting and organ processing.

Chapter 3. Identifying novel virulence determinants of *S. aureus* by phenotypic:genotypic analysis

3.1 Introduction

Despite a wealth of recent work, the genetic attributes that fully determine the pathogenicity of *S. aureus* remain poorly understood. Whilst many individual bacterial virulence determinants have been described, the pool of as yet unknown genetic determinants of *S. aureus* disease is far from exhausted. Reverse genetic approaches can be used to unlock phenotypic information associated with certain genes (Fey et al., 2013) yet high-throughput *in vitro* screens of, for example, transposon libraries most notably lack the dynamic interplay of genes with a host. Furthermore, key virulence factors of laboratory strains compared with circulating clinical strains may vary and correlating information between distinct strains must be done with caution (Nair et al., 2011).

Investigation of putative virulence determinants of *S. aureus* has advanced significantly in recent years, most notably with the introduction of accessible whole genome sequencing (WGS) data. With the advent of high-throughput WGS, specific and detailed genomic information is now available for both prokaryotes and eukaryotes. Prior to this, clinical strain populations of *S. aureus* were exhaustively investigated using forward genetic approaches i.e. by comparing phenotype (*in vitro* or *in vivo*) with genotype by linking the presence of certain bacterial genes with clinical phenotypes by PCR analysis (Peacock et al., 2002; Jarraud et al., 2002), array comparative genomic hybridization (aGCH) (Gill et al., 2011; Lindsay et al., 2006) and multi-locus sequence typing (MLST) (Fowler et al., 2007).

These established methods have contributed to the cumulative knowledge on gene combinations that are necessary for pathogenesis but WGS now provides the capability to expand this further as it enables investigation of polymorphisms of known genes but also to mine currently unknown loci. However, since the first bacterial WGS was published (Fleischmann et al., 1995), whilst many applications of these massive datasets have been used for descriptive epidemiological studies (Köser et al., 2012; Harris et al., 2013), functional phenotype:genotype studies remain in their infancy. This may be in

part because the generation of huge amounts of sequencing data far exceeds our current ability to assign gene function. Approaches to elucidate phenotype:genotype relationships are needed with software to analyse large data sets and high throughput, translational *in vivo* models to interrogate phenotypic effects are beginning to emerge.

One approach that has been successfully used is Tn-seq, a method that applies deep sequencing to monitor insertion of transposon-generated mutants allowing construction of genome wide maps of genomic areas important in phenotypes of interest. Using this approach, transposon generated mutant libraries of *Streptococcus pneumoniae*, have been evaluated under a range of *in vivo* and *in vitro* conditions, leading to new assignments of gene function and identification of novel therapeutic targets e.g. a transcriptional regulator of pyrimidine synthesis (van Opijnen and Camilli, 2012). Similar techniques of sequencing and comparative pathogenomics in the zebrafish embryo model, have been used to identify novel fitness determinants of Extraintestinal Pathogenic *E. coli* (ExPEC) (Wiles et al., 2013). Deleting the identified candidate genes lead to an attenuated fitness phenotype in fish and murine models. Regarding *S. aureus*, a transposon mutant library of livestock associated MRSA (LA-MRSA), ST398, was created and analysed by transposon directed insertion site sequencing (TraDIS). When mutants were screened for growth and survival in whole porcine blood, 23 mutants exhibited attenuated bacterial fitness, the majority of which were involved in metabolism (Christiansen et al., 2014).

However, much bacterial pathogenesis research focuses on large genetic differences, within genes or genomic regions and less work been done on the impact of more subtle genetic differences such as single nucleotide polymorphisms (SNPs). The availability of whole genome sequencing now provides the tools for this approach. For example, genome wide analysis of hundreds of clinical strains of *Streptococcus pyogenes*, alongside clinical data, identified that a reduced incidence of necrotising fasciitis was associated with the presence of a single SNP which resulted in a premature stop codon in the metal dependent regulator, *mtsR* (Olsen et al., 2010). Further analysis revealed *mtsR* inactivation indirectly decreased secreted protease activity, which diminishes the necrotising fasciitis capacity of this bacterium, linking the WGS data to functional impact. Using a similar approach, whole genome sequences for a range of clonal complex 33 *S. aureus* isolates were compared and it was shown that the more contemporary healthcare associated strains contained a SNP that inserts a premature

stop codon in the alpha-haemolysin gene (*hla*), unlike community acquired strains and more historic strains (DeLeo et al., 2011). When this mutation was recreated in a historic strain, virulence was significantly attenuated in a mouse bacteraemia model highlighting how related strains can subtly differ yet lead to a substantially altered phenotype.

Genome-wide association studies (GWAS) are now emerging as an application of WGS data to reveal virulence determinants. Combining GWAS and a machine learning approach, virulence was predicted from genome sequences of *S. aureus* clinical isolates. Genetic fingerprints associated with phenotypes of interest such as toxin production and adhesiveness were assigned yet the clinical implications of these remain to be explored (Laabei et al., 2014). Most recently, convergent adaptation of a distinct MRSA clade introduced to Australia from Asia with mutations in key regulatory systems was reported to be responsible for persistence of this particular strain in the nosocomial environment (Baines et al., 2015).

Clonal evolution of strains provides insight into key virulence determinants and allows interrogation of virulence traits enabling invasive disease. Prospectively collecting large numbers of clinical *S. aureus* strains, coupled with high-throughput DNA sequencing, allows genome wide comparisons to be made and the relationship with cellular physiology and pathogenesis to be established (Harris et al., 2010). The vertebrate zebrafish embryo model of *S. aureus* infection is a crucial adjunct to mammalian studies, which facilitates screening of large numbers of strains in a fashion not possible with murine models. Using our high-throughput model of systemic *S. aureus* infection in zebrafish embryos (Prajsnar et al., 2008), closely related *S. aureus* strains can be screened for differences in pathogenesis. Identified potential virulence determinants can then be functionally analysed.

3.2 Aims of this chapter

i. To screen a clinically characterised and genome sequenced collection of hospital acquired MRSA strains using a high-throughput zebrafish model to determine relative pathogenicity
ii. To use bioinformatic comparisons on whole genome sequences of clinical strains to identify potential genetic determinants that correlate with disease

iii. To test the role of novel genetic determinants of disease *in vitro* and *in vivo*.

3.3 Results

3.3.1 Selection of whole genome sequenced clinical strain collections

S. aureus is a major contributor to hospital-acquired infection and a high prevalence of hospital-acquired MRSA (HA-MRSA) infection has numerous adverse effects (Boucher et al., 2010). Focusing on HA-MRSA, two clinical strain collections were initially selected. Firstly, WGS data was available for a collection of 63 related ST239 MRSA strains, which included both a global collection spanning 20 years and samples from a single northeastern Thailand hospital attained over 7 months, all associated with hospital-acquired infection (Harris et al., 2010). At the time of the Harris study, the majority of HA-MRSA isolates from this region, came from a limited pool of widely disseminated clones including MRSA ST239. This internationally significant clone is multiply antibiotic resistant and accounts for a large proportion of HA-MRSA in parts of Asia but has also been detected in South America and Eastern Europe (Feil et al., 2008). Therefore, this collection was designated 'global ST239 strains' in the present study.

Secondly, a separate but related collection containing variants of MRSA ST239 causing an outbreak in the intensive care unit (ICU) of a London hospital, was also selected. This collection was designated 'local ST239 strains' in the present study. Both invasive and non-invasive *S. aureus* isolates were collected from patients and subject to further analysis, including WGS (Edgeworth et al., 2007). In comparison to the first collection, these outbreak strains were genetically very similar, being differentiated by low numbers of single nucleotide polymorphisms (SNPs). Important to this combined genomic and *in vivo* modeling approach is the selection of clinical strains sets that are genetically closely related. This will allow a tangible number of genetic targets for functional analysis, after phenotypic differences are ascribed. Should the strains be too genetically distinct, it may prove too difficult to hone in on candidate genes.

3.3.2 Annotation of the whole genome sequence data

Whole-genome sequencing was carried out using an Illumina MiSeq (Illumina, USA), which generated short sequence reads (150 bp) for analysis. Next generation sequencing technology (see Section 1.11.7) allows genome-wide SNPs to be mapped to a reference strain. As one of the earliest isolates to be collected (October 2003), ST239 strain TW20, was chosen as the reference isolate for both strain collections and it has been fully sequenced, assembled and annotated (Holden et al., 2009). After template preparation, reads are accumulated and compared to the same segment in TW20, in order to identify SNPs. As phylogenetic interpretation can be confounded by mobile genetic elements (MGE) capable of horizontal transfer, 'core' SNPs are distinguished from 'accessory' SNPs. Variable sites in the core genome were used to produce phylogenetic trees (Figure 3.1 and Figure 3.2).

The horizontal dimension of the tree displays the amount of genetic change, with the horizontal lines being termed 'branches'. The longer the branch, the greater the change. The scale bar quantifies this change indicating that there are 0.02 nucleotide substitutions per site (i.e. the number of 'substitutions' per the length of the sequence). As seen in Figure 3.1 (inset), the tree contains orientators i.e. nodes which represent the likely ancestors (blue circle) and tips which are names of the isolates (often assigned at sample collection or the sequencing facility). A short black line on the left hand side of the tree indicates the root, the likely last common ancestor.

As strains were sequenced off-site, as part of a larger sequencing project, some strains were not relevant to this project so those sections are 'collapsed' down for ease of viewing. The reference isolate, TW20, was an isolate of particular interest to other groups and up to 100 other closely related strains were sequenced (some of which are displayed in the 'local ST239 strains' phylogenetic tree, Figure 3.2). Therefore, to allow viewing of the investigated isolates, the region containing TW20 is marked but collapsed down on Figure 3.1.

From these collections, strain relatedness was used to select a preliminary set of strains to test for relative pathogenesis in the zebrafish embryo model of infection for 'global ST239 strains' (Figure 3.1) and 'local ST239 strains' (Figure 3.2).

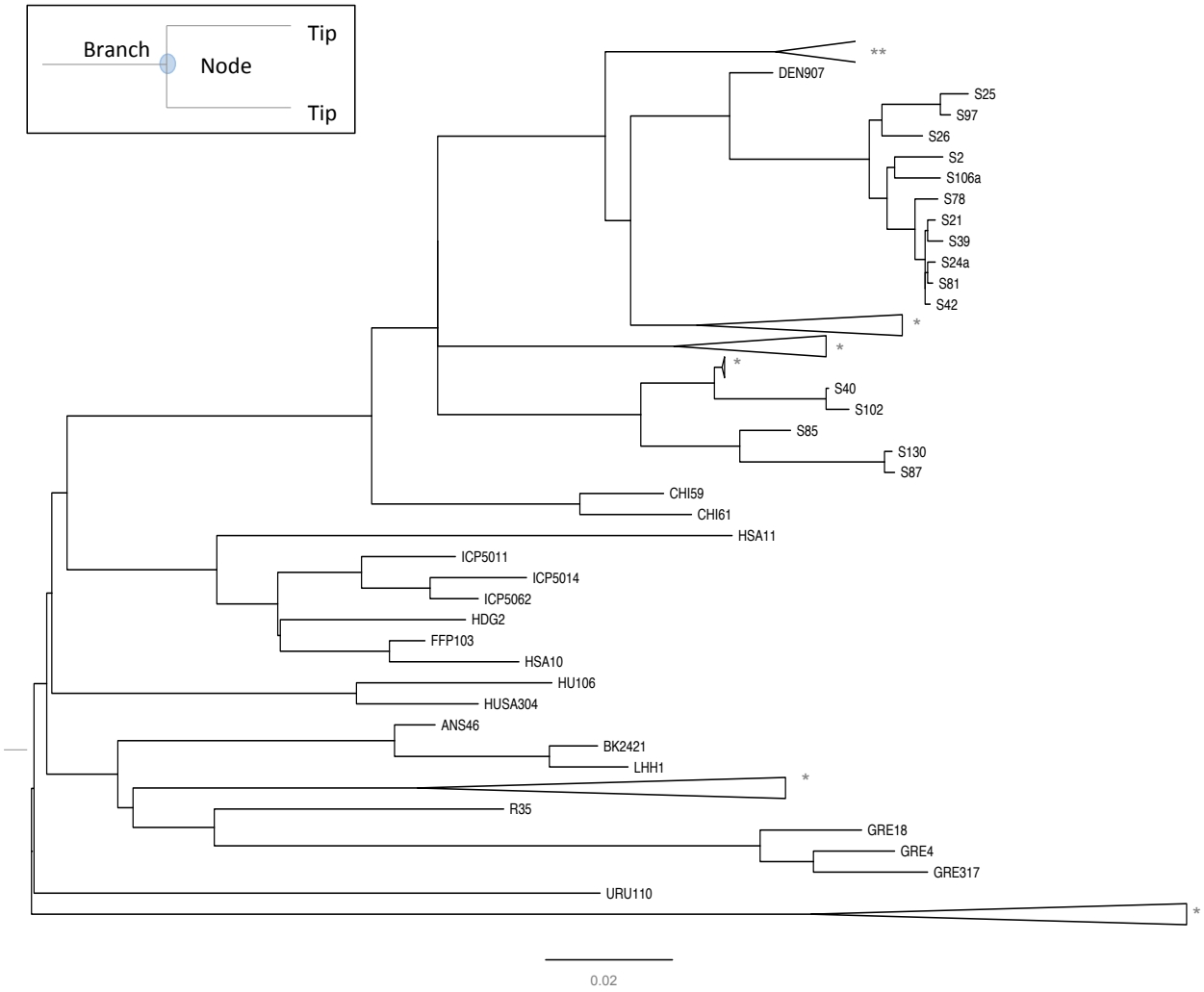


Figure 3.1 Maximum likelihood phylogenetic tree of MRSA 'global ST239 strains' based on core genome SNPs

Genome sequence data for each isolate were mapped against the reference isolate TW20 and variable sites in the core genome were assigned as described in Harris *et al* (2010). Inset displays the terminology for tree orientation.

The scale bar represents substitutions per SNP site.

* isolates not investigated in this collection are displayed as collapsed sections

** collapsed section containing reference isolate, TW20

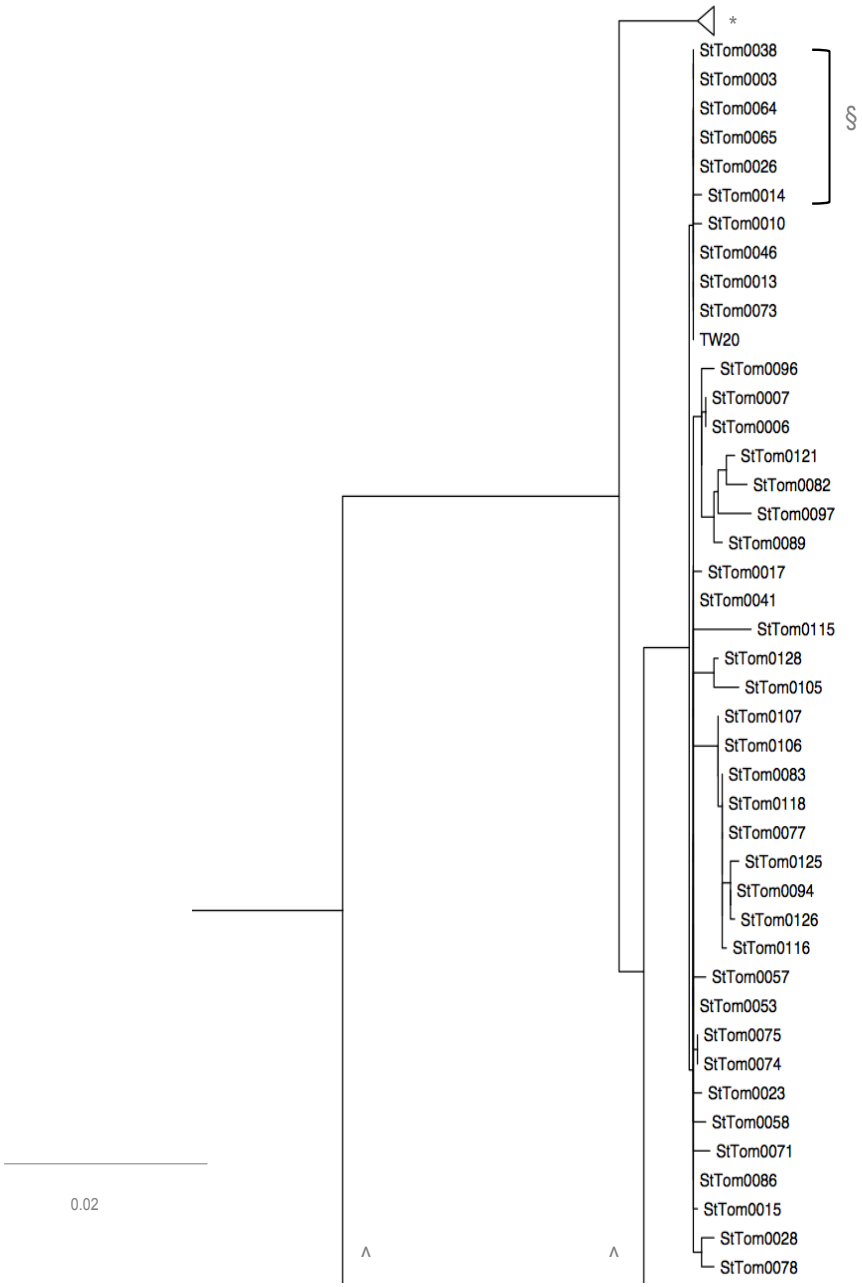


Figure 3.2 Maximum likelihood phylogenetic tree of MRSA 'local ST239 strains', based on core genome SNPs

Genome sequence data for each isolate were mapped against the reference isolate TW20 and variable sites in the core genome were assigned as described in Harris *et al* (2010). The scale bar represents substitutions per SNP site.

* isolates not investigated in this collection are displayed as collapsed sections

§ where branches are not seen between isolates, no SNP differences exist

^ remaining parts of the phylogenetic tree not relevant in this study

3.3.3 Determining relative pathogenicity of clinical strains

Previous work done by Dr Tomasz Prajsnar (University of Sheffield) demonstrated a dose-dependent relationship between *S. aureus* CFU injected per zebrafish embryo and mortality. For doses in excess of 5000 CFU, the zebrafish innate immune system is overwhelmed and approximately 50% of zebrafish are dead within 48 hours (Prajsnar et al., 2008).

Different strains of *S. aureus* are known to have variable virulence in the zebrafish model of infection (Prajsnar et al., 2008). Key laboratory strains SH1000 and Newman have been tested as well as the MRSA isolate COL. To achieve overall 5 day survival rates of 50% in the zebrafish model, a dose of approximately 1500 CFU is commonly used (Prajsnar et al., 2008). Previous work carried out by Mr Alexander Williams (University of Sheffield) investigated the optimal CFU per embryo that would produce 50% survival of embryos at termination of experiment in the ST239 clinical strain collections. 2500 CFU was selected as the optimum dose (data not shown) and survival was monitored for four days post infection.

Embryos were injected at 30 hpf as important cellular components of the innate immune system are present in the blood circulation at this time (Herbomel et al., 1999). Unless otherwise stated, London Wildtype zebrafish (LWT) were used and are designated as 'embryos' throughout the experiments (0-120 hpf). For each experiment, strains were injected in groups of 3 or 4 according to genetic relatedness. After micro-injection, embryos were incubated individually at 28°C in 96 well plates until the end of the experiment.

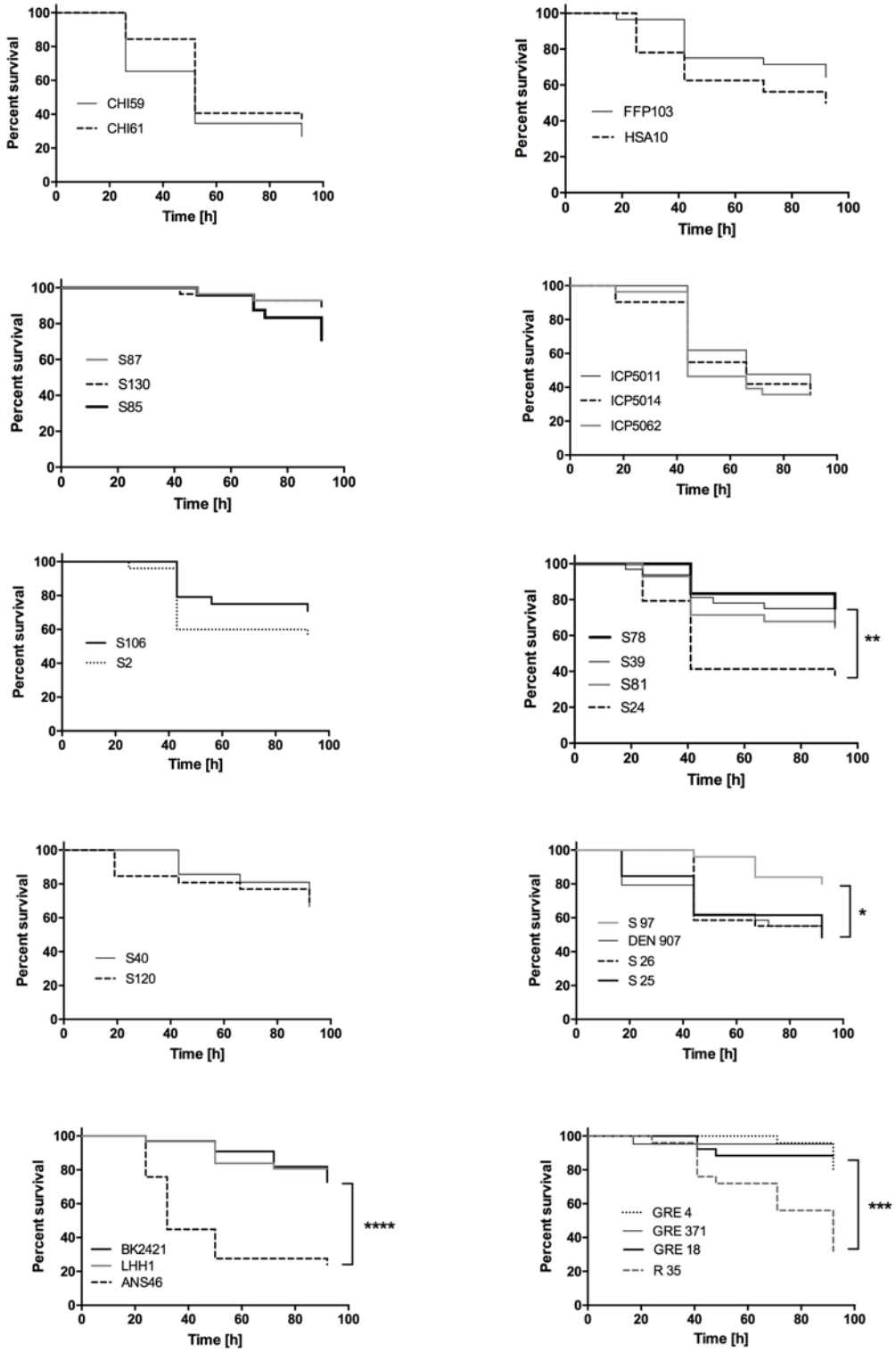


Figure 3.3 MRSA 'global ST239 strains' show variable virulence phenotypes when injected into the zebrafish circulation valley

Groups of up to 4 isolates of 'global ST239 strains' were injected into LWT zebrafish embryos at a dose of 2500 CFU (n= 20-30 per strain). Each strain was assessed in duplicate experiments and the survival curves shown above are representative of the two experiments. Pairwise comparisons of neighbouring strain virulence differences for each experiment are shown in Table 3.1.

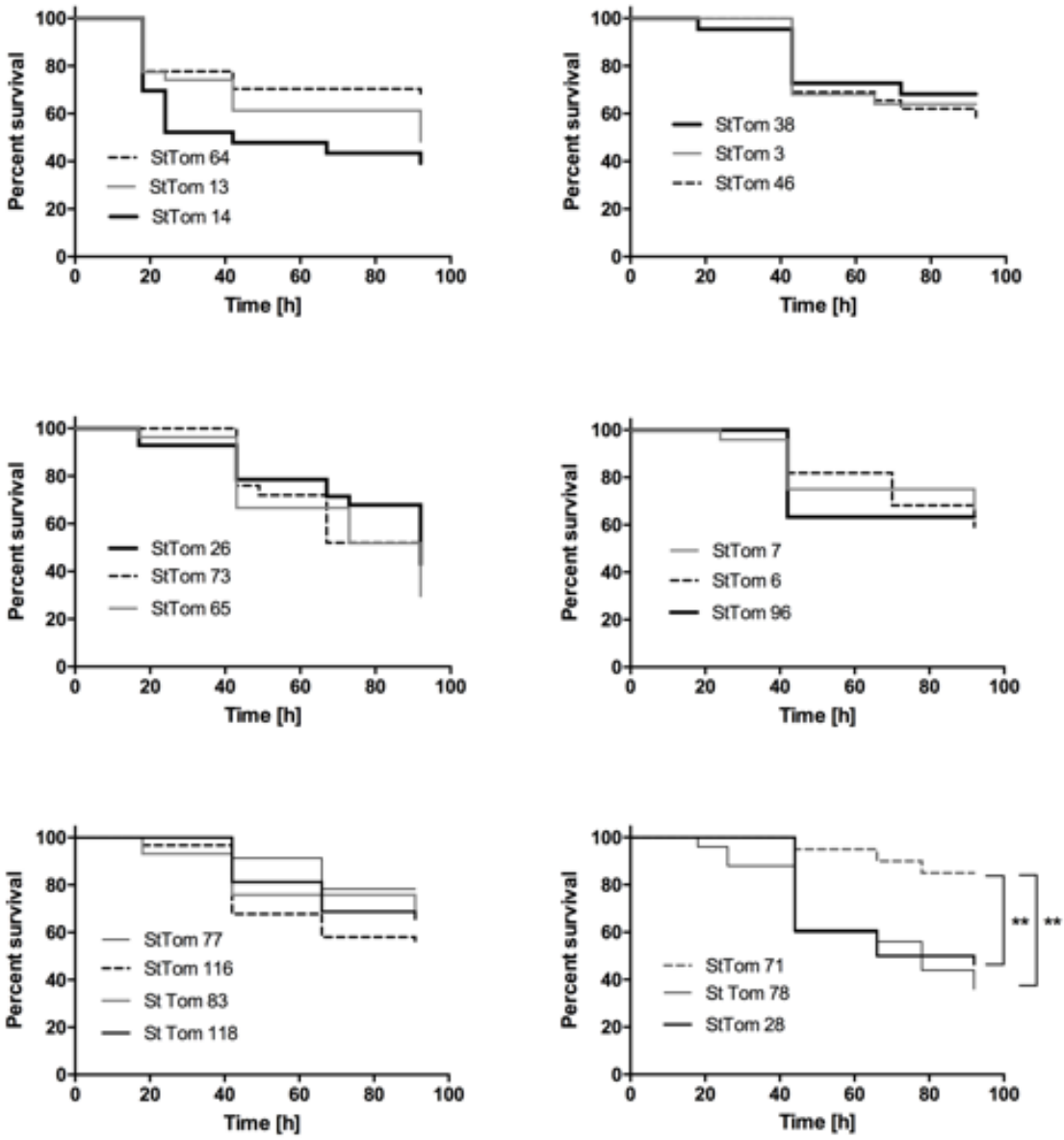


Figure 3.4 MRSA 'local ST239 strains' show variable virulence phenotypes when injected into the zebrafish circulation valley

Groups of up to 4 isolates of 'local ST239 strains' were injected into LWT zebrafish embryos at a dose of 2500 CFU (n= 20-30 per strain). Each of the strains above was assessed in duplicate experiments and the survival curves shown above are representative of the two experiments. Pairwise comparisons of neighbouring strain virulence differences for each experiment are shown in Table 3.2.

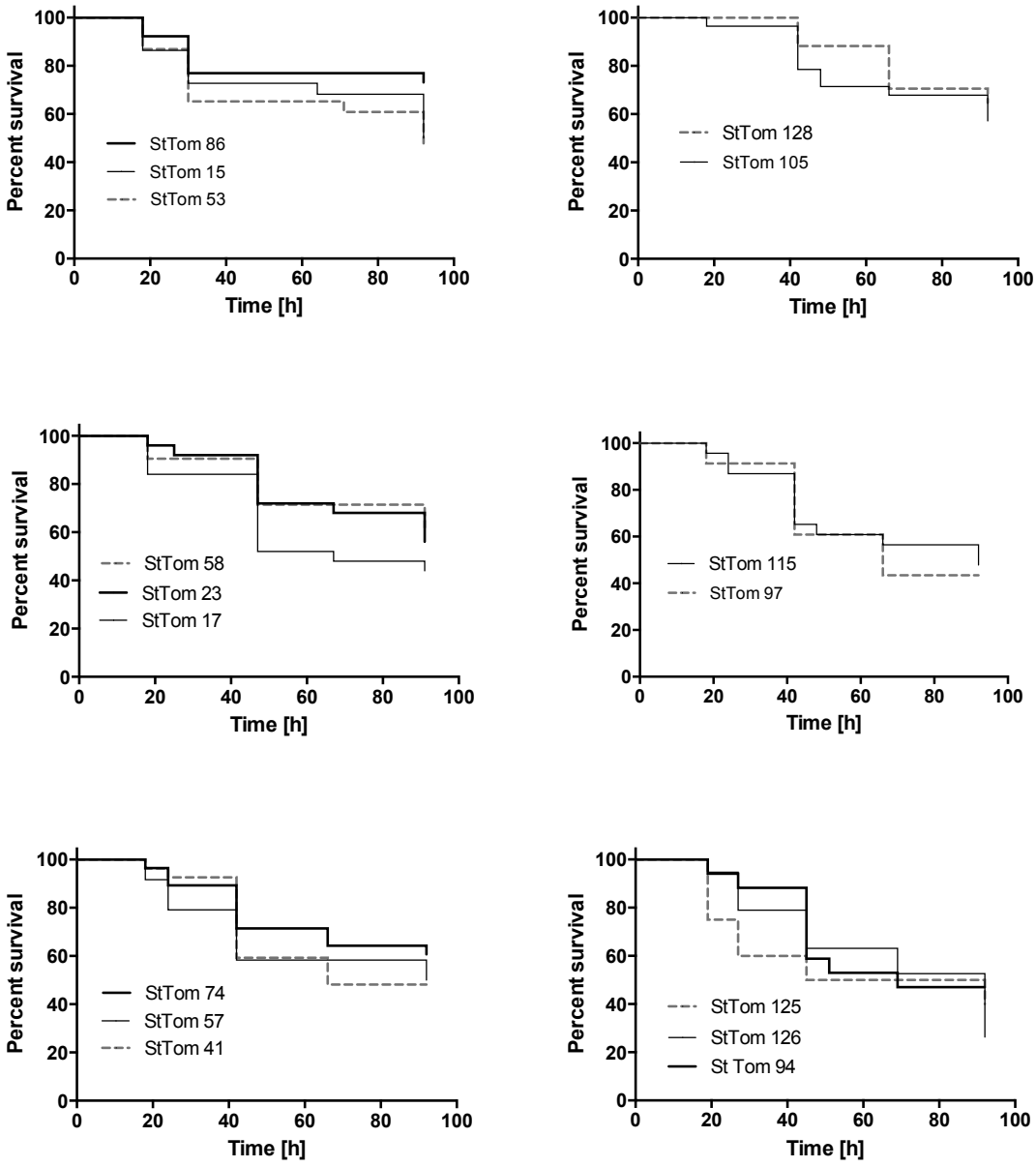


Figure 3.5 MRSA 'local ST239 strains' show similar virulence phenotypes when injected into the zebrafish circulation valley

Groups of up to 3 isolates of 'local ST239 strains' were injected into LWT zebrafish embryos at a dose of 2500 CFU (n= 20-30 per strain). Each of the strains above was assessed in a single experiment as minimal phenotypic differences were noted. Survival curves are shown above and pairwise comparisons of neighbouring strain virulence differences for each experiment are shown in Table 3.3.

Strain comparisons	1st experiment	2nd experiment
CHI59 vs CHI61	0.22	0.17
FFP103 vs HSA10	0.2	0.53
S87 vs S130	0.64	0.20
S87 vs S85	0.04	0.56
S130 vs S85	0.10	0.48
ICP5011 vs ICP5014	0.48	0.74
ICP5011 vs ICP5062	0.48	0.16
ICP5014 vs ICP5062	0.97	0.31
S106 vs S2	0.47	0.54
S40 vs S120	0.98	0.15
S78 vs S39	0.42	-
S78 vs S81	0.35	0.14
S78 vs S24	0.004	0.88
S81 vs S39	0.86	0.77
S39 vs S24	0.02	-
S81 vs S24	0.04	0.69
S97 vs DEN907	**0.01**	**0.05**
S97 vs S26	**0.01**	**0.02**
S97 vs S25	**0.02**	**0.01**
DEN907 vs S26	0.70	0.73
DEN907 vs S25	0.82	0.1
S25 vs S26	0.87	0.89
BK2421 vs LHH1	0.53	0.04
BK2421 vs ANS46	**<0.0001**	**0.01**

LHH1 vs ANS46	**<0.0001**	**0.0005**
GRE4 vs GRE 317	0.14	0.64
GRE4 vs G18	0.46	0.54
GRE 4 vs R35	**0.0003**	**0.01**
GRE 317 vs GRE18	0.44	0.31
GRE317 vs R35	**0.0003**	**0.02**
R35 vs GRE18	**<0.0001**	**0.004**

Table 3.1 Pairwise comparisons across the MRSA 'global ST239 strain' collection

p values are shown for the log rank test pair-wise comparisons between neighbouring 'global ST239 strains'. Isolates taken forward for genomic analysis are highlighted in **bold**.

Strain comparisons	1st experiment	2nd experiment
StTom 64 vs StTom 13	0.21	0.91
StTom 64 vs StTom 14	0.05	0.20
StTom 13 vs StTom 14	0.31	0.12
StTom 38 vs StTom 3	0.82	0.76
StTom 38 vs StTom 46	0.56	0.21
StTom 3 vs StTom 46	0.71	0.24
StTom26 vs StTom 73	0.84	-
StTom 26 vs StTom 65	0.29	-
StTom 73 vs StTom 65	0.46	0.68
StTom 6 vs StTom 7	0.68	0.05
StTom 6 vs StTom 96	0.87	0.63
StTom 7 vs StTom 96	0.85	0.17
StTom 77 vs StTom 116	0.06	0.07
StTom 77 vs StTom 83	0.41	0.02
StTom 77 vs StTom 118	0.30	0.44
StTom 116 vs StTom 83	0.30	0.72
StTom 116 vs StTom 118	0.33	0.28
StTom 118 vs StTom 83	0.88	0.14
StTom 71 vs StTom 78	**0.001**	**0.05**
StTom 71 vs StTom 28	**0.006**	**0.07**
StTom 78 vs StTom 28	0.41	0.77

Table 3.2 Pairwise comparisons of the MRSA 'local ST239 strain' collection

p values are shown for the log rank test pair-wise comparisons between neighbouring 'local ST239 strains'. Isolates taken forward for genomic analysis are highlighted in **bold**.

Strain comparisons	1st experiment
StTom 74 vs StTom 57	0.39
StTom 74 vs StTom 41	0.40
StTom 57 vs StTom 41	0.91
StTom 53 vs StTom 15	0.83
StTom 53 vs StTom 86	0.08
StTom 15 vs StTom 86	0.13
StTom 128 vs StTom 105	0.56
StTom 58 vs StTom 23	0.74
StTom 58 vs StTom 17	0.21
StTom 23 vs StTom 17	0.30
StTom 115 vs StTom 97	0.82
StTom 74 vs StTom 57	0.39
StTom 74 vs StTom 41	0.40
StTom 57 vs StTom 41	0.91
StTom 125 vs StTom 94	0.41
StTom 125 vs StTom 126	0.85
StTom 94 vs StTom 126	0.46

Table 3.3 Pairwise comparisons of the strains from the MRSA 'local ST239 strain' collection which showed minimal virulence differences

p values are shown for the log rank test pair-wise comparisons of neighbouring 'local ST239 strains'.

In total, 64 MRSA strains were screened for virulence differences in the zebrafish model comprising 29 from the 'global ST239 strain' collection and 35 from the 'local ST239 strain' collection. Whilst the number of surviving fish varied more between strain comparisons within the 'global ST239 strain' collection when compared to the 'local ST239 strain' collection, many comparisons, across both collections, yielded no significant reproducible differences.

However, four groups of isolates were found to reproducibly contain attenuated isolates compared to the neighbouring strain/s. Attenuated isolate/s are listed first in bold:

Global ST239 strains:

- **S97** vs DEN 907, S26, S25 (designated Group 1)
- **LHH1** and **BK2421** vs ANS46 (designated Group 2)
- **GRE 4, GRE 18, GRE 317** vs R35 (designated Group 3)

Local ST239 strains:

- **StTom 71** vs StTom 78 and StTom 28 (designated Group 4)

Bioinformatic analysis of genomic differences between strains within each Group was undertaken.

3.3.4 Bioinformatic analysis of whole genome sequence data

Every base in the sequence reads from the isolate being tested, which differs from the reference genome, is designated as a SNP. Reads are only mapped if they match the reference strain with >90% identity. Using the variable sites in the core genome, phylogenetic reconstruction of the strain collections was carried out (by Dr Matthew Holden, University of St Andrews). Software was then employed to view these phylogenies (http://tree.bio.ed.ac.uk/software/figtree) and annotate genetic relatedness with the number of unique SNPs compared to neighbouring strains, as shown in Figure 3.6.

Using Artemis bioinformatics software, comprehensive information pertaining to each SNP can be obtained by searching between either the relevant nodes or between nodes and tips (isolates) (Rutherford et al., 2000; Carver et al., 2012). Insertions or deletions (indels) were then identified using methods as per Croucher et al. (2011).

In the 'local ST239 strain' collection, small numbers of SNPs were identified relative to the reference genome so in Group 4 only 4 SNPs were relevant to investigate. However, in the 'global ST239 strains', in some cases, there was large differences in SNPs, which would be impossible to fully pursue. Therefore, it was decided that in Group 1, whilst there is a total of 131 SNPs that differ between DEN 907, S25, S26 and S97 (calculated by adding together the number of distinguishing SNPs above each branch on Figure 3.7), only those between node 120 and strain S97 were pursued as those 4 SNPs are most likely to lead to a loss of function mutation causing attenuated virulence.

In Group 2, as both BK2421 and LHH1 were attenuated, SNPs that differed between those two strains (19 + 31 = 50 SNPs in total) were not pursued. From node 93 to 95, 61 SNPs in the branch leading to these isolates were reviewed as a loss of function mutation here may explain the attenuated virulence (compared to ANS46) (Figure 3.7).

In Group 3, all three GRE strains were attenuated so SNP differences between these individual strains were not pursued but the 215 SNPs in branches leading to these isolates were investigated (Figure 3.7). In both groups 2 & 3, it could be argued that a gain of function mutation may lead to the ability of either ANS46 or R35 to cause zebrafish mortality but this was not further explored.

A summary of the results is shown in Table 3.4. Highlighted in bold are the genetic targets taken forward for further analysis including mutant recreation and complementation.

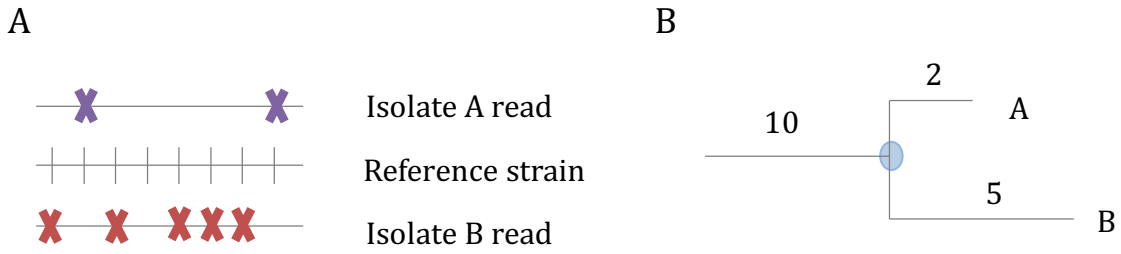
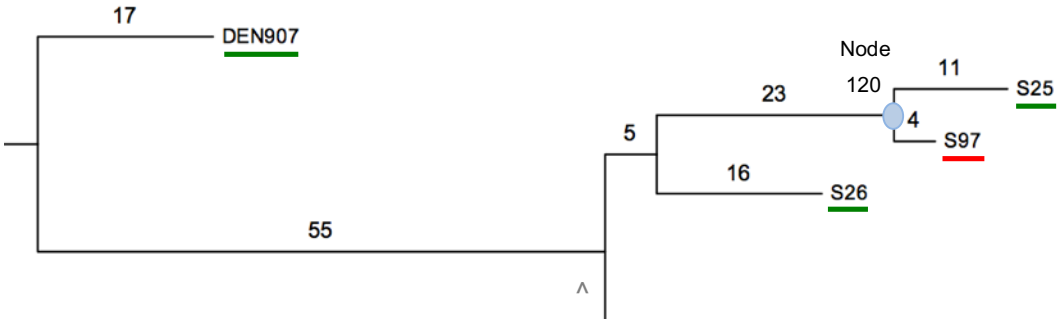


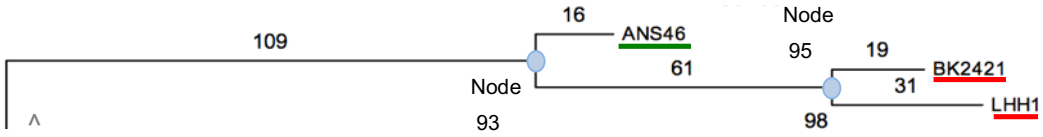
Figure 3.6 Representation of SNP designation compared to the reference strain

A Comparison of isolate sequence to that of the reference strain

B In this example, all the SNPs before final branch point (node shown as blue circle) are common to both isolates whereas isolate A has 2 unique SNPs and isolate B has 5 unique SNPs.



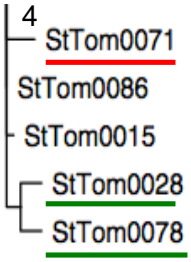
Group 1



Group 2



Group 3



Group 4

Figure 3.7 Distinguishing SNPs between neighbouring strains

Relevant nodes are annotated. The number of distinguishing SNPs is shown above each branch. The attenuated strain/s (compared to neighbouring strains underlined in green) are underlined in red.

^ remaining parts of the phylogenetic tree not relevant in this study

Group 1	**Node 120 → strain S97**		**Global ST239 strains**
	Type of SNP	Gene name	Function
	Indel	***isaB***	**immunodominant antigen B**
	NS		hypothetical protein SATW20_01120
	NS and indel		**hypothetical protein SATW20_13140**
	S		DNA polymerase III (beta chain)
	I		downstream of SATW20_11510
Group 2	**Node 93 → node 95**		**Global ST239 strains**
	Type of SNP	Gene name	Function
	SNOP	*esaA*	unknown function
	SNOP	*epiD*	lantibiotic decarboxylase
	SNOP		nitroreductase family protein
	NS		conserved hypothetical protein
	NS		putative membrane protein
	NS		putative N-acetylmannosamine phosphate
	NS	*rpsR*	30S ribosomal protein S18
	NS		tetrapyrrole (corrin/porphyrin) methylase
	NS	*rplA*	50S ribosomal protein L1
	NS		conserved hypothetical protein
	NS	*dltD*	putative LTA biosynthesis protein
	NS		conserved hypothetical protein
	NS		putative succinyl-CoA ligase
	NS		radical SAM superfamily protein
	NS	*odhB/citM*	dihydrolioamide succinyltransferase
	NS	*ebh*	very large surface anchored protein
	NS		putative membrane protein
	NS		putative peptidase
	NS	*dnaK*	chaperone protein
	NS	*rplU*	50S ribosomal protein L21
	NS	*folC*	putative folylpolyglutamate synthetase
	NS	*sasC*	LPXTG surface protein
	NS		putative surface protein
	NS		putative aminopeptidase

	NS	*agrC*	
	NS		hypothetical protein
	NS	*fmtB/mrp*	LPXTG surface-anchored protein
	NS		putative exported protein
	NS	*mqo1*	putative malate:quinone oxidoreductase 1
	NS		putative cobalt transport protein
	NS	*sirB*	putative siderophore permease
	NS	*capP*	capsular polysaccharide synthesis enzyme
	NS		ABC transporter ATP binding protein
Group 3	**Node 108 → node 110**		**Global ST239 strains**
	Type of SNP	Gene name	Function
	STIP	***saeS***	**histidine kinase protein SaeS**
	SNOP		putative membrane protein
	SNOP		hypothetical protein
	SNOP	*gltB*	glutamate synthase small subunit
Group 4	**Strain TW20 → strain StTom0071**		**Local ST239 strains**
	Type of SNP	Gene name	Function
	NS	***htrA2***	**putative serine protease**
	S		hypothetical protein SATW20_10750
	I		putative membrane protein SATW20_10750
	I		hypothetical protein SATW20_18920

Table 3.4 Bioinformatic analysis of core genome SNP differences and indels between nodes and/or isolates in the 'global ST239 strain' and 'local ST239 strain' collection compared to the reference genome, TW20

Abbreviations: Indel – insertion/deletion; NS – non-synonymous amino acid substitution; S – synonymous amino acid substitution; I – intergenic region; SNOP – non-stop codon changed to stop codon; STIP – stop codon changed to non-stop codon.

Accessory genome analysis was performed by comparing the *de novo* assemblies of the genome of interest with the reference genome (TW20) facilitated by Artemis Comparison Tool (ACT) (Carver et al., 2005). No accessory genome differences were found between the isolates in Groups 1 and 4. Some potential differences in the accessory genome were noted between isolates in Group 2 and 3 but it was not possible to pursue these further due to lack of effective software at that time.

For each of the groups 1-4, genetic targets within the core genome, for molecular biological manipulation, were chosen as shown in bold in Table 3.4. Intergenic and synonymous SNPs were not explored further as priority was given to SNPs that would cause a change in amino acid insertion during translation. When such non-synonymous SNPs would lead to insertion of a premature stop codon (SNOP) or removal of a stop codon at the end of the gene (STIP), these were preferentially chosen due to the predicted impact on protein translation and therefore function. The potential functional impact of identified mutations on candidate genes is shown in Table 3.5.

In group 1, a total of 4 unique SNPs and 2 deletions (indels) were identified between node 120 and the attenuated isolate S97. Of these, hypothetical protein, SATW20_01120, contained a non-synonymous mutation. Using the NCBI protein database, the translated protein was predicted to contain a region with homology to superfamily I DNA and RNA helicases and helicase subunits. Studies suggest that such helicase domains may have a role in pathogenesis as such proteins are needed for genome maintenance when DNA damage occurs (Sharma and Rao, 2012).

However, the strain alignment tool within Geneious® software showed the location of this gene within the clinical strain background was not only surrounded by incomplete phage genes, suggesting a phage region of the genome, but when this gene was aligned across multiple different genetic backgrounds, there was huge sequence variation with little conservation (94% identity at the DNA level) between genomes. Therefore, this protein was not pursued further as it may represent a redundant and non-functional part of the genome.

Also within group 1, a second hypothetical protein, SATW20_13140, was found to be in a stable part of the chromosome and highly conserved across genomic backgrounds

(99.7% identity at the DNA level). This gene contained two mutations – an indel, which constituted a deletion of a single base (guanine) at position 1404529 and a non-synonymous mutation at base position 1404535. The indel would cause a frame shift making it unlikely that the non-synonymous mutation would be translated further downstream. The frame shift would truncate the protein from 96 to 44 amino acids. Therefore, recreation of the mutation in gene SATW20_13140 was attempted and designated SATW20_13140$^{\Delta Gdel}$. The second 'indel' found in this group was in immunodominant antigen B (*isaB*). The adenine base at 2953589 bp is deleted causing a frameshift after amino acid position 141, leading to a shortened translated protein of 149 amino acids. This mutation was designated *isaB*$^{\Delta Adel}$.

In group 2, bioinformatic analysis was carried out between the nodes 93 to 95 as both strains branching off node 95 were attenuated compared to strain ANS46 (Figure 3.7). In total, 61 SNPs were identified and all nonsynonymous SNPs were recorded in Table 3.4. Due to the large number of potentially important SNPs, *esaA*, was initially selected for further analysis as there are reports suggesting this gene may have a role in virulence in *S. aureus* and other organisms such as *Mycobacterium tuberculosis* (Volkman et al., 2010; Anderson et al., 2013; Zhang et al., 2015). An ESAT-6 like secretion system, within which *esaA* is one of eight putative genes, has been described in *S. aureus* but its exact function remains unknown (Burts et al., 2005). However, strain alignment showed *esaA* to have multiple SNP differences between genetic backgrounds, which would produce chimeric proteins if the mutant was recreated in the standard laboratory strain *S. aureus* SH1000. Therefore, this gene was not pursued further.

As two additional genes were also identified as having premature stop codons (SNOPs), lantibiotic decarboxylase (*epiD*) and a nitroreductase family protein, existing transposon mutants of these genes were further investigated. Whilst mutants from the recently acquired Nebraska transposon library result in knock-out of such genes rather than SNP variation, the transposon mutants would only serve as an proxy indicator of mutant phenotype in a different genetic background (Fey et al., 2013). However, compared to the genetic background of the transposon library, USA300 JE2, neither lantibiotic decarboxylase (NE 1856) and nitroreductase family protein (NE 414) were attenuated in the zebrafish embryo virulence assay so no further work was carried out on these genes (data not shown).

In group 3, bioinformatic analysis between nodes 108 and 110 showed 215 SNPs that may account for attenuation of the three isolates (GRE 4, GRE 317 and GRE 18) branching from node 110 (Table 3.4 lists only the STIP and SNOP mutations). Given the large number of differences, *saeS*, was selected for further work as it is a known virulence determinant regulator and confirmation of the role of this gene in the attenuated strains would help prove the principle of this novel approach. The particular SNP identified was located at the 3' end of the *saeS* gene, preventing ribosomal insertion of a stop codon (STIP) in the standard position. This was predicted to extend the mRNA transcript and increase the length of the protein product by an additional 7 amino acids. This mutation was designated $saeS^{\Delta A \rightarrow T}$.

Finally, in group 4, four SNPs were identified but only one described a non-synonymous mutation. The identified gene, *htrA2*, is a putative serine protease of 774 amino acids. This SNP would change the arginine at amino acid position 103 to a lysine. This mutation was designated $htrA2^{\Delta G \rightarrow A}$.

Group	Gene name and position	Wildtype amino acid (aa) length	Amino acid change	Likely impact
1	SATW20_13140	96	Base deletion and frameshift	Truncated to 44 aa
1	*isaB* SATW20_27760	175	Base deletion and frameshift	Truncated to 149 aa
3	*saeS* SATW20_07800	351	Loss of stop codon	Elongated by 7 aa
4	*htrA2* SATW20_10190	774	Arginine changed to lysine at aa position 103	Unknown

Table 3.5 Potential functional impact of identified mutations on candidate genes

(aa – amino acid)

3.3.5 Candidate genes

3.3.5.1 SATW20_13140

Using the curated database for protein families (pfam) this 96 amino acid product was found to have a conserved domain from amino acid 1-93 of a putative toxin 64, a predicted RNase toxin (Zhang et al., 2012). No further literature is available on this hypothetical protein although it is highly conserved across genomic backgrounds of *S. aureus*. Given the small number of SNPs identified as different between S97 vs DEN 907, S26, S25 in Group 1, this represented a potentially novel virulence determinant to be further explored.

3.3.5.2 *isaB*

The *S. aureus* immunodominant antigen B protein, IsaB, has no known homologs in other bacteria but was shown to elicit an immune response during MRSA bacteraemia, as part of a study to identify new vaccine targets (Lorenz et al., 2000). Being both secreted and cell surface associated, the protein has been shown to bind nucleic acid and is expressed only during infection and not colonization (Mackey-Lawrence et al., 2009). Whilst its role in virulence remains unclear, *isaB* gene expression appears responsive to external stimuli e.g. neutrophil exposure and the regulatory protein, staphylococcal accessory regulator A (*sarA)* is able to act as a repressor (Mackey-Lawrence and Jefferson, 2013).

3.3.5.3 *saeS*

The gene, *saeS,* is a well-known to be involved in virulence, as part of a two-component histidine kinase system, *saeRS* (Schafer et al., 2009; Sun et al., 2010). Such systems allow expression of genes to be regulated by diverse environmental stimuli. For example, when the *saeRS* system is activated, expression of α-haemolysin, β-haemolysin and coagulase are upregulated mediating *S. aureus* tissue invasion (Giraudo et al., 1999). Inactivation of *saeS* has been shown *in vitro* to decrease bacterium-associated host cell apoptosis (Liang et al., 2006) and *in vivo*, multiple studies demonstrate attenuated virulent phenotypes across a range of model systems (Benton et al., 2004; Prajsnar et al., 2008).

3.3.5.4 *htrA2*

The surface serine protease, *htrA* (high temperature requirement), was first described in *E. coli* and is highly conserved amongst kingdoms. It has been shown to be a virulence factor in several pathogens and has a role in degrading damaged proteins and resisting stress (Skorko-Glonek et al., 2008). There are two *htrA* genes in *S. aureus*, *htrA1* and *htrA2* and using a rat model of endocarditis, it has been shown that a single mutation resulting in loss of *htrA* alone did not affect bacterial density in infected tissues but a double knockout strain was significantly attenuated. However, this was only seen in the RN3690 genetic background and not COL highlighting the lack of understanding of these genes in pathogenesis (Rigoulay et al., 2005).

3.3.6 Antibiotic susceptibility of ST239 clinical strains

S. aureus are naturally poorly transformable with only a few strains, such as laboratory strains SH1000 and Newman, being commonly used for genetic manipulation (Baba et al., 2008; O'Neill, 2010). Clinical *S. aureus* strains have variable antibiotic resistance patterns, which limits the choice of suitable cloning vectors. Of the available plasmid vectors used for unmarked allelic exchange via homologous recombination, temperature sensitive vectors such as pMAD (Arnaud et al., 2004) and pIMAY (Monk et al., 2012) are increasingly used. Employing a two-step recombination method, involving single cross-over integration of the vector into the *S. aureus* chromosome, followed by a second cross-over event which excises the plasmid DNA from the host strain chromosome, these vectors have improved the efficiency of targeted allelic exchange of homologous genes. The newly developed pIMAY and pIMAY-lacZ vectors, further described in Section 2.16, use chloramphenicol as the antibiotic selection marker whereas pMAD incorporates erythromycin resistance. To allow recreation of target mutations in the clinical strain background, the antibiotic resistance profiles were therefore tested.

Antibiotic susceptibility was tested by both disc diffusion (Figure 3.8) and incorporation of antibiotic into BHI agar plates (Table 3.6). As shown, the resistance profile of the ST239 strains was extensive and variable, with chloramphenicol being the only antibiotic to which the majority of strains were susceptible. Unfortunately, isolate

GRE18 (which also represented GRE 4 and GRE 317) was resistant to chloramphenicol, which prevented a single antibiotic resistance cassette being possible for further genetic analysis. Of note, GRE18 tested sensitive to erythromycin on solid agar when a disc containing 15 μg ml^{-1} of antibiotic but was resistant when a lower concentration of 5 μg ml^{-1} was employed. The latter would be the antibiotic concentration employed during plasmid usage, rendering the use of pMAD not possible. Cadmium chloride susceptibility was also tested as vectors carrying cadium resistance genes are available (Kornblum et al., 1986). However all strains tested were resistant to cadmium (Table 3.6).

These phenotypic data were confirmed by resistome analysis which compares genes with known resistance mechanisms to sequenced genomes (analysis performed by Dr Matthew Holden, Unviersity of St. Andrews). Previous studies have used similar techniques and shown complete concordance between genotypic predictions of antibiotic resistance and phenotypic data (Köser et al., 2012).

Given the antibiotic resistance profile of these clinical ST239 strains, the vector pIMAY was chosen to allow recreation of the mutant in the neighbouring strain background.

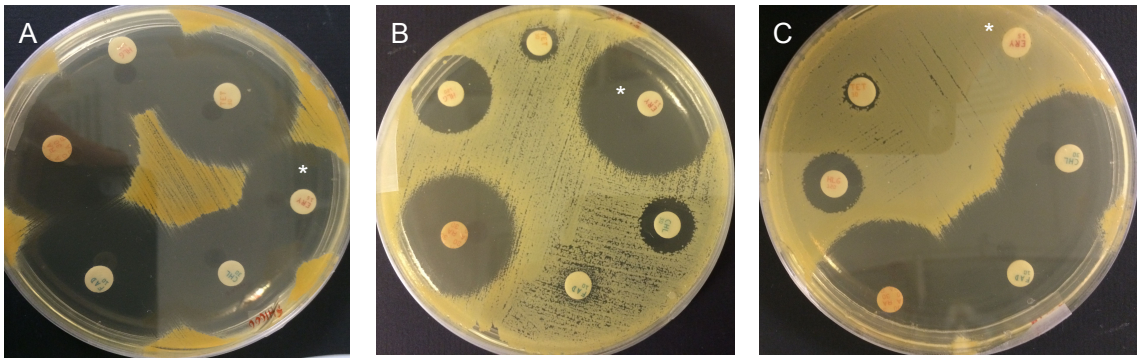


Figure 3.8 Antibiotic susceptibility of (A) SH1000, (B) GRE18 and (C) R35 as tested by disc diffusion on BHI media

Antibiotic discs (μg ml^{-1}) clockwise from white asterix are: erythromycin 15, chloramphenicol 30, fusidic acid 10, rifampicin 30, gentamicin 120 and tetracycline 10.

Strain	Ery/Lin (5/25 μg ml^{-1})	Tet (5 μg ml^{-1})	Kan (50 μg ml^{-1})	$CdCl_2$ (250 μg ml^{-1})	Cm (10 μg ml^{-1})
SH1000	S	S	S	-	S
TW20	R	R	R	-	S
R35	R	R	R	R	S
GRE18	R	R	R	R	R
S97	R	R	-	R	S
S25	R	R	-	R	S
StTom71	R	R	-	R	S

Table 3.6 Table of antibiotic and heavy metal susceptibility of *S. aureus* strains

Strains requiring genetic manipulation were tested by antibiotic incorporation into BHI agar plates at the concentrations stated in each column.

Ery/Lin – erythromycin/lincomycin; Tet – tetracycline; Kan – kanamycin; Cd – cadmium chloride; Cm – chloramphenicol.

(- represents conditions that were not tested)

3.3.7 Phenotypic analysis of *S. aureus* strains

Of the four genetic targets – SATW20_13140, *isaB*, *saeS* and *htrA2*, further phenotypic analysis was sought to examine the impact of the identified SNPs on gene function. Due to the paucity of data on the function of SATW20_13140, *htrA2* and *isaB* in the literature, no robust phenotypic analysis was available for these genes.

The gene, *saeS*, however, is a global regulator of virulence, required for the expression of a myriad of virulence factors, including haemolysins. Alpha-haemolysin production is positively regulated by *saeS*, allowing strains possessing a functional copy of *saeS* to haemolyse red blood cells as seen during growth on blood containing agar plates. GRE18, GRE4 and GRE317 are attenuated strains that possess a SNP in *saeS* that is predicted to elongate the protein. This may lead to a dysfunctional protein and decrease in haemolysis compared to the neighbouring strain, R35, which contains the functional wildtype *saeS* gene. A reduction in red blood cell (RBC) haemolysis in the mutant strain (GRE18) was seen compared to the neighbouring strain (R35) and the positive control (SH1000) on both defibrinated horse and rabbit blood agar plates as demonstrated in Figure 3.9 and 3.10 respectively.

Quantitative haemolysis assays were also performed as per the protocol described in Section 2.3.2. However, levels of haemolysis in the SH1000 and clinical strains were below the level of detection of the spectrophotometer. Previously in our lab, liquid haemolysis assays have been carried out using strains such as *S. aureus* 8325-4. This strain originates from 8325 lineage but has been cured of its three prophages (Novick, 1967) whereas SH1000 is further modified by a repair of the *rsbU* gene, a sigma factor B regulator. The reinstating of a functional *rsbU* gene resulted in decreased exoprotein expression including alpha-haemolysin (Horsburgh et al., 2002). It is possible that the clinical MRSA strains also have relatively low levels of haemolysin which prevent measurement by liquid assay. Indeed it has been shown that significant differences in toxin expression can exist between HA-MRSA and CA-MRSA strains, purportedly due to cell wall differences between the two types of MRSA and *agr* quorum sensing ability (Rudkin et al., 2012).

A

B

C

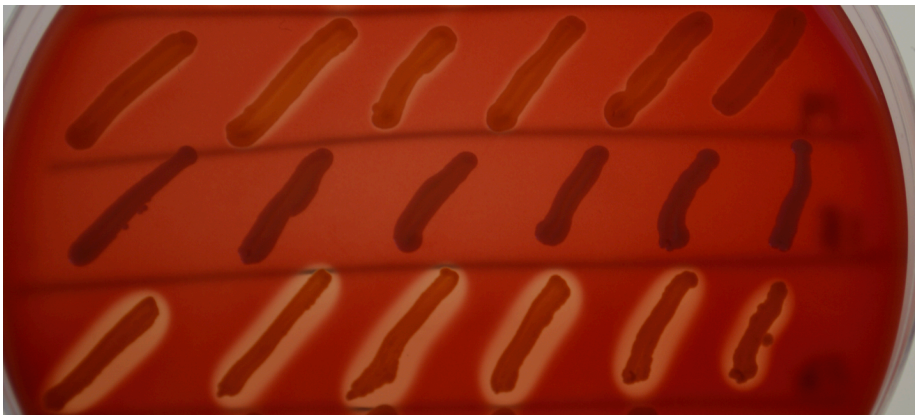


Figure 3.9 Extent of RBC haemolysis between strains on defibrinated horse blood agar

A R35
B GRE18
C SH1000 (positive control)

Six bacterial streaks, each from different colonies, were plated to ensure plate location did not affect results.

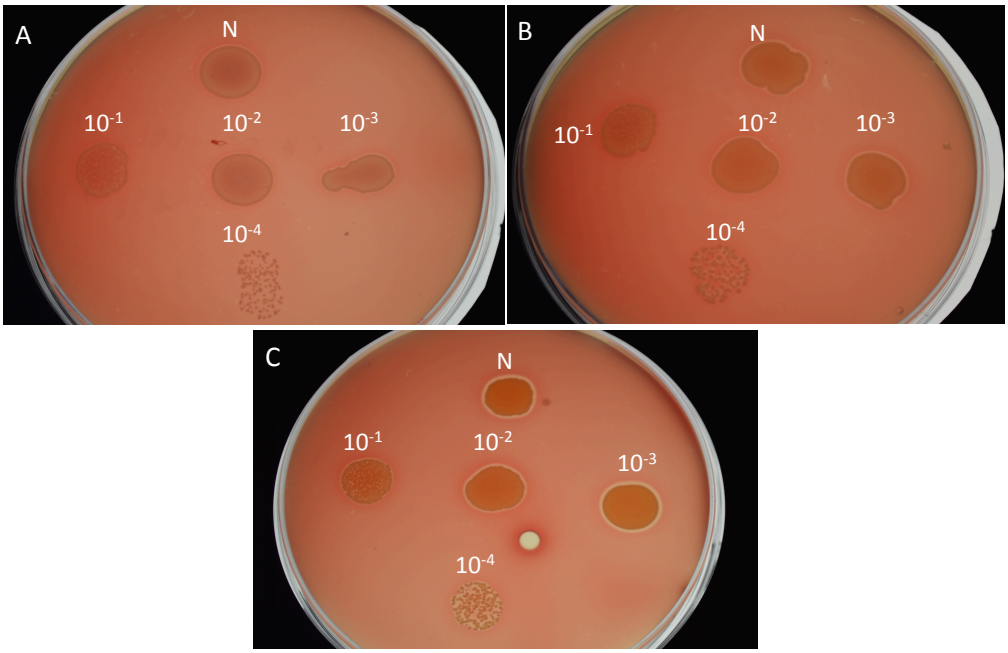


Figure 3.10 Extent of RBC haemolysis between (A) GRE18, (B) R35 and (C) SH1000 (positive control) strains on defibrinated rabbit blood agar

Bacterial cultures were applied to the rabbit blood agar plates either neat (N) or diluted as shown (10^{-1} – 10^{-4}). The presence and extent of the zones of clearing (haemolysis) were qualitatively recorded.

3.3.8 Construction of *S. aureus* mutants

Attempts were made to recreate the 4 identified SNPs as unmarked, in-frame, allelic exchanges of the representative genomic region in the respective neighbouring strains: *saeS* – strain R35; *htrA2* – strain StTom78; *isaB* – strain S25 and SATW20_13140 – strain S25. In this project, *E. coli* DC10B was employed as the intermediate cloning host during mutant recreation in the *S. aureus* clinical strain background.

3.3.8.1 Construction of *S. aureus saeS* mutant

A pair of primers was designed to amplify a region containing the SNP of interest and 1-Kb of DNA either side. The primers were designed to include an overlapping region of 15-20 bp with the linearized vector, to allow construction of the plasmid using Gibson Assembly cloning. Primer pair EJ1/EJ2 (*saeS*) were used and the 2-Kb region was amplified from the GRE18 genomic DNA producing a PCR product of the expected size of 2032 bp (2001 bp insert and 15 bp forward primer vector overlap region and 16 bp reverse primer overlap region) as shown in Figure 3.11A. The vector, pIMAY-Z, was digested with *Not*I-HF and *Kpn*I-HF (8815 bp – 89 bp = 8726 bp) and gel extracted (Figure 3.12 E) before the vector and insert were ligated using the Gibson Assembly method as described in Section 2.13.3. The construct was transformed into electrocompetent *E. coli* DC10B cells. Positive transformants were selected on LB + chloramphenicol (15 μg ml^{-1}) + X-Gal at 37°C and dark blue colonies were further analysed by PCR using primer pair EJ1/EJ2 and extracted plasmid as template DNA and separation in a 1% (w/v) agarose gel (Figure 3.12 B). Putative positive clones were also verified by DNA sequencing (GATC Biotech AG, Germany). The plasmid was designated pEJ1.

Five micrograms of pEJ1 was then transformed separately into electro-competent *S. aureus* clinical strain R35 and as a positive control, *S. aureus* RN4220. Transformants were selected on BHI + chloramphenicol (10 μg ml^{-1}) + X-Gal at 25°C for 48 h. Putative positive blue clones were individually patched on to BHI + chloramphenicol (10 μg ml^{-1}) + X-Gal at 25°C and pEJ1 verified as present by PCR using primer pair MCS FWD/MSC REV, using extracted plasmid as template DNA and separation in a 1% (w/v) agarose gel (Figure 3.12 C). As the plasmid was successfully transformed

directly into the clinical strain R35 (R35-pEJ1), no further work was done with RN4220-pEJ1.

Integration of R35-pEJ1 into the *S. aureus* chromosome was attempted by selecting a single colony containing R35-EJ1, re-suspending in 200 µl BHI and serially diluting from 10^{-1} to 10^{-6}. Fifty microlitres from each dilution was plated out on to BHI + chloramphenicol (10 µg ml^{-1}) + X-Gal and incubated at 37°C overnight. When single-cross over integration into the chromosome has occurred, colonies should be light blue in colour, due to the single copy of *lacZ*. As no light blue colonies were seen after the overnight incubation at 37°C, colonies were patched onto BHI + chloramphenicol (10 µg ml^{-1}) + X-Gal plates and incubated again at 37°C. All colonies remained dark blue in colour indicating that the plasmid remained present and replicating. Genomic DNA was extracted from 10 colonies and the template DNA was PCR analysed with primer pair MCS FWD/MCS REV to screen for loss of replicating plasmid. All colonies screened showed the presence of replicating plasmid, indicating that the integration was unsuccessful (Figure 3.12 D).

Integration was then attempted at the higher temperature of 39°C but all colonies remained dark blue with no loss of replicating plasmid. A final integration attempt using a liquid culture method was performed (Bae and Schneewind, 2006). In short, one colony containing R35-pEJ1 plasmid was grown overnight at 30°C in BHI broth containing chloramphenicol (10 µg ml^{-1}). Five microliters of overnight culture was inoculated into 5 ml pre-warmed BHI + chloramphenicol (10 µg ml^{-1}) and incubated overnight at the non-permissive temperature, 37°C with shaking at 250 rpm. Five microliters of this overnight culture was inoculated into 5 ml pre-warmed BHI broth with a lower concentration of chloramphenicol (7.5 µg ml^{-1}) at 37°C. After overnight incubation, 50 µl aliquots were plated onto BHI + chloramphenicol (10 µg ml^{-1}) and re-incubated at 37°C. Colonies were then inoculated into 5ml BHI + chloramphenicol (10 µg ml^{-1}) and incubated at 30°C overnight to facilitate plasmid excision. Cultures were 10^6 fold diluted with dH_20 and spread onto BHI containing X-gal only. Unfortunately, no light-blue colonies were seen.

A possible explanation for the inability to successfully integrate the plasmid is the occurrence of a spontaneous mutation in the $repA^{TS}$ gene which would prevent

temperature sensitivity. When the pIMAY-Z vector alone, containing no inserts, was transformed into *S. aureus* RN4220 and incubated at 37°C, dark blue colonies were seen after one day. If the temperature sensitive plasmid was functioning correctly, no plasmid replication should occur at 37°C. Alternatively, it is possible that the clinical strain background is not amenable to integration. However, successful integration of pIMAY has been described into clinical strains (Monk et al., 2012; Heilbronner et al., 2013; Chua et al., 2014) whereas the more recently developed pIMAY-Z has been less frequently employed.

Therefore, pIMAY was used instead of pIMAY-Z and the same method was employed. In short, the construct was produced using the Gibson assembly method (Figure 3.13). After electroporation into *E. coli* DC10B cells, positive putative clones were confirmed by PCR analysis with MCS FWD/MSC REV and separation by 1% (w/v) agarose gel electrophoresis (Figure 3.14 A). The verified plasmid, pEJ2 was concentrated and 5 µl of DNA (~ 2.5 µg) was used to transform electro-competent *S. aureus* R35 with selection on BHI + chloramphenicol (10 µg ml^{-1}) at 28°C for 48 hours. Resulting colonies were streaked onto BHI + chloramphenicol (10 µg ml^{-1}) at 28°C for 48 hours to obtain pure clones. The presence of pEJ2 in R35 was confirmed by PCR analysis (MCS FWD/MCS REV) and separation by 1% (w/v) agarose gel electrophoresis (data not shown).

Integration of plasmid was attempted as described above with overnight incubation in the presence of antibiotics at 37°C. Loss of replicating plasmid would indicate successful plasmid integration and was screened for by PCR analysis with plasmid primers (MCS FWD/MCS REV) and agarose gel separation. No PCR products, or very faint PCR products (interpreted as false positives) were seen for the majority of clones (data not shown). Further confirmation of plasmid integration was carried out by PCR analysis. Primer pair, EJ3 OUT/MCS REV (upstream integration) and MCS FWD/EJ4 OUT (downstream integration) were used for PCR before separation of products by 1% (w/v) agarose gel electrophoresis. Figure 3.15 shows the potential outcomes of either an upstream or downstream integration of the plasmid. Upstream integration was confirmed, as the expected PCR product size was 2606 bp and 2353 bp for primer pairs EJ3 OUT/MCS REV and MCS FWD/EJ4 OUT respectively (Figure 3.14 B, C). Figure

3.16 shows the possible outcomes of plasmid excision following an upstream integration relative to the SNP.

To excise the plasmid, one successfully integrated clone was grown overnight without antibiotics at 28°C. Serial dilutions of this culture were made from 10^{-1} to 10^{-6} and 50 µl was plated out onto BHI + anhydrotetracycline (1 µg ml^{-1}) and incubated at 28°C for 48 hours. Anhydrotetracycline induces antisense *secY* RNA expression, which inhibits *secY*, a protein essential for bacterial growth. Cells that contain integrated plasmid will be unable to grow in the presence of anhydrotetracycline, allowing selection for those clones that have undergone a double cross-over event. This second recombination event leads to plasmid resolution and depending on the site of plasmid excision, either the wildtype or the mutant copy of the targeted DNA remains only. Clones present after incubation on BHI + anhydrotetracycline (1 µg ml^{-1}) were then patched onto BHI + chloramphenicol (10 µg ml^{-1}) and BHI + anhydrotetracycline (1 µg ml^{-1}) and incubated at the non-permissive temperature 37°C, to screen for chloramphenicol sensitive, anhydrotetracycline resistant clones that no longer contain integrated plasmid. Despite screening over 1000 colonies, none exhibited the desired phenotype and all colonies remained chloramphenicol resistant. It is unclear why plasmid excision and mutant recreation was not possible in the R35 strain, but RM system strain differences may play a part.

The ideal background in which to recreate the mutant is the clinical strain neighbouring background, R35. However, in order to functionally analyse the role of this particular SNP in the *saeS* gene, an attempt was made to recreate the mutant in the *S. aureus* SH1000 genomic background.

The plasmid DC10B-pEJ2 was successfully transformed into *S. aureus* RN4220 and replicating plasmid was confirmed by PCR analysis with primer pair MCS FWD/MCS REV (data not shown). Direct transformation of 5 µl DC10B-pEJ2 was attempted into electrocompetent SH1000 at 28°C and approximately 30 colonies were seen across all plates. Concurrently, a φ11 phage lysate of RN4220-pEJ2 was made and used to transduce the plasmid into *S. aureus* SH1000 which also yielded many colonies on the selective agar plates. After patching onto BHI + chloramphenicol (10 µg ml^{-1}) at 28°C for 48 hours to obtain pure colonies, the presence of SH1000-pEJ2 was confirmed by

PCR analysis (MCS FWD/MCS REV) and separation by 1% (w/v) agarose gel electrophoresis (data not shown).

Integration of the plasmid was attempted with both a transformed and transduced clone as described above with overnight incubation in the presence of antibiotics at 37°C. Growth of potential single cross-over integrants from transduction was more efficient than that achieved by transformation and therefore these clones used for the rest of the protocol. Confirmation of plasmid integration was done by PCR analysis using primer pair, MCS FWD/EJ4 OUT before separation of PCR products on a 1% (w/v) agarose gel and upstream integration was confirmed as the PCR product size was 2353 bp (Figure 3.17 A).

As attempted previously, one successfully integrated clone was grown overnight without antibiotics at 28°C. Serial dilutions of this culture were made from 10^{-1} to 10^{-6} and 50 µl was plated onto BHI. The anhydrotetracycline was omitted during this attempt as it did not seem to reduce the number of clones to screen when used previously. Clones were then patched onto BHI only and BHI + chloramphenicol (10 µg ml^{-1}) and incubated at the non-permissive temperature 37°C, to screen for chloramphenicol sensitive clones that no longer contain integrated plasmid. The number of chloramphenicol sensitive colonies was low (1/1200) with only one chloramphenicol sensitive colony found (Figure 3.17 B). Genomic DNA was extracted and this clone was sent for sequencing. The putative mutant was confirmed as having the same SNP in the codon as the original strain GRE18 (TTA, leucine) rather than the wildtype SH1000 *saeS* stop-codon, TAA, at the same position. No other base pair changes were detected between the wildtype and mutant *saeS* gene (Figure 3.17 C).

As the recreation of the mutant was successful in the SH1000 background, albeit with exceedingly low efficiency, a final attempt was made to recreate the mutant in the originally intended background, ST239 R35 strain. Having screened 1000 colonies for chloramphenicol sensitive clones previously, colonies that were confirmed as having upstream single cross-over integration were re-streaked from the bead. Plasmid excision was attempted and a further 1400 colonies were patched onto BHI only and BHI + chloramphenicol (10 µg ml^{-1}) however, no chloramphenicol sensitive colonies were observed and further attempts were abandoned.

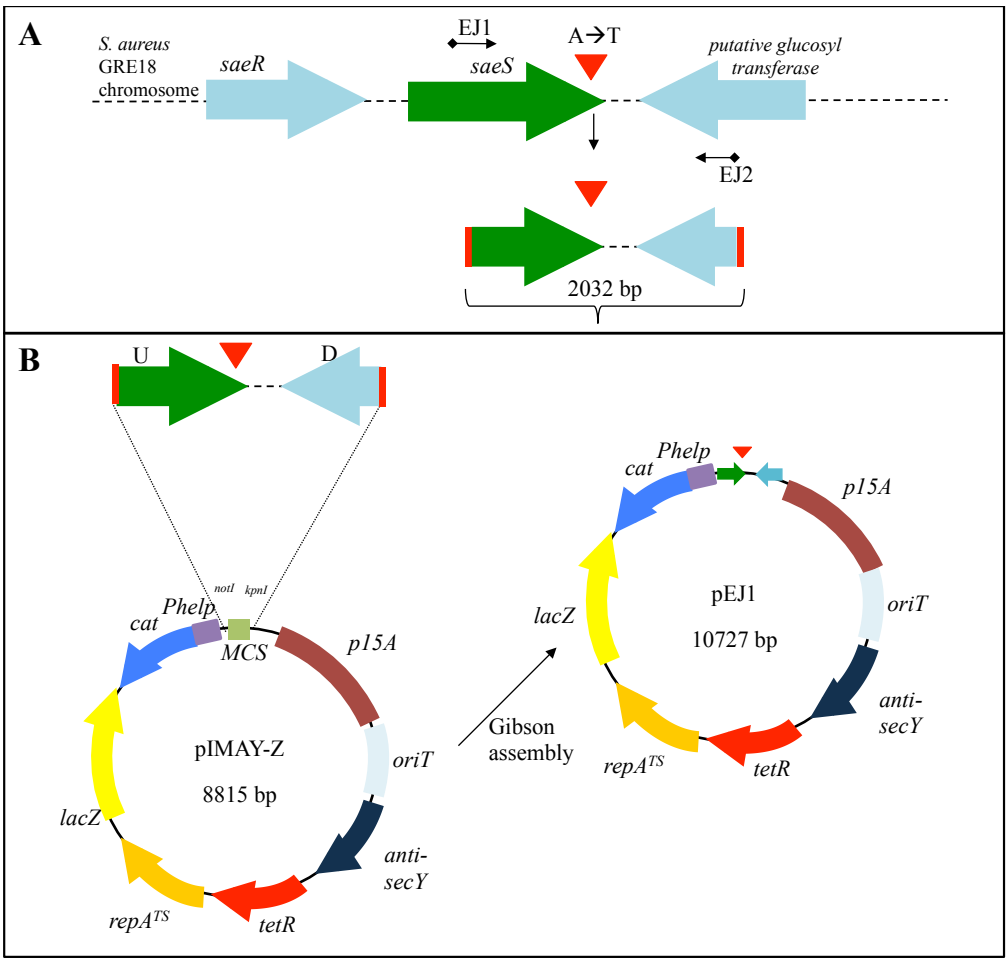


Figure 3.11 Construction of the *S. aureus saeS*$^{\Delta A \rightarrow T}$ plasmid, pEJ1

A Amplification of 1 Kb flanking regions of the *saeS*$^{\Delta A \rightarrow T}$ cloned from the GRE18 genome. The overlap sequence from the vector was added to the primers used to generate the insert (thin red box either side of amplification region). Primer binding sites for EJ1/EJ2 are shown. ◆ on the 5' end of each primer signifies the vector overlap region. U – upstream flanking region of SNP; D – downstream flanking region of SNP. The red triangle highlights the position of the SNP of interest.

B Diagrammatic representation of the PCR fragment inserted into the shuttle vector pIMAY-Z at the MCS using Gibson Assembly. The vector was digested with *NotI*-HF and *Kpn*I-HF. The resulting plasmid pEJ1 is shown.

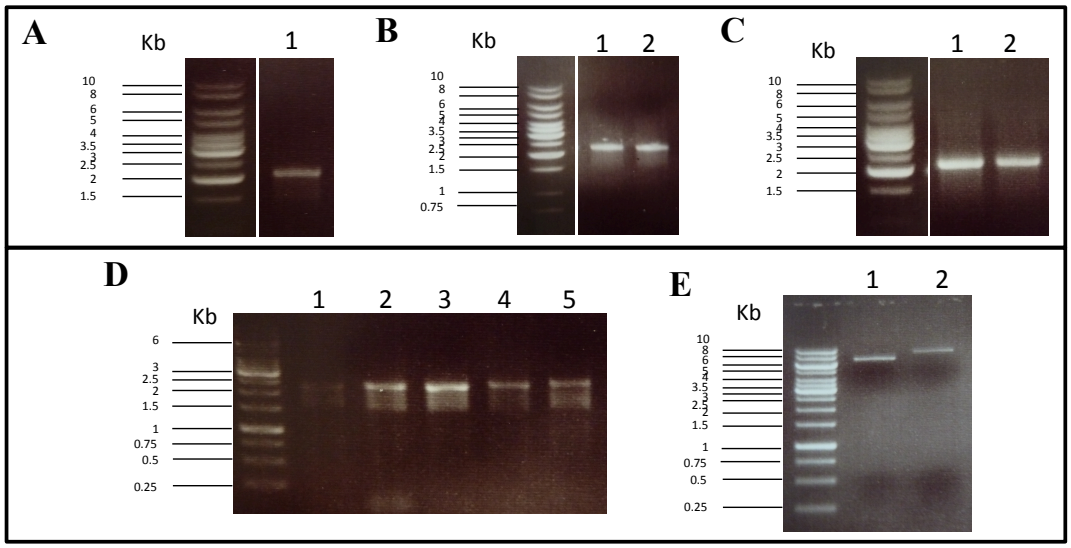


Figure 3.12 PCR products of *S. aureus saeS*$^{\Delta A \rightarrow T}$ mutant recreation in pIMAY-Z.

A The PCR product of *saeS*$^{\Delta A->T}$ with 1000 bp both upstream and downstream, was amplified with primer pair EJ1/EJ2 (lane 1), with an expected size of 2032 bp as shown by 1% (w/v) TAE agarose gel electrophoresis.

B 1% (w/v) TAE agarose gel showing PCR amplification of the *saeS* region within pEJ1 DNA extracted from two randomly selected *E. coli* DC10B transformants (lane 1 and 2) with primer pair EJ1/EJ2. The expected insert size of 2032 bp is seen.

C 1% (w/v) TAE agarose gel showing PCR amplification of the *saeS* region within pEJ1 plasmid DNA extracted from a randomly selected *S. aureus* R35 transformants (lane 1) using MCS FWD/MCS REV primers. Lane 2 shows PCR amplification of the same regions within pEJ1 plasmid DNA extracted a clone of *S. aureus* RN4220 putative transformants using the same primers. Expected sizes are 2232 bp in both genomic backgrounds.

D PCR amplification of genomic DNA extracted from putative R35 integrants using primers MCS FWD/MCS REV as seen on a 1% TAE agarose gel. Lane 1 contains plasmid DNA extracted from pEJ1 as a positive control. Lanes 2-5 were expected to show no PCR product if the plasmid has integrated into the chromosome.

E 1% (w/v) TAE agarose gel showing *Not*I-HF and *Kpn*I-HF restriction digest of pIMAY (lane 1) and pIMAY-Z (lane 2). Expected sizes are 5654 bp and 8726 bp respectively.

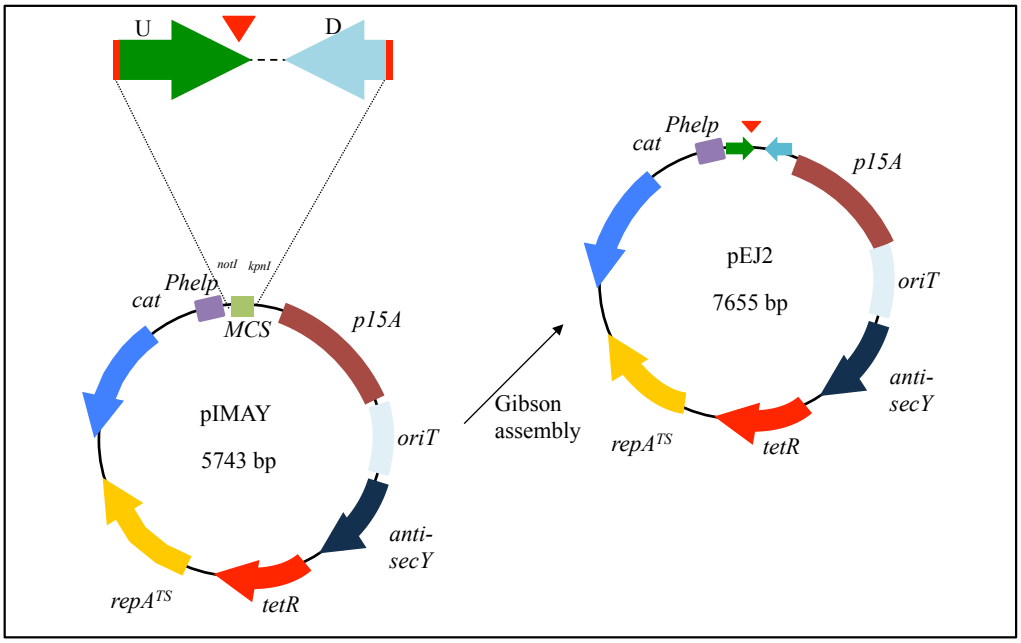


Figure 3.13 Construction of the *S. aureus saeS*$^{\Delta A \rightarrow T}$ plasmid, pEJ2

Diagrammatic representation of the fragment (*saeS*$^{\Delta A \rightarrow T}$ cloned from the GRE18 genome) inserted into the shuttle vector pIMAY at the MCS using Gibson Assembly. The vector was digested with *Not*I-HF and *Kpn*I-HF (5654 bp). The resulting plasmid pEJ2 is shown. The red triangle highlights the position of the SNP of interest. The overlap sequence from the vector was added to the primers used to generate the insert (thin red box either side of amplification region).

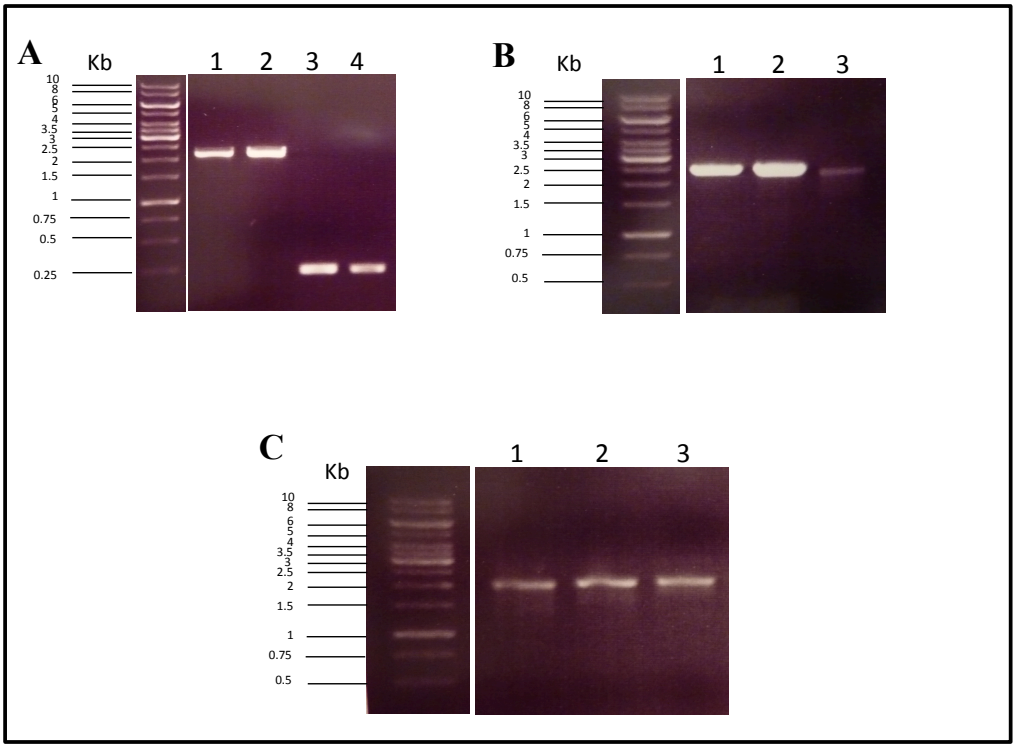


Figure 3.14 PCR products of *S. aureus saeS*$^{\Delta A \rightarrow T}$ mutant recreation using pIMAY

A 1% (w/v) TAE agarose gel showing PCR amplification of the *saeS*$^{\Delta A \rightarrow T}$ region within pEJ2 DNA extracted from four randomly selected *E. coli* DC10B transformants with primers MCS FWD/MCS REV. After successful transformation, expected PCR products of 2232 bp indicate correct insertion into pIMAY. Transformants lacking the construct show a PCR product for the MCS region only (173 bp) (lanes 3 and 4). Two out of four putative positive transformants (lanes 1 and 2) show the correct product size (2232 bp).

B R35 clones that had lost replicating plasmid were screened for confirmation of integration using primer pair EJ3 OUT (chromosomal) and MCS REV (plasmid). Upstream integration would yield a product of size of 2606 bp, as seen in both clones tested (lanes 1-2). A positive control was included in lane 3 using pEJ1 as template DNA and primer pair MCS FWD/ MCS REV producing a product size of 2232 bp.

C Further confirmation of upstream integration within R35 was shown by using genomic DNA from presumed integrants and performing PCR analysis with primer pair MCS FWD (plasmid) and EJ4 OUT (chromosomal) to give an expected product size of 2353 bp. All of the clones had successfully integrated upstream (lanes 2 and 3) and a positive control (same as for B) was run in Lane 1.

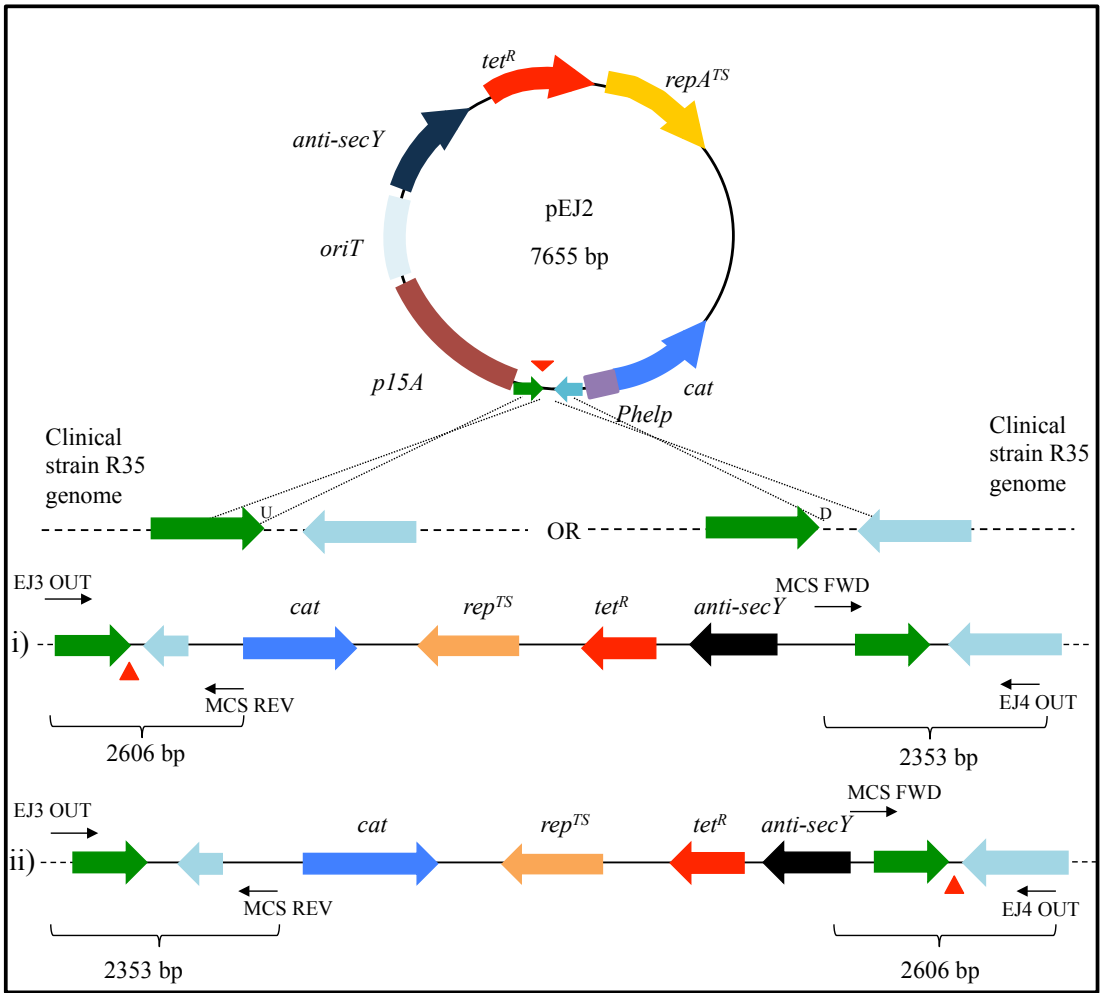


Figure 3.15 Diagrammatic representation of the likely outcomes of a single cross over recombination event of pEJ2 into the *S. aureus* R35 chromosome

An upstream arm recombination event would lead to the outcome shown in i) and a downstream arm recombination would lead to the outcome shown in ii).
Primer annealing sites are indicated.

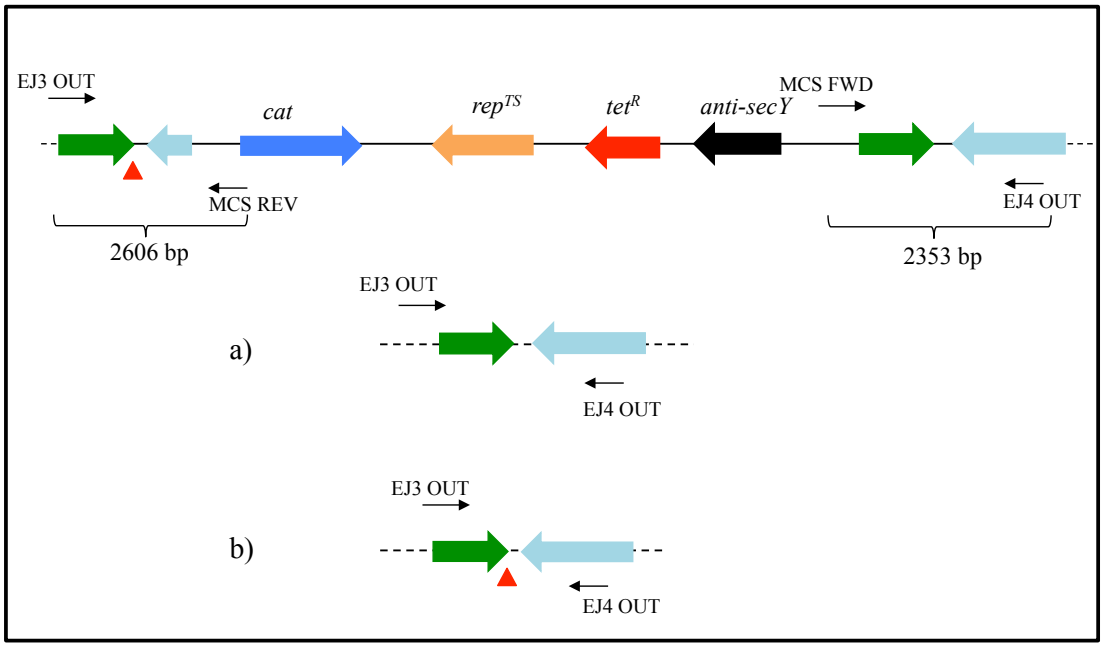


Figure 3.16 Diagrammatic representation of the outcomes of the double cross over excision event after upstream integration

a) upstream excision would yield the wildtype SNP

b) downstream excision would recreate the mutation (*saeS*$^{\Delta A \rightarrow T}$). Both products would be the same size so cannot be differentiated using PCR.

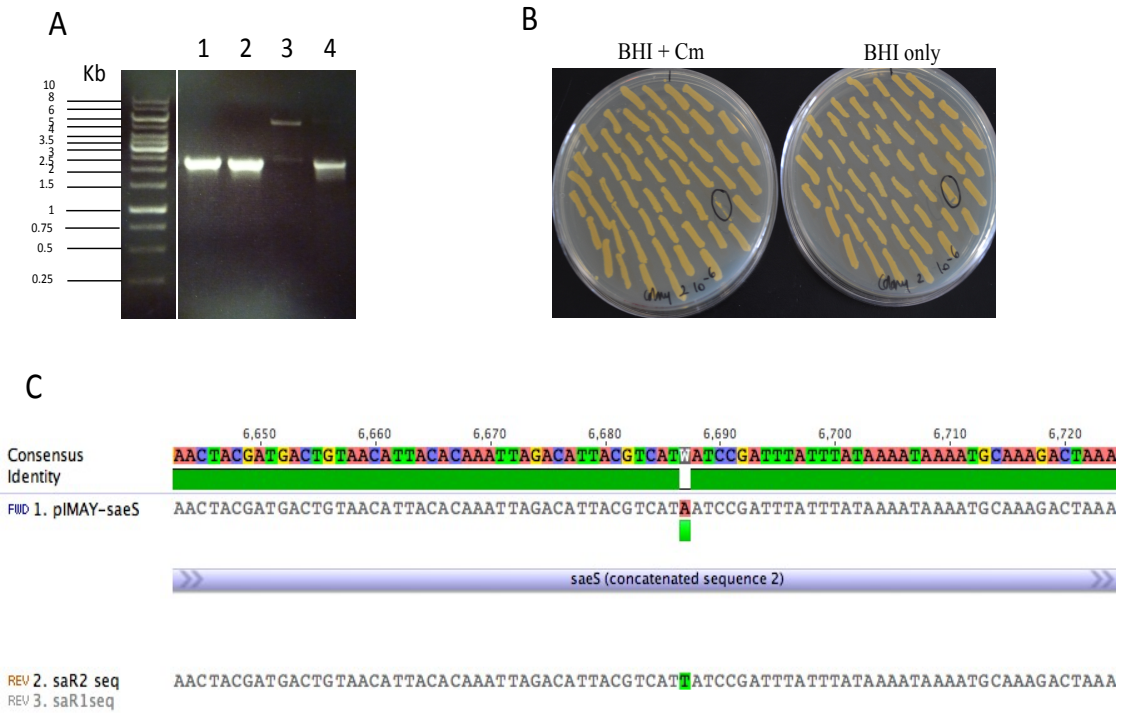


Figure 3.17 Final steps of recreating mutant SH1000 *saeS*$^{\Delta A \rightarrow T}$

A Clones were tested for site of integration with primers MCS FWD (plasmid) and EJ4 OUT (chromosomal). Using these primers, upstream integration yields a product of 2353 bp and downstream 2606 bp. Tested clones underwent upstream integration (lanes 1, 2). Lane 3 contains a negative control of a PCR reaction containing plasmid primers EJ3 OUT/MCS REV with SH1000 wildtype gDNA and lane 4 contains a positive control of MCS FWD/MCS REV primers from extracted plasmid DC10B-pEJ1 (expected product size 2232 bp).

B Patching of potential double cross-over colonies onto BHI + chloramphenicol (Cm) (10 µg ml^{-1}) or BHI only. The single chloramphenicol sensitive colony is circled.

C Results of sequencing of the chloramphenicol sensitive colony. The top line of base pair reads displays the wildtype copy of *saeS* amino acid number 351 as TAA (stop codon) and underneath is the SNP change to a non-stop codon, TTA (leucine) in the recreated mutant in the SH1000 background (saR2 seq). No other base pair changes were detected between the wildtype and mutant copy.

3.3.8.1.1 Phenotypic analysis of SH1000 *saeS*$^{A->T}$ *in vitro* and *in vivo*

Recreation of a mutant with the same SNP as identified in the initial whole genome sequence data permits testing to establish if that SNP is responsible for the decreased haemolysis *in vitro* and attenuated virulence phenotype in the zebrafish embryo model of infection.

As it was only possible to recreate the mutant in a standard laboratory genetic background, SH1000, this wildtype strain was used as a positive control and strain SH1000*saeS*::*ery* (Tn551 insertion containing an erythromycin resistance cassette, SJF 1293) was used for comparison. To test for haemolysis differences, strains were grown for 12 h in 5 ml BHI with 250 rpm rotary shaking. After centrifugation to remove cells, the supernatant was filter-sterilised and 10 µl of neat or ten fold dilutions were spotted onto rabbit blood agar plates. After overnight incubation at 37 °C, the plate was photographed as shown in Figure 3.18.

There was intermediate haemolytic activity (haemolysis seen at 1/100 dilution) in the qualitative assay of SH1000*saeS*$^{A->T}$ compared to SH1000 (haemolysis seen at 1/1000 dilution) and SH1000*saeS*::ery (haemolysis seen at 1/10 dilution only). This suggests that the specific SNP, which inserts near to the 3' end of the *saeS* gene, is exerting an affect on exotoxin production, in particular on alpha-haemolysin but to a lesser extent compared to knockout of the gene by a erythromycin resistance cassette containing transposon.

When injected into the zebrafish embryos, no difference was seen in virulence between the wildtype SH1000 and the recreated mutant SH1000*saeS*$^{A->T}$ with both producing approximately 50% embryo death. As seen previously, SH1000*saeS*::ery can show diminished virulence (Figure 3.19 B, $p = 0.004$) but is inconsistent and can vary between experiments (Figure 3.19 A, $p = 0.42$) (Prajsnar, 2009).

Recreation of the *saeS* mutation in the clinical strain background, ST239, proved unsuccessful. With the antibiotic resistance of the clinical strain background and the unknown RM systems, genetic manipulation was not possible despite recent advances in transforming previously recalcitrant strains. Furthermore, the attenuated *in vivo*

phenotype predicted to be caused by the *saeS* SNP difference between the GRE 4, GRE 18, GRE 317 strains compared to the neighbouring strain R35, could not be established by changing this SNP in the *saeS gene* within the SH1000 background. This may be due to pre-existing large genomic differences between ST239 MRSA strains and the ST8 MSSA SH1000 strain. However, it could also be due to differences specifically in exotoxin expression and role of such toxins in virulence across different genetic backgrounds.

However, another or additional explanation may be that whilst strains in the 'global ST239 strain' collection were ordered phylogenetically, in many cases, there remained sizeable genomic differences between neighbouring strains. This made subsequent bioinformatic analysis difficult, as the number of SNPs that could be potentially contributing to the phenotype was large. For example, in Group 3, there were a total of 215 core SNP differences between nodes 108 and 110 which could have accounted for the virulence differences. In addition, we purposefully omitted to investigate any gain of function mutations between node 108 and strain R35 (Figure 3.7). There were many significant potential loss of function mutants between 108 and 110 and we chose to further explore *saeS* only to prove the principle of this approach. Therefore, it is possible that a combination of mutations or a genetic 'fingerprint' is responsible for the attenuation in virulence between these strains and this may explain why an attenuated phenotype in the zebrafish model was not seen by re-creating the single *saeS* SNP mutation in an MSSA background. As no phenotype was seen, there was no merit in pursuing this work any further.

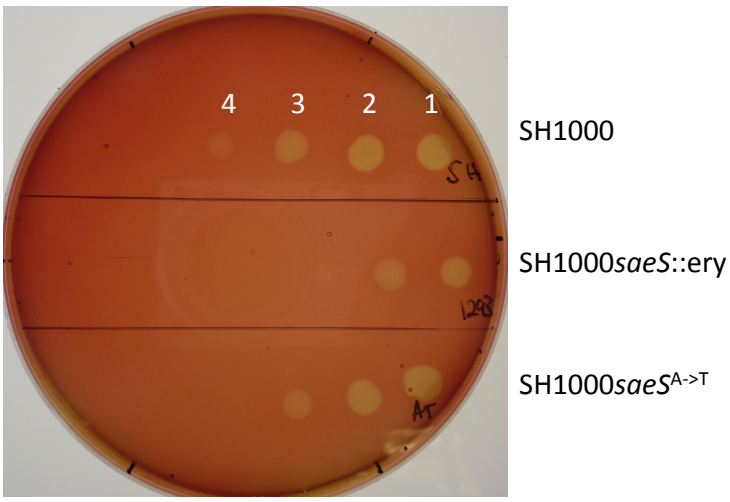


Figure 3.18 Haemolysis caused by BHI culture supernatants of SH1000 (wildtype) and two mutants of *saeS* at various dilutions on rabbit blood agar

Dilutions (from right to left): 1 – neat; 2 - 1/10; 3 - 1/100 and 4 - 1/1000.
Photograph representative of two independent experiments.

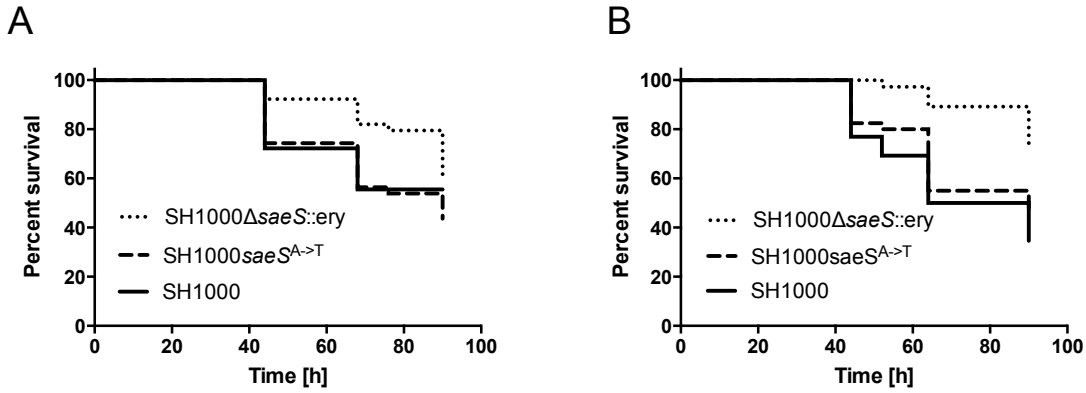


Figure 3.19 Zebrafish embryo survival rates upon bacterial circulation injection of SH1000 (wildtype) and two mutants of *saeS*

Two independent experiments of SH1000, SH1000*saeS*::ery and SH1000*saeS*$^{A->T}$ injected into the embryo circulation valley at 1500 CFU (n=30). Survival of fish injected with SH1000*saeS*$^{A->T}$ was not statistically different from fish injected with SH1000 (A) $p = 0.43$ and (B) $p = 0.37$.

3.3.8.2 Construction of *S. aureus htrA2* mutant

A pair of primers was designed to amplify a region containing the SNP of interest and 1-Kb of DNA either side (Figure 3.20 A). The primers were designed to include an overlapping region of 15-20 bp with the linearized vector, to allow construction of the plasmid using Gibson Assembly cloning. Primer pair EJ5/EJ6 (*htrA2*) was used and the 2-Kb region was amplified from the StTom71 genomic DNA and produced a PCR product of 2032 bp (2001 bp insert and 15 bp forward primer vector overlap region and 16 bp reverse primer overlap region) (Figure 3.22 A). The vector, pIMAY-Z, was digested with *NotI*-HF and *KpnI*-HF, gel extracted and the vector and insert were ligated using the Gibson Assembly method (Figure 3.20 B). The construct was transformed into electrocompetent *E. coli* DC10B cells, giving the plasmid, pEJ3. Positive transformants were selected on LB + chloramphenicol (15 μg ml^{-1}) + X-Gal at 37°C and dark blue colonies were further analysed by primer pair EJ5/EJ6 using extracted plasmid as template DNA and separation in a 1% (w/v) agarose gel (Figure 3.22 B). Putative positive clones were sent for DNA sequencing (GATC Biotech AG, Germany).

Unfortunately, there were multiple base pair differences between the *htrA2* region (SNP +/- 1000 bp) mapped by sequencing data from the clinical strain StTom 71 and the pEJ3 DNA. This was later found to be due to a mismatch in the sequencing data originally supplied by the Wellcome Trust Sanger Centre as repeat sequencing of the same isolates yielded incomparable results. This may be due to incorrect strains being stocked, sequenced, distributed but the root of the problem was not identified. No further work was conducted on this gene as the phenotypic-genotypic analysis is no longer valid.

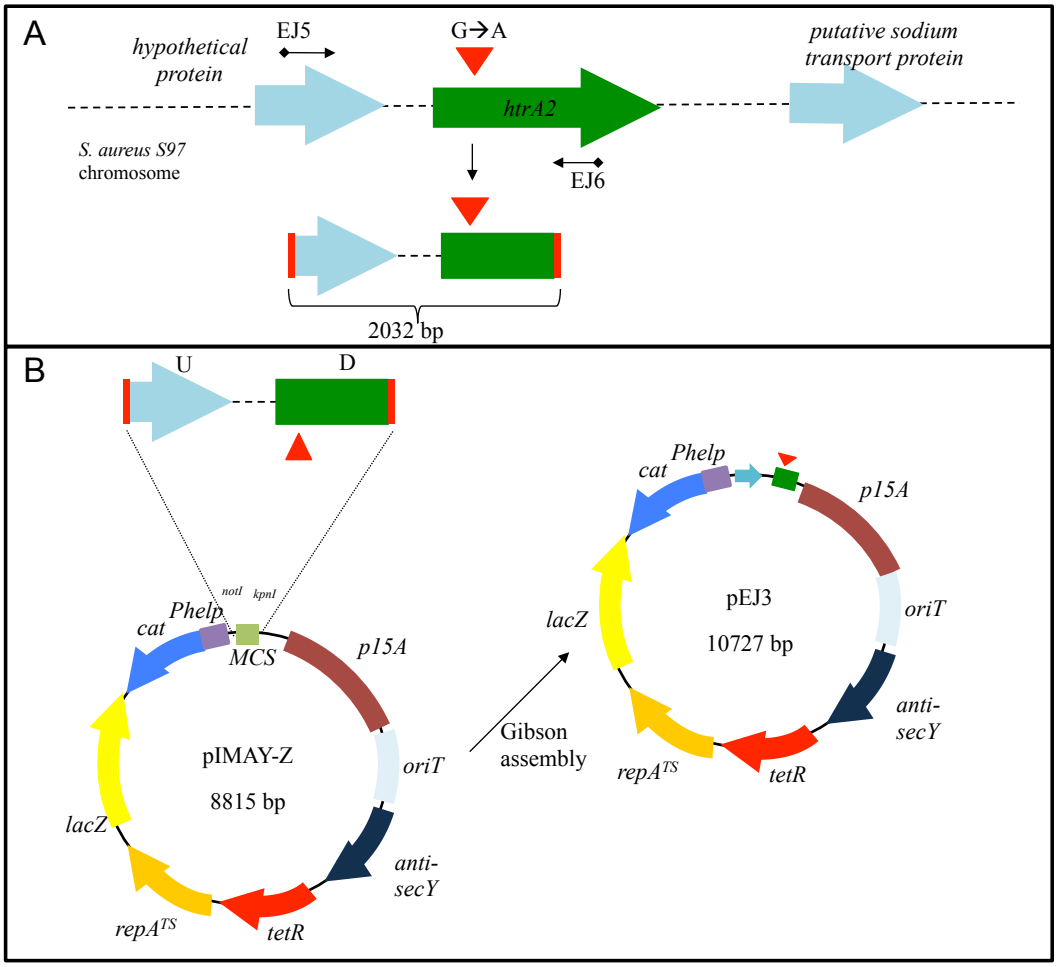


Figure 3.20 Construction of the *S. aureus htrA2*$^{\Delta G \rightarrow A}$ plasmid, pEJ3

A Amplification of 1 Kb flanking regions of the *htrA2*$^{\Delta G \rightarrow A}$ cloned from the St Tom71 genome. The overlap sequence from the vector was added to the primers used to generate the insert (thin red box either side of amplification region). Primer binding sites for EJ5/EJ6 are shown. ◆ on the 5' end of each primer signifies the vector overlap region. U – upstream flanking region of SNP; D – downstream flanking region of SNP. The red triangle highlights the position of the SNP of interest.

B Diagrammatic representation of the PCR fragment inserted into the shuttle vector pIMAY-Z at the MCS using Gibson Assembly. The vector was digested with *Not*I-HF and *Kpn*I-HF. The resulting plasmid pEJ3 is shown.

3.3.8.3 Construction of *S. aureus isaB* mutant

A pair of primers was designed to amplify a region containing the SNP of interest and 1-Kb of DNA either side (Figure 3.21 A). The primers were designed to include an overlapping region of 15-20 bp to the linearized vector, to allow construction of the plasmid using Gibson Assembly cloning. Primer pair EJ7/EJ8 (*isaB*) was used and the 2-Kb region was amplified from the S97 genomic DNA and produced a PCR product of 2032 bp (2001 bp insert and 15 bp forward primer vector overlap region and 16 bp reverse primer overlap region (Figure 3.22 C). The vector, pIMAY-Z, was digested with *NotI*-HF and *KpnI*-HF, gel extracted and the vector and insert were ligated using the Gibson Assembly method to construct pEJ4 (Figure 3.21 B). The construct was transformed into electrocompetent *E. coli* DC10B cells, giving the plasmid pEJ4). Positive transformants were selected on LB + chloramphenicol (15 μg ml^{-1}) + X-Gal at 37°C and dark blue colonies were further analysed by primer pair EJ7/EJ8 using extracted plasmid as template DNA and separation in a 1% (w/v) agarose gel (Figure 3.22 D). Putative positive clones were sent for DNA sequencing (GATC Biotech AG, Germany).

Unfortunately, the expected SNP at 1084364 (deletion of A) was not present as expected. This was also later found to be due to a mismatch in the sequencing data originally supplied by the Wellcome Trust Sanger Centre as repeat sequencing of the same isolates yielded incomparable results. No further work was conducted on this gene as the phenotypic-genotypic analysis is no longer valid.

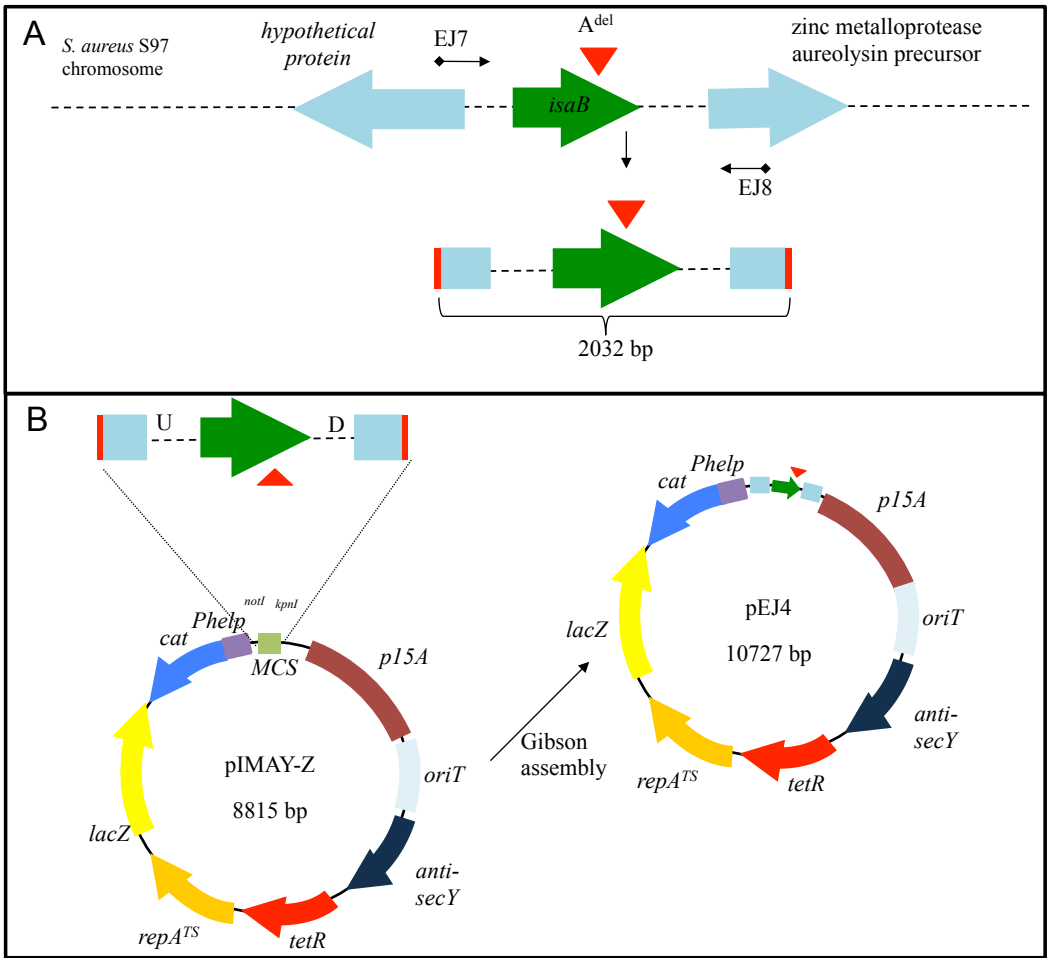


Figure 3.21 Construction of the *S. aureus isaB* plasmid, pEJ4

A Amplification of 1 Kb flanking regions of the *isaB*$^{\Delta A del}$ cloned from the S97 genome. The overlap sequence from the vector was added to the primers used to generate the insert (thin red box either side of amplification region). Primer binding sites for EJ7/EJ8 are shown. ◆ on the 5' end of each primer signifies the vector overlap region. U – upstream flanking region of SNP; D – downstream flanking region of SNP. The red triangle highlights the position of the SNP of interest.

B Diagrammatic representation of the PCR fragment inserted into the shuttle vector pIMAY-Z at the MCS using Gibson Assembly. The vector was digested with *Kpn*I-HF and *NotI*-HF. The resulting plasmid pEJ4 is shown.

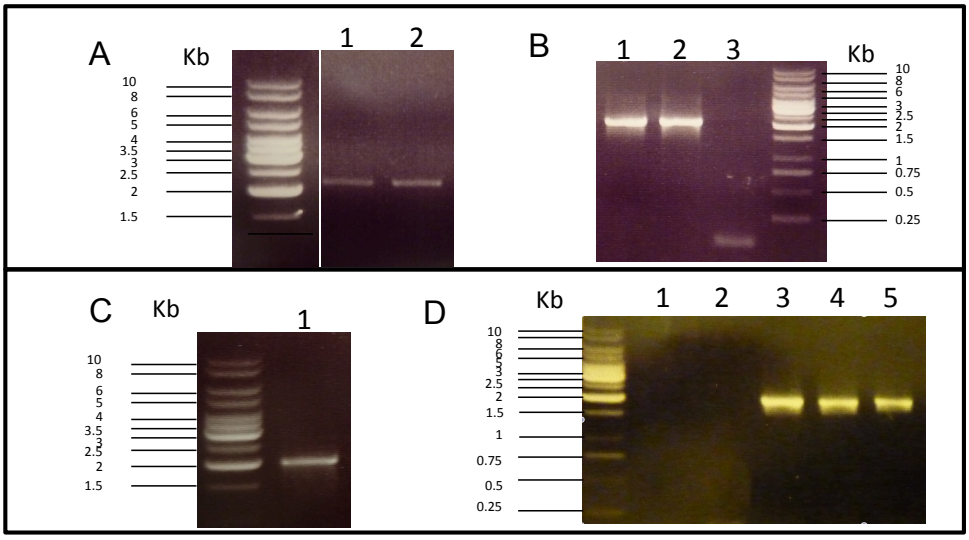


Figure 3.22 PCR products of various *S. aureus* mutants

A 1% (w/v) TAE agarose gel showing products of PCR amplification of the *htrA2*$^{\Delta G \rightarrow A}$ with 1000 bp both upstream and downstream regions using primers EJ5 and EJ6. Expected size of 2032 bp is seen (lanes 1 and 2)

B 1% (w/v) TAE agarose gel showing PCR amplification of the *htrA2* region within pEJ3 DNA extracted from putative *E. coli* DC10B transformants with primer pair EJ5/EJ6. After successful transformation, expected PCR products of 2032 bp indicate correct insertion of this region into pIMAY-Z (lanes 1 and 2). Lane 3 shows an unsuccessful transformant lacking the insert DNA.

C 1% (w/v) TAE agarose gel showing products of PCR amplification of the *isaB*$^{\Delta A del}$ with 1000 bp both upstream and downstream regions using primer pair EJ7 and EJ8. Expected size of 2032 bp is seen (lane 1)

D 1% (w/v) TAE agarose gel showing PCR amplification of the *isaB* region within pEJ4 DNA extracted from putative *E. coli* DC10B transformants with primer pair EJ7/EJ8. After successful transformation, expected PCR products of 2032 bp indicate correct insertion of the selected region into pIMAY-Z (lanes 3-5). Lanes 1 and 2 shows an unsuccessful transformant lacking the insert DNA.

3.3.8.4 Construction of *S. aureus* SATW20_13140 mutant

A pair of primers was designed to amplify a region containing the SNP of interest and 1-Kb of DNA either side (Figure 3.23 A). The primers were designed to include an overlapping region of 15-20 bp to the linearized vector, to allow construction of the plasmid using Gibson Assembly cloning. Primer pair EJ9/EJ10 was used and the 2-Kb region was amplified from the S97 genomic DNA and produced a PCR product of 2032 bp (2001 bp insert and 15 bp forward primer vector overlap region and 16 bp reverse primer overlap region). The vector, pIMAY-Z, was digested with *NotI*-HF and *KpnI*-HF, gel extracted and the vector and insert were ligated using the Gibson Assembly method as described above to construct pEJ5 (Figure 3.23 B). The construct was transformed into electrocompetent *E. coli* DC10B cells, giving the plasmid pEJ5. Positive transformants were selected on LB + chloramphenicol (15 μg ml^{-1}) + X-Gal at 37°C and dark blue colonies were further analysed by primer pair EJ9/EJ10 using extracted plasmid as template DNA and separation in a 1% (w/v) agarose gel. The expected band of 2032 bp was seen but there were two non-specific bands also seen at a size of 750 bp and 2500 bp (data not shown).

Unfortunately, it was apparent that the original genomic sequencing data (Wellcome Trust Sanger Centre) was also incorrect for these strains and no further work was conducted on this gene.

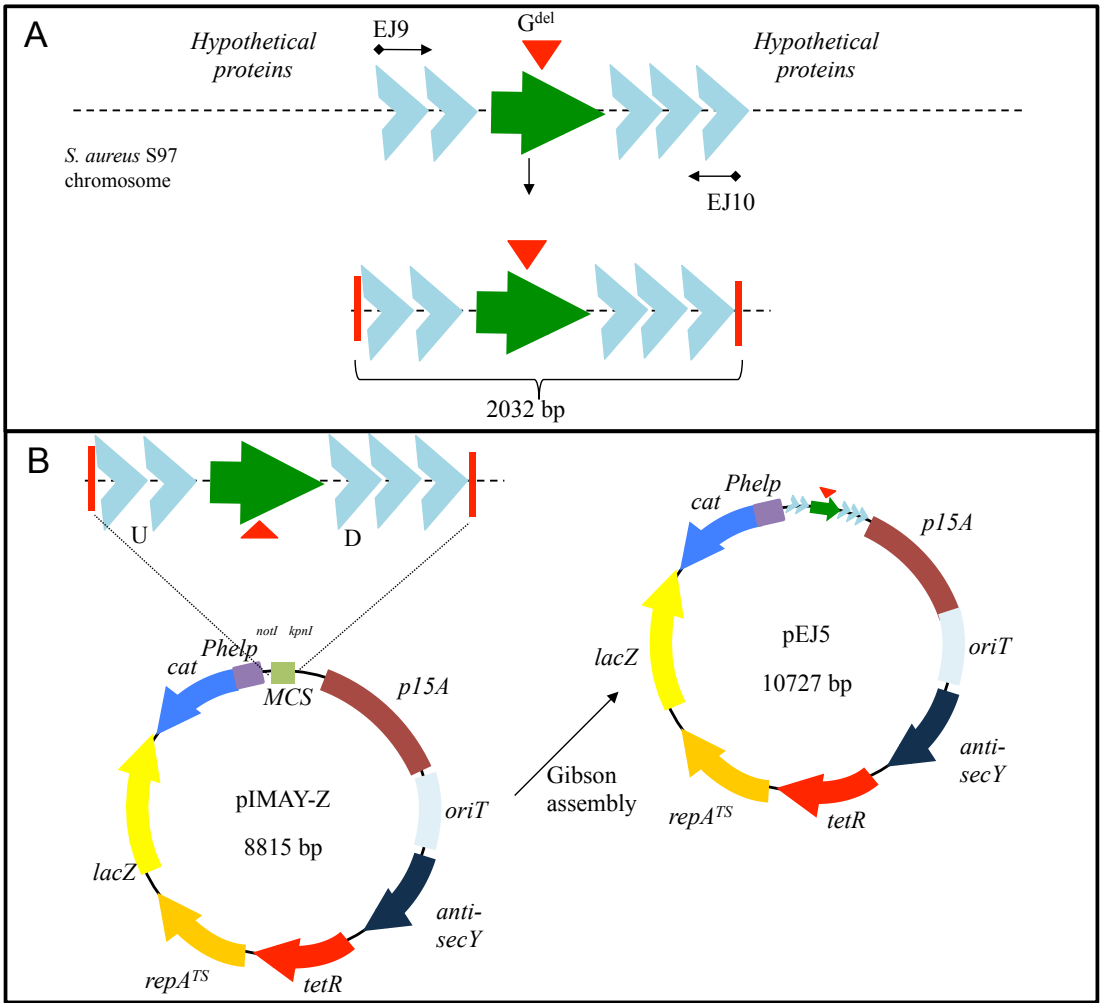


Figure 3.23 Construction of the *S. aureus* SATW20_13140$^{\Delta Gdel}$ plasmid, pEJ5

A Amplification of 1 Kb flanking regions of SATW20_13140$^{\Delta Gdel}$ (large green arrow) cloned from the S97 genome. The overlap sequence from the vector was added to the primers used to generate the insert (red blue box either side of amplification region). Primer binding sites for EJ9/EJ10 are shown. ◆ on the 5' end of each primer signifies the vector overlap region. U – upstream flanking region of SNP; D – downstream flanking region of SNP. The red triangle highlights the position of the SNP of interest.

B Diagrammatic representation of the PCR fragment inserted into the shuttle vector pIMAY-Z at the MCS using Gibson Assembly. The vector was digested with *Kpn*I-HF and *NotI*-HF. The resulting plasmid pEJ5 is shown.

3.3.9 Virulence screen of additional clinical strain collections

Following the genomic sequencing problems described above, it still remained to be seen whether a phenotypic:genotypic screen approach can be utilised to identify novel virulence determinants. The main failing was the errors within the sequencing data, which could be remedied by prospective reliable sequencing of a different collection, yet difficulties would remain when attempting to recreate mutants in the clinical strain background. Another consideration is the extent of genotypic differences between strains being screened through the *in vivo* model. Above, in the 'global ST239 strain' collection, phenotypic differences were seen between genetically similar strains but the number of SNPs potentially involved was too extensive to fully interrogate. In contrast, in the 'local ST239 strain' collection, there were minimal genetic differences between strains as the isolates were originally from a single nosocomial outbreak. As such, phenotypic differences between these strains were less common and so fewer genetic targets were identified.

It was therefore reasoned that there could be an 'optimum' strain collection for this type of approach i.e. one that had limited genomic variation between strains. As such, two new clinical strain collections were selected based on this criteria and screened for virulence through the zebrafish model. Any neighbouring strains with significantly different virulence would be pursued further and the WGS data would be analysed. After discussion with collaborators at the University of Cambridge and the Wellcome Trust Sanger Institute, new strain collections were selected.

3.3.9.1 MRSA outbreak collection from a Neonatal Intensive Care Unit

This relatively small ST22 MRSA outbreak occurred in the Neonatal Intensive Therapy Unit (NITU) at Cambridge University National Health Service Foundation Trust in 2009. Patient 1, the index case, is designated 1B in the strain collection and the remaining 5 samples received (7 C, 8 C, 10 C, 11 C, 12 C) were colonised individuals (Köser et al., 2012). As described in the publication, an unrooted maximum likelihood tree was constructed (Figure 3.24). All six strains were injected (in duplicate experiments) into the zebrafish circulation valley at 1500 CFU of 1-day-old embryos and mortality was observed until 90 hpf.

As shown in Figure 3.25 A-C, overall the strains were less virulent than previous strain collections. Strain 12C was prone to clumping and needle blocking hence the maximum dose achieved was only 1000 CFU in both experiments so cannot be used for meaningful comparisons.

Strain 10C and 11C appear attenuated compared to 1B, 7C and 8C although the difference in virulence between these strains is small particularly when compared to the initial screen of the ST 239 population (Section 3.3.3) which yielded marked virulence differences. For example, percentage survival of zebrafish injected with strain ST239 R35 was approximately 30% compared to those injected with strain ST239 GRE 18 with a survival of 80%. These large differences justified further bioinformatics and molecular interrogation (Harris et al., 2010). The very small differences in virulence between the ST22 strains are too modest to justify molecular manipulation of any identified genetic targets. It is likely that the sensitivity of this infection model is not sufficient to identify marked and reproducible virulence differences in this strain collection so no further work was conducted.

3.3.9.2 MRSA outbreak collection from a Special Care Baby Unit

This MRSA outbreak in 2011 occurred in the Special Care Baby Unit (SCBU) of the Cambridge University NHS Foundation Trust and involved a newly identified sequence type, ST 2371, which is closely related to the epidemic-MRSA (E-MRSA) strain type 22 (Harris et al., 2013). As highlighted by the red boxes on the phylogenetic tree (Figure 3.26), 24 strains were selected for *in vivo* phenotypic analysis and results are shown in Figure 3.27.

There were no significant phenotypic differences between the 24 SCBU MRSA isolates screened using the zebrafish embryo infection model. This is likely due to the limited number of genetic differences, in some cases only 1 or 2 core genome SNP differences, between neighbouring strains. Therefore, no further bioinformatic analysis or molecular genetic work was carried out.

The outcomes of both the NITU and SCBU strain collection screening may serve to confirm that this approach using phenotypic:genotypic analysis to identify novel

virulence determinants will only work for an optimally sized strain collection. A collection which has small numbers of SNP differences (5-10) between strains may be better suited to such an approach rather than either far more differences (e.g. ‘global ST239 strain’ collection) or much less/no differences (e.g. ‘local ST239 strain’ collection and the NITU and SCBU collections).

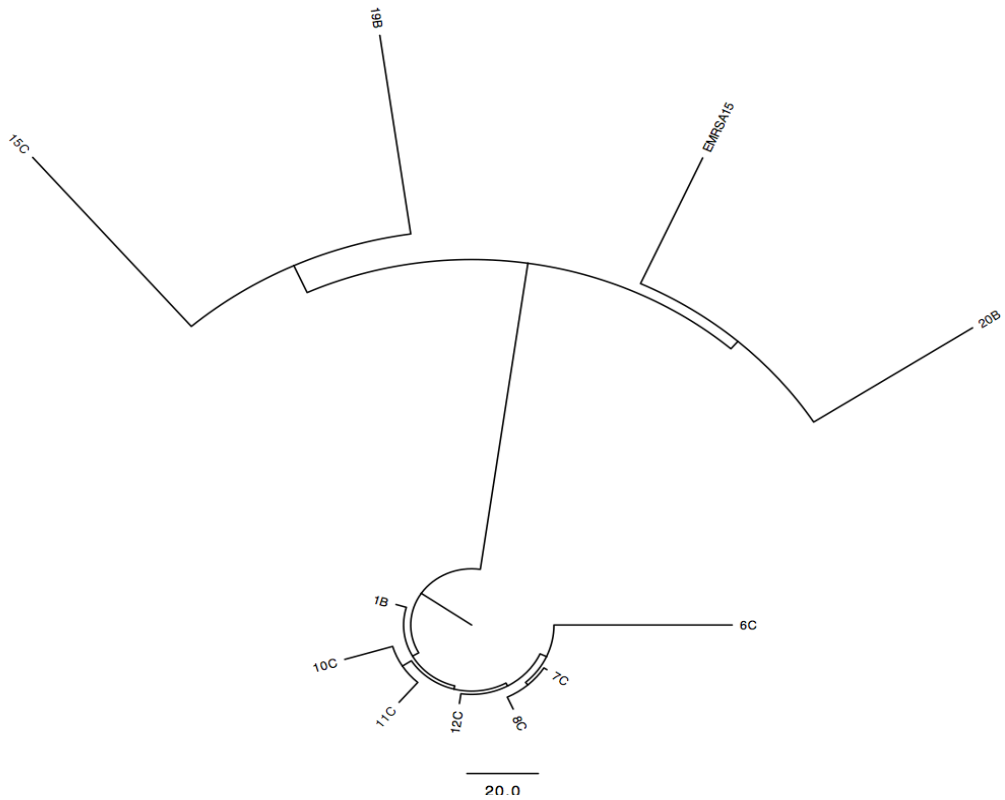


Figure 3.24 Maximum likelihood phylogenetic tree of MRSA ST22 NITU strains, based on core genome SNPs

Genome sequence data for each isolate were mapped against a reference isolate ST22 (HO 5096 0412) and variable sites in the core genome were assigned as described in Harris et al. (2010). The scale bar represents the number of SNP differences per site.

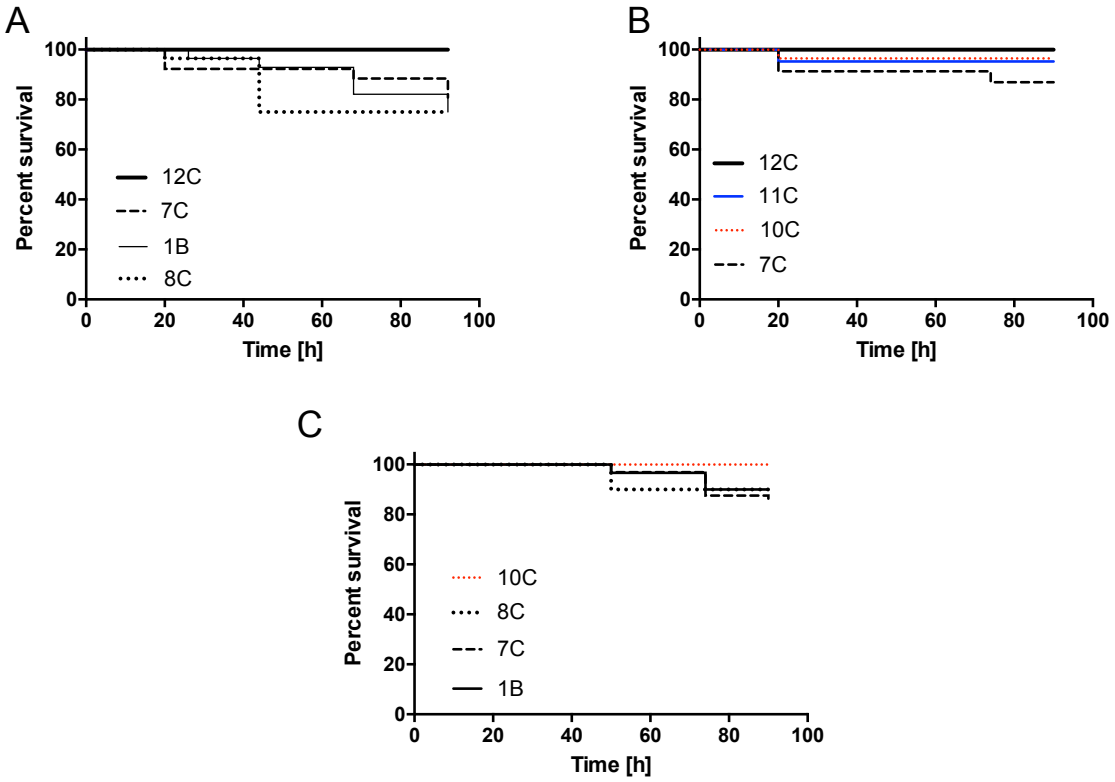


Figure 3.25 Results from the phenotypic assay from the small ST22 MRSA outbreak

A Survival rate of zebrafish embryos injected with various strains (n=30). Log rank test pairwise comparisons showed 1B or 7C or 8C vs. 12C $p < 0.05$.

B Survival rate of zebrafish embryos injected with various strains (n=30). Log rank test pairwise comparisons showed 7C vs. 12C $p = 0.05$; 7C vs 10C/11C $p=0.34$.

C Survival rate of zebrafish embryos injected with various strains (n=30). Log rank testspairwise comparisons showed 10C vs. 1B $p = 0.11$; 10C vs. 7C $p = 0.04$; 10C vs. 8C $p= 0.11$.

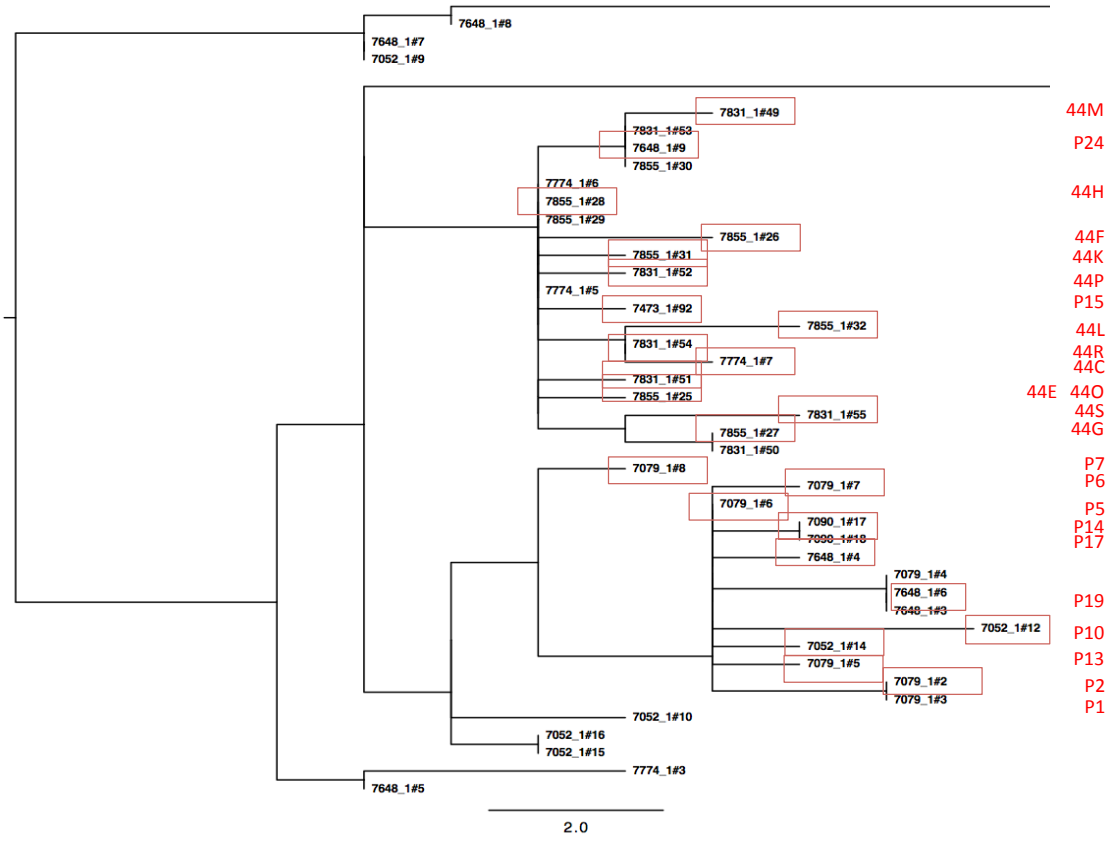


Figure 3.26 Maximum likelihood phylogenetic tree of MRSA ST2173 SCBU strains, based on core genome SNPs

Genome sequence data for each isolate were mapped against a reference isolate ST22 (HO 5096 0412) and variable sites in the core genome were assigned as described in Harris *et al*. (2010). The scale bar represents the number of SNP differences per site. The red boxes highlight the strains selected for *in vivo* phenotypic analysis. The letter/number combinations on the right-hand side are the anonymous patient identifiers related to each strain.

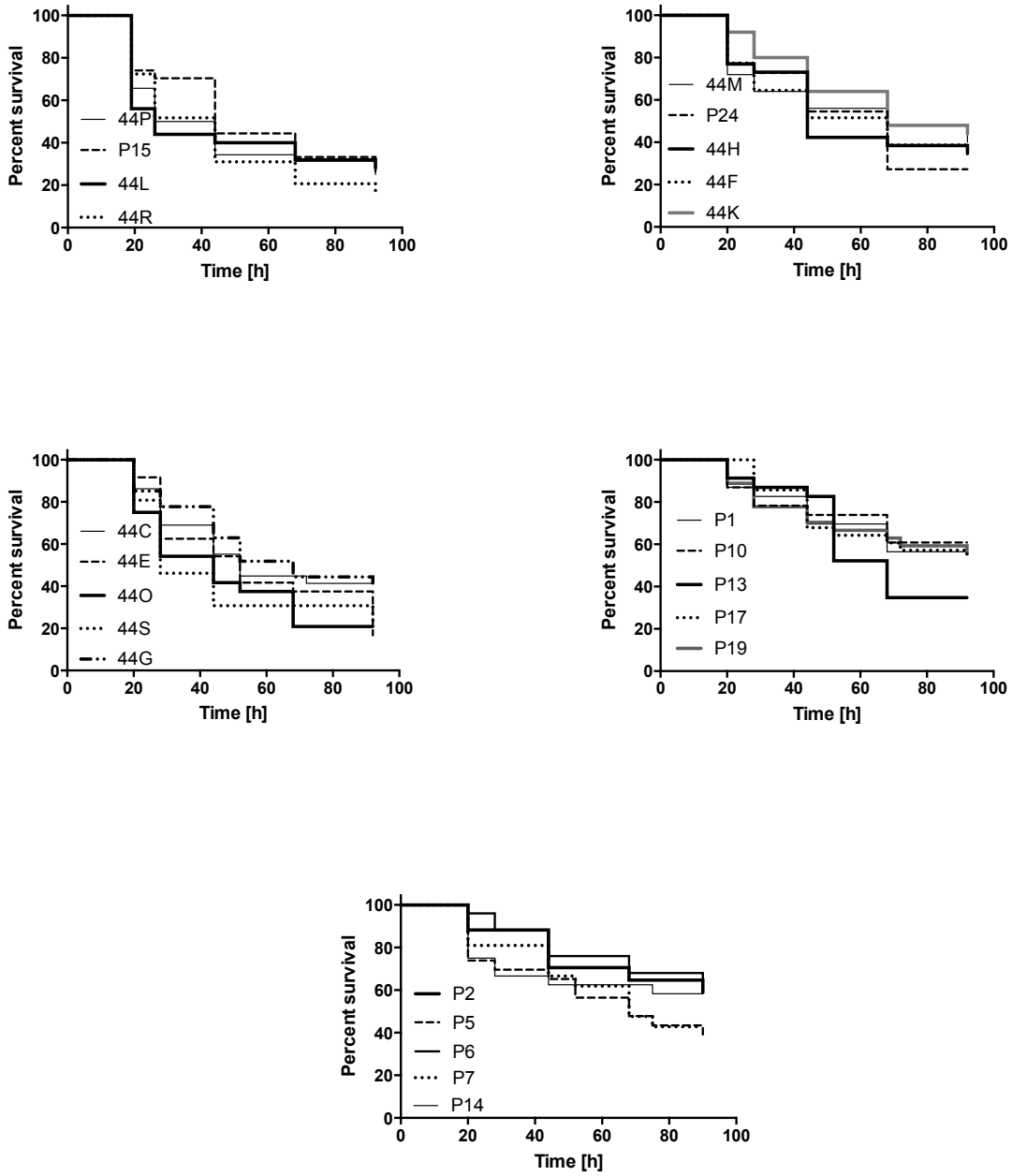


Figure 3.27 Survival rate of zebrafish embryos injected with various strains from the SCBU ST 2371 MRSA outbreak

Each experiment was performed once and no statistically significant differences were seen by pairwise comparison (n=30).

3.4 Discussion

To date, no method exists to enable clinicians to accurately predict *S. aureus* disease course and outcome in an individual patient. It is imperative to better understand microbial determinants of virulence to establish more effective clinical management. The aim of this chapter was to align clear differences in pathogenesis between related *S. aureus* strains with in-depth genomic data to reveal candidate genomic fingerprints associated with virulence. The output from such a model could have wide applications ranging from the proposal of new vaccine or anti-staphylococcal therapy targets tailored to individual bacterial strains through to predictive ability of host outcome using novel information regarding host:pathogen interactions.

Currently, 40% of the *S. aureus* genome has unknown function (personal communication, Dr Matthew Holden, University of St. Andrews). Whilst it is possible to mine the genome for genes that correlate with severe disease at certain sites, as has led to the discovery of phenol soluble modulins (PSMs), translating those data across the range of clonal complexes and types of infection is difficult (Wang et al., 2007). A major strength of our approach was the use of an *in vivo* screening model, the zebrafish embryo, which has a functional innate immune system. More specifically, this is the only vertebrate model that allows a high level of throughput in the absence of host variation. Another advantage is the unbiased approach of a representative set of clinical MRSA strains that enabled pursuit of unknown virulence determinants. To prove the principle of this approach, a well-characterised collection of ST239 MRSA strains were chosen. A comprehensive picture of the population genetic structure of HA-MRSA is not yet known but knowledge in this area is expanding (Holden et al., 2013; Harris et al., 2013).

By using this novel approach to phenotypic:genotypic analysis, this project aimed to supersede the more standard screens for novel virulence determinants in well known pathogens (Shin et al., 2006). Curiosity as to why certain strains of *S. aureus* are more virulent is longstanding and acknowledging this difference led to the recent discovery of novel cytolytic peptides in CA-MRSA (Wang et al., 2007). This was prompted by the recognition of such peptides in *S. epidermidis*. Whilst such approaches are necessary and fruitful, in this project, a vertebrate *in vivo* model of infection was coupled to

genomic information. Unfortunately, this approach was unsuccessful for two main reasons: i) genetically related strains with virulence differences in the zebrafish assay often had multiple SNP differences and the difficulty in recreating such mutations, within a particularly genetically recalcitrant background, was under-estimated; ii) genomic sequencing data for ¾ of the initial strains taken forward for further interrogation was inaccurate and therefore, further analysis could not be conducted.

The errors in the sequencing data could be a result of several factors. The strains were collected from various hospitals and sent to the Wellcome Trust Sanger Institute. The arrangements were not consistent and in some instances, genomic DNA was sent from the donor institution and in other cases, the strain itself was sent on agar slopes. Recording and stocking in the Sanger Institute library would have occurred by different people over an extended period of time. Therefore identifying potential error pathways is challenging and time-consuming. When sequence data from the constructed plasmids pEJ3, pEJ4 and pEJ5 did not match the SNPs expected according to the original WGS data, all strains of interest were sent for re-sequencing. Three quarters of the groups of the strains with significant differences in the virulence assays i.e. Groups 1 and 4, had a completely un-matching repeat sequence. For example, the sequence was from unrelated ST strains or possibly contaminated with DNA from other organisms. Therefore, to still use the phenotypic data would require re-analysis of the potentially important SNPs. But perhaps more importantly, as the strains were received in Sheffield from the Sanger strain collection, it is possible that the incorrect strains were sent originally and so re-analysis of the virulence phenotype would also be prudent. Given the inconvenience and time-scale involved, two smaller, correctly stocked and verified sequenced strain collections were interrogated but unfortunately did not yield any significant phenotypic differences to pursue further. This is likely because the number of SNP differences between strains from these nosocomial outbreak collections was extremely small (Figures 3.24 and 3.26).

As this project was collaborative, the strains were kindly delivered in batches and the sequencing runs were carried out off site (Wellcome Trust Sanger Centre). Whilst many similar collaborations are fruitful, reliance on external parties in this project in part contributed to its failings. From the outset, it would have been helpful to re-confirm that the correct ST239 MRSA strains were sent and that the sequencing data that was

heavily used throughout the project corresponded with such strains. As the original sequencing of these isolates dated back to before 2010, it would have been prudent to re-sequence key isolates at the outset.

Other hurdles encountered during the project included the limited number of strains that can be phenotypically screened in the zebrafish model in a given experiment. It is important that strains are injected within a 2 hour time window, otherwise the development stage of the embryos could impact on outcomes as the immune system matures. Despite being relatively high throughput compared to murine models, day to day batch variation in the embryos can occur and a standard strain of known virulence could not be incorporated into every experiment as otherwise, genetically similar strains could not be screened in the identified groups of 3 or 4. Another caveat is that *S. aureus* is known to possess human specific virulence factors that would not have been picked up using this type of screen. Humanised murine and zebrafish models are currently in development (Knop et al., 2015).

Regarding the difficulties in recreating mutants in the clinical strain background, it is feasible that incompatible RM systems prevented plasmid DNA from pEJ02 integrating into the ST239 R35 genome. Since work on this project ceased, more impediments to genetic manipulation have been overcome. The host derived methylation patterns that protect DNA from being degraded are specific to clonal complexes. Clonal complex specific *E. coli* cloning hosts that express type I RM genes now allow direct transformation into a wider repertoire of lineages (Jones et al., 2015; Monk et al., 2015). However, even with such technology, homologous recombination events that allow mutations consisting of a single SNP are difficult to achieve in different genetic backgrounds. The chromosomal copy of the area of interest must be identical in both genetic backgrounds otherwise, a mosaic of the area of interest could be created once single cross-over integration has occurred.

The aim of the screen was to identify a tangible number of genetic targets to further investigate but one of the main problems with the global ST239 strain collection was that neighbouring strains were not necessarily genetically similar. As demonstrated in Table 3.4, large numbers of genetic differences between strains were identified and it was not feasible to pursue them all. It may be that many of the synonymous SNPs had little functional impact but only thorough molecular biological analysis could this be

proved. The large number of SNP differences was not anticipated at the outset and perhaps a different approach as detailed below would be better served to analyse polymorphisms that may explain phenotypic differences across a large number of distinct strains. One advantage of identifying the *saeS* gene was that a notable phenotype i.e. change in haemolysis could be investigated in neighbouring strains. The other identified mutants had ill defined phenotypes which was encouraging insofar as they may have represented novel virulence factors but phenotypic characterisation other that the zebrafish virulence assay was not available.

Notwithstanding the problems faced during this specific approach to identifying novel virulence determinants of *S. aureus*, it remains an important goal to marry phenotypic and genotypic data in this genomic era. Predicted genomes lack functional annotation and other approaches could be used to progress in this area. As aforementioned, microbial genome wide association studies (GWAS) have gained popularity in recent years. Prior to this, it was eukaryotic geneticists who mainly used this technique. In short, it allows testing of large numbers of SNPs within a population of organisms for statistically significant differences related to a particular phenotype (Read and Massey, 2014). In *S. aureus*, phenotypes such as *in vitro* cytotoxicity and vancomycin-intermediate resistance have been used in GWAS studies and association with certain polymorphisms has been noted (Laabei et al., 2014; Alam et al., 2014). It is likely that if sufficiently high throughout techniques with *in vivo* models are developed, this approach could also be undertaken using zebrafish assays for example.

However, as has been done in other organisms, genetic fingerprint identification is not only limited to using whole genome sequencing data. Employing comparative genomic hybridisation in *Entamoeba*, analysis of divergent regions allowed identification of certain patterns associated with more or less virulent strains (Shah et al., 2005). A consideration to this approach may be that organisms constituting part of the colonising microbiome such as *S. aureus*, are likely to have very similar genomes to those that go on to cause infection, not least because the majority of patients are infected with their own colonising strain (Gordon and Lowy, 2008). *Streptococcus suis* is not a human commensal but can cause zoonotic infections through ingestion of poorly cooked pork products (Hughes et al., 2009). A recently published study used *S. suis* WGS and clinical data to undertake discriminant analysis of principal components (DAPC). The

severity of infection corresponded with particular genomic patterns, suggesting that the outcome of interaction of this bacteria with a host is, at least in part, dependent on the bacterial genome. For commensal organisms such as *S. aureus,* such direct associations are likely to be more difficult to describe, as commensal strains may be genetically similar to invasive strains but simply seizing the opportunity to enter the host.

This ability for the human host to co-exist with *S. aureus* in the absence of infection no doubt contributes to the difficulty faced when attempting to unravel host-pathogen interactions. Once a colonising strain takes advantage of a portal of entry such as a skin wound or during surgery, it must then diversify its functions in order to survive and cause an infection. It therefore follows that any analysis of genetic polymorphisms must take into account rapid changes that occur under selective pressure i.e. during *in vivo* infection (Jenkins et al., 2015).

Finally, in addition to GWAS, other approaches that could be considered to achieve our initial aim include Rapid Virulence Annotation (RVA), which aims to identify virulence determinants through simultaneous screening of bacterial DNA through multiple (invertebrate and vertebrate) infection models. Conserved regions of importance are identified and correlated across the different models yielding potential virulence loci within the bacteria. Using the emerging human pathogen, *Photorhabdus asymbiotica,* the authors of this approach are now attempting to understand the biological significance of the identified loci (Waterfield et al., 2008).

Given the level of human disease caused by *S. aureus*, it would be remiss to not consider host factors. It is well established that host susceptibility limits or promotes infection with *S. aureus* but the picture is far from simple (Shukla et al., 2015). In a recent attempt at evaluating the entire human genome for variants that promote for susceptibility to severe *S. aureus* infection, no single polymorphism reached statistical significance highlighting the underlying complexity of individual immune responses to *S. aureus* (Nelson et al., 2014). Identification of novel virulence determinants and host:pathogen interactions in non-human infection models is the first step, but translation to the human host is the ultimate goal.

In this chapter, it has been demonstrated that novel virulence determinants could not be identified using the approach. The attempt has highlighted that multiple SNPs are likely

to account for virulence differences between even related strains and genetic background differences must be borne in mind when extrapolating data from other clonal complexes. Addressing how best to functionally annotate the wealth of emerging 'omics' data remains a significant challenge.

Chapter 4. Identification of *S. aureus* genes required for growth on human blood

4.1 Introduction

The pathogenicity of *S. aureus* requires a multitude of virulence factors that are intricately co-ordinated and regulated. Several excellent reviews exist which summarise the breadth of factors that are required to ensure the pathogen is successful within the human host (Gordon and Lowy, 2008; Powers and Wardenburg, 2014). In addition to the more 'classic' virulence factors such as pore-forming toxins and superantigens, fundamental metabolic processes of bacteria have also been recognised as a prerequisite for virulence. Many of the current therapeutic strategies against microbes focus on disrupting essential metabolic processes such as protein synthesis (Chopra and Roberts, 2001); DNA synthesis (Drlica et al., 2008); cell wall biosynthesis (Schneider and Sahl, 2010) and folate synthesis (Proctor, 2008). However, improved understanding of the correlations between such essential processes and virulence may provide further therapeutic strategies to be explored.

Microbial fitness during pathogenesis requires efficient utilisation of available nutrients and a requirement for *de novo* synthesis remains as bacteria are auxotrophic for certain components (Brown and Stocker, 1987; McFarland and Stocker, 1987; Faith et al., 2012). The link between metabolism and pathogenesis however, extends further. Dynamically altering metabolic status, such as occurs during persister formation can improve survival under antibiotic exposure (Keren et al., 2004). In addition, strategies to overcome the nutrient limited environment *in vivo* are well described (Hammer and Skaar, 2011) as are upregulation of peptide or amino acid transport mechanisms across a range of animal models (Coulter et al., 1998). Investigating the enteric pathogen *Yersinia enterocolitica*, it was revealed that global regulatory systems can respond to environmental cues and adjust metabolism to enhance virulence (Heroven and Dersch, 2014).

Survival and growth in human blood is critical to *S. aureus* pathogenesis (Alonzo et al., 2012). There are many disparate *in vivo* environments to which the bacteria must adapt

and flexible metabolic capability is paramount. Knowledge of the bacterial genes critical for growth of *S. aureus* in human blood would provide improved understanding of the substrates and biosynthetic pathways necessary for disease. The ultimate goal would be the identification of potential novel targets for treatment of invasive infections. Previously, nucleotide biosynthesis has been identified as being critical for growth of *S. aureus* and other bacteria specifically in human blood (Samant et al., 2008). Using human serum, the authors identified purine and pyrimidine biosynthesis as essential for the success of the pathogen as *de novo* synthesis was needed *in vivo* due to the presumed scarcity of such nucleobases in human blood.

Previously, the transcriptome of the *S. aureus* USA300 LAC strain was analysed during a 2-hour incubation in 100% heparinised human blood. However, the study predominantly focused on upregulation of host inflammatory cytokines and receptors and detailed studies of the growth requirements of *S. aureus* on human blood are lacking (Malachowa et al., 2011). A mutagenized library of MSSA strain HG03 was constructed and all strains were represented in an inoculum to assess competitive growth in *ex vivo* whole human blood or an *in vivo* mouse abscess infection model (Valentino et al., 2014). Bacteria were recovered and transposon insertions were identified relative to a nutrient broth outgrowth control. Providing an internal control, many genes known for their importance in *S. aureus* pathogenicity were identified but importantly, metabolic pathways were described including nucleotide biosynthesis *in vivo* and in *ex vivo* fluids. Whilst this study itemized many metabolic genes of potential importance during infection, further interrogation or biological validation was not carried out. The aim of this chapter therefore was to screen a *S. aureus* transposon (Tn) mutant library in order to identify genes associated with virulence. The hypothesis was that establishing human infection i.e. a bacteraemia would require not only immune evasion strategies but also mechanisms to acquire scarce nutrients in this hostile environment.

Transposition based systems for *S. aureus* mutants have been available for many years allowing chromosomal genes to be disrupted before phenotypic testing is carried out. The frequency and randomness of transposon insertion is key to the usefulness of the created mutant library. Tn917 has been used successfully in both *S. aureus* and *S. epidermidis*, but hot spots for insertion were seen, rendering this transposon sub optimal

as rounds of enrichment may be needed (McDevitt et al., 1994). As such in 2004, Bae *et al.* transformed *S. aureus* strain Newman with two plasmids: pFA545 which encodes the *mariner* transposase in addition to tetracycline and ampicillin resistance markers; and pBursa containing a minimariner transposable element (*Bursa aurealis*), a temperature sensitive plasmid replicon and chloramphenicol resistance gene. *Bursa aurealis* is 3.2 Kb encompassing the mariner terminal inverted repeats (TIR), a promotorless *Aequorea victoria* green fluorescent protein (*gfp*), the R6K replication origin and the erythromycin resistance cassette (*ermB*) (Bae et al., 2004). Using erythromycin as the selectable marker and temperature variation to encourage chromosomal insertion, DNA fragments were PCR amplified using transposon primers. Sequence preference was not seen unlike when Tn917 was used. Using this Tn library in a nematode infection assay, 70% of mutants that caused decreased host killing carried insertions in metabolic genes. Not surprisingly, many of these showed normal growth in the nutrient rich laboratory media, tryptic soy broth, highlighting the need for assays that better recapitulate the *in vivo* complexity of host:pathogen interactions.

To further support studies of pathogenesis, the Nebraska Transposon Mutant Library (NTML) was recently constructed in the CA-MRSA USA300 JE2 strain, deposited in the Network on Antimicrobial Resistance in *S. aureus* (NARSA) strain repository and is freely available to registered users. This library has also been created using the *mariner* based transposon (*bursa aurealis)* using the same methodology as Bae and colleagues in 2004 (Fey et al., 2013). After transposon integration into the chromosome, genomic DNA was extracted from putative mutants to determine the Tn insertion sites by sequencing the nucleotides containing the end of the transposon in addition to those adjacent. The precise location of each transposon insertion was identified by comparison with the USA300_FPR3757 genome sequence and genes with the Tn inserted near to the 5' end were included in the final library (www.narsa.net). The choice of strain for this transposon library is topical. USA300 JE2 has been a major circulating MRSA strain, particularly in the USA for over a decade and its complete genome has been published (Diep et al., 2006). The prevalence of this strain and the global goal of establishing improving control strategies support the use of JE2 in this Tn library. JE2 is a plasmid cured derivative of Los Angeles County (LAC) jail USA300 strain enabling genetic manipulation (Kennedy et al., 2008).

To date, the NTML library has been used to carry out diverse screens to identify genes involved in *S. aureus* antibiotic persistence *in vitro* (Yee et al., 2015); altered haemolytic activity on rabbit blood agar (Fey et al., 2013; Bose et al., 2014); polymicrobial interactions (Michelsen et al., 2015) and hyaluronidase activity (Ibberson et al., 2014). Therefore a high throughput comprehensive approach to identify genes involved in the growth of *S. aureus* on human blood was undertaken using this ordered Tn library of non-essential genes.

4.2 Aims of this chapter

i. to identify genes that are required for growth on human blood
ii. to use infection models to assay pathogenesis of identified mutants *in vivo*
iii. to interrogate how microbial survival is influenced by its environment.

4.3 Results

4.3.1 Phenotypic screen of the NTML *in vitro*

The entire NTML (kindly received from Dr Kenneth Bayles, University of Nebraska Medical Centre) was deconvoluted to 96-well plates and individual bead stocks. Each mutant was recorded in a database with the corresponding 96-well plate co-ordinates and strain ID number that matched the NARSA strain ID. For example, enterotoxin K (*sek*; USA300_0800) has strain ID NE 1255 and is located on plate 4B, well A7. This work was conducted in collaboration with Dr John Connolly (University of Sheffield).

Using the method described in Section 2.18, the library was screened by inoculation on the solid media listed below (i-iv). The main phenotype of interest was growth on anti-coagulated human blood agar i.e. the only source of nutrients being the blood itself. The rationale for including other media was that if a human blood growth phenotype was identified, further information might be extracted from the ability or inability of the mutant to grow on serum or haemolyse red blood cells (RBCs). Bovine serum agar provided an alternative to human serum, which reduced the number of human donors required for the screen. Growth was examined only on this media. In addition to human blood, haemolysis was also assessed on the standardised medium of 5% (v/v) sheep blood with Columbia agar as has been previously used (Chow et al., 1983). Columbia

agar provides a rich nutrient source to enable bacterial growth. Pilot data demonstrated that the optimal media to use in screening for these phenotypes were (Connolly, 2016):

i. 30% (v/v) human blood agar incubated anaerobically for 48 hours
ii. 50% (v/v) bovine serum agar incubated aerobically 37°C for 48 hours
iii. 5% (v/v) sheep blood with Columbia agar incubated aerobically at 37°C for 16 hours followed by 4°C for 4 hours to allow for beta-haemolysis
iv. BHI agar containing erythromycin (5 μg ml^{-1}) and lincomycin (25 μg ml^{-1}) to ensure there were no contaminants and to indicate that the transposon was likely to be present.

After incubation, all strain phenotypes were recorded according to colony morphology, growth and haemolysis (Connolly, 2016).

A flow diagram displaying the screening and selection of strains for further analysis is shown in Figure 4.1. From the 1,920 tested, 100 strains had a growth or haemolysis phenotype in one or all conditions tested and these were individually selected and patched again onto the various media to confirm the phenotype. Of these, 68 retained the original phenotype on the three media. Only the 46 strains which had a phenotype on human blood only (23 strains) or human blood plus other media (23 strains) were taken forward for further work (Table 4.1).

As secondary site mutations may occur during Tn library generation, attempts were made to transduce all 46 strains of interest into both the existing genomic background, USA300 JE2 CA-MRSA strain and the well-used laboratory strain, SH1000. In total, 33 out of 46 strains produced colonies on selective plates after transduction but only 31 were confirmed as containing the Tn in the expected gene by PCR using primer pairs designed 400 bp upstream (forward primer) and downstream (reverse primer) of the recorded transposon insertion site (Connolly, 2016). Separation of PCR products by 1% (w/v) agarose gel electrophoresis gave product sizes of approximately 4 Kb in transposon mutants (3.2 Kb transposon insertion plus 800 bp from the primer design). To better distinguish clear phenotypes in growth and haemolysis, further patching onto either 30% (v/v) human or rabbit blood was done to assess growth and either 5% (v/v) human or sheep blood plus Columbia agar to look for haemolysis differences. Only 9

out of 31 mutants retained the initial phenotype suggesting that the phenotypes in the other 22 mutants may not be the result of the transposon insertion and possibly due to disruption in unrelated parts of the genome. Therefore, these 9 mutants were selected for further analysis due to their distinct phenotypes (Table 4.2). Encouragingly, mutants known to play a significant role in haemolysis (*agr*, *sae*, *hla*) were identified with a haemolysis phenotype in the screen (dark grey boxes) but as these are already characterised virulence determinants, they were not pursued further in this project (Xiong et al., 2006).

4.3.2 Initial analysis of strains of interest both *in vitro* and *in vivo*

As seen in Table 4.2, various phenotypic combinations were seen across the different media tested, in the now confirmed and transduced mutants. In particular, three (white boxes) showed interesting growth phenotypes, *purA*, *purB* and *pabA,* and were extensively pursued further both *in vitro* (Section 4.3.2.1 and Section 4.3.2.4) and *in vivo* (Section 4.3.2.2 and Section 4.3.2.5). In addition, six strains (light grey boxes) displayed haemolysis phenotypes of interest on human blood and were further examined *in vivo* using the zebrafish embryo model of infection as described in Section 4.3.2.3 (Figure 4.7).

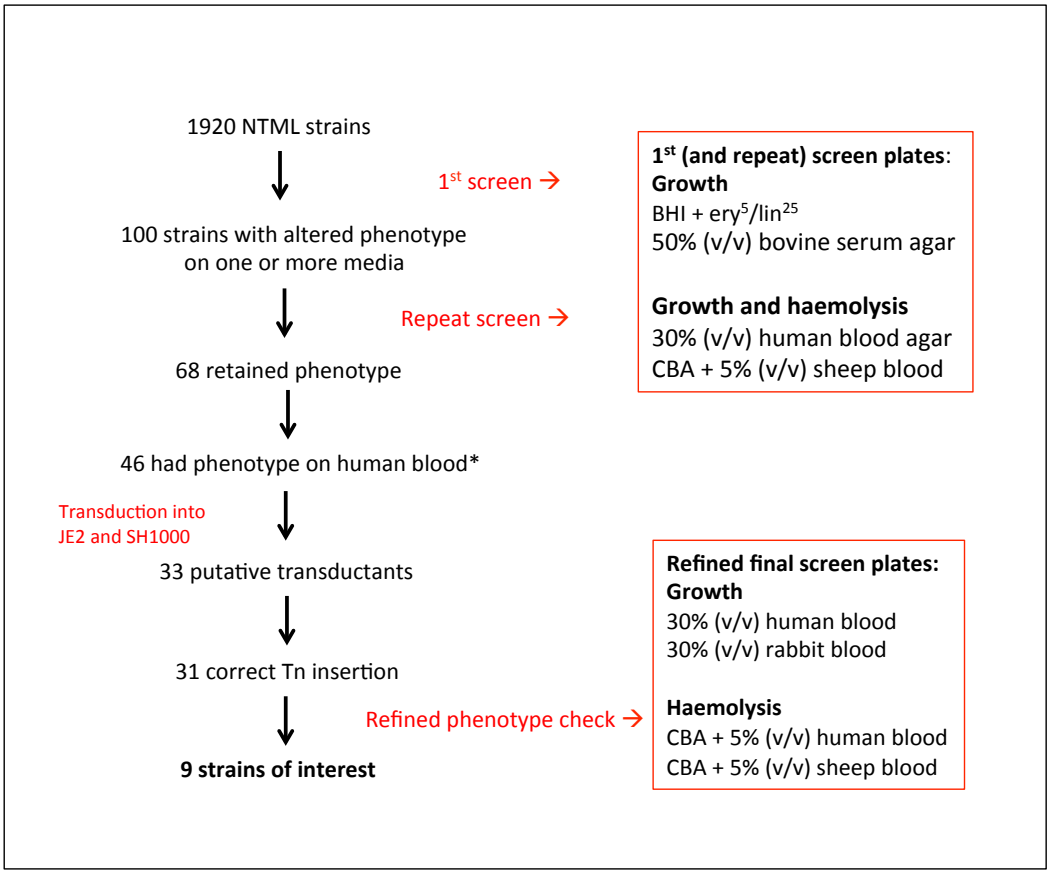


Figure 4.1 Workflow chart displaying NTML phenotypic screen to identify strains of interest

* Human blood and/or at least one of the other media

Superscript numbers shown antibiotic concentrations used.

NARSA #	Gene Name	Screen Conditions		
		30% Human Blood Agar	5% Sheep Blood + Columbia Agar	50% Bovine Serum Agar
NE27	*nos*	Slightly reduced growth	------	------
NE92	*qoxA*	Reduced growth. No haemolysis	------	------
NE95	*agrB*	No haemolysis. Opaque pigmentation	No haemolysis	------
NE229	-	Reduced growth and haemolysis	Highly reduced haemolysis	------
NE427	*fumC*	No haemolysis. Opaque pigmentation	------	------
NE460	*atl*	Opaque pigmentation	------	------
NE522	*purB*	Reduced growth	Reduced haemolysis and growth	Highly reduced growth
NE529	*purA*	Reduced growth	Increased haemolysis	Highly reduced growth
NE547	*odhA*	Reduced growth	------	------
NE552	*nikD*	Slightly reduced growth	------	------
NE573	*ribBA*	Slightly reduced growth	------	White opaque pigmentation
NE594	*gltA*	Slightly reduced growth	------	------
NE635	*ribE*	Reduced growth	------	------
NE821	*pabA*	Reduced growth	------	------
NE857	*nirB*	Opaque pigmentation	------	------
NE873	*agrC*	No haemolysis. Opaque pigmentation	No haemolysis	------
NE884	*nikC*	Reduced haemolysis and slightly reduced growth	------	------
NE896	-	No haemolysis	------	------
NE912	*clpP*	Reduced growth	Reduced haemolysis and growth	Reduced growth
NE945	*brnQ*	Highly reduced haemolysis.	------	------
NE1048	*pyrP*	No haemolysis	------	Slightly reduced growth
NE1063	*pabB*	Increased haemolysis and reduced growth	------	------
NE1236	-	Increased haemolysis	------	------
NE1253	*murQ*	Increased haemolysis	------	------
NE1260	*pckA*	Increased haemolysis	------	------
NE1267	-	Increased haemolysis	Increased haemolysis	------
NE1296	*saeS*	No haemolysis	Highly reduced haemolysis	------
NE1299	-	Increased haemolysis	------	------
NE1304	*araC*	No haemolysis	------	------
NE1315	*mecA*	Increased haemolysis	------	------
NE1354	*hla*	No haemolysis	Highly reduced haemolysis	------
NE1391	*odhB*	Reduced growth	Highly increased haemolysis	------
NE1404	*mreC*	Highly reduced haemolysis.	------	------
NE1434	*ctaB*	No haemolysis. Reduced growth	------	------

NE1509	*abcA*	Reduced haemolysis. Opaque pigmentation	------	------
NE1532	*agrA*	No haemolysis. Opaque pigmentation	None haemolysis	------
NE1536	*gcvH*	Reduced growth	Increased haemolysis	------
NE1543	*qoxC*	No haemolysis. Slightly reduced growth	------	------
NE1604	*nikE*	Slightly reduced growth	------	------
NE1610	*lpdA*	Highly reduced growth	Reduced growth and reduced haemolysis	Reduced growth
NE1622	*saeR*	No haemolysis	Highly reduced haemolysis	------
NE1659	-	Highly increased haemolysis	Highly increased haemolysis	------
NE1751	-	Highly reduced growth	------	Slightly reduced growth
NE1770	*sucD*	Highly reduced growth	Reduced growth	------
NE1775	*lipA*	Highly increased haemolysis. Slightly reduced growth	Increased haemolysis	------
NE1908	-	None haemolysis. Opaque pigmentation	No haemolysis	White opaque pigmentation

Table 4.1 Strains identified as having an altered phenotype on human blood agar

----- = No altered phenotype found.

Strain (NARSA #)	Growth Phenotype		Haemolysis Phenotype	
	30% Human Blood	**30% Rabbit Blood**	**5% Human Blood + Columbia Agar**	**5% Sheep Blood + Columbia Agar**
purB (522)	Reduced Growth	Reduced Growth	Increased Haemolysis	Reduced Haemolysis
purA (529)	Reduced Growth	Reduced Growth	Increased Haemolysis	Slightly Increased Haemolysis
pabA (821)	Highly Reduced Growth	Slightly Reduced Growth	------	------
atl (460)	Opaque Colony	Opaque Colony	Increased Haemolysis	------
murQ (1253)	------	------	Increased Haemolysis	Increased Haemolysis
araC (1304)	------	------	Reduced Haemolysis	------
mecA (1315)	------	------	Reduced Haemolysis	Slightly Reduced Haemolysis
odhB (1391)	Slightly Reduced Growth	Slightly Reduced Growth	Increased Haemolysis	Increased Haemolysis
lipA (1775)	Slightly Reduced Growth	------	Increased Haemolysis	------
agrB (95)	------	------	------	Reduced Haemolysis
agrC (873)	------	------	Slightly Reduced Haemolysis	No Haemolysis
saeS (1296)	------	------	------	No Haemolysis
hla (1354)	------	------	------	No Haemolysis
agrA (1532)	------	------	Reduced Haemolysis	No Haemolysis
saeR (1622)	------	------	------	No Haemolysis

Table 4.2 Summary of JE2 strains with altered phenotype changes than remained post-transduction

----- denotes no difference compared to parent

NARSA strain ID shown in brackets

White boxes: strains with a defect in growth on human blood agar which were investigated further

Light grey boxes: strains with altered haemolysis on human blood agar which were investigated further

Dark grey boxes: strains that would be expected to show a haemolysis phenotype due to extensive published literature and hence were not explored further.

4.3.2.1 Analysis of purine biosynthesis mutants *in vitro*

4.3.2.1.1 Growth in nutrient variable liquid media

When grown on 50% (v/v) bovine serum agar or 30% (v/v) human or rabbit blood agar (Table 4.1 and 4.2), both *purA* and *purB* mutants were shown to have significant growth defects. In liquid growth assays, both mutants grew as per the wildtype in rich nutrient broth (BHI) but when in either bovine or human serum no growth was measured indicating that the required nutrients are not present in sufficient quantities in mammalian serum (Figure 4.2).

Much of what is known about purine biosynthesis in *S. aureus* is predicted from purine metabolic pathways that have been characterised in other organisms. *S. aureus*, like other bacteria, are able to synthesis nucleotides *de novo* in addition to using exogenous sources and salvage pathways, the latter of which are more energy conservative (Sonenshein et al., 1993). Even at low concentrations, exogenous purines are preferentially used and synthesise of *de novo* enzymes is reduced. Similar to the genome of *Bacillus subtilis* a purine biosynthesis operon (*purEKCSQLFMNHD)* and purine biosynthesis genes (*purA* and *purB)* exist in *S. aureus.* Although gene topography is similar between the two organisms, *purB* is encoded within the *pur* operon in *B. subtilis*, whereas in *S. aureus* it is located separately (Fox et al., 2007). Other differences in the purine pathways between Gram-positive organisms have also been identified. For example, in *Lactococcus lactis*, *purR* has 80% DNA sequence identity with the same gene in *B. subtilis* yet performs the function of transcriptional activator rather than a repressor in the latter (Kilstrup and Martinussen, 1998).

Due to ongoing salvage, free bases are not usually found intracellularly but extracellular concentration can vary widely depending on the environment. An abscess *in vivo* would provide a rich source for fundamental components of nucleotides released from dying cells and *S. aureus* has transporters to enable efficient uptake of pyrimidine and purine bases from its surroundings. Many factors are involved in regulation of nucleobase uptake, and if amino acid deprivation occurs, the stringent response is activated in *B. subtilis* and purine uptake is inhibited (Beaman et al., 1983).

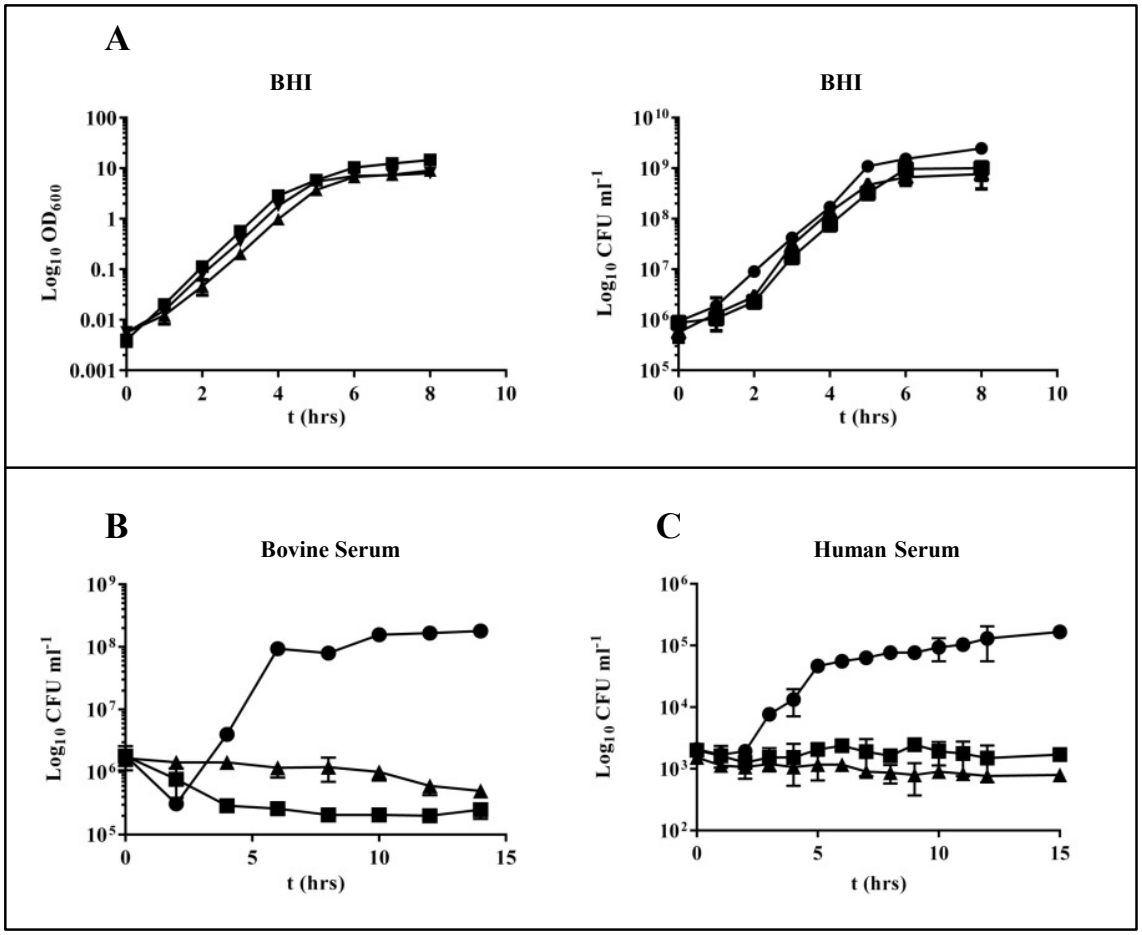


Figure 4.2 Purine biosynthesis mutant growth is prevented in mammalian serum

A Purine biosynthesis mutants have comparable growth to JE2 measured by OD_{600} or CFU in BHI broth.

Purine biosynthesis mutants show reduced growth in bovine serum **(B)** and human serum **(C)**, relative to JE2.

These data represent three independent repeats, error bars represent standard errors.

● = JE2, ■ = JE2-*purB*, ▲ = JE2-*purA*

The purine biosynthetic pathway of *S. aureus* is shown in Figure 4.3. Purines are not synthesized as free bases and the first purine formed is inosine monophosphate (IMP). Nucleic acid bases (purines: adenine, guanine; pyrimidines: cytosine, thymine and uracil) are linked to ribose sugars through N-glycosidic linkages forming nucleosides e.g. adenosine or thymidine. One or more phosphate groups are then bonded to carbon atoms with the sugar molecule forming a nucleotide (e.g. adenosine monophosphate). If the ribose lacks a 2' OH group, then a deoxyribonucleotide is formed e.g. deoxythymidine monophosphate (dTMP) that goes on to be incorporated into DNA. Nucleotides have important functions in addition to being monomers for nucleic acid polymers, such as providing key energy sources for the bacteria and they are also component parts in many cofactors (Todar's Online Textbook of Bacteriology, 2006).

Adenylosuccinate synthetase (PurA) is the enzyme that converts IMP to adenylo-succinate which is converted to adenosine monophosphate by the enzyme adenylosuccinate lyase (PurB). PurB also features upstream in this pathway converting 5'- phosphoribosyl-4-(N-succinocarboxamide)-5-aminoimidazole (SAICAIR) to 5-amino-1-(5-phospho-D-ribosyl)imidazole-4-carboxamide (AICAIR) prior to the conversion of AIRCAIR to IMP via PurH. Therefore, it was hypothesised that the reduced growth of the purine biosynthesis mutants on nutrient poor media *in vitro* resulted from lack of AMP (*purA* mutant) and AMP and GMP (*purB* mutant) implying that exogenous supply would rescue the phenotype.

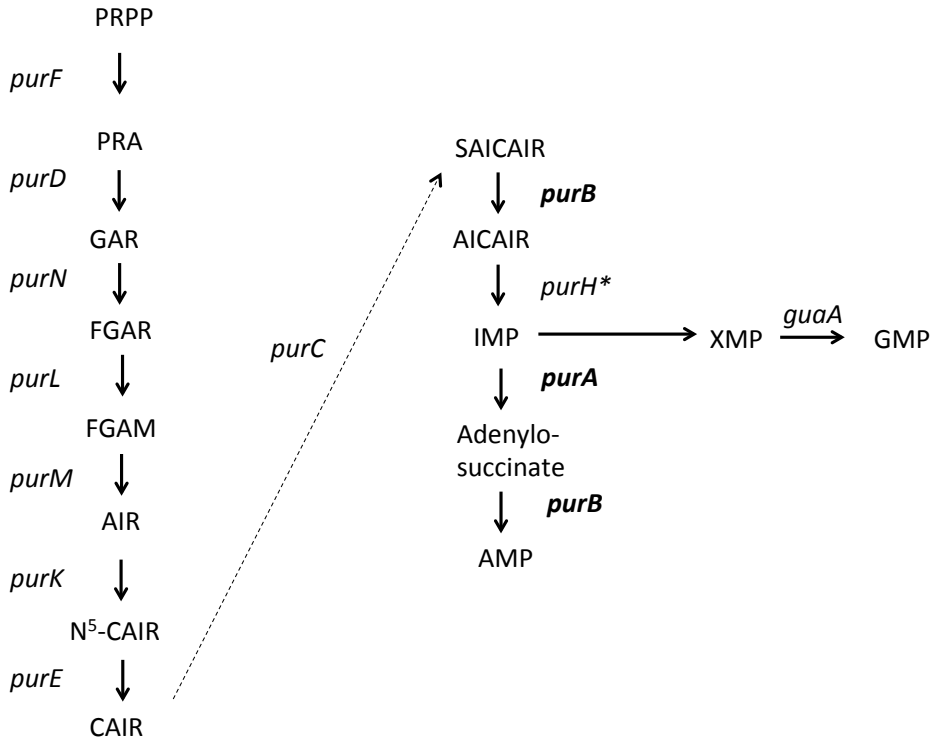


Figure 4.3 The purine *de novo* biosynthesis pathway

(using Kegg and Biocyc websites)

*THF co factor required

purA and *purB* are shown in bold

PRPP 5-phospho-α-D-ribose 1-diphosphate
PRA 5-phospho-β-D-ribosylamine
GAR N1-(5-phospho-β-D- ribosyl)glycinamide
FGAR, N2-formyl-N1-(5-phospho-β-D-ribosyl)glycinamide
FGAM 2-(formamido)-N1-(5-phospho-β-D-ribosyl)acetamidine
AIR 5-amino-1-(5- phospho-β-D-ribosyl)imidazole
N5-CAIR N5-carboxyaminoimidazole ribonucleotide
CAIR 5-amino-1-(5-phospho-D-ribosyl)imidazole-4-carboxylate
SAICAIR 5'- phosphoribosyl-4-(N-succinocarboxamide)-5-aminoimidazole
AICAIR 5-amino-1-(5-phospho-D-ribosyl)imidazole-4-carboxamide
FAICAIR 5-formamido-1-(5- phospho-D-ribosyl)-imidazole-4-carboxamide
IMP inosine monophosphate
Adenylo-succinate N6-(1,2-dicarboxyethyl)-AMP
AMP adenosine-monophosphate.

4.3.2.1.2 Biochemical complementation of purine biosynthesis mutants *in vitro*

To test this hypothesis, chemically defined solid media (CDM) were used to characterise the auxotrophy of these mutants. Adenine or guanine were first tested and as expected from their biosynthetic pathway positions, addition of adenine alone to CDM complemented the *purA* growth back to parental levels but both adenine and guanine were required to re-establish *purB* growth (Figure 4.4 and Table 4.3). Alternatively, a combination of adenine and inosine could complement the growth defect of *purB* (data not shown).

4.3.2.2 Analysis of the role of purine biosynthesis *in vivo*

4.3.2.2.1 Virulence phenotype in the zebrafish assay

Having identified both *purA* and *purB* as having poor growth on human blood, *in vivo* characterisation was sought using the zebrafish embryo model (Prajsnar et al., 2008). *purA* and *purB* were found to be significantly attenuated compared to the wildtype in both the MSSA SH1000 and MRSA JE2 background (Figure 4.5 A, B). In the SH1000 background, neither mutant, when injected at 1500 CFU into the circulation valley of the zebrafish at 30 hpf, caused embryo mortality. The JE2 parental strain is more virulent compared to SH1000 in the zebrafish infection model and thus it was not unexpected that JE2-*purA* and JE2-*purB* caused some host death (<10%). To analyse bacterial kinetics during infection, six live embryos (and all dead embryos) were collected, homogenised and plated out for bacterial CFU enumeration as described in Section 2.19.9 (Figure 4.5 C, D). Neither SH1000-*purA* nor SH1000-*purB* was able to replicate *in vivo* and bacterial numbers decreased during the course of the experiment. This is in stark contrast to the bacterial kinetics observed when parental *S. aureus* is injected at the same dose (1500 CFU) (Figure 4.5 E). In addition, the effect of the neutrophil and macrophage depletion on growth of the mutants was investigated using *pu*.1 morphant embryos as described in Section 2.19.10. As shown in Figure 4.5 F, upon injecting 30 embryos, approximately 10 embryos (30%) remained alive at 90 hpi despite embryos having no neutrophils or macrophages for the first 36-48 hours. In the embryos injected with 1500 CFU of parental *S. aureus*, all embryos had succumbed by 20 hpi as, with no functional immune system, the embryos are overwhelmed with uncontrolled and increasing bacterial numbers as has been previously published (Prajsnar et al., 2008).

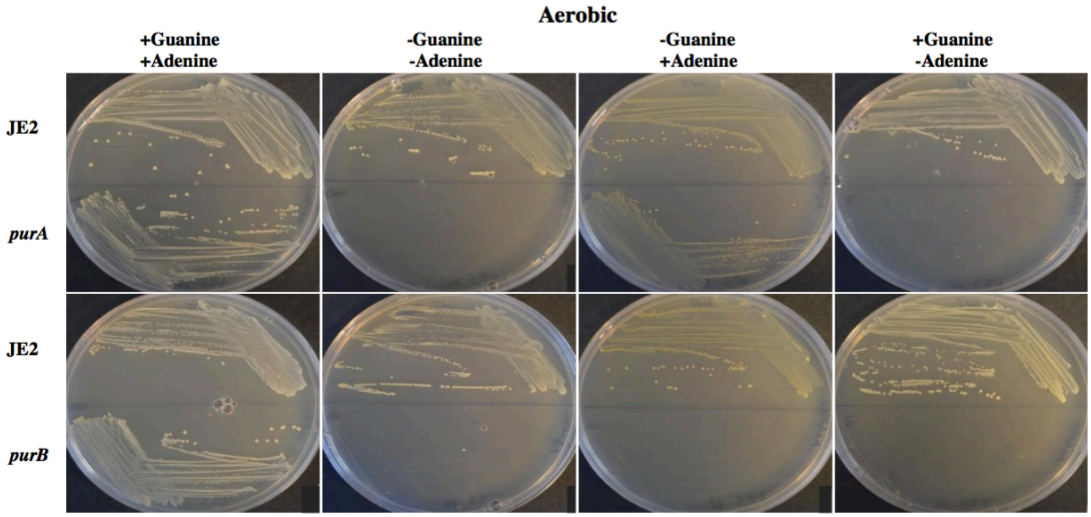


Figure 4.4 Role of adenine and guanine in the growth, on solid media, of purine biosynthesis mutants

CDM solid media must contain adenine for *purA* growth and both adenine and guanine for *purB* growth. Adenine 20 µg ml^{-1}; guanine 20 µg ml^{-1}, plates were incubated aerobically for 24 hours.

Strain	Chemically Defined Media			
	+Adenine +Guanine	-Adenine -Guanine	+Adenine -Guanine	-Adenine +Guanine
Aerobic Growth				
JE2	+	+	+	+
purB	+	-	-	-
purA	+	-	+	-

Table 4.3 Growth analysis on solid media of JE2-*purA* and JE2-*purB* in the presence or absence of adenine and guanine

Adenine 20 µg ml^{-1}; guanine 20 µg ml^{-1}; + growth; - no growth

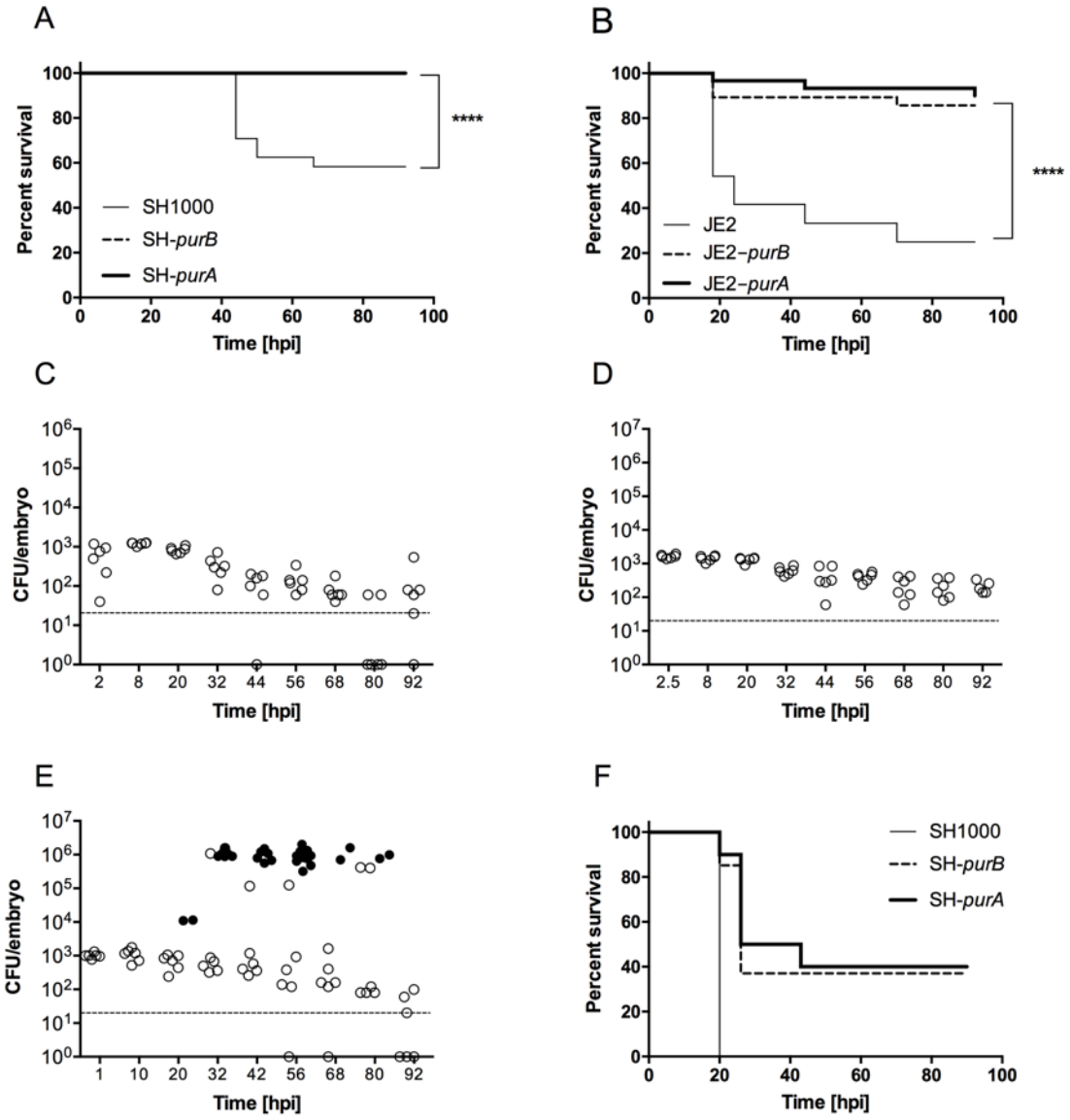


Figure 4.5 *In vivo* attributes of purine biosynthesis mutants in the zebrafish infection model

A Survival curves demonstrating attenuation of SH-*purA* and SH-*purB* compared to SH1000 (n = 30, **** $p < 0.0001$). NB Overlapping data points are seen.

B Survival curves demonstrating attenuation of JE2-*purA* and JE2-*purB* compared to JE2 (n = 30 **** $p < 0.0001$).

Bacterial CFU were determined at regular time points after injection of **C** SH-*purA*; **D** SH-*purB* and **E** SH1000 (n = 60-90). The dashed line represents the limit of detection of the assay (20 CFU). Open circles: live embryos, filled circles: dead embryos.

F Survival of *pu.*1 morphant embryos injected with SH1000, SH-*purA* or SH-*purB* (n=30).

4.3.2.2.2 Biochemical complementation of purine biosynthesis mutants *in vivo*

Next, *in vivo* complementation was attempted by immediate immersion of injected wildtype embryos in purine containing solutions. Guanine could not be used for immersion experiments, as it is only soluble in 5 M hydrochloric acid, which would be toxic to the zebrafish and attempts at neutralising the pH caused the solution to precipitate. Therefore, as was done *in vitro*, inosine was used as it is soluble in water and could be used in conjunction with the optimal fish media. 300 μg ml^{-1} adenine was unable to rescue the virulence phenotype of SH-*purA* (Figure 4.6 A). Adenine and inosine (300 μg ml^{-1} and 400 μg ml^{-1} respectively) combined had no effect on virulence of SH-*purB* (Fig 4.6 B). These doses were chosen because they are approximately 10 times the purine content of CDM. The inability of adenine and/or inosine to biochemically complement virulence *in vivo* may be because such compounds do not penetrate the zebrafish exterior and gain access to the bloodstream and phagocytes, where the bacteria are likely to be residing. In similar work, Ivánovics and colleagues, showed that co-localisation of purine dependent bacteria and purine compounds cannot alone restore virulence in a mouse model of infection (Ivánovics et al., 1968). After injecting adenine biosynthesis deficient mutants of *Bacillus anthracis* into the peritoneal cavity, the authors were unable to rescue the attenuated phenotype by co-injecting adenine at the site of bacterial injection. It may be possible to co-inject the bacteria and adenine/inosine into the circulation valley of the zebrafish embryo but this was not attempted.

It is well established that *de novo* synthesis of purines represents a strict requirement for bacterial growth and persistence in the host i.e. nucleotide limited conditions. Purine auxotrophy attenuates many pathogenic bacteria (Mahan et al., 1993). The NTML screen for growth phenotypes on human blood and the *in vivo* work presented here is in agreement with this prior knowledge. Therefore, it was deemed unnecessary to pursue this work further as it would only serve to confirm previously documented observations.

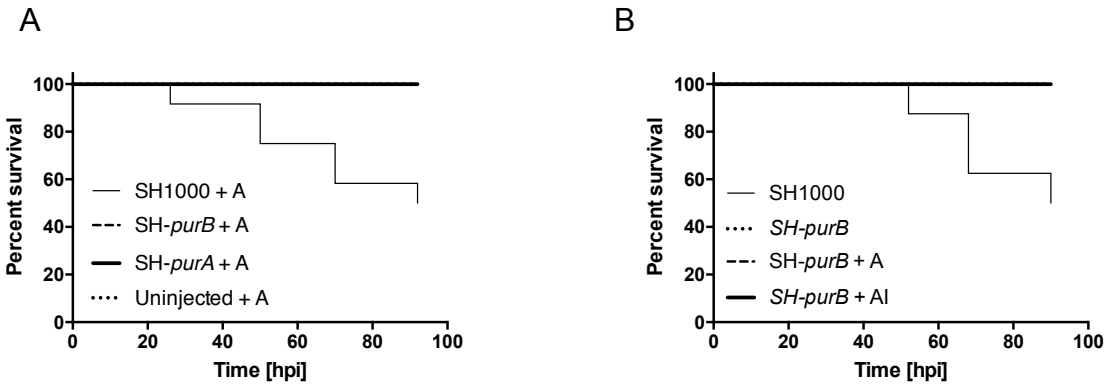


Figure 4.6 *In vivo* complementation of purine biosynthesis mutants in the zebrafish embryo model of infection

A Survival curves after injection of parental SH1000, SH-*purA*, SH-*purB* or uninjected controls and immediate immersion in E3 medium supplemented with adenine (A) 300 μg ml^{-1} (overlapping data points).

B Survival curves after injection of parental SH1000 or SH-*purB* and immediate immersion in E3 medium supplemented with adenine 300 μg ml^{-1} (A) or adenine 300 μg ml^{-1} plus 400 μg ml^{-1} inosine (AI, overlapping data points).

n=30 embryos per group, approximately 1500 CFU bacteria per embryo.

4.3.2.3 Further analysis of the haemolytic strains from the NTML screen

Six strains were identified in the NTML screen as having differences in haemolysis on human blood agar. As pursuing all of these mutants, in addition to the purine and folate biosynthesis mutants, would be too time-consuming, it was decided that the zebrafish infection model would be used to prioritise attenuated mutants to pursue further.

As such, each mutant, alongside the parent JE2, was injected at approximately 1500 CFU in the zebrafish circulation valley at 30 hpf. As shown in Figure 4.7 (A, B), all of the mutants had virulence comparable to the parent. Therefore, in the absence of attenuation *in vivo*, these were not pursued further.

4.3.2.4 Analysis of *pabA in vitro*

pabA is a key gene involved in folate production. Unlike in humans, bacteria *de novo* synthesise folate via the *pab* operon which contains three genes, *pabA, pabB* and *pabC*, converting chorismate to para-aminobenzoic acid (PABA) (Figure 4.8). The active forms of folate, dihydrofolate (DHF) and tetrahydrofolate (THF), are synthesized further downstream. The roles of THF in *S. aureus* metabolism are listed in Table 4.4.

4.3.2.4.1 Unusual growth phenotype of *pabA* on blood vs. blood components

Identified in the initial screen, the *pabA* Tn mutant, had a unique growth phenotype. Growth was highly reduced on 30% (v/v) human blood but had only slightly reduced growth on 30% (v/v) rabbit blood (Table 4.2). This prompted assaying growth on other mammalian species blood agar, which demonstrated that *pabA* grows well on both sheep and horse blood agar (Figure 4.9). To test if specific human blood components might affect *pabA* growth, the parent and mutant were inoculated onto whole blood or blood component agar (Figure 4.9). *pabA* displayed good growth on 50% (v/v) human clotted serum or 50% (v/v) plasma agar but not on 30% (v/v) whole human blood.

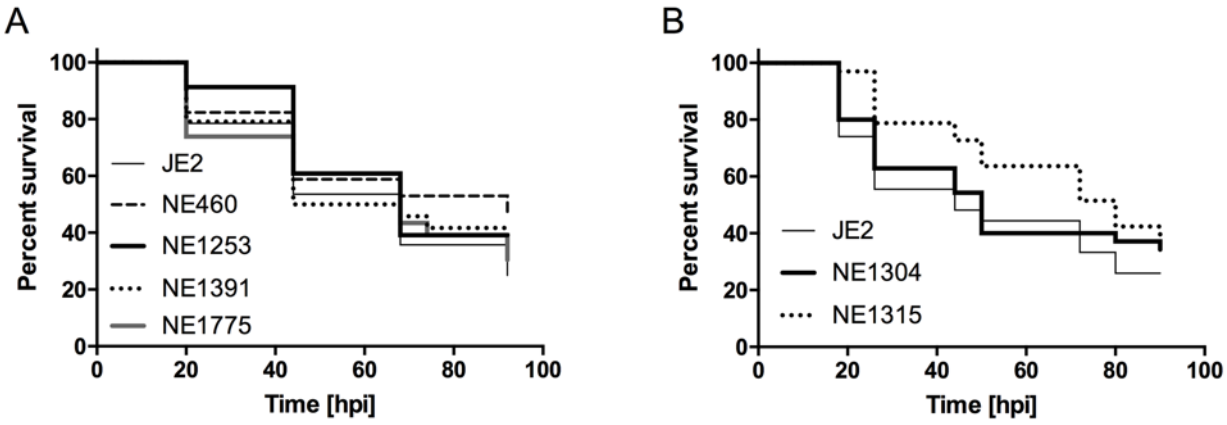


Figure 4.7 Virulence of haemolytic NTML strains in the zebrafish infection model

A Survival curves demonstrating equivalent virulence of 1500 CFU JE2, NE460, NE1253, NE1391 and NE1775 (all mutants vs. JE2 – NS).

B Survival curves demonstrating equivalent virulence of 1500 CFU JE2, NE1304 and NE1315 (all mutants vs. JE2 – NS).

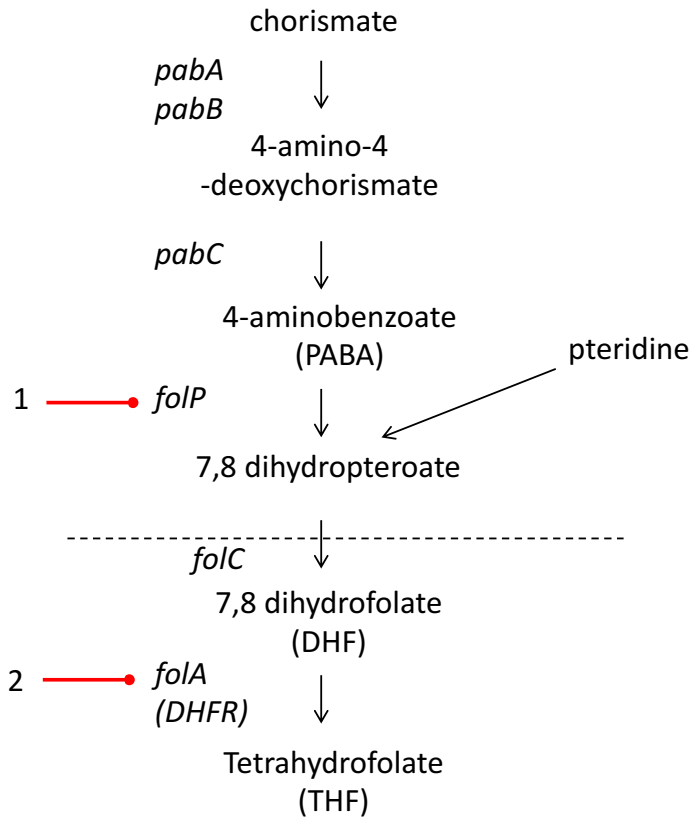


Figure 4.8 The *de novo* folate biosynthesis pathway in *S. aureus*

Below the dotted line represents the part of the pathway present in humans

Red lines highlight the sites of antibiotic action: (1) sulphonamides target *folP* – sulphonamides; (2) trimethoprim targets *folA*

DHFR – dihydrofolate reductase

pabA para-aminobenzoate synthase

pabB para-aminobenzoate synthase

pabC 4-amino-4-deoxychorismate lyase

folP Dihydropteroate synthase

folC Folylpolyglutamate synthase

folA Dihydrofolate reductase.

Action	**Gene involved**
Serine/glycine interconversion	*glyA*
Vitamin B5 (pantothenate) biosynthesis	*panB*
dUMP → dTTP	*thyA*
5,10-methylene-THF → 5-methyl-THF	*metF*
L-homocysteine → methionine	*metH*
THF → 10-formyl-THF	*fhs*
Synthesis of formylate L-methionine charged tRNA	*fmt*
AIRCAIR → FAICAIR	*purH*

Table 4.4 A summary of the roles of folate in *S. aureus* metabolism

glyA serine hydroxymethyltransferase
panB 3-methyl-2-oxobutanoate hydroxymethyltransferase
dUMP deoxyuracilmonophosphate
dTTP deoxythyminemonophosphate
thyA thymidylate synthase
metF 5,10-methylenetetrahydrofolate reductase
metH 5-methyltetrahydrofolate--homocysteine methyltransferase
fhs formate tetrahydrofolate ligase
fmt Methionyl-tRNA formyltransferase
AICAIR 5-amino-1-(5-phospho-D-ribosyl)imidazole-4-carboxamide
FAICAIR, 5-formamido-1-(5-phospho-D-ribosyl)-imidazole-4-carboxamide
purH bifunctional purine biosynthesis protein

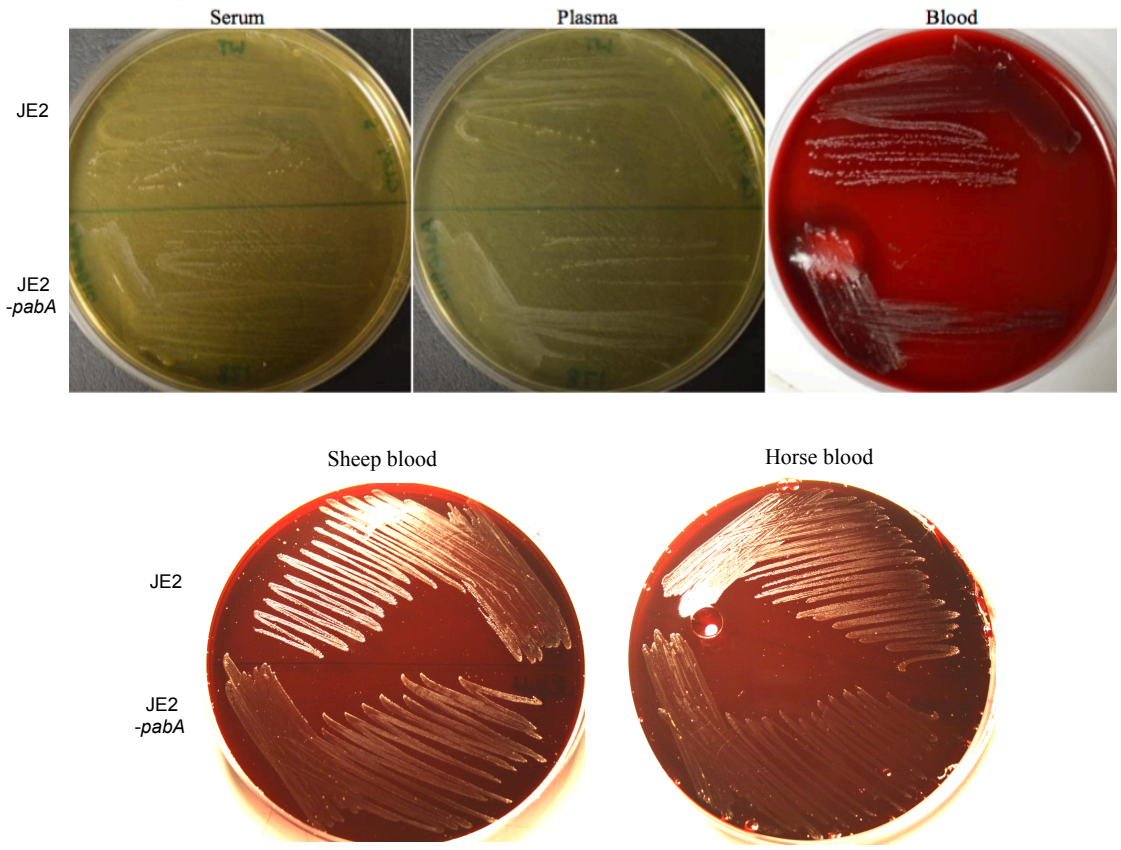


Figure 4.9 Growth of parent and *pabA* strains on human blood/components or mammalian whole blood agar

Human serum and plasma were separated from whole blood samples as described in Section 2.1.6. Plates (50% v/v human serum, 50% v/v human plasma, 30% v/v human, sheep or horse blood agar) were inoculated and incubated aerobically for 24 hours at 37°C.

Colony growth was seen on human blood agar for the parent strain but not *pabA*. Both parent and *pabA* showed good growth on human serum, plasma, sheep and horse blood agar.

In liquid culture, *pabA* growth was not different to that of the wildtype in both BHI, bovine and human serum (data not shown). This is in contrast to the purine biosynthesis mutants, which grew well in liquid BHI but poorly in both bovine human serum where essential nutrients may be lacking. It was reasoned that perhaps the reduced amount of human serum in the 30% (v/v) whole blood agar plates was too low to support growth. Plasma content in the whole blood plates would only be 15% (v/v) as plasma constitutes 50% of whole blood, with the remaining 50% provided by the cellular components, but increasing the plasma volume in whole blood agar plates did not support *pabA* growth (data not shown).

It was next considered that reduced growth on human blood could be due to lack of certain nutrients that are required by a THF-lacking strain. As THF is essential for a variety of biochemical reactions (Table 4.4) to further characterise the auxotroph, CDM was used to understand the mechanism underpinning the lack of *pabA* growth on human blood. Of course, this approach would only yield significant information if the mechanism was, indeed, related to nutritional deficiency.

4.3.2.4.2 Biochemical complementation of *pabA in vitro*

Chemically defined solid media was used to characterise the auxotrophy of *pabA*. CDM agar was made as described in Section 2.1.5 but omitting purines, serine and glycine. Individual plates were made with various combinations of nutrients added back as outlined in Table 4.5. In the absence of all components, both wildtype and mutant grew very poorly. On CDM agar plates lacking 20 μg ml^{-1} adenine and guanine (serine and glycine present) mutant growth was comparable to the wildtype suggesting that unlike in a *pab* deficient *L. lactis*, purine synthesis is not critical for growth (Wegkamp et al., 2007).

In the presence of serine (100 μg ml^{-1}), both parent and *pabA* grew poorly yet in the presence of glycine (100 μg ml^{-1}), *pabA* had a very slight growth defect only (+++ vs. ++++). PABA is a folate synthetic intermediate and has been used in *E. coli* and *S. aureus* to bypass folate deficiency caused by genetic knockout of *pabA* or addition of folate antagonists (Tran and Nichols, 1991; Phetsang et al., 2013). When PABA (20 μg ml^{-1}) was added in addition to glycine, growth of both the parent and mutant were

restored. However, the addition of PABA to CDM did not support parental level growth in the absence of serine and glycine. Furthermore, CDM containing both serine and glycine supported growth of both the parent and mutant to the same degree. This suggests that glycine is critical for *S. aureus* growth which is in agreement with other studies (Townsend et al., 1996). Methionine (50 µg ml^{-1}) was noted to be essential for growth of both the parent and mutant and therefore not pursued further. Vitamin B5 (pantothenate, 400 ng ml^{-1}) was not able to restore growth of *pabA* (data not shown). The addition of thymine (40 µg ml^{-1}) to CDM did not restore full growth of the mutant to parent levels (+++ growth remained) and pyrimidines are not routinely added to standard CDM (unlike purines) as wildtype bacteria have alternative dTMP synthetic pathways.

Interestingly, addition of folic acid to CDM did not restore growth, even in the presence of glycine (data not shown). This may be due to a lack of uptake of folic acid by the bacteria which has been noted in *E. coli* (Tran and Nichols, 1991). It would seem plausible that as bacteria are capable of *de novo* synthesis of THF, transport of exogenous folates is not needed. In a study examining inhibition of folate-targeting antibiotics such as trimethoprim, exogenous folic acid, folinic acid, DHF and THF were not able to antagonise the effect of the antibiotic, suggesting that cellular uptake is not occurring (Hamilton-Miller, 1988).

Overall, it must be noted that growth differences seen on CDM between the parent and mutant, using the various compound combinations, were modest compared to the stark difference in growth on human blood i.e. good parental growth and essentially no growth of the mutant. However, whilst the CDM agar plate experiments provided useful results as to which nutritional requirements the mutant may have, it was considered that subtle growth defects would be difficult to see on solid agar plates so liquid CDM growth assays were also carried out (Figure 4.10). Conducting liquid assays would also eliminate the possibility that useful by-products from the parent, for example, PABA, were leeching across to the mutant on solid agar and aiding growth, which has been reported to occur in *E. coli* parental and mutant strains (Huang and Pittard, 1967).

Using CDM base media lacking purines, serine and glycine, nutrient combinations were added back in growth experiments (Figure 4.10). Only the addition of purines, serine

and glycine could restore growth of the mutant to parental levels (as measured by maximum OD_{600} reached) but the growth rate was slightly reduced compared to the parent (Fig 4.10 G and H). This is in contrast to the outcome of the CDM solid agar experiments where purines were not seen to be necessary.

However, these experiments informed attempts at biochemical complementation of *pabA* on human blood *in vitro*, with the aim of restoring *pabA* growth. As results suggested that a combination of serine, glycine and purines was necessary, those components (purines 20 μg ml^{-1}; serine 100 μg ml^{-1}; glycine 100 μg ml^{-1}) were added to 30% (v/v) human blood agar plates. However, added separately or together, the growth of *pabA* on blood remained poor compared to the parental strain (data not shown). Addition of PABA did complement growth fully (Figure 4.11) as would be expected from the CDM experiments and similar work done in *L. lactis* (Wegkamp et al., 2007).

Despite not having an impact in the CDM experiments, methionine (50 μg ml^{-1}) or thymine was added to human blood plates as both are known to be downstream effectors requiring folate. Methionine had no affect on *pabA* growth (data not shown), but remarkably, the addition of thymine improved mutant growth when added at concentration equivalent to purines used in CDM i.e. 40 μg ml^{-1}. Furthermore, increasing the amount of thymine ten fold in the human blood plates increased growth almost to the level of the parent (Fig 4.11). This was also seen if thymidine (400 μg ml^{-1}) was supplemented instead, indicating that firstly pyrimidines are taken up by *S. aureus* and secondly, that pyrimidines may play an important role in the reduced *pabA* growth on human blood and will be explored further in Section 4.3.5.

Added*	**JE2**	**JE2-*pabA***
-	+	~ +
Purine	+	+
Purines + PABA	+	+
PABA	+	~ +
Serine	+	+
Serine + PABA	+	+
Glycine	++++	+++
Glycine + PABA	++++	++++
Serine + glycine	++++	++++
Serine + glycine + PABA	++++	++++
Methionine	++	++
Methionine + PABA	++	++
Thymine	++++	+++
Thymine + PABA	++++	++++

Table 4.5 Growth of wildtype and mutant on solid CDM base agar with various nutrient combinations

Individual CDM plates were made with various combinations of nutrients added back and incubated for 48 hours at 37°C.

*Doses – purines 20 μg ml^{-1}; serine 100 μg ml^{-1}; glycine 100 μg ml^{-1}; PABA 20 μg ml^{-1}; methionine 50 μg ml^{-1}; thymine 40 μg ml^{-1}.

+ Very poor growth
++ Poor growth
+++ Slightly reduced growth
++++ Normal growth

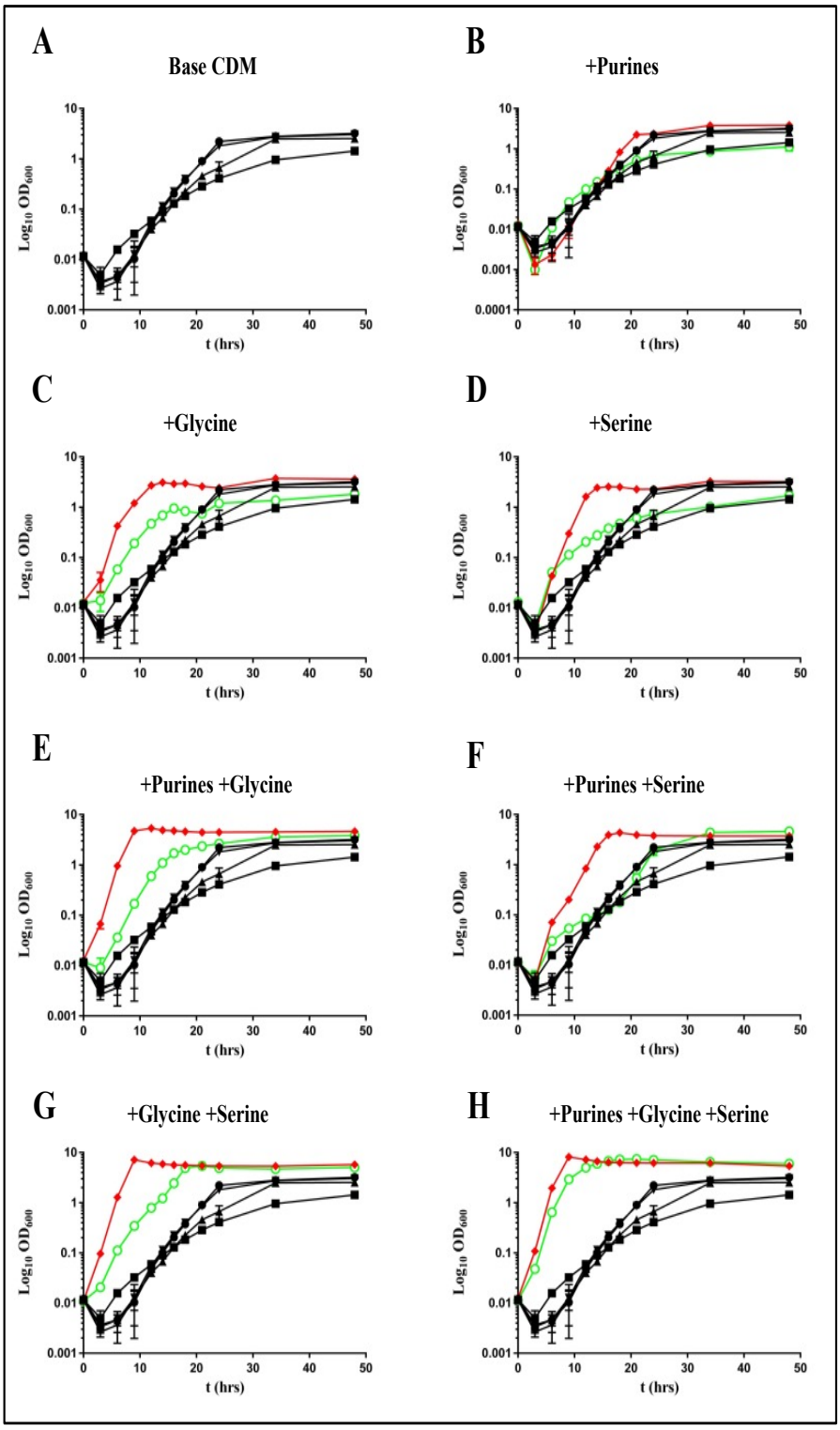


Figure 4.10 Analysis of the JE2-*pabA* phenotype in liquid CDM

Growth of JE2-*pabA* was compared with the parent in CDM base with various nutrient combinations as shown.

● = JE2, ■ = JE2-*pabA*, ▼ = JE2 +PABA, ▲ = JE2-*pabA*+PABA, ♦ = JE2 +nutrients above graph, ○ = JE2-*pabA* +nutrients above graph.

These data represent three independent repeats, error bars show standard errors.

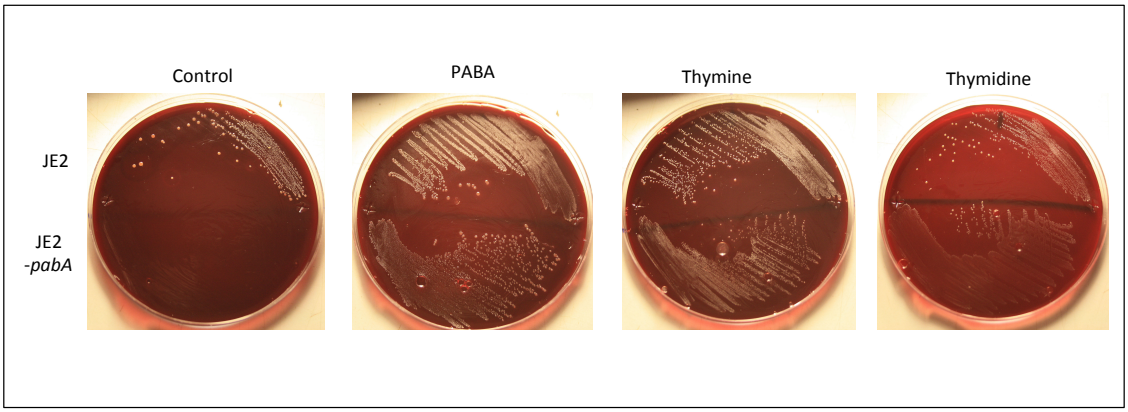


Figure 4.11 Growth of JE2 and JE2-*pabA* on 30% (v/v) human blood agar plates with or without pyrimidines

Plates include: un-supplemented (control); or supplemented with PABA (20 µg ml^{-1}); thymine (400 µg ml^{-1}) or thymidine (400 µg ml^{-1}).

4.3.2.5 Analysis of *pabA in vivo*

4.3.2.5.1 Virulence phenotype of *pabA* in the zebrafish assay

There are no *in vivo* data available regarding the role of *pabA* in *S. aureus* pathogenesis but other species have been examined. Investigating the fungal pathogen, *Aspergillus fumigatus,* a signature tagged mutagenesis and mouse model screen isolated an attenuated strain displaying a mutation in the promoter of *pabA*, highlighting the need for intact folate synthesis during pathogenesis (Brown et al., 2000). Interestingly, whilst *in vitro* folate supplements did not support *pabA* growth, PABA supplementation in the drinking water of infected mice restored virulence *in vivo* but only when given continuously throughout the experiment. Therefore, to investigate the behaviour of the *S. aureus pabA* mutant further, two models of infection were employed.

In the zebrafish embryo, at a dose of 1500 CFU, *S. aureus pabA* was found to be significantly attenuated compared to the wildtype SH1000 or JE2 (Figure 4.12 A, B). To analyse bacterial kinetics during infection, six live embryos (and any dead embryos) were collected, homogenised and plated out for bacterial CFU enumeration (Figure 4.12 C). *pabA* was able to cause a low number of host deaths and those fish that succumb had high bacterial numbers (10^6 CFU) suggesting that *pabA* has the ability to subvert phagocyte containment and replicate in the host. Genetic complementation of the *pab* operon restored virulence *in vivo* (Section 4.3.4.1, Figure 4.17).

Approximately 30 *pu*.1 morphant embryos (as described Section 2.19.10) were injected with 1500 CFU of SH1000-*pabA* or parent SH1000. In the absence of phagocytes, *pabA* was restored to virulence in a similar fashion to the parental strain but with a slight temporal delay. By 20 hpi, all embryos injected with SH1000, and 80% of the SH-*pabA* injected embryos, had succumbed. The remaining SH-*pabA* injected embryos died over the following 24 hr (Figure 4.12 D). The restoration of *pabA* virulence in the *pu.1* embryos suggests that the mutant is not able to access the required nutrients in the phagocyte but if uncontained by phagocytes in knock down embryos, *pabA* can replicate and overwhelm the host before reconstitution of the immune system occurs.

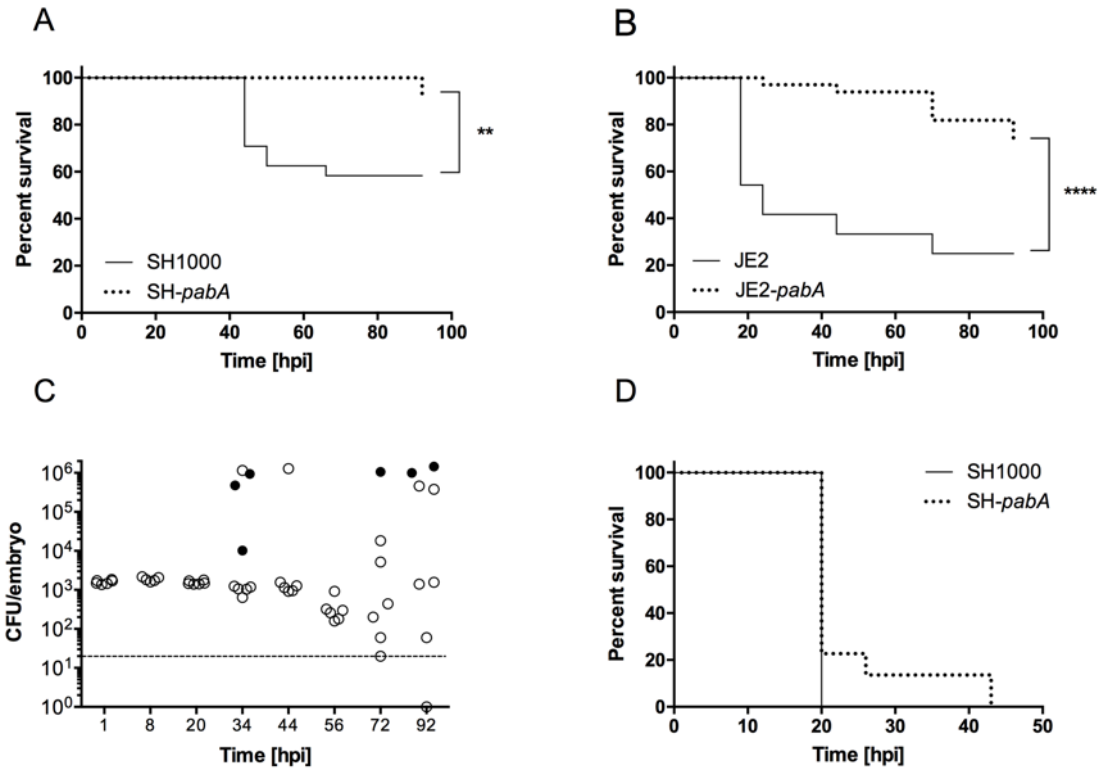


Figure 4.12 *In vivo* attributes of *pabA* in the zebrafish infection model

A Survivals curves demonstrating attenuation of 1500 CFU SH-*pabA* compared to SH1000 (** $p = 0.006$, $n = 30$).

B Survival curves demonstrating attenuation of 1500 CFU JE2-*pabA* compared to JE2 (**** $p < 0.0001$, $n = 30$).

C Bacterial CFU recovered from embryos at regular time points after injection of 1500 CFU SH-*pabA* (n=60) The dashed line represents the limit of detection of th2 assay (20 CFU). Open circles are live embryos, filled circles are dead embryos.

D Survival of *pu.*1 morphant embryos injected with 1500 CFU SH1000 or SH-*pabA* (n = 30).

4.3.2.5.2 Virulence of *pabA* in the murine sepsis model of infection

In addition to the zebrafish embryo model of infection, the murine sepsis model was also employed as described in Section 2.21. Mice were injected with 2 x 10^7 CFU of the wildtype, SH1000, or 4 x 10^7 CFU of SH-*pabA* (n=10 per group). At 72 hpi, a statistically significant decrease in weight of mice infected with parental *S. aureus* was seen compared to the mutant and bacterial numbers were significantly higher in kidneys from these animals (Figure 4.13, p = 0.001). Bacterial numbers in the liver were higher in the SH-*pabA* injected mice (p = 0.006). This is the first demonstration of *S. aureus pabA* attenuation in a mammalian host.

4.3.2.5.3 Biochemical complementation of *pabA* in the zebrafish model

Given the known defects caused by disruption of the *pabA* gene, attempts were made to characterise which components (e.g. PABA, purines, pyrimidines, amino acids, vitamins etc.) would enable biochemical complementation *in vivo*. All compounds were solubilised in E3 zebrafish medium and pH corrected to between 6.5-7.5 prior to use. Toxicity tests were carried out on un-injected 30 hpf embryos by immersion to ensure any effects seen on injected embryos would not be due to toxicity by the compounds themselves. Concentrations of serine and glycine initially chosen matched the concentration used in CDM (100 μg ml^{-1}) and no toxicity was seen (Figure 4.14, un-injected fish). The PABA concentration was also chosen to reflect that used in the CDM experiments (20 μg ml^{-1}), but as this compound is soluble only in 100% (v/v) ethanol, the dose was titrated down to as low as possible (7 μg ml^{-1}). As shown in Figure 4.14 B, serine, glycine and PABA when added simultaneously into E3 medium restored virulence of SH-*pabA* (1500 CFU). However, PABA alone also restored virulence of *pabA* (Figure 4.14 C). Therefore, restoration of virulence was likely to stem from PABA bypassing the need for folate production in the mutant as addition of serine and glycine alone to the embryos did not restore virulence (data not shown).

Negative controls were unaffected throughout (un-injected embryos) and importantly, addition of all three compounds or just PABA alone did not increase the level of killing seen by the parental strain, SH1000 (1500 CFU).

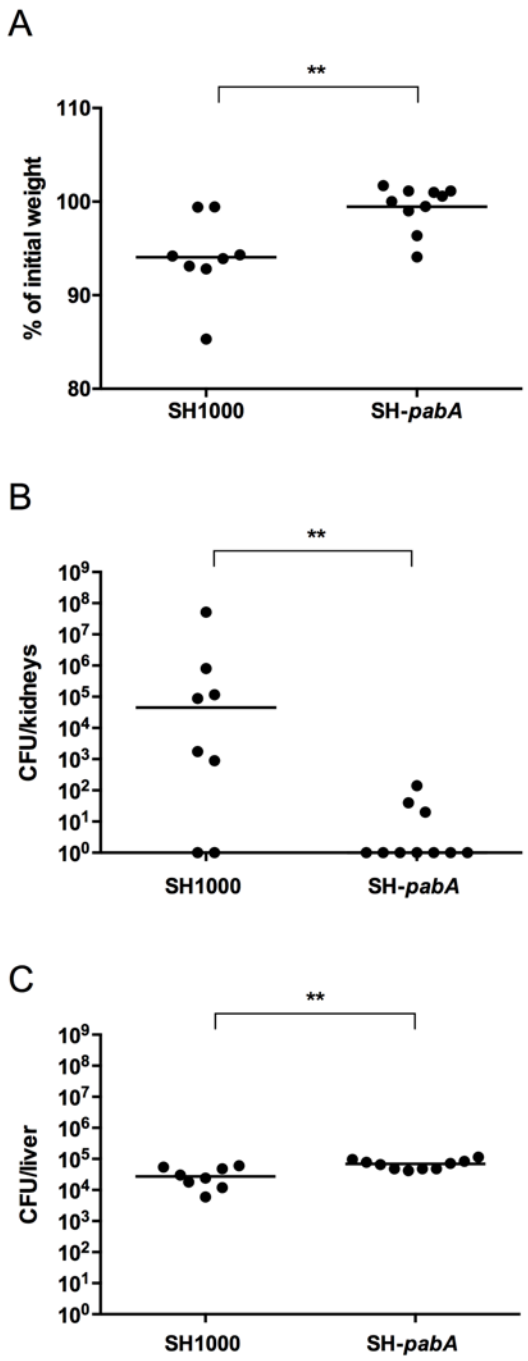


Figure 4.13 Virulence of SH-*pabA* in the murine sepsis model of infection

2 x 10^7 CFU SH1000 or 4 x 10^7 CFU SH1000-*pabA* were injected intravenously into BALB/c mice (n=10). Weight loss (**A** ** p = 0.003), CFU in kidneys (**B** ** p = 0.001) and liver (**C** ** p = 0.006) were recorded. Mice were culled at 72 hpi.

Limit of detection of the assay: kidneys - 400 CFU, livers - 500 CFU.

Next, as purines were potentially thought to be important from the CDM experiment data, described in Section 4.3.2.4.2 above, embryos were injected with either mutant or parent and immediately immersed in inosine 300 μg ml^{-1}. In addition, negative control embryos were not injected but immersed at the same stage of development. Inosine alone was unable to restore virulence *in vivo* (Figure 4.14 D). A combination of serine and glycine and pantothenate (290 ng ml^{-1}, Figure 4.14 E) was tried but was also unsuccessful. It was next thought possible that a full combination of the downstream effectors of folate metabolism might be needed to restore virulence so a combination of serine (1 mg ml^{-1}), glycine (1 mg ml^{-1}), methionine (1 mg ml^{-1}), pantothenate (2.9 μg ml^{-1}) and inosine (1 mg ml^{-1}) was attempted. Despite using higher doses than in previous experiments, no significant host death was observed in the *pabA* injected embryos (Figure 4.14 G).

Even though folic acid was unable to complement *in vitro*, an immersion experiment was attempted with 50 μM folic acid but no complementation was seen (Figure 4.14 H). This may due to an inability of this compound to cross zebrafish and/or bacterial membranes. However, used as a positive control in immersion experiments, the upstream intermediate of folate, PABA, restored virulence in the zebrafish model. This is in agreement with data from other organisms whereby PABA has been shown to complement intracellular growth of *Burkholderia pseudomallei pabB in vitro* using cell monolayers (Pilatz et al., 2006).

As growth on human blood was only possible by supplementation with one specific end product of folate metabolism, the ability of thymidine to complement SH-*pabA in vivo* was tested (Figure 4.15). Thymidine was chosen instead of thymine, as the former is soluble in water unlike thymine, which is soluble only in 1 M NaOH, creating a pH that may be toxic to the zebrafish. Toxicity tests were carried out on un-injected embryos over a range of thymidine concentrations to ensure embryos were not affected by the compound alone. As there are no data available to guide the optimal dose for such experiments, it was reasoned that the CDM concentration (40 μg ml^{-1}) might be too low *in vivo* as when antibiotics are added in immersion experiments, often high doses are required compared to the known MIC of each antibiotic (McVicker et al., 2014). Therefore, 20 times the CDM concentration (800 μg ml^{-1}) was used unless otherwise stated.

As seen in Figure 4.15 A, PABA was able to restore virulence of SH-*pabA*. When thymidine was added to the E3 solution, unfortunately, the SH1000 injected control group only had 13 embryos due to technical difficulties on the day of the experiment. As such the percentage of survival in the SH1000 group was 70% (higher than would normally be expected) compared to 78% in the SH-*pabA* group ($p = 0.71$). It could be that, in this experiment, the similar levels of killing between the two strains was more likely due to the small sample size and less than expected killing by the wildtype, rather than biochemical complementation. The other genetic background, JE2, was also tested. Embryo death was not significantly different between JE2 and JE2-*pabA* in the presence of PABA (Figure 4.15 C) and high levels of killing (50-70%) were seen in both groups. In the presence of thymidine, embryo mortality was also similar between the groups (Figure 4.15 D) however, in control experiments with E3 medium, JE2-*pabA* can cause death of some embryos (Figure 4.12). Therefore, biochemical complementation in this genetic background, which has overall higher virulence in the zebrafish model *per se*, was difficult to confirm.

As such, bacterial kinetic *in vivo* experiments were conducted in the SH1000 background. Embryos were injected with 1500 CFU of SH-*pabA* and immersed in either PABA (Figure 4.15 E) or thymidine (Figure 4.15 F). Host death was negligible in the latter compared to those immersed in PABA despite using 40 x CDM concentration of thymidine. Therefore, it was concluded that thymidine was unable to biochemically complement *pabA in vivo* by immersion. Although *in vivo* complementation could not be achieved using downstream effectors of folate metabolism, the importance of pyrimidines in the *pabA* phenotype was further explored below in Section 4.3.5.

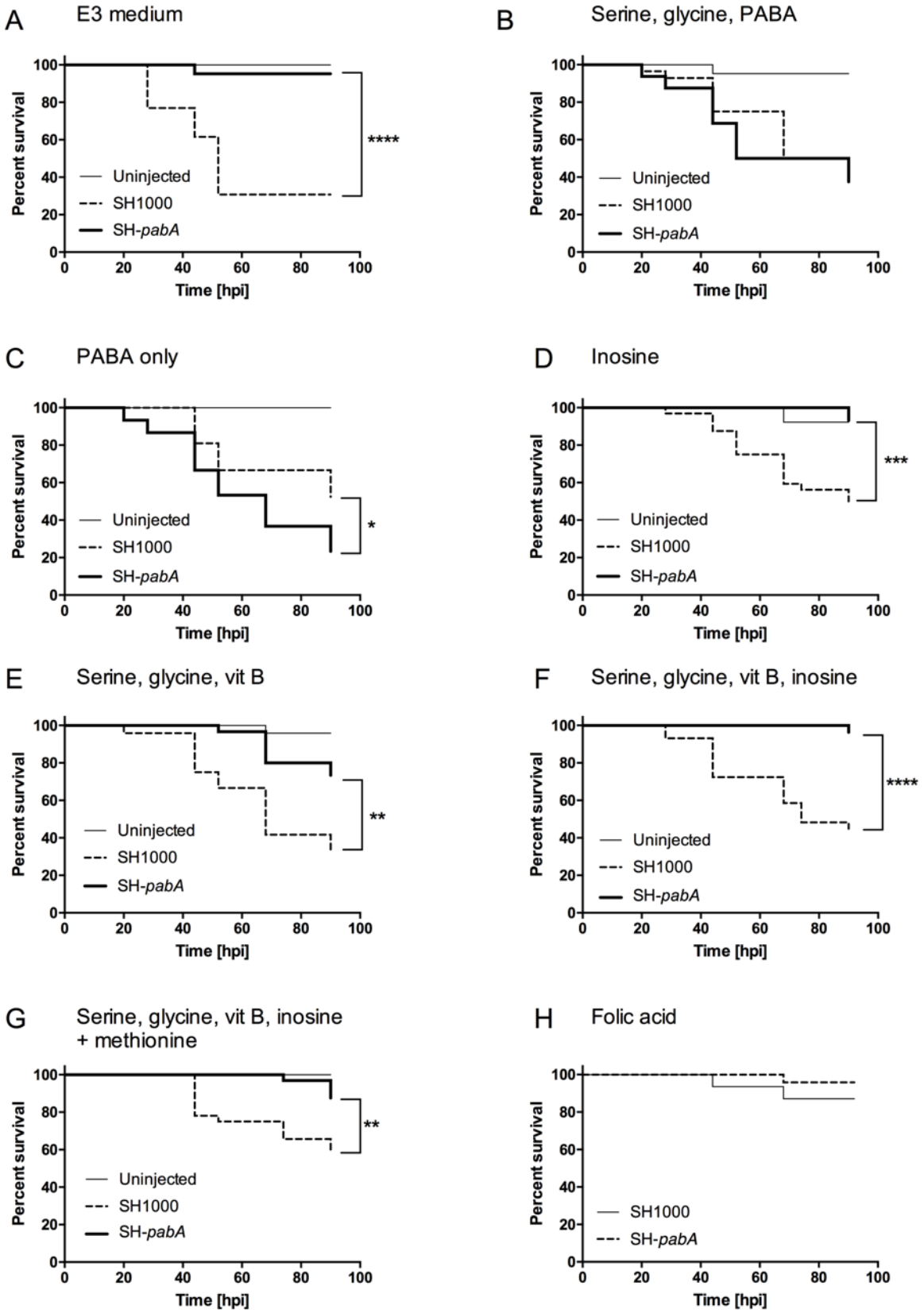

A
E3 medium
Percent survival
Time [hpi]
Uninjected
SH1000
SH-pabA
****
B
Serine, glycine, PABA
C
PABA only
*
D
Inosine
***
E
Serine, glycine, vit B
**
F
Serine, glycine, vit B, inosine
****
G
Serine, glycine, vit B, inosine
+ methionine
**
H
Folic acid

Figure 4.14 Survival curves demonstrating biochemical complementation of SH-*pabA* in the zebrafish embryo infection model

1500 CFU *S. aureus* SH1000 or SH-*pabA* injected systemically into embryos followed by immediate immersion:

A in E3 medium ($p < 0.0001$)
B 100 μg ml^{-1} serine, 100 μg ml^{-1} glycine and 7 μg ml^{-1} PABA (NS)
C 7 μg ml^{-1} PABA ($p = 0.031$)
D 300 μg ml^{-1} inosine ($p = 0.0001$)
E 100 μg ml^{-1} serine, 100 μg ml^{-1} glycine and 290 ng ml^{-1} pantothenic acid ($p= 0.001$)
F 100 μg ml^{-1} serine, 100 μg ml^{-1}glycine, 290 ng ml^{-1} pantothenic acid and 300 μg ml^{-1} inosine (NB overlapping data points, $p < 0.0001$)
G 1 mg ml^{-1} serine, 1 mg ml^{-1} glycine, 2.9 μg ml^{-1} pantothenic acid, 1 mg ml^{-1} methionine and 1 mg ml^{-1} inosine ($p = 0.0067$)
H 50 μM folic acid (NS).

Virulence of SH1000 was compared to that of SH-*pabA* generating p values, or non-significance (NS) as noted.

Uninjected zebrafish were included as negative controls in panels A-G (n per group = 25-30).

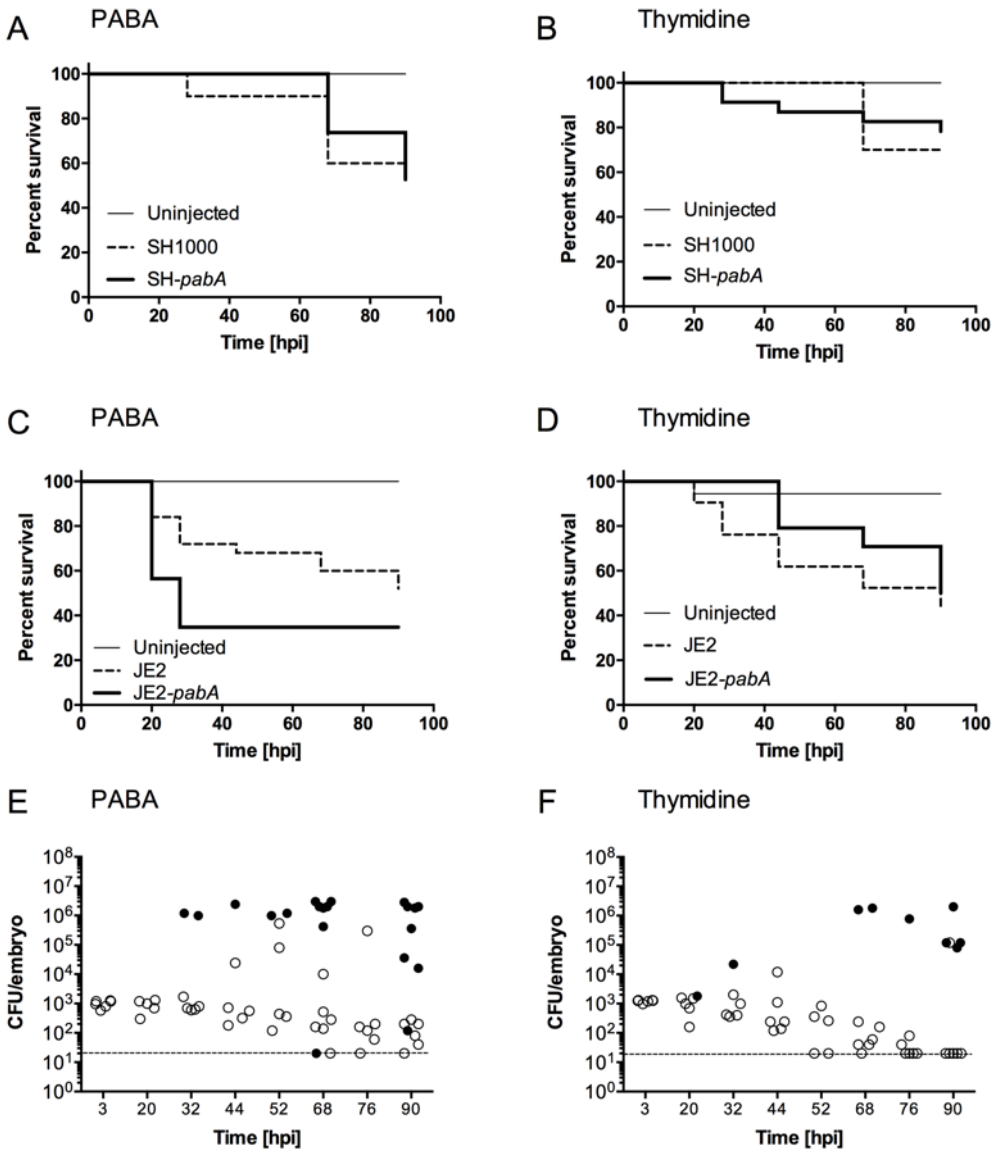


Figure 4.15 Biochemical complementation of SH-*pabA* with pyrimidines in the zebrafish model of infection

1500 CFU SH1000 or SH-*pabA* was injected systemically into embryos followed by immediate immersion in 7 μg ml^{-1} PABA (**A**) or 800 μg ml^{-1} thymidine (**B**). In both experiments, SH-pabA vs. SH1000 – NS. Uninjected zebrafish were included as negative controls (n per group = 25-30).
1500 CFU JE2 or JE2-*pabA* was injected systemically into embryos followed by immediate immersion in 7 μg ml^{-1} PABA (**C**) or 800 μg ml^{-1} thymidine (**D**). In both experiments, JE2-*pabA* vs. JE2 – NS. Uninjected zebrafish were included as negative controls (n per group = 25-30).

Bacterial CFU in live (open circles) and dead fish (filled circles) was enumerated at regular time points after injection of SH-*pabA* (n = 60-90) and immediate immersion in: 7 μg ml^{-1} PABA (**E**) or 1.6 mg ml^{-1} thymidine (**F**). The dashed line represents the limit of detection of the assay (20 CFU).

4.3.3 Role of other genes in the *pab* operon during pathogenesis

As *pabA* is located within the *pab* operon (also containing *pabB* and *pabC*), it would be prudent to revisit the initial screen and check if a similar phenotype to *pabA* was seen for the *pabB* and *pabC* mutants. Indeed, there was reduced growth on human blood of *pabB* in the original screen but multiple attempts to transduce this into the JE2 background were unsuccessful (data not shown). However, transduction was possible into SH1000. Although not originally isolated in the screen, revisiting the photographs of the original screening plates showed a slight reduction in growth on human blood of *pabC* (data not shown).

Both mutants were assayed for virulence in the zebrafish model and found to be significantly attenuated compared to the parent (Figure 4.16 A, B) as would be expected as the genes are in an operonic structure.

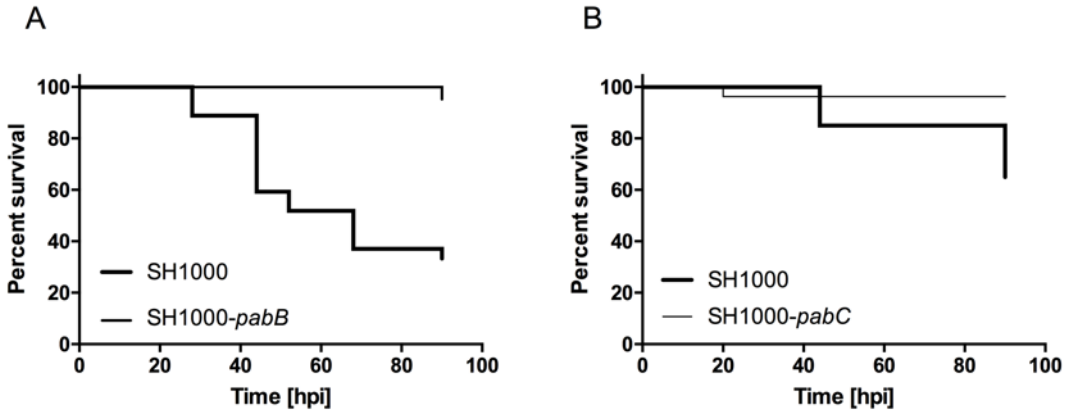


Figure 4.16 Virulence of *pabB* and *pabC* in the zebrafish infection model

A Survival curves demonstrating attenuated virulence of 1500 CFU SH-*pabB* compared to SH1000 ($p < 0.0001$).
B Survival curves demonstrating attenuated virulence of 1500 CFU SH-*pabC* compared to SH1000 ($p < 0.001$).

n = 30

4.3.4 Confirmation of the role of *pabA*, *glyA* and PABA in *S. aureus* virulence in the zebrafish embryo model

4.3.4.1 Genetic complementation of the *pab* operon

As shown in Figure 4.17 A, to confirm that the attenuation of SH-*pabA in vivo* is due to disruption of *pabA*, virulence assays were carried out in the zebrafish embryo model of infection. As seen previously, SH-*pabA* is attenuated compared to the parent ($p < 0.0001$). A negative control strain, SH-*pabA* + pKASBAR (designated strain reference JC011), containing integrated backbone but does not contain the *pab* operon was also attenuated as would be expected ($p<0.0001$). However, genetic complementation of SH-*pabA* with the *pab* operon inserted at lipase (designated strain reference JC010) had restored virulence causing similar host mortality as the parent. This confirmed that the avirulent phenotype of *pabA* is mediated by disruption of the *pab* locus.

4.3.4.2 Serine-glycine inter-conversion and pathogenesis *in vivo*

Interconversion of serine and glycine produces one carbon units that are transferred to THF as an intermediate carrier. THF, as a cofactor, can then donate the single carbon units to biosynthetic intermediates (Massaro and Rogers, 2002). The cleavage of serine to glycine via *glyA* is a major source of one carbon units so it was hypothesised that a *glyA* mutant may be attenuated *in vivo* due to its central role in metabolism. However, 1500 CFU of SH-*glyA* had similar virulence to 1500 CFU SH1000 and so this was not explored further (Figure 4.17 B).

4.3.4.3 Specificity of PABA to rescue virulence of folate deficient mutants

It was important to confirm that the biochemical complementation of SH-*pabA in vivo* was not the result of a generic toxic effect on the embryos that would potentially cause increased non-specific host mortality. Therefore, an unrelated attenuated mutant, *phePsaeR*, was injected into the circulation valley of the zebrafish at an approximate dose of 1500 CFU in parallel with a parent *S. aureus*, SH1000. The strain, *phePsaeR,* has both a disrupted phenylalanine transport (*pheP*) and virulence factor regulator (*saeR*) gene and is avirulent in this infection model (Chapter 5). Neither mutation should be affected by the availability of PABA as they have functional THF producing

pathways. After injection, both the parent and mutant were immediately immersed in either E3 solution or 7 μg ml^{-1} PABA and survival was followed over the subsequent 90 hours. The virulence of *phePsaeR* did not change and the parent strain caused approximately 50% host death as expected (Figure 4.17, C & D).

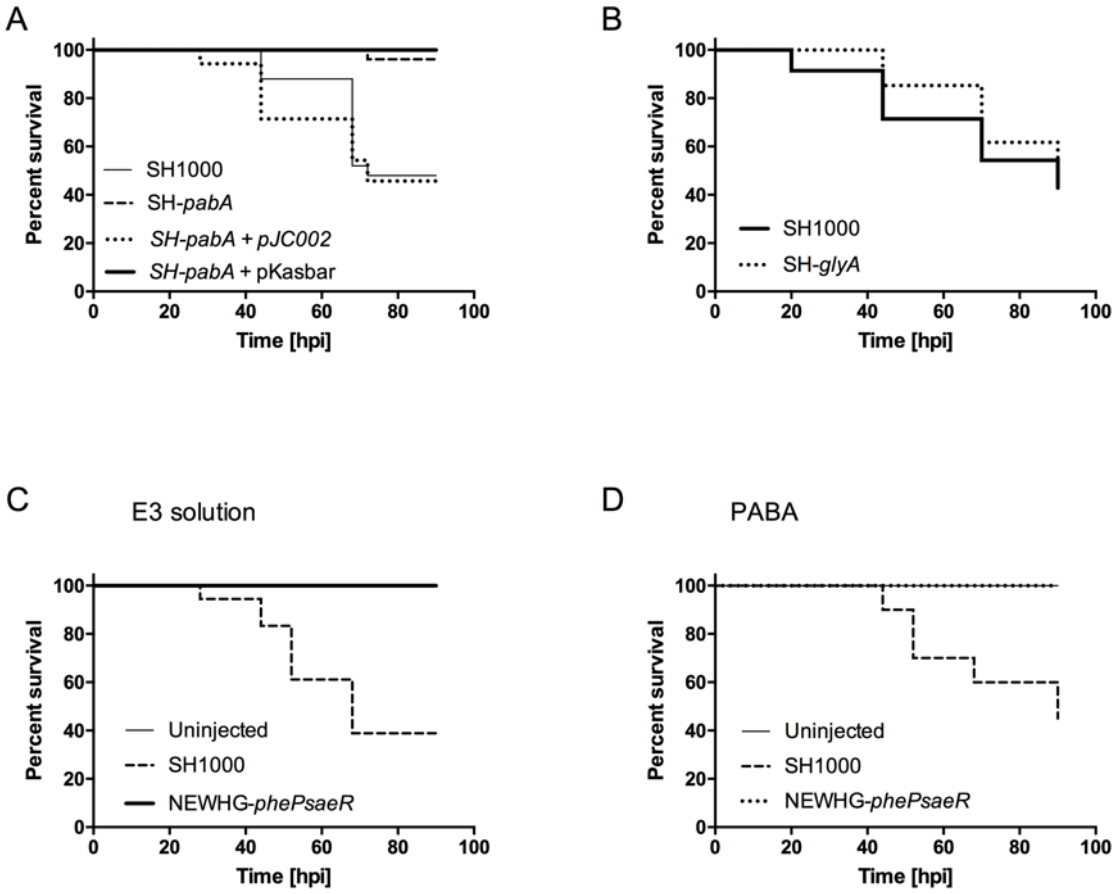


Figure 4.17 Investigation of the role of the *pab* operon, *glyA* and PABA in *S. aureus* pathogenesis in the zebrafish embryo infection model

A Genetic complementation of *pab* operon restores virulence of SH-*pabA* (SH-*pabA* + pJC002) compared to SH-*pabA* or SH-*pabA* with plasmid backbone only (SH-*pabA* = pKasbar) (p = NS, 1500 CFU injected in all groups, n=30).

B Survival curves demonstrating equivalent virulence of 1500 CFU SH-*glyA* compared to 1500 CFU SH1000 (p = NS).

1500 CFU SH1000 or 1500 CFU NewHG-*phePsaeR* injected systemically into embryos followed by immediate immersion in E3 solution (**C**, $p < 0.0001$, NB overlapping data points) or 7 μg ml^{-1} PABA (**D**, $p < 0.0001$, NB overlapping data points).

4.3.5 Investigating the mechanism underlying the *pabA* growth phenotype

4.3.5.1 Analysis of the role of red blood cells

The reason for *pabA* growth being inhibited on human blood but not on human serum and plasma was further investigated. The relevance of pyrimidines to the potential underlying mechanism was also evaluated.

One hypothesis tested considered that *pabA* was unable to grow on whole blood plates as a critical growth factor or nutrient was sequestered intracellularly, possibly in red blood cells (RBCs). During the process of preparing serum and plasma to incorporate into solid agar plates (Section 2.1.6), it was considered that low levels of RBC haemolysis might occur, releasing factors that enable *pabA* growth. To test this, chocolate agar (whole blood heated to 70°C for 10 minutes before being cooled and mixed with agar) was made, as this process should lyse RBCs, thereby releasing potential nutrients. However, mutant growth was not restored indicating that sequestration of substances by RBCs was not responsible for the lack of *pabA* growth specifically on human blood (data not shown).

Next, the converse of the above hypothesis was considered that as *pabA* grows to the same extent as the parent if plated onto human serum or plasma, perhaps the cellular component of blood may itself be playing an inhibitory role. Whilst care is taken not to disrupt RBCs during phlebotomy and later plate preparation, it is likely that some lysis of RBCs occurs. The mutant grows well on animal blood including sheep and horse, which suggests a human specific inhibitory phenomenon. As the addition of pyrimidines to human blood agar restored growth of *pabA*, it was hypothesised that, in the event of DNA damage (e.g. by RBC lysis products), *pabA* would be unable to respond as the parental strain. The deficiency in the folate pathway might prevent upregulation of dTMP levels, hence explaining why exogenous pyrimidines can rescue *pabA* growth on human blood.

To first test if RBC lysis products are inhibitory, RBCs in whole blood were purposefully lysed to make ‘red plasma’ (the blood for is vortexed for 3 minutes prior to separating plasma by centrifugation as described in Section 2.1.6.2). The ‘red plasma’ (so called due to the colour caused by containing products of RBC lysis) was added to

normally produced plasma in increasing amounts e.g. standard plates were 50% plasma which was reduced to 45%, 37.5% and 25% by substitution with 'red plasma'. Even a small addition of vortexed red plasma, i.e. comprising only 5% of the total plate content, prevented growth of the mutant (Figure 4.18). This suggested that RBC lysis products may be inhibitory and to hone in on the inhibitory factor, the major constituent of RBC, haemoglobin was first investigated.

50% (v/v) plasma agar was supplemented with increasing concentrations of bovine haemin (data not shown), bovine haemoglobin (data not shown) or human haemoglobin (Figure 4.19). Human haemin is difficult to source and therefore could not be tested. However, no inhibition of JE2-*pabA* growth was seen using any of the three components.

It remained possible that *pabA* was more sensitive to heme toxicity compared to the parent. The role of heme toxicity was explored further by adding free iron (Fe^{2+}) to human blood which would reduce the need for heme cellular uptake and degradation, thus removing the potentially toxic insult. Increasing concentrations of ammonium ferrous sulphate were added to human blood containing agar at levels ranging from 6 μg ml^{-1} to 60 μg ml^{-1} but restoration of *pabA* growth was not seen suggesting that iron homeostasis does not affecting the growth of *pabA* (data not shown).

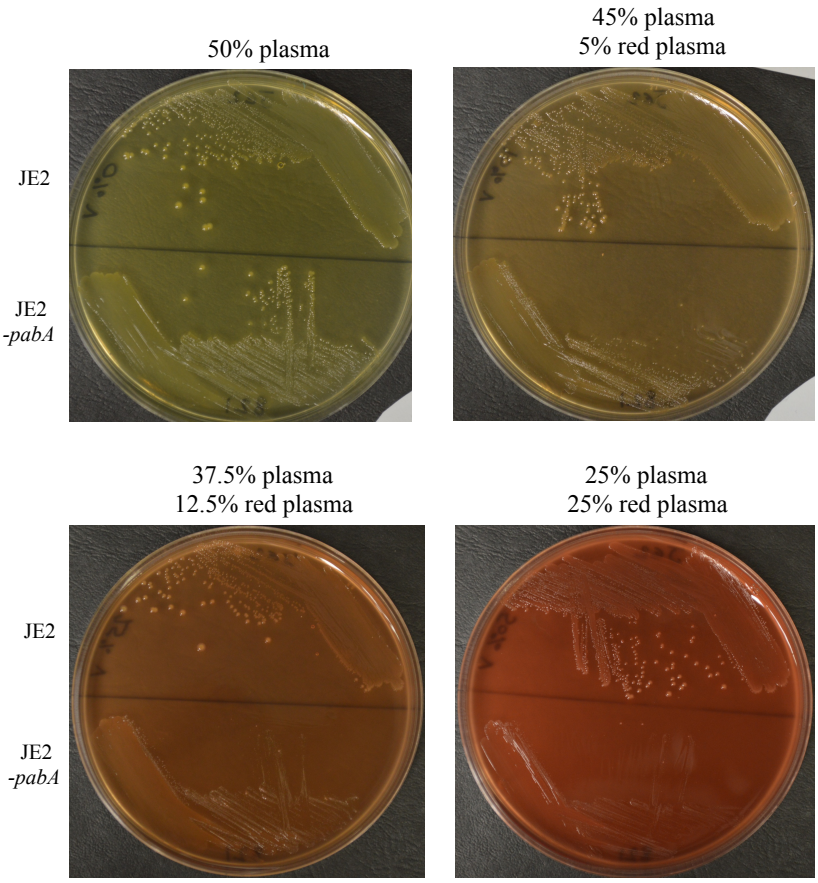


Figure 4.18 Growth of parent or mutant on plasma agar with increasing amounts of vortexed red plasma

Increasing concentrations of 'red plasma' was added to normal plasma agar plates and growth of JE2-*pabA* was diminished dose dependently. Plates were incubated at 37°C for 48 h.

'Red plasma', so called due to the colour caused by RBC lysis, was obtained by vortexing blood and separating plasma by centrifugation.

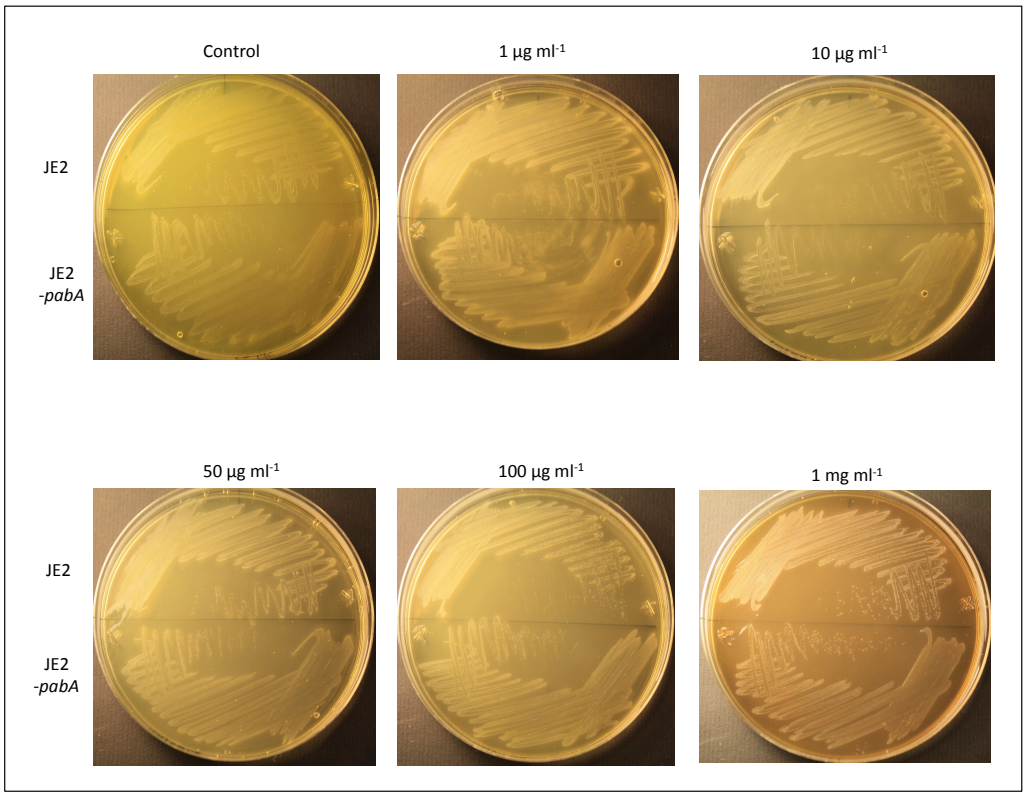


Figure 4.19 Analysis of the effect of human haemoglobin on JE2-*pabA* growth

Growth of JE2 and JE2-*pabA* on 50% (v/v) plasma plates either unsupplemented (control); or supplemented with increasing concentrations of human haemoglobin. Plates were incubated at 37°C for 48 h.

4.3.5.2 Analysis of the role of white blood cells and platelets

Other possibilities for sources of toxicity in whole blood included substances released from platelets or white blood cells (WBCs) or simply the cellular presence itself. As such, both platelet poor plasma (PPP) and platelet rich plasma (PRP) were tested for *pabA* growth but showed the same level of growth for parent and mutant indicating that this was not responsible (data not shown).

As seen in Figure 4.20 in the absence of THF, alternative salvage pathways for nucleotide synthesis are used, as *thyA* no longer has the cofactor it requires to convert deoxyuracilmonophosphate (dUMP) to deoxythyminemonophosphate (dTMP). According to biocyc information of metabolic pathways in *S. aureus* (http://biocyc.org), an alternative pathway is present which firstly requires uptake of the nucleobases (thymine) into the cell and then conversion to dTMP by two enzymes, pyrimidine nucleoside phosphorylase (Pdp) and thymidine kinase (Tdk). Pdp converts thymine to thymidine and Tdk converts thymidine to dTMP. These enzymes do not require THF.

The role of platelets and WBCs in the *pabA* growth phenotype were therefore explored further as both are known to contain high levels of thymidine phosphorylase (Schneider et al., 1973; van Kuilenburg and Zoetekouw, 2006). It was hypothesised that lysis of such cells would enhance the breakdown of thymidine to thymine and thus prevent Tdk being able to convert thymidine into the required dTMP.

After plasma sample preparation, the WBCs were added back to a plasma sample (PPP + WBC). A PRP sample was also included and the samples were subjected to repeat freeze-thawing in liquid nitrogen. After five cycles, the samples were thawed and 50% (v/v) plasma agar plates were made as described in Section 2.1.6.3. Parent and mutant were streaked onto each plate as shown in Figure 4.21. Both strains grew well on all plates indicating that lysis of non-RBC cellular components was unlikely to explain why *pabA* grows well on plasma but not blood. However, it should be noted that the degree of cell lysis was not able to be verified so the extent of intact cells could be playing a role.

Putting together the positive findings thus far, it is clear that thymine/thymidine is able to complement *pabA* growth on human blood and that growth on plasma is restricted when RBC lysis occurs. Therefore new hypotheses were that the mutant grows poorly on human blood due to:

i) an as yet unproven toxicity by haemoglobin or other RBC lysis factors
ii) in the absence of folate, a requirement for pyrimidine salvage pathways, which are perhaps inhibited in blood
iii) an increased demand for pyrimidines (for example if a competitive inhibition process is occurring).

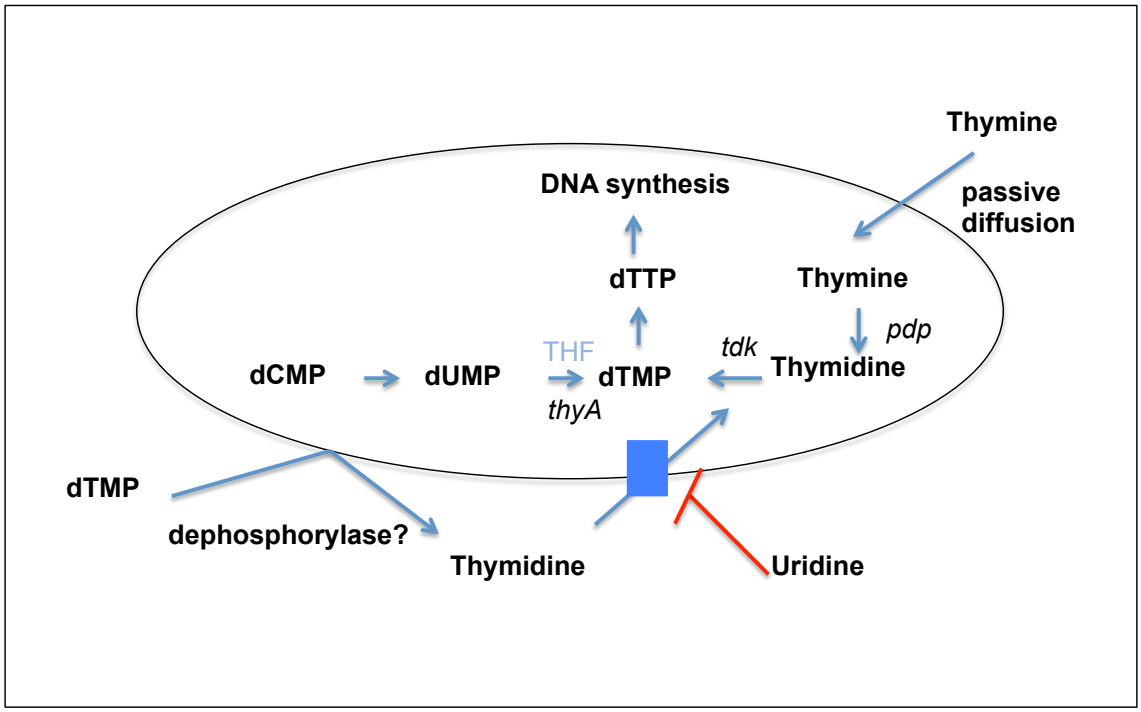


Figure 4.20 Metabolic pathways associated with dTTP production

Genes are shown in italics

Blue box – pyrimidine transporter

Red line – inhibitor of transporter

dCMP - Deoxycytidine monophosphate

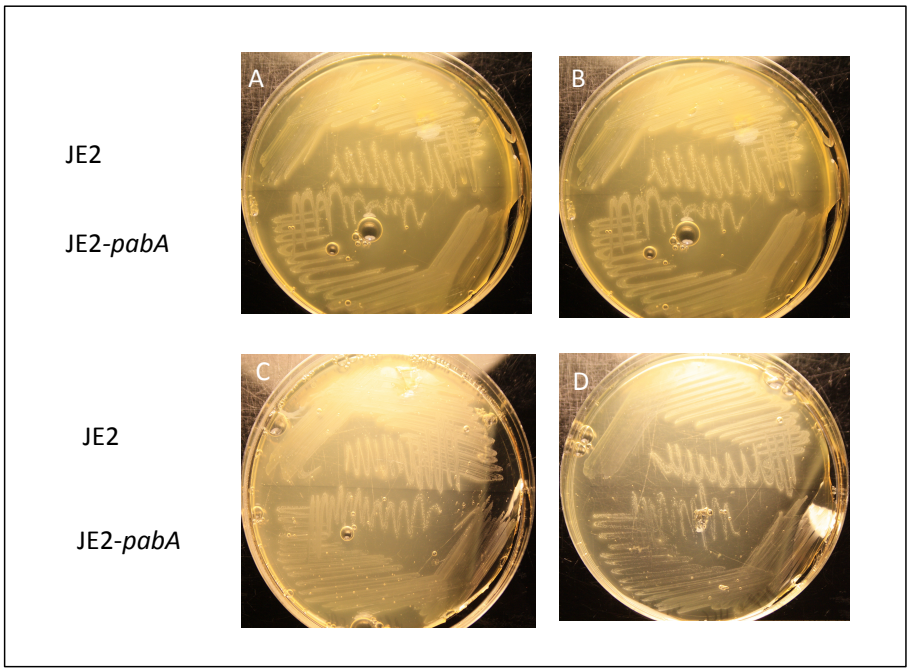


Figure 4.21 Analysis of the effect of non-RBC components on JE2-*pabA* growth

Growth of JE2 and JE2-*pabA* on 50% (v/v) plasma plates without or with platelet or WBC lysis. Plates were incubated at 37°C for 48 h.

A Platelet rich plasma (PRP)

B Platelet rich plasma (PRP) subjected to freeze-thaw cycles

C Platelet poor plasma (PPP) + WBCs

D Platelet poor plasma (PPP) + WBCs subjected to freeze-thaw cycles

4.3.5.3 Use of chemically defined media to assess the importance of pyrimidines

To prove or disprove the hypotheses (ii) and (iii), CDM agar was used to probe how essential thymine/thymidine was to growth of *pabA*. Pyrimidines are not included in the standard *S. aureus* CDM as wildtype *S. aureus* can *de novo* synthesise the deoxyribonucleosides which are essential to DNA replication, using the folate requiring *thyA* pathway.

Presuming a complete knock out of THF production due to the disrupted *pab* operon, *pabA* should be unable to grow on CDM as exogenous pyrimidines are not supplied. However, as seen in Table 4.5, *pabA* grew as per the parent on CDM solid agar when serine and glycine were present. This biochemical complementation was re-visited using CDM and combinations of added serine, glycine, and pyrimidines (Table 4.6). PABA (50 μg ml^{-1}) was used as the positive control.

As seen in Figure 4.22, *pabA* growth was permitted to the same extent as the parent in the presence of serine and glycine as seen previously. The presence of thymidine alone did not support growth and suppressor mutation colony formation was seen. Suppressor mutations are an additional mutation that restores function lost by an already existing mutation, thereby 'suppressing' the mutant phenotype. A combination of serine, glycine and thymidine did allow growth but as serine and glycine alone achieved this, no further growth augmentation was possible with thymidine. This is in agreement with previous CDM results (Section 4.3.2.4.2). It remained to be seen what the roles of pyrimidine salvage pathways are in the *pabA* human blood growth phenotype and this was further investigated.

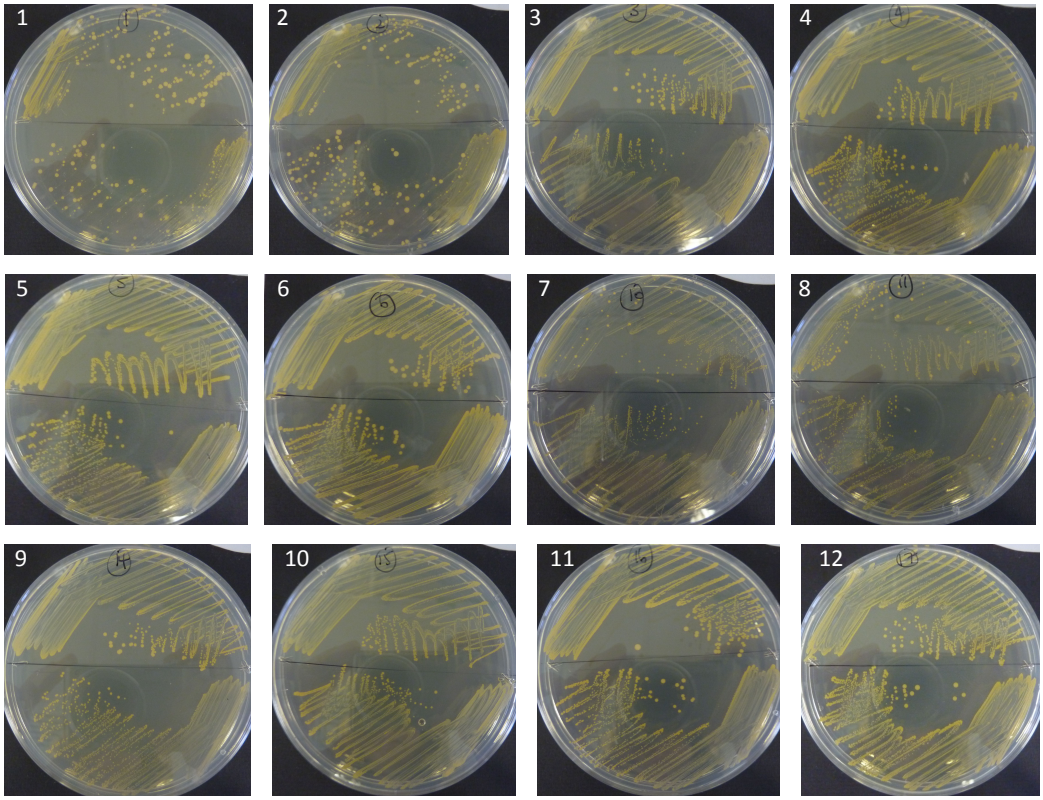


Figure 4.22 Role of serine, glycine and thymidine on growth of JE2 (top half) and JE2-*pabA* (bottom half)

Plate number	Added*:	JE2	JE2-*pabA*
1	Serine	++	++
2	Serine + PABA	++	++
3	Glycine	++++	+++
4	Glycine + PABA	++++	++++
5	Serine + Glycine	++++	++++
6	Serine + Glycine + PABA	++++	++++
7	Thymidine	++	++
8	Thymidine + PABA	++	++
9	Glycine + Thymidine	++++	+++
10	Glycine + Thymidine + PABA	+++	+++
11	Serine + Glycine + Thymidine	++++	++++
12	Serine + Glycine + Thymidine + PABA	++++	++++

Table 4.6 Pyrimidine contribution to growth of *pabA* in nutrient poor media
* Serine 100 µg ml^{-1}; glycine 100 µg ml^{-1}; thymidine 400 µg ml^{-1}; PABA 50 µg ml^{-1}. Plates were inoculated with JE2 (top half) and JE2-*pabA* (bottom half) and incubated at 37°C for 48 h. Growth: + very poor, ++ poor, +++ slightly reduced, ++++ normal.

4.3.5.4 Investigation of the role of pyrimidine salvage pathways in growth on human blood

Synthesis of dTMP can occur via a THF-dependent route, or nucleotide salvage pathways requiring thymine or thymidine (Figure 4.20). On any media tested, with the exception of human whole blood, *pabA* growth was permitted suggesting that the nucleotide salvage pathways provide enough dTMP for DNA synthesis and growth. It was hypothesised therefore, that pyrimidine salvage pathways may be competitively inhibited by blood, which high levels of thymine/thymidine are required to overcome.

4.3.5.4.1 Construction of multiple mutant strains

To assess the contribution of pyrimidine salvage to *pabA*, double mutants were constructed SH1000*pabAnupC*, SH1000*pabApdp* and SH1000*pabAtdk*. The three Tn mutants, *nupC* (NE544), *pdp* (NE424) and *tdk* (NE277) were taken from the NTML library and used to make ϕ11 phage lysates as described in Section 2.15. SH-*pabA* contains the *bursa aurealis* transposon carrying the *ermB* cassette. Thus, in order for double mutants to be produced, the erythromycin resistance was replaced with another antibiotic using allelic exchange and homologous recombination. An NTML genetic toolbox is available to facilitate this and the plasmid containing a spectinomycin resistance cassette (pSPC) was chosen. As this is 1 Kb smaller than the *ermB* cassette, the mariner transposon size reduces to 2.2 Kb using this plasmid.

pSPC contains pE194ts, a temperature sensitive origin of replication, anhydrotetracycline marker for counter selection (100 ng ml^{-1}), chloramphenicol resistance gene (Cm^R, 10 μg ml^{-1}), spectinomycin resistance cassette (Spc^R, 1 mg ml^{-1}) and homologous DNA regions to *bursa aurealis* (Figure 4.23 A). The plasmid was transduced into SH-*pabA*^{ery} by selection onto LK containing citrate (0.02 M) and spectinomycin (1 mg ml^{-1}) and incubated at 30°C for 48 hours. A colony was then inoculated into BHI broth containing chloramphenicol (10 μg ml^{-1}) and incubated at 44°C overnight without shaking. Chloramphenicol resistant colonies were patched onto BHI + chloramphenicol (10 μg ml^{-1}) agar plate and incubated overnight at 44°C to promote plasmid integration. Colonies showing good growth the following day were inoculated into BHI broth and incubated at 30°C shaking at 250 rpm. Subculture into

fresh BHI was performed for 3 consecutive days. After this time, the subculture was plated with serial dilutions up to 10^{-7} onto BHI agar plates. Large colonies were replica patched onto agar plates with either BHI only, BHI agar containing chloramphenicol (10 μg ml^{-1}), BHI containing erythromycin (5 μg ml^{-1}) and BHI containing spectinomycin (1 mg ml^{-1}) and incubated at 37°C for 24 hours. Double recombinants i.e. those which have should have excised and lost the plasmid from the chromosome, displayed erythromycin and chloramphenicol susceptibility yet spectinomycin resistance. Resistance cassette swap was confirmed by PCR amplification using a primer pair flanking the Tn insertion site in the *pabA* gene and the expected product size of 3 Kb was seen (2.2 Kb + ~600 bp, Figure 4.23 B) confirming construction of SH-*pabA*^{spc}. Finally, SH-*pabA*^{spc} was transduced with each lysate to yield the desired double mutants and selected on LK + citrate (0.02 M) + erythromycin (4 μg ml^{-1}) + spectinomycin (150 μg ml^{-1}). A lower antibiotic concentration was employed to minimise bacterial stress. To verify successful double mutants, PCR amplification using gene specific primer pairs which anneal either side of the Tn insertion site was carried out to verify the double mutants (Figure 4.23 C). Mutants were streaked onto various media with or without thymine or thymidine supplementation.

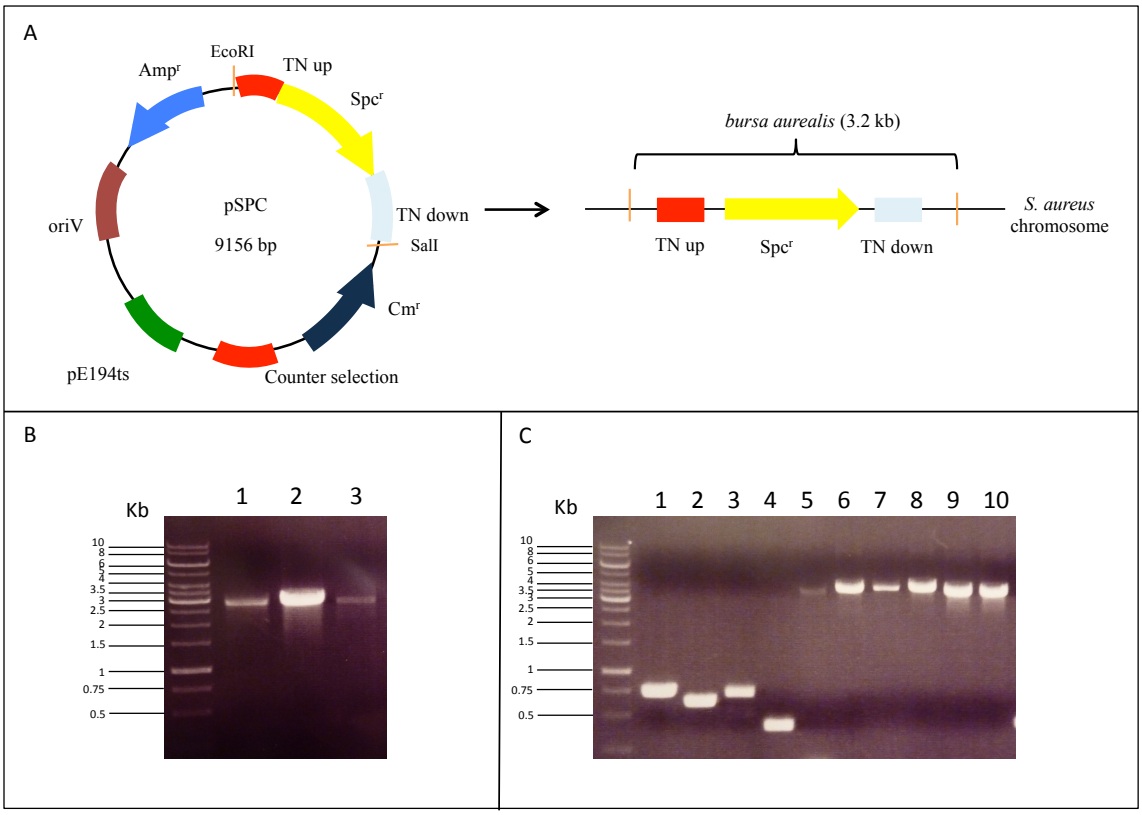


Figure 4.23 Resistance cassette replacement in Tn mutants

A Diagrammatic representation of pSPC and its integration into the *S. aureus* chromosome through allelic exchange (via the Tn up/down regions) and plasmid excision.

B 1% (w/v) TAE agarose gel showing products of PCR amplification of *pabA* after replacement of the erythromycin resistance cassette for the spectinomycin cassette for 3 putative colonies. All showed the expected size of ~ 3 Kb.

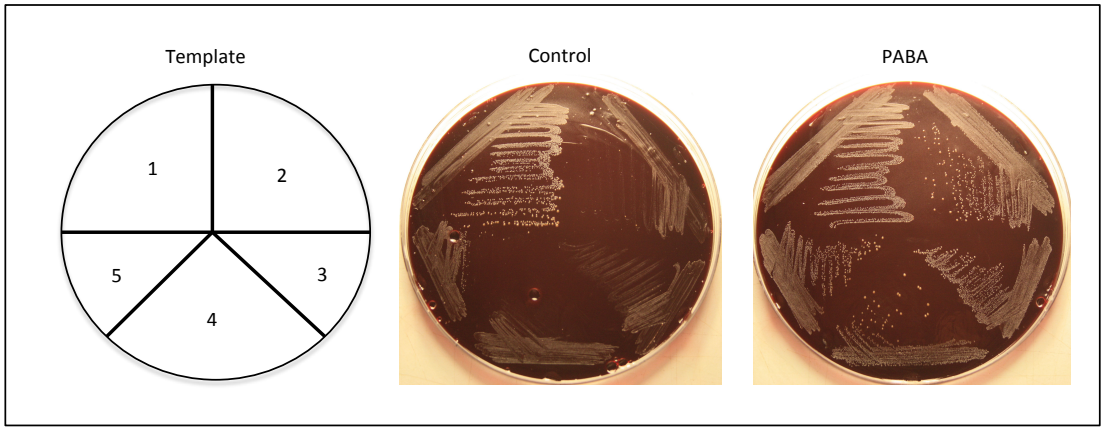
C 1% (w/v) TAE agarose gel showing products of PCR amplification of wildtype genes in *pabA* (lane 1, 750 bp)**,** *pdp* (lane 2, 632 bp), *nupC* (lane 3, 717 bp) and *tdk* (lane 4, 400 bp). Lanes 5-10 contain the Tn mutant showing 3.2 Kb erythromycin containing Tn in the double mutants: SH*pabAnupC* 3.2 + 0.7 = 3.9 kb (lane 5), SH*pabApdp* 3.2 + 0.6 = 3.8 kb (lanes 6-8) and SH*pabAtdk* 3.2 + 0.4 = 3.6 kb (lane 9,10).

On rich media such as BHI, both *pabAnupC* and *pabApdp* had comparable growth to the parent indicating the required nutrients were available in these media. However, although growth of *pabAtdk* was seen on BHI, there was evidence of suppressor mutation colony formation, in response to the inadequate dTMP production by this double mutant. However, as some growth was seen, in contrast to the complete absence of *pabA* growth on human blood, it was hypothesised that in the absence of potentially inhibitory lysed RBC products, the alternative salvage pathways (via *tdk*) can work well enough to afford low level growth. However, it is also possible that other necessary metabolites e.g. dTMP itself is provided in complex media such as BHI as the exact constituents are not well-characterised. As expected, all three double mutants had poor growth on 30% human blood plates but were fully complemented by the addition of PABA, as expected (Figure 4.24).

As NupC is thought to be the dominant pyrimidine transporter in *S. aureus* (Kriegeskorte et al., 2014), it is of interest that *pabAnupC* was still able to grow in the presence of thymidine on human blood, suggesting other pyrimidine transporters may be allowing uptake (Figure 4.24). In the same publication, Kriegeskorte and colleagues identified three putative nucleoside transporters in *S. aureus* but only investigated NupC due to its high sequence identity to NupC in *B. subtilis*. *pabApdp* grew well on human blood in the presence of thymine or thymidine, which was unexpected as it was hypothesised that only thymidine supplementation would support growth. This is because if thymine is supplied, it would be unable to be converted to thymidine (given the absence of Pdp) yet if thymidine is given, as the Tdk enzyme is intact, conversion from thymidine to dTMP can take place. It is unclear why the double mutant can grow in the presence of thymine.

pabAtdk was not complemented by addition of either thymine or thymidine to human blood demonstrating that the loss of a functional Tdk enzyme prevents the salvage pathway from maintaining dTMP levels (Figure 4.24). This suggested that if there is an inhibitory factor in blood, Tdk may be the target. Competitive inhibition of Tdk could be overcome by exogenous pyrimidines, allowing *pabA* growth. However, NTML Tn mutants may impact on other genes in addition to those which contain the transposon. Operon structures have been predicted *in silico* and documented experimentally (ten Broeke-Smits et al., 2010). *nupC* is not situated within an operon; *pdp* is thought to be

transcribed with a hypothetical protein (USA300HOU_2125) and *tdk* may be in a large operon containing up to 20 genes. This may impact on the validity of these results and so genetic complementation of *tdk* was attempted by the construction of SH1000*pabAtdk::tdk*. This work was conducted in collaboration with Mr Sam Fenn (Research Technician, University of Sheffield). To date, successful construction of the complementation plasmid has not been achieved so this will be continued as future work.



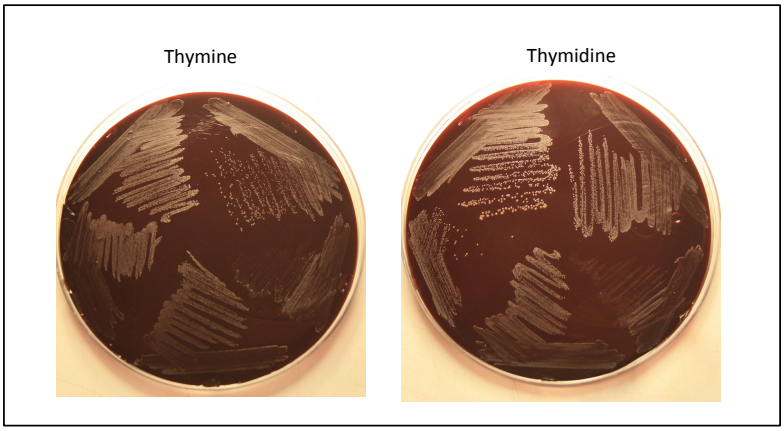


Figure 4.24 Role of PABA and other components in growth on human blood with or without pyrimidine supplementation

(1) SH1000

(2) SH-*pabA*

(3) SH*pabA*^{spc}*tdk*^{ery}

(4) SH*pabA*^{spc}*pdp*^{ery}

(5) SH*pabA*^{spc}*nupC*^{ery}

30% (v/v) human blood plates either unsupplemented (control); or supplemented with PABA (20 µg ml^{-1}); thymine (400 µg ml^{-1}) or thymidine (400 µg ml^{-1}).

4.3.5.4.2 Investigating the effect of Tdk inhibitors on *pabA* growth

As Tdk inhibition appears to play an important role in preventing exogenous pyrimidines from rescuing *pabA* growth on human blood, other methods of inhibiting Tdk were explored to substantiate these findings.

Of all the metabolic pathways enlisted by bacteria to promote survival, the folate pathway is of particular interest as efficacious antibiotics targeting this pathway are commonly used. As with all antibiotics introduced, resistance mechanisms have arisen and in patients treated long-term with sulphonamides or the DHFR antagonist, trimethoprim, many resistant strains have been isolated (Eliopoulos and Huovinen, 2001). Changes to the amino acids of the DHFR enzyme often account for the resistance, preventing trimethoprim from binding effectively (Vickers et al., 2009). However, other mechanisms of treatment failure with folate antagonists exist because if folate biosynthesis cannot take place, salvage pathways can still be used to ensure dTTP synthesis continues. Extracellular amounts of pyrimidine bases vary with body sites and host systemic status (Besier et al., 2008) and the limiting factor for this process in the human host is the lack of available pyrimidines whereas other species, aside from equine hosts, have far higher levels of thymidine in blood (Table 4.7). In particular, rodent blood has exceedingly high levels of thymidine and this underpins why *in vivo* activity of folate antagonists using a rodent model of infection is not recommended (Entenza et al., 2009). In the same study, a *tdk* mutant was shown to remain susceptible to iclaprim, a new DHFR antagonist, even in the presence of rodent serum, highlighting that the highest levels of exogenous thymidine cannot be effective in the absence of Tdk. The same effect has also been seen using a *tdk* mutant in *E. coli* (Tokunaga et al., 1997).

Whilst human blood in the physiological state has a minimal thymidine concentration, pathological processes such as necrotic cells and pus from patients with cystic fibrosis can have elevated thymidine levels (Besier et al., 2008). This has clinical relevance as novel therapeutic strategies can be developed which concurrently inhibit both the *de novo* folate biosynthesis pathway and the salvage *tdk* pathway (Zander et al., 2010a). To achieve this goal, non-toxic thymidine kinase inhibitors have been sought. Nucleoside analogues such as halogenated 2-deoxyuridine derivatives have been shown to inhibit *S. aureus* Tdk but can also cause DNA damage in host cells. Alternatives have been

identified using a multistep virtual screening approach to identify novel compounds with activity against Tdk (Zander et al., 2010b).

To test the hypothesis that Tdk inhibition, mediated by a component of human blood is preventing *pabA* growth on human blood, two of the most active Tdk inhibitors from the virtual screen were selected for testing: compound A which, in the presence of folate antagonists and thymidine, had a MIC of 0.25 mg L^{-1} against *S. aureus* strain ATCC 700699; and compound B which had a MIC of 1 mg L^{-1}. Each compound was received from Ambinter (France) and resuspended in 1% (v/v) DMSO (Figure 4.25). A disc impregnated with DMSO (1% v/v) was included as a control (data not shown).

Compound A (Amb2716238) and compound B (Amb1042771) at a range of concentrations were impregnated onto sterile discs (Sigma-Aldrich) prior to placement on a lawn of JE2-*pabA*. To create the correct inoculum, one colony was suspended in 2 ml dH_2O before evenly spreading onto the agar plate using a sterile swab. For this experiment, human blood agar was supplemented with thymidine (400 μg ml^{-1}) to support *pabA* growth. It was thought that in the presence of the Tdk inhibitor, *pabA*, even in the presence of thymidine would be prevented from growing but this was not seen (Figure 4.25). Unaffected growth of *pabA* may be due to poor efficacy of the novel Tdk inhibitors so the same experiment was conducted using the halogenated derivative, 5-iodo-2`-deoxyuridine (5-IdU) but no growth inhibition was seen (data not shown).

In an effort to understand this further, compound A and B at high concentration (1 mg ml^{-1}) were impregnated onto sterile discs and placed onto a lawn of parent, JE2, either side of a folate antagonist gradient strip, trimethoprim E-test® (bioMérieux). The human blood agar plate contained no supplements, as the parent grows well on 30% (v/v) human blood. Although the gradient strip displayed the expected MIC of trimethoprim against JE2, the Tdk inhibitors did not augment this inhibition (Figure 4.25 B). It may be that the Tdk inhibitors are not effective on solid media or that Tdk inhibition *per se* is not solely responsible for *pabA* growth inhibition and a competitive inhibition with thymidine is occurring.

Species (source)	**Serum thymidine ($\mu g\ ml^{-1}$)**
Mouse*	0.166
Rat *	0.266
Rabbit**	0.042
Human	~0.010
Beef	0.064
Sheep	0.077
Horse	<0.028

Table 4.7 Concentrations of thymidine measured in the serum of various mammals

* pool of 40 animals

** mean of 7 animals

Adapted from (Nottebrock and Then, 1977)

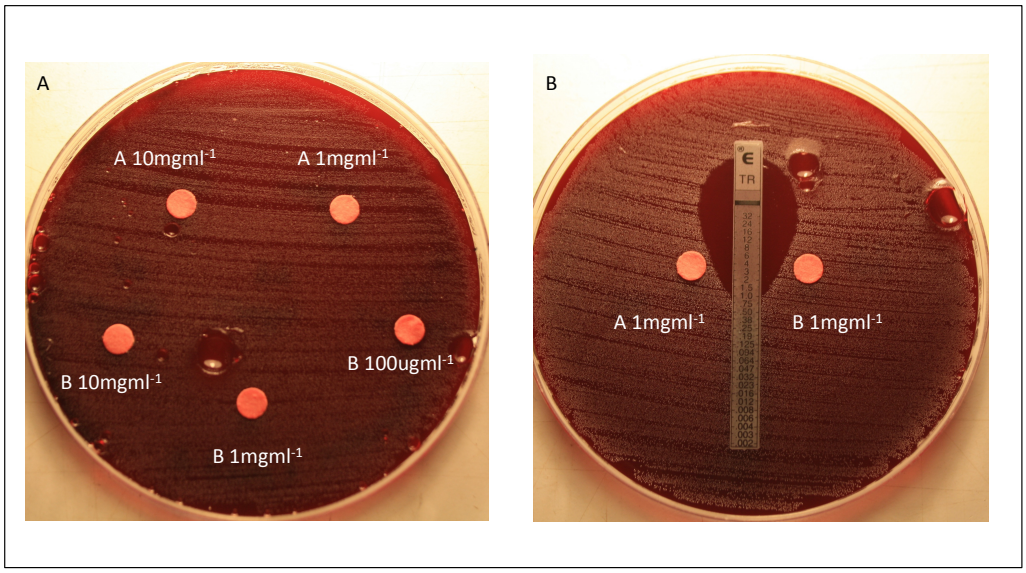


Figure 4.25 Effect of Tdk inhibitors on parent and *pabA* growth on human blood

A Compound A (Amb2716238) and compound B (Amb1042771) at concentrations as shown were impregnated onto sterile discs prior to placement on a lawn of JE2-*pabA*. Human blood agar contained thymidine (400 µg ml^{-1}).

B Compound A (Amb2716238) and compound B (Amb1042771) (1 mg ml^{-1}) were impregnated onto sterile discs and placed onto a lawn of parent, JE2, in the presence of trimethoprim E-test®. Human blood agar contained no supplements.

Plates were incubated at 37°C for 24 hr.

4.3.5.4.3 Metal ion chelation and Tdk activity

Another route of exploring Tdk inhibition was attempted. Tdk is a deoxyribonucleoside kinase composed of 199 amino acids including 4 zinc ion-binding sites (www.uniprot.org). The details of *S. aureus* Tdk are not well known but are documented to be more closely related to the eukaryotic thymidine kinase 1 (TK1) than those in Gram-negative bacteria (Sandrini et al., 2006). Taking mammalian TK1 as a guide, it is thought that although Tdk is not a zinc metalloenzyme but zinc atoms are needed for regulation of transcription of the enzyme (Chesters et al., 1990).

Given the potential reliance of Tdk on zinc, divalent cation chelation would potentially render the enzyme unregulated and disturb its normal function. Commonly used chelators were tested including ethylenediaminetetraacetic acid (EDTA), ethylene glycol tetraacetic acid (EGTA) and dipyridyl as there are varying affinity of zinc ions to each chelator (Auld, 1988). These compounds were tested at 1 M against both mutant and parent on 50% (v/v) plasma agar plates but no affect on growth of the mutant was seen (data not shown).

Conversely, addition of zinc ions to human blood might enable *pabA* to grow if blood is a zinc poor environment. It was hypothesised that components in blood, perhaps released from cells, may chelate zinc, thus rendering Tdk inactive and preventing *pabA* growth specifically on human blood. A review of the literature identified neutrophil derived calprotectin as a host protein able to chelate manganese and zinc. This immune defence strategy inhibits microbial growth by creating metal poor environments in which bacteria are less able to proliferate (Corbin et al., 2008). However, it was not possible to obtain calprotectin in sufficient quantity as recombinant human calprotectin is expensive and scarce.

Therefore, to test this hypothesis, a complementation experiment was instead conducted. Zinc chloride (Sigma) with a dose range from 10 mM to 1 M was added to human blood agar on sterile discs. Each plate was spread with either the parent, JE2-*pabA* or JE2-*tdk*. At the highest concentration (1 M), zinc chloride caused precipitation (large white ring around disc) of proteins in the blood which has been described previously (Zaworski and Gill, 1988). A small zone of clearing was seen around the 100

mM zinc disc in the parent. No *pabA* growth was seen on unsupplemented agar highlighting that exogenous thymidine remains a requirement for growth, even when Tdk is potentially aided by the presence of excess zinc ions (Figure 4.26). Growth similar to the parent was seen for JE2-*tdk.*

Therefore, zinc availability is not playing a major role in the prevention of *pabA* growth on human blood.

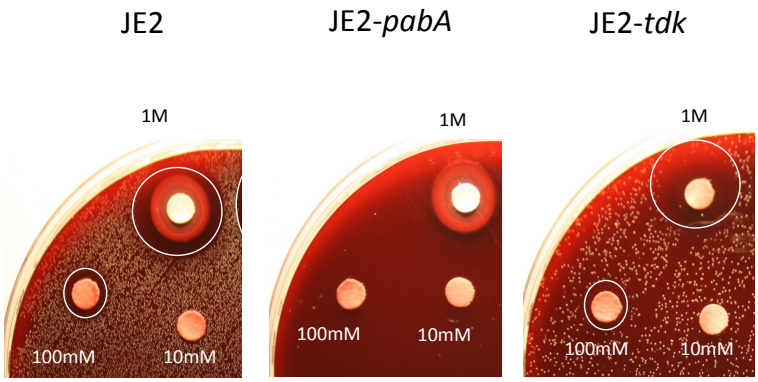


Figure 4.26 Effect of zinc chloride on bacterial growth on human blood

JE2, JE2-*pabA* and JE2-*tdk* are lawned onto 30% (v/v) human blood agar plates and zinc chloride impregnated discs are added. Plates were incubated at 37°C for 24 hr.

Thin white circles show a zone of clearing around the disc.

4.3.5.5 Investigation of antibiotics targeting folate metabolism

In order to further explore the relationship between disturbed thymidine production via folate and the amount of thymidine available, experiments were designed to include a different mode of folate antagonism. As aforementioned, trimethoprim targets the bacterial DHFR enzyme preventing production of THF, limiting bacterial survival during infection.

The strains of interest were spread onto BHI agar plates before the addition of a Trimethoprim E-test®. The *tdk* mutant should be unable to incorporate exogenous thymidine and in combination with an inability to produce folate, was expected to be remain susceptible to antibiotics. This was confirmed on BHI, a high nutrient medium, as addition of thymidine made no difference to the MIC value (0.25 mg L^{-1}) (Figure 4.27). In contrast, the parent and SH-*pabA* were susceptible to trimethoprim in the absence of thymidine supplementation (MIC 1 mg L^{-1}) but resistant in the presence of extra thymidine (MIC > 32 mg L^{-1}) demonstrating that levels of thymidine can gravely affect the ability of antibiotics to halt bacterial growth.

The same set of experiments was carried out on 30% (v/v) human blood agar except that JE2-*pabA* was not spread in the absence of thymidine as it is not able to grow. As seen in Figure 4.28, as for BHI medium, both the parent, JE2, and JE2-*pabA* were fully resistant to trimethoprim in the presence of exogenous thymidine whereas JE2-*tdk* remained susceptible. It was important to compare these findings to growth phenotypes seen when animal blood was used, as in the initial screen. Agar plates containing 30% (v/v) sheep or horse blood were made and the same strains were spread in the absence or presence of thymidine. As shown in Table 4.7, sheep blood is known to contain high levels of thymidine so it was predicted that addition of exogenous thymidine would have minimal effect on strain growth for the parent and *pabA*. This was confirmed experimentally as MIC values of > 32 mg L^{-1} were observed for JE2 and JE2-*pabA* with or without thymidine. JE2-*tdk* however remained unable to use thymidine and was shown to be susceptible to trimethoprim regardless of thymidine availability (Figure 4.29). Thymidine levels in horse blood are lower than in sheep and this is reported to be due to the presence of pyrimidine phosphorylase (Pdp) in horse red blood cells which, when released, converts free thymidine to thymine thus reducing the substrate pool of

thymidine available for the Tdk pathway (Amyes and Smith, 1974). It was predicted that the experiments using horse blood agar would yield results similar to human blood due to the lower natural thymidine content. As seen in Figure 4.30, JE2 was resistant to trimethoprim in the presence of thymidine on horse blood agar. The same was seen for JE2-*pabA* but interestingly, in the absence of thymidine, *pabA* is exquisitely sensitive to trimethoprim on horse blood with growth only being visible at the edge of the plate. This may be due to a degree of RBC lysis in the horse blood, releasing Pdp and lowering thymidine concentrations to levels that barely support *pabA* growth. It has been shown that as little as 0.25% RBC lysis was required to sufficiently lower thymidine levels in whole blood agar (Darrell et al., 1968).

Healthy human blood contains low thymidine levels (Table 4.7). However, there are pathological human conditions where the levels dramatically rise. Mitochondrial neurogastrointestinal encephalomyopathy (MNGIE) is a rare autosomal recessive disease caused by mutations in the thymidine phosphorylase (TP) gene (Spinazzola et al., 2002). Similar to Pdp in bacteria, TP catalyses the reversible phosphorolysis of thymidine to thymine. Less than 200 people worldwide are known to be or have been affected by this condition and diagnosis is based on elevated plasma thymidine levels and genetic testing for mutations in the TP gene.

Taken altogether, these data shed light on the potential mechanism for inhibition of *pabA* growth on human blood. Firstly, it is unlikely that thymidine levels vary significantly between plasma and whole blood. Indeed, the diagnostic test for elevated thymidine uses plasma measurements (https://rarediseases.org/rare-diseases/mitochondrial-neurogastrointestinal-encephalopathy/). On human blood agar, *pabA* is dependent on exogenous thymidine yet grows well on unsupplemented human plasma which raises the concept of varying thymidine requirements on different media. Competitive inhibition of Tdk by blood or an increased requirement for dTMP, which cannot be supported without increasing the thymine/thymidine concentration are both potential underlying mechanisms of poor *pabA* growth on human blood agar.

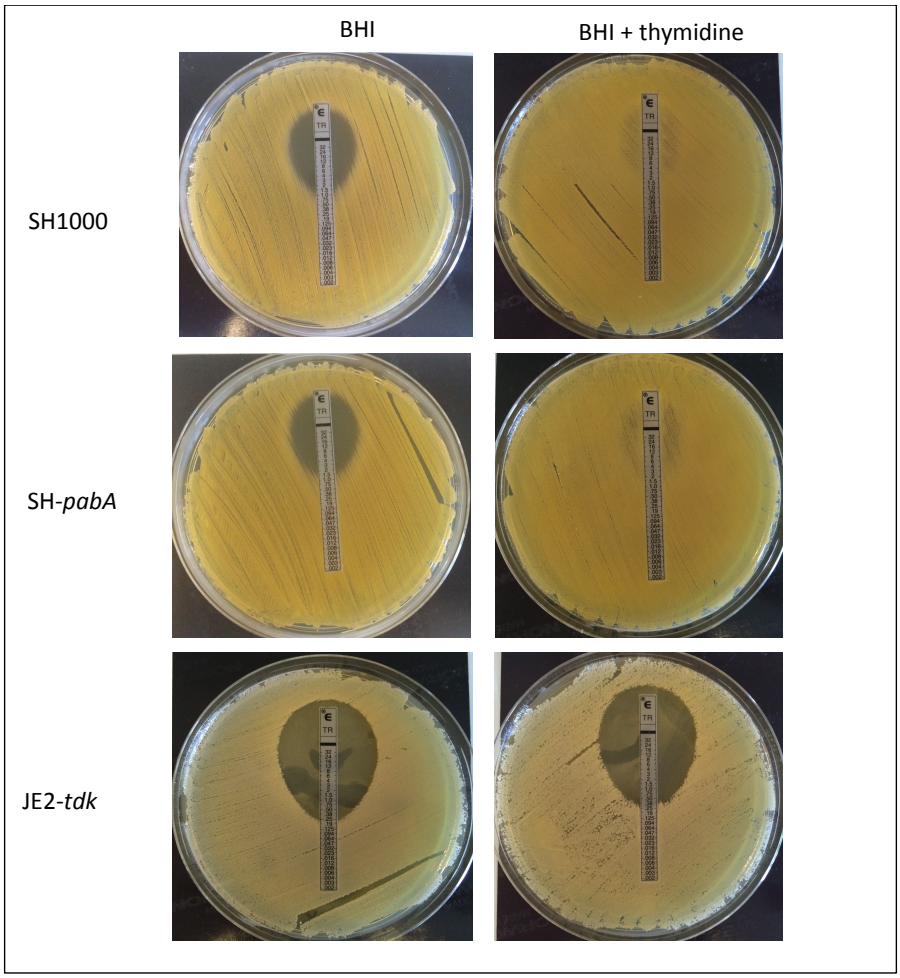


Figure 4.27 Strain susceptibility to trimethoprim with or without exogenous thymidine on BHI media

SH1000, SH-*pabA* and JE2-*tdk* were spread onto BHI plates either unsupplemented or with the addition of thymidine (400 μg ml^{-1}). Trimethoprim E-tests® were added for MIC determination. Plates were incubated at 37°C for 24 hr.

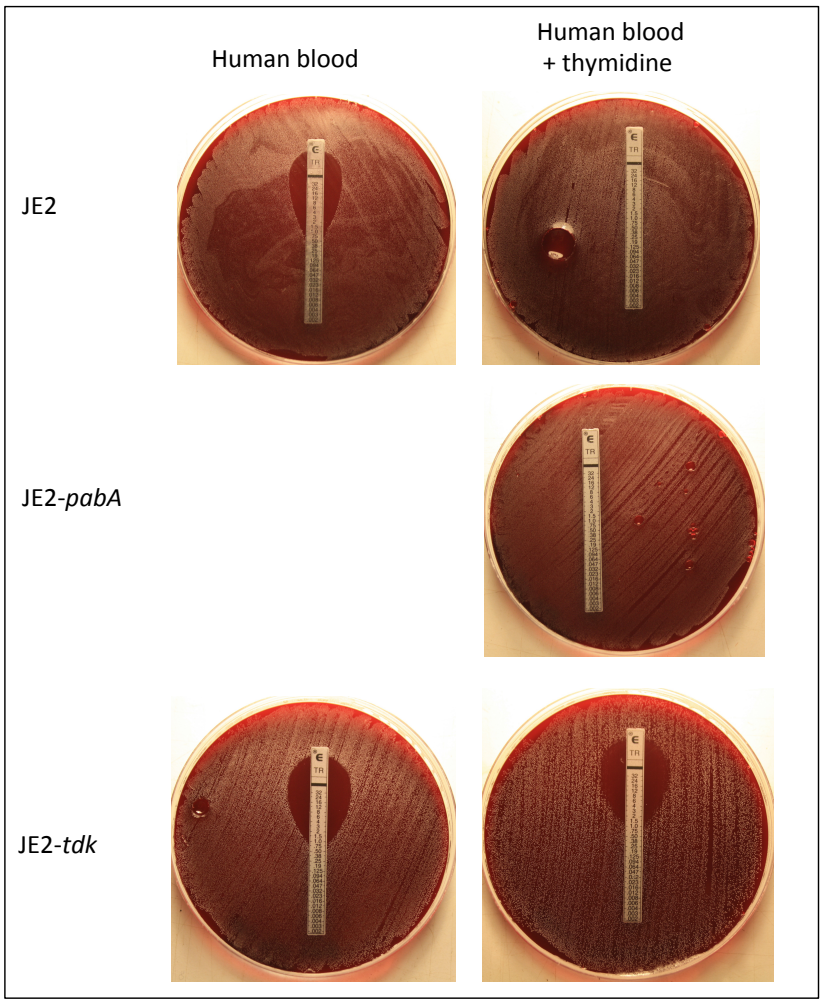


Figure 4.28 Strain susceptibility to trimethoprim with or without exogenous thymidine on 30% (v/v) human blood agar

JE2 and JE2-*tdk* were spread onto human blood agar either unsupplemented or with the addition of thymidine (400 µg ml^{-1}). JE2-*pabA* was only grown in the presence of thymidine. Trimethoprim E-tests® were added for MIC determination. Plates were incubated at 37°C for 24 hr.

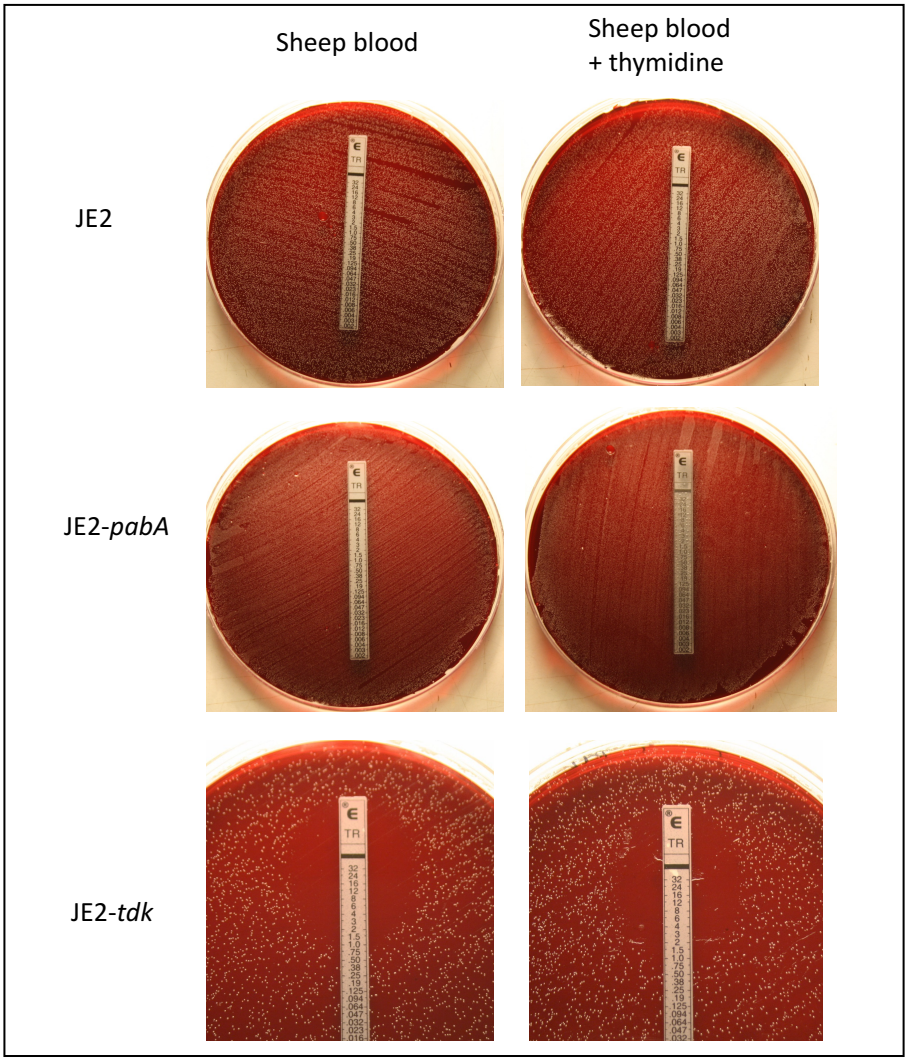


Figure 4.29 Strain susceptibility to trimethoprim with or without exogenous thymidine on 30% (v/v) sheep blood agar

JE2, JE2-*pabA* and JE2-*tdk* were spread onto sheep blood agar either unsupplemented or with the addition of thymidine (400 µg ml^{-1}). Trimethoprim E-tests® were added for MIC determination. Plates were incubated at 37°C for 24 hr.

JE2-*tdk* images are enlarged and cropped to aid viewing.

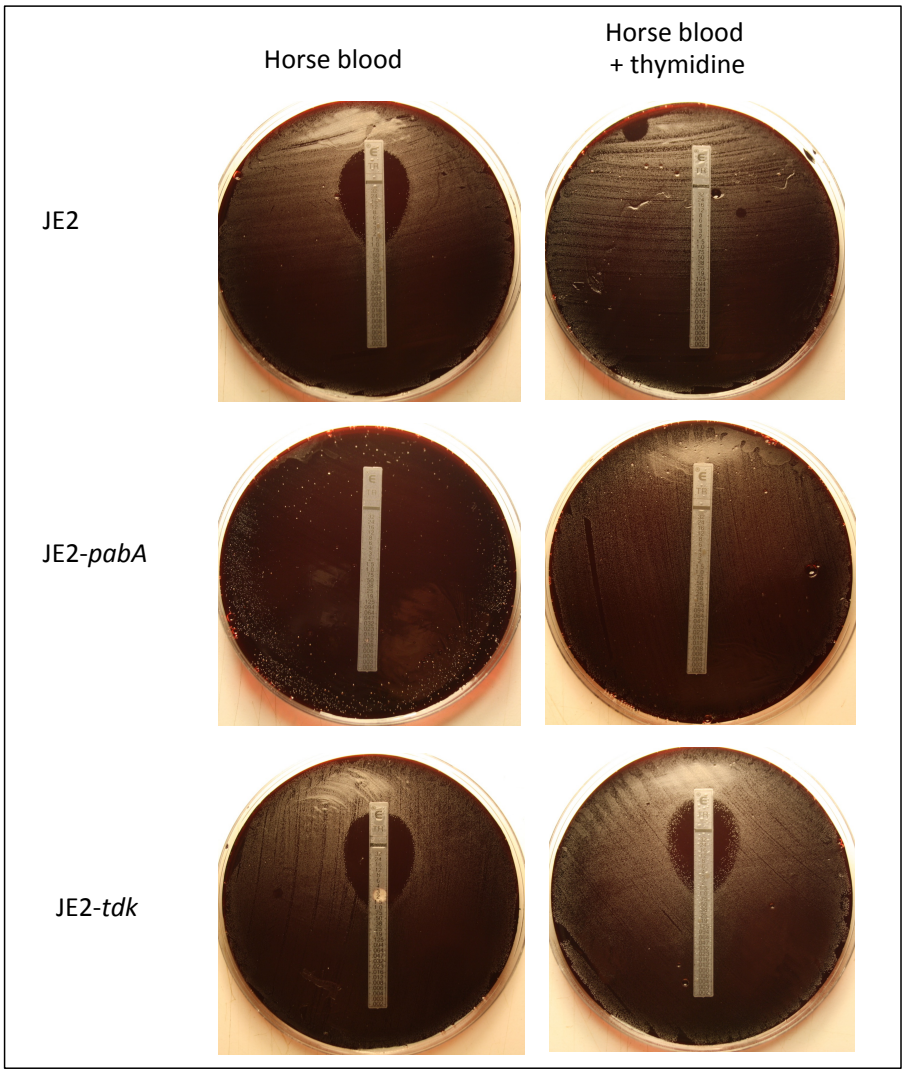


Figure 4.30 Strain susceptibility to trimethoprim with or without exogenous thymidine on 30% (v/v) horse blood agar

JE2, JE2-*pabA* and JE2-*tdk* were spread onto horse blood agar either unsupplemented or with the addition of thymidine (400 μg ml^{-1}). Trimethoprim E-tests® were added for MIC determination. Plates were incubated at 37°C for 24 hr.

4.3.5.6 Comparison of *pabA* with *thyA*

Mechanisms of 'classic' *S. aureus* resistance to antibiotics such as trimethoprim have been described e.g. mutations in the key enzyme, DHFR (Eliopoulos and Huovinen, 2001). However, another type of 'phenotypic' resistance also occurs whereby a subpopulation of *S. aureus* grow slowly and display as pinpoint size colonies on unsupplemented media (Proctor et al., 1998). Usually arising after prolonged exposure to antibiotics, many of these 'small colony variants' (SCVs) are hemin or menadione auxotrophs but thymidine-dependent SCVs are also found (Gilligan et al., 1987; Kahl et al., 2003).

These SCVs are able to cause persistent infections as they are multiply antibiotic resistant and have altered virulence factor expression (Proctor et al., 2006). More recently, it was discovered that thymidine-dependent SCVs are caused by mutations in thymidylate synthase (*thyA*) which requires THF as a cofactor (Chatterjee et al., 2008). As these strains are unable to convert dUMP into dTMP, to avoid dTMP depletion, they utilise extracellular thymidine (as is found in a cystic fibrosis lung burdened with pus and dead cells) via Tdk, hence being thymidine dependent (Besier et al., 2008). Strains with disrupted *thyA* are non-susceptible to the anti-folate antibiotics as the major THF requiring byproduct, dTMP, can be made by the alternative salvage pathways, providing sufficient thymidine is available.

Comparing and contrasting *pabA* and *thyA* may yield some insight into mechanisms for *pabA* growth inhibition. However, it should be noted that *pabA* is not a small colony variant as it grows with a normal morphology.

4.3.5.6.1 Growth of *pabA* and *thyA* on Mueller-Hinton agar

The SH1000-*thyA* mutant was kindly provided by Professor Barbara Kahl, University of Münster, Germany. The *thyA* replacement mutant was constructed using pBT9-*thyA*::*ermB* (pBT9 is a shuttle vector able to replicate in *E. coli* and staphylococci) (Kriegeskorte et al., 2014).

Mueller-Hinton (MH) agar is known to be low in thymidine and recommended for accurate testing of folate antagonist MIC values (Haltiner et al., 1980). As shown in Figure 4.31, the parent grew well on MH agar and was susceptible to trimethoprim unless thymidine was added. Although a zone of clearing appears to be seen around the trimethoprim gradient strip with thymidine added, colonies can be seen growing up to the disc on closer inspection. Interestingly, *pabA* grew well on MH agar. When thymidine was added, growth of *pabA* was seen up to the trimethoprim gradient strip indicating resistance. Finally, *thyA* was unable to grow on MH which is compatible with published data (Kriegeskorte et al., 2014). *thyA* grows when thymidine is added but is not affected by trimethoprim.

4.3.5.6.2 Growth of *pabA* and *thyA* on sheep and horse blood

Next, the growth of both mutants was tested alongside the parent for growth patterns on 30% (v/v) sheep blood with Columbia agar (which should contain high levels of thymidine) and Iso-sensitest agar with 5% (v/v) lysed horse blood (Oxoid) (which should contain very low levels of thymidine due to release of Pdp).

After overnight incubation at 37°C, only the parental strain and SH-*pabA* grew on the agar containing lysed horse blood, confirming the thymidine dependency of SH-*thyA*. In contrast, all three mutants grew on sheep blood containing agar, but the morphology of SH-*thyA* was in keeping with that of an SCV (Figure 4.32). The sheep blood agar plates were then placed at 4°C for 6 hours to examine for beta-haemolysis and it can be clearly seen that both the parent and SH-*pabA* display marked haemolytic activity whereas SH-*thyA* does not. This is in agreement with studies, which have demonstrated decreased activity of the accessory gene regulator (*agr*) in SCVs due to an absence of RNAIII. The latter is the effector molecule of the quorum-sensing regulon, *agr*, and promotes production of toxins including haemolysins (Proctor et al., 2014).

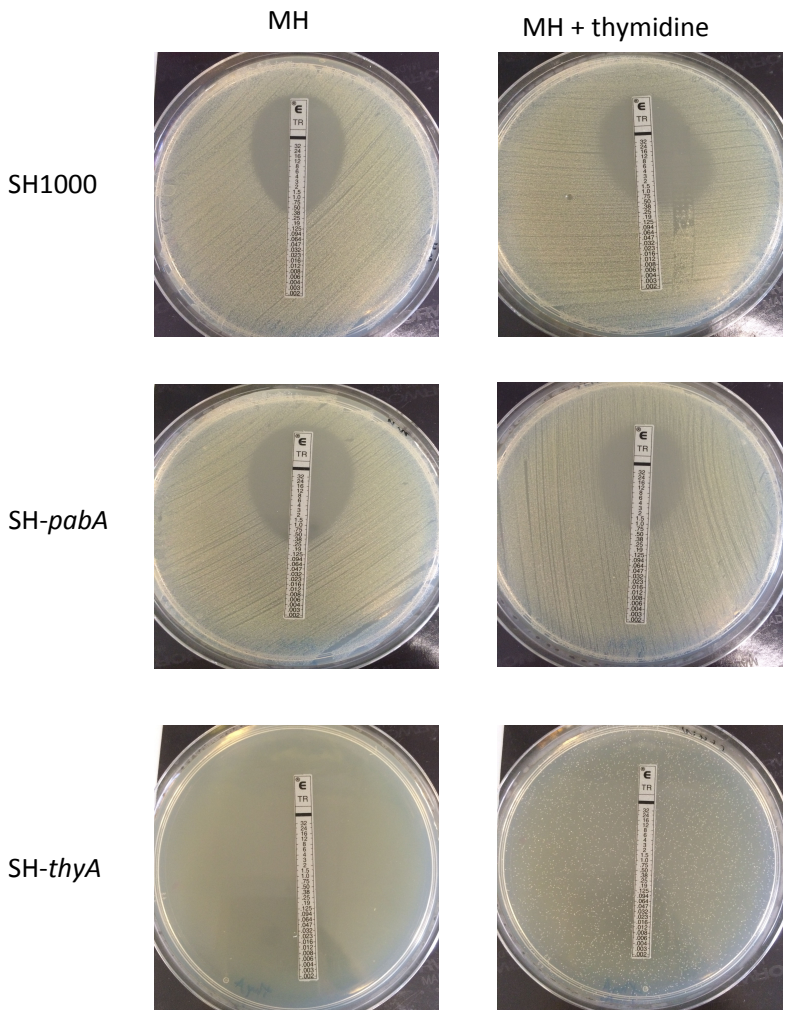


Figure 4.31 Strain susceptibility to trimethoprim with or without exogenous thymidine on Mueller-Hinton agar

SH1000, SH-*pabA* and SH-*tdk* were spread onto Mueller-Hinton agar either unsupplemented or with the addition of thymidine (400 μg ml^{-1}). Trimethoprim E-tests® were added for MIC determination. Plates were incubated at 37°C for 24 hr.

4.3.5.6.3 Comparison of *pabA* and *thyA* growth on human blood agar

The two mutants were next streaked onto 30% (v/v) human blood agar with or without thymidine at various concentrations. In the absence of thymidine, only SH1000 was able to grow. When thymidine (400 μg ml^{-1}) was added, SH-*pabA* growth was seen but SH-*thyA* was barely able to grow (Figure 4.33 C). There was minimal growth of the small SCV colonies (in the inoculum pool) but also evidence of suppressor colony formation, the latter being due to reversion from the SCV to a parent phenotype. In a recent publication, revertants were found to contain point mutations at the initially identified mutation site allowing the *thyA* gene to function once again (Kriegeskorte et al., 2015).

SH-*thyA* is dependent on thymidine availability as evidenced by good growth on sheep blood agar and poor growth on horse and human blood. If competitive inhibition of Tdk is responsible for restricting *pabA* growth on human blood but can be overcome by supplementary pyrimidine, it would follow that supplemental thymidine should also complement growth of *thyA*, which also depends on Tdk and pyrimidine salvage pathways for viability. Therefore, three times the standard thymidine concentration was added to human blood agar (1.2 mg ml^{-1}) and *thyA* growth was observed (Figure 4.33 D). This provides support for the hypothesis that a component of human blood is competitively inhibiting Tdk in *S. aureus*. The thymidine content of media plays an important role as overcoming this inhibition is dependent on adequate exogenous thymidine which acts as a substrate for the enzyme and ultimately yields dTTP.

As *pabA* growth is permitted on human blood with lower thymidine supplementation compared to *thyA*, this may suggest that there is residual enzymatic activity in the absence of the co-factor THF in the *pabA* mutant.

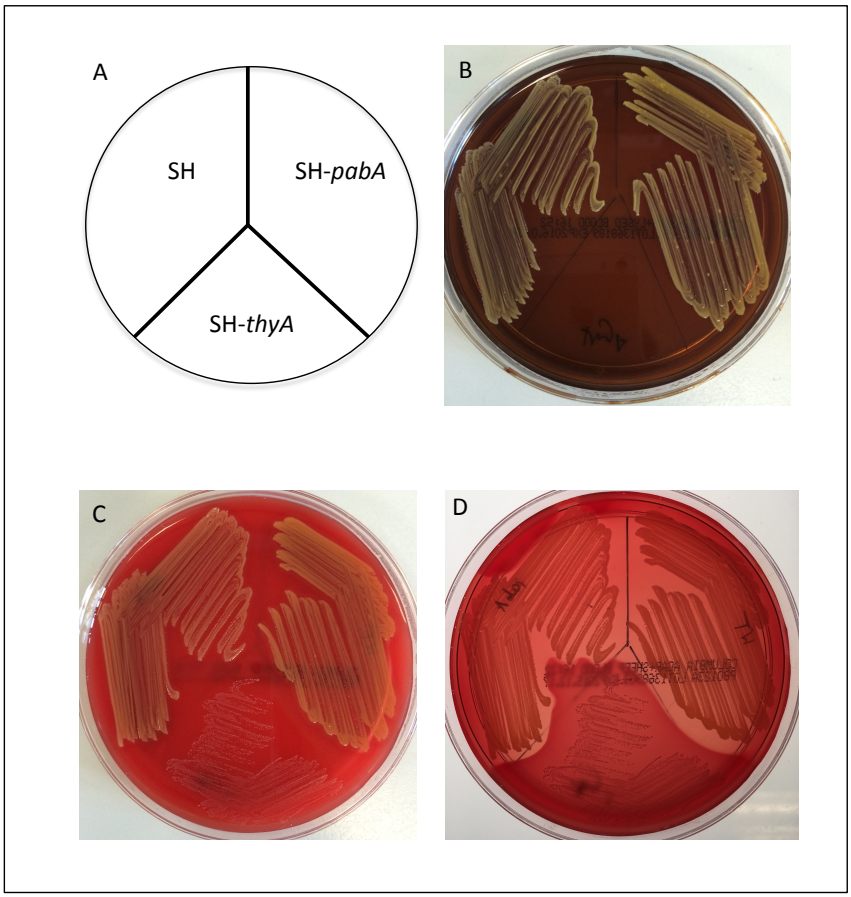


Figure 4.32 Growth of parent and mutants on whole or lysed animal blood agar

A Position of streaked strains

B Iso-sensitest agar with 5% (v/v) lysed horse blood

C 30% (v/v) sheep blood with Columbia agar to observe for growth

D 30% (v/v) sheep blood with Columbia agar to observe for beta-haemolysis

Plates were incubated at 37°C for 24 hr. Sheep blood agar plates were then placed at 4°C for 6 hours for beta-haemolysis.

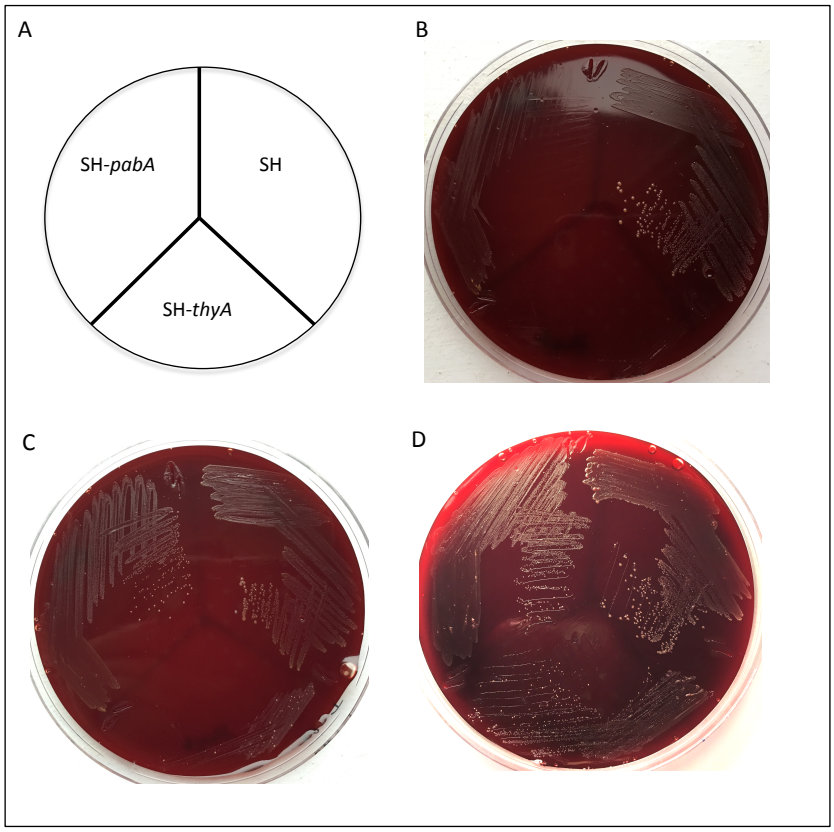


Figure 4.33 Growth of parent and mutants on whole human blood agar with varying levels of thymidine

A Position of streaked strains

B 30% (v/v) whole human blood agar (unsupplemented)

C 30% (v/v) whole human blood agar + thymidine (400 µg ml^{-1})

D 30% (v/v) whole human blood agar + thymidine (1.2 mg ml^{-1})

Plates were incubated at 37°C for 24 hr.

4.3.5.6.4 Effect of lysed human RBCS on *thyA* growth

If Tdk inhibition prevents *pabA* growth on human blood, the inhibitory compound is proposed to originate from within RBCs as *pabA* growth is inhibited on plasma by a small amount of vortexed 'red plasma' (from lysed RBCs). It could follow therefore, that lysis of RBCs is a limiting factor for folate deficient strains such as *pabA* or *thyA*. It is already established in the literature that *thyA* mutants persist intracellularly and reduce toxin and protease production (Besier et al., 2008). It was considered therefore that this may be a strategy to reduce the possibility of lysing RBCs. Once lysed, the RBCs may release the as yet unidentified inhibitory factor which would then inhibit the Tdk enzyme that is required for *thyA* survival.

To test this, MH agar was supplemented with thymidine (400 μg ml^{-1}) and evenly spread with either the parent or SH-*thyA*. Both PPP and whole human blood were vortexed for 3 minutes to achieve partial RBC lysis in the latter (the plasma was vortexed as a control). To achieve full lysis, another aliquot of whole human blood was placed at -80°C for 30 minutes before returning to room temperature for thawing. Sterile discs were soaked in each substance as shown in Figure 4.34 and incubated overnight at 37°C. The products of RBC lysis affected neither growth of the parent or *thyA* during this experiment. The formation and persistence of *S. aureus* thymidine dependent SCVs is complex and not yet fully understood. This experiment has shown that SH-*thyA* is able to grow in the presence of lysed RBCs disproving the hypothesis above.

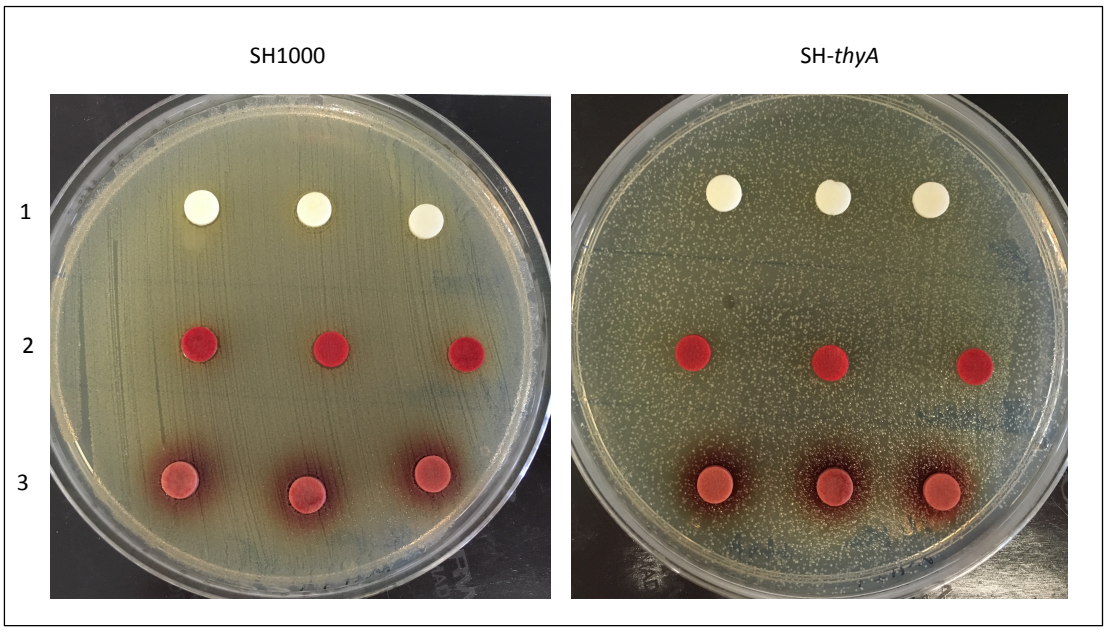


Figure 4.34 Growth of parent or *pabA* on Mueller-Hinton agar supplemented with thymidine with addition of discs impregnated with blood components

1. vortexed PPP
2. vortexed whole blood (to promote partial RBC lysis)
3. freeze-thawed whole blood (to promote complete RBC lysis)

Growth was seen up to all discs for both parent and mutant. Plates were incubated at 37°C for 24 hr.

Thymidine content - 400 μg ml^{-1}.

4.3.5.7 Investigating cellular stress caused by heme toxicity

In the host environment, when innate immune cells encounter bacteria, reactive oxygen species (ROS) are generated such as superoxide and nitric oxide (Nunoshiba et al., 1995). Oxidative damage to DNA bases has serious potential consequences for bacteria. Bacteria have developed sophisticated mechanisms to resist oxidative stress and can repair DNA affected by oxidative damage (Gaupp et al., 2012). Paraquat (methyl viologen) is a widely used herbicide that reduces oxygen to superoxide anion radicals intracellularly, mimicking superoxide stress conditions *in vivo*. Although the exact mechanisms of heme toxicity to bacteria are poorly understood, monooxygenase like activity has been suggested to cause direct DNA damage (Lin and Everse, 1987). Heme acquisition however is a necessity for *S. aureus* survival in the tightly controlled host environment (Anzaldi and Skaar, 2010).

It was suspected that RBC lysis products were causing detrimental effects to *pabA*, in excess of that caused to the parent. It was hypothesised that released heme might be a significant cause of bacterial oxidative stress requiring increased dTTP requirements for DNA repair. Therefore, a strain unable to acquire heme due to a disrupted iron-regulated surface determinant (Isd) system and heme transport system (Hts) was kindly provided by Dr Sean Nair (LS1Δ*isdE*Δ*htsA*, University College London). The *pabA* mutation was transduced into this strain using φ 11 phage and successful transductants were confirmed by PCR. The triple mutant (LS1Δ*isdE*Δ*htsApabA*) was inoculated onto 30% (v/v) human blood agar to determine if the removal of potential heme toxicity would restore growth. No growth was observed for *pabA* or Δ*isdE*Δ*htsApabA* on unsupplemented blood agar but both strains displayed good growth in the presence of exogeneous pyrimidines (data not shown). Therefore, it remains unconfirmed if oxidative stress induced by heme toxicity plays a role in the *pabA* growth phenotype on human blood.

4.4 Discussion

The NTML was screened for gene disruptions causing growth and haemolysis defects on agar containing human blood as the only nutrient source. Of the 9 mutants taken forward for further study, three (*purA*, *purB* and *pabA*) showed distinct *in vitro* and *in vivo* phenotypes. The reduced growth and virulence phenotype of the purine biosynthesis mutants was due to purine requirements not readily available in human blood. The reduced growth of *pabA in vitro* was intriguing as it was specific to human blood and was only complemented by pyrimidine supplementation. Despite good growth on human plasma, the addition of lysed RBC components abrogated growth implying a potent inhibitor of *pabA* growth was present in the RBC component of human blood. In the absence of THF dependent pyrimidine synthesis via *thyA*, nucleotide salvage pathways are essential for growth of *pabA*. The current proposal is that either a factor in whole blood competitively inhibits these nucleotide salvage pathway enzymes, or that growth on human blood requires increased levels of dTMP, for example due to heme toxicity, which cannot be supported without increasing the thymine/thymidine concentration. The nature of RBC lysis toxicity remains to be identified but human haemoglobin did not prevent growth of *pabA* on plasma. The ability of *pabA* to grow on MH or CDM agar suggests necessary compounds persist in the media or that residual activity of *thyA* occurs in the absence of THF.

4.4.1 Purine biosynthesis mutants

The availability of essential nutrients during host infection is a dynamic process and poorly characterised. In a study detailing the non-essential genes involved in growth of *E. coli* or *Salmonella enterica* in human serum using a microarray-based system, the majority of mutants identified were involved in purine or pyrimidine biosynthesis (Samant et al., 2008). This suggests a scarcity of nucleotides *in vivo,* which bacteria counteract by being equipped with energy costly metabolic pathways leading to *de novo* synthesis. It is interesting that not all bacteria have *de novo* synthesis pathways and one such pathogen, *Helicobacter pylori*, has been shown to breakdown extracellular host DNA to use as a purine source (Liechti and Goldberg, 2013). Humans also rely on adequate nucleotide levels and rarely incorporate nucleotides from dietary sources including offal or meat (Van Buren and Rudolph, 1997). Synthesised primarily in the

liver, purine and pyrimidine biosynthesis pathways in eukaryotes share similarities with those in prokaryotes (Kappock et al., 2000). Being essential for cellular metabolism, anti-metabolites including purine analogues are commonly used as cancer treatment strategies, e.g. 6-mercaptopurine and 6-thioguanine, which inhibit the conversion of IMP to adenine and guanine (Nelson et al., 1975). The major downfall of this strategy is the lack of specificity to tumour cells as the drugs also affect these key pathways in healthy rapidly dividing cells. However, purine antagonists have also been developed as anti-bacterial agents in the past but none have been extensively tested in humans nor used clinically (Gottlieb and Shaw, 2013), although 6-thioguanine has been shown to reduce bacterial loads in both liver and kidney of a *S. aureus* murine renal abscess model (Lan et al., 2010). To be a successful anti-staphylococcal strategy, bacterium-selective small molecule inhibitors of nucleotide biosynthesis would be required.

An important benefit of further understanding purine metabolic processes is the wider effect disruptions in these pathways may have on the pathogen. Purine biosynthesis mutants displayed increased carotenoid pigment production which reduced recovery of the strains in a murine abscess model of infection (Lan et al., 2010). This was reported to be due to *purA* displaying decreased proteolytic activity and downregulating several virulence regulatory genes. Furthermore, adenosine synthase A (AdsA), a nucleotidase cell wall anchored enzyme that converts AMP to adenosine, has been identified as a virulence factor in *S. aureus* (Thammavongsa et al., 2009). Whilst the mechanisms are not fully elucidated, there is evidence that adenosine reduces the killing ability of neutrophils thus allowing unconstrained *S. aureus* proliferation.

These data and the work from this project highlight that host systemic infection is dynamic and bacteria must readily adapt to changing environments ranging from the intra-phagocyte niche to extracellular dissemination.

4.4.2 Analysis of *pabA*

4.4.2.1 Attempting to identify the mechanism for the distinctive *in vitro pabA* growth phenotype

There is no available literature on the role of *pabA* specifically in *S. aureus* but other Gram-positive organisms have been studied (Wegkamp et al., 2007). The ability of *pabA* to grow on human serum and plasma but not on human blood suggested that a component in blood is inhibiting a non-THF requiring pathway that leads to production of dTMP. In such alternative pathways, thymidine is converted to dTMP (via Tdk) and ultimately dTTP, which is necessary for DNA replication. In the presence of pyrimidines, *pabA* growth is permitted on human blood but a genetic knockout of *tdk* eliminates this biochemical complementation. This infers that exogenous pyrimidines added to blood are taken up by *pabA* and used to produce dTMP. The target of the inhibition on human blood agar may be Tdk, as in its absence, thymidine can no longer be converted to dTMP in the mutant strain. An absolute lack of thymidine was considered as playing a role as human blood is known to have low levels, but growth of *pabA* on other thymidine poor media suggest this not to be the case. It is possible that whilst every effort is made to ensure these media do not contain interfering factors, this has been documented to occur. In a *L. lactis pab* deletion mutant, poor growth but not no growth was seen in CDM without serine, glycine and nucleobases. If spent CDM media was used (filtered and glucose added back) no growth could be seen unless PABA was added. Therefore, trace amounts of required nutrients may inadvertently be present (Wegkamp et al., 2007). However, it is more likely that an increased requirement for thymidine, possibly due to oxidative stress in blood is necessary to support growth specifically on human blood.

Unlike other bacteria, *S. aureus* requires a complex combination of amino acids for growth (Emmett and Kloos, 1975). Those most frequently required include arginine, valine, leucine, cysteine and proline. In the absence of a full complement of amino acids, suppressors can be seen and it has been documented that suppressors are most commonly seen when alanine, glycine, proline, trytophan or valine are removed (Townsend et al., 1996). This was seen in the experiments described in this project, as auxotrophic strains exhibited large isolated colonies against a poor growth background (Figure 4.22, panels 1 and 2). Therefore, it may be that in these CDM experiments, the

essential requirements for either the parent or mutant are being tested. For example, both the parent and mutant grow poorly in the absence of serine or glycine and the absence of serine alone cannot be fully complemented by PABA even in parent bacteria. When serine and glycine are both present, the parent and mutant grow well and it would be difficult to see any added benefit from extra factors such as pyrimidines. Conversely, growth inhibition on human blood could not be rescued with any compounds except pyrimidines suggesting that all other necessary factors to bypass the lack of THF, are present in both plasma and whole blood. Intriguingly, in *E. coli*, the absence of folate, mediated by DHFR antagonists such as sulphonamides, but in the presence of other factors (e.g. serine, glycine and purines), a lack of thymine is deleterious and prevents growth in blood. This is referred to as thymine-less death (Then and Angehrn, 1973). The same phenomenon has also been reported in *S. aureus* (Mathieu et al., 1968). Thymine-less death is thought to occur due to the generation of toxic metabolites if DNA replication stops but RNA and protein synthesis continues (Ostrer et al., 2015). It is unclear why a thymine-less death phenomenon was not seen in this project. However, the studies described above all used folate antagonist antibiotics, rather than a *pabA* mutant. In both cases, preventing folate synthesis abrogates the use of folate requiring pyrimidine metabolic pathways but it may be that antibiotics have subtly different effects on these metabolic pathways, compared to a lack of a functional copy of the *pabA* gene. Alternatively, there may be residual enzymatic activity in the absence of THF. Notwithstanding, the concept of 'thymine-less' death highlights the fundamental importance of pyrimidines in bacterial survival, over and above the other downstream effectors of THF (Then and Angehrn, 1973). The main difference between plasma and blood is therefore presumed to be a lack of an inhibitory factor from lysed RBCs in the former.

Ultimately, it is not yet known whether the requirement for supplementation of thymine or thymidine on human blood to allow *pabA* growth is to prevent competitive inhibition of Tdk or to compensate for an increased pyrimidine requirement due to oxidative stress and DNA damage in human blood (Figure 4.35). It remains for the component of blood that competitively inhibits the Tdk enzyme, to be identified and further evidence that human blood causes an increased demand for dTMP, which cannot be met by the THF deficient *pabA* is also required.

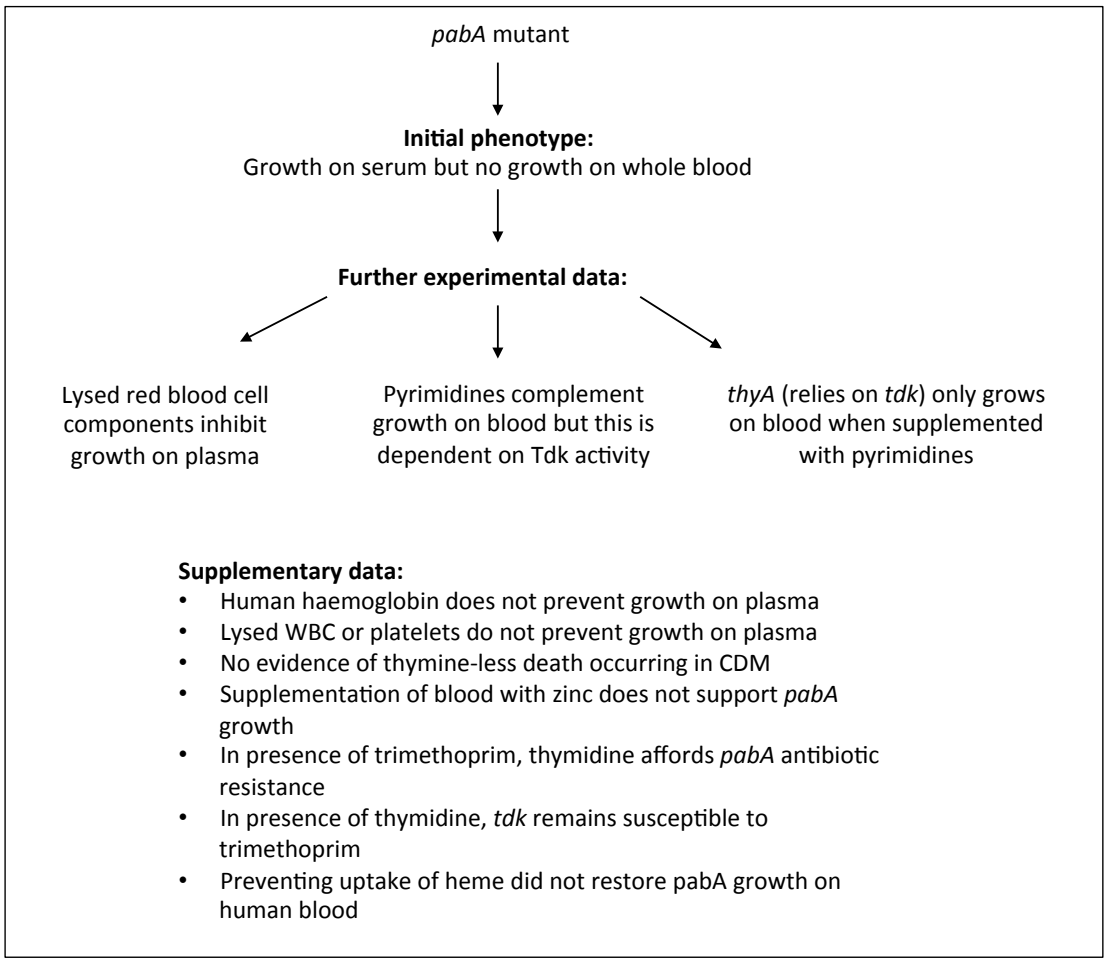


Figure 4.35 Summary of data on potential mechanisms of the *pabA* growth phenotype

4.4.2.2 Further considerations and future work

To date, a *pabA* phenotype has not been described in *S. aureus*. In another Gram-positive organism, *Streptococcus pneumoniae*, a *pabB* mutant, was employed in vaccine research so understanding such pathways may inform future prophylactic strategies against *S. aureus* (Chimalapati et al., 2011). Knowledge of immune responses elicited by attenuated mutants, may lead to the identification of improved vaccine strain candidates for *S. aureus*, which are intensively sought. This work also highlights the need for the correct use of animal models in research on metabolic mutants as demonstrated by the stark differences in thymidine serum concentration between mammals (Table 4.7).

Bacteria have evolved mechanisms for the efficient transport of exogenous nucleotides, as *de novo* synthesis carries an energy cost. *pabA* has been shown to be attenuated in two *in vivo* infection models, yet in a small number of zebrafish embryos, the mutant was still able to replicate inside the host and cause death (Figure 4.12). This implies that acquisition of necessary nutrients can occur when available.

As discussed in Section 4.3.5.5, trimethoprim is commonly used in the control of *S. aureus* infections clinically and long-standing treatment can lead to failure due to development of antibiotic resistance (Zander et al., 2010a). In this context, *thyA* mutations are usually observed in the resistant subpopulation and such mutations cause formation of thymidine dependent SCVs which rely on pyrimidine salvage pathways (via Pdp and Tdk) (Kriegeskorte et al., 2014). However, pyrimidine availability is key as these antibiotics remain bacteriocidal unless a thymidine rich environment exists such as damaged host tissues which allow such bacteria to utilise pyrimidine via Tdk. Understanding these pathways has clinical relevance as the uptake of thymidine and conversion to dTMP antagonises the action of folate pathway targeted anti-microbials. Yet as wild-type *S. aureus* can make dTMP via the THF-dependent route, Tdk inhibition or more novel approaches such as restricting thymidine uptake by transporter analogues to overcome thymidine dependent strains, would be of limited benefit in clinical practice except for treatment of resistant subpopulations towards specific antibiotics i.e. SCVs with *thyA* mutations. Little is known about the clinical prevalence or relevance of *pabA* mutations and this could be explored further.

It is interesting that, although both are potentially deficient in dTMP production, *pabA* and *thyA* mutants have stark differences. Most notably, *pabA* is not an SCV. In addition, when thymidine dependent strains are identified clinically, all isolates sequenced so far have mutations in *thyA*, rather than other THF pathway enzymes. This suggests that *thyA* is essential which is corroborated by published studies (Chaudhuri et al., 2009). The mechanisms that trigger SCV formation have been elucidated and dTMP is proposed to be the intracellular trigger as SCVs had little dTMP measured intracellularly compared to colonies with a normal morphology (Zander et al., 2008). It would therefore be of interest to measure dTMP levels of *pabA* to further compare and contrast these two mutants.

There is scarce literature on the exact mechanisms of pyrimidine and purine uptake by *S. aureus* but three putative pyrimidine transporters are described. Nucleoside permease, NupC, is documented to be the major transporter of thymidine (Kriegeskorte et al., 2014). Nucleotides e.g. dTMP cannot be transported *per se* but if cell surface enzymes are present to enable dephosphorylation, free thymidine or thymine can enter the cell (Zander et al., 2010a). It is thought, from work in *B. subtilis* and *E. coli*, that thymine is able to enter bacteria through passive diffusion before being converted by Pdp to thymidine. In wildtype cells this reaction rarely occurs due to the lack of a necessary pool of deoxyribose 1 phosphate (d1p) (Sonenshein et al., 1993; Itsko and Schaaper, 2011). However, if dTTP cannot be made through the normal pathways e.g. *thyA*-requiring THF, it is proposed that a pool of dUMP builds up which may increase the availability of the otherwise scarce, deoxyribose 1 phosphate. Together, the *de novo* synthesis and salvage pathways ensure that optimal amounts of the canonical dNTPs are available. Other further work could include investigation of pyrimidine transporters, as work from this project suggests transporters other than NupC may play a role in pyrimidine salvage (Section 4.3.5.4.1). Two remaining putative pyrimidine transporters have been identified and not yet investigated.

The purchased Tdk inhibitors did not prevent *pabA* growth on human blood (in the presence of thymidine) or growth of parent in the presence of trimethoprim. In the publication describing the identification of these inhibitors, liquid assays were conducted in MH media (Zander et al., 2010b). It may be that the Tdk inhibitors exert

their action in liquid and development of liquid whole blood assays to further test these and other potential Tdk inhibitors could be attempted.

Alternatively, bacterial spectrophotometric Tdk assays are described (Sanghvi et al., 2013). Measurement of *S. aureus* Tdk activity in complex media e.g. BHI compared to human plasma and blood for both the parent and *pabA* would confirm if disrupted Tdk activity was occurring in human blood and not the other media. A range of thymidine concentrations could also be tested to investigate for the competitive nature of Tdk inhibition that is proposed here.

Potential inhibitory factors in blood could be further explored. Haemoglobin is the most abundant hemoprotein in humans and is a complex of four heme groups. Heme is an iron containing ring structure and but usage of heme as an iron source can be toxic to bacteria due to its active redox potential, though the mechanisms underlying this are not fully understood (Anzaldi and Skaar, 2010). Liberation of iron from heme by *S. aureus* is achieved by lysis of RBCs with toxicity being reduced by the two component heme-regulated transporter (*hrtAB*) (Hammer and Skaar, 2011). Although human haemoglobin was not shown to be important in preventing *pabA* growth on plasma in this project, commercially purchased human haemoglobin is reported to be unstable (Pishchany et al., 2013). The method for freshly purifying haemoglobin from human blood could be used instead of commercial preparations.

Finally, the role of calprotectin could be investigated if significant quantities can be acquired. Using mass spectroscopy to identify proteins specifically expressed in abscesses of *S. aureus* infected mice, the metal ion chelating protein, calprotectin, was identified and noted to make up 40% of the cytosolic protein content of neutrophils (Corbin et al., 2008). Due to its ability to chelate ions such as zinc and manganese, calprotectin displays broad antimicrobial activity and *S. aureus* growth is completely inhibited *in vitro* at 75 μg ml^{-1}. The link between Tdk and zinc chelation could be explored further.

Chapter 5. Augmentation of *S. aureus* pathogenesis

5.1 Introduction

Precise host-pathogen dynamics during *S. aureus* infection are poorly understood, both in animal models and human disease. Using animal models including zebrafish and mammals, high doses of this pathogen are required to establish infection (Clarke et al., 2007; Prajsnar et al., 2008) yet the dose required to establish human infection is unknown but suggested to be far less (Elek and Conen, 1957). At the time patients present to hospital with symptoms and signs of *S. aureus* sepsis, and blood cultures are taken to establish the causative agent, quantitative measurements of bacterial numbers are no longer representative of the initial inoculum. In addition, the dose of *S. aureus* sufficient to establish an infection may vary widely depending on host susceptibility (Shukla et al., 2015). Factors such as route of entry of bacteria and *S. aureus* colonisation status also play a role (von Eiff et al., 2001).

Previously considered to be primarily an extracellular pathogen, increasing evidence now supports a viable intracellular stage for *S. aureus*, during which both survival and replication are possible (Kubica et al., 2008; Thwaites and Gant, 2011). It is concerning that *S. aureus* can persist within professional phagocytes for multiple days whilst not causing overt damage, allowing these 'Trojan horses' to disseminate the pathogen widely throughout the host. Previous work in our laboratory using the zebrafish embryo model of infection has demonstrated that *S. aureus* is efficiently phagocytosed within minutes of systemic injection, by professional phagocytes. Yet this engulfment does not always lead to effective bacterial killing as the host remains at risk of succumbing to infection (Prajsnar et al., 2008). The abscesses that form in infected hosts are founded from single or small numbers of bacteria, despite a large inoculum initially injected (Prajsnar et al., 2012). This 'bottleneck' denotes a phenomenon whereby the final diversity of a population is limited to a small founding population. From a large initial inoculum, this small founder population undergoes clonal expansion and goes on to cause host morbidity and mortality. The bottleneck has been shown to be immunological as evidenced by the knockdown of phagocytes abolishing this phenomenon and rendering the embryos susceptible to death with less than 10 CFU (personal communication, Dr Tomasz Prajsnar). As the removal of phagocytes

abolishes this clonal phenomenon, it was hypothesised that intracellular phagocytic niches are established from which a small number of bacteria can escape and ultimately found the fatal infection.

However, the basic mechanisms and regulation of this bottleneck are poorly understood. By co-injecting antibiotic resistant or fluorescently tagged, but otherwise isogenic, strains of *S. aureus* into the zebrafish embryo model, bacterial numbers from each subpopulation can be quantified or abscesses visualised. If a mixed population (1:1) was injected, a skewing of the strain ratios was observed with one strain often predominating and causing host death (Prajsnar et al., 2012). Importantly, adventitious mutations arising in a particular strain was ruled out as re-inoculating dominant strains back as part of the mixture did not increase the chances of that particular strain predominating again.

Early literature supports these findings of stochastic clonal expansion. Gorrill and colleagues conducted mixed inoculum mouse injections and found that individual abscesses are 'derived from a single bacterial unit, with little evidence for mutual support' (Gorrill, 1958). This has also been confirmed recently in the murine sepsis model where three isogenic strains (antibiotic resistance tagged) were injected systemically into the tail vein of BALB/c mice. Mice were culled at various time points throughout the experiment and bacterial numbers in individual organs enumerated (McVicker et al., 2014). Clonal expansion of individual strains was evident, particularly in the kidneys indicating again that, despite high dose inocula used in animal models, marked bottlenecks are playing a role in the ultimate infection outcome. When considering mixed populations of bacteria, there are several hypotheses pertaining to host pathogen interactions such as the 'model of independent action' whereby only a single or few bacteria are able to clonally expand as described above or 'augmentation synergism' which requires the integrated action of the population (Meynell and Stocker, 1957). Available evidence suggests that the first of these hypotheses is at play in *S. aureus* infection.

Other groups have noted similar clonal phenomenon when using a mixed infection of three isogenic *Streptococcus pneumoniae* strains to intravenously inoculate mice. They went on to delineate host and microbial factors involved in the clonal selection of

bacteria at the initiation of septicaemia (Gerlini et al., 2014). However, the concept of *in vivo* population bottlenecks leading to stochastic release of founder bacteria that successfully replicate beyond the capacity of host control, is not limited to Gram-positive bacteria. Using 'wild-type isogenic tagged strains' (WITS) of *Salmonella Typhimurium*, a mixed infection was orally administered to mice and over the course of 96 hours, a marked reduction in tag diversity was noted within the intestinal tract (Maier et al., 2014). Using the same pathogen, other groups noted an early 'non-Darwinian' selection of a few bacteria upon initial infection in the gut yet other organs contain bacteria from an independent pool (Lim et al., 2014). *Borrelia* species are also documented to undergo bottlenecks and after inoculation with an isogenic but heterogeneously tagged population of clones complexity of these strains diminished, in a stochastic manner, as the infection was established (Rego et al., 2014).

Processes that govern this stochastic, bacterial clone dominance within the phagocyte are being actively explored. Preliminary work conducted by Dr Justyna Serba (University of Sheffield) observed that clonal expansion occurs within phagocytes. By injecting zebrafish with a 1:1 ratio of CFP and YFP expressing *S. aureus* strains, the numbers of each type of bacteria could be quantified within phagocytes. At early time points (3 hpi) a fifth of phagocytes contained a single colour, indicating loss of the other strain. By 6 hpi, the percentage of phagocytes containing only once colour fraction had increased to 45% (Serba, 2015).

S. aureus disease does not always occur as a mono-infection. For example, skin and soft tissue infections can be dual-infected with *Streptococcus pyogenes* or other streptococci whilst invasive *S. aureus* infections can occur in combination with other bacteria or yeast e.g. *Candida* species (Boon and Beale, 1987; Schlecht et al., 2015). Studying mixed infections is challenging and uncommon, especially in animal models mimicking systemic infections. In the field of *S. aureus*, one of the most studied combinations is *S. aureus* and *Pseudomonas aeruginosa* infections in the lungs of cystic fibrosis patients yet many other polymicrobial combinations and sites of infection exist clinically (Mashburn et al., 2005).

Aside from mixed infections, other bacteria are likely to be simply present at the time of *S. aureus* infection, particularly in the skin and soft tissues. Resident colonising flora

e.g. *S. epidermidis*, *M. luteus*, *Corynebacterium* species can be protective by preventing adherence of pathogens such as *S. aureus* but equally such organisms have the ability to be pathogens in certain clinical contexts (Bibel et al., 1983). Recently, it was demonstrated that pro-inflammatory cytokines released from monocytes exposed to the secretome of *S. aureus* were dampened by concurrent exposure to the secretome of *S. epidermidis* which limited inflammation by promoting release of anti-inflammatory cytokines (Laborel-Préneron et al., 2015). However, it is not known whether these colonisers can also be detrimental to the host during the initiation of invasive *S. aureus* infection.

To interrogate the clonal expansion phenomenon further in *S. aureus*, mixed strain inocula including varying ratios of virulent, avirulent bacteria or bacterial cell components, were tested in both the zebrafish embryo and murine models of systemic infection. In particular, the roles of peptidoglycan and skin commensal organisms were examined and attempts at unraveling the underlying mechanism are documented.

5.2 Aims

i. To understand the breadth and parameters of augmentation of *S. aureus* pathogenesis *in vivo*
ii. To interrogate the mechanism of the augmentation phenomenon *in vivo.*

5.3 Results

5.3.1 Identification of an augmentation phenomenon during *S. aureus* infection

5.3.1.1 Co-injection of antibiotic sensitive and resistant strains

Previous work has established that sub-curative doses of antibiotics, which may be found in the environment or if patients do not take the full course of antibiotics, can confer a significant advantage to an antibiotic resistant strain *in vivo* when inoculated at a 1:1 ratio with an antibiotic sensitive counterpart (McVicker et al., 2014). The mechanism underlying the skewed strain ratios that result from the presence of low antibiotic concentrations, has not been elucidated yet the phenomenon is abolished in phagocyte depleted zebrafish embryos. The necessity of phagocytes for controlling *S. aureus* infection is well established but the ability for *S. aureus* to take advantage of specific conditions or niches to avoid killing by the innate immune system has also been described (Guide et al., 2003; Kubica et al., 2008).

The data described by McVicker and colleagues (McVicker et al., 2014) presented an opportunity to explore the requirement of high dose inocula to establish infection. It was hypothesised that not all bacteria within the injected population were behaving in the same manner and perhaps host:pathogen or pathogen:pathogen interactions were affecting outcome. If only a few bacteria escape to establish the fatal infection, what is the role of all the remaining bacteria? Using antibiotics to manipulate populations of sensitive and resistant bacteria provided a method of examining the bacterial population further *in vivo*.

Pilot experiments were conducted in collaboration with Mr Alexander Williams (Research Technician, University of Sheffield) to determine if, in a mixed population of antibiotic resistant and antibiotic sensitive strains, the presence of curative dose antibiotics would affect the pathogenesis of the antibiotic susceptible bacterial population. Experiments were conducted in the zebrafish embryo as described in Section 2.19.

A virulent strain of *S. aureus*, Newman, at high dose of approximately 1500 CFU caused 50% embryo mortality during 90 hours post infection. The majority of embryos were alive at 24 hpi and thereafter, two distinct outcomes were seen whereby embryos

either survive infection with low numbers of bacteria or they are overwhelmed by replicating bacteria and succumb. However, mortality is dose dependent and strains injected at a lower dose of 150 CFU show a significantly reduced mortality rate (approximately 80-90% survival) as the majority of embryos survive with reducing numbers of bacteria. In this experiment, zebrafish embryos were infected with Newman at a 1:9 ratio of approximately 150 CFU (low dose) tetracycline-resistant, Tet^R, and 1350 CFU (high dose) erythromycin/lincomycin-resistant, Ery^R, mixed inoculum, with or without a curative dose of tetracycline (50 μg ml^{-1}). Low dose (150 CFU) *S. aureus* was injected alone as a control. These strains are otherwise isogenic and show no virulence differences when injected separately in high dose in the zebrafish model (Prajsnar et al., 2012). The Ery^R strain retains sensitivity to tetracycline so erythromycin resistance can be used as a strain marker in order to later delineate the two bacterial populations on selective agar. Once injected, the zebrafish were monitored for 90 hours and any embryo that succumbed to infection, as detected by cessation of heartbeat or large abscess formation and tissue destruction, was individually collected in order that total and relative bacterial numbers of strains could be quantified.

Low dose bacteria (dotted line) caused significantly less killing than high dose (dashed line, Figure 5.1 A). 50 μg ml^{-1} tetracycline, administered by immersion in the E3 zebrafish medium, has been shown previously to prevent growth of the Ery^R bacteria (McVicker et al., 2014). In the mixed inoculum group, in the presence of tetracycline, there was significant mortality compared to the low dose alone ($p = 0.0018$). In the absence of antibiotics, a total inoculum of 1500 CFU i.e. low dose susceptible bacteria (150 CFU) plus antibiotic resistant bacteria (1350 CFU) caused approximately 50% mortality. To ensure this was not a Newman strain specific phenomenon, the same experiments were carried out using the SH1000 laboratory strain background and similar results were obtained (Figure 5.1 B).

Bacterial CFU burden in living embryos (5 embryos per group per time-point) at 2 and 18 hours post infection and every 12 hours thereafter, were determined (Figure 5.1 C & D, open circles). At each time-point, bacterial CFUs from dead embryos were also determined (Figure 5.1 C & D, filled circles). Analysing the bacterial kinetics of each population in this manner demonstrated that, in the absence of antibiotics, embryos are more likely to succumb to the Ery^R strain (red filled circles), simply because a higher

initial number was injected (1350 CFU) compared to the Tet^R strain (150 CFU) (Figure 5.1 C). In the presence of tetracycline however, embryos that have succumbed contain approximately 10^6 CFU of the Tet^R strain (black filled circles in 5.1 D). The antibiotic prevents growth of the antibiotic sensitive strain as low numbers of antibiotic sensitive (Ery^R) strain were recovered from embryos but the antibiotic sensitive strain was not completely eradicated from the host (open red circles, Figure 5.1 D). This might be due to residual *S. aureus* burden within phagocytes that are unable to effectively kill the bacteria (Gresham et al., 2000) and such niches may be protected from antibiotics (Jacobs and Wilson, 1983). This suggested that in the presence of antibiotic susceptible bacteria, low numbers of Tet^R bacteria were more successful in causing host death. Without the Ery^R bacteria being present i.e. the low dose 150 CFU only control group, this level of killing was not seen, implying that the antibiotic susceptible bacterial population may play a role. It is not yet known how these 'bystanders' promote this effect.

This led to the conclusion that in this model, virulent bacteria inoculated at a dose too low to otherwise cause infection may be helped by the presence of other bacteria, even if those bacteria are not able to proliferate. Understanding this process may provide insight into why high dose inocula are required in animal models to establish infection. Going forward, it is hoped that such knowledge would inform clinical infection processes in humans.

Therefore, a wider hypothesis was developed which considered that non-proliferative or avirulent bacteria or even just bacterial components, may be able to augment pathogenesis of low dose *S. aureus* (low enough that when injected alone, no significant mortality is seen) leading to increased host mortality. Using antibiotics to explore this phenomenon was limiting as only certain antibiotics can be reliably and reproducibly used with immersion methods in the zebrafish. Investigation of different antibiotics would require intravenous administration necessitating sequential bacterial then antibiotic injections. This was avoided due to risk of zebrafish damage. Therefore, in order to expand the experimental repertoire, avirulent *S. aureus* strains were used to interrogate this augmentation phenomenon further.

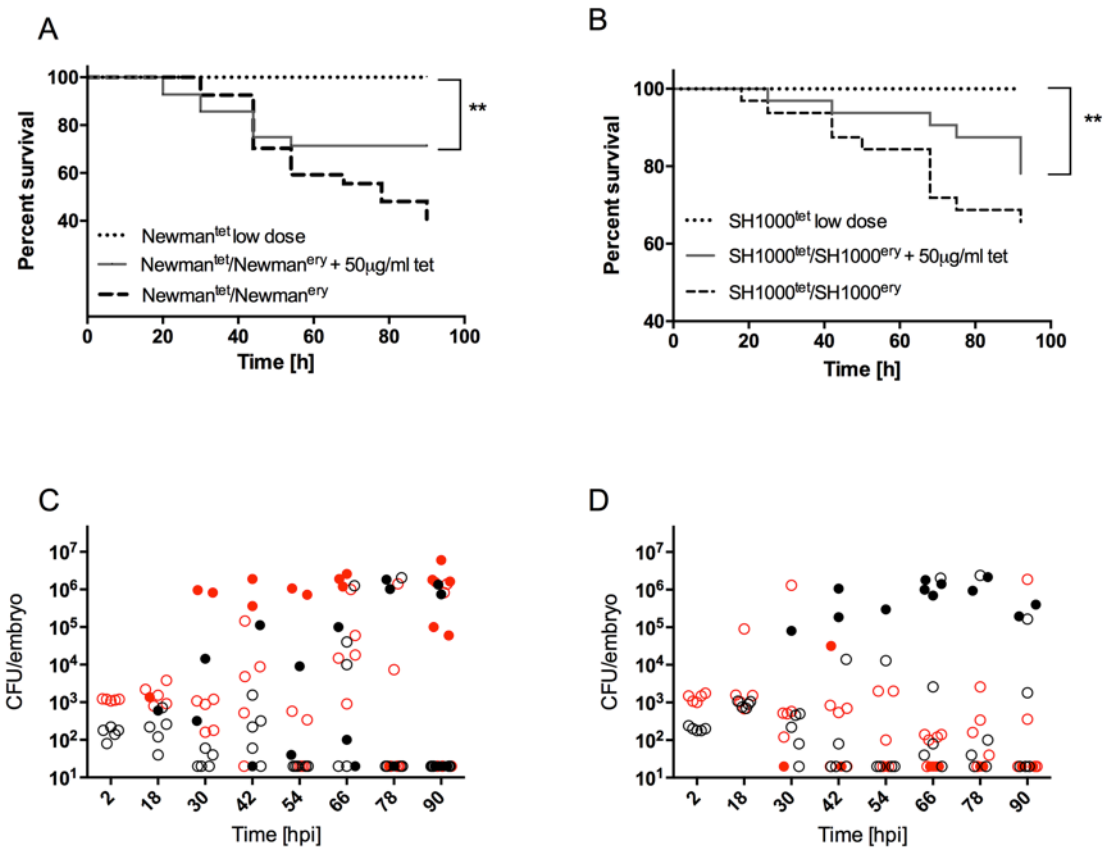


Figure 5.1 Co-injection of tetracycline resistant and sensitive strains in a 1:9 ratio followed by the administration of tetracycline

A Injection of a mixture of low dose Newman Tet^R (150 CFU) with Newman Ery^R (1350 CFU) caused augmented host killing in the presence of 50 µg ml^{-1} tetracycline (log rank test; ** p = 0.0014).

B Injection of a mixture of low dose SH1000 Tet^R (150 CFU) with SH1000 Ery^R (1350 CFU) caused augmented host killing in the presence of 50 µg ml^{-1} tetracycline (log rank test; ** p = 0.0071).

C & D Growth of each bacterial population within zebrafish embryos. At each time point, 5 living embryos and any dead embryos were processed for CFU per embryo. Open circles represent living embryos and filled circles show dead embryos. Red colour represents the Ery^R population and black, the Tet^R population. At each time point, an individual fish is represented by both a red and black circle as both populations were co-injected.

Injection of a mixture of low dose Newman Tet^R (150 CFU) with Newman Ery^R (1350) without the addition of antibiotics (**C**) or followed immediately by the addition of 50 µg ml^{-1} tetracycline (**D**).

5.3.1.2 Co-injection of attenuated and parent *S. aureus* strains

A range of attenuated mutants was used to determine if they would augment pathogenesis by the parent strain. The strains chosen are described in Table 5.1. SH1000*pheP* has reduced virulence in both a *Drosophila melanogaster* infection model and murine abscess model (Horsburgh et al., 2004). When injected at high dose (1500 CFU) in the zebrafish embryo model at 30 hpf, approximately 80% of embryos survived (data not shown). Similarly, several studies have shown the importance of the *sae* locus in pathogenesis but although *saeR* mutants show attenuated virulence *in vivo*, they are not avirulent (Goerke et al., 2005; Prajsnar et al., 2008). If the mutant itself caused low-level killing and a low dose parent also caused low-level killing, it would be possible that combined inocula mortality would reflect the addition of each strains virulence, thus making any augmentation phenomenon harder to discern. In order for this assay to be used, the avirulent strains tested should cause no or very little mortality when injected at high dose alone.

Therefore, *pheP* was transduced into SH1000*saeR* using φ 11 phage to produce a double mutant. SH1000*phePsaeR* was shown to be avirulent at high dose (1500 CFU) in the zebrafish embryo model of infection (Figure 5.2 A). SH1000*sagB* has not previously been tested for virulence *in vivo* but has recently been shown to have increased peptidoglycan strand length and perturbation of protein secretion (Wheeler et al., 2015; Chan et al., 2016). Injected at 1500 CFU into the zebrafish embryo model, SH1000*sagB* was found to be highly attenuated (Figure 5.2 B). Purine biosynthesis mutants, such as SH1000*purB*, display reduced virulence in mouse abscess models and indeed were avirulent in the zebrafish infection model in this project (Chapter 4). Finally, SH1000*pabA* was also chosen as it was also identified as having reduced virulence in the zebrafish embryo model (Chapter 4).

Co-injecting parent bacteria (150 CFU) and *phePsaeR* (1350 CFU) in a 1:9 strain ratio (total dose of 1500 CFU) produced mortality far in excess of low dose parent alone ($p=0.0016$) (Figure 5.2 A). Testing the remaining mutants (*sagB*, *purB* and *pabA*) at a 1:9 (parent:mutant) ratio, it was demonstrated that not all attenuated mutants were able to augment host death in combination with low dose parent strain (Figure 5.2 B – D). This is perhaps not surprising as attenuated mutants *in vivo* may act in different ways,

with respect to intracellular growth dynamics (Grant et al., 2012). Understanding the augmentation phenomenon is important as it could shed light on the mechanisms underlying stochastic bacterial escape from phagocytes leading to clonal abscesses. The avirulent strain *phePsaeR* may help the parent strain to establish infection, despite low numbers, due to this specific double mutation. For example, enhanced escape from the phagocyte may ensue if the phagocyte is concurrently dealing with strains of varying virulence. Additionally, the *sae* operon is a key global regulator of exotoxin production and may play a role in resistance of *S. aureus* to myeloid cell killing (Geiger et al., 2008). It was hypothesised that strains with *sae* locus mutations may skew the host pathogen dynamics in favour of the host allowing uncontrolled proliferation of the parent strain.

Therefore, double mutants were created combining a *sae* mutation with another avirulent mutation, *purB*, (which was not able to augment). A *purB* φ11 phage lysate was used to transduce this mutation into the *pheP* mutant background. *purB* contains a Tn containing erythromycin resistance whilst the *pheP* mutant contains a Tn with tetracycline resistance so a double mutant was easily produced. The *saeR* mutant used to construct the *phePsaeR* mutant however, contains an erythromycin resistance cassette so an alterative *sae* mutant was used in which the entire *sae* locus was replaced with a kanamycin cassette (Mainiero et al., 2010). An *sae* φ80 phage lysate was used to transduce this mutation into the recipient *pheP* strain. Transductants were confirmed by PCR (data not shown). SH1000*phePpurB* and SH1000*saeRpurB* were then tested under the same experimental protocol. No pathogenesis augmentation was seen in combination with the low dose parent suggesting the *sae* locus is not responsible for this phenomenon (Figure 5.3).

The requirement for *phePsaeR* to be alive was next tested by heat killing the strain by incubation at 70°C for 30 minutes. The same experimental protocol was used as for live *phePsaeR*. Compared to mixed inocula with viable *phePsaeR*, the augmentation phenomenon was abolished with heat-killed bacteria (Figure 5.4). Therefore, the mutant must be alive to enhance zebrafish mortality. An augmentation phenomenon has now been demonstrated under two conditions (antibiotic and attenuated mutant mediated). Further host:pathogen dynamics of this phenomenon were investigated using *phePsaeR*.

Strain (SH1000)	**Description**	**Reference**
pheP	Deficient in amino acid permease	(Horsburgh et al., 2004)
saeR	Global regulator of virulence factors	(Prajsnar et al., 2008)
sagB	Deficient in glucosaminidase leading to increased glycan chain length	(Wheeler et al., 2015) (Chan et al., 2016)
purB	Disruption of purine biosynthesis	This study (Chapter 4)
pabA	Disruption of folate biosynthesis	This study (Chapter 4)

Table 5.1 Description of attenuated mutant strains

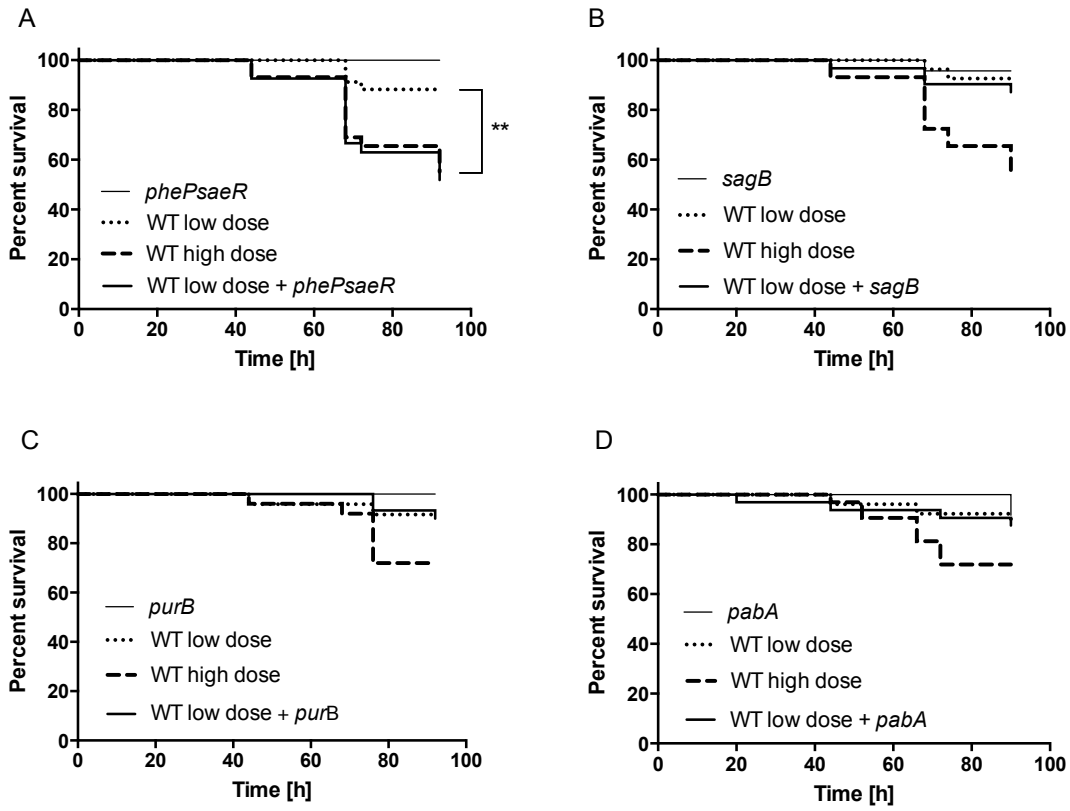


Figure 5.2 The effect of attenuated strains on *S. aureus* SH1000 pathogenesis in the zebrafish infection model

The mutant strains at 1500 CFU (high dose, thin black line) are attenuated in the zebrafish model. Low dose SH1000 (dotted line) at 150 CFU is attenuated whilst high dose SH1000 (dashed line) causes up to 50% mortality (n = 28 embryos per group).

A Injection of a mixture of low dose SH1000 (150 CFU) with SH1000*phePsaeR* (1350) caused augmented host killing compared to low dose SH1000 injected alone (log rank test; ** p = 0.0016).

Injection of a mixture of low dose SH1000 (150 CFU) with the following mutants (1350 CFU) did not augment host killing compared to low dose SH1000 injected alone:

B SH1000*sagB* (log rank test; p=0.48)
C SH1000*purB* (log rank test; p=0.87)
D SH1000*pabA* (log rank test; p=0.90)

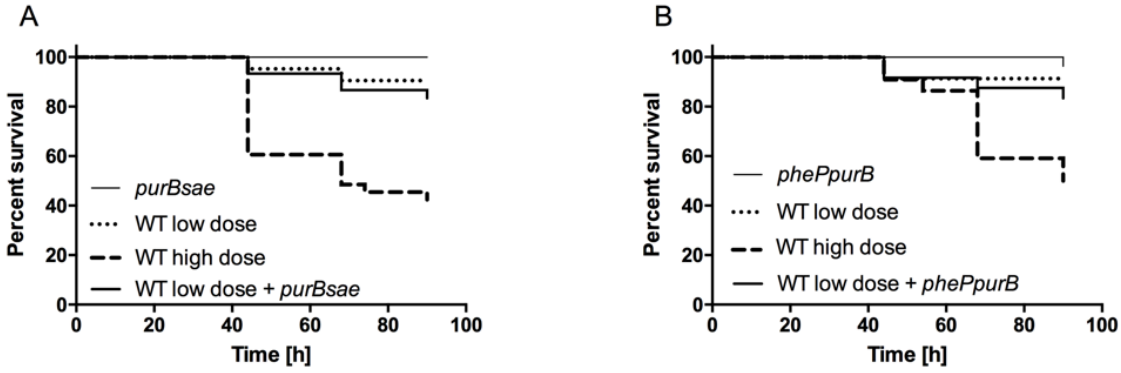


Figure 5.3 Combining *purB* or *pheP* with *sae*Δ did not permit augmentation of pathogenesis in the zebrafish infection model

A SH1000*purBsae* caused no host death alone (thin black line) or in combination with low dose parent (thick black line).

B SH1000*phePpurB* caused no host death alone (thin black line) or in combination with low dose parent (thick black line).

In both experiments, low dose SH1000 (150 CFU, dotted line) killed few hosts compared to high dose (1500 CFU, dashed line).

n=30 per group

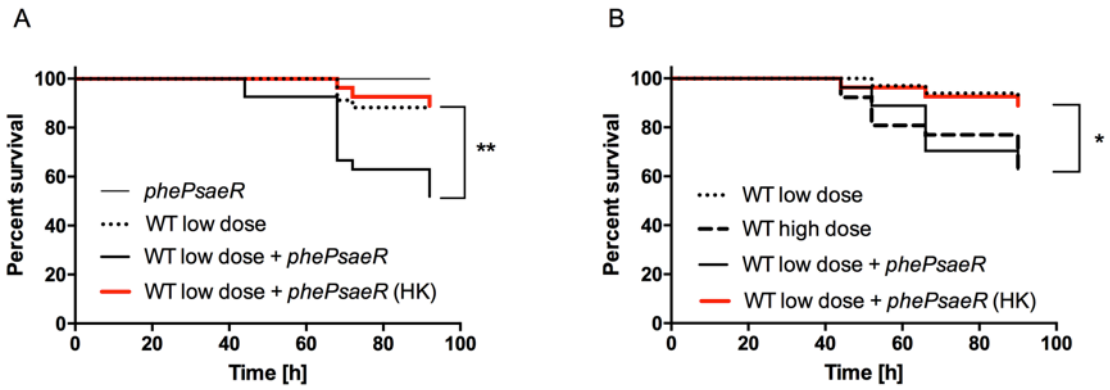


Figure 5.4 Non-viable *phePsaeR* was unable to augment host death in the zebrafish infection model

SH1000*phePsaeR* caused no host death alone. Low dose SH1000 (150 CFU, dotted line) killed few hosts compared to high dose (1500 CFU, dashed line); n=30 per group.

The increased host death seen with a mixture of low dose SH1000 (150 CFU) and SH1000Δ*phePsaeR* (1350 CFU) was abolished by heat killing (HK) the mutant (red line).

A & B are repeat experiments.

A ** p = 0.0025
B * p = 0.028

5.3.2 Host pathogen dynamics during pathogenesis augmentation with attenuated mutant mixed inocula

5.3.2.1 Bacterial growth kinetics of mixed inocula *in vivo*

To establish the pathogen dynamics of mixed inocula at a 1:9 ratio (low dose SH1000, 150 CFU and *phePsaeR* 1350 CFU) zebrafish were injected in large numbers and at 2 hpi, 8 hpi, and then every 12 hours, 5 live fish and any dead fish were individually collected. An isogenic antibiotic resistance tagged strain of SH1000 was used in this experiment, containing a kanamycin resistance cassette (SH1000 Kan^R) in order than the *phePsaeR* mutant (containing both erythromycin/lincoymycin and tetracycline resistance cassettes) could be distinguished on selective media. The collected fish were homogenized and serially diluted onto either kanamycin 50 μg ml^{-1} agar plates or erythromycin 5 μg ml^{-1}/ lincomycin 25 μg ml^{-1} agar plates and total and relative strain CFUs were calculated.

Zebrafish injected with low dose SH1000 Kan^R alone show a general reduction in bacterial numbers over time until the limit of detection of the assay (20 CFU) is reached (Figure 5.5 A). When high dose parent is injected alone, many more embryos were killed as indicated by the high number of filled circles in Figure 5.5 B. When the *phePsaeR* mutant was injected at 1.5 $x10^3$ CFU, in the majority of embryos, the bacteria were eradicated during the course of the experiment (Figure 5.5 C). However, when both low dose SH1000 Kan^R and high dose mutant are co-injected, the majority of dead embryos were overwhelmed by low dose SH1000 Kan^R growth to 10^6 CFU, rather than by that of the mutant. Some of those fish also contained $10^3/10^4$ CFU of the mutant strain (Figure 5.5 D) but those numbers fall short of the 10^6 CFU threshold that appears to be required for embryo death as has been previously reported (Prajsnar et al., 2008). Depicted as percentage CFU of each strain per embryo, Figure 5.5 E demonstrates again that in each dead embryo, the overwhelming bacterial burden arose from the SH1000 Kan^R strain rather than the mutant. This shows that the host was unable to cope with an otherwise innocuous low dose of *S. aureus*, when concurrently injected with avirulent bacteria.

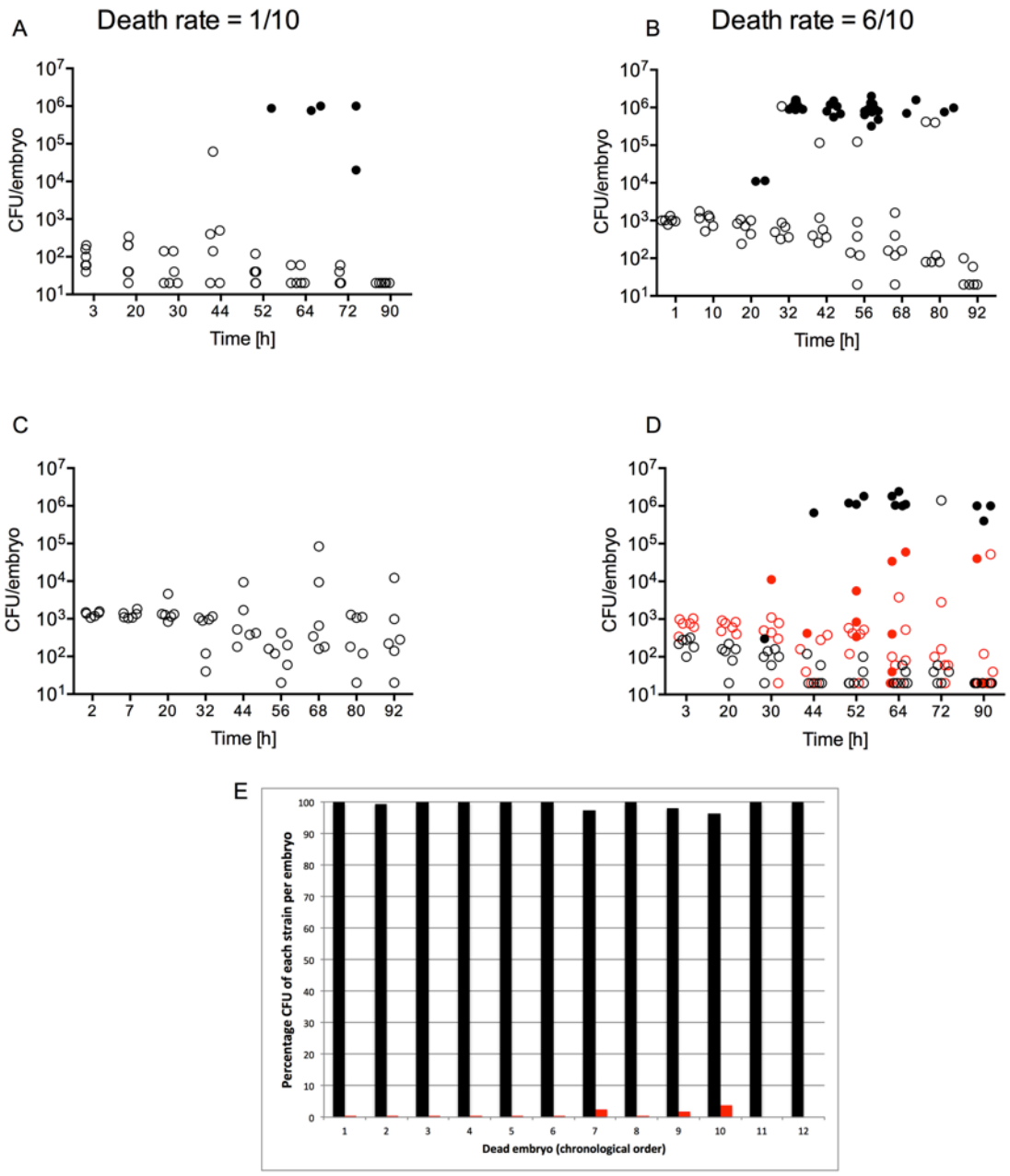


Figure 5.5 Population dynamics of bacterial strains in single and mixed infections in the zebrafish infection model

Injection of low dose SH1000 parent (150 CFU) **(A)**; high dose SH1000 parent (1500 CFU) **(B)**, high dose *phePsaeR* (1500 CFU) **(C)** or injection of parent (150 CFU) and *phePsaeR* (1400 CFU) into the zebrafish circulation **(D)** (open and closed black circles – parent strain; open red and closed red circles – mutant strain). Open circles indicate individual live fish; filled circles are dead fish; n=45-90. **E** Relative bacterial numbers at time of host death from panel D (black bars – parent strain; red bars – mutant strain). NB The zebrafish death that occurred at 30 hrs was excluded as this was not due to overwhelming bacterial numbers and likely died from other factors.

5.3.2.2 The role of phagocytes in mediating augmentation of pathogenesis in the zebrafish embryo model of infection

5.3.2.2.1 Investigation of *phePsaeR* growth in the absence of phagocytes

Using a knock-down approach, it has previously been established than a temporary delay in phagocytic cells development renders the zebrafish embryo susceptible to over-whelming bacterial replication and host death (Prajsnar et al., 2008). In wildtype embryos, primitive macrophages arise at 30 hpf from the anterior lateral plate mesoderm and then circulate and seed to various tissues (Herbomel et al., 1999). Granulocytic cells appear between 32-48 hpf to complete the first wave of phagocytic influx but definitive haematopoesis occurs in the caudal haemopoeitic tissue (CHT) (Lieschke et al., 2001; Yoo and Huttenlocher, 2011).

Chemically modified anti-sense oligonucleotides (morpholinos) are used to target the translational start site of the transcription factor, *pu.1*, thus preventing protein production. As is also found in mice, *pu.1* is required for myeloid cell development and injection of the *pu.1* morpholino at the 1-4 cell zebrafish embryo stage leads to a delay in the appearance of neutrophils until 36 hpf and macrophages until 48 hpf (McKercher et al., 1996; Rhodes et al., 2005).

It was not possible to interrogate augmentation during *S. aureus* pathogenesis using *pu.1* knock down approaches, as in the absence of phagocytes and a total inoculum of 1500 CFU, the host would rapidly succumb. However, injecting the mutant *phePsaeR* alone into embryos at 1500 CFU demonstrated that, similar to the parent, this strain was restored to almost full virulence in the absence of phagocytes, with over 80% of the embryos dead at 40 hpi with 10^6 CFU (Figure 5.6 A, B). Compared to injection of low dose (150 CFU) parent strain alone, there was slightly delayed killing but nonetheless this demonstrates that, in wildtype zebrafish, the *phePsaeR* mutant was controlled by phagocytes.

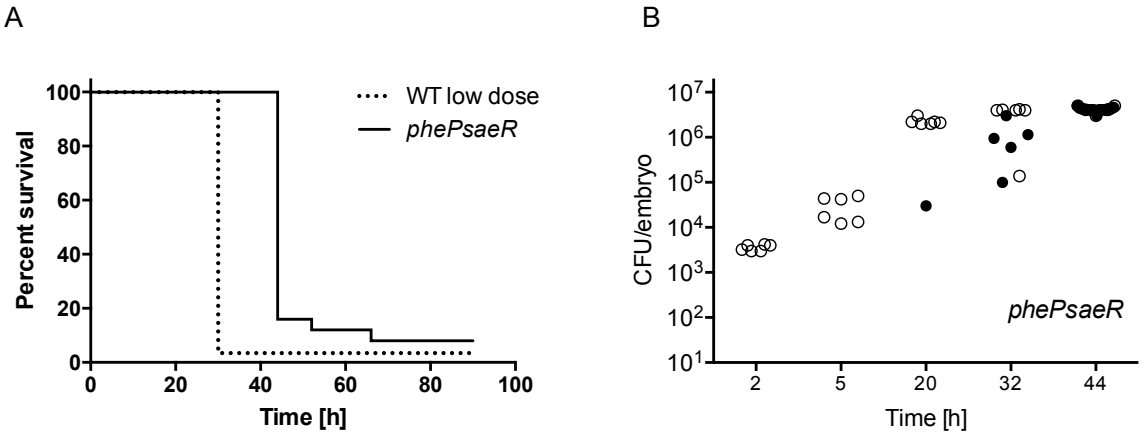


Figure 5.6 Myeloid depleted zebrafish embryos show susceptibility to both the parent and *phePsaeR* mutant

A Survival of *pu.1* knock-down embryos after injection with low dose (150 CFU) parent SH1000 or 1500 CFU *phePsaeR* into the zebrafish circulation (n=28).

B Growth of *phePsaeR* (1500 CFU) within myeloid depleted embryos after injection into the zebrafish circulation. At each time point, 5 living embryos and any dead embryos were processed for CFU per embryo. Open circles represent living embryos, filled circles show dead embryos (n=71).

5.3.2.2.2 *In vivo* zebrafish imaging of phagocytosis of *S. aureus* mixed strains during pathogenesis

Zebrafish are transparent in the early stages of development with pigment developing from around 36 hpf (Kimmel et al., 1995). They are therefore amenable to microscopy to study host:pathogen interactions (Henry et al., 2013). It has been shown that physical aspects of phagocyte vacuoles containing virulent strains appear differently using electron microscopy, compared to those containing attenuated strains (Gresham et al., 2000). It is possible that the two strains used in these experiments are being trafficked differently *in vivo*, for example, by asynchronous phagocytosis or occupation of different niches within the phagocyte. Therefore, to explore if phagocytes deal with the parent and *phePsaeR* mutant differently after injection, fluorescently tagged parental strain, SH1000 carrying pMV158-GFP (SJF4405, unpublished) was co-injected with red fluorescent cell wall stained (pHrodo™, Life Technologies) *phePsaeR* mutant.

pHrodo™ is a pH-sensitive dye that fluoresces red at a pH below 5. Once engulfed by phagocytes, bacteria are delivered to the intracellular organelle known as a phagosome. Fusion events with lysosomes generate phagolysosomes which have an acidic pH and contain hydrolytic enzymes (Stuart and Ezekowitz, 2005). As such, *S. aureus* stained with pHrodo™ can be visualised within these acidic intraphagocyte compartments (Zhu et al., 2015). SH1000*phePsaeR* was incubated for 30 minutes with 2mM pHrodo™ as described in Section 2.19.11.3. Zebrafish were injected at 30 hpf with 150 CFU SH1000-GFP and 1350 CFU of pHrodo™ stained *phePsaeR*, incubated at 28°C for 1-2 hours before imaging by confocal microscopy. Unlike erythrocytes which are moving rapidly around the circulation, phagocytes remain anchored to the plasma membrane of the yolk sac or the outer epidermal layer (Herbomel et al., 1999) (Figure 1.7). Due to the strain ratios used, many more phagocytes could be visualised with red fluorescent bacteria indicating that the mutant was phagocytosed and transported to acidic compartments, such as the phagolysosome. In a small number of phagocytes, green fluorescent bacteria were seen indicating phagocytosis of the GFP expressing parental strain. In a few phagocytes, both red fluorescent and green fluorescent bacteria were co-localised in an individual phagocyte (Figure 5.7 A and B). Therefore, this does not provide evidence for the parental and mutant strain being differentially phagocytosed or trafficked as the explanation for augmentation of *S. aureus* pathogenesis.

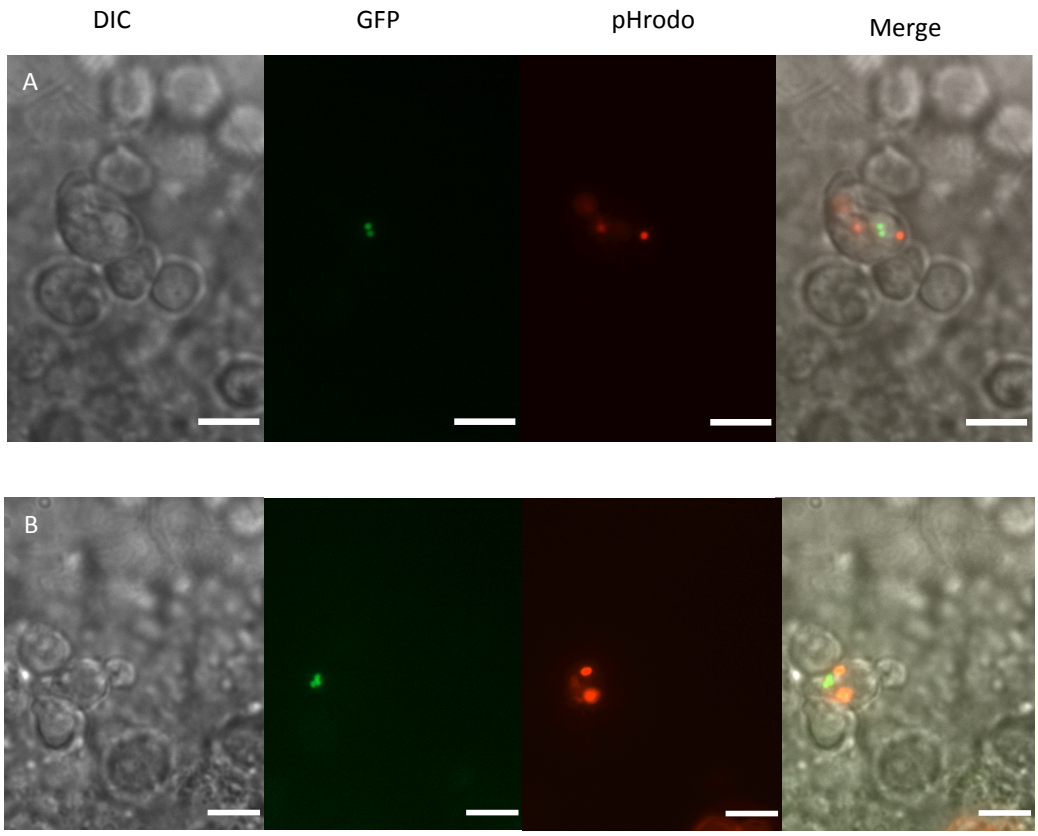


Figure 5.7 Parental GFP-labelled *S. aureus* and red fluorescent *phePsaeR* were internalised by zebrafish phagocytes

Embryos were injected at 30 hpf with 150 CFU SH1000-GFP and 1350 CFU of pHrodo™ stained SH1000*phePsaeR* and imaged after 1-2 hours by confocal microscopy.

Five embryos were imaged, A and B represent data from two individual embryos. Across all embryos, GFP *S. aureus* was observed alone in a phagocyte twice; pHrodo *phePsaeR* was observed alone 16 times and co-localisation of both strains was seen in 6 phagocytes.

Scale bar represents 10 μm.

5.3.3 Population dynamics of mixed inocula that do not augment pathogenesis

The SH1000 mutants that were unable to augment low dose parental bacterial pathogenesis were further interrogated. Firstly, bacterial growth dynamic experiments were carried out both for the mutants alone and then in combination with low dose parent *S. aureus*. As shown in Figure 5.8 A, when injected at 1500 CFU the *purB* mutant was unable to grow *in vivo* and all the embryos survived until 90 hpi. The number of bacteria recovered from living fish diminished over time. When *purB* was combined with low dose bacteria, similar kinetics were as seen for the *purB* mutant alone and the only fish that succumb during the 90-hour experiment were overwhelmed by parent bacteria (black closed circles, Figure 5.8 B).

When injected alone at 1500 CFU, the *sagB* mutant, could, at late timepoints, achieve high bacterial numbers, in some instances and in rare cases, the embryos succumbbed (filled black circles, Figure 5.8 C). Other embryos remained alive, despite high bacterial numbers, which had not been previously seen (open black circles, Figure 5.8 C). In all previous work to date, it has been shown that when bacterial numbers reach 10^6 CFU, the embryo dies. As the experiment must be terminated at 90 hpi to comply with Home Office licence regulations, it is not possible to know what might happen to these embryos with high *sagB* numbers that survive to the end of the experiment. Interestingly, in the absence of phagocytes achieved by using the *pu.1* morpholino, 1500 CFU *sagB* caused death rates similar to that seen in the *phePsaeR* mutant i.e. delayed death compared to the parental strain but virulence was restored and fish overwhelmed with 10^6 CFU (personal communication, Nelly Wagner, University of Sheffield).

As seen in Figure 5.8 D, when *sagB* is combined with low dose *S. aureus*, the majority of embryos had low numbers of *sagB* (open red circles) and low parental numbers (open black circles). Embryos that died had high levels of parental strain with low levels of mutant (Figure 5.8 E, diamond and triangle matching pairs); or high levels of both bacteria (Figure 5.8 E, star and square matching pairs) or more surprisingly, a high level of *sagB* and almost undetectable parental CFUs (Figure 5.8 E, upside down triangle pair).

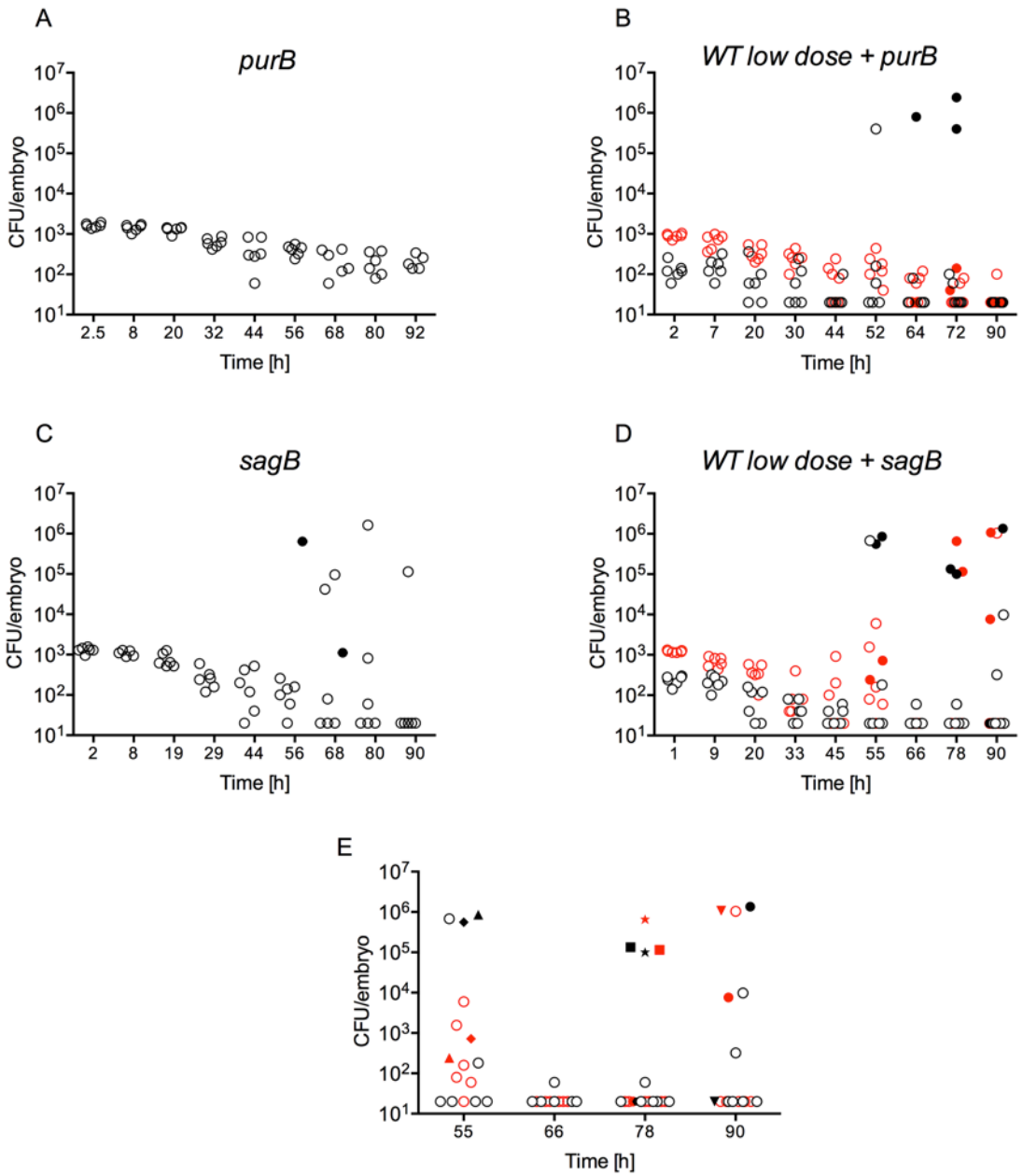


Figure 5.8 Population dynamics of *purB* and *sagB* in single and mixed infections in the zebrafish infection model

Open circles indicate live fish; filled circles are dead fish, n=50-80. Open and filled black circles – parent strain, open red and filled red circles - mutant strain.

A Injection of *purB* (1500 CFU)

B Injection of parent (150 CFU) and *purB* (1350 CFU)

C Injection of *sagB* (1500 CFU)

D Injection of parent (150 CFU) and *sagB* (1350 CFU)

E Subject matched (displayed by matching symbols) embryos showing each bacterial population, at the later time points, from panel D.

5.3.4 Determining the breadth of the augmentation phenomenon in zebrafish embryos

5.3.4.1 Using latex fluorescent beads

One hypothesis for the augmentation of killing by the low dose parent strain in the presence of the attenuated mutant would be that the maximum capacity of a particular niche, i.e. a phagocyte, has been reached. This would allow parent strains to perhaps more easily escape from such phagocytes, employing their repertoire of virulence factors and establishing infection. This has already been tested by performing experiments with either heat killed attenuated mutant *phePsaeR* as above (Figure 5.4) or different *S. aureus* avirulent mutants. However, this was further explored by injecting inert latex beads in place of the mutant. Latex beads were prepared as described in Section 2.20.

In the first experiment, zebrafish were injected with approximately 1500 green fluorescent amine-modified beads and six fish were imaged at 2 hpi on the confocal microscope. At 2 hpi, all amine-modified beads were visualised within phagocytes (Figure 5.9 A). The remaining embryos were followed for survival over 90 hours as per the standard protocol. For all types of beads, survival data showed that the beads injected alone cause no mortality in the embryo, suggesting they are non-toxic (Figure 5.11). However, when green fluorescent carboxylate-modified beads or non-fluorescent latex beads were injected at the same dose, phagocytosis was not seen suggesting that the outer charge on these beads may affect engulfment (Figure 5.9 B and C). Phagocyte:bead interactions may be affected by these charges and perhaps the beads adhere to the vessel endothelium, preventing phagocytosis. As such, mixed inocula experiments were primarily carried out using amine-modified beads. *S. aureus* SH1000 carrying pmV158-mCherry (SJF4308) was used and this has been shown to have the same virulence as SH1000 lacking the plasmid (personal communication, Dr Tomasz Prajsnar). Zebrafish were co-injected with low dose *S. aureus* at a 1:9 ratio with amine-modified green fluorescent beads. Imaging 2 hpi showed bacteria and beads had been phagocytosed into both neutrophils and macrophages and in some cases, co-localised in the same immune cell (Figure 5.10). However, the presence of the latex beads was not able to augment host death by *S. aureus* (Figure 5.11 A, B). Similar data was observed

if carboxylate modified or unmodified beads were injected with low dose *S. aureus* (Figure 5.11 D) but these beads were not phagocytosed.

Therefore, pathogenesis augmentation with low dose bacteria cannot be recapitulated using latex beads implying that the mechanism is not simply niche filling. Taken together with the data that the avirulent strain must be alive, this suggests a dynamic interaction with the host immune system. The physical presence of the latex beads did not hinder *S. aureus* infection as high dose (1500 CFU) injected together with latex beads (approximately 1500) caused equal mortality compared to high dose *S. aureus* alone (Figure 5.11 B). Equally, a large amount of beads (approximately 9000) was unable to augment *S. aureus* pathogenesis (Figure 5.11 C).

During these experiments, it was noted that all types of beads appeared to adhere to the microcentrifuge tube walls during the washing steps mentioned above. This occurred to a greater or lesser degree depending on the type and concentration of the bead used. To overcome this, a quenching reaction was carried out after the first dilution step. 30 mM glycine and 1% (w/v) bovine serum albumin (BSA), both filter sterilised, were added and left to incubate at room temperature for 30 minutes. Thereafter, the beads were centrifuged at top speed, before replacement of the buffer with sterile PBS. This process prevented the beads from adhering and increased enumeration accuracy. Glycine is documented to block the unbound areas of the beads and thus reduce unwanted reactions (Ng et al., 2013). Once quenched, unmodified latex polystyrene beads were shown to be phagocytosed but once again, did not increase pathogenesis when injected with low dose *S. aureus* (data not shown).

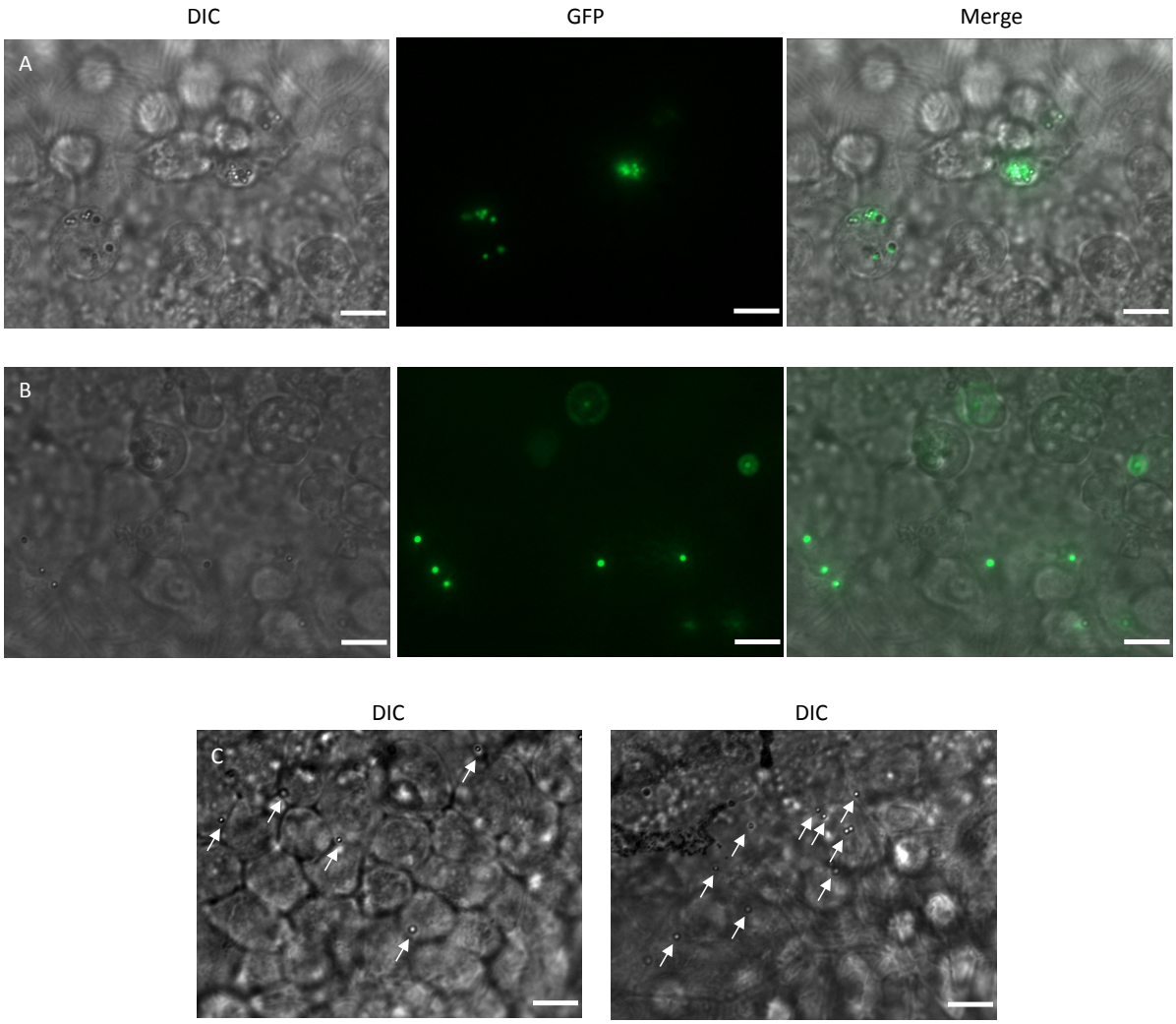


Figure 5.9 Microscopy of 1 µm latex beads injected into the zebrafish embryo circulation valley

Embryos were injected at 30 hpf with approximately 1500 (**A**) amine-modified green fluorescent polystyrene beads; (**B**) carboxylate-modified green fluorescent or (**C**) polystyrene beads and imaged after 1-2 hours by confocal microscopy (white arrows identify individual beads. 3-5 embryos were imaged and images are representative.

DIC - differential interference contrast microscopy (to enhance contrast)

Scale bar represents 10 µm.

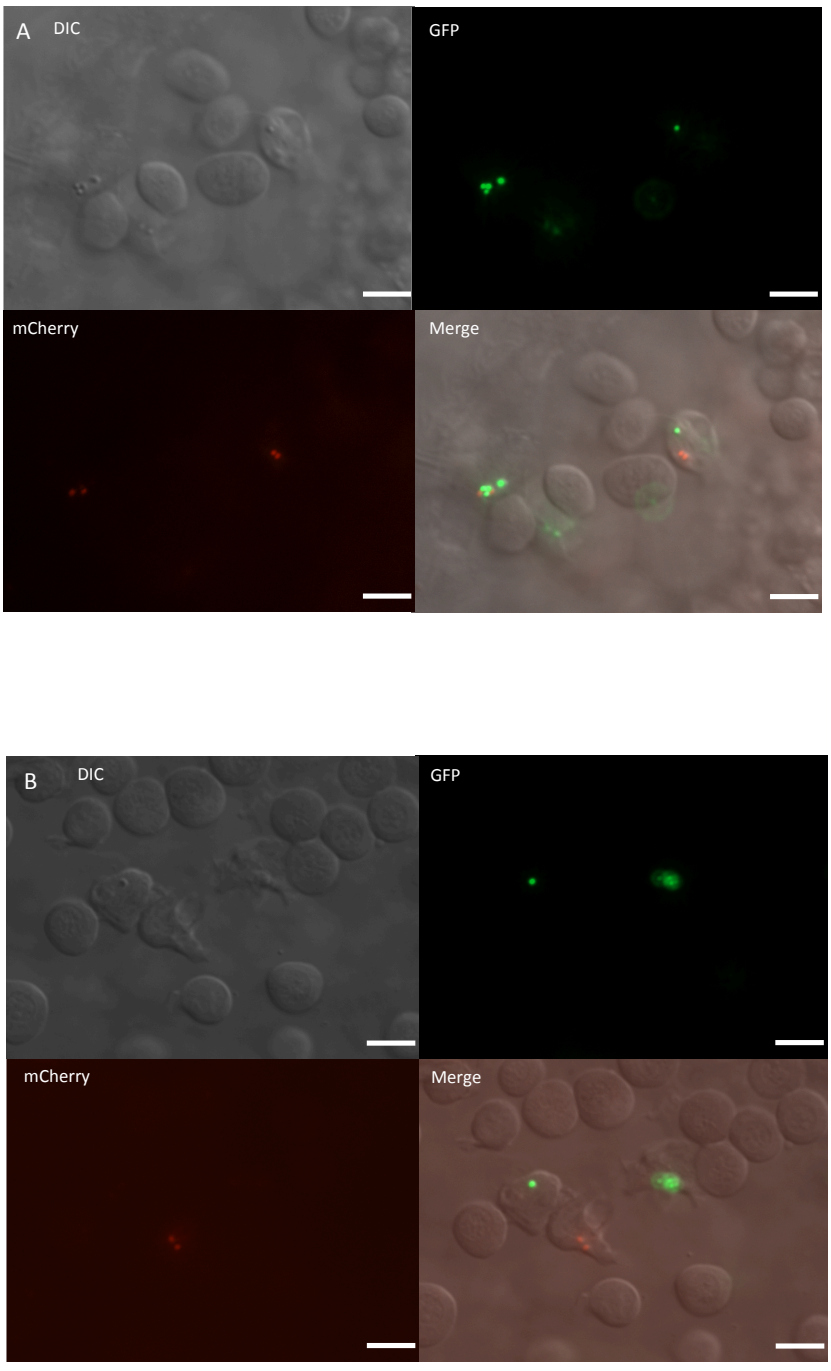


Figure 5.10 Microscopy of 'low dose' *S. aureus* and 1 µm latex beads co-injected into the zebrafish embryo circulation valley

Embryos were injected at 30 hpf with approximately 150 CFU mCherry-SH1000 and 1350 amine-modified green fluorescent polystyrene beads and imaged after 1-2 hours using confocal microscopy. Up to five embryos were imaged and panels A and B are from two representative embryos. Scale bar represents 10 µm

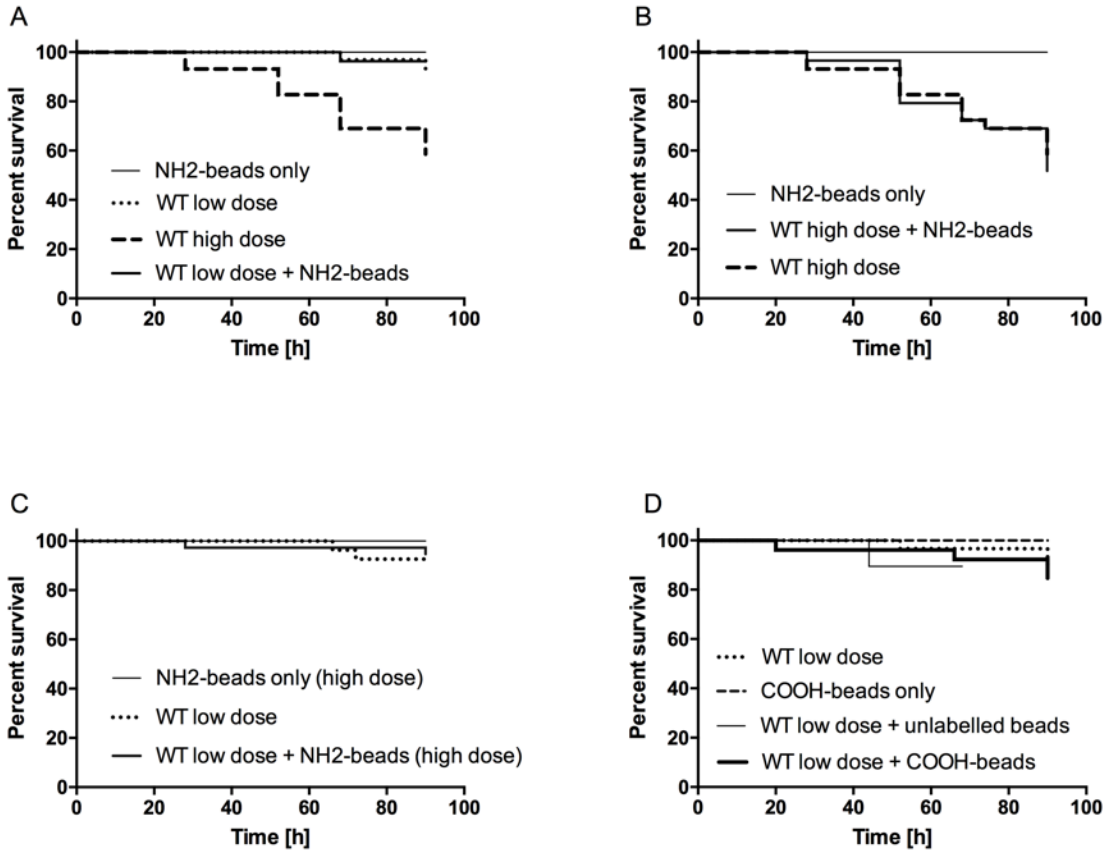


Figure 5.11 Effect of beads on *S. aureus* pathogenesis in the zebrafish infection model

Zebrafish embryos were injected systemically at 30 hpf with *S. aureus* SH1000, latex beads or a combination, n=28.

A Survival of embryos after injection with approximately 1500 amine-modified green fluorescent polystyrene beads (NH2-beads), low dose (150 CFU) mCherry-SH1000, high dose (1500 CFU) mCherry-SH1000 or low dose (150 CFU) mCherry-SH1000 plus 1350 NH2-beads.
B Survival of embryos after injection with approximately 1500 NH2-beads, 1500 CFU mCherry-SH1000 plus 1350 NH2-beads or high dose (1500 CFU) mCherry-SH1000.
C Survival of embryos after injection with approximately 9000 (high dose) NH2-beads, low dose (150 CFU) mCherry-SH1000 or and low dose (150 CFU) mCherry-SH1000 plus 9000 (high dose) NH2-beads.
D Survival of embryos after injection with low dose (150 CFU) mCherry-SH1000, approximately 1500 carboxylate-modified green fluorescent polystyrene beads (COOH-beads) (dashed line), low dose (150 CFU) mCherry-SH1000 plus approximately 1350 polystyrene beads (thin black line, this group was terminated early due to technical reasons with the incubator) or low dose (150 CFU) mCherry-SH1000 plus approximately 1350 COOH-beads (thick black line).

5.3.4.2 Investigation of the effect of commensal skin bacteria on *S. aureus* pathogenesis in the zebrafish infection model

To examine the breadth of this augmentation phenomenon, avirulent bacteria were tested, to more closely mirror the local environment that might be present at the time of *S. aureus* infection. The skin milieu consists of many commensal bacteria including *S. epidermidis*, *M. luteus* and *Bacillus* species (Cogen et al., 2008). These organisms do not have the vast repertoire of immune evasion strategies and toxin production of *S. aureus* and whilst they can be recognised as invasive, it is often in specific clinical circumstances such as immuno-compromised individuals or prosthetic device associated infections (Otto, 2009). *S. epidermidis* is predominantly a human skin commensal. *M. luteus* is part of the human skin microflora but is also found in the external environment. *B. subtilis* is a soil organism. These bacterial species are Gram-positive and have polymeric cell wall peptidoglycan.

The following experiments were conducted in collaboration with Dr Tomasz Prajsnar (University of Sheffield). Previously, preliminary experiments injecting varying doses of *B. subtilis* (ranging from 750 CFU to 6000 CFU per nl) into the zebrafish circulation valley at 30 hpf were carried out and no mortality was seen (data not shown). In addition, *S. epidermidis* was also injected alone at both 2000 CFU and 3700 CFU whilst *M. luteus* was injected up to 3800 CFU and no host mortality was observed. Therefore, mixed inoculum assays were performed and as shown in Figure 5.12 A, *B. subtilis* live bacteria injected at 1000 CFU together with *S. aureus* SH1000 at 150 CFU per embryo was able to augment host death compared to low dose *S. aureus* injected alone (n=30 embryos per group, $p = 0.034$). However, when this experiment was repeated, although the trend remained, statistical comparison of the mixed group vs. low dose alone using the log rank test, was not significant ($p = 0.13$, data not shown). *M. luteus* live bacteria in the same protocol, revealed a highly reproducible and significant augmentation phenomenon (Figure 5.12 B, $p = 0.0001$). Low dose *S. aureus* killed very few hosts but the combined inocula caused 40-50% mortality. Interestingly, *S. epidermidis* bacteria were unable to synergise with low dose SH1000 bacteria as shown in Figure 5.12 C.

M. luteus showed the most striking augmentation of *S. aureus* pathogenesis and therefore was further pursued. To ascertain if heat killing *M. luteus* would abolish this

phenomenon, *M. luteus* bacteria were subjected to 70°C for 30 minutes and the duplicate experiments revealed that heat killed *M. luteus*, in combination with low dose *S. aureus*, caused increased host death compared to low dose alone (heat killed *M. luteus* vs. low dose *S. aureus* $p = 0.063$ and $p = 0.009$ for experiment 1 and 2 respectively, Figure 5.12 D). This suggested that heat stable elements of *M. luteus* may be responsible for modulating the host response or interacting with the *S. aureus* such that host susceptibility is increased to the pathogen.

Taking an example of a bacterium that could augment pathogenesis, *M. luteus*, and one that cannot, *S. epidermidis*, bacterial kinetic studies were carried out. It was considered that perhaps the embryo immune system might deal with avirulent non-staphylococcal species in a different way to, for example, avirulent *S. aureus* mutants. For the latter, it has been previously shown (Figure 5.5), that even when high inocula are injected into the zebrafish, avirulent strain numbers diminish throughout the 90-hour time course. Using mixed inocula, in order for the two populations to be delineated, *M. luteus* was serially passaged on BHI media with or without rifampicin (0.03 μg ml^{-1}) and incubated at 30°C until a rifampicin resistant derivative was identified. The same was conducted for *S. epidermidis*. *M. luteus*^{rif} and *S. epidermidis*^{rif} were injected with the standard mixed inocula (1:9 *S. aureus*:commensal ratio) alone into 60 embryos at 30 hpf. At various time points, 5 embryos were collected and bacterial numbers were determined. The population dynamics of *S. epidermidis*^{rif} and *M. luteus*^{rif} are shown in Figure 5.12 E and F respectively (red open circles). After injection at 1350 CFU, bacterial numbers rapidly declined by 7 hpi and reach the limits of detection of the assay by 20 hpi (*M. luteus*) and 44 hpi (*S. epidermidis*). *S. epidermidis* did not permit increased host death from low dose *S. aureus* as depicted by the small number of dead embryos (black closed circles) in Figure 5.12 E. However, in the presence of *M. luteus*, low dose *S. aureus* was able to proliferate and cause significant host death, far in excess of when low dose *S. aureus* was injected alone (Figure 5.12 F).

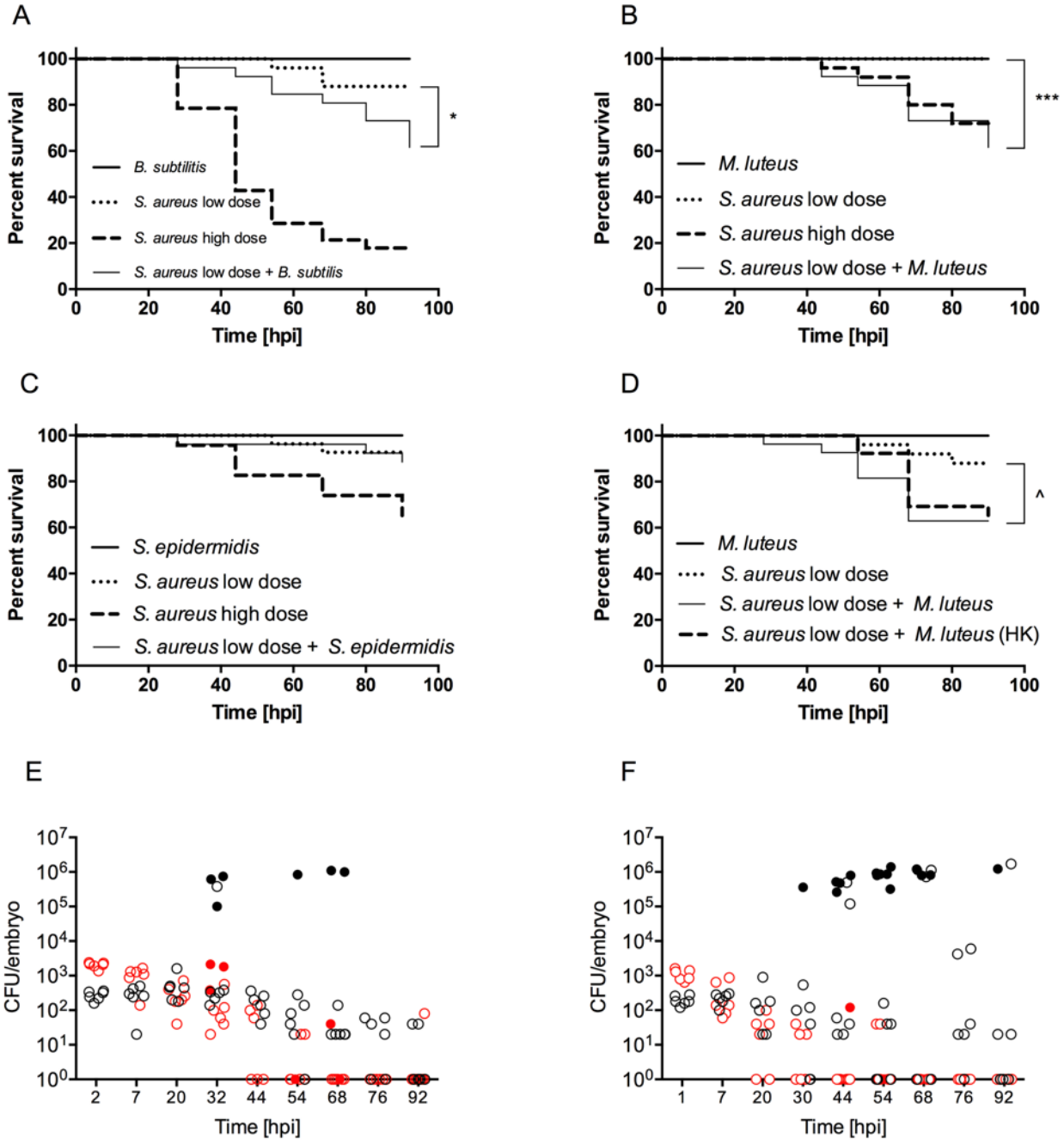

A
Percent survival
Time [hpi]
B. subtilitis
S. aureus low dose
S. aureus high dose
S. aureus low dose + B. subtilis
*
B
Percent survival
Time [hpi]
M. luteus
S. aureus low dose
S. aureus high dose
S. aureus low dose + M. luteus
***
C
Percent survival
Time [hpi]
S. epidermidis
S. aureus low dose
S. aureus high dose
S. aureus low dose + S. epidermidis
D
Percent survival
Time [hpi]
M. luteus
S. aureus low dose
S. aureus low dose + M. luteus
S. aureus low dose + M. luteus (HK)
^
E
CFU/embryo
Time [hpi]
F
CFU/embryo
Time [hpi]

Figure 5.12 Gram-positive nonpathogenic bacteria are able to augment pathogenesis with low dose *S. aureus* in the zebrafish infection model

Survival of zebrafish in the systemic model of *S. aureus* infection was determined (n=28).

A Injection of *B. subtilis* (1000 CFU), low dose *S. aureus* (150 CFU), high dose *S. aureus* (1500 CFU) or low dose *S. aureus* (150 CFU) plus *B. subtilis* (1000 CFU) (* p = 0.034).

B Injection of *M. luteus* (1500 CFU), low dose *S. aureus* (150 CFU), high dose *S. aureus* (1500 CFU) or low dose *S. aureus* (150 CFU) plus *M. luteus* (1350 CFU) (*** p = 0.0001)

C Injection of *S. epidermidis* (1500 CFU), low dose *S. aureus* (150 CFU), high dose *S. aureus* (1500 CFU) or low dose *S. aureus* (150 CFU) plus *S. epidermidis* (1350 CFU).

D Injection of *M. luteus* (approximately 1350 CFU) either live or heat killed (HK) and low dose *S. aureus* (150 CFU) into the zebrafish circulation (^ HK vs. low dose p = 0.063, live vs. low dose p = 0.034).

Population dynamics were determined in the zebrafish embryo infection model. Open circles represent live embryos, filled circles represent dead fish (n=80).

E Injection of *S. epidermidis* (1350 CFU, open red and filled red circles) and *S. aureus* (150 CFU, open and filled black circles).

F Injection of *M. luteus* (1350 CFU, open red and filled red circles) and *S. aureus* (150 CFU, open and filled black circles).

Next, microscopy was carried out to assess the extent of phagocytosis of the nonpathogenic bacteria when co-injected with *S. aureus*. Cell wall staining of either *M. luteus* or *S. epidermidis* live bacteria was undertaken using pHrodo™. Firstly, SH1000-GFP (150 CFU) and pHrodo™ stained *S. epidermidis* (1350 CFU) were co-injected into 30 embryos at 30 hpf and at 2 hpi, 6 embryos were removed for live imaging by confocal microscopy. A further experiment investigated SH1000-GFP (150 CFU) and pHrodo™ stained *M. luteus* (1350 CFU). In each experiment, the remaining embryos were kept for the full 90-hour time course and survival was monitored. In addition, as for all experiments, post injection into the embryo, a microcentrifuge tube containing PBS was inoculated with the same micro injection needle so an accurate count of injected bacteria could be calculated after plating onto selective media and overnight incubation. This was particularly important to ensure pHrodo™ toxicity was not occurring.

As seen in Figure 5.13 A (*S. epidermidis* + low dose *S. aureus*) and B (*M. luteus* + low dose *S. aureus*), cell wall stained nonpathogenic bacteria and SH1000-GFP are phagocytosed and can reside within the same phagocyte. It is not possible with this experiment to accurately deduce if the occupied compartments of the two populations are different but this confirms that the augmentation phenomenon is not mediated by nonpathogenic bacteria, preventing *S. aureus* phagocytosis, for example. It can be clearly seen that stained *M. luteus* and *S. epidermidis* display red fluorescence indicating localization within an acidified environment, such as the phagolysosome.

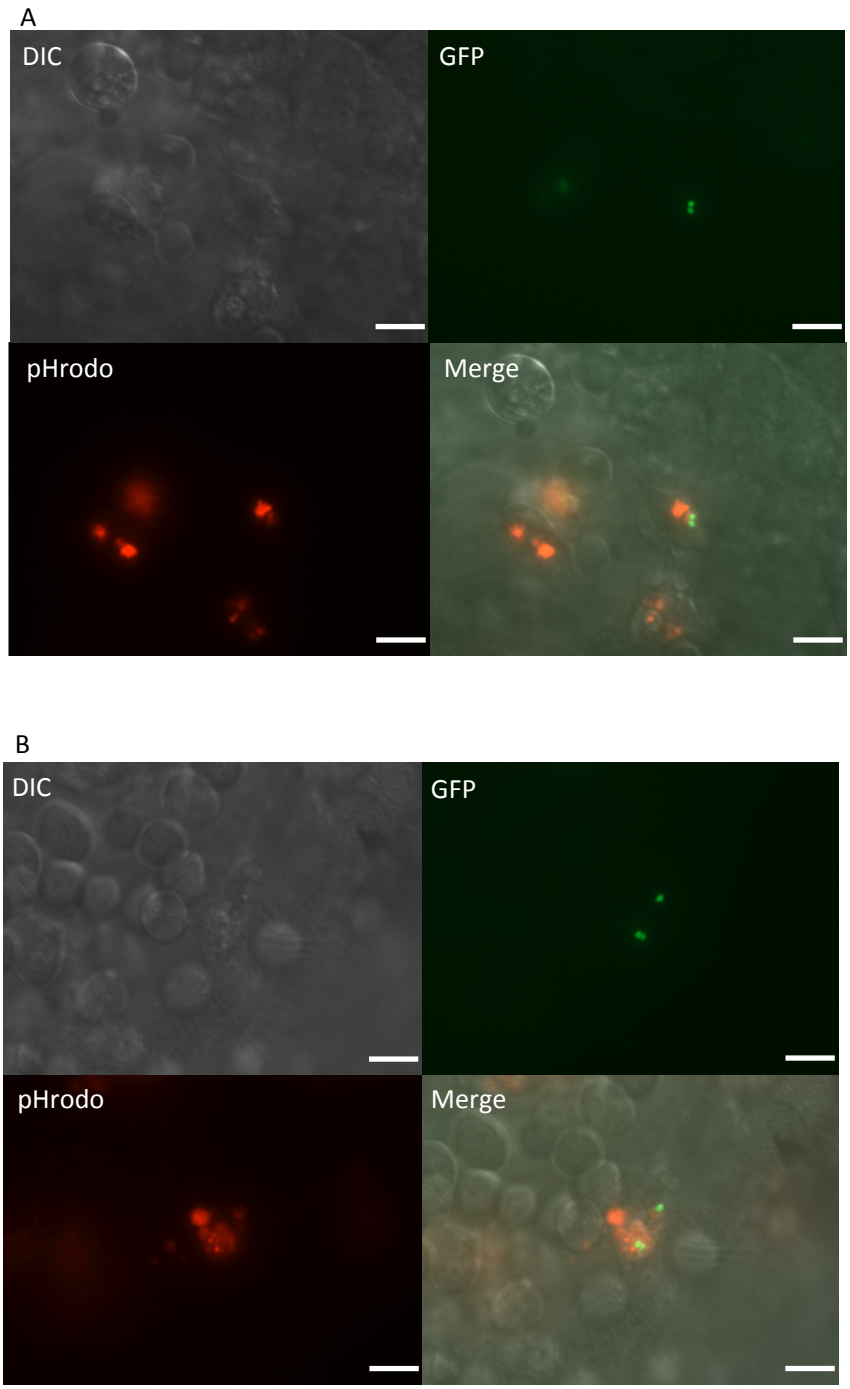


Figure 5.13 Microscopy of low dose *S. aureus* SH1000 coinjected with other Gram-positive bacteria

S. epidermidis (**A**) or *M. luteus* (**B**) were co-injected with *S. aureus* into the zebrafish embryo circulation valley.

Embryos were injected at 30 hpf with low dose (150 CFU) GFP-SH1000 and 1350 CFU live *S. epidermidis* or *M. luteus* labelled with pHrodo and imaged after 1-2 hours by confocal microscopy. Images are representative of the five embryos examined. Scale bar represents 10 μm.

5.3.4.3 Is there a common mechanism underlying the augmentation phenomenon?

In summary of the data so far, whilst certain avirulent mutants such as *phePsaeR* can enhance *S. aureus* pathogenesis, a glucosaminidase mutant affecting peptidoglycan composition cannot. In addition, the Gram-positive commensal bacterium, *M. luteus*, can augment pathogenesis, even after undergoing heat killing indicating a heat stable component may be involved. This allowed a further hypothesis to be developed: that fundamental parts of Gram-positive bacteria, such as the cell wall constituents, may be interacting within the host to modify capability to control an otherwise innocuous infective dose. This would not explain the underlying mechanism in full, as *S. epidermidis,* which has a similar peptidoglycan composition to *S. aureus* bacteria (Tipper and Berman, 1969), and perhaps even heat killed *phePsaeR* might also be expected to do so. However, there may be dose dependent effects occurring, multiple different phenomenon or more subtle underlying mechanisms that may be seen with further investigation.

Gram-positive cell walls are largely made up of peptidoglycan. As discussed in Section 1.9, peptidoglycan is a large polymer composed of sugars and amino acids. The glycan chain backbone consists of alternating N-acetylglucosamine and N-acetylmuramic acid with the peptide side chains allowing crosslinking. Whilst controversy exists in the literature with regard to which component of peptidoglycan is immuno-stimulatory, it is widely known to play a role in *S. aureus* pathogenesis (McDonald et al., 2005). Therefore, purified peptidoglycan preparations were tested for the ability to augment *S. aureus* pathogenesis.

5.3.4.3.1 The cell wall component, peptidoglycan, can augment *S. aureus* pathogenesis

In order to test this new hypothesis, purified peptidoglycan, from different species of Gram-positive bacteria, were individually injected systemically into the embryos. As described in Section 2.24, the peptidoglycan injected was purified to ensure removal of potential confounding immuno-stimulatory molecules. After several purification steps, peptidoglycan was incubated with 48% (v/v) hydrofluoric acid to ensure no wall

teichoic acids remain. As described in Section 2.24.4, peptidoglycan from 2 x 10^8 CFU weighs approximately 26 μg. Therefore, 1500 CFU per nl embryo injection is equivalent to 0.2 ng of peptidoglycan. As this is a very rough approximation, the amount of peptidoglycan injected into embryos for augmentation experiments ranged from 3-10 ng.

Injecting 25 embryos per group, 5 ng peptidoglycan alone from *S. aureus* (SH1000), *M. luteus, B. subtilis, Streptococcus mutans* or *C. flaccumfaciens* was unable to cause any host mortality (Figure 5.14). *C. flaccumfaciens* is a Gram-positive organism that is known to be a plant pathogen but is nonpathogenic to humans (Francis et al., 2011). In combination with a low dose of the *S. aureus* (150 CFU), none of those tested showed a significant increase in host mortality except for *M. luteus* and *S. epidermidis* peptidoglycan (Figure 5.15). It is interesting that not all peptidoglycan can cause augmentation of pathogenesis with low dose *S. aureus*. This may be due to specific ligands or motifs that each peptidoglycan displays *in vivo*. The glycan chain of peptidoglycan is highly conserved between species but the amino acid side chains and peptide bridges vary and this has been proposed to affect pathogenesis (Myhre et al., 2004). *M. luteus* peptidoglycan architecture differs from *S. aureus* as shown in Figure 5.16. Whilst the amino acid side chains are identical, the peptide bridge consists of D-alanine, L-lysine, D-glutamine and L-alanine rather than the pentaglycine chain found in *S. aureus* (Schleifer and Kandler, 1972). Interestingly, live *S. epidermidis* was unable to cause augmentation yet peptidoglycan did augment host death. This may be due to differences in ligand presentation to the host between live cells and purified material.

To confirm that decreased embryo survival was due to overwhelming proliferation of the low dose bacteria, *in vivo* bacterial kinetics experiments were conducted for *S. aureus* or *M. luteus* peptidoglycan in combination with 150 CFU *S. aureus* bacteria. As shown in Figure 5.17, there was far higher mortality seen when *M. luteus* peptidoglycan was co-injected compared to *S. aureus* peptidoglycan. Embryos, which succumbed, contained 10^6 CFU *S. aureus*.

Synergistic interactions between bacterial cell wall components have been documented previously. LTA from *S. aureus* was able to synergise with peptidoglycan from *B. subtilis* (Kengatharan et al., 1998). This suggests that peptidoglycan, independent of its

species origin, can act to stimulate immune responses caused by other bacterial components. This might explain the findings in this project that non-pathogenic commensal peptidoglycan, in the presence of live *S. aureus* bacteria, reduces the ability of the immune system to control the pathogen.

It was possible that augmentation of host death seen by addition of purified *M. luteus* or *S. epidermidis* peptidoglycan may be acting by a different mechanism than that of the avirulent strains. To further explore this, it was next necessary to ascertain if the co-injected peptidoglycan was phagocytosed in a similar way to whole bacteria.

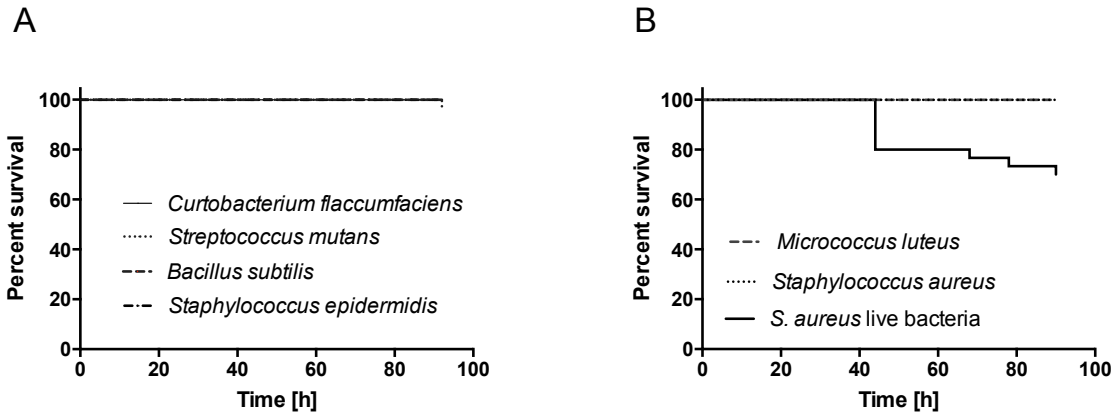


Figure 5.14 Peptidoglycan alone was unable to kill the zebrafish embryo host

A and B Purified peptidoglycan (5 ng) from a range of species was unable to cause host death compared to live *S. aureus* bacteria injected at 1500 CFU (positive control).

NB Overlapping data points are present in both graphs.
(n = 25 per group)

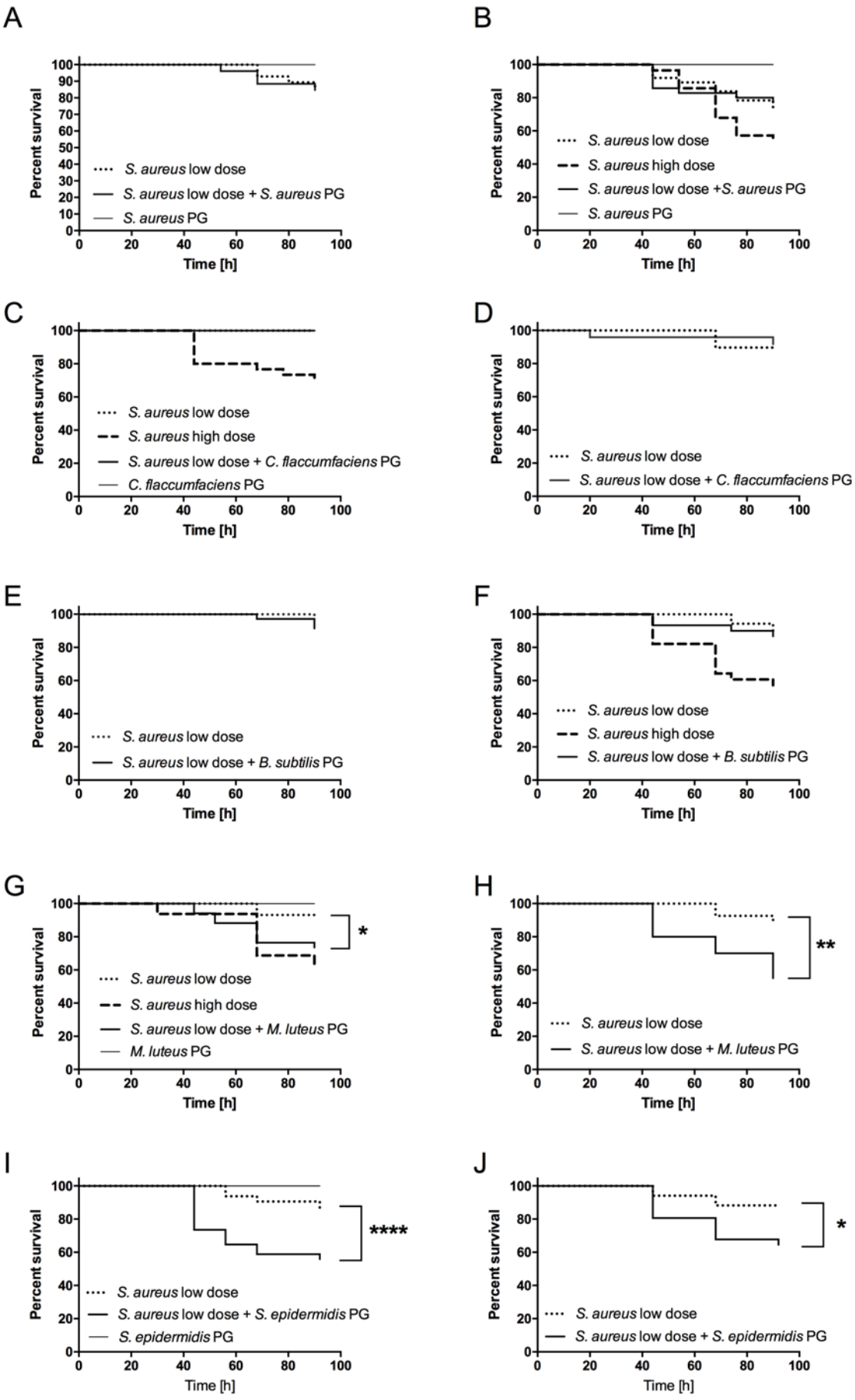

A
Percent survival
Time [h]
S. aureus low dose
S. aureus low dose + S. aureus PG
S. aureus PG
B
Percent survival
Time [h]
S. aureus low dose
S. aureus high dose
S. aureus low dose +S. aureus PG
S. aureus PG
C
Percent survival
Time [h]
S. aureus low dose
S. aureus high dose
S. aureus low dose + C. flaccumfaciens PG
C. flaccumfaciens PG
D
Percent survival
Time [h]
S. aureus low dose
S. aureus low dose + C. flaccumfaciens PG
E
Percent survival
Time [h]
S. aureus low dose
S. aureus low dose + B. subtilis PG
F
Percent survival
Time [h]
S. aureus low dose
S. aureus high dose
S. aureus low dose + B. subtilis PG
G
Percent survival
Time [h]
*
S. aureus low dose
S. aureus high dose
S. aureus low dose + M. luteus PG
M. luteus PG
H
Percent survival
Time [h]
**
S. aureus low dose
S. aureus low dose + M. luteus PG
I
Percent survival
Time [h]
****
S. aureus low dose
S. aureus low dose + S. epidermidis PG
S. epidermidis PG
J
Percent survival
Time [h]
*
S. aureus low dose
S. aureus low dose + S. epidermidis PG

Figure 5.15 Effect of co-injection of peptidoglycan from various species with low dose *S. aureus* bacteria

The effect of peptidoglycan (5 ng) on *S. aureus* pathogenesis in the zebrafish systemic model was tested.

A Co-injection of low dose (150 CFU) *S. aureus* with *S. aureus* purified peptidoglycan.
B Co-injection of low dose (150 CFU) *S. aureus* with *S. aureus* purified peptidoglycan. High dose (1500 CFU) *S. aureus* was injected as a control group.
C Co-injection of low dose (150 CFU) *S. aureus* with *C. flaccumfaciens* purified peptidoglycan. High dose (1500 CFU) *S. aureus* was injected as a control group.
D Co-injection of low dose (150 CFU) *S. aureus* with *C. flaccumfaciens* purified peptidoglycan.
E Co-injection of low dose (150 CFU) *S. aureus* with *B. subtilis* purified peptidoglycan.
F Co-injection of low dose (150 CFU) *S. aureus* with *B. subtilis* purified peptidoglycan. High dose (1500 CFU) *S. aureus* was injected as a control group.
G Co-injection of low dose (150 CFU) *S. aureus* with *M. luteus* purified peptidoglycan. High dose (1500 CFU) *S. aureus* was injected as a control group. Low dose *S. aureus* (dotted line) caused minimal death compared to high dose (dashed line). Low dose *S. aureus* compared to low dose *S. aureus* plus *M. luteus* peptidoglycan caused increased host death (*p = 0.04).
H Co-injection of low dose (150 CFU) *S. aureus* with *M. luteus* purified peptidoglycan. Low dose *S. aureus* compared to low dose *S. aureus* plus *M. luteus* peptidoglycan caused increased host death (** p = 0.006).
I and J Co-injection of low dose (150 CFU) *S. aureus* with *S. epidermidis* purified peptidoglycan. Low dose *S. aureus* (dotted line) caused minimal death compared to high dose (dashed line). Low dose *S. aureus* compared to low dose *S. aureus* plus *S. epidermidis* peptidoglycan caused increased host death (I ****p < 0.0001 and J *p = 0.025).

NB Overlapping data points occur in graph C.
(n = 28 embryos per group)

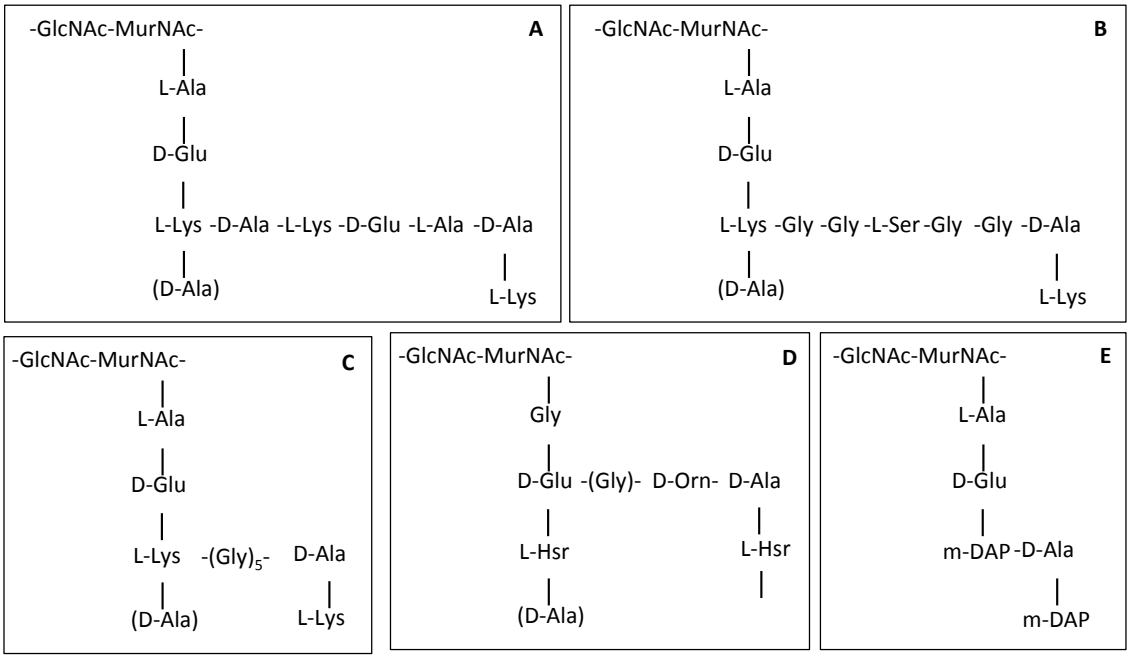


Figure 5.16 Composition of peptidoglycan from various Gram-positive bacteria

A *M. luteus*
B *S. epidermidis*
C *S. aureus*
D *C. flaccumfaciens*
E *B. subtilis*

Adapted from (Schleifer and Kandler, 1972; Myhre et al., 2004)

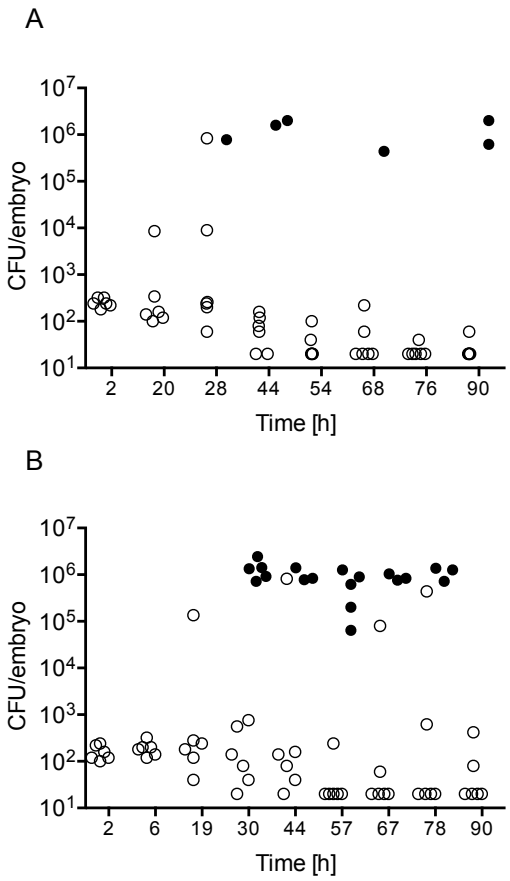


Figure 5.17 Bacterial kinetics when low dose *S. aureus* was co-injected with peptidoglycan in the zebrafish pathogenesis model

A Injection of *S. aureus* low dose (150 CFU) and 5 ng *S. aureus* peptidoglycan into the zebrafish circulation valley (open circle – live embryo; filled circle – dead embryo).

B A Injection of *S. aureus* low dose (150 CFU) and 5 ng *M. luteus* peptidoglycan into the zebrafish circulation valley (open circle – live embryo; filled circle – dead embryo).

n = 90 embryos per group

5.3.4.3.2 Microscopy imaging of the fate of fluorescently labelled peptidoglycan with and without live bacteria in the zebrafish infection model

It was investigated whether purified peptidoglycan was phagocytosed in a similar way to bacteria. It is likely that purified peptidoglycan preparations are composed of a range of particle sizes, as cell breakage will occur to varying degrees. Firstly, *M. luteus* or *S. aureus* peptidoglycan were both stained with a combination of pHrodo™ and Fluorescein-NHS ester in order that any phagocytosed material could be visualised with the red fluorescent pH sensitive pHrodo and non-phagocytosed material with the green fluorescent second stain. 3 ng of peptidoglycan was injected into the circulation valley of 30 hpf zebrafish embryos and imaging was acquired by confocal microscopy. As shown in Figure 5.18, the vast majority of *M. luteus* peptidoglycan was found within in the acidic compartments of phagocytes. A small amount of unphagocytosed material could be seen free-flowing in the blood circulation. The same results were found when *S. aureus* SH1000 purified peptidoglycan was labelled and injected. However, the small amount of unphagocytosed material observed outside of phagocytes was not free-flowing as for *M. luteus*. Interestingly, the material appeared to be adhered to the vessel walls (data not shown as only evident on moving images). It is not yet known why this difference may exist but variations in charge or binding affinities of the two peptidoglycans may be involved.

Next, a mixed inocula experiment was carried out, with *M. luteus* peptidoglycan incubated with the fluorescent cell wall stain Alexa Fluor® 647 NHS ester, a bright and photostable far red dye. Low dose *S. aureus*-GFP (150 CFU) was co-injected with 5 ng of stained *M. luteus* peptidoglycan. As shown in Figure 5.19, A and B, both *S. aureus* and *M. luteus* peptidoglycan appear co-localised within phagocytes confirming that polymeric peptidoglycan is phagocytosed alongside live bacteria.

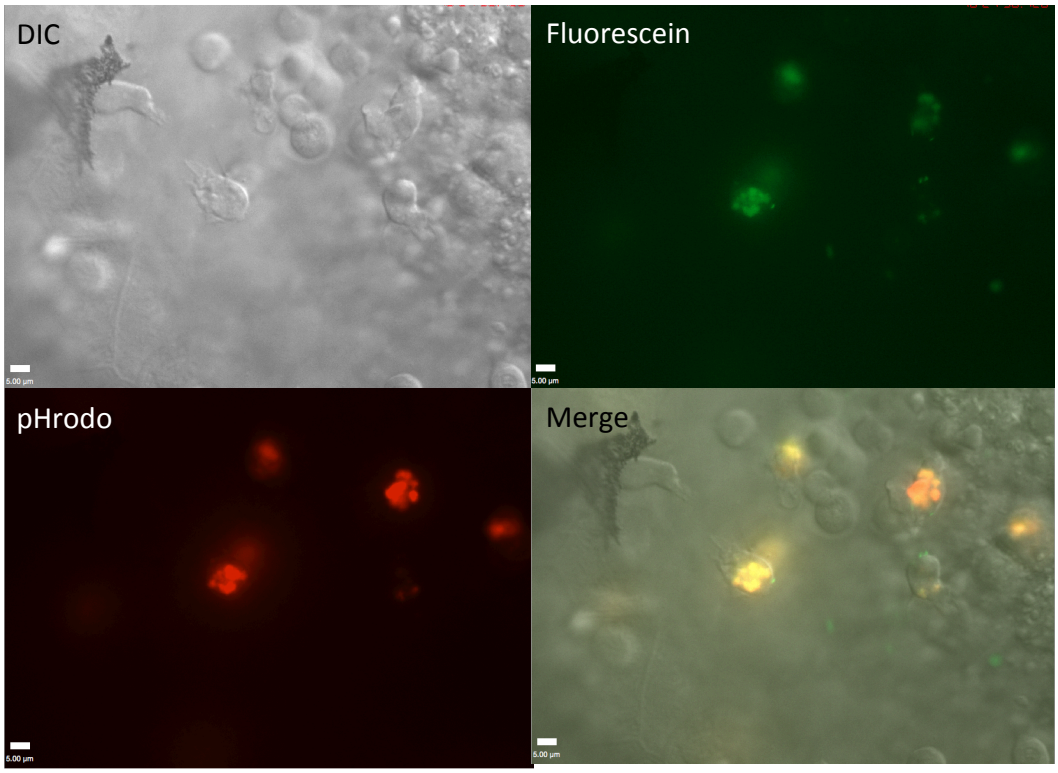


Figure 5.18 Microscopy of phagocytosed labelled *M. luteus* peptidoglycan in live zebrafish

Embryos were injected at 30 hpf with dual labelled (Fluorescein and pHrodo) *M. luteus* purified peptidoglycan (3 ng) and imaged after 1-2 hours by confocal microscopy. Images are representative of the five embryos examined.

Scale bar represents 5 µm.

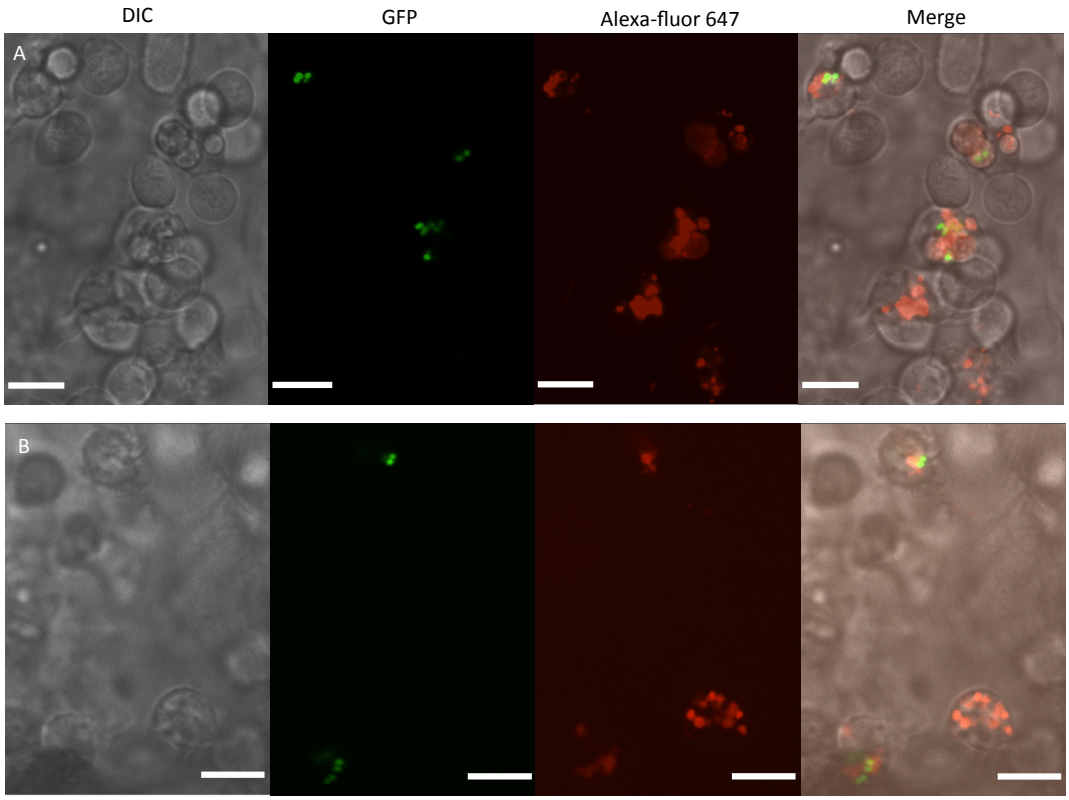


Figure 5.19 Microscopy of phagocytosed labelled *M. luteus* peptidoglycan and live *S. aureus* within live zebrafish

Embryos were injected at 30 hpf with Alexa-fluor 647 labelled *M. luteus* purified peptidoglycan (5 ng) and low dose (150 CFU) SH1000-GFP and imaged after 1-2 hours by confocal microscopy. Images are representative of the five embryos examined. Panels A and B are from individual embryos.

Scale bar represents 10 μm.

5.3.4.3.3 Is the structural integrity of peptidoglycan important in augmentation of pathogenesis?

Effective phagocytosis by professional phagocytes is in part governed by particle size. Given the small particle size of digested soluble peptidoglycan, it is unlikely to be directly phagocytosed. The importance of the structural integrity of the peptidoglycan to the pathogenesis augmentation phenomenon was investigated by digesting peptidoglycan with the hydrolytic enzyme, mutanolysin, which cleaves the glycan backbone after each MurNAc residue, rendering the peptidoglycan soluble (Mesnage et al., 2014). Purified *M. luteus* peptidoglycan (5 ng) was digested as described in Section 2.24.3. Either insoluble or soluble *M. luteus* peptidoglycan was co-injected with low dose (150 CFU) *S. aureus*, using the standard experimental protocol. In the first experiment, solublised peptidoglycan combined with low dose *S. aureus* did not cause augmentation of host death, unlike insoluble peptidoglycan (Figure 5.20 A, $p = 0.047$) suggesting that the structural integrity of this polymer is crucial. In the second experiment, soluble peptidoglycan augmented host death but to a lesser extent than insoluble peptidoglycan (Figure 5.20 B).

Therefore, important underlying mechanisms of this augmentation phenomenon may include effective phagocytosis and further intra-phagocyte processing of peptidoglycan, in order that the immune milieu is altered sufficiently to allow low dose *S. aureus* to cause significant host death.

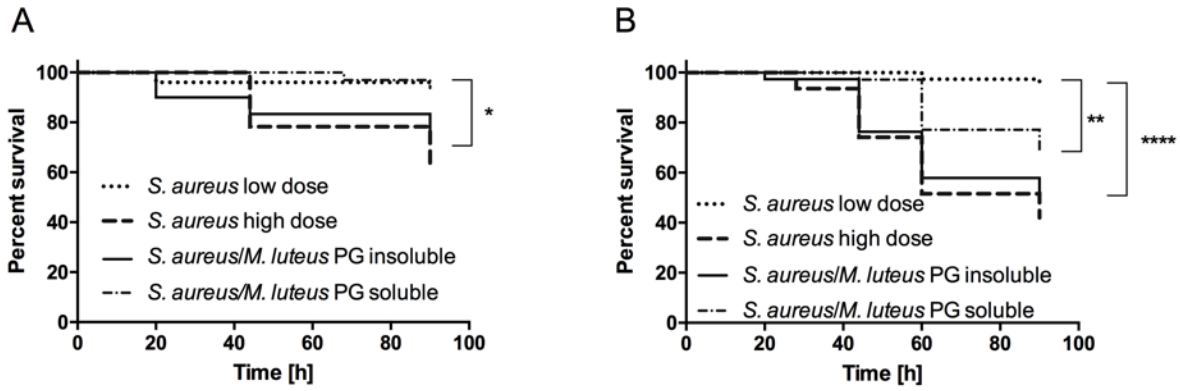


Figure 5.20 Disruption of the peptidoglycan backbone may be important during augmentation of zebrafish infection

A and B Survival curves for zebrafish co-injected with soluble or insoluble *M. luteus* peptidoglycan (5 ng) and low dose (150 CFU) *S. aureus* (thick grey line) from two independent experiments (A * p = 0.047, B ** p = 0.0034, **** p = <0.0001). Low dose (150 CFU) *S. aureus* or high dose *S. aureus* (1500 CFU) were injected as control groups.

n = 30 per group

5.3.5 Investigation of the pathogenesis augmentation phenomenon in the murine sepsis model

5.3.5.1 Co-injection of attenuated mutant *phePsaeR* and low dose *S. aureus*

Experimental evidence from the zebrafish model of infection has successfully been used to inform mammalian studies in our laboratory (McVicker et al., 2014). As such, it was sought to establish if the augmentation phenomenon could be replicated in the murine model. As there is 90% homology between the mouse and human genome, data from this model could help to inform understanding of infective processes in humans. The septic arthritis model is a gold standard model of intravenous *S. aureus* infection in the mouse and has been extensively used (Bremell et al., 1991; Clarke et al., 2007). Initially used to investigate aspects of septic arthritis, the model was found to reproducibly cause systemic infection with reliable end points such as animal health (based on a wellbeing scoring system) and bacterial CFUs in various organs (Nilsson et al., 1996). However, as for the zebrafish experiments, high dose inocula are required to establish infection with the standard intravenous dose being around 10^{7-8} CFU in this specific model. It was sought therefore to determine if lower doses, in addition to either attenuated mutants or cell wall components, could cause infection as has been demonstrated in the zebrafish model.

Unless otherwise stated, in the following murine experiments, the limit of detection of the assay was 20 CFU for kidneys and 30 CFU for liver. On the graphs, solid lines indicate median values and non-parametric statistical tests were used with the same p value cut offs as described (Section 2.26).

A pilot experiment was conducted initially to investigate the establishment of infection at a given dose using *S. aureus* strain NewHG. This strain is a derivative of Newman, a commonly used clinical strain isolated in 1952 (Duthie and Lorenz, 1952). Whilst Newman is widely used in murine studies of *S. aureus* disease a single amino acid change in the *saeS* gene, a global virulence gene regulator, results in high levels of toxin expression (Mainiero et al., 2010). NewHG has a repaired copy of *saeS*, resulting in a level of gene expression similar to many other *S. aureus* strains. The double mutant *phePsaeR* was transduced from SH1000 into the NewHG background using φ11. The parental NewHG carries a kanamycin resistance cassette (Kan^R) so that the parent and

mutant strains could be distinguished to determine bacterial CFUs. NewHG and NewHG Kan^R are otherwise isogenic and have been shown to have equivalent virulence in both zebrafish and murine infection models (McVicker et al., 2014).

Based on prior data from our group and pilot data collected in this project, a dose of $1x10^6$ CFU per mouse (n=10) was chosen as a low dose of *S. aureus* NewHG. A dose of $1x10^7$ CFU per mouse (n=10) was used for the high dose positive control injections with parental *S. aureus* and also for the dose of *phePsaeR*, both alone (n=10) and in combination with low dose parent (n=10).

As shown in Figure 5.21, the majority of mice injected with low dose *S. aureus* did not lose weight and had low bacterial numbers in the kidneys and livers at 3 dpi. However, it remains evident that even at low dose, a small number of mice do lose weight and often those mice have high CFU recovery from the organs. This stochastic infective process has been noted by our group and can be explained by the clonal expansion data previously acquired (Prajsnar et al., 2012). As expected, weight loss up to 20% and high CFU recovery from both kidneys and liver were obtained when $9.3x10^6$ CFU of parental bacteria were injected. Conversely, *phePsaeR* injected alone at $6.2x10^6$ CFU mutant was shown to be attenuated by the lack of weight loss in this group and almost complete eradication of this strain from the kidneys and liver. In the mixed group, low dose NewHG at $1x10^6$ CFU and $6.6x10^6$ CFU NewHG*phePsaeR* were co-injected. Whilst overall there was a significant decrease in weight amongst these mice ($p = 0.009$) compared to low dose alone, there was no difference in parental bacterial CFUs recovered from organs (Figure 5.21 A, black circles). Bacterial numbers of *phePsaeR* recovered from either the kidneys or the liver of the mixed group was low (Figure 5.21 A, orange circles).

It may be that the strain ratios were not optimal to demonstrate augmentation or perhaps the mammalian immune system is functioning in a different way to that of zebrafish. A repeat experiment with increased doses of *phePsaeR* was warranted to investigate this further. Therefore, $3.1x10^7$ CFU *phePsaeR* was injected with low dose *S. aureus* (Figure 5.21 B) but no increased weight loss or higher number of parental CFUs in either liver or kidneys was seen in the mixed group compared to the low dose control ($1.7x10^6$ CFU). Interestingly, in this particular experiment, bacterial numbers in the

liver were higher than expected for the low dose group, with a median of 10^6 CFU, which highlights the variability that can arise within the model (Figure 5.21 B, black circles). Bacterial numbers of *phePsaeR* recovered from either the kidneys or the liver of the mixed group or mutant only groups were low (Figure 5.21 B, orange circles) demonstrating that neither organ retains high numbers of the mutant and it is eradicated from the host.

Therefore, it was not possible to replicate the augmentation phenomenon seen with attenuated *S. aureus* strains and low dose parental *S. aureus* in the zebrafish embryo model of infection, in this murine model. The attenuated strain did not cause infection in the mouse model and in the absence of intravital imaging, the presumption is made that the attenuated strain is phagocytosed as was seen in the zebrafish. However, perhaps the strains are processed differently by the murine phagocytes, preventing the mechanism underlying augmentation from taking place. Virulent and avirulent strains residing in different phagocyte vacuoles have been previously reported (Gresham et al., 2000). Or perhaps the augmentation phenomenon using these mixed inocula is limited to zebrafish. Therefore, other mediators of the phenomenon were investigated including purified peptidoglycan.

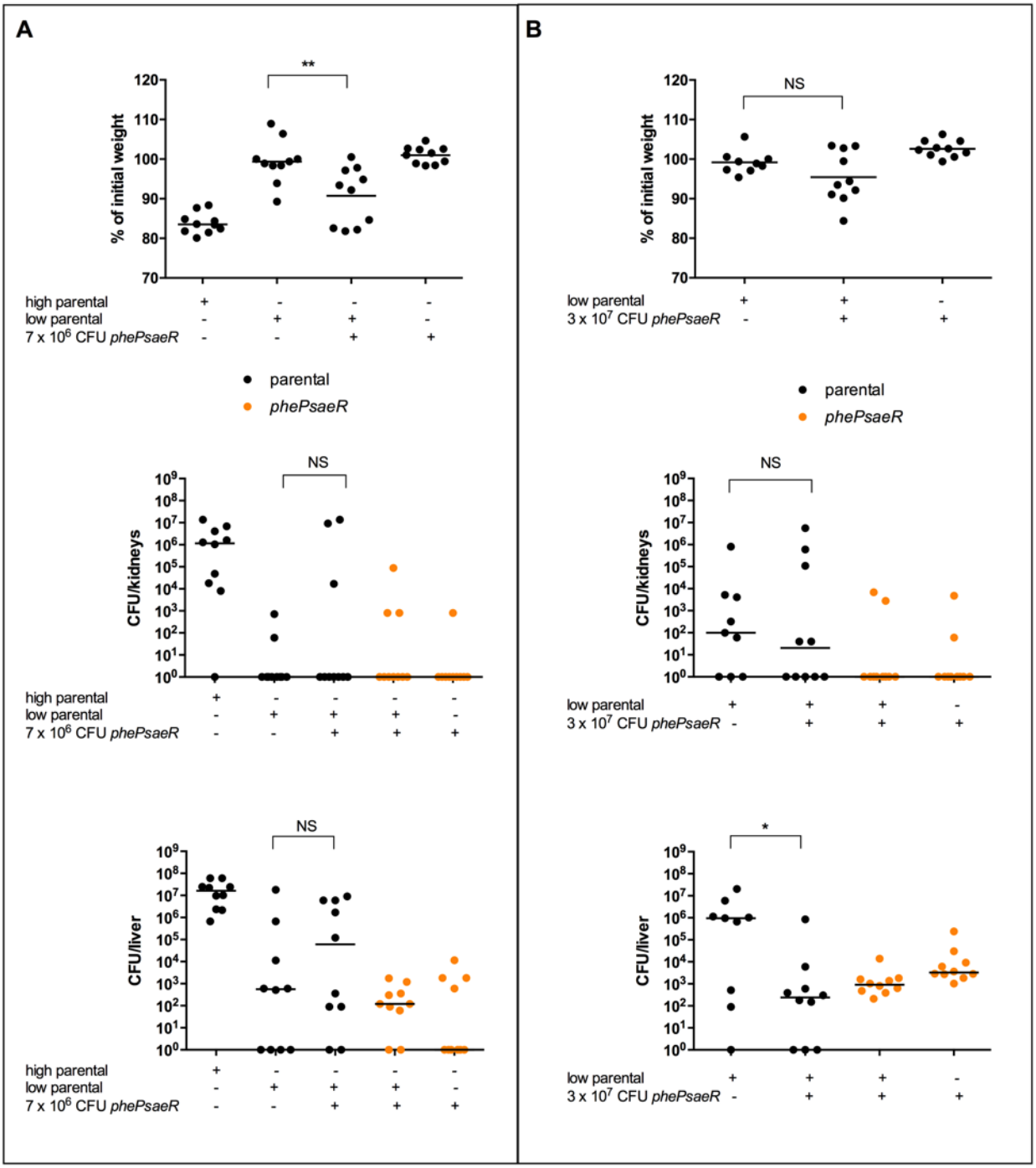

A
B
% of initial weight
**
NS
high parental
low parental
7 x 10^6 CFU phePsaeR
3 x 10^7 CFU phePsaeR
parental
phePsaeR
CFU/kidneys
CFU/liver
*

Figure 5.21 Mixed inocula with *phePsaeR* does not elicit an augmentation phenomenon in the murine sepsis model

A High dose ($9.3x10^6$ CFU) parental strain, low dose ($1x10^6$ CFU) parental strain, low dose ($1.3x10^6$ CFU) parental strain plus 6.6×10^6 CFU NewHG*phePsaeR* or 6.2×10^6 CFU NewHG*phePsaeR* only were injected intravenously (n=10). Weight loss and CFU in kidneys and liver were recorded (parental strain – black circles, *phePsaeR* – orange circles, ** p = 0.009).

B Low dose ($1.7x10^6$ CFU) parental strain, low dose ($1.5x10^6$ CFU) parental strain plus 3.1×10^7 CFU NewHG*phePsaeR* or 3.6×10^7 CFU NewHG*phePsaeR* only were injected intravenously (n=10). Weight loss and CFU in kidneys and liver were recorded (parental strain – black circles, *phePsaeR* – orange circles, * p = 0.037).

5.3.5.2 Establishing the augmentation phenomenon in the murine host using purified peptidoglycan

5.3.5.2.1 Investigating murine host response to purified peptidoglycan alone

In order to test the augmentation phenomenon in the murine model of infection using peptidoglycan, it was first established if peptidoglycan alone would cause host morbidity.

In keeping with rodent data from the literature, a dose dependent systemic effect was seen, as determined by animal health and weight loss, when peptidoglycan was administered intravenously. Interestingly, *S. aureus* peptidoglycan was more potent at eliciting weight loss compared to *M. luteus* but a dose dependent decrease in weight was seen with both peptidoglycans (Figure 5.22 A). Mice receiving 1 mg *S. aureus* peptidoglycan reached culling limits at 24 hpi whereas mice receiving 1 mg *M. luteus* peptidoglycan lost more weight than if lower doses were administered but all animals were healthy throughout the 72-hour experiment. Peptidoglycan from *B. subtilis*, *C. flaccumfaciens*, *S. epidermidis* and non-hydrofluoric acid treated *S. aureus* were all tested (500 μg) and shown to cause minimal weight loss. Whilst there were small differences between weight loss according to type of peptidoglycan, it was important that overall, minimal health disturbances were seen when peptidoglycan was injected alone so that pathogenesis augmentation could be clearly seen, over and above any additive effects. Doses of 200 μg *S. aureus* peptidoglycan and 500 μg *M. luteus* peptidoglycan were chosen for the further experiments, unless otherwise stated.

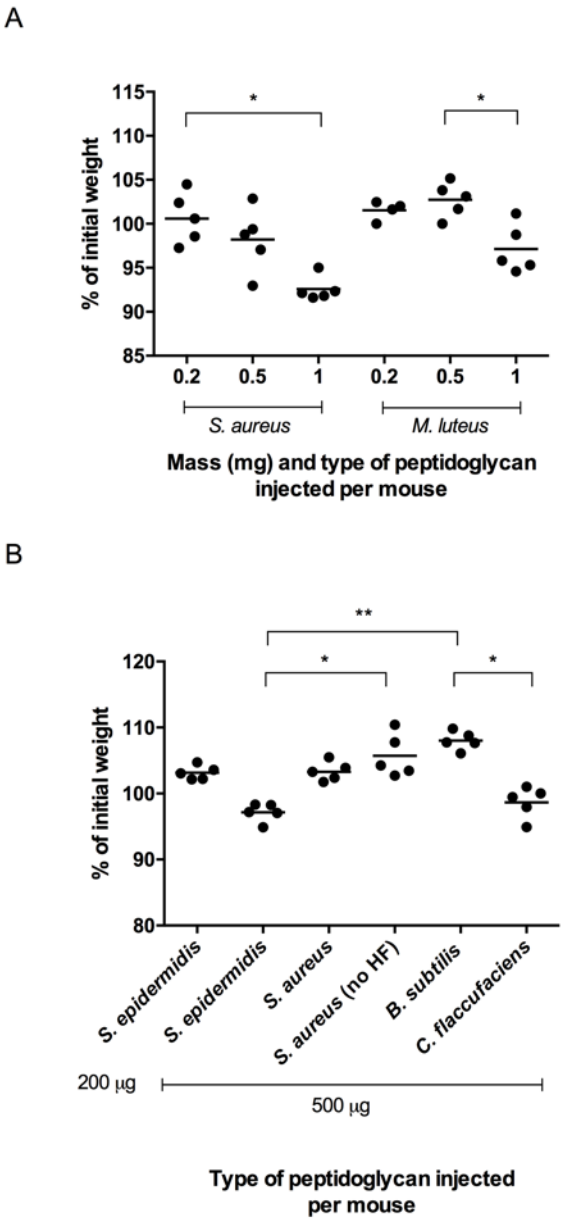


Figure 5.22 Mouse health in response to different doses and types of peptidoglycan

A Various doses of purified *S. aureus* or *M. luteus* peptidoglycan injected into groups of 5 mice. Mice receiving 1 mg *S. aureus* peptidoglycan were culled at 24 hpi (* $p < 0.05$, adjusted for multiple comparisons).

B Various doses and types of purified peptidoglycan injected into groups of 5 mice. *S. aureus* peptidoglycan (no HF) was purified as per the standard protocol but the incubation step with 48% (v/v) hydrofluoric acid was omitted (* $p < 0.05$, ** $p < 0.01$, adjusted for multiple comparisons).

5.3.5.2.2 Co-injection of *M. luteus* peptidoglycan and low dose *S. aureus* in the murine sepsis model

It was next investigated if co-inoculation of *M. luteus* peptidoglycan and low dose *S. aureus* could augment pathogenesis in this murine sepsis model. As had been established during pilot experiments, high dose *S. aureus* ($1x10^7$ CFU) caused significantly more weight loss and higher bacterial CFUs compared to low dose ($1x10^6$ CFU). Mixed inocula consisted of *S. aureus* NewHG Kan^R ($1.2x10^6$ CFU) and 500 μg *M. luteus* peptidoglycan. High ($8.8x10^6$ CFU) and low dose ($8.8x10^5$ CFU) *S. aureus* alone and peptidoglycan (500 μg) only were included as controls (Figure 5.23 A). Mice receiving the mixed inocula lost significantly more weight than low dose controls ($p < 0.0001$) with two mice requiring culling at 44 hpi due to reaching illness severity limits. A second mouse in the mixed group was found dead at 44 hpi. In the high dose *S. aureus* only group, mice also lost up to 20% body weight and one mouse was culled at 24 hpi after reaching severity limits. However, it is likely this mouse did not have a severe *S. aureus* infection due to the undetectable CFU recovered from the organs (red circle, Figure 5.23 A). One mouse in the low dose group also required culling at 44 hpi consistent with the observation that a stochastic infection process can still occur, albeit much less commonly, when lower numbers of bacteria are injected. Peptidoglycan alone caused no weight loss.

Significantly higher CFUs were recovered from the kidneys of mice in the mixed group ($p=0.012$) compared to low dose alone but the most striking result was the exceedingly high numbers (between 10^8 and 10^9 CFUs) recovered from the livers in the mixed group compared to that in the low group ($p < 0.0001$). Even the high dose group liver CFUs did not exceed 10^7 CFU, despite the mice in this group having ten times the initial *S. aureus* load. This experiment was repeated but an additional mixed group was included which contained low dose ($9.3x10^5$ CFU) *S. aureus* in addition to mutanolysin-digested *M. luteus* soluble peptidoglycan (sPGN, 500 μg). As shown in Figure 5.23 B, only mice in the group co-injected with low dose ($9x10^5$ CFU) *S. aureus* polymeric *M. luteus* peptidoglycan (pPGN, 500 μg) demonstrated significant weight loss, with two mice requiring culling at 24 hpi (red circles, Figure 5.23 B) and a further 6 mice were culled at 48 hpi for also reaching severity limits (green circles, Figure 5.23 B). Once again, liver CFU recovered from the pPGN mixed group were extremely high compared to the

low dose control ($p<0.0001$) whereas the sPGN mixed group CFUs were comparable to the low dose control group. In this experiment, CFUs recovered from the kidney were similar across all groups. Therefore, the augmentation phenomenon between peptidoglycan and *S. aureus* found initially in the zebrafish model can be replicated in the mouse model. Indeed, it seems the effect is even more pronounced in the mammalian system with extremely high liver bacterial numbers.

Therefore, given the significant perturbation primarily involving the liver in the mixed pPGN group, it was hypothesised that after phagocytosis of both peptidoglycan and bacteria, the Kupffer cells lose control of *S. aureus*, despite the low dose inocula. Possible mechanisms include local or systemic cytokine perturbation, altered bacteria intra-phagocyte trafficking and/or a reduced ability of phagocytes to kill the bacteria. Other hypotheses include changes in immune cell recruitment or killing efficacy.

The stark abolition of the effect when soluble peptidoglycan was used instead of intact polymer confirms the findings from zebrafish experiments that the structural integrity of peptidoglycan is essential for the process to occur.

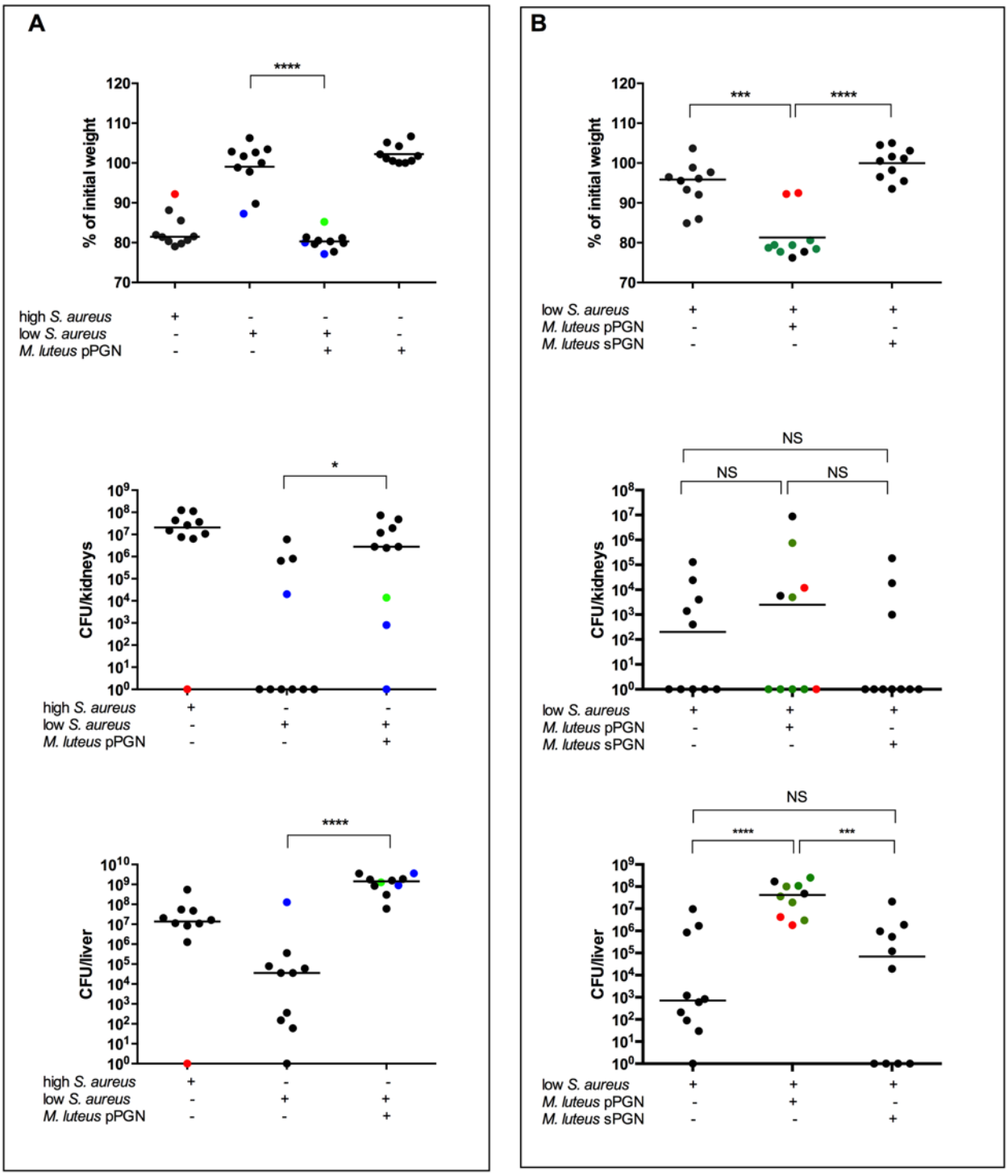

A
% of initial weight
****
high S. aureus
low S. aureus
M. luteus pPGN
CFU/kidneys
*
CFU/liver
****
B
% of initial weight
***
****
low S. aureus
M. luteus pPGN
M. luteus sPGN
CFU/kidneys
NS
NS
NS
CFU/liver
NS
****
***

Figure 5.23 Co-inoculation of *M. luteus* peptidoglycan with a low dose of *S. aureus* promotes recovery of high bacterial numbers from the murine liver

A High dose ($8.8x10^6$ CFU) bacteria, low dose ($8.8x10^5$ CFU) bacteria, low dose ($1.2x10^6$ CFU) bacteria plus 500 µg *M. luteus* peptidoglycan or 500 µg *M. luteus* peptidoglycan only were injected intravenously (n=10). Weight loss and CFU in kidneys and liver were recorded. Red circle – mouse culled at 24 hpi; green circle – mouse found dead at 44 hpi; blue circles – mice culled at 44 hpi (**** $p < 0.0001$, * $p = 0.012$).

B Low dose ($8x10^5$ CFU) bacteria, low dose ($9x10^5$ CFU) bacteria plus 500 µg *M. luteus* insoluble peptidoglycan (pPGN) or 500 µg soluble peptidoglycan (sPGN) were injected intravenously (n=10). Weight loss (*** $p = 0.0003$, **** $p < 0.0001$) and CFU in kidneys and liver (**** $p < 0.0001$, $p = 0.0002$) were recorded. Red circle – mouse culled at 24 hpi; green circles – mice culled at 48 hpi.

5.3.5.2.3 Co-injection of *S. aureus* peptidoglycan and *S. aureus* bacteria in a murine sepsis model

To determine the specificity of the peptidoglycan, pathogenesis augmentation phenomenon, other Gram-positive peptidoglycan was investigated mirroring those in the zebrafish model. *S. aureus* SH1000 derived peptidoglycan (200 μg) was combined with low dose ($1.5x10^6$ CFU) *S. aureus* bacteria. Results closely mirrored those seen with *M. luteus* peptidoglycan, with marked weight loss and hugely increased bacterial numbers in the liver as compared to low dose ($1.5x10^6$ CFU) alone (Figure 5.24 A). Furthermore, this augmented pathogenesis remained if the peptidoglycan was not treated with 48% (v/v) hydrofluoric acid (Figure 5.24 B). As this step removes secondary polysaccharides that are anchored, via phosphodiester bonds, to the peptidoglycan including capsule and teichoic acids, these components are unlikely to be responsible for mediating augmentation.

Lipoproteins are now thought to be the main immunostimulatory compound associated with cell wall immune activation via TLR2 (Section 1.9.3.1). To investigate lipoproteins as mediators of the augmentation phenomenon, a lipoprotein diacylglyceryl transferase (*lgt*) deficient mutant was kindly received from Professor F. Gotz (University of Tubingen). Originally in the *S. aureus* SA113 background, the mutation was transduced using φ11 into the SH1000 strain. This mutant is unable to carry out the lipid modification of prelipoproteins and releases large amounts of unmodified prelipoproteins as discussed in Section 1.9.3.1 (Stoll et al., 2005). Whilst macrophage cell line infection assays demonstrated that wildtype *S. aureus* provoked a strong immune response compared to the *lgt* mutant, cytokine induction in fresh human blood was similar for both wildtype and mutant. This suggests that in more physiological conditions, complex interactions, in addition to a lipoprotein-mediated phenomenon are occurring. In keeping with the latter, mixed inocula containing peptidoglycan from SH1000Δ*lgt*, did not abolish the augmentation phenomenon and significant weight loss, kidney and liver CFUs were seen compared to the low dose ($1.3x10^6$ CFU) control (Figure 5.25). However, as for *M. luteus* peptidoglycan, disrupting the glycan backbone of peptidoglycan by digestion with mutanolysin abolished the effect.

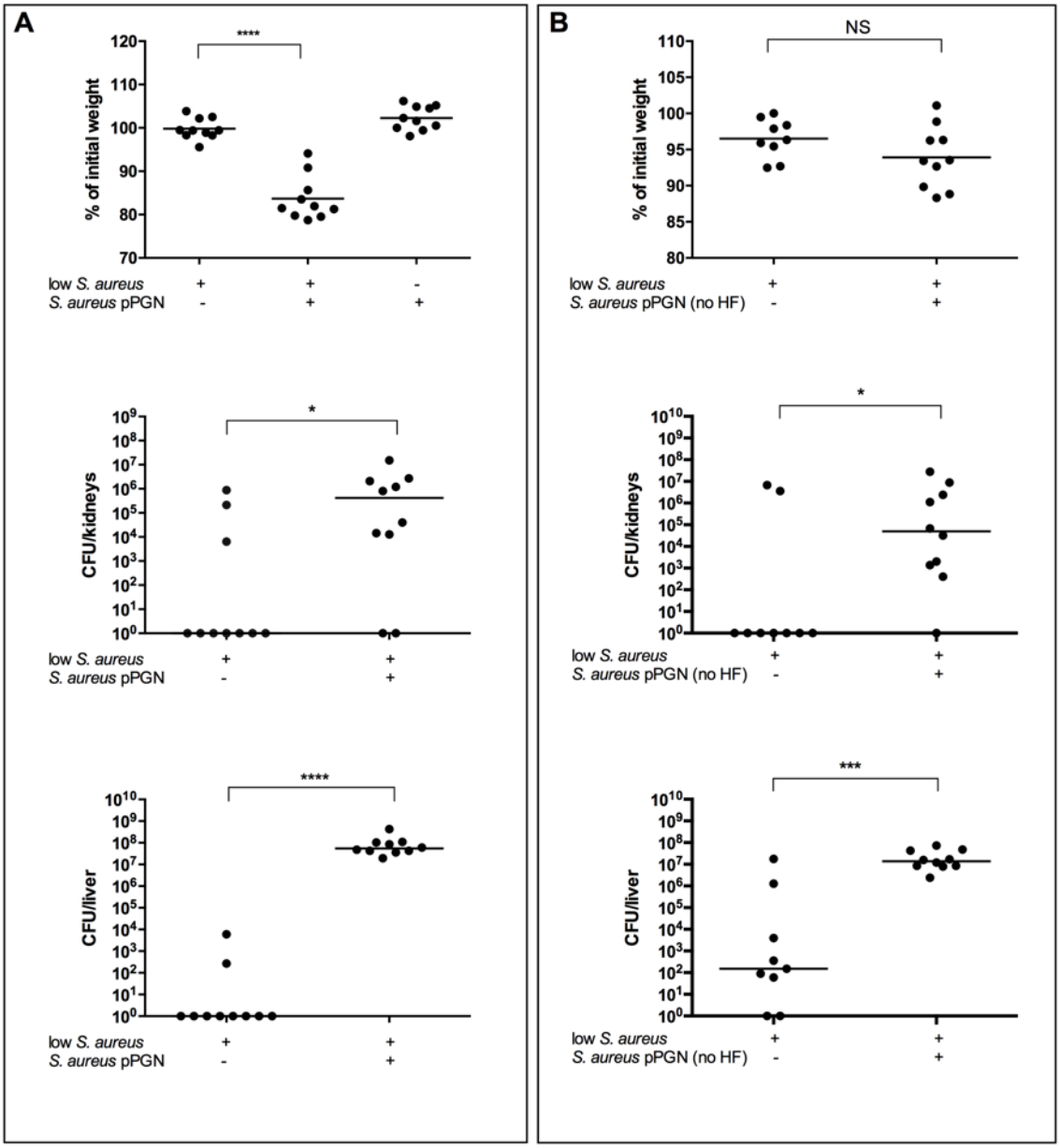


Figure 5.24 Co-inoculation of *S. aureus* peptidoglycan and low dose of *S. aureus* promotes recovery of high bacterial numbers from the murine liver

A Low dose ($1.5x10^6$ CFU) bacteria, low dose ($1.5x10^6$ CFU) bacteria plus 200 µg *S. aureus* insoluble peptidoglycan (pPGN) or 200 µg *S. aureus* pPGN alone were injected intravenously (n=10). Weight loss and CFU in kidneys and liver were recorded (**** $p < 0.0001$,* $p = 0.017$).

B Low dose ($6.5x10^5$ CFU) bacteria, low dose ($5.5x10^5$ CFU) bacteria plus 200 µg *S. aureus* pPGN or 200 µg *S. aureus* pPGN alone were injected intravenously (n=10). NB the peptidoglycan in this experiment was not treated with 48% v/v hydrofluoric acid. Weight loss and CFU in kidneys and liver were recorded (* $p = 0.03$, *** $p = 0.0004$).

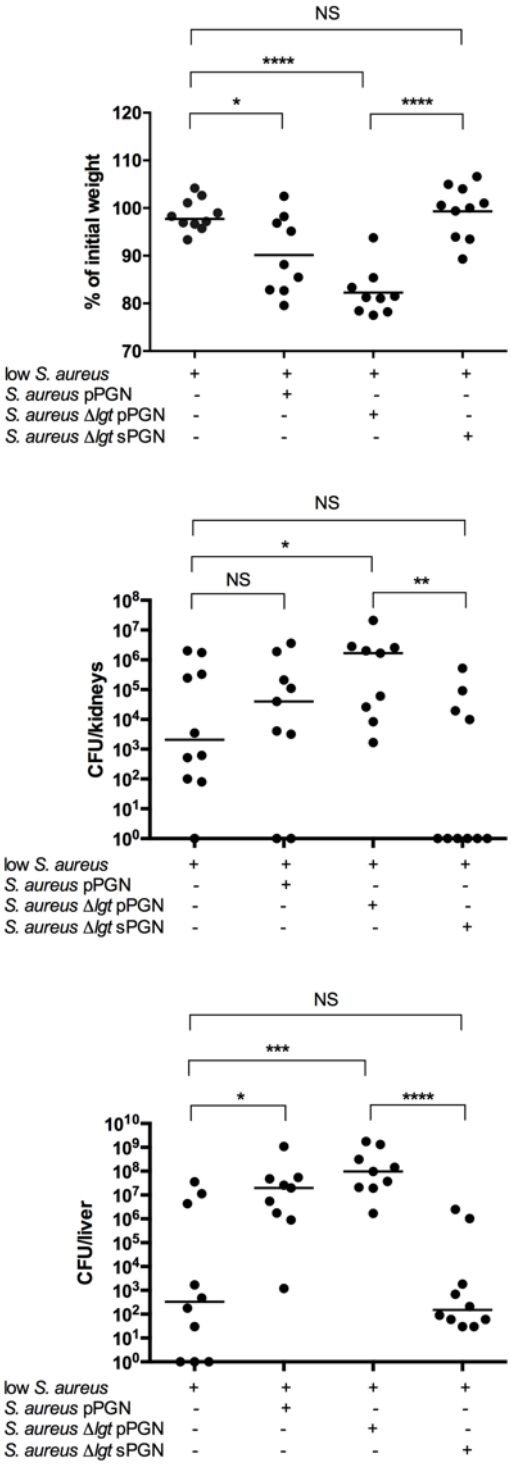


Figure 5.25 Lipoproteins are not responsible for augmentation of pathogenesis by peptidoglycan

Low dose ($1.3x10^6$ CFU) bacteria, low dose ($1.6x10^6$ CFU) bacteria plus 200 µg *S. aureus* SH1000 insoluble peptidoglycan (pPGN), low dose ($1.1x10^6$ CFU) bacteria plus either 200 µg *S. aureus* SH1000Δ*lgt* pPGN or soluble peptidoglycan (sPGN) were injected intravenously (n=10). Weight loss (**** $p < 0.0001$, * $p = 0.02$); CFU in kidneys (* $p = 0.036$, ** $p = 0.0046$) and liver were recorded (* $p = 0.01$, *** $p = 0.0004$, $p < 0.0001$).

5.3.5.3 Examining the extent of the augmentation phenomenon in the murine sepsis model

5.3.5.3.1 Is the composition of peptidoglycan important?

It has so far been established that peptidoglycan from *S. aureus* or *M. luteus* can augment pathogenesis with low dose bacteria. It has also been shown that for *S. aureus* peptidoglycan neither teichoic acids nor lipoproteins are responsible for exerting this effect. It was hypothesised that as the glycan chain backbone of peptidoglycan is highly conserved between species, the composition of the amino acid side chains and crosslinking stem peptides, which vary significantly, may impact on the augmentation phenomenon. To understand the impact of the amino acids to this process, peptidoglycans from *C. flaccumfaciens*, *B. subtilis* and *S. epidermidis* were chosen as they have markedly different forms. *C. flaccumfaciens* is a well known plant pathogen and like *M. luteus* grows optimally at 30°C (Francis et al., 2011). Its peptidoglycan is unusual as instead of L-alanine as the first peptide in the side chain, glycine is present. *B. subtilis* contains meso-diaminopimelic acid (m-DAP) at position 3, an amino acid commonly found in the cell wall peptidoglycan of Gram-negative bacteria (Schleifer and Kandler, 1972). Peptidoglycan from *S. epidermidis* however is very similar to that from *S. aureus*, the only difference being altered composition of the crosslinking side chains (Figure 5.16). It has been shown previously that peptidoglycan from different bacterial species can induce cytokine production *ex vivo* in human blood which suggests that a specific stem peptide composition is not necessary for immune stimulation (Myhre et al., 2004).

Another reason for investigating peptidoglycan from these particular bacteria refers back to the underlying clinical importance of this work. It was hypothesised that the likelihood of acquiring a clinical infection from *S. aureus* may be enhanced by surrounding skin commensal and/or environmental bacteria. Such bacteria themselves are non-pathogenic but their presence at the portal of entry of *S. aureus* via a wound, for example, may enhance the ability of low dose *S. aureus* to cause disease.

To investigate this further, low dose (6.5 x 10^5 CFU) *S. aureus* alone or low dose (5.6 x 10^5 CFU) *S. aureus* plus 500 μg *C. flaccumfaciens* peptidoglycan were injected into groups of 10 mice. As shown in Figure 5.26 A, although there appeared to be a trend to increased weight loss in the mixed inocula group, this was not statistically significant. However, markedly increased CFUs were recovered from both the kidneys and liver in the mixed group. This disassociation of systemic health effects and bacterial burden in the organs has not been noted previously.

When *B. subtilis* peptidoglycan was combined with low dose (1 x 10^6 CFU) *S. aureus*, stark differences in weight loss where seen over the three day experiment. One mouse reached severity limits and required culling at 44 hpi (green circle). Of note, unlike that seen in any previous experiment, 30 minutes post injection with low dose *S. aureus* and 500 μg *B. subtilis* peptidoglycan, animals appeared hunched with ruffled fur and decreased movement. All animals in the low dose (7.9x10^5 CFU) only group were healthy throughout. Increased monitoring was established for the mixed group and the animals continued to deteriorate in well-being scores through the experiment but remained above culling limits until the final time-point. The mixed group had bacterial CFUs in both kidneys and liver far in excess of those recovered from the low dose alone animals (Figure 5.26 B).

Due to the immediate sickness of animals in the *B. subtilis* peptidoglycan mixed group, for the next experiment using *S. epidermidis* peptidoglycan, a peptidoglycan (200 μg) only control group was added back. As expected, animals in either the low dose (1.1 x 10^6 CFU) or peptidoglycan only group lost very little weight with some animals gaining weight as would be expected for a healthy animal ingesting food daily (Figure 5.27). Significantly more weight loss was seen in animals receiving low dose (1.2 x 10^6 CFU) *S. aureus* plus 200 μg *S. epidermidis* peptidoglycan ($p = 0.001$). Markedly increased CFUs were recovered from the liver in the mixed group ($p < 0.0001$) but kidney CFUs were similar in both groups (possibly due to fairly high CFUs recovered from the low group).

It may be therefore that a conserved part of Gram-positive peptidoglycan is responsible for the augmentation phenomenon, as differences in stem and cross-linking peptides did not alter the phenotype. It is interesting that animals appeared unwell very rapidly in the

B. subtilis mixed group perhaps indicating a rapid immuno-stimulatory response to this particular peptidoglycan, more in-keeping with a shock response as has been reported previously (Kengatharan et al., 1998). 'Shock' occurs if bacterial exotoxins or other bacterial components crosslink major histocompatibility complex class II molecules on APCs with T cell receptors, leading to a massive, unconstrained release of cytokines such as TNF-α which damages the host. This was not followed up further but additional experiments could include serum cytokine measurements to follow the systemic reaction and lowering the peptidoglycan dose to see if the effect could be titrated.

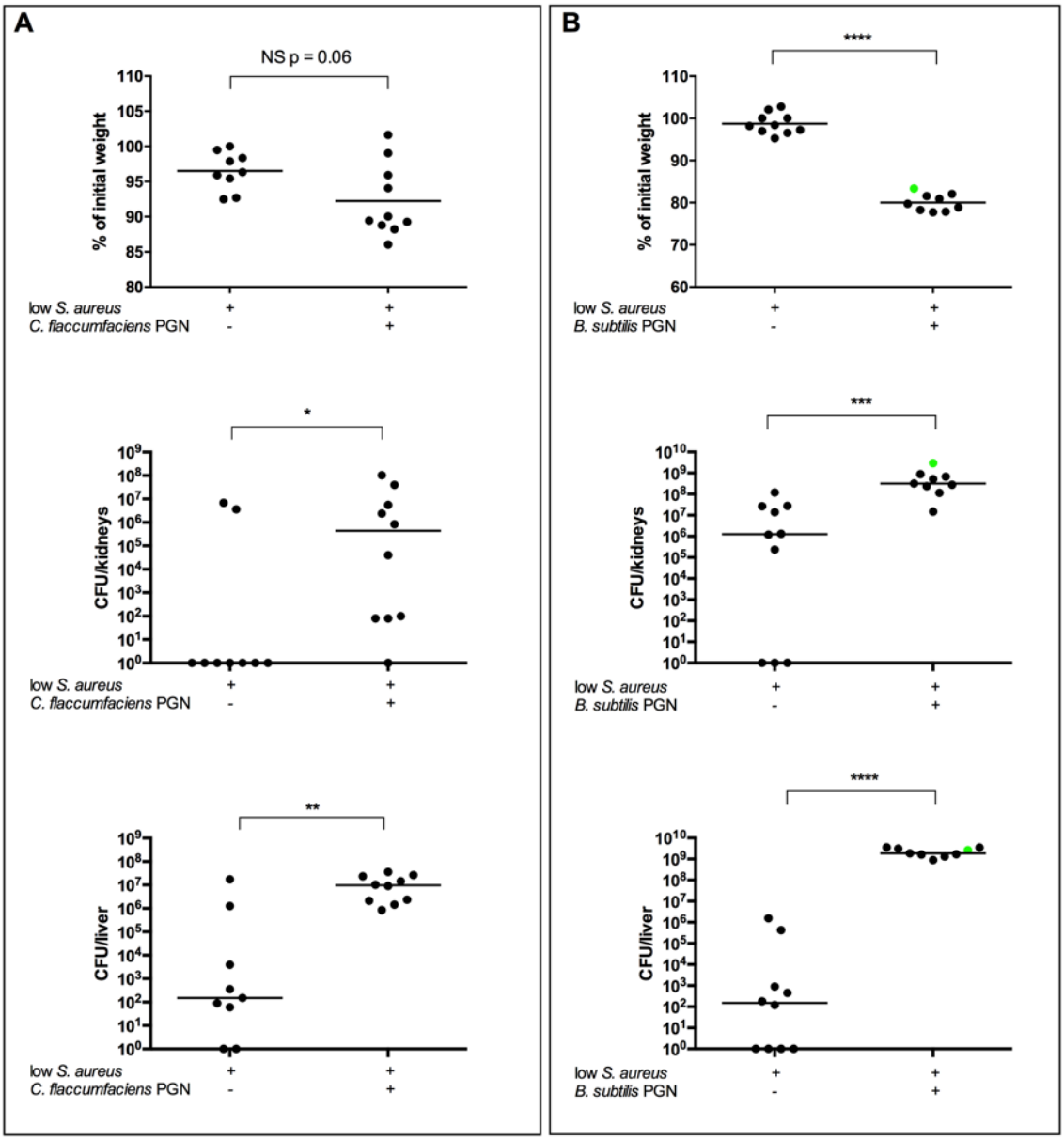


Figure 5.26 *C. flaccumfaciens* or *B. subtilis* peptidoglycan can enhance *S. aureus* pathogenesis

A Low dose ($6.5x10^5$ CFU) bacteria alone or low dose ($5.6x10^5$ CFU) bacteria plus 500 µg *C. flaccumfaciens* insoluble peptidoglycan were injected intravenously (n=10). Weight loss and CFU in kidneys and liver were recorded (* $p = 0.024$; ** $p = 0.0014$).

B Low dose ($7.9x10^5$ CFU) bacteria alone or low dose ($1x10^6$ CFU) bacteria plus 500 µg *B. subtilis* peptidoglycan were injected intravenously (n=10). Weight loss and CFU in kidneys and liver were recorded (**** $p < 0.0001$, *** $p = 0.0003$). Green circle indicates a mouse that reached severity limits at 44 hpi.

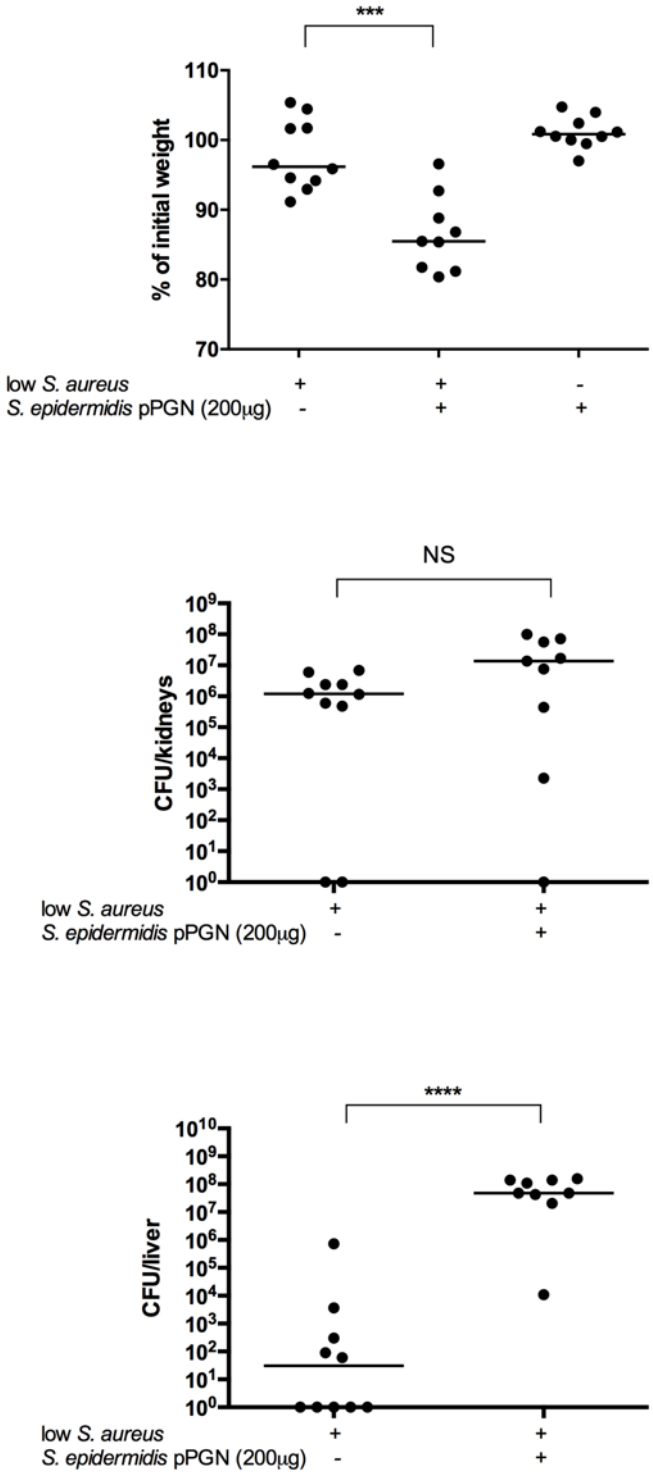


Figure 5.27 *S. epidermidis* peptidoglycan can enhance *S. aureus* pathogenesis

Low dose ($1.1x10^6$ CFU) bacteria alone, low dose ($1.2x10^6$ CFU) bacteria plus 200 µg *S. epidermidis* peptidoglycan or 200 µg *S. epidermidis* peptidoglycan alone were injected intravenously (n=10). Weight loss and CFU in kidneys and liver were recorded (*** $p = 0.001$, **** $p < 0.0001$).

5.3.5.3.2 Can any particulate material augment pathogenesis in the murine sepsis model?

As for the zebrafish model, it was next investigated if any particle, either inert or biological, was able to perturb immune homeostasis and render animals more susceptible to *S. aureus*.

Regarding *S. aureus*, both insoluble peptidoglycan and live bacteria are known to be phagocytosed and *in vitro*, peptidoglycan particles are shown to remain within the phagolysosome, post phagocytosis (Shimada et al., 2010). Live *S. aureus* can escape the phagolysosome (Grosz et al., 2014) so subtle differences in handling are likely between the two. Furthermore, delivery of degraded peptidoglycan products such as MDP, by phagolysosomes into the cytosol may occur in a way that cannot be easily mimicked by direct addition of soluble peptidoglycan to *in vitro* assays. The mechanism by which addition of both peptidoglycan and live bacteria enhances infection is unknown yet it was important to test if inert particles could also do so. As shown in the zebrafish assays, latex beads are phagocytosed and for the murine experiments a large number was chosen (1×10^8 beads), to ensure that the augmentation phenomenon was not simply due to overwhelming the phagocytic capability of the host nor particulate activation of the inflammasome.

Therefore, inert latex polystyrene beads (1 μm, Sigma) were quenched with 30 mM glycine and 1% (w/v) BSA prior to injection. Beads were diluted to 1×10^9 per ml allowing each animal in the control group to receive 1×10^8 beads in the 100 μl injection volume. This dose was chosen to represent approximately the number of particles of peptidoglycan injected in previous experiments. Mice receiving beads alone remained healthy throughout the experiment, losing no weight. Mice receiving either low dose (7.9×10^5 CFU) alone or low dose (8.9×10^5 CFU) *S. aureus* plus beads also maintained their weight and there were no significant differences in either kidney or liver numbers between the groups. Once again, kidneys CFUs in the low group were higher than expected. There was wide variation in the liver CFUs recovered from the mixed group as seen by the spread of the data (Figure 5.28).

Therefore, in keeping with the literature described above, particles cannot cause infection augmentation in a similar fashion to biological material. This also provides evidence that the underlying mechanism of this phenomenon is not merely due to overwhelming the phagocytes thus preventing them engulfing and killing bacteria. If this was the case, the bead presence should augment pathogenesis yet this was not seen.

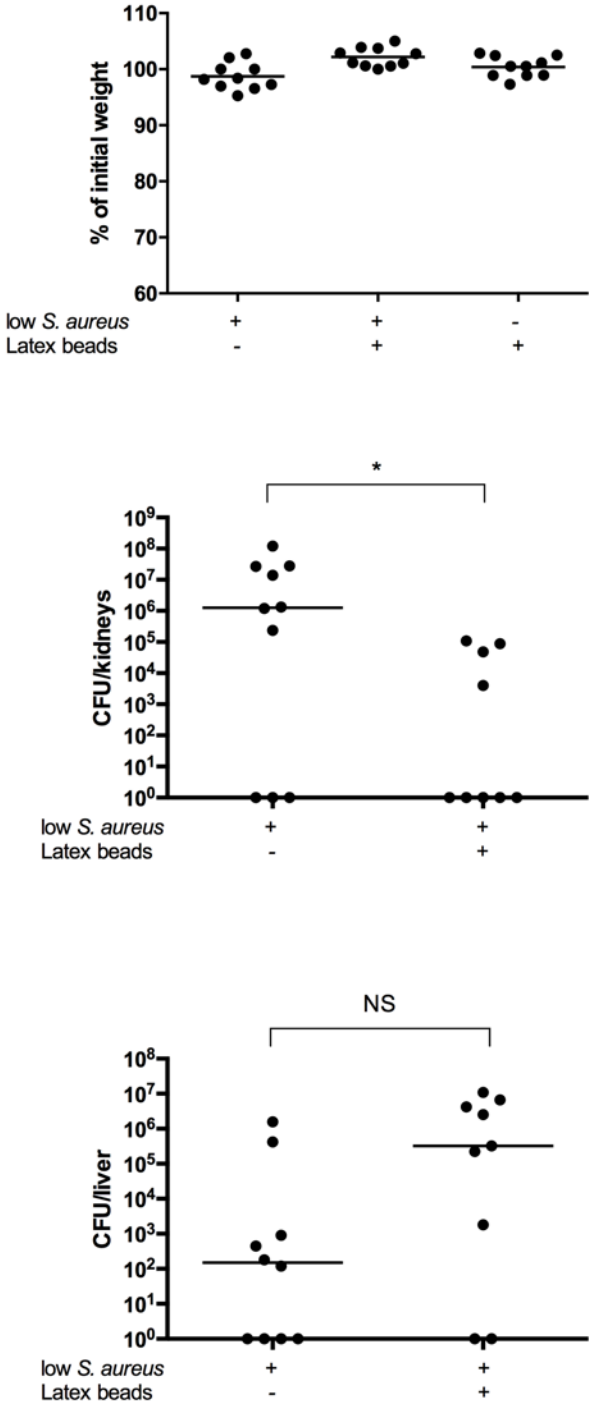


Figure 5.28 Polystyrene latex beads cannot augment pathogenesis of *S. aureus* in the murine sepsis model

Low dose ($7.9x10^5$ CFU) bacteria, low dose ($8.9x10^5$ CFU) bacteria plus $1x10^8$ 1 μm polystyrene latex beads or $1x10^8$ latex beads alone were injected intravenously (n=10). Weight loss and CFU in kidneys and liver were recorded (* p = 0.029).

5.3.5.3.3 Macroscopic images and histopathological analysis of murine livers

In keeping with the high liver CFUs recovered from animals injected with peptidoglycan and *S. aureus*, it was observed macroscopically that the livers were peppered with multiple, small abscesses (Figure 5.29). This was not seen in the low dose group alone and it has not been previously seen when high dose *S. aureus* was injected. In the latter, it is common to see a few large abscesses, predominantly in the kidney at 3 dpi and only occasionally in the liver.

As this was a novel finding, microscopic histopathological analysis was undertaken of control and experimental animals. Instead of processing the organs for CFU numbers as for other experiments, organs were harvested from animals injected with low dose ($9.6x10^5$ CFU) *S. aureus* or low dose ($8.5x10^5$ CFU) plus *M. luteus* peptidoglycan (500 μg), high dose ($9.8x10^6$ CFU) *S. aureus* or peptidoglycan only (500 μg) and cryopreserved (Section 2.22).

Liver parenchyma from peptidoglycan only animals was macroscopically and histologically normal (Figure 5.29 A, C and D). Animals receiving low dose ($9.6x10^5$ CFU) *S. aureus* had very few abscesses and in most organs, none at all (data not shown). High dose ($9.8x10^6$ CFU) *S. aureus* infected animals had occasional large abscesses seen in mainly in kidneys but also the liver (data not shown). Mixed inocula appear to modify the host handling of *S. aureus*, particularly in the liver. Animals in the mixed group had multiple abscesses throughout the liver (Figure 5.29 E, F) and also in some kidneys. At 72 hpi, *S. aureus* attracted a dense neutrophilic infiltrate and extracellular *S. aureus* was observed towards the centre of the abscess, in agreement with other studies (Cheng et al., 2009).

Abscesses are an important pathophysiological marker of *S. aureus* disease. The structure of a *S. aureus* abscess is similar regardless of the location but species and tissue specific aspects exist (Kobayashi et al., 2015). The appearance of multiple, small hepatic abscesses at late time points is novel as when high *S. aureus* doses are administered, bacteria are initially recovered from the liver at the starting inoculum dose but then taper off except in the kidneys where large abscesses are seen at later time points (Holtfreter et al., 2013; McVicker et al., 2014; Wang et al., 2015).

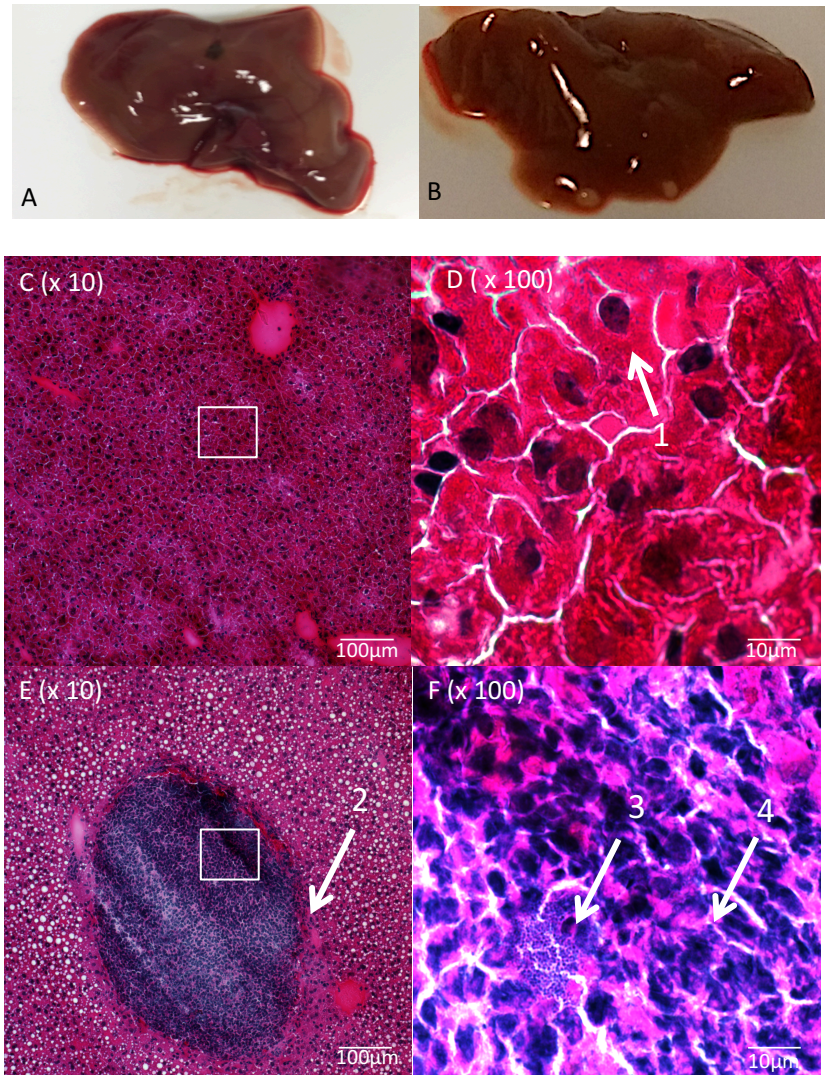


Figure 5.29 Macroscopic images and histopathology of murine livers

Macroscopic image of a liver harvested from a mouse injected with:

A 500 µg *M. luteus* peptidoglycan only (healthy)

B Low dose ($9.6x10^5$ CFU) *S. aureus* plus 500 µg *M. luteus* peptidoglycan (multiple small abscesses can be seen)

Thin-sectioned, H&E stained organs from a mouse injected with 500 µg *M. luteus* peptidoglycan only (C, D) or low dose ($9.6x10^5$ CFU) *S. aureus* plus 500 µg *M. luteus* peptidoglycan (E, F) were imaged at either x 10 (C, E) or x 100 (D, F). Region of interest imaged at x100 is shown in the x10 image (white box).

1 healthy hepatocytes with central nucleus
2 large abscess within liver parenchyma
3 accumulation of extracellular *S. aureus*
4 dense infiltrate of polymorphonuclear leukocytes (PMNs)

5.3.5.3.4 Titration of bacteria or peptidoglycan dose in pathogenesis augmentation in the murine sepsis model

The standard low dose *S. aureus* used in all experiments so far has been 1 x 10^6 CFU thus it was investigated whether lower doses could also cause infection in the presence of *M. luteus* peptidoglycan. In these experiments, 5 mice were injected per group.

Firstly, ten fold dilutions of the standard dose were injected i.e. approximately 1 x 10^5 CFU and 1 x 10^4 CFU both alone and in combination with peptidoglycan. Significant weight loss was seen using NewHG 10^5 CFU but not 10^4 CFU with 500 μg *M. luteus* peptidoglycan yet surprisingly, large liver bacterial numbers were seen in both groups (Figure 5.30 A). The extent of the phenomenon gradually waned as the bacterial dose was reduced. Even at a bacterial dose of 5 x 10^3 and 7 x 10^2 CFU in combination with peptidoglycan, two and one mouse of out five, respectively, showed 10^5-10^6 CFU in the liver compared to complete clearance without peptidoglycan.

Taken together, these data suggest that a threshold of bacterial numbers exist in the region of 5000 – 10000 CFU whereby the augmentation phenomenon can be seen. This is a staggering finding as throughout the literature on *S. aureus* murine (BALB/c) infection models using IV tail vein injection, high inocula are needed to establish infection (Clarke et al., 2007; von Kockritz-Blickwede et al., 2008; Jenkins et al., 2015). It appears that in the presence of bacterial components, the infectious dose of *S. aureus* is drastically lowered. This not only has implications for how disease is established and what prophylactic or therapeutic strategies might be considered but also presents an alternative mouse sepsis model, perhaps more akin to the clinical situation.

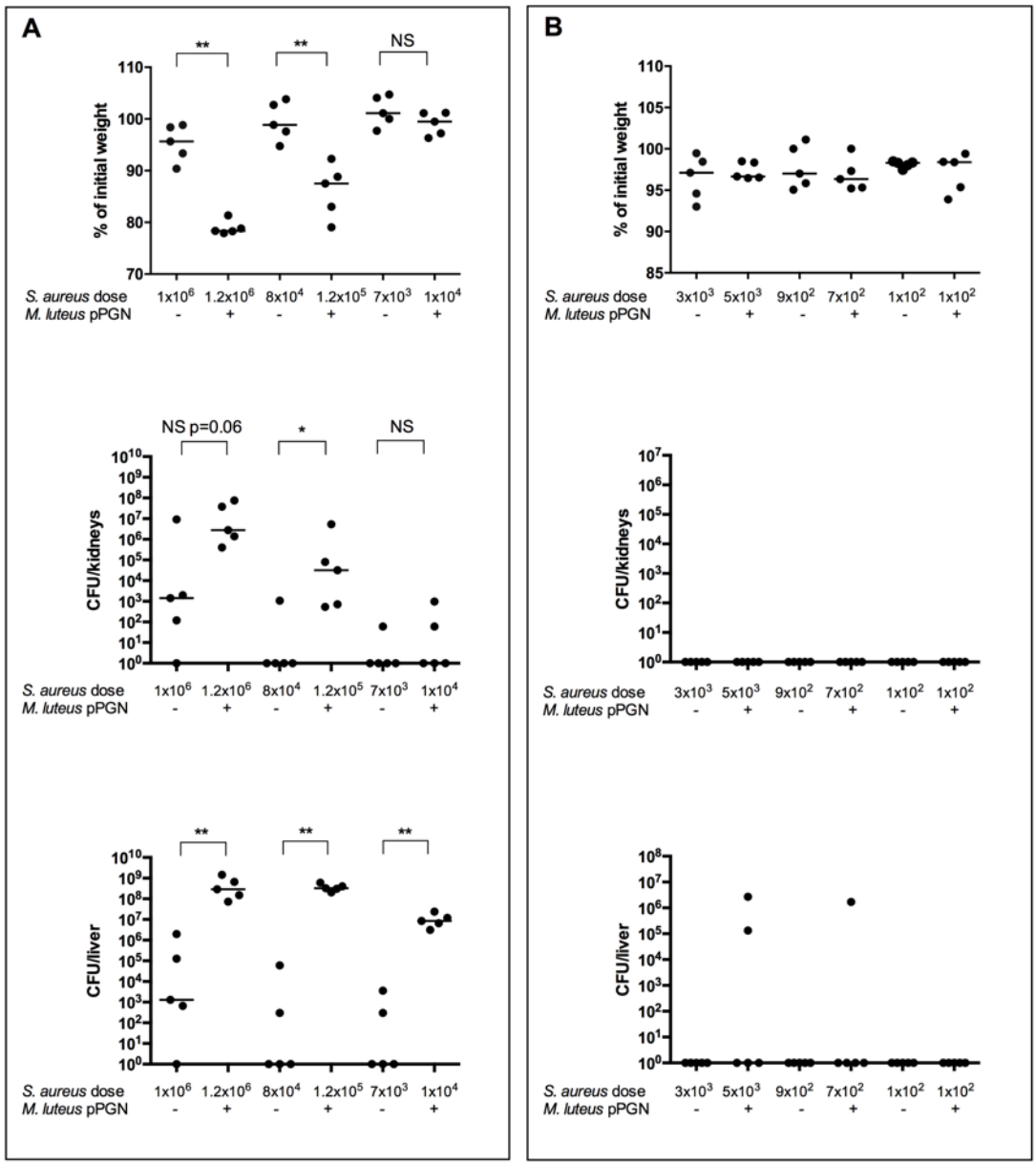


Figure 5.30 Titration of *S. aureus* dose in mixed inocula during *S. aureus* pathogenesis in the murine sepsis model

A Low dose *S. aureus* ranging from 1 x 10^6 - 1 x 10^4 CFU per mouse, without or with *M. luteus* peptidoglycan (500 µg) were injected intravenously (n=5). Weight loss and CFU in kidneys and liver were recorded (* $p = 0.024$; ** $p < 0.01$).

B Low dose *S. aureus* ranging from 1 x 10^4 - 1 x 10^2 CFU per mouse, without or with *M. luteus* peptidoglycan (500 µg) were injected intravenously (n=5). Weight loss and CFU in kidneys and liver were recorded.

Next, it was investigated if the amount of *M. luteus* peptidoglycan could be titrated down from 500 μg to either 250 μg or 50 μg. *M. luteus* peptidoglycan injected at 500 μg in the mixed inocula caused significant weight loss but not if lower doses were co-administered though a dose dependent trend could be noted. No significant differences were seen in kidney numbers even at the highest dose of 500 μg, which is consistent with previous data. However, half the standard amount of *M. luteus* peptidoglycan, 250 μg, in combination with 1 x 10^6 CFU *S. aureus* caused high liver CFUs (Figure 5.31). Indeed, co-injecting only 50 μg of peptidoglycan caused a trend to higher liver bacterial numbers compared to low dose alone.

As for zebrafish peptidoglycan experiments, attempts were made to calculate the amount of staphylococcal cells that would be equivalent to the peptidoglycan injected into each mouse. Data from this project approximated that 26 μg peptidoglycan equates to around 2 x 10^8 staphylococcal cells (Section 2.24.4). Injecting 200 μg of *S. aureus* peptidoglycan is equivalent to 1.5 x 10^9 *S. aureus* cells. The OD_{600}:CFU ratio for *S. epidermidis* is documented as 0.68 x 10^9 CFU/ml per OD_{600} (Kronforst et al., 2012). Using the same method as for *S. aureus*, peptidoglycan mass for 1 ml of culture at OD_{600} 1, was approximately 33 μg. Therefore, 200 μg *S. epidermidis* peptidoglycan equates to 4.1 x 10^9 CFU equivalent. Finally, the same was carried out for *M. luteus* and the OD_{600}:CFU ratio for *M. luteus* was presumed to be 5 x 10^7 CFU/ml per OD_{600} (Matsuura et al., 2013). 1 ml culture at OD_{600} 1 had a peptidoglycan weight of approximately 19 μg, so injecting 500 μg of peptidoglycan is similar to 1.3 x 10^9 CFU *M. luteus* cells.

Determining precise amounts of peptidoglycan that is yielded from a known concentration of *S. aureus* is difficult and prone to error, not least because the purification process will inevitably cause material loss. It is also not possible to know the quantification of the bioburden on the skin or in the environment that may be present concurrently with *S. aureus*. However, it is encouraging that relatively lower amounts of peptidoglycan can still cause augmentation of *S. aureus* pathogenesis.

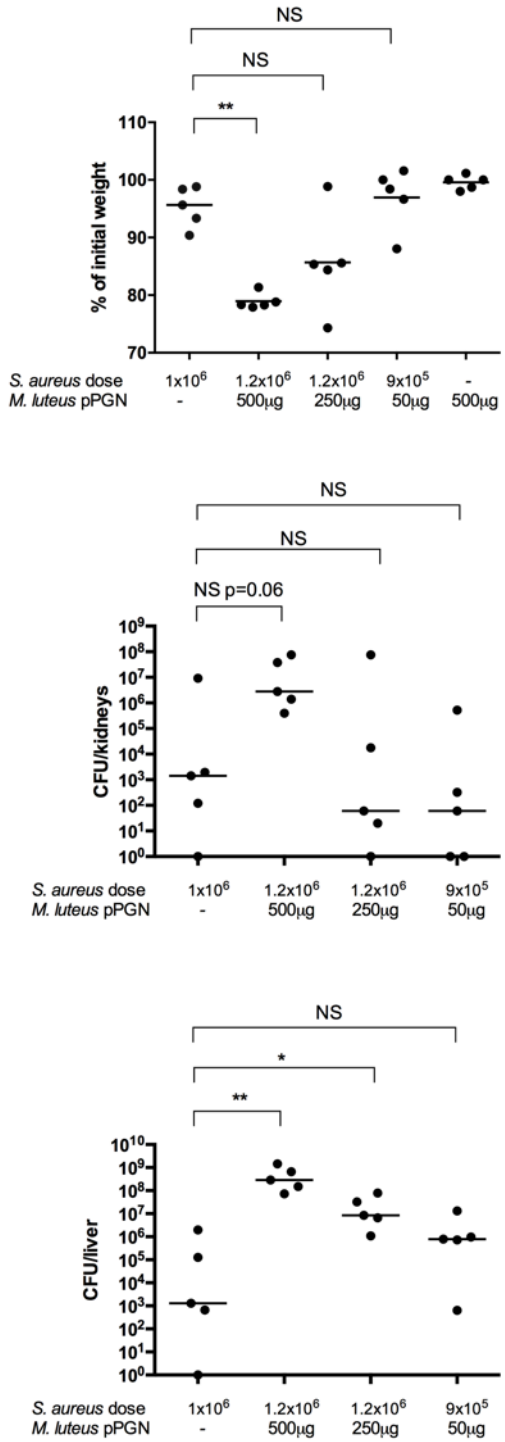


Figure 5.31 Titration of *M. luteus* peptidoglycan dose in mixed inocula during *S. aureus* pathogenesis

Low dose *S. aureus* (1 x 10^6 per mouse), without or with *M. luteus* peptidoglycan at either 500 µg, 250 µg or 50 µg were injected intravenously in the murine sepsis model (n=5). Weight loss and CFU in kidneys and liver were recorded (* $p = 0.016$; ** $p < 0.01$).

5.3.5.3.5 Is the augmentation phenomenon bacterial strain specific?

Thus far, *S. aureus* laboratory strain NewHG has been used in all murine experiments. Next the phenomenon was investigated in a clinical strain background, USA300, JE2 (strain is discussed in Chapter 4). This would determine if the process was bacterial strain specific or common to multiple *S. aureus* lineages. Pilot data was first obtained to ascertain optimal dosing of JE2 that would resemble phenotypes from previous experiments. Based on data collected by colleagues, the dose of JE2 to achieve 'low dose' and 'high dose' would be lower than that used for NewHG (personal communication, Dr E Pollitt, University of Sheffield).

In pilot experiments, using only 5 animals per group, approximately JE2 5 x 10^5 CFU caused a trend towards less weight loss and lower organ CFUs compared to a ten fold higher dose, JE2 5 x 10^6 CFU (Figure 5.32 A). Due to small numbers of animals used in these pilot experiments and variation in the data, statistical significance was not seen. It was decided therefore to use JE2 5 x 10^5 CFU as the low dose. As seen in Figure 5.32 B, mice receiving JE2 4 x 10^5 CFU plus 500 μg *M. luteus* peptidoglycan lost more weight than low dose (5 x 10^5 CFU) only controls but interestingly, bacterial liver numbers were very similar between the two groups (n=10). One mouse in the low dose only group reached severity limits at 48 hpi and was culled. This mouse was subsequently found to have very high bacterial numbers recovered from both kidneys and liver indicating a large *S. aureus* disease burden.

Comparing kidney CFU counts between groups demonstrated a significantly higher number recovered from the mixed group compared to low dose alone. However, the majority of mice in the low dose alone group had CFUs between 10^5 and 10^7, suggesting bacterial replication. Previously, when low dose control animals have had CFUs of those values, there was no difference when compared to the mixed group (for example, see Figure 5.27). However, kidney numbers recovered from the mixed group in this experiment were higher still (between 10^7 and 10^9) as shown in Figure 5.32 B. Whilst augmentation of pathogenesis is seen using the clinical strain JE2 in combination with peptidoglycan, the tissue tropism of the phenomenon has changed. This may be a JE2-specific effect and it remains to be determined whether the underlying mechanism is the same between different bacterial strains.

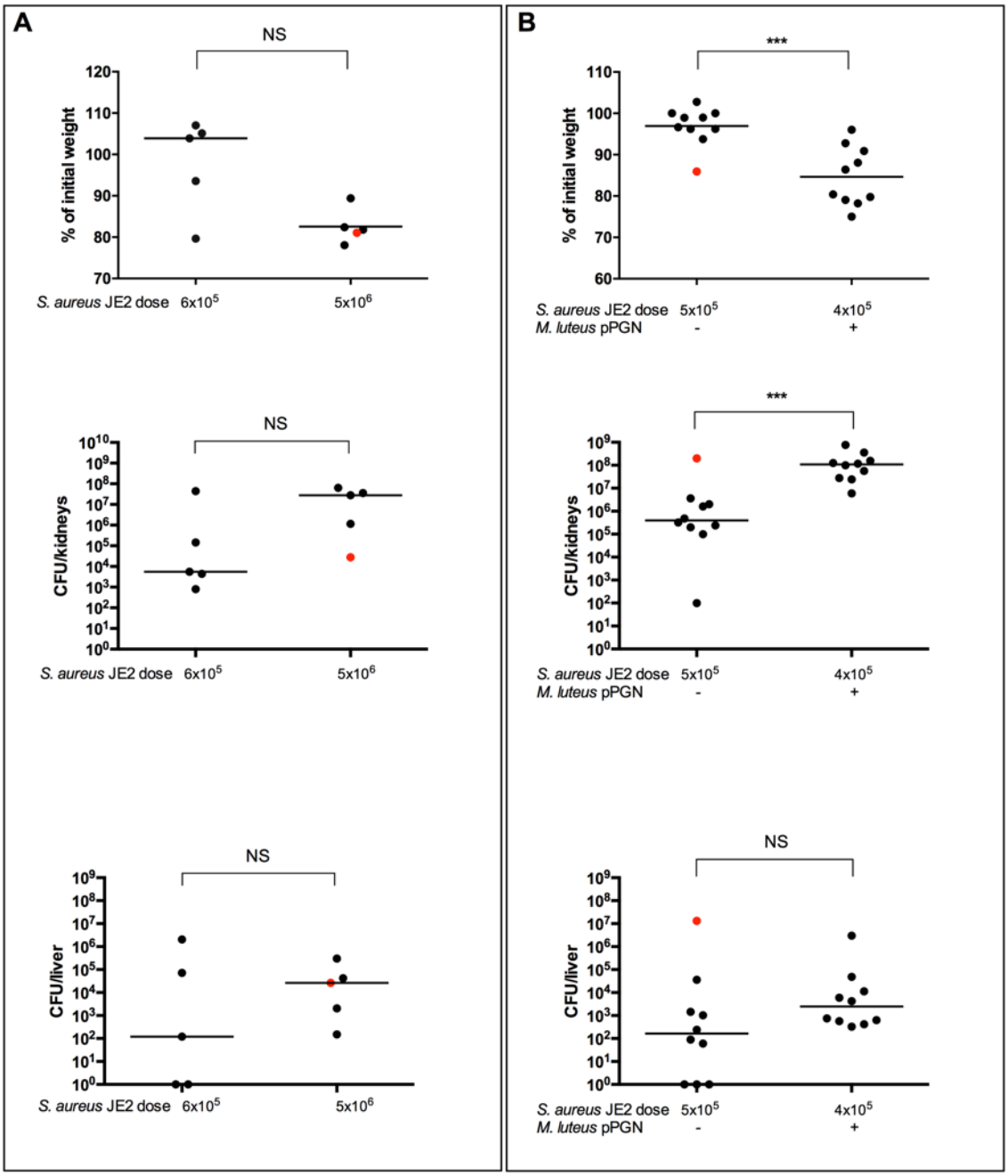


Figure 5.32 *S. aureus* strain specific effects may play a role in augmentation of murine infection

A Low dose *S. aureus* JE2 (6 x 10^5 per mouse), or high dose *S. aureus* JE2 (5 x 10^6 per mouse) were injected intravenously (n=5). Weight loss and CFU in kidneys and liver were recorded. One mouse reached severity limits at 48 hpi (red circle).

B Low dose *S. aureus* JE2 (5 x 10^5 per mouse) without or with 500 µg *M. luteus* peptidoglycan was injected intravenously (n=10). Weight loss and CFU in kidneys and liver were recorded. One mouse reached severity limits at 48 hpi (red circle).
***p = 0.0003 (weight); *** p = 0.0007 (kidneys)

5.3.5.3.6 Investigating if the augmentation phenomenon is mouse strain specific

Host susceptibility to *S. aureus* is an important disease determinant in humans and the same is true for different mouse strains. The majority of laboratory mouse strains are inbred with varying degrees of susceptibility to bacterial pathogens including *S. pneumoniae* (Gingles et al., 2001) and *S. aureus* (von Kockritz-Blickwede et al., 2008). Using the laboratory strain of *S. aureus* SH1000 at a dose of 4 x 10^7 CFU, BALB/c, A/J and DBA/2 mice were highly susceptible, succumbing between 1 and 7 days post infection. Several other mouse strains showed intermediate susceptibility whilst C57BL/6 mice were very resistant to infection, showing only 10% mortality at 14 days. Underlying mechanisms were determined to be partly due to differences in macrophage chemokine production and innate immune cell recruitment.

To examine for mouse strain specific effects, mice reported to be the most resistant to *S. aureus* infection, C57BL/6, were purchased (Envigo Laboratories). *S. aureus* strain NewHG was injected in pilot experiments (n = 5) and three different doses were initially chosen: 1 x 10^7, 5 x 10^7 and 2 x 10^8 CFU per mouse. It was thought that NewHG may behave in a similar fashion to SH1000 (von Kockritz-Blickwede et al., 2008) in this mouse strain so high doses were injected to establish the spectrum of tolerable doses in C57BL/6 mice. Unfortunately, all 5 animals in the highest dose group (actual dose injected was 1.4 x 10^8 CFU) were found dead the following morning (20 hpi). Mice in the middle dose group (5 x 10^7 CFU) were extremely unwell at 20 hpi and required culling (red circles). Mice in the lowest dose group (1 x 10^7 CFU) remained healthy throughout the 72-hour experiment and displayed few signs of illness. This group however consistently lost weight at each time point, up to 30% of their initial weight (Figure 5.33 A). Animals in the middle dose group had high CFUs recovered from the liver but less so from the kidneys. In the lowest dose group, liver numbers were also high and a wide range of counts was found in the kidneys (Figure 5.33 B).

The aim of the pilot experiment was to establish the optimum 'low dose' for further experiments i.e. that which would not affect the health status of the animals. This was not achieved as all doses used caused morbidity or mortality. This was unexpected as the literature suggests that this strain of mouse has increased resistance to *S. aureus* infection. It may be that bacterial strain differences play a role as NewHG is not a

widely used strain and no documentation can be found in the literature of this bacterial strain being used in this mouse strain. Alternatively, despite carrying the same mouse strain name, there is likely to be variations in the mice purchased from different suppliers. However, it was clear that a lower dose than 1 x 10^7 CFU should be used in the mixed inocula experiments and 4 x 10^6 CFU was chosen.

In addition to testing the *S. aureus* dose in C57BL/6 mice, peptidoglycan doses were also titrated in the pilot experiment (Figure 5.33 A). Regardless of the amount injected (500 µg, 1 mg or 2 mg *M. luteus* peptidoglycan), minimal weight loss was seen and the mice appeared healthy throughout.

Therefore, using 10 animals per group, low dose alone (3.6 x 10^6 CFU) or low dose (4.3 x 10^6 CFU) plus 1 mg *M. luteus* peptidoglycan was injected into C57BL/6 mice via the tail vein. A higher peptidoglycan dose was chosen due to the reported increased susceptibility of this mouse strain to *S. aureus*. Animals in both groups lost weight but far more was lost in the mixed group. All mice in the mixed group showed signs of illness at 1 dpi and continued to deteriorate to reach severity limits at 44 hpi (Figure 5.33 C). The low dose only group was culled at 67 hpi. Liver CFUs were high in both groups (approximately 10^7 – 10^8 CFUs) indicating bacterial replication but interestingly, a marked difference between the groups was seen in recovered CFUs from the kidneys (Figure 5.33 D, E).

Similar to when a different bacterial *S. aureus* strain was used, although an augmentation phenomenon was seen using this mouse strain, it did not exactly replicate data seen previously and the tissue tropism appeared to be different. Due to the high liver CFUs recovered from both groups, this experiment was repeated using a lower dose of NewHG (2 x 10^6 CFU) with or without 1 mg *M. luteus* peptidoglycan. As for the previous experiment, animals in both the low dose control group and mixed inocula group lost weight but weight loss was exaggerated in the mixed group (Figure 5.33 F). In the kidneys, there was no significant difference in CFU between the two groups (Figure 5.33 G). High liver bacterial numbers were seen in both groups at 72 hpi yet higher CFUs were recovered from the mixed group animals (Figure 5.33 H). It may be that optimal doses to evaluate the phenomenon in this mouse strain have not been achieved and further titrations may be warranted as future work. The advantages of

establishing the phenomenon in this mouse strain are two fold: firstly to strengthen the data collected by demonstrating effects independent of the mouse strain background but secondly, to further hone in on the mechanism. Many transgenic knockout mice are only available in this mouse strain background and having a robust assay in the C57BL/6 mice would expand the repertoire of hypothesis testing experiments. For example, TLR2, Nod2, and inflammasome components such as NALP3 knock out mice could be used to dissect the immune influence on augmentation of infection.

Comparing and contrasting genetic or phenotypic differences between mouse strains is more accessible due to the development of The Mouse Phenome Database (Maddatu et al., 2012). However, these datasets are vast and not necessarily specific to the pathogen of interest. It is perhaps not surprising that mirroring the BALB/c phenotype is difficult in the C57BL/6 background. Although in general C57BL/6 mice are considered more resistant to *S. aureus* infection, using a subcutaneous *S. aureus* infection model, C57BL/6 mice were more susceptible than BALB/c so assumptions as to strain susceptibility are likely to be error prone (Nippe et al., 2011). Recent advances in developing humanised mice may add vital information to this complex area (Knop et al., 2015).

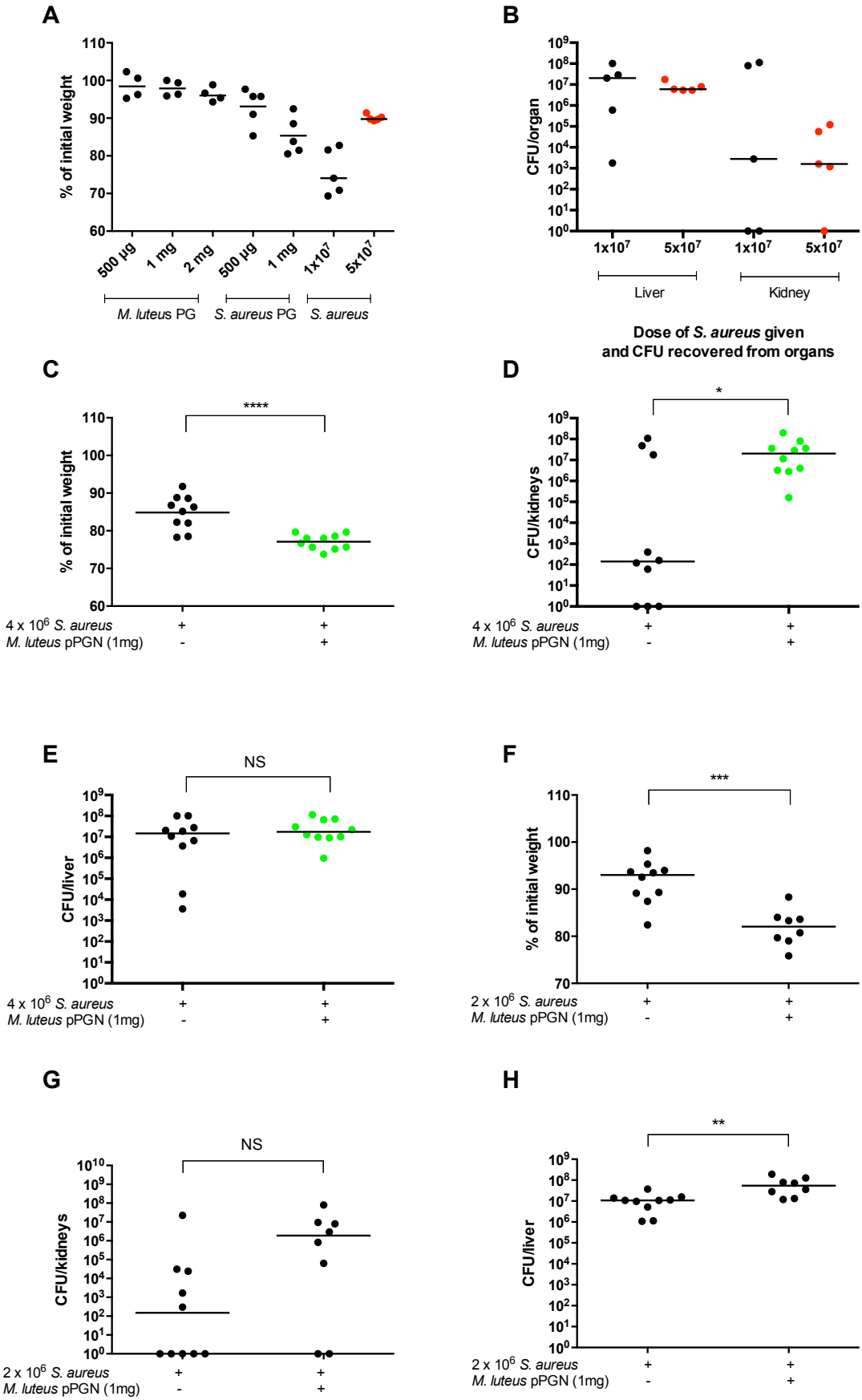

A
% of initial weight
110
100
90
80
70
60
500 µg
1 mg
2 mg
500 µg
1 mg
1x10^7
5x10^7
M. luteus PG
S. aureus PG
S. aureus
B
CFU/organ
10^9
10^8
10^7
10^6
10^5
10^4
10^3
10^2
10^1
10^0
1x10^7
5x10^7
1x10^7
5x10^7
Liver
Kidney
Dose of S. aureus given
and CFU recovered from organs
C
% of initial weight
****
4 x 10^6 S. aureus + +
M. luteus pPGN (1mg) - +
D
CFU/kidneys
*
4 x 10^6 S. aureus + +
M. luteus pPGN (1mg) - +
E
CFU/liver
NS
4 x 10^6 S. aureus + +
M. luteus pPGN (1mg) - +
F
% of initial weight
***
2 x 10^6 S. aureus + +
M. luteus pPGN (1mg) - +
G
CFU/kidneys
NS
2 x 10^6 S. aureus + +
M. luteus pPGN (1mg) - +
H
CFU/liver
**
2 x 10^6 S. aureus + +
M. luteus pPGN (1mg) - +

Figure 5.33 Use of the C57BL/6 mouse strain to demonstrate the pathogenesis augmentation phenomenon

A and B Pilot experiment to determine optimum *S. aureus* and peptidoglycan dose in C57BL/6 mice (n=4-5). Weight loss and CFU in kidneys and liver were recorded (red circles – mice reaching severity limits).

Low dose *S. aureus* (4×10^6 per mouse) without or with 1 mg *M. luteus* peptidoglycan was injected intravenously (n=10). Weight loss (**C**) and CFU in kidneys (**D**) and liver (**E**) were recorded (**** $p < 0.0001$, * $p = 0.033$).
Green circles – mice culled at 44 hpi

Low dose *S. aureus* (2×10^6 per mouse) without or with 1 mg *M. luteus* peptidoglycan was injected intravenously (n=10). Weight loss (**F**) and CFU in kidneys (**G**) and liver (**H**) were recorded (*** $p = 0.0009$, ** $p = 0.029$).

5.3.5.3.7 Effect of live commensal bacteria on *S. aureus* pathogenesis in the murine sepsis model

Firstly, *S. epidermidis* was investigated and a pilot experiment was carried out to ensure that when injected alone, live *S. epidermidis* was not detrimental to the mouse. Firstly, 5 BALB/c mice were injected intravenously with $1.3x10^7$, $1.9x10^8$ or $4.7x10^8$ CFU *S. epidermidis* (Figure 5.34 A). Both lower doses caused no weight loss or change in animal health status score. The highest dose ($5x10^8$ CFU) caused 10-20% weight loss by 72 hpi and animals appeared scruffy with signs of systemic illness. Correspondingly, the two lower doses of *S. epidermidis* were either cleared or found in low numbers in both kidneys and liver (10^4 CFU) yet high levels of *S. epidermidis* are recovered from the liver of the $5x10^8$ CFU group. As such the dose of $1x10^8$ CFU was chosen for the mixed inocula experiment. *S. epidermidis* 138, a clinical strain was used that had been serially passaged onto agar containing rifampicin to obtain a spontaneous Rif^R derivative. This antibiotic resistance marker (Rif^R) was used to distinguish the *S. epidermidis* from the *S. aureus* strain (NewHG Kan^R).

Conducted as a pilot experiment, $1x10^6$ CFU NewHG Kan^R with and without $1x10^8$ CFU *S. epidermidis* Rif^R or $1x10^8$ CFU *S. epidermidis* Rif^R alone was injected into each group of mice (n=5, Figure 5.34 B). There was significantly more weight loss in the group receiving the mixed inoculum. *S. aureus* CFUs recovered from the kidneys were similar between low dose control and mixed groups yet, as was seen when co-injecting peptidoglycan, significantly higher *S. aureus* was found in the liver of animals injected with live *S. epidermidis* and low dose *S. aureus* (p=0.0079). *S. epidermidis* numbers are low in both the mixed and *S. epidermidis* only group, representing the clearance of this organism from the host (dark red circles). The experiment was then repeated with ten mice per group and similar findings were seen (Figure 5.35) confirming live *S. epidermidis* is able to augment *S. aureus* pathogenesis.

Next, 5 BALB/c mice were injected intravenously with $3.8x10^7$, $1.9x10^8$ or $2.9x10^8$ CFU of *M. luteus* (Figure 5.36 A). All doses caused no weight loss or change in animal health status score. Low dose ($2x10^6$ CFU) NewHG Kan^R with and without $2.8x10^8$ CFU *M. luteus* or $2.8x10^8$ CFU *M. luteus* alone was injected into each group of mice (n=5, Figure 5.36 A). For enumeration, the two bacterial species were differentiated by

colony growth rate and appearance. Mice receiving *S. aureus* in combination with *M. luteus* lost more weight than those receiving low dose *S. aureus* alone (p=0.023). *S. aureus* CFUs recovered from the kidneys were similar between low dose control and mixed groups but significantly higher *S. aureus* was recovered from the liver of animals injected with live *M. luteus* and low dose *S. aureus* (p=0.024). *M. luteus* was not recovered from any of the harvested organs indicating eradication from the host. The experiment was then repeated with ten mice per group and augmentation of *S. aureus* pathogenesis was seen even when the live *M. luteus* dose administered was lowered to $1x10^7$ CFU in mixed inocula (p = 0.018, Figure 5.35 B).

In summary, it is compelling that as little as $1x10^7$ CFU of live *M. luteus* can augment *S. aureus* pathogenesis. This may well represent the physiological magnitude of *M. luteus* skin burden in a localised area though accurate studies of commensal organism bioburden are lacking. Quite how co-inoculation of these commensal organisms, as might occur during wounds or skin trauma, alongside low dose *S. aureus* alters pathogenesis is not known but data from this project suggests significant augmentation of infection occurs.

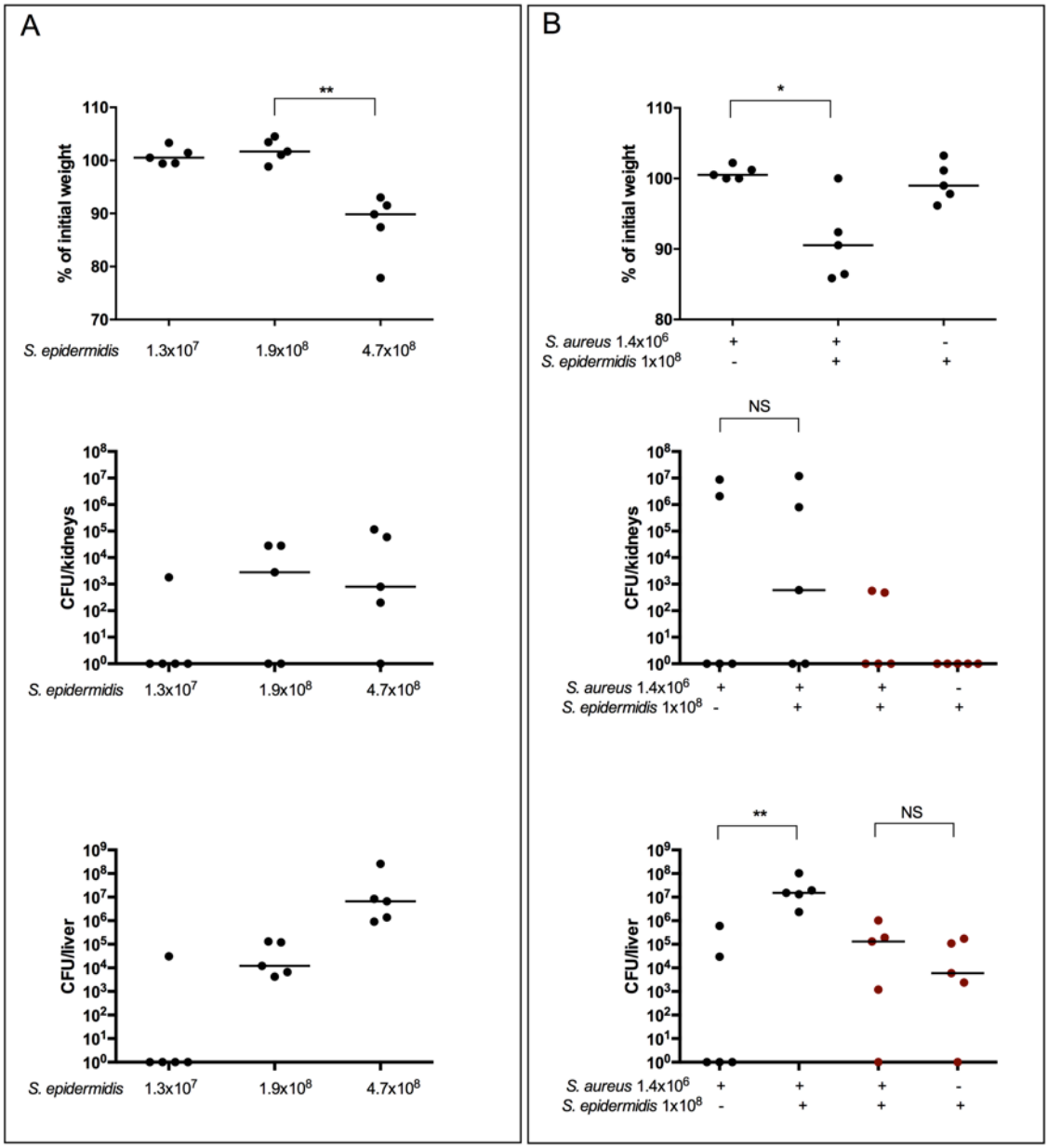


Figure 5.34 Co-injection of live *S. epidermidis* and low dose *S. aureus* pathogenesis in the murine sepsis model

A *S. epidermidis* dose titration (n=5). Weight loss and CFU in kidneys and liver were recorded (** p = 0.0079)

B Low dose ($1.4x10^6$ CFU) *S. aureus* without or with or $1x10^8$ CFU *S. epidermidis* or $1x10^8$ CFU *S. epidermidis* alone was injected intravenously (n=5). Weight loss and organ CFUs were recorded (* p = 0.0238; ** p = 0.0079). Red circle – *S. epidermidis*; black circle – *S. aureus*.

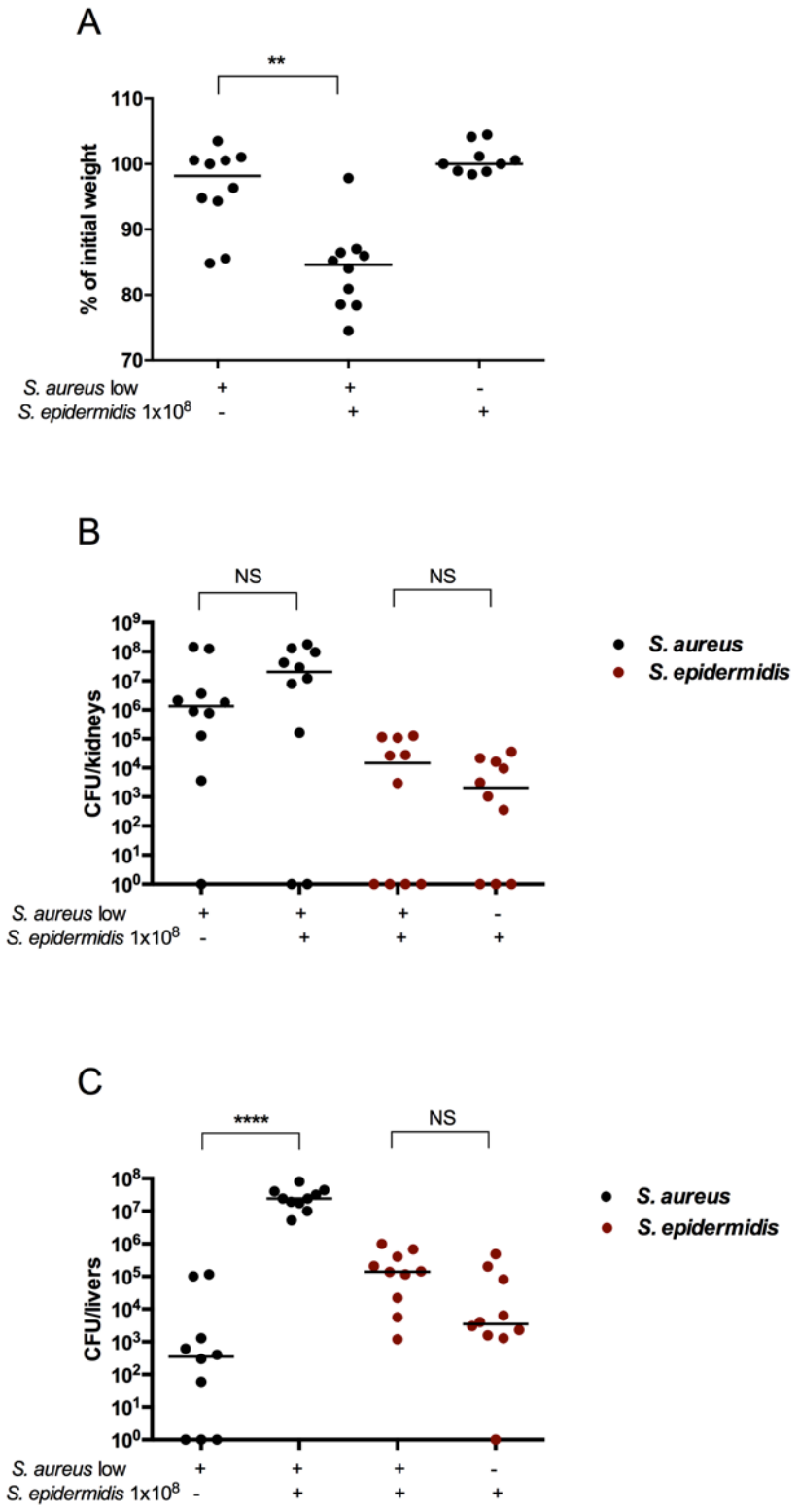


Figure 5.35 Co-injection of live *S. epidermidis* augments low dose *S. aureus* pathogenesis in the murine sepsis model

Low dose ($1x10^6$ CFU) *S. aureus* without or with or $1x10^8$ CFU *S. epidermidis* or $1x10^8$ CFU *S. epidermidis* alone was injected intravenously (n=10). Weight loss (**A**) and organ CFUs were recorded (**B** kidneys; **C** liver; ** $p = 0.0029$, **** $p < 0.0001$).

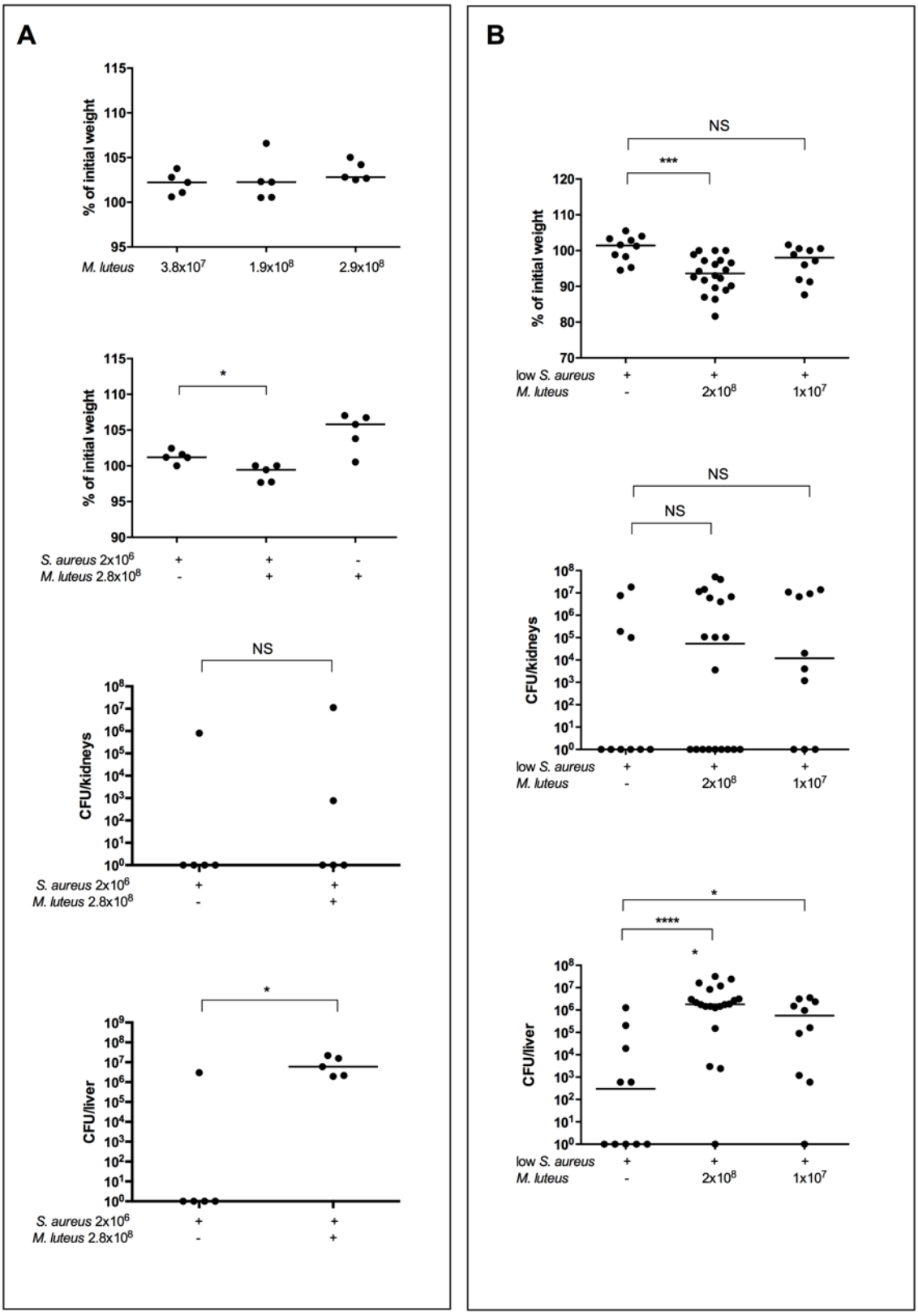

A
% of initial weight
M. luteus 3.8x10^7 1.9x10^8 2.9x10^8
*
S. aureus 2x10^6 + + -
M. luteus 2.8x10^8 - + +
NS
CFU/kidneys
S. aureus 2x10^6 + +
M. luteus 2.8x10^8 - +
*
CFU/liver
S. aureus 2x10^6 + +
M. luteus 2.8x10^8 - +
B
NS
***
% of initial weight
low S. aureus + + +
M. luteus - 2x10^8 1x10^7
NS
NS
CFU/kidneys
low S. aureus + + +
M. luteus - 2x10^8 1x10^7
*
****
*
CFU/liver
low S. aureus + + +
M. luteus - 2x10^8 1x10^7

Figure 5.36 Co-injection of live *M. luteus* augments low dose *S. aureus* pathogenesis in the murine sepsis model

A *M. luteus* dose titration ($3.8x10^7$, $1.9x10^8$ or $2.9x10^8$ CFU); low dose ($2x10^6$ CFU) *S. aureus* without or with or $2.8x10^8$ CFU *M. luteus* or $2.8x10^8$ CFU *M. luteus* alone was injected intravenously (n=5). Weight loss and organ CFUs were recorded (* $p = 0.023$ - weight loss, * $p = 0.024$ – liver).

B Low dose ($8.2x10^5$ CFU) *S. aureus* alone or low dose ($1.3x10^6$ CFU, n=10) *S. aureus* with either $2x10^8$ CFU (n=20) or $1x10^7$ CFU (n=10) *M. luteus* was injected intravenously. Weight loss and organ CFUs were recorded (*** $p = 0.0005$, * $p = 0.0018$; **** $p < 0.0001$).

5.3.5.4 Interrogating the mechanism of pathogenesis augmentation

5.3.5.4.1 Population dynamics following mixed inocula administration

It was hypothesised that in the presence of peptidoglycan, the immune bottleneck may be distorted permitting release of many bacteria from innate immune cells. As such, strain predominance would be abolished, perhaps accounting for the high liver CFUs recovered from mice injected with mixed inocula. To test this and record the population dynamics of *S. aureus* in the presence of peptidoglycan, 32 animals were injected with 1 x 10^6 CFU NewHG (1:1:1 SJF3679-81) alone and 32 animals received 1 x 10^6 CFU NewHG (1:1:1 SJF3679-81) plus 500 µg *M. luteus* peptidoglycan (total volume of 100 µl). At 30 minutes post injection, 8 animals from low dose and 8 from the mixed group were culled and organs (liver, kidneys and spleen) were harvested. The same was carried out at 10 and 40 hours post infection and the final 16 animals were culled at 70 hours. There was significantly more weight loss in the mixed group animals, at both 40 and 70 hpi, compared to low dose (Figure 5.37 A). Even at ten hours, there were higher numbers of bacteria in animals receiving mixed inocula in all organs and the two groups diverged further at later time points (Figure 5.37 B, C, D). Unfortunately, two animals in the low dose group and one from the mixed group were found dead at 69 hpi and were excluded from analysis. Two animals in the mixed group were culled at 52 hpi (red circle) and 69 hpi (green circle) respectively after reaching severity limits.

It can be seen that immediately after injection, the majority of the inoculum is found in the liver and in the absence of peptidoglycan, bacterial numbers subsequently decline. In the presence of peptidoglycan, bacterial numbers are maintained and then increase. Similar results are seen in the kidneys although the spread of the data is larger. In the spleen, bacteria are eradicated in the low dose group but remain around 10^4 CFU in the mixed group throughout. Up to 10 hours, there was no overall increase in bacterial numbers throughout the organs either demonstrating that minimal bacterial growth is occurring, perhaps due to innate immune system control mechanisms, or that any bacterial growth is offset by host killing. These data suggest the latter is more likely as numbers are maintained in the mixed group where an immune perturbation is perhaps occurring. The augmentation process has rapid onset however, providing further insight into the early infection dynamics.

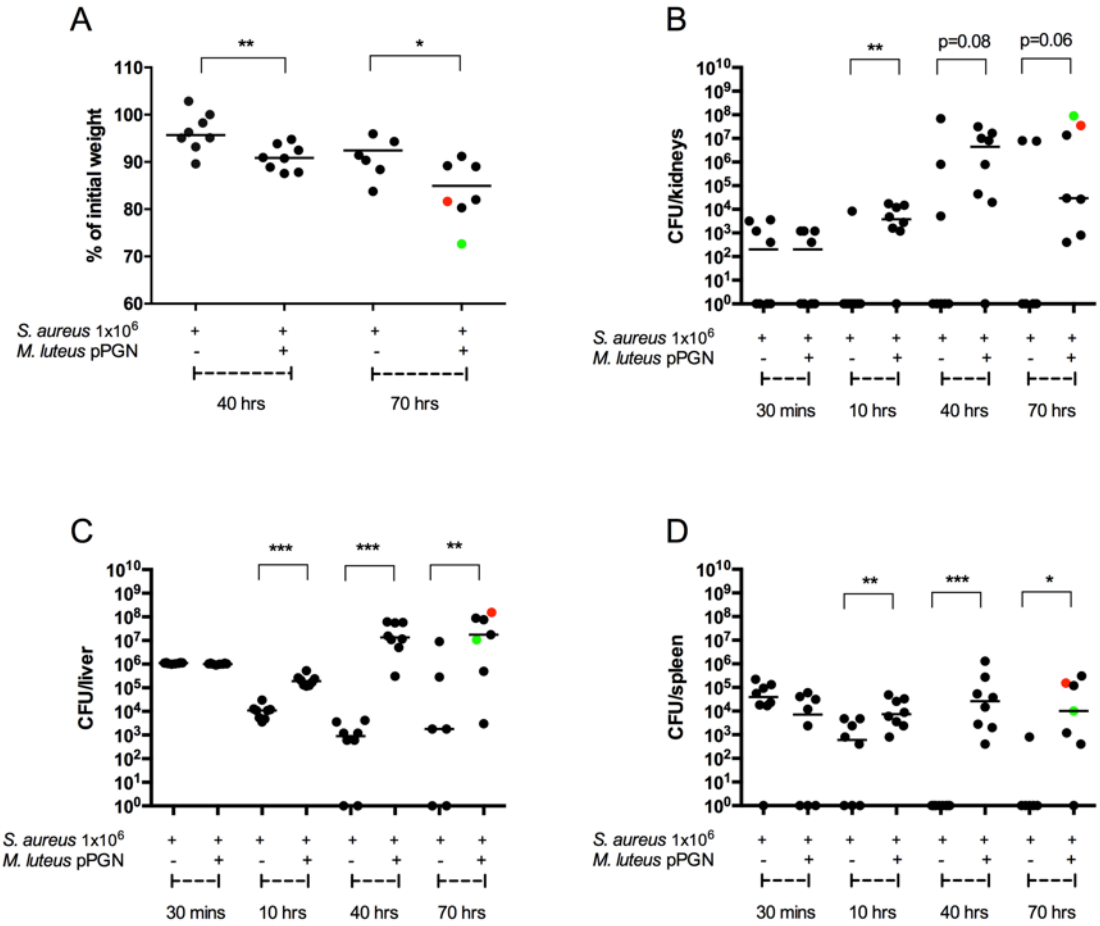


Figure 5.37 Distribution of bacterial load in mouse organs at various time points during infection

Low dose (1 x 10^6) *S. aureus* without or with 500 µg *M. luteus* peptidoglycan was injected intravenously (n=8).

A Weight loss (* p = 0.010, ** p = 0.007)
B CFU in kidneys (red circles – mice reaching B severity limits; ** p = 0.0064)
C CFU in liver (*** p = 0.0002 [10 hours], *** p = 0.0002 [40 hours], ** p = 0.0076)
D CFU in spleen (** p = 0.0093, *** p = 0.0002, * p = 0.014)

Red circle – mouse culled at 52 hpi; green circle – mouse culled at 69 hpi.

In addition to total bacterial numbers per organ, this experiment was designed to monitor strain variance during infection. The recovered CFUs of the three strains was determined by organ homogenisation, and plating on selective antibiotic media after serial dilution. Where total bacterial load was low, strain distribution is not reflective of strain dominance and therefore not given (denoted as less than limit of detection of the assay, <LoD).

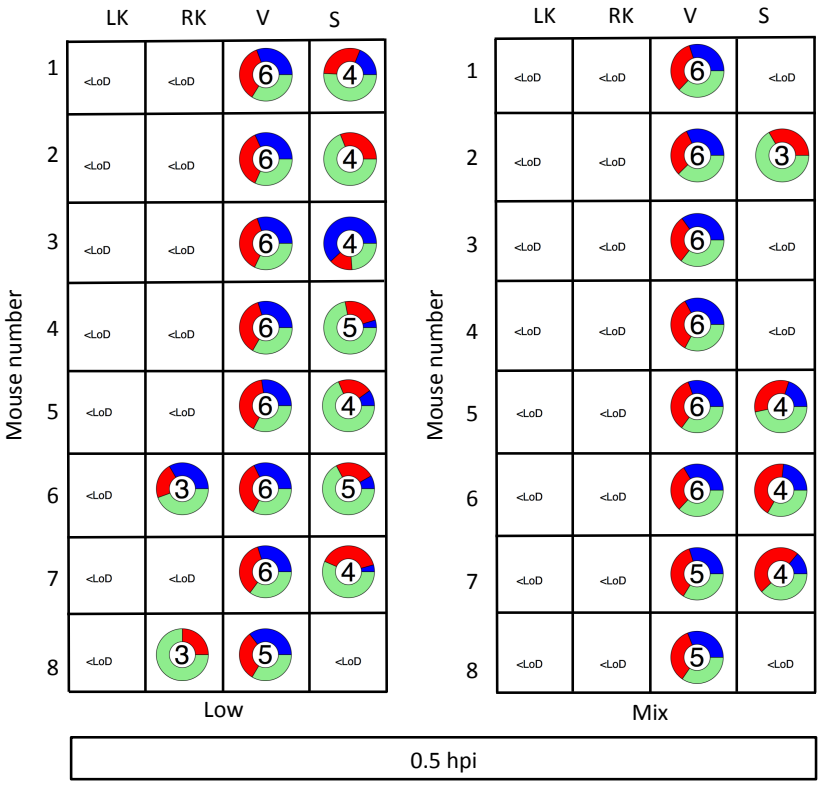
At 30 minutes post infection, all three strains, in equal proportion, at the starting inoculum dose, are seen in the liver of all animals (where animals have log 5 CFU, total organ CFU was no less than 9 x 10^5 CFU). Strain variance did not change dramatically by 10 hpi but total bacterial numbers were less as discussed above. For the low dose group, at both 40 hpi and 70 hpi, few animals have detectable bacteria, but when bacteria are recovered, dominance by one strain is often seen (Figure 5.38). This mirrors previously published work (McVicker et al., 2014). In the mixed group at 40 hpi and 72 hpi, clonal expansion of one or two strains can be observed in the kidneys and possibly also in the spleen, although as low overall numbers are recovered from the spleen in some animals, it may be that strains are being eradicated over different time periods rather than true clonal expansion *per se*.

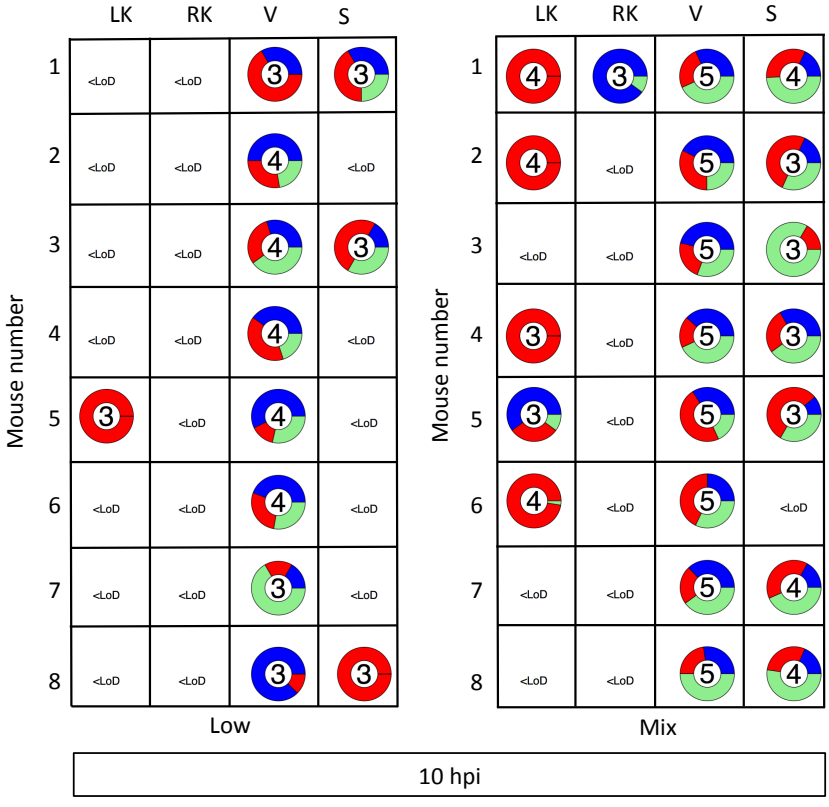
In mice receiving mixed inocula, liver numbers increase throughout, yet at 40 hpi, whilst the proportions of each strain have changed, complete loss of a strain is not seen. By 70 hpi, loss of a strain is observed only in mice 5, 6 and 7. To analyse these data further, species evenness (or diversity index) was calculated for liver CFUs from mice in the mixed group. This quantifies how equal a population is and assumes that each strain has an equal chance of becoming dominant. Values are constrained between 1 (even) and 0 (not even) so at the beginning of the experiment, species evenness in the liver organs is 1. At later time points, species evenness values are lower and this relationship can be plotted as a linear regression (Figure 5.39 A). The R^2 value for species evenness over time in the livers of these animals is 0.44 ($p < 0.0001$) denoting that clonality is occurring over time. Similar regressions have not been done for kidneys as only the later time points have detectable bacterial numbers. Organs harvested from animals in the low dose group were also not analysed for species evenness for the same reasons.

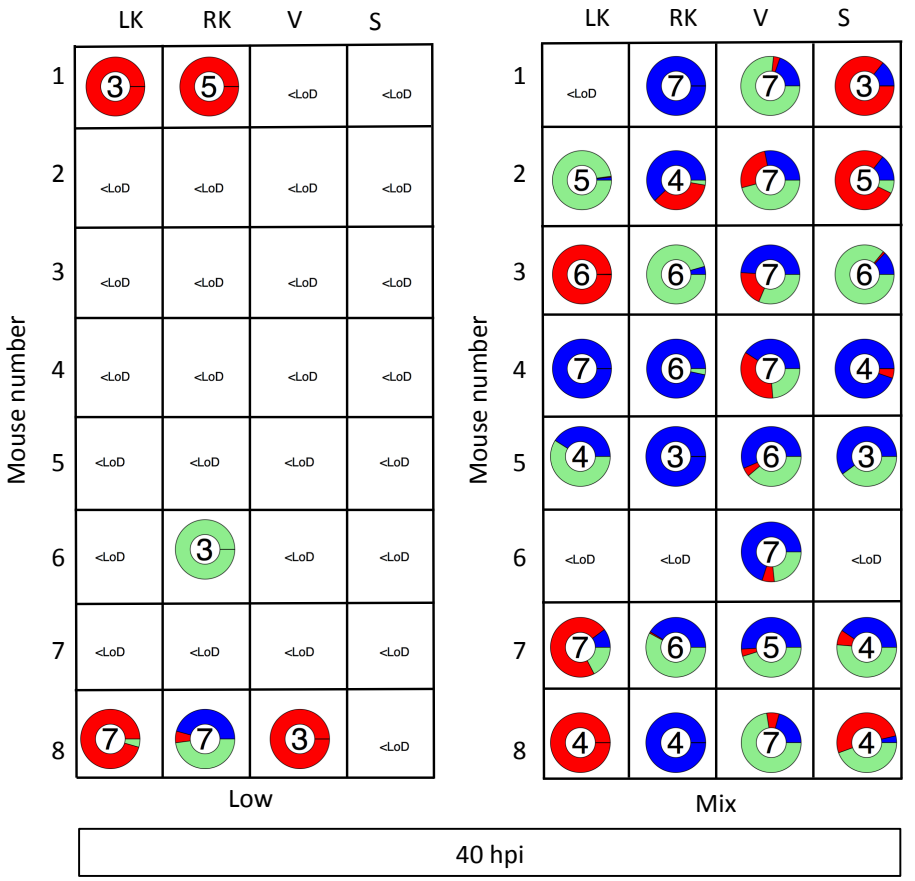
The aim of this experiment was to assess if the immunological bottleneck was significantly perturbed when *S. aureus* plus peptidoglycan was injected. From observing clonal expansion in the kidneys and liver (Figure 5.38) and species evenness calculations (Figure 5.39 A), it has been shown that the bottleneck remains and clonal expansion occurs. This is important, as abolishing the bottleneck would render the animal unable to control infection via the normal mechanisms. Interpreting data from such animals would deviate from physiological parameters.

However, this experiment does not allow an assessment of the degree of clonality i.e. compared to the initial, equally proportioned inocula (1:1:1), clonality would appear to occur with even small proportional changes yet is that indicative of true clonality? To answer this question, a separate experiment was undertaken using the same 1:1:1 *S. aureus* but either at low dose ($1.6x10^6$ CFU) plus 500 μg *M. luteus* peptidoglycan or high dose ($1.8x10^7$ CFU) *S. aureus* alone. Once organs were harvested at 72 hpi, each organ was analysed for species evenness and the two groups were then compared. As shown in Figure 5.39 B, there is no difference in the degree of clonality between the two groups, with spread seen in both. This shows that the bottleneck that occurs in the liver during a more standard high dose infection is not different to that occurring in in the presence of peptidoglycan.

Overall, this large experiment shows that the process from inoculation to *S. aureus* infection with or without peptidoglycan is not a 'free for all'. The innate immune system is able to control the majority of bacteria but small numbers can escape this control and found successful bacterial populations, including abscess formation. Quite what governs this process is largely unknown. This experiment demonstrates that in the presence of peptidoglycan, more bacteria seem able to escape host control, particularly in the liver and found abscesses. It was hypothesised that, whilst the liver CFUs at late time point consist of multiple strains, each individual abscess would be founded by a single bacteria. To test this, *S. aureus* (1:1:1) 1 $x10^6$ CFU plus 500 μg *M. luteus* peptidoglycan was injected into five mice. Individual abscesses were dissected from infected livers, homogenised, serially diluted and plated onto selective antibiotic media. Data shows that this hypothesis is true, with each abscess being initiated by a single bacterium, which goes onto clonally expand (Figure 5.39 C).


LK
RK
V
S
Mouse number
1
2
3
4
5
6
7
8
<LoD
Low
Mix
0.5 hpi


LK
RK
V
S
Mouse number
1
2
3
4
5
6
7
8
<LoD
Low
Mix
10 hpi


LK
RK
V
S
Mouse number
1
2
3
4
5
6
7
8
<LoD
Low
Mix
40 hpi

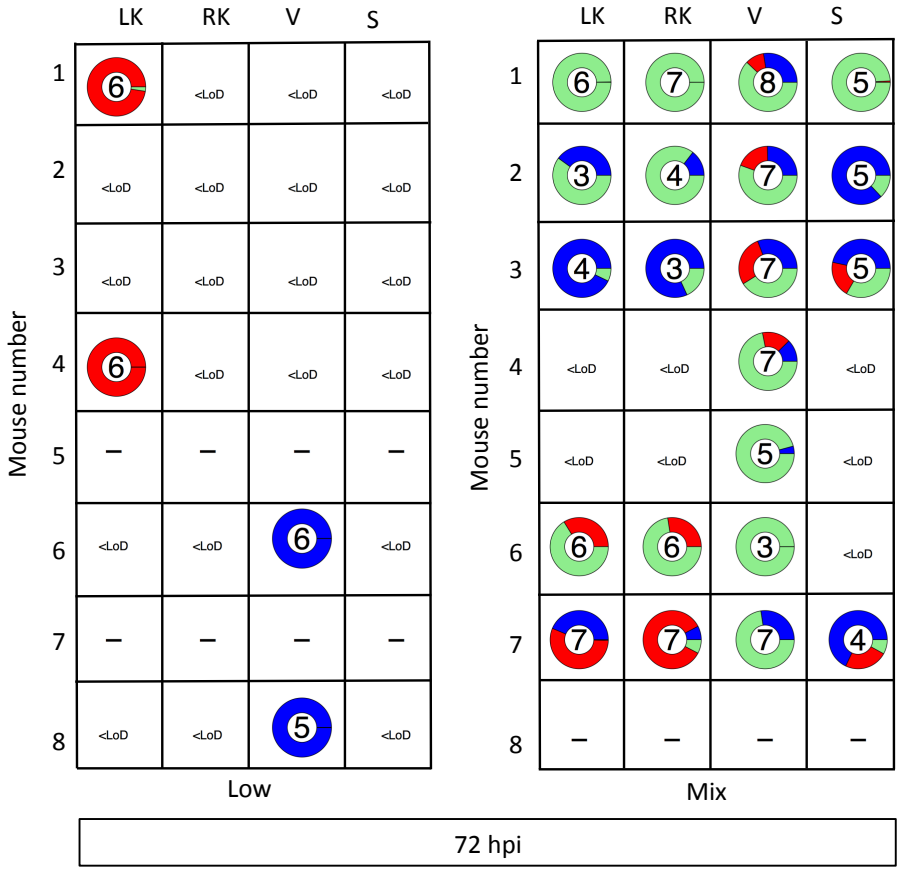

LK
RK
V
S
Mouse number
1
2
3
4
5
6
7
8
<LoD
–
Low
Mix
72 hpi

Figure 5.38 The pattern of *S. aureus* clonal expansion observed with and without peptidoglycan during murine infection

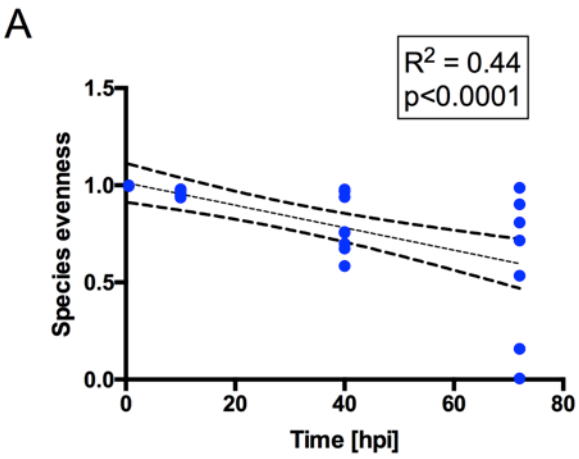
Animals (8 per group) were injected with 1 x 10^6 CFU NewHG alone (**Low**) or 1 x 10^6 CFU NewHG plus 500 µg *M. luteus* peptidoglycan (**Mix**). 8 animals from low dose and 8 from the mixed group were culled at 0.5, 10, 40 or 72 hpi.

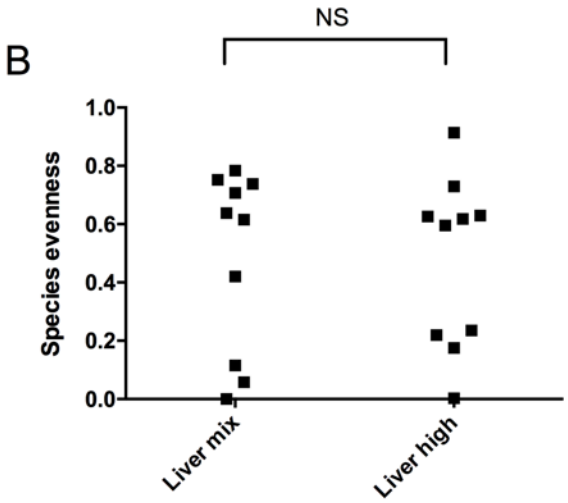
Pie charts display the proportion of the three strains in left kidney (LK), right kidney (RK), liver (V) or spleen (S) for each mouse (mice are numbered 1-8 in each group at the time points shown). The $\log_{10}$(CFU) in each organ is shown within each circle.

Red – Ery^R, green – Kan^R, blue – Tet^R.

<LoD signifies the limit of detection of the assay (2000 CFU in kidneys or spleens and 3000 CFU in livers).

Mouse marked as – were not included in analysis.


A
R^2 = 0.44
p<0.0001
Species evenness
1.5
1.0
0.5
0.0
0
20
40
60
80
Time [hpi]


B
NS
Species evenness
1.0
0.8
0.6
0.4
0.2
0.0
Liver mix
Liver high

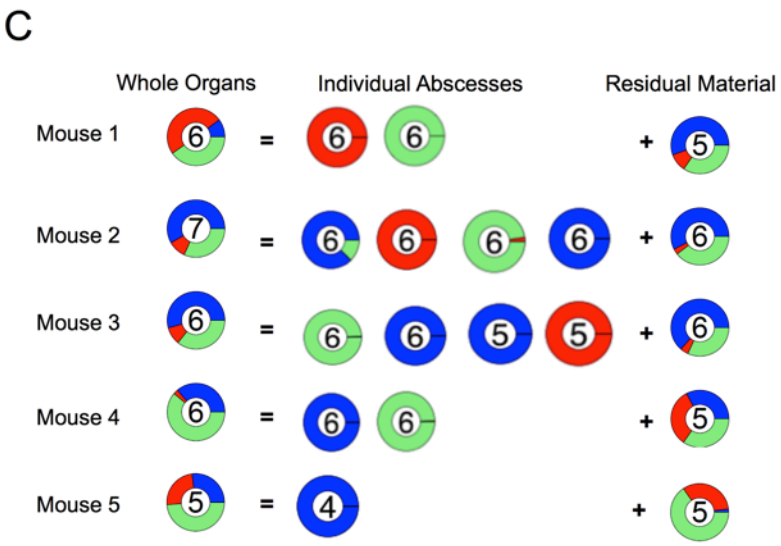

C
Whole Organs
Individual Abscesses
Residual Material
Mouse 1
Mouse 2
Mouse 3
Mouse 4
Mouse 5

Figure 5.39 Assessment of the degree of clonality in murine liver abscesses

A Linear regression of species evenness over time for bacteria recovered from livers of mice challenged with low dose ($1x10^6$ CFU) *S. aureus* plus 500 μg *M. luteus* peptidoglycan. Blue circles represent the species evenness value for individual livers (---- represents line of best fit; ---- represents 95% confidence intervals)

B Species evenness values for individual livers from animals injected with low dose ($1.6x10^6$ CFU) *S. aureus* plus 500 μg *M. luteus* peptidoglycan or high dose (1.8×10^7 CFU) *S. aureus* alone.

C For mice injected with low dose ($1x10^6$ CFU; 1:1:1) *S. aureus* plus 500 μg *M. luteus* peptidoglycan, individual abscesses were dissected from the livers, homogenised and plated onto selective agar to demonstrate abscess clonality. For each mouse, liver bacterial CFUs are separated into counts from individual abscesses and residual liver tissue post dissection.

5.3.5.4.2 Cytokine analysis of mouse serum

Understanding cytokine changes during *S. aureus* infection is incomplete and translation into novel therapeutic opportunities has been disappointing. Neutralisation of pro-inflammatory cytokines in sepsis was shown in animal models to be protective (Beutler et al., 1985). However, this effect did not translate to human clinical trials (Abraham et al., 1995). One hypothesis for the mechanism of pathogenesis augmentation was that the presence of peptidoglycan perturbs the cytokine milieu allowing less effective host control of low dose *S. aureus*. To hone in on the responsible mechanism for augmentation of *S. aureus* pathogenesis, murine serum cytokines were measured (as described in Section 2.23) at baseline (three days prior to injection), six hours post injection and 48 hours post injection. Mice were either injected with low dose (1.7×10^6 CFU) *S. aureus*, high dose (1.8×10^7 CFU) *S. aureus*, 500 μg *M. luteus* peptidoglycan alone or a mixed inoculum of low dose (1.6×10^6 CFU) plus 500 μg *M. luteus* peptidoglycan (n=10). At the time points described, superficial venesection of the tail vein was conducted and a range of pro and anti-inflammatory cytokine/chemokines were measured including IFN-gamma, IL-1β, IL-6, IL-10, IL-12, CXCL1, IL-17A, TNF, CCL2 and CCL4.

As shown in Figure 5.40, for the majority of cytokines, no discernable differences were noted between low dose *S. aureus* alone or in combination with peptidoglycan. Importantly, mice receiving peptidoglycan only had cytokine levels similar to those seen at baseline, three days prior to infection. Serum from mice receiving mixed inocula had significantly higher levels of CCL2 (Figure 5.40 I). This response was rapid and short-lived, with high dose *S. aureus* also causing a significant peak, in excess of that caused by low dose *S. aureus* and peptidoglycan in combination.

The question arises therefore, as to why higher levels of CCL2 might be detrimental to the host. The clonal expansion theory suggests that single bacteria escape phagocytes, establish a niche and proliferate to a collective size that is too large to be phagocytosed. Systemically unwell mice have low levels of *S. aureus* in the bloodstream suggesting death occurs by toxaemia rather than overwhelming bacterial burden *per se* (Gorrill, 1958). Increasing innate immune cell recruitment through the chemokine up-regulation actually may be advantageous to the bacteria, by providing, for example, intraphagocyte

niches in which *S. aureus* is capable of surviving (Thwaites and Gant, 2011; Grosz et al., 2014). Alternatively, CCL2 dependent variation in the type of immune cell response may have an impact. A rapid rise and fall of CCL2 post human challenge with endotoxin has been recorded (Sylvester et al., 1993). Similar temporal dynamics were seen in mouse models where systemic inflammatory systemic response (SIRS) was induced (Tsuda et al., 2004). Such mice have increased susceptibility to secondary bacterial infections, mediated by CCL2 release. The chemokine converted resident macrophages to alternatively activated macrophages and impaired resistance to infection.

The potential links between bacteria/peptidoglycan and CCL2 production are not fully understood but associations have been documented. Nod2 mediated, CCL2-dependent eradication of the bacteria from the intestine has been shown in a mouse model of pathogenic *E. coli* infection (Kim et al., 2011). In Nod2 knockout mice, increased bacterial burden was caused by a reduction in CCL2 leading to less monocyte recruitment. Although data from this augmentation project showed increased CCL2, aberrant Nod2 signalling in the presence of peptidoglycan cannot be ruled out.

It must however be considered that these mouse serum cytokine data are from systemic blood samples and this may overlook more subtle local cytokine perturbations between the different mouse groups. The temporal and spatial dynamics of cytokine release and effects are complex. TNF-α, as a mediator of inflammation, is constitutively transcribed in Kupffer cells to ensure rapid release upon challenge with pathogens. Not all cytokines are pre-transcribed but other pro-inflammatory mediators such as IL-1 and IL-6 can be swiftly released from these cells. (Fox et al., 1989). A comprehensive organ specific, temporal surveillance of serum cytokines would be desirable but was not practically possible within this project.

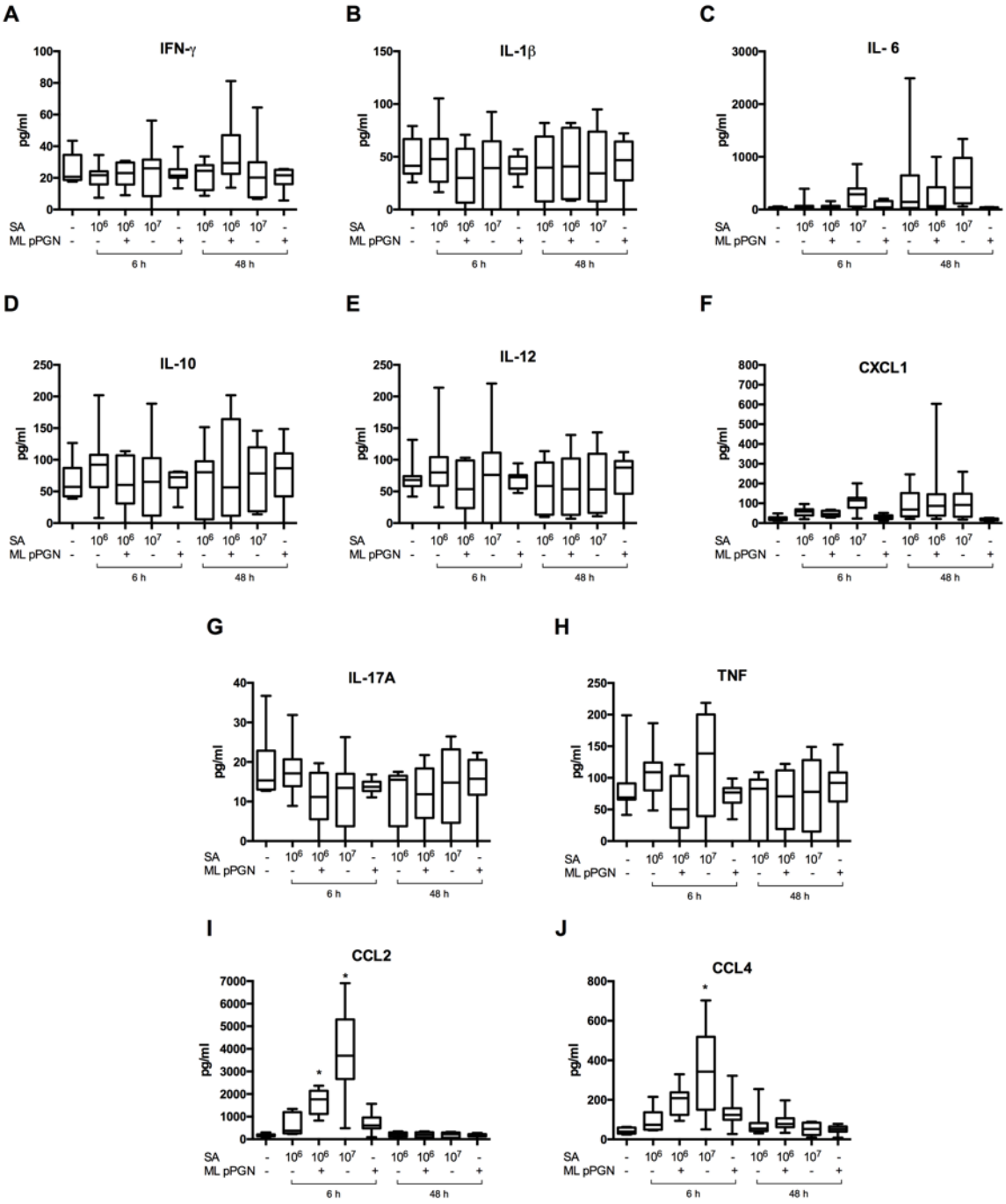


Figure 5.40 Cytokine measurements from mouse serum at baseline, 6 and 48 hours post intravenous injection with *S. aureus* and/or peptidoglycan

Mice were injected (n=10) with low dose ($1.7x10^6$ CFU) bacteria, low dose ($1.6x10^6$ CFU) bacteria plus 500 µg *M. luteus* peptidoglycan, high dose ($1.8x10^7$ CFU) bacteria or 500 µg *M. luteus* peptidoglycan alone. Blood sampling via tail vein injury was carried out three days prior to injection (baseline) and again at 6 and 48 hpi. 10 cytokines were measured **(A-J)**: IFN-gamma, IL-1β, IL-6, IL-10, IL-12, CXCL1, IL-17A, TNF, CCL2 and CCL4 (* $p < 0.05$, adjusted for multiple comparisons).

5.4 Discussion

Mammalian models of *S. aureus* infection are generally characterized by the requirement for a large bacterial inoculum (approximately 1x 10^7 CFU in the sepsis model). The reason for this has remained unknown although recently it has been demonstrated that during infection single bacteria within the population found the abscesses that can eventually lead to host mortality (Prajsnar et al., 2012; McVicker et al., 2014). This changed the dogma that *S. aureus* worked like a pack organism, with increasing bacterial numbers allowing accumulation of toxins, which, in sufficient concentrations would then cause host damage. It also raised the question as to whether the rest of the population performs an active role or simply provides numbers to get through the immunological bottleneck.

In the zebrafish model of infection, attenuated mutants of *S. aureus* can augment pathogenesis of the wildtype (i.e. low numbers of wildtype will cause disease in the presence of high numbers of avirulent mutants). It is of interest that a strain such as *sagB* was unable to augment pathogenesis by *S. aureus*. It was hypothesised that immune system recognition of the glucosaminidase mutant, *sagB*, might be different to that of the parental strain as the peptidoglycan structure is altered. Indeed, it is already known that the longer glycan strands found in the *sagB* mutant interfere with phagocyte receptor binding (Wheeler et al., 2015). Preliminary work conducted by Nelly Wagner (PhD student, University of Sheffield) has since suggested that *sagB* activates the immune response more than *phePsaeR*, as measured by in-situ IL-1β assays in zebrafish embryos. It may be that by activating the immune system to a lesser degree, parent bacteria, even at low dose, gain an advantage during mixed inocula infections with *phePsaeR*. If *sagB* induces higher levels of immune stimulation, this may promote for eradication of the low dose parental *S. aureus*. Further work as to the implications of this are ongoing but outside the scope of this project.

Purified, particulate bacterial cell wall peptidoglycan was also able to augment *S. aureus* pathogenesis but inert particulate beads or solubilised peptidoglycan did not. Commensal and environmental bacteria, that do not cause disease in their own right, were also able to augment pathogenesis of low numbers of wildtype *S. aureus*.

In the murine model, significant pathogenesis augmentation by the addition of purified peptidoglycan from non-pathogenic Gram-positive organisms or intact commensal organisms was observed. The infective dose could be lowered from 10^7 to 10^4 CFU in the presence of these potentiators and the liver appears to be the focal point of loss of immune control. Rather than occasional large abscesses, multiple small abscesses were seen, each founded by a single bacterium. Yet again, inert beads or monomeric peptidoglycan could not reproduce this phenomenon. A significant rise in macrophage chemokines CCL2 was measured in the presence of co-injected peptidoglycan and low dose pathogen indicating a perturbation of innate immune cells may play a role.

Together, these results have important ramifications for human *S. aureus* disease as it may begin to explain how initiation of infection occurs as *S. aureus* primarily enters via a wound or invasive procedure (Naber, 2009). The bacterial burden however will never be a pure culture but in conjunction with organisms that are associated with the skin or environmental microflora (Grice and Segre, 2011). These data demonstrate that other bacteria (and even their components) enable *S. aureus* to initiate infection. The other bacteria in themselves cannot cause disease but contribute to infection by the pathogen. Given that standard models of *S. aureus* infection often employ 10^7 CFU to establish infection, it is striking that 10^7 live *M. luteus*, in combination with 10^6 *S. aureus* can cause significant host morbidity.

5.4.1 Potential mechanisms of augmentation of *S. aureus* infection

This study interrogated the *S. aureus* population that is required to cause disease in animal models. It is not yet clear which additional aberrant processes are occurring to lower the infectious doses by 1000 fold in the presence of the potentiators examined here, but peptidoglycan appears to be a key mediator of the augmentation phenomenon. Either purified peptidoglycan or live bacteria surrounded by peptidoglycan exacerbate *S. aureus* infection.

Associated with a bacterial cell or not, polymeric peptidoglycan is phagocytosed whereas soluble peptidoglycan is unlikely to be so. Once engulfed by phagocytes, the degree of sensitivity to host enzymes can shape the inflammatory response (Vollmer et al., 2008a). *M. luteus* peptidoglycan is sensitive to lysozyme found within host

phagocytes whereas *S. aureus* and *S. epidermidis* peptidoglycan is resistant (Bera et al., 2006). As both *M. luteus* and *S. epidermidis* peptidoglycan were able to augment pathogenesis, a direct mechanistic link to lysozyme sensitivity cannot be made but susceptibility to and degradation products released from other host enzymes is not known and cannot be ruled out. Indeed, IL-1β release from macrophages challenged with *S. aureus* peptidoglycan *in vitro* was entirely abolished by the addition of a lysozyme inhibitor (Shimada et al., 2010). The authors suggested that some residual lysozyme sensitivity may exist depending on the degree of O-acetylation in *S. aureus* or that the enzymatic efficiency could be increased in intraphagocyte acidified compartments. Interestingly, IL-1β levels were not significantly lower in Nod2 knockout mice indicating that cytosolic sensing of *S. aureus* ligands may be Nod2 independent.

If degradation does happen within the phagosome, transit to the cytosol must occur if intracellular receptors are to have access to the products of digestion. Pore-forming toxins from many species including *S. aureus* have been shown to facilitate the transit of microbial products from phagosomes to the cytoplasm (Ratner et al., 2007; Davis et al., 2011; Grosz et al., 2014). Recognition by intracellular Nod receptors also requires digestion of polymeric peptidoglycan to Nod ligands e.g. MDP or other monomeric components. In *S. pneumoniae*, host enzymes such as lysozyme can cause sufficient release of specific ligands for Nod sensing (Davis et al., 2011). Cytosolic sensing of these products then leads to cytokine and chemokine production, with the aim of eradicating the invading organism.

Aberrant cytokine signalling in the presence of mixed inocula could explain the augmentation phenomenon found in this project. Increased levels of CCL2 were detected in serum from animals injected with *S. aureus* and peptidoglycan. CCL2 (alternatively known as monocyte chemotactic protein 1, MCP1) is a chemokine able to recruit monocytes, macrophages, neutrophils and lymphocytes by enhancing migration through the vascular endothelium (Deshmane et al., 2009). NF-κB production leads to the release of macrophage chemokine CCL2 (Ueda et al., 1997) which is required for host defense against a range of pathogens including *S. pneumoniae* (Davis et al., 2011) and *L. monocytogenes* (Serbina et al., 2008). Given the importance of CCL2 in controlling infection however, it is difficult to link the high levels of macrophage

chemoattractants and reduced *S. aureus* clearance. It is feasible that these data are masking information regarding the local cytokine requirements or perhaps an overzealous macrophage recruitment response is detrimental to the host, reducing the capacity to control infection and initiating septic shock type responses. Assessment of innate immune cell recruitment and killing efficacy should be explored both *in vitro*, *ex vivo* and *in vivo* to aid in resolving this conundrum. If Nod2 signalling is to be further interrogated in this phenomenon, the experiments could be performed in the Nod2 knockout mouse background.

Understanding host response to peptidoglycan alone is problematic so attempting to unravel the intricacies of these mixed inocula is demanding. Surprisingly, studies on mixed infections are rare. Ratner and colleagues hypothesised that host detection and response to multiple colonising organisms may be different to that of single species in isolation. *Haemophilius influenzae* peptidoglycan was better able to enter epithelial cells in the presence of the pore forming toxin, pneumolysin, from *S. pneumoniae.* Alpha toxin from *S. aureus* also allowed peptidoglycan entry. Nod1 was required for the enhanced epithelial cytokine response highlighting the impact of a polymicrobial presence on the innate immune system (Ratner et al., 2007). The same group demonstrated that competitive interactions between colonising flora can determine success or failure of certain pathogens (Lysenko et al., 2005). Co-colonisation of *S. pneumoniae* and *H. influenza*e resulted in striking clearance of *S. pneumoniae*, which was abolished if neutrophil or complement depletion by cobra venom factor, was undertaken, hinting at the underlying mechanisms. Finally, *S. aureus* has been shown to hijack a skin commensal, *Propionibacterium acnes*, by using a secreted factor, Christie, Atkins, Munch-Peterson (CAMP), to enhance haemolysis and cytokine induction at the initiation of skin infection (Lo et al., 2011).

It has been shown that under normal circumstances, Nod2 activation by MDP negatively regulates TLR responses. In the absence of this, a pro-inflammatory Th1 milieu ensues which is detrimental to the host by causing experimental colitis (Watanabe et al., 2008). It is also reported that monomeric peptidoglycan can directly activate the inflammasome, independent of TLR and Nod2 (Martinon et al., 2004). Therefore, it should be considered that low dose *S. aureus* is handled or trafficked distinctively if peptidoglycan products from commensal bacteria are present.

Intraphagocyte signalling, cytokine/chemokine release may be contrasting to that which occurs with high dose *S. aureus* alone but the exact mechanisms of this phenomenon remain to be determined.

5.4.2 Clinical importance of infection potentiation

This project sought to better understand if infection is caused by a critical mass of bacteria gaining opportunistic entry into a wound or if exogenous factors/adjuvants are involved? A 3-log reduction in the infective dose was achieved in the murine sepsis model by addition of peptidoglycan or commensal microflora. It is improbable that the large dose required to cause infection in animal models are mirrored in human infection. An early publication commented that 'a nasal droplet of 100 μm diameter could not accommodate this number, even if it consisted entirely of staphylococci' (Elek and Conen, 1957). Therefore, the role of 'adjuvants' has been explored. Using human volunteers, *S. aureus* was given intra-dermally, sub-cutaneously, via a scratch or incision. Sharing the same natural habitat, the nares, *S. aureus* was co-administered with mucin but no enhancement of infection occurred. Mucin is a heavily glycosylated protein found in gel-like form on mucous surfaces of mammals (Voynow and Rubin, 2009). Remarkably, it has been extensively investigated for its ability to lower resistance to pathogens when co-administered (Olitzki, 1948). The underlying mechanism was purported to be inhibition of phagocytosis and ineffective phagocytic killing though the exact chemical entity causing this effect remains unknown (Smith, 1950). Other potential adjuvants such as starch (present in surgical glove powder) and suture material were also tested with the latter being shown to significantly lower the infective dose. In the presence of suture material, *S. aureus* wound infection could be caused by 10^3 CFU rather than 10^7 CFU (James and MacLeod, 1961). *Corynebacterium parvum* (also known as *P. acnes*) is a Gram-positive human commensal which stimulates the reticulo-endothelial system. If heat killed and administered 4-7 days before an intra-peritoneal *S. aureus* challenge, resistance to infection was promoted (Adlam et al., 1972). This protection is reminiscent of a vaccine mediated effect and bacterial cell components, including peptidoglycan have been examined as vaccine candidates (Capparelli et al., 2011). However, the timing of administration of immunostimulatory products such as killed *Mycobacterium bovis* bacillus Calmette–Guérin (BCG) cells is absolutely crucial in establishing distinct

phenotypes. When injected (via the intra-peritoneal route) 14 days prior to intravenous *S. aureus,* increased resistance to *S. aureus* infection was described (Dubos and Schaedler, 1957; Sher et al., 1975). However, if both BCG and *S. aureus* were co-administered intravenously, mouse mortality rate increased significantly (Schaedler and Dubos, 1957). Furthermore, when BCG was given, mice with chronic staphylococci infections showed acute activation of the infectious process, with high bacterial numbers noted in both kidneys and liver. The authors comment on the unusual finding of high *S. aureus* numbers in the liver, which is not normally seen as *S. aureus* is usually clearly from the liver rapidly (McVicker et al., 2014). Finally, cell walls from *Bacterium coli* (*E. coli*) caused increased susceptibility to the live organism if administered 30 minutes apart but protection against infection was seen if a 24 hour delay was permitted (Rowley, 1956). The authors concluded that LPS was mediating these responses and later studies have also made an association between endotoxin and heterologous infection resistance and implicated humoral and cellular factors in the mechanism (Michael and Massell, 1962; Pindak, 1970).

Taken together, the literature, particularly from around 1950-60s provides data from experiments with similarities but also differences compared to the data from this project. Notably, co-injection of biological material augments infection yet LPS cannot be the causative agent as endotoxin levels were similar across all preparations, including soluble peptidoglycan, which cannot augment infection (data not shown).

It is evident how important timing of exogenous factor and pathogen administration is in determining protection or resistance towards the pathogen. This highlights the diversity and flexibility of the immune response and may start to explain the complexity underlying clinical *S. aureus* disease. If skin trauma or environmental contamination were to introduce skin commensals such as *M. luteus* and *S. epidermidis* concurrently with the opportunist *S. aureus*, a higher likelihood of infection may arise. However, if the inoculation of *S. aureus* occurred hours or days later, perhaps these microflora evoke protection. Furthermore, the distinction between commensal and pathogenic bacteria is blurred and exact definitions of each are problematic. *S. aureus* can be considered a skin commensal, though its usual site of colonisation is the nares yet it is more renowned for its tissue damaging and life-threatening potential. *S. epidermidis* is considered the benign cousin of *S. aureus* yet its propensity to cause opportunistic

disease is documented (Otto, 2009). Studies addressing direct interactions between these two bacteria exist though none question the outcome of intravenous co-injection of both in the murine model host. A study showed direct interactions occurring as serine proteases from *S. epidermidis* were shown to degrade biofilms caused by *S. aureus* (Vandecandelaere et al., 2014). Using a *C. elegans S. aureus* virulence model, increased survival was described when serine protease from *S. epidermidis* was added to the microtiter plate. Different commensal skin organisms have been shown to uniquely modulate skin immunity (Naik et al., 2015). Colonisation with *S. epidermidis* induced IL-17 $CD8^+$ T cells and limited invasion with *Candida albicans* which was applied to sandpaper-treated dorsal skin 11 days later. This heterologous protection was suggested to be an evolutionary adaptation allowing commensal organisms to 'calibrate barrier immunity'. The impact of surrounding commensals on *S. aureus* colonisation has also been investigated in humans. Children who received the pneumococcal vaccine had higher rates of *S. aureus* colonisation and associated infections (Regev-Yochay et al., 2004).

Understanding these fundamental processes is of clinical importance and has translational potential. Nosocomial infections make up a sizeable portion of total *S. aureus* disease burden. Optimising skin microflora or modifying host immune responses could reduce vulnerability to infection during routine procedures such as intravenous cannulation or incisions made during surgery. Diseases with a propensity for *S. aureus* infection e.g. atopic dermatitis, diabetes, could also be targeted to ascertain if local application of immune modifying compounds could avert infection.

5.4.3 Further work

Spinning disc confocal intravital microscopy of murine livers will be used to image host:pathogen dynamics in real time. The heavy bacterial burden noted in the liver, manifest as multiple small abscesses, is the striking pathology observed by co-injection of bacteria and peptidoglycan. Collaborators at the University of Calgary (Alberta, Canada) use fluorescent imaging to delineate Kupffer cells, neutrophils and *S. aureus* (Kolaczkowska et al., 2015). Alexa-fluor 647 NHS ester will be used to stain peptidoglycan and intravital imaging will be acquired for *S. aureus* alone and *S. aureus* plus peptidoglycan. Preliminary work suggests that peptidoglycan is phagocytosed by

Kupffer cells along with the bacteria within 10 minutes of injection but unlike if bacteria are injected alone, bacteria are later seen (around 8 hpi) adjacent to phagocytes having escaped and gone on to form an abscess. These first experiments were conducted in the same mouse strain as in this project, BALB/c, but attempts were also made to establish the phenomenon in C57BL/6 mice as this would allow interrogation of knock out mice, due to the vast repertoire of transgenic mice available in this strain background.

Although the data is not shown, it was briefly explored whether other cell wall components of Gram-positive bacteria e.g. lipoteichoic acids (LTA) were also able to augment host death as such components have previously been shown to synergise with peptidoglycan *in vivo* (Kengatharan et al., 1998). However, injection of low dose *S. aureus* and 10 ng LTA into the zebrafish circulation valley at 30 hpf did not augment pathogenesis. It would be interesting to explore if this is due to a lack of access of LTA to the intracellular phagocyte environment and this could be explored further by attaching such components to latex beads. Other components from Gram-negative organisms e.g. LPS or even fungal pathogens e.g. cryptococcal capsule could also be tested. A wide variety of commensal and pathogen combinations will occur in the clinical context and the polymicrobial influence on pathogen success is under explored.

Attempts should be made to explore the intraphagocyte processing of peptidoglycan further. Covalently attaching soluble peptidoglycan, which is not phagocytosed, to the phagocytosed latex beads would provide a way of interrogating if soluble peptidoglycan can augment pathogenesis, once it gains intracellular access. Using a repertoire of host enzymes to cleave peptidoglycan in distinct locations, the exact moiety of peptidoglycan required could be determined. Lysozyme inhibitors such as N,N′,N″-Triacetylchitotriose (triNAG) could be investigated to explore the link between peptidoglycan degradation and inflammatory signalling (Shimada et al., 2010). Other tools to distinguish between Nod receptor binding, inflammasome activation and local cytokine release should be investigated to aid in unraveling the immune components involved.

Some preliminary *in vitro* work assessing complement receptor activation on human monocytes by ELISA assay (personal communication, Ms Daria Shamarina) suggested

that peptidoglycan activates both C5a and C3a. Lysenko and colleagues demonstrated that in the presence of *H. influenzae*, clearance of *S. pneumoniae* was abolished by complement depletion (Lysenko et al., 2005). Cobra venom factor (CVF) is a potent activator of the complement system leading to depletion of the complement cascade. Intra-peritoneal injections of CVF are well-tolerated by mice and enhanced mortality to subsequent *S. aureus* infection is not seen (Sakiniene et al., 1999). Preventing activation of the complement system and then injecting low dose *S. aureus* plus peptidoglycan could reveal if complement activation is a mediator.

As $1x10^7$ CFU of live *M. luteus* in combination with low dose ($1x10^6$ CFU) *S. aureus* caused augmentation of infection by the pathogen, it would be important to assess if the *S. aureus* dose can be lowered further to ascertain the limit of this phenomenon. Titration of the amount of *S. epidermidis* that can still augment pathogenesis should also be carried out along with serum sampling for cytokine analysis. It would be interesting to know if similar cytokine perturbations are noted with live commensal bacteria compared to peptidoglycan. Heat-killed *S. epidermidis* could also be investigated as unique ligands may be generated, influencing the host response. Finally, other skin commensal organisms could be investigated such as *Propionibacterium* and *Corynebacterium* species.

Precise host pathogen interactions remain poorly understood at the cellular level. Improved understanding of these dynamic interactions will inform better design of vaccines, antibiotics and enhance insight into the interplay between polymicrobial presence and *S. aureus* pathogenesis.

Chapter 6. General discussion

In 1959, David E Rogers, an Associate Professor of Medicine published an article entitled 'Observation of the nature of staphylococcal infections' (Rogers, 1959). Four key areas were highlighted as being of importance in *S. aureus* pathogenesis:

1) The intracellular phase of the *S. aureus* life cycle
2) Organ tropism in animal models compared to human infection
3) Persistence preventing infection eradication
4) A lack of effective humoral immunity.

Notwithstanding the 57 years since, many of these areas remain hot topics of modern research. Survival of *S. aureus* within host cells and professional phagocytes poses a real threat. A strategy for how best to therapeutically intervene to prevent these phagocytic cells from acting as 'Trojan horses' for bacterial dissemination is actively sought. The hypothesis that abolishing intracellular *S. aureus* may be the Achilles heel in host control has recently been tested (Lehar et al., 2015). After confirming that commonly used antibiotics are unable to kill bacteria contained within macrophages and distant dissemination occurs despite antibiotic administration *in vivo*, a novel therapeutic containing a covalently linked antibody-antibiotic conjugate was developed. Opsonisation and subsequent phagocytosis of bacteria coated in this conjugate readily eradicated intracellular *S. aureus*. Importantly, the antibiotic chosen was able to kill antibiotic resistant persister cells. Such novel therapeutics are encouraging and should be fast-tracked to clinical studies but this approach highlights the immense multi-disciplinary input required from biology, physics, chemistry, immunology, bio-engineering, pharmacology and industry in order to generate the next wave of weapons against multi-drug resistant pathogens such as *S. aureus*.

Tissue tropism of *S. aureus* also remains an area of interest. Clinically, both diagnosis and confirmation that initial treatment is effective relies on blood sampling for automated bacterial culture. Whilst kidney and liver biochemical parameters are measured, such as urea, creatinine and aspartate aminotransferase (AST), assessment of bacterial burden in these organs is not routine practice. Conversely, the mainstay model of mammalian invasive *S. aureus* disease, the mouse, uses kidney abscess formation

and kidney bacterial CFU as a standard output. In Chapter 5, significant perturbation of liver control of *S. aureus* was noted when mixed inocula were injected, yet again, the significance and existence of this organ specific response in human disease is unknown. In 1957, Elek and Conen suggested that 'the advent of penicillin and other antibiotics has rendered direct inoculation in volunteers relatively safe' (Elek and Conen, 1957), referring to subcutaneous or intradermal administration of *S. aureus*. However, for obvious ethical reasons, invasive infections cannot be studied directly thus preventing sufficient understanding of the correlates between animal models and human infection.

To advance understanding of the processes governing infection, this project set out to analyse *S. aureus* virulence and has taken three distinct approaches. Aligning phenotype to genotype using the zebrafish embryo model of infection, characterising growth requirements in human blood *ex vivo* and investigating mixed inocula, all yielding interesting findings. Firstly, the advent of highly sophisticated sequencing technology does not easily reveal biologically relevant phenotypic information regarding strains. Secondly, high-throughput *in vitro* screens conducted in enriched media may not predict phenotype in the restricted host environment. Thirdly, examining *S. aureus* pathogenesis *in vivo* in isolation of the other microbiome constituents may camouflage clinically relevant host microbe interactions.

Pursuing three strands of investigation into host:pathogen interaction has demonstrated the complexities of deciphering *S. aureus* pathogenesis. Ranging from simply assigning nomenclature, to testing hypotheses about multifactorial *in vivo* processes using confined animal models, is challenging.

6.1 Defining the 'players'

Particularly for an organism such as *S. aureus*, the annotation of being a commensal or pathogen is better represented as a continuum rather than distinct entities. If the human host is thought of as a 'human-microbe hybrid' (Goodacre, 2007), it has been said that pathogenesis simply represents the disruption of homeostasis (Ehrlich et al., 2008). For *S. aureus*, this may manifest as disturbances that promote for or protect against colonisation. The relationship between host and *S. aureus* may be individualised as colonisation status can appear predetermined (Brown et al., 2014). Persistent carriers

are often re-colonised with the same *S. aureus* strain, despite decolonisation (Mody et al., 2003) whereas non-carriers often maintain that status despite artificial inoculation (Nouwen et al., 2004a). The degree of homeostasis within the nares will vary between individuals and the same strain of *S. aureus* may behave as a commensal in one host yet an invasive pathogen in another, depending on local and systemic 'opportunities'. The bioburden is known to influence pathogenicity as persistent, compared to intermittent, carriers can carry up to 1000 times more *S. aureus*, which increases the risk of acquiring infection (Nouwen et al., 2004b).

Clonal expansion should now be considered one of the hallmarks of *S. aureus* infection and this phenomenon is demonstrated in other pathogens (Moxon and Murphy, 1978; Prajsnar et al., 2008). Microbial colonisation, however, is polyclonal with multiple strains from multiple species including *S. epidermidis* (Ueta et al., 2007). It is also possible for multiple *S. aureus* strains to colonise the nares with mathematical modeling predicting this happens in 6.6% of *S. aureus* colonised individuals (Cespedes et al., 2005).

Therefore, definitions of the 'players' are fluid and will vary from host to host. The commonly used inbred murine strains within this project and many others are no doubt poor mimics of human genetic susceptibility to infection. However, most studies will seek to define and provide controls to demonstrate which populations are considered the commensal or pathogen. Whether that reflects the *in vivo* situation remains to be fully elucidated.

6.2 Understanding the requirements for disease

To expose the intricacies of *S. aureus* host:pathogen interaction, it is imperative to understand the current shortfalls in studies. The metazoan mammalian host is a single entity comprised of heterotrophic eukaryotic cells, organized into tissues and organs. The prokaryotic pathogen is seldom found alone and in the persistent carrier, up to 10^7 organisms can be detected in the nares (Verhoeven et al., 2012). This large population is naturally heterogeneous despite being founded by a single strain and bacterial phenotypic and genotypic changes occur during growth. The most infamous phenotypic switch is termed a persister cell, whereby the addition of antibiotics causes the majority

of cells to die yet a small, distinct subpopulation persists (Bigger, 1944; Conlon, 2014). These form in stark contrast to genetically antibiotic resistant strains, usually by mutation or horizontal gene transfer. Despite divergent origins, antibiotic resistant subpopulations are associated with poor outcome (Mulcahy et al., 2010; Hanberger et al., 2011). Therefore, the dynamics of a bacterial infection are multifaceted and intimately integrated with the host and competition for survival against therapeutic interventions.

Precisely recapitulating this interface *in vitro* is impossible and the choice of *S. aureus* strain used for analysis and translation to the mammalian context is often oversimplified (Land et al., 2015). Interestingly, laboratory strains have far less phenotypic uniformity *in vitro* compared to clinical strains demonstrating an evolutionary pressure on strains most recently retrieved from hosts. Furthermore, the common practice of examining individual virulence factors and inferring importance in, for example, vaccine development, has so far proved futile (Bagnoli et al., 2012). More recently, antagonism between different leukotoxins released from *S. aureus* has been described (Yoong and Torres, 2015). LukSF-PV and LukED were shown to inhibit each other by forming inactive hybrid toxins that prevent cytoxicity and haemolysis by the bona fide toxin. This is interesting as these strategies aid in nutrient acquisition for *S. aureus*, which serve to combat the nutritional immunity encountered in the host. The authors suggest that this is a sophisticated mechanism whereby counter inhibition between leukotoxins promotes for long-term persistent states and colonisation by reducing host damage. Analysing each of these toxins in isolation would fail to detect such subtle but important interactions.

The importance of the microbiome as integral for optimal immune system development is increasingly recognised (Yamamoto et al., 2012). Indeed, the therapeutic potential of manipulating the microbiome is an area of active research (Peterson et al., 2015). This aim is underpinned by the need for detailed understanding of the host and pathogen and interspecies interactions within local microbial ecosystems (Piters and Bogaert, 2016). For example, the commensal bacterium, *Corynebacterium accolens*, hydrolyses host fat into free fatty acids that are detrimental to the co-coloniser *S. pneumoniae in vitro*. How these molecular epidemiological findings relate to the *in vivo* setting remains to be seen

as the plethora of other bacterial species present may also have an impact (Bomar et al., 2016).

Another aspect of commensal and pathogen interaction with the immune system is the concept that commensals must be tolerated in order to avoid causing excessive and tissue damaging inflammation. Levels of 10^4 CFU/cm^2 *S. epidermidis* have been recorded (Noble and Pitcher, 1978). Skin colonisation by *S. epidermidis* was shown to be important for the development of tolerance during neonatal life, mediated by regulatory T cells (Scharschmidt et al., 2015). During skin wounding or trauma, increased exposure to skin commensals presumably occurs and the interplay between immune recognition and control of pathogens such as *S. aureus* in addition to recognising the commensal bacterial burden is currently unknown. In work related to that discussed in Chapter 5, in the presence of TLR2 stimulants such as *S. aureus* LTA, peptidoglycan monomer acted as a co-stimulant for the release of pro-inflammatory cytokines, via the intracellular Nod2 receptor (Volz et al., 2010). This is interesting as peptidoglycan monomer, common to all Gram-positive organisms including commensal skin flora, is unable to elicit an immune response unless an extracellular signal is transduced from a pathogen. The authors suggest this may represent a host inflammation safety mechanism to avoid immune stimulation by the presence of harmless commensal flora.

All of the factors listed, and countless more, have ramifications for our understanding of the requirements of disease. It is ambitious to design experiments that take account of such multifactorial processes but using a range of animal models including innovative attempts at humanisation and complementary sophisticated *in vitro* analyses, addressing such complexities is compelling. This project has demonstrated the unique ability of the zebrafish embryo model to test hypotheses that would be difficult to establish directly in the murine model. Developing a robust assay of virulence in the zebrafish has been key to refining hypotheses that are later tested in the murine host. This clarity also ensures that the right questions are being asked, taking in account as many physiological factors and parameters as possible, in order to more closely recapitulate human disease.

6.3 Understanding the effects of disease

In this project, either a systemic zebrafish infection model or a murine sepsis model was used. The former used death as an outcome whereas in the latter, experiments are terminated at given time-points or when substantial severity limits are reached. Most often, the zebrafish experiments therefore provide a binary outcome i.e. alive or dead but bacterial CFU dynamics within the host and detailed microscopic imaging are notable advantages to using this model. In mice with markers of significant *S. aureus* infection, high bacterial burden is not recovered from the blood, despite the initial inoculum being administered via the tail vein. Instead, abscess formation with corresponding high CFU in the kidneys is the standard signature of the uncontrolled infectious process. This is consistent with previous reports which ruled out breakdown of abscesses and generalized bacteraemia as the cause of death in *S. aureus* infected mice, as the CFU counts in the blood at time of cull were low (Gorrill, 1958).

In patients treated for *S. aureus* disease, it might be assumed that outgrowth of antibiotic resistant strains could explain morbidity and mortality but this is rarely seen. Compared to other pathogens, mortality rate from invasive *S. aureus* disease is high. Predictors of mortality include age (Lamagni et al., 2011), immune status (although the exact nature of protective vs. susceptible factors is poorly defined) (Hal et al., 2012), co-morbidities including renal failure required haemodialysis (Kaech et al., 2006) or liver cirrhosis (Kang et al., 2010), source of infection (i.e. high risk includes endovascular or central nervous system) (Soriano et al., 2000) and perhaps most notable, presence of shock/sepsis (Turnidge et al., 2009). Of course, bacterial factors such as toxin production also play a role, as does optimal patient management including promptness and appropriateness of antibiotic therapy.

Septic shock was previously defined as ‘hemodynamic instability with two systemic inflammatory response syndrome criteria’ (Bone et al., 1992) but this has recently been updated (Shankar-Hari M et al., 2016). Sepsis is now defined as ‘life-threatening organ dysfunction due to a dysregulated host response to infection’ and septic shock is ‘a subset of sepsis in which underlying circulatory and cellular/metabolic abnormalities are profound enough to substantially increase mortality’. In both the mouse and human infection, death likely occurs due to sepsis leading to septic shock. As the host response

to the infection is dysregulated, the impact of the pathogen directly on mortality is difficult to estimate. The immunostimulatory effects of the pathogen may tip the balance in favour of the host, by creating a pro-inflammatory over-zealous immune response but lack of a response at all is also likely to be detrimental. Understanding of this immune balance is lacking. Antibiotic induced *S. aureus* cell wall damage by addition of vancomycin increased bacterial degradation and increased cytokine responses (Wolf et al., 2011) whereas subcutaneous injection of *M. luteus* into mice with lysozyme deficiency caused prolonged inflammation as bacterial degradation was required to deactivate the pro-inflammatory peptidoglycan causing tissue damage (Ganz et al., 2003). Understanding this fine balance is crucial to furthering our ability to prevent death from *S. aureus* infection.

6.4 Further considerations

In the past 100 years, mortality from communicable diseases has been replaced by that from non-communicable diseases but the battle against infectious agents is not over (www.who.int). Emerging new pathogens and novel resistance mechanisms of known pathogens will account for huge numbers of deaths over the coming years. The inspiration for understanding the fundamentals of pathogen biology at the host interface is that exposing new therapies can have huge impact – infectious diseases by their very nature spread between hosts so successful interventions will have impact far beyond the individual. In some aspects of course, intervention after infection is already too late. With current and emerging technology, obtaining and analysing large bacterial genomic datasets will be possible. These could then be cross-referenced with strain-specific virulence data to develop the holy grail of effective diagnostics - powerful clinical prognostic indicators (Ehrlich et al., 2008).

With regards to this project, further translational work will continue as discussed in Chapter 5. Investigation into the initiation of infection and the consequences of mixed inocula will be expanded to include organisms commonly found in *S. aureus* niches. As peptidoglycan is only present in prokaryotes and therefore represents a good therapeutic target, work will be done to elucidate the important pattern recognition receptors that recognise peptidoglycan and the specific biochemical moieties that are recognised by the host intracellularly. Advanced imaging techniques such as light sheet microscopy,

which offers high optical resolution with planar illumination, will hopefully allow visualisation of the clonal expansion phenomenon, which so far has not possible (Weber et al., 2014). Accordingly, identification of novel virulence determinants and clarification of the role of those that are already described will continue unabated.

References

Abdelnour, A., Arvidson, S., Bremell, T., Rydén, C., and Tarkowski, A. (1993). The accessory gene regulator (*agr*) controls *Staphylococcus aureus* virulence in a murine arthritis model. Infect. Immun. *61*, 3879–3885.

Abraham, E.P., and Chain, E. (1988). An enzyme from bacteria able to destroy penicillin. 1940. Rev. Infect. Dis. *10*, 677–678.

Abraham, E., Wunderink, R., Silverman, H., Perl, T.M., Nasraway, S., Levy, H., Bone, R., Wenzel, R.P., Balk, R., and Allred, R. (1995). Efficacy and safety of monoclonal antibody to human tumor necrosis factor alpha in patients with sepsis syndrome. A randomized, controlled, double-blind, multicenter clinical trial. TNF-alpha MAb Sepsis Study Group. JAMA *273*, 934–941.

Adlam, C., Broughton, E.S., and Scott, M.T. (1972). Enhanced Resistance of Mice to Infection with Bacteria following Pre-treatment with *Corynebacterium parvum*. Nature *235*, 219–220.

Alam, M.T., Petit, R.A., Crispell, E.K., Thornton, T.A., Conneely, K.N., Jiang, Y., Satola, S.W., and Read, T.D. (2014). Dissecting vancomycin-intermediate resistance in *Staphylococcus aureus* using genome-wide association. Genome Biol. Evol. *6*, 1174–1185.

Alber, G., Hammer, D.K., and Fleischer, B. (1990). Relationship between enterotoxic- and T lymphocyte-stimulating activity of staphylococcal enterotoxin B. J. Immunol. *144*, 4501–4506.

Alberts, B., Johnson, A., Lewis, J., Raff, M., Roberts, K., and Walter, P. (2002). Innate Immunity. Garland Science.

Alonzo, F., Benson, M.A., Chen, J., Novick, R.P., Shopsin, B., and Torres, V.J. (2012). *Staphylococcus aureus* leucocidin ED contributes to systemic infection by targeting neutrophils and promoting bacterial growth *in vivo*. Mol. Microbiol. *83*, 423–435.

Amyes, S.G., and Smith, J.T. (1974). Trimethoprim-sensitivity testing and thymineless mutants. J. Med. Microbiol. *7*, 143–153.

Anderson, M., Aly, K.A., Chen, Y.-H., and Missiakas, D. (2013). Secretion of atypical protein subtrates by the ESAT-6 Secretion System of *Staphylococcus aureus*: ESAT-6 secretion in *S. aureus*. Mol. Microbiol. *90*, 734-743.

Anzaldi, L.L., and Skaar, E.P. (2010). Overcoming the Heme Paradox: Heme Toxicity and Tolerance in Bacterial Pathogens. Infect. Immun. *78*, 4977–4989.

Arnaud, M., Chastanet, A., and Debarbouille, M. (2004). New Vector for Efficient Allelic Replacement in Naturally Nontransformable, Low-GC-Content, Gram-Positive Bacteria. Appl. Environ. Microbiol. *70*, 6887–6891.

Askarian, F., van Sorge, N.M., Sangvik, M., Beasley, F.C., Henriksen, J.R., Sollid, J.U.E., van Strijp, J.A.G., Nizet, V., and Johannessen, M. (2014). A *Staphylococcus*

aureus TIR domain protein virulence factor blocks TLR2-mediated NF-κB signaling. J. Innate Immun. *6*, 485–498.

Auld, D.S. (1988). Use of chelating agents to inhibit enzymes. Methods Enzymol. *158*, 110–114.

Baba, T., Bae, T., Schneewind, O., Takeuchi, F., and Hiramatsu, K. (2008). Genome sequence of *Staphylococcus aureus* strain Newman and comparative analysis of staphylococcal genomes: polymorphism and evolution of two major pathogenicity islands. J. Bacteriol. *190*, 300–310.

Bae, T., and Schneewind, O. (2006). Allelic replacement in *Staphylococcus aureus* with inducible counter-selection. Plasmid *55*, 58–63.

Bae, T., Banger, A.K., Wallace, A., Glass, E.M., Åslund, F., Schneewind, O., and Missiakas, D.M. (2004). *Staphylococcus aureus* virulence genes identified by bursa aurealis mutagenesis and nematode killing. Proc. Natl. Acad. Sci. *101*, 12312–12317.

Bagnoli, F., Bertholet, S., and Grandi, G. (2012). Inferring Reasons for the Failure of *Staphylococcus aureus* Vaccines in Clinical Trials. Front. Cell. Infect. Microbiol. *2,* 16.

Baichoo, N., Wang, T., Ye, R., and Helmann, J.D. (2002). Global analysis of the *Bacillus subtilis* Fur regulon and the iron starvation stimulon. Mol. Microbiol. *45*, 1613–1629.

Baines, S.L., Holt, K.E., Schultz, M.B., Seemann, T., Howden, B.O., Jensen, S.O., Hal, S.J. van, Coombs, G.W., Firth, N., Powell, D.R., et al. (2015). Convergent Adaptation in the Dominant Global Hospital Clone ST239 of Methicillin-Resistant *Staphylococcus aureus*. mBio *6*, e00080–15.

Bassett, A.R., Tibbit, C., Ponting, C.P., and Liu, J.-L. (2013). Highly Efficient Targeted Mutagenesis of Drosophila with the CRISPR/Cas9 System. Cell Rep. *4*, 220–228.

Beaman, T.C., Hitchins, A.D., Ochi, K., Vasantha, N., Endo, T., and Freese, E. (1983). Specificity and control of uptake of purines and other compounds in *Bacillus subtilis*. J. Bacteriol. *156*, 1107–1117.

Becker, S., Frankel, M.B., Schneewind, O., and Missiakas, D. (2014). Release of protein A from the cell wall of *Staphylococcus aureus*. Proc. Natl. Acad. Sci. *111*, 1574-1579.

Beenken, K.E., Mrak, L.N., Zielinska, A.K., Atwood, D.N., Loughran, A.J., Griffin, L.M., Matthews, K.A., Anthony, A.M., Spencer, H.J., Skinner, R.A., et al. (2014). Impact of the functional status of s*aeRS* on *in vivo* phenotypes of *Staphylococcus aureus sarA* mutants. Mol. Microbiol. *92*, 1299-1312.

Benacerraf, B., Sebestyen, M.M., and Schlossman, S. (1959). A quantitative study of the kinetics of blood clearance of P32-labelled *Escherichia coli* and Staphylococci by the reticuloendothelial system. J. Exp. Med. *110*, 27–48.

Benson, M.A., Ohneck, E.A., Ryan, C., Alonzo, F., Smith, H., Narechania, A., Kolokotronis, S.-O., Satola, S.W., Uhlemann, A.-C., Sebra, R., et al. (2014). Evolution of hypervirulence by a MRSA clone through acquisition of a transposable element. Mol. Microbiol. *93*, 664-681.

Benton, B.M., Zhang, J.P., Bond, S., Pope, C., Christian, T., Lee, L., Winterberg, K.M., Schmid, M.B., and Buysse, J.M. (2004). Large-Scale Identification of Genes Required for Full Virulence of *Staphylococcus aureus*. J. Bacteriol. *186*, 8478–8489.

Bera, A., Herbert, S., Jakob, A., Vollmer, W., and Götz, F. (2005). Why are pathogenic staphylococci so lysozyme resistant? The peptidoglycan O-acetyltransferase OatA is the major determinant for lysozyme resistance of *Staphylococcus aureus*. Mol. Microbiol. *55*, 778–787.

Bera, A., Biswas, R., Herbert, S., and Götz, F. (2006). The presence of peptidoglycan O-acetyltransferase in various staphylococcal species correlates with lysozyme resistance and pathogenicity. Infect. Immun. *74*, 4598–4604.

Bermingham, A., and Derrick, J.P. (2002). The folic acid biosynthesis pathway in bacteria: evaluation of potential for antibacterial drug discovery. BioEssays News Rev. Mol. Cell. Dev. Biol. *24*, 637–648.

Berube, B.J., and Bubeck Wardenburg, J. (2013). *Staphylococcus aureus* α-Toxin: Nearly a Century of Intrigue. Toxins *5*, 1140–1166.

Besier, S., Zander, J., Siegel, E., Saum, S.H., Hunfeld, K.-P., Ehrhart, A., Brade, V., and Wichelhaus, T.A. (2008). Thymidine-Dependent *Staphylococcus aureus* Small-Colony Variants: Human Pathogens That Are Relevant Not Only in Cases of Cystic Fibrosis Lung Disease. J. Clin. Microbiol. *46*, 3829–3832.

Beutler, B., Milsark, I.W., and Cerami, A.C. (1985). Passive immunization against cachectin/tumor necrosis factor protects mice from lethal effect of endotoxin. Science *229*, 869–871.

Bibel, D.J., Aly, R., Shinefield, H.R., and Maibach, H.I. (1983). The *Staphylococcus aureus* receptor for fibronectin. J. Invest. Dermatol. *80*, 494–496.

Bigger, J. (1944). Treatment of staphylococcal infections with penicillin by intermittent sterilisation. The Lancet *244*, 497–500.

Bilan, D.S., Pase, L., Joosen, L., Gorokhovatsky, A.Y., Ermakova, Y.G., Gadella, T.W.J., Grabher, C., Schultz, C., Lukyanov, S., and Belousov, V.V. (2013). HyPer-3: a genetically encoded H(2)O(2) probe with improved performance for ratiometric and fluorescence lifetime imaging. ACS Chem. Biol. *8*, 535–542.

Bjornson, A.B., Bjornson, H.S., Lincoln, N.A., and Altemeier, W.A. (1984). Relative roles of burn injury, wound colonization, and wound infection in induction of alterations of complement function in a guinea pig model of burn injury. J. Trauma *24*, 106–115.

Bomar, L., Brugger, S.D., Yost, B.H., Davies, S.S., and Lemon, K.P. (2016). *Corynebacterium accolens* Releases Antipneumococcal Free Fatty Acids from Human Nostril and Skin Surface Triacylglycerols. mBio *7,* e01725-15.

Bone, R.C., Balk, R.A., Cerra, F.B., Dellinger, R.P., Fein, A.M., Knaus, W.A., Schein, R.M.H., and Sibbald, W.J. (1992). Definitions for Sepsis and Organ Failure and Guidelines for the Use of Innovative Therapies in Sepsis. Chest *101*, 1644–1655.

Boon, R.J., and Beale, A.S. (1987). Response of *Streptococcus pyogenes* to therapy with amoxicillin or amoxicillin-clavulanic acid in a mouse model of mixed infection caused by *Staphylococcus aureus* and *Streptococcus pyogenes*. Antimicrob. Agents Chemother. *31*, 1204–1209.

Borregaard, N., and Cowland, J.B. (1997). Granules of the human neutrophilic polymorphonuclear leukocyte. Blood *89*, 3503–3521.

Bose, J.L., Daly, S.M., Hall, P.R., and Bayles, K.W. (2014). Identification of the *vfrAB* operon in *Staphylococcus aureus*: a novel virulence factor regulatory locus. Infect. Immun. *82*, 1813-22.

Boucher, H.W., and Corey, G.R. (2008). Epidemiology of Methicillin-Resistant *Staphylococcus aureus*. Clin. Infect. Dis. *46*, S344–S349.

Bremell, T., Lange, S., Yacoub, A., Rydén, C., and Tarkowski, A. (1991). Experimental *Staphylococcus aureus* arthritis in mice. Infect. Immun. *59*, 2615–2623.

Brinkmann, V., Reichard, U., Goosmann, C., Fauler, B., Uhlemann, Y., Weiss, D.S., Weinrauch, Y., and Zychlinsky, A. (2004). Neutrophil extracellular traps kill bacteria. Science *303*, 1532–1535.

Bronner, S., Monteil, H., and Prévost, G. (2004). Regulation of virulence determinants in *Staphylococcus aureus*: complexity and applications. FEMS Microbiol. Rev. *28*, 183–200.

Brothers, K.M., Newman, Z.R., and Wheeler, R.T. (2011). Live imaging of disseminated candidiasis in zebrafish reveals role of phagocyte oxidase in limiting filamentous growth. Eukaryot. Cell *10*, 932–944.

Brown, D.F., and Reynolds, P.E. (1980). Intrinsic resistance to beta-lactam antibiotics in *Staphylococcus aureus*. FEBS Lett. *122*, 275–278.

Brown, R.F., and Stocker, B.A. (1987). *Salmonella typhi* 205aTy, a strain with two attenuating auxotrophic characters, for use in laboratory teaching. Infect. Immun. *55*, 892–898.

Brown, A.F., Leech, J.M., Rogers, T.R., and McLoughlin, R.M. (2014). *Staphylococcus aureus* Colonization: Modulation of Host Immune Response and Impact on Human Vaccine Design. Front. Immunol. *4,* 507.

Brown, J.S., Aufauvre-Brown, A., Brown, J., Jennings, J.M., Arst, H., and Holden, D.W. (2000). Signature-tagged and directed mutagenesis identify PABA synthetase as essential for *Aspergillus fumigatus* pathogenicity. Mol. Microbiol. *36*, 1371–1380.

Brown, K.A., Khanafer, N., Daneman, N., and Fisman, D.N. (2013). Meta-Analysis of Antibiotics and the Risk of Community-Associated Clostridium difficile Infection. Antimicrob. Agents Chemother. *57*, 2326–2332.

Bubeck Wardenburg, J., Williams, W.A., and Missiakas, D. (2006). Host defenses against *Staphylococcus aureus* infection require recognition of bacterial lipoproteins. Proc. Natl. Acad. Sci. *103*, 13831–13836.

Buckingham, S.C., McDougal, L.K., Cathey, L.D., Comeaux, K., Craig, A.S., Fridkin, S.K., and Tenover, F.C. (2004). Emergence of community-associated methicillin-resistant *Staphylococcus aureus* at a Memphis, Tennessee Children's Hospital. Pediatr. Infect. Dis. J. *23*, 619–624.

Buer, J., and Balling, R. (2003). Mice, microbes and models of infection. Nat. Rev. Genet. *4*, 195–205.

Bunce, C., Wheeler, L., Reed, G., Musser, J., and Barg, N. (1992). Murine model of cutaneous infection with Gram-positive cocci. Infect. Immun. *60*, 2636–2640.

Burts, M.L., Williams, W.A., DeBord, K., and Missiakas, D.M. (2005). EsxA and EsxB are secreted by an ESAT-6-like system that is required for the pathogenesis of *Staphylococcus aureus* infections. Proc. Natl. Acad. Sci. *102*, 1169–1174.

Capparelli, R., Nocerino, N., Medaglia, C., Blaiotta, G., Bonelli, P., and Iannelli, D. (2011). The *Staphylococcus aureus* Peptidoglycan Protects Mice against the Pathogen and Eradicates Experimentally Induced Infection. PLoS ONE *6*, e28377.

Cartron, M.L., England, S.R., Chiriac, A.I., Josten, M., Turner, R., Rauter, Y., Hurd, A., Sahl, H.-G., Jones, S., and Foster, S.J. (2014). Bactericidal Activity of the Human Skin Fatty Acid cis-6-Hexadecanoic Acid on *Staphylococcus aureus*. Antimicrob. Agents Chemother. *58*, 3599–3609.

Carver, T., Harris, S.R., Berriman, M., Parkhill, J., and McQuillan, J.A. (2012). Artemis: an integrated platform for visualization and analysis of high-throughput sequence-based experimental data. Bioinformatics *28*, 464–469.

Carver, T.J., Rutherford, K.M., Berriman, M., Rajandream, M.-A., Barrell, B.G., and Parkhill, J. (2005). ACT: the Artemis Comparison Tool. Bioinforma. *21*, 3422–3423.

Casadevall, A., and Pirofski, L. (1999). Host-Pathogen Interactions: Redefining the Basic Concepts of Virulence and Pathogenicity. Infect. Immun. *67*, 3703–3713.

Cespedes, C., Said-Salim, B., Miller, M., Lo, S.-H., Kreiswirth, B.N., Gordon, R.J., Vavagiakis, P., Klein, R.S., and Lowy, F.D. (2005). The clonality of *Staphylococcus aureus* nasal carriage. J. Infect. Dis. *191*, 444–452.

Chaffin, D.O., Taylor, D., Skerrett, S.J., and Rubens, C.E. (2012). Changes in the *Staphylococcus aureus* Transcriptome during Early Adaptation to the Lung. PLoS ONE *7*, e41329.

Chaibenjawong, P., and Foster, S.J. (2011). Desiccation tolerance in *Staphylococcus aureus*. Arch. Microbiol. *193*, 125–135.

Chambers, H.F., and DeLeo, F.R. (2009). Waves of resistance: *Staphylococcus aureus* in the antibiotic era. Nat. Rev. Microbiol. *7*, 629–641.

Champion, J.A., Katare, Y.K., and Mitragotri, S. (2007). Particle shape: a new design parameter for micro- and nanoscale drug delivery carriers. J. Control. *121*, 3–9.

Champion, J.A., Walker, A., and Mitragotri, S. (2008). Role of particle size in phagocytosis of polymeric microspheres. Pharm. Res. *25*, 1815–1821.

Chan, L.C., Chaili, S., Filler, S.G., Barr, K., Wang, H., Kupferwasser, D., Edwards, J.E., Xiong, Y.Q., Ibrahim, A.S., Miller, L.S., et al. (2015). Nonredundant Roles of Interleukin-17A (IL-17A) and IL-22 in Murine Host Defense against Cutaneous and Hematogenous Infection Due to Methicillin-Resistant *Staphylococcus aureus*. Infect. Immun. *83*, 4427–4437.

Chan, Y.G.Y., Frankel, M.B., Missiakas, D., and Schneewind, O. (2016). SagB Glucosaminidase Is a Determinant of *Staphylococcus aureus* Glycan Chain Length, Antibiotic Susceptibility, and Protein Secretion. J. Bacteriol. *198*, 1123–1136.

Chang, S., Sievert, D.M., Hageman, J.C., Boulton, M.L., Tenover, F.C., Downes, F.P., Shah, S., Rudrik, J.T., Pupp, G.R., Brown, W.J., et al. (2003). Infection with vancomycin-resistant *Staphylococcus aureus* containing the *vanA* resistance gene. N. Engl. J. Med. *348*, 1342–1347.

Chapman, G.H., Berens, C., Peters, A., and Curcio, L. (1934). Coagulase and Hemolysin Tests as Measures of the Pathogenicity of Staphylococci. J. Bacteriol. *28*, 343–363.

Chatterjee, I., Kriegeskorte, A., Fischer, A., Deiwick, S., Theimann, N., Proctor, R.A., Peters, G., Herrmann, M., and Kahl, B.C. (2008). *In vivo* mutations of thymidylate synthase (encoded by *thyA*) are responsible for thymidine dependency in clinical small-colony variants of *Staphylococcus aureus*. J. Bacteriol. *190*, 834–842.

Chaudhuri, R.R., Allen, A.G., Owen, P.J., Shalom, G., Stone, K., Harrison, M., Burgis, T.A., Lockyer, M., Garcia-Lara, J., Foster, S.J., et al. (2009). Comprehensive identification of essential *Staphylococcus aureus* genes using Transposon-Mediated Differential Hybridisation (TMDH). BMC Genomics *10*, 291.

Cheng, A.G., Kim, H.K., Burts, M.L., Krausz, T., Schneewind, O., and Missiakas, D.M. (2009). Genetic requirements for *Staphylococcus aureus* abscess formation and persistence in host tissues. FASEB J. *23*, 3393–3404.

Chesney, P.J., Bergdoll, M.S., Davis, J.P., and Vergeront, J.M. (1984). The disease spectrum, epidemiology, and etiology of toxic-shock syndrome. Annu. Rev. Microbiol. *38*, 315–338.

Chesters, J.K., Petrie, L., and Travis, A.J. (1990). A requirement for Zn2+ for the induction of thymidine kinase but not ornithine decarboxylase in 3T3 cells stimulated from quiescence. Biochem. J. *272*, 525–527.

Cheung, A.L., Eberhardt, K.J., Chung, E., Yeaman, M.R., Sullam, P.M., Ramos, M., and Bayer, A.S. (1994). Diminished virulence of a *sar*/*agr* mutant of *Staphylococcus aureus* in the rabbit model of endocarditis. J. Clin. Invest. *94*, 1815–1822.

Cheung, G.Y.C., Joo, H.-S., Chatterjee, S.S., and Otto, M. (2014). Phenol-soluble modulins – critical determinants of staphylococcal virulence. FEMS Microbiol. Rev. *38*, 698–719.

Chiller, K., Selkin, B.A., and Murakawa, G.J. (2001). Skin Microflora and Bacterial Infections of the Skin. J. Investig. Dermatol. *6*, 170–174.

Chimalapati, S., Cohen, J., Camberlein, E., Durmort, C., Baxendale, H., de Vogel, C., van Belkum, A., and Brown, J.S. (2011). Infection with Conditionally Virulent *Streptococcus pneumoniae pab* Strains Induces Antibody to Conserved Protein Antigens but Does Not Protect against Systemic Infection with Heterologous Strains. Infect Immun. *79*, 4965-4976.

Chopra, I., and Roberts, M. (2001). Tetracycline Antibiotics: Mode of Action, Applications, Molecular Biology, and Epidemiology of Bacterial Resistance. Microbiol. Mol. Biol. Rev. *65*, 232–260.

Chow, A.W., Gribble, M.J., and Bartlett, K.H. (1983). Characterization of the hemolytic activity of *Staphylococcus aureus* strains associated with toxic shock syndrome. J. Clin. Microbiol. *17*, 524–528.

Christiansen, M.T., Kaas, R.S., Chaudhuri, R.R., Holmes, M.A., Hasman, H., and Aarestrup, F.M. (2014). Genome-wide high-throughput screening to investigate essential genes involved in methicillin-resistant *Staphylococcus aureus* Sequence Type 398 survival. PloS One *9*, e89018.

Chua, K.Y., Monk, I.R., Lin, Y.-H., Seemann, T., Tuck, K.L., Porter, J.L., Stepnell, J., Coombs, G.W., Davies, J.K., Stinear, T.P., et al. (2014). Hyperexpression of α-hemolysin explains enhanced virulence of sequence type 93 community-associated methicillin-resistant *Staphylococcus aureus*. BMC Microbiol. *14*, 31.

Chua, K.Y.L., Stinear, T.P., and Howden, B.P. (2013). Functional genomics of *Staphylococcus aureus*. Brief. Funct. Genomics *12*, 305–315.

Clarke, S.R., Brummell, K.J., Horsburgh, M.J., McDowell, P.W., Mohamad, S.A.S., Stapleton, M.R., Acevedo, J., Read, R.C., Day, N.P., and Peacock, S.J. (2006). Identification of *in vivo*–expressed antigens of *Staphylococcus aureus* and their use in vaccinations for protection against nasal carriage. J. Infect. Dis. *193*, 1098–1108.

Clarke, S.R., Mohamed, R., Bian, L., Routh, A.F., Kokai-Kun, J.F., Mond, J.J., Tarkowski, A., and Foster, S.J. (2007). The *Staphylococcus aureus* Surface Protein IsdA Mediates Resistance to Innate Defenses of Human Skin. Cell Host Microbe *1*, 199–212.

Clauditz, A., Resch, A., Wieland, K.-P., Peschel, A., and Gotz, F. (2006). Staphyloxanthin Plays a Role in the Fitness of *Staphylococcus aureus* and Its Ability To Cope with Oxidative Stress. Infect. Immun. *74*, 4950–4953.

Cogen, A.L., Nizet, V., and Gallo, R.L. (2008). Skin microbiota: a source of disease or defence? Br. J. Dermatol. *158*, 442–455.

Colucci-Guyon, E., Tinevez, J.-Y., Renshaw, S.A., and Herbomel, P. (2011). Strategies of professional phagocytes in vivo: unlike macrophages, neutrophils engulf only surface-associated microbes. J. Cell Sci. *124*, 3053–3059.

Conlon, B.P. (2014). *Staphylococcus aureus* chronic and relapsing infections: Evidence of a role for persister cells: An investigation of persister cells, their formation and their role in *S. aureus* disease. BioEssays *36*, 991-996.

Connolly, J. (2016). Analysis of *Staphylococcus aureus* Virulence Determinants. PhD thesis. University of Sheffield.

Cooper, M.D., and Alder, M.N. (2006). The evolution of adaptive immune systems. Cell *124*, 815–822.

Corbin, B.D., Seeley, E.H., Raab, A., Feldmann, J., Miller, M.R., Torres, V.J., Anderson, K.L., Dattilo, B.M., Dunman, P.M., Gerads, R., et al. (2008). Metal Chelation and Inhibition of Bacterial Growth in Tissue Abscesses. Science *319*, 962–965.

Corrigan, R.M., Miajlovic, H., and Foster, T.J. (2009). Surface proteins that promote adherence of *Staphylococcus aureus* to human desquamated nasal epithelial cells. BMC Microbiol. *9*, 22.

Corvaglia, A.R., François, P., Hernandez, D., Perron, K., Linder, P., and Schrenzel, J. (2010). A type III-like restriction endonuclease functions as a major barrier to horizontal gene transfer in clinical *Staphylococcus aureus* strains. Proc. Natl. Acad. Sci. *107*, 11954–11958.

Cosgrove, S.E., Sakoulas, G., Perencevich, E.N., Schwaber, M.J., Karchmer, A.W., and Carmeli, Y. (2003). Comparison of Mortality Associated with Methicillin-Resistant and Methicillin-Susceptible *Staphylococcus aureus* Bacteremia: A Meta-analysis. Clin. Infect. Dis. *36*, 53–59.

Coulombe, F., Divangahi, M., Veyrier, F., de Léséleuc, L., Gleason, J.L., Yang, Y., Kelliher, M.A., Pandey, A.K., Sassetti, C.M., Reed, M.B., et al. (2009). Increased NOD2-mediated recognition of N-glycolyl muramyl dipeptide. J. Exp. Med. *206*, 1709–1716.

Coulter, S.N., Schwan, W.R., Ng, E.Y.W., Langhorne, M.H., Ritchie, H.D., Westbrock-Wadman, S., Hufnagle, W.O., Folger, K.R., Bayer, A.S., and Stover, C.K. (1998). *Staphylococcus aureus* genetic loci impacting growth and survival in multiple infection environments. Mol. Microbiol. *30*, 393–404.

Crisóstomo, M.I., Vollmer, W., Kharat, A.S., Inhülsen, S., Gehre, F., Buckenmaier, S., and Tomasz, A. (2006). Attenuation of penicillin resistance in a peptidoglycan O-acetyl transferase mutant of *Streptococcus pneumoniae*. Mol. Microbiol. *61*, 1497–1509.

Croucher, N.J., Harris, S.R., Fraser, C., Quail, M.A., Burton, J., van der Linden, M., McGee, L., von Gottberg, A., Song, J.H., Ko, K.S., et al. (2011). Rapid pneumococcal evolution in response to clinical interventions. Science *331*, 430–434.

Crowhurst, M.O., Layton, J.E., and Lieschke, G.J. (2002). Developmental biology of zebrafish myeloid cells. Int. J. Dev. Biol. *46*, 483–492.

Cui, L., Ma, X., Sato, K., Okuma, K., Tenover, F.C., Mamizuka, E.M., Gemmell, C.G., Kim, M.-N., Ploy, M.-C., Solh, N.E., et al. (2003). Cell Wall Thickening Is a Common Feature of Vancomycin Resistance in *Staphylococcus aureus*. J. Clin. Microbiol. *41*, 5–14.

Dancer, S. J. (2008). The effects of antibiotics on methicillin-resistant *Staphylococcus aureus*. J. Antimicrob Chemother. *61*, 246-253.

Darrell, J.H., Garrod, L.P., and Waterworth, P.M. (1968). Trimethoprim: laboratory and clinical studies. J. Clin. Pathol. *21*, 202–209.

David, M.Z., and Daum, R.S. (2010). Community-Associated Methicillin-Resistant *Staphylococcus aureus*: Epidemiology and Clinical Consequences of an Emerging Epidemic. Clin. Microbiol. Rev. *23*, 616–687.

David, M.Z., Daum, R.S., Bayer, A.S., Chambers, H.F., Fowler, V.G., Miller, L.G., Ostrowsky, B., Baesa, A., Boyle-Vavra, S., Eells, S.J., et al. (2014). *Staphylococcus aureus* Bacteremia at 5 US Academic Medical Centers, 2008–2011: Significant Geographic Variation in Community-Onset Infections. Clin. Infect. Dis. *59*, 798–807.

Davis, K.M., Nakamura, S., and Weiser, J.N. (2011). Nod2 sensing of lysozyme-digested peptidoglycan promotes macrophage recruitment and clearance of *S. pneumoniae* colonization in mice. J. Clin. Invest. *121*, 3666–3676.

DeLeo, F.R., Kennedy, A.D., Chen, L., Wardenburg, J.B., Kobayashi, S.D., Mathema, B., Braughton, K.R., Whitney, A.R., Villaruz, A.E., Martens, C.A., et al. (2011). Molecular differentiation of historic phage-type 80/81 and contemporary epidemic *Staphylococcus aureus*. Proc. Natl. Acad. Sci. *108*, 18091–18096.

Deshmane, S.L., Kremlev, S., Amini, S., and Sawaya, B.E. (2009). Monocyte Chemoattractant Protein-1 (MCP-1): An Overview. J. Interferon Cytokine Res. *29*, 313–326.

Diep, B.A., Gill, S.R., Chang, R.F., Phan, T.H., Chen, J.H., Davidson, M.G., Lin, F., Lin, J., Carleton, H.A., Mongodin, E.F., et al. (2006). Complete genome sequence of USA300, an epidemic clone of community-acquired meticillin-resistant *Staphylococcus aureus*. Lancet *367*, 731–739.

Dostert, C., Pétrilli, V., Van Bruggen, R., Steele, C., Mossman, B.T., and Tschopp, J. (2008). Innate immune activation through Nalp3 inflammasome sensing of asbestos and silica. Science *320*, 674–677.

Douady, C.J., Delsuc, F., Boucher, Y., Doolittle, W.F., and Douzery, E.J.P. (2003). Comparison of Bayesian and maximum likelihood bootstrap measures of phylogenetic reliability. Mol. Biol. Evol. *20*, 248–254.

Drlica, K., Malik, M., Kerns, R.J., and Zhao, X. (2008). Quinolone-Mediated Bacterial Death. Antimicrob. Agents Chemother. *52*, 385–392.

Dubos, R.J., and Schaedler, R.W. (1957). Effects of cellular constituents of mycobacteria on the resistance of mice to heterologous infections I. Protective effects. J. Exp. Med. *106*, 703–717.

DuMont, A.L., Yoong, P., Day, C.J., Alonzo, F., McDonald, W.H., Jennings, M.P., and Torres, V.J. (2013). *Staphylococcus aureus* LukAB cytotoxin kills human neutrophils by targeting the CD11b subunit of the integrin Mac-1. Proc. Natl. Acad. Sci. *110*, 10794–10799.

Duthie, E.S., and Lorenz, L.L. (1952). Staphylococcal Coagulase: Mode of Action and Antigenicity. J. Gen. Microbiol. *6*, 95–107.

Dziarski, R., and Gupta, D. (2005). *Staphylococcus aureus* Peptidoglycan Is a Toll-Like Receptor 2 Activator: a Reevaluation. Infect. Immun. *73*, 5212–5216.

Edgeworth, J.D., Yadegarfar, G., Pathak, S., Batra, R., Cockfield, J.D., Wyncoll, D., Beale, R., and Lindsay, J.A. (2007). An Outbreak in an Intensive Care Unit of a Strain of Methicillin-Resistant *Staphylococcus aureus* Sequence Type 239 Associated with an Increased Rate of Vascular Access Device—Related Bacteremia. Clin. Infect. Dis. *44*, 493–501.

Ehrlich, G.D., Hiller, N.L., and Hu, F.Z. (2008). What makes pathogens pathogenic. Genome Biol. *9*, 225.

Elek, S.D., and Conen, P.E. (1957). The virulence of Staphylococcus pyogenes for man; a study of the problems of wound infection. Br. J. Exp. Pathol. *38*, 573–586.

Eliopoulos, G.M., and Huovinen, P. (2001). Resistance to Trimethoprim-Sulfamethoxazole. Clin. Infect. Dis. *32*, 1608–1614.

Ellett, F., Pase, L., Hayman, J.W., Andrianopoulos, A., and Lieschke, G.J. (2011). mpeg1 promoter transgenes direct macrophage-lineage expression in zebrafish. Blood *117*, e49–e56.

Emmett, M., and Kloos, W.E. (1975). Amino acid requirements of staphylococci isolated from human skin. Can. J. Microbiol. *21*, 729–733.

Entenza, J.M., Haldimann, A., Giddey, M., Lociuro, S., Hawser, S., and Moreillon, P. (2009). Efficacy of iclaprim against wild-type and thymidine kinase-deficient methicillin-resistant *Staphylococcus aureus* isolates in an *in vitro* fibrin clot model. Antimicrob. Agents Chemother. *53*, 3635–3641.

Ewbank, J.J. (2002). Tackling both sides of the host–pathogen equation with *Caenorhabditis elegans*. Microbes Infect. *4*, 247–256.

Faith, N.G., Kim, J.-W., Azizoglu, R., Kathariou, S., and Czuprynski, C. (2012). Purine biosynthesis mutants (*purA* and *purB*) of serotype 4b Listeria monocytogenes are severely attenuated for systemic infection in intragastrically inoculated A/J Mice. Foodborne Pathog. Dis. *9*, 480–486.

Falugi, F., Kim, H.K., Missiakas, D.M., and Schneewind, O. (2013). Role of Protein A in the Evasion of Host Adaptive Immune Responses by *Staphylococcus aureus*. mBio *4*, e00575–13.

Fattom, A.I., Sarwar, J., Ortiz, A., and Naso, R. (1996). A *Staphylococcus aureus* capsular polysaccharide (CP) vaccine and CP-specific antibodies protect mice against bacterial challenge. Infect. Immun. *64*, 1659–1665.

Faustin, B., Lartigue, L., Bruey, J.-M., Luciano, F., Sergienko, E., Bailly-Maitre, B., Volkmann, N., Hanein, D., Rouiller, I., and Reed, J.C. (2007). Reconstituted NALP1 inflammasome reveals two-step mechanism of caspase-1 activation. Mol. Cell *25*, 713–724.

Feil, E.J., Cooper, J.E., Grundmann, H., Robinson, D.A., Enright, M.C., Berendt, T., Peacock, S.J., Smith, J.M., Murphy, M., Spratt, B.G., et al. (2003). How Clonal Is *Staphylococcus aureus*? J. Bacteriol. *185*, 3307–3316.

Feil, E.J., Nickerson, E.K., Chantratita, N., Wuthiekanun, V., Srisomang, P., Cousins, R., Pan, W., Zhang, G., Xu, B., Day, N.P.J., et al. (2008). Rapid Detection of the Pandemic Methicillin-Resistant *Staphylococcus aureus* Clone ST 239, a Dominant Strain in Asian Hospitals. J. Clin. Microbiol. *46*, 1520–1522.

Fey, P.D., Endres, J.L., Yajjala, V.K., Widhelm, T.J., Boissy, R.J., Bose, J.L., and Bayles, K.W. (2013). A Genetic Resource for Rapid and Comprehensive Phenotype Screening of Nonessential *Staphylococcus aureus* Genes. mBio *4*, e00537–12.

Filkins, L.M., Graber, J.A., Olson, D.G., Dolben, E.L., Lynd, L.R., Bhuju, S., and O'Toole, G.A. (2015). Coculture of *Staphylococcus aureus* with *Pseudomonas aeruginosa* Drives *S. aureus* towards Fermentative Metabolism and Reduced Viability in a Cystic Fibrosis Model. J. Bacteriol. *197*, 2252–2264.

Flajnik, M.F., and Kasahara, M. (2010). Origin and evolution of the adaptive immune system: genetic events and selective pressures. Nat. Rev. Genet. *11*, 47–59.

Fleischmann, R.D., Adams, M.D., White, O., Clayton, R.A., Kirkness, E.F., Kerlavage, A.R., Bult, C.J., Tomb, J.F., Dougherty, B.A., and Merrick, J.M. (1995). Whole-genome random sequencing and assembly of *Haemophilus influenzae* Science *269*, 496–512.

Foletti, D., Strop, P., Shaughnessy, L., Hasa-Moreno, A., Casas, M.G., Russell, M., Bee, C., Wu, S., Pham, A., Zeng, Z., et al. (2013). Mechanism of Action and *In vivo* Efficacy of a Human-Derived Antibody against *Staphylococcus aureus* α-Hemolysin. J. Mol. Biol. *425*, 1641–1654.

Foster, S.J. (1995). Molecular characterization and functional analysis of the major autolysin of *Staphylococcus aureus* 8325/4. J. Bacteriol. *177*, 5723–5725.

Foster, T. (1996). *Staphylococcus* In Medical Microbiology. (Galveston (TX): University of Texas Medical Branch at Galveston),

Foster, T.J. (2005). Immune evasion by staphylococci. Nat. Rev. Microbiol. *3*, 948–958.

Foster, T.J., and Höök, M. (1998). Surface protein adhesins of *Staphylococcus aureus*. Trends Microbiol. *6*, 484–488.

Fournier, B., and Philpott, D.J. (2005). Recognition of *Staphylococcus aureus* by the Innate Immune System. *8*, 521–540

Fowler, V.G., Jr, Nelson, C.L., McIntyre, L.M., Kreiswirth, B.N., Monk, A., Archer, G.L., Federspiel, J., Naidich, S., Remortel, B., Rude, T., et al. (2007). Potential associations between hematogenous complications and bacterial genotype in *Staphylococcus aureus* infection. J. Infect. Dis. *196*, 738–747.

Fox, E.S., Thomas, P., and Broitman, S.A. (1989). Clearance of gut-derived endotoxins by the liver. Release and modification of 3H, 14C-lipopolysaccharide by isolated rat Kupffer cells. Gastroenterology *96*, 456–461.

Fox, P.M., Climo, M.W., and Archer, G.L. (2007). Lack of Relationship between Purine Biosynthesis and Vancomycin Resistance in *Staphylococcus aureus*: a Cautionary Tale for Microarray Interpretation. Antimicrob. Agents Chemother. *51*, 1274–1280.

Francis, M.J., Doherty, R.R., Patel, M., Hamblin, J.F., Ojaimi, S., and Korman, T.M. (2011). *Curtobacterium flaccumfaciens* Septic Arthritis following Puncture with a Coxspur Hawthorn Thorn. J. Clin. Microbiol. *49*, 2759–2760.

Freeman, A.F., and Holland, S.M. (2008). The Hyper IgE Syndromes. Immunol. Allergy Clin. *28*, 277.

Fricke, W.F., and Rasko, D.A. (2014). Bacterial genome sequencing in the clinic: bioinformatic challenges and solutions. Nat. Rev. Genet. *15*, 49–55.

Ganz, T., Gabayan, V., Liao, H.-I., Liu, L., Oren, A., Graf, T., and Cole, A.M. (2003). Increased inflammation in lysozyme M-deficient mice in response to *Micrococcus luteus* and its peptidoglycan. Blood *101*, 2388–2392.

Garrison, P.K., and Freedman, L.R. (1970). Experimental endocarditis I. Staphylococcal endocarditis in rabbits resulting from placement of a polyethylene catheter in the right side of the heart. Yale J. Biol. Med. *42*, 394–410.

Garsin, D.A., Sifri, C.D., Mylonakis, E., Qin, X., Singh, K.V., Murray, B.E., Calderwood, S.B., and Ausubel, F.M. (2001). A simple model host for identifying Gram-positive virulence factors. Proc. Natl. Acad. Sci. *98*, 10892–10897.

Gaupp, R., Ledala, N., and Somerville, G.A. (2012). Staphylococcal response to oxidative stress. Front. Cell. Infect. Microbiol. *2,* 33.

Geiger, T., Goerke, C., Mainiero, M., Kraus, D., and Wolz, C. (2008). The Virulence Regulator Sae of *Staphylococcus aureus*: Promoter Activities and Response to Phagocytosis-Related Signals. J. Bacteriol. *190*, 3419–3428.

Geiger, T., Francois, P., Liebeke, M., Fraunholz, M., Goerke, C., Krismer, B., Schrenzel, J., Lalk, M., and Wolz, C. (2012). The Stringent Response of *Staphylococcus aureus* and Its Impact on Survival after Phagocytosis through the Induction of Intracellular PSMs Expression. PLoS Pathog *8*, e1003016.

Georgoutsou-Spyridonos, M., Ricklin, D., Pratsinis, H., Perivolioti, E., Pirmettis, I., Garcia, B.L., Geisbrecht, B.V., Foukas, P.G., Lambris, J.D., Mastellos, D.C., et al. (2015). Attenuation of *Staphylococcus aureus*-Induced Bacteremia by Human Mini-Antibodies Targeting the Complement Inhibitory Protein Efb. J. Immunol. *195*, 3946–3958.

Gerlini, A., Colomba, L., Furi, L., Braccini, T., Manso, A.S., Pammolli, A., Wang, B., Vivi, A., Tassini, M., van Rooijen, N., et al. (2014). The Role of Host and Microbial Factors in the Pathogenesis of Pneumococcal Bacteraemia Arising from a Single Bacterial Cell Bottleneck. PLoS Pathog *10*, e1004026.

Gibson, D.G., Young, L., Chuang, R.-Y., Venter, J.C., Hutchison, C.A., and Smith, H.O. (2009). Enzymatic assembly of DNA molecules up to several hundred kilobases. Nat. Methods *6*, 343–345.

Gill, S.R., McIntyre, L.M., Nelson, C.L., Remortel, B., Rude, T., Reller, L.B., and Fowler, V.G., Jr. (2011). Potential Associations between Severity of Infection and the Presence of Virulence-Associated Genes in Clinical Strains of *Staphylococcus aureus*. PLoS ONE *6*, e18673.

Gillet, Y., Issartel, B., Vanhems, P., Fournet, J.-C., Lina, G., Bes, M., Vandenesch, F., Piémont, Y., Brousse, N., Floret, D., et al. (2002). Association between *Staphylococcus aureus* strains carrying gene for Panton-Valentine leukocidin and highly lethal necrotising pneumonia in young immunocompetent patients. Lancet *359*, 753–759.

Gilligan, P.H., Gage, P.A., Welch, D.F., Muszynski, M.J., and Wait, K.R. (1987). Prevalence of thymidine-dependent *Staphylococcus aureus* in patients with cystic fibrosis. J. Clin. Microbiol. *25*, 1258–1261.

Gingles, N.A., Alexander, J.E., Kadioglu, A., Andrew, P.W., Kerr, A., Mitchell, T.J., Hopes, E., Denny, P., Brown, S., Jones, H.B., et al. (2001). Role of genetic resistance in invasive pneumococcal infection: identification and study of susceptibility and resistance in inbred mouse strains. Infect. Immun. *69*, 426–434.

Girardin, S.E., Boneca, I.G., Viala, J., Chamaillard, M., Labigne, A., Thomas, G., Philpott, D.J., and Sansonetti, P.J. (2003a). Nod2 is a general sensor of peptidoglycan through muramyl dipeptide (MDP) detection. J. Biol. Chem. *278*, 8869–8872.

Girardin, S.E., Boneca, I.G., Carneiro, L.A.M., Antignac, A., Jéhanno, M., Viala, J., Tedin, K., Taha, M.-K., Labigne, A., Zähringer, U., et al. (2003b). Nod1 detects a unique muropeptide from gram-negative bacterial peptidoglycan. Science *300*, 1584–1587.

Giraudo, A.T., Raspanti, C.G., Calzolari, A., and Nagel, R. (1994). Characterization of a Tn551-mutant of *Staphylococcus aureus* defective in the production of several exoproteins. Can. J. Microbiol. *40*, 677–681.

Giraudo, A.T., Calzolari, A., Cataldi, A.A., Bogni, C., and Nagel, R. (1999). The *sae* locus of *Staphylococcus aureus* encodes a two-component regulatory system. FEMS Microbiol. Lett. *177*, 15–22.

Goerke, C., Fluckiger, U., Steinhuber, A., Bisanzio, V., Ulrich, M., Bischoff, M., Patti, J.M., and Wolz, C. (2005). Role of *Staphylococcus aureus* Global Regulators *sae* and sigma (B) in Virulence Gene Expression during Device-Related Infection. Infect. Immun. *73*, 3415–3421.

Goodacre, R. (2007). Metabolomics of a superorganism. J. Nutr. *137*, 259S – 266S.

Gordon, R.J., and Lowy, F.D. (2008). Pathogenesis of Methicillin-Resistant *Staphylococcus aureus* Infection. Clin. Infect. Dis. *46*, S350–S359.

Gorrill, R.H. (1958). The establishment of staphylococcal abscesses in the mouse kidney. Br. J. Exp. Pathol. *39*, 203–212.

Gottlieb, D., and Shaw, P.D. (2013). Antibiotics: Volume I Mechanism of Action (Springer).

Grant, A.J., Morgan, F.J.E., McKinley, T.J., Foster, G.L., Maskell, D.J., and Mastroeni, P. (2012). Attenuated *Salmonella Typhimurium* Lacking the Pathogenicity Island-2 Type 3 Secretion System Grow to High Bacterial Numbers inside Phagocytes in Mice. PLoS Pathog *8*, e1003070.

Gresham, H.D., Lowrance, J.H., Caver, T.E., Wilson, B.S., Cheung, A.L., and Lindberg, F.P. (2000). Survival of *Staphylococcus aureus* Inside Neutrophils Contributes to Infection. J. Immunol. *164*, 3713–3722.

Grice, E.A., and Segre, J.A. (2011). The skin microbiome. Nat. Rev. Microbiol. *9*, 244–253.

Grosz, M., Kolter, J., Paprotka, K., Winkler, A.-C., Schafer, D., Chatterjee, S.S., Geiger, T., Wolz, C., Ohlsen, K., Otto, M., et al. (2014). Cytoplasmic replication of *Staphylococcus aureus* upon phagosomal escape triggered by phenol-soluble modulin α. Cell. Microbiol. *16*, 451–465.

Guide, S.V., Stock, F., Gill, V.J., Anderson, V.L., Malech, H.L., Gallin, J.I., and Holland, S.M. (2003). Reinfection, Rather than Persistent Infection, in Patients with Chronic Granulomatous Disease. J. Infect. Dis. *187*, 845–853.

Guryev, V., Koudijs, M.J., Berezikov, E., Johnson, S.L., Plasterk, R.H.A., van Eeden, F.J.M., and Cuppen, E. (2006). Genetic variation in the zebrafish. Genome Res. *16*, 491–497.

Haas, P.-J., de Haas, C.J.C., Poppelier, M.J.J.C., van Kessel, K.P.M., van Strijp, J.A.G., Dijkstra, K., Scheek, R.M., Fan, H., Kruijtzer, J.A.W., Liskamp, R.M.J., et al. (2005). The structure of the C5a receptor-blocking domain of chemotaxis inhibitory protein of *Staphylococcus aureus* is related to a group of immune evasive molecules. J. Mol. Biol. *353*, 859–872.

Haggar, A., Ehrnfelt, C., Holgersson, J., and Flock, J.-I. (2004). The Extracellular Adherence Protein from *Staphylococcus aureus* Inhibits Neutrophil Binding to Endothelial Cells. Infect. Immun. *72*, 6164–6167.

Hal, S.J. van, Jensen, S.O., Vaska, V.L., Espedido, B.A., Paterson, D.L., and Gosbell, I.B. (2012). Predictors of Mortality in *Staphylococcus aureus* Bacteremia. Clin. Microbiol. Rev. *25*, 362–386.

Haltiner, R.C., Migneault, P.C., and Robertson, R.G. (1980). Incidence of thymidine-dependent enterococci detected on Mueller-Hinton agar with low thymidine content. Antimicrob. Agents Chemother. *18*, 365–368.

Hamilton-Miller, J.M.T. (1988). Reversal of activity of trimethoprim against Gram-positive cocci by thymidine, thymine and "folates." J. Antimicrob. Chemother. *22*, 35–39.

Hammer, N.D., and Skaar, E.P. (2011). Molecular mechanisms of *Staphylococcus aureus* iron acquisition. Annu. Rev. Microbiol. *65*.

Hampele, I.C., D'Arcy, A., Dale, G.E., Kostrewa, D., Nielsen, J., Oefner, C., Page, M.G.P., Schönfeld, H.-J., Stüber, D., and Then, R.L. (1997). Structure and function of the dihydropteroate synthase from *Staphylococcus aureus*. J. Mol. Biol. *268*, 21–30.

Hanberger, H., Walther, S., Leone, M., Barie, P.S., Rello, J., Lipman, J., Marshall, J.C., Anzueto, A., Sakr, Y., Pickkers, P., et al. (2011). Increased mortality associated with methicillin-resistant *Staphylococcus aureus* (MRSA) infection in the intensive care unit: results from the EPIC II study. Int. J. Antimicrob. Agents *38*, 331–335.

Hanses, F., Roux, C., Dunman, P.M., Salzberger, B., and Lee, J.C. (2014). *Staphylococcus aureus* gene expression in a rat model of infective endocarditis. Genome Med. *6*, 93.

Harrington, L.E., Hatton, R.D., Mangan, P.R., Turner, H., Murphy, T.L., Murphy, K.M., and Weaver, C.T. (2005). Interleukin 17-producing CD4+ effector T cells develop via a lineage distinct from the T helper type 1 and 2 lineages. Nat. Immunol. *6*, 1123–1132.

Harris, S.R., Feil, E.J., Holden, M.T.G., Quail, M.A., Nickerson, E.K., Chantratita, N., Gardete, S., Tavares, A., Day, N., Lindsay, J.A., et al. (2010). Evolution of MRSA During Hospital Transmission and Intercontinental Spread. Science *327*, 469–474.

Harris, S.R., Cartwright, E.J., Torok, M.E., Holden, M.T., Brown, N.M., Ogilvy-Stuart, A.L., Ellington, M.J., Quail, M.A., Bentley, S.D., Parkhill, J., et al. (2013). Whole-genome sequencing for analysis of an outbreak of meticillin-resistant *Staphylococcus aureus*: a descriptive study. Lancet Infect. Dis. *13*, 130–136.

Hashimoto, M., Tawaratsumida, K., Kariya, H., Kiyohara, A., Suda, Y., Krikae, F., Kirikae, T., and Gotz, F. (2006). Not Lipoteichoic Acid but Lipoproteins Appear to Be the Dominant Immunobiologically Active Compounds in *Staphylococcus aureus*. J. Immunol. *177*, 3162–3169.

Hayashi, F., Means, T.K., and Luster, A.D. (2003). Toll-like receptors stimulate human neutrophil function. Blood *102*, 2660–2669.

Hébert, L., Courtin, P., Torelli, R., Sanguinetti, M., Chapot-Chartier, M.-P., Auffray, Y., and Benachour, A. (2007). *Enterococcus faecalis* constitutes an unusual bacterial model in lysozyme resistance. Infect. Immun. *75*, 5390–5398.

Heilbronner, S., Monk, I.R., and Foster, T.J. (2013). The phage integrase vector pIPI03 allows RecA-independent, site-specific labelling of *Staphylococcus lugdunensis* strains. Plasmid *70*, 377–384.

Henry, K.M., Loynes, C.A., Whyte, M.K.B., and Renshaw, S.A. (2013). Zebrafish as a model for the study of neutrophil biology. J. Leukoc. Biol. *94*, 633–642.

Herbert, S., Bera, A., Nerz, C., Kraus, D., Peschel, A., Goerke, C., Meehl, M., Cheung, A., and Götz, F. (2007). Molecular basis of resistance to muramidase and cationic antimicrobial peptide activity of lysozyme in staphylococci. PLoS Pathog. *3*, e102.

Herbomel, P., Thisse, B., and Thisse, C. (1999). Ontogeny and behaviour of early macrophages in the zebrafish embryo. Dev. *126*, 3735–3745.

Herbomel, P., Thisse, B., and Thisse, C. (2001). Zebrafish Early Macrophages Colonize Cephalic Mesenchyme and Developing Brain, Retina, and Epidermis through a M-CSF Receptor-Dependent Invasive Process. Dev. Biol. *238*, 274–288.

Heroven, A.K., and Dersch, P. (2014). Coregulation of host-adapted metabolism and virulence by pathogenic yersiniae. Front. Cell. Infect. Microbiol. *4*, 146.

Hetru, C., and Hoffmann, J.A. (2009). NF-kappaB in the immune response of Drosophila. Cold Spring Harb. Perspect. Biol. *1*, a000232.

Hiramatsu, K., Hanaki, H., Ino, T., Yabuta, K., Oguri, T., and Tenover, F.C. (1997). Methicillin-resistant *Staphylococcus aureus* clinical strain with reduced vancomycin susceptibility. J. Antimicrob. Chemother. *40*, 135–136.

Holden, M.T.G., Lindsay, J.A., Corton, C., Quail, M.A., Cockfield, J.D., Pathak, S., Batra, R., Parkhill, J., Bentley, S.D., and Edgeworth, J.D. (2009). Genome Sequence of a Recently Emerged, Highly Transmissible, Multi-Antibiotic- and Antiseptic-Resistant Variant of Methicillin-Resistant *Staphylococcus aureus*, Sequence Type 239 (TW). J. Bacteriol. *192*, 888–892.

Holden, M.T.G., Hsu, L.-Y., Kurt, K., Weinert, L.A., Mather, A.E., Harris, S.R., Strommenger, B., Layer, F., Witte, W., de Lencastre, H., et al. (2013). A genomic portrait of the emergence, evolution, and global spread of a methicillin-resistant *Staphylococcus aureus* pandemic. Genome Res. *23*, 653–664.

Holtfreter, S., Radcliff, F.J., Grumann, D., Read, H., Johnson, S., Monecke, S., Ritchie, S., Clow, F., Goerke, C., Bröker, B.M., et al. (2013). Characterization of a mouse-adapted *Staphylococcus aureus* strain. PloS One *8*, e71142.

Hornung, V., Bauernfeind, F., Halle, A., Samstad, E.O., Kono, H., Rock, K.L., Fitzgerald, K.A., and Latz, E. (2008). Silica crystals and aluminum salts activate the NALP3 inflammasome through phagosomal destabilization. Nat. Immunol. *9*, 847–856.

Horsburgh, M.J., Aish, J.L., White, I.J., Shaw, L., Lithgow, J.K., and Foster, S.J. (2002). Sigma B Modulates Virulence Determinant Expression and Stress Resistance: Characterization of a Functional *rsbU* Strain Derived from *Staphylococcus aureus* 8325-4. J. Bacteriol. *184*, 5457–5467.

Horsburgh, M.J., Wiltshire, M.D., Crossley, H., Ingham, E., and Foster, S.J. (2004). PheP, a Putative Amino Acid Permease of *Staphylococcus aureus*, Contributes to Survival *In vivo* and during Starvation. Infect. Immun. *72*, 3073–3076.

Hoshino, K., Takeuchi, O., Kawai, T., Sanjo, H., Ogawa, T., Takeda, Y., Takeda, K., and Akira, S. (1999). Cutting edge: Toll-like receptor 4 (TLR4)-deficient mice are hyporesponsive to lipopolysaccharide: evidence for TLR4 as the Lps gene product. J. Immunol. *162*, 3749–3752.

Huang, M., and Pittard, J. (1967). Genetic Analysis of Mutant Strains of *Escherichia coli* Requiring p-Aminobenzoic Acid for Growth. J. Bacteriol. *93*, 1938–1942.

Hughes, J.M., Wilson, M.E., Wertheim, H.F.L., Nghia, H.D.T., Taylor, W., and Schultsz, C. (2009). *Streptococcus suis*: An Emerging Human Pathogen. Clin. Infect. Dis. *48*, 617–625.

Humann, J., and Lenz, L.L. (2009). Bacterial peptidoglycan degrading enzymes and their impact on host muropeptide detection. J. Innate Immun. *1*, 88–97.

Ibberson, C.B., Jones, C.L., Singh, S., Wise, M.C., Hart, M.E., Zurawski, D.V., and Horswill, A.R. (2014). *Staphylococcus aureus* hyaluronidase is a CodY-regulated virulence factor. Infect. Immun. *82*, 4253-4256

Ibrahim, H.R., Matsuzaki, T., and Aoki, T. (2001). Genetic evidence that antibacterial activity of lysozyme is independent of its catalytic function. FEBS Lett. *506*, 27–32.

Ip, W.E., Sokolovska, A., Charriere, G.M., Boyer, L., Dejardin, S., Cappillino, M.P., Yantosca, L.M., Takahashi, K., Moore, K.J., Lacy-Hulbert, A., et al. (2010). Phagocytosis and phagosome acidification are required for pathogen processing and MyD88-dependent responses to *Staphylococcus aureus*. J. Immunol. *184*, 7071–7081.

Itsko, M., and Schaaper, R.M. (2011). The dgt gene of *Escherichia coli* facilitates thymine utilization in thymine-requiring strains. Mol. Microbiol. *81*, 1221–1232.

Ivánovics, G., Marjai, E., and Dobozy, A. (1968). The Growth of Purine Mutants of *Bacillus anthracis* in the Body of the Mouse. J. Gen. Microbiol. *53*, 147–162.

Iyer, J.K., and Coggeshall, K.M. (2011). Primary innate immune cells respond efficiently to polymeric peptidoglycan but not to peptidoglycan monomers. J. Immunol. *186*, 3841–3845.

Iyer, J.K., Khurana, T., Langer, M., West, C.M., Ballard, J.D., Metcalf, J.P., Merkel, T.J., and Coggeshall, K.M. (2010). Inflammatory cytokine response to *Bacillus anthracis* peptidoglycan requires phagocytosis and lysosomal trafficking. Infect. Immun. *78*, 2418–2428.

Jackson, A.N., McLure, C.A., Dawkins, R.L., and Keating, P.J. (2007). Mannose binding lectin (MBL) copy number polymorphism in Zebrafish (*D. rerio*) and identification of haplotypes resistant to *L. anguillarum*. Immunogenetics *59*, 861–872.

Jacobs, R.F., and Wilson, C.B. (1983). Intracellular penetration and antimicrobial activity of antibiotics. J. Antimicrob. Chemother. *12*, 13–20.

Jacobson, M.A., Gellermann, H., and Chambers, H. (1988). *Staphylococcus aureus* bacteremia and recurrent staphylococcal infection in patients with acquired immunodeficiency syndrome and AIDS-related complex. Am. J. Med. *85*, 172–176.

James, R.C., and MacLeod, C.J. (1961). Induction of Staphylococcal Infections in Mice with Small Inocula Introduced on Sutures. Br. J. Exp. Pathol. *42*, 266–277.

Janeway, C.A., Travers, P., Walport, M., and Shlomchik, M.J. (2001). The complement system and innate immunity. Garland Science.

Jarraud, S., Mougel, C., Thioulouse, J., Lina, G., Meugnier, H., Forey, F., Nesme, X., Etienne, J., and Vandenesch, F. (2002). Relationships between *Staphylococcus aureus* genetic background, virulence factors, agr groups (alleles), and human disease. Infect. Immun. *70*, 631–641.

Jenkins, A., Diep, B.A., Mai, T.T., Vo, N.H., Warrener, P., Suzich, J., Stover, C.K., and Sellman, B.R. (2015). Differential expression and roles of *Staphylococcus aureus* virulence determinants during colonization and disease. mBio *6*, e02272–02214.

Jiménez, J.N., Ocampo, A.M., Vanegas, J.M., Rodriguez, E.A., Mediavilla, J.R., Chen, L., Muskus, C.E., A. Vélez, L., Rojas, C., Restrepo, A.V., et al. (2012). CC8 MRSA Strains Harboring SCCmec Type IVc are Predominant in Colombian Hospitals. PLoS ONE *7*, e38576.

Johnson, A.P., Aucken, H.M., Cavendish, S., Ganner, M., Wale, M.C.J., Warner, M., Livermore, D.M., Cookson, B.D., and Participants, the U.E. (2001). Dominance of EMRSA-15 and -16 among MRSA causing nosocomial bacteraemia in the UK: analysis of isolates from the European Antimicrobial Resistance Surveillance System (EARSS). J. Antimicrob. Chemother. *48*, 143–144.

Jones, M.J., Donegan, N.P., Mikheyeva, I.V., and Cheung, A.L. (2015). Improving Transformation of *Staphylococcus aureus* Belonging to the CC1, CC5 and CC8 Clonal Complexes. PLoS ONE *10*, e0119487.

Kaech, C., Elzi, L., Sendi, P., Frei, R., Laifer, G., Bassetti, S., and Fluckiger, U. (2006). Course and outcome of *Staphylococcus aureus* bacteraemia: a retrospective analysis of 308 episodes in a Swiss tertiary-care centre. Clin. Microbiol. Infect. *12*, 345–352.

Kahl, B.C., Belling, G., Reichelt, R., Herrmann, M., Proctor, R.A., and Peters, G. (2003). Thymidine-Dependent Small-Colony Variants of *Staphylococcus aureus* Exhibit Gross Morphological and Ultrastructural Changes Consistent with Impaired Cell Separation. J. Clin. Microbiol. *41*, 410–413.

Kaiko, G.E., Horvat, J.C., Beagley, K.W., and Hansbro, P.M. (2008). Immunological decision-making: how does the immune system decide to mount a helper T-cell response? Immunology *123*, 326–338.

Kang, C.I., Song, J.H., Chung, D.R., Peck, K.R., Ko, K.S., Yeom, J.S., Kim, S.W., Chang, H.H., Kim, Y.S., Jung, S.I., et al. (2010). Clinical impact of methicillin resistance on outcome of patients with *Staphylococcus aureus* infection: a stratified analysis according to underlying diseases and sites of infection in a large prospective cohort. J. Infect. *61*, 299–306.

Kaplan, G. (1977). Differences in the mode of phagocytosis with Fc and C3 receptors in macrophages. Scand. J. Immunol. *6*, 797–807.

Kappock, T.J., Ealick, S.E., and Stubbe, J. (2000). Modular evolution of the purine biosynthetic pathway. Curr. Opin. Chem. Biol. *4*, 567–572.

Karauzum, H., and Datta, S.K. (2016). Adaptive Immunity Against *Staphylococcus aureus*. (Springer Berlin Heidelberg).

Kengatharan, K.M., De Kimpe, S., Robson, C., Foster, S.J., and Thiemermann, C. (1998). Mechanism of Gram-positive shock: identification of peptidoglycan and lipoteichoic acid moieties essential in the induction of nitric oxide synthase, shock, and multiple organ failure. J. Exp. Med. *188*, 305–315.

Kennedy, A.D., Otto, M., Braughton, K.R., Whitney, A.R., Chen, L., Mathema, B., Mediavilla, J.R., Byrne, K.A., Parkins, L.D., Tenover, F.C., et al. (2008). Epidemic community-associated methicillin-resistant *Staphylococcus aureus*: Recent clonal expansion and diversification. Proc. Natl. Acad. Sci. *105*, 1327–1332.

Keren, I., Shah, D., Spoering, A., Kaldalu, N., and Lewis, K. (2004). Specialized Persister Cells and the Mechanism of Multidrug Tolerance in *Escherichia coli*. J. Bacteriol. *186*, 8172–8180.

Kielian, T., Barry, B., and Hickey, W.F. (2001). CXC Chemokine Receptor-2 Ligands Are Required for Neutrophil-Mediated Host Defense in Experimental Brain Abscesses. J. Immunol. *166*, 4634–4643.

Kilstrup, M., and Martinussen, J. (1998). A transcriptional activator, homologous to the *Bacillus subtilis* PurR repressor, is required for expression of purine biosynthetic genes in *Lactococcus lactis*. J. Bacteriol. *180*, 3907–3916.

Kim, H.K., Falugi, F., Thomer, L., Missiakas, D.M., and Schneewind, O. (2015). Protein A suppresses immune responses during *Staphylococcus aureus* bloodstream infection in guinea pigs. mBio *6*, e02369-14.

Kim, Y.-G., Kamada, N., Shaw, M.H., Warner, N., Chen, G.Y., Franchi, L., and Núñez, G. (2011). The Nod2 sensor promotes intestinal pathogen eradication via the chemokine CCL2-dependent recruitment of inflammatory monocytes. Immunity *34*, 769–780.

Kimmel, C.B., Ballard, W.W., Kimmel, S.R., Ullmann, B., and Schilling, T.F. (1995). Stages of embryonic development of the zebrafish. Dev. Dyn. *203*, 253–310.

Kimpe, S.J.D., Kengatharan, M., Thiemermann, C., and Vane, J.R. (1995). The cell wall components peptidoglycan and lipoteichoic acid from *Staphylococcus aureus* act in synergy to cause shock and multiple organ failure. Proc. Natl. Acad. Sci. *92*, 10359–10363.

Kimura, Y., Hisano, Y., Kawahara, A., and Higashijima, S. (2014). Efficient generation of knock-in transgenic zebrafish carrying reporter/driver genes by CRISPR/Cas9-mediated genome engineering. Sci. Rep. *4,* 6545.

Kinkel, T.L., Roux, C.M., Dunman, P.M., and Fang, F.C. (2013). The *Staphylococcus aureus* SrrAB two-component system promotes resistance to nitrosative stress and hypoxia. mBio *4*, e00696–00613.

Kirst, H.A., Thompson, D.G., and Nicas, T.I. (1998). Historical Yearly Usage of Vancomycin. Antimicrob. Agents Chemother. *42*, 1303–1304.

Klebanoff, S.J., Kettle, A.J., Rosen, H., Winterbourn, C.C., and Nauseef, W.M. (2013). Myeloperoxidase: a front-line defender against phagocytosed microorganisms. J. Leukoc. Biol. *93*, 185–198.

Klemsz, M.J., McKercher, S.R., Celada, A., Van Beveren, C., and Maki, R.A. (1990). The macrophage and B cell-specific transcription factor PU.1 is related to the ets oncogene. Cell *61*, 113–124.

Knolle, P., Schlaak, J., Uhrig, A., Kempf, P., Meyer zum Büschenfelde, K.H., and Gerken, G. (1995). Human Kupffer cells secrete IL-10 in response to lipopolysaccharide (LPS) challenge. J. Hepatol. *22*, 226–229.

Knop, J., Hanses, F., Leist, T., Archin, N.M., Buchholz, S., Gläsner, J., Gessner, A., and Wege, A.K. (2015). *Staphylococcus aureus* infection in Humanized Mice: a new model to study pathogenicity associated with human immune response. J. Infect. Dis. *212*, 435-344.

Kobayashi, K., Inohara, N., Hernandez, L.D., Galán, J.E., Núñez, G., Janeway, C.A., Medzhitov, R., and Flavell, R.A. (2002). RICK/Rip2/CARDIAK mediates signalling for receptors of the innate and adaptive immune systems. Nature *416*, 194–199.

Kobayashi, S.D., Malachowa, N., and DeLeo, F.R. (2015). Infectious Disease Theme Issue: Pathogenesis of *Staphylococcus aureus* Abscesses. Am. J. Pathol. *185*, 1518–1527.

Kok, F.O., Shin, M., Ni, C.-W., Gupta, A., Grosse, A.S., van Impel, A., Kirchmaier, B.C., Peterson-Maduro, J., Kourkoulis, G., Male, I., et al. (2015). Reverse genetic screening reveals poor correlation between morpholino-induced and mutant phenotypes in zebrafish. Dev. Cell *32*, 97–108.

Kokai-Kun, J.F. (2008). The Cotton Rat as a Model for *Staphylococcus aureus* nasal colonization in humans: cotton rat *S. aureus* nasal colonization model. Methods Mol. Biol. *431*, 241–254.

Kokai-Kun, J.F., Walsh, S.M., Chanturiya, T., and Mond, J.J. (2003). Lysostaphin Cream Eradicates *Staphylococcus aureus* Nasal Colonization in a Cotton Rat Model. Antimicrob. Agents Chemother. *47*, 1589–1597.

Kolaczkowska, E., Jenne, C.N., Surewaard, B.G.J., Thanabalasuriar, A., Lee, W.-Y., Sanz, M.-J., Mowen, K., Opdenakker, G., and Kubes, P. (2015). Molecular mechanisms of NET formation and degradation revealed by intravital imaging in the liver vasculature. Nat. Commun. *6*, 6673.

Kolar, S.L., Antonio Ibarra, J., Rivera, F.E., Mootz, J.M., Davenport, J.E., Stevens, S.M., Horswill, A.R., and Shaw, L.N. (2013). Extracellular proteases are key mediators of *Staphylococcus aureus* virulence via the global modulation of virulence-determinant stability. Microbiology. *2*, 18–34.

Kornblum, J., Hartman, B.J., Novick, R.P., and Tomasz, A. (1986). Conversion of a homogeneously methicillin-resistant strain of *Staphylococcus aureus* to heterogeneous resistance by Tn551-mediated insertional inactivation. Eur. J. Clin. Microbiol. *5*, 714–718.

Köser, C.U., Holden, M.T., Ellington, M.J., Cartwright, E.J., Brown, N.M., Ogilvy-Stuart, A.L., Hsu, L.Y., Chewapreecha, C., Croucher, N.J., and Harris, S.R. (2012). Rapid whole-genome sequencing for investigation of a neonatal MRSA outbreak. N. Engl. J. Med. *366*, 2267–2275.

Kovacs-Simon, A., Titball, R.W., and Michell, S.L. (2011). Lipoproteins of Bacterial Pathogens. Infect. Immun. *79*, 548–561.

Koziel, J., Maciag-Gudowska, A., Mikolajczyk, T., Bzowska, M., Sturdevant, D.E., Whitney, A.R., Shaw, L.N., DeLeo, F.R., and Potempa, J. (2009). Phagocytosis of *Staphylococcus aureus* by Macrophages Exerts Cytoprotective Effects Manifested by the Upregulation of Antiapoptotic Factors. PLoS ONE *4*, e5210.

Kreiswirth, B., Löfdahl, S., Betley, M.J., O'Reilly, M., Schlievert, P.M., Bergdoll, M.S., and Novick, R.P. (1983). The toxic shock syndrome exotoxin structural gene is not detectably transmitted by a prophage. Nature *305*, 709–712.

Kriegeskorte, A., Block, D., Drescher, M., Windmüller, N., Mellmann, A., Baum, C., Neumann, C., Lorè, N.I., Bragonzi, A., Liebau, E., et al. (2014). Inactivation of *thyA* in *Staphylococcus aureus* Attenuates Virulence and Has a Strong Impact on Metabolism and Virulence Gene Expression. mBio *5, e01447-14*.

Kriegeskorte, A., Lorè, N.I., Bragonzi, A., Riva, C., Kelkenberg, M., Becker, K., Proctor, R.A., Peters, G., and Kahl, B.C. (2015). Thymidine-Dependent *Staphylococcus aureus* Small-Colony Variants Are Induced by Trimethoprim-Sulfamethoxazole (SXT) and Have Increased Fitness during SXT Challenge. Antimicrob. Agents Chemother. *59*, 7265–7272.

Krismer, B., Liebeke, M., Janek, D., Nega, M., Rautenberg, M., Hornig, G., Unger, C., Weidenmaier, C., Lalk, M., and Peschel, A. (2014). Nutrient Limitation Governs *Staphylococcus aureus* Metabolism and Niche Adaptation in the Human Nose. PLoS Pathog *10*, e1003862.

Kronforst, K.D., Mancuso, C.J., Pettengill, M., Ninkovic, J., Coombs, M.R.P., Stevens, C., Otto, M., Mallard, C., Wang, X., Goldmann, D., et al. (2012). A Neonatal Model of Intravenous *Staphylococcus epidermidis* Infection in Mice at 24hr Old Enables Characterization of Early Innate Immune Responses. PLOS ONE *7*, e43897.

Kubica, M., Guzik, K., Koziel, J., Zarebski, M., Richter, W., Gajkowska, B., Golda, A., Maciag-Gudowska, A., Brix, K., Shaw, L., et al. (2008). A Potential New Pathway for *Staphylococcus aureus* Dissemination: The Silent Survival of *S. aureus* Phagocytosed by Human Monocyte-Derived Macrophages. PLoS ONE *3*, e1409.

Kuklin, N.A., Clark, D.J., Secore, S., Cook, J., Cope, L.D., McNeely, T., Noble, L., Brown, M.J., Zorman, J.K., Wang, X.M., et al. (2006). A Novel *Staphylococcus aureus* Vaccine: Iron Surface Determinant B Induces Rapid Antibody Responses in Rhesus Macaques and Specific Increased Survival in a Murine *S. aureus* Sepsis Model. Infect. Immun. *74*, 2215–2223.

Kuroda, M., Ohta, T., Uchiyama, I., Baba, T., Yuzawa, H., Kobayashi, I., Cui, L., Oguchi, A., Aoki, K., Nagai, Y., et al. (2001). Whole genome sequencing of meticillin-resistant *Staphylococcus aureus*. The Lancet *357*, 1225–1240.

Laabei, M., Recker, M., Rudkin, J.K., Aldeljawi, M., Gulay, Z., Sloan, T.J., Williams, P., Endres, J.L., Bayles, K.W., Fey, P.D., et al. (2014). Predicting the virulence of MRSA from its genome sequence. Genome Res. *24*, 839–849.

Laborel-Préneron, E., Bianchi, P., Boralevi, F., Lehours, P., Fraysse, F., Morice-Picard, F., Sugai, M., Sato'o, Y., Badiou, C., Lina, G., et al. (2015). Effects of the *Staphylococcus aureus* and *Staphylococcus epidermidis* Secretomes Isolated from the Skin Microbiota of Atopic Children on CD4 + T Cell Activation. PLOS ONE *10*, e0141067.

Lacey, R.W. (1975). Antibiotic resistance plasmids of *Staphylococcus aureus* and their clinical importance. Bacteriol. Rev. *39*, 1–32.

Laing, K.J., Purcell, M.K., Winton, J.R., and Hansen, J.D. (2008). A genomic view of the NOD-like receptor family in teleost fish: identification of a novel NLR subfamily in zebrafish. BMC Evol. Biol. *8*, 42.

Lam, S.H., Chua, H.L., Gong, Z., Lam, T.J., and Sin, Y.M. (2004). Development and maturation of the immune system in zebrafish, *Danio rerio*: a gene expression profiling, in situ hybridization and immunological study. Dev. Comp. Immunol. *28*, 9–28.

Lamagni, T.L., Potz, N., Powell, D., Pebody, R., Wilson, J., and Duckworth, G. (2011). Mortality in patients with meticillin-resistant *Staphylococcus aureus* bacteraemia, England 2004-2005. J. Hosp. Infect. *77*, 16–20.

Lambein, L. (2015). An *in vivo* anti-staphylococcal drug screen using a zebrafish infection model implicates host autophagy in *Staphylococcus aureus* survival. PhD thesis, University of Sheffield.

Lambert, P.A., Worthington, T., Tebbs, S.E., and Elliott, T.S. (2000). Lipid S, a novel *Staphylococcus epidermidis* exocellular antigen with potential for the serodiagnosis of infections. FEMS Immunol. Med. Microbiol. *29*, 195–202.

Lamkanfi, M., Malireddi, R.K.S., and Kanneganti, T.-D. (2009). Fungal zymosan and mannan activate the cryopyrin inflammasome. J. Biol. Chem. *284*, 20574–20581.

Lan, L., Cheng, A., Dunman, P.M., Missiakas, D., and He, C. (2010). Golden Pigment Production and Virulence Gene Expression Are Affected by Metabolisms in *Staphylococcus aureus*. J. Bacteriol. *192*, 3068–3077.

Land, A.D., Hogan, P., Fritz, S., and Levin, P.A. (2015). Phenotypic Variation Is Almost Entirely Independent of the Host-Pathogen Relationship in Clinical Isolates of *S. aureus*. PLoS ONE *10*, e0129670.

Lanza, F. (1998). Clinical manifestation of myeloperoxidase deficiency. J. Mol. Med. *76*, 676–681.

Laupland, K.B., Ross, T., and Gregson, D.B. (2008). *Staphylococcus aureus* bloodstream infections: risk factors, outcomes, and the influence of methicillin resistance in Calgary, Canada, 2000-2006. J. Infect. Dis. *198*, 336–343.

Lautt, W.W. (2009). Hepatic Circulation: Physiology and Pathophysiology (Morgan & Claypool Life Sciences).

Lee, C.Y., and Iandolo, J.J. (1986). Integration of staphylococcal phage L54a occurs by site-specific recombination: structural analysis of the attachment sites. Proc. Natl. Acad. Sci. *83*, 5474–5478.

Lee, L.Y.L., Höök, M., Haviland, D., Wetsel, R.A., Yonter, E.O., Syribeys, P., Vernachio, J., and Brown, E.L. (2004). Inhibition of Complement Activation by a Secreted *Staphylococcus aureus* Protein. J. Infect. Dis. *190*, 571–579.

Lehar, S.M., Pillow, T., Xu, M., Staben, L., Kajihara, K.K., Vandlen, R., DePalatis, L., Raab, H., Hazenbos, W.L., Hiroshi Morisaki, J., et al. (2015). Novel antibody–antibiotic conjugate eliminates intracellular *S. aureus*. Nature *527*, 323–328.

de Lencastre, H., Sa Figueiredo, A.M., Urban, C., Rahal, J., and Tomasz, A. (1991). Multiple mechanisms of methicillin resistance and improved methods for detection in clinical isolates of *Staphylococcus aureus*. Antimicrob. Agents Chemother. *35*, 632–639.

Li, D., and Cheung, A. (2008). Repression of *hla* by *rot* Is Dependent on *sae* in *Staphylococcus aureus*. Infect. Immun. *76*, 1068–1075.

Liang, X., Yu, C., Sun, J., Liu, H., Landwehr, C., Holmes, D., and Ji, Y. (2006). Inactivation of a Two-Component Signal Transduction System, SaeRS, Eliminates Adherence and Attenuates Virulence of *Staphylococcus aureus*. Infect. Immun. *74*, 4655–4665.

Liechti, G.W., and Goldberg, J.B. (2013). *Helicobacter pylori* Salvages Purines from Extracellular Host Cell DNA Utilizing the Outer Membrane-Associated Nuclease NucT. J. Bacteriol. *195*, 4387–4398.

Lieschke, G.J., Oates, A.C., Crowhurst, M.O., Ward, A.C., and Layton, J.E. (2001). Morphologic and functional characterization of granulocytes and macrophages in embryonic and adult zebrafish. Blood *98*, 3087–3096.

Lim, C.H., Voedisch, S., Wahl, B., Rouf, S.F., Geffers, R., Rhen, M., and Pabst, O. (2014). Independent bottlenecks characterize colonization of systemic compartments and gut lymphoid tissue by *Salmonella*. PLoS Pathog. *10*, e1004270.

Lin, H., and Everse, J. (1987). The cytotoxic activity of hematoheme: evidence for two different mechanisms. Anal. Biochem. *161*, 323–331.

Lin, L., Ibrahim, A.S., Xu, X., Farber, J.M., Avanesian, V., Baquir, B., Fu, Y., French, S.W., Edwards, J.E., and Spellberg, B. (2009). Th1-Th17 cells mediate protective adaptive immunity against *Staphylococcus aureus* and *Candida albicans* infection in mice. PLoS Pathog. *5*, e1000703.

Lindsay, J.A. (2008). *Staphylococcus*: Molecular Genetics (Horizon Scientific Press).

Lindsay, J.A., and Holden, M.T.G. (2004). *Staphylococcus aureus*: superbug, super genome? Trends Microbiol. *12*, 378–385.

Lindsay, J.A., Moore, C.E., Day, N.P., Peacock, S.J., Witney, A.A., Stabler, R.A., Husain, S.E., Butcher, P.D., and Hinds, J. (2006). Microarrays Reveal that Each of the Ten Dominant Lineages of *Staphylococcus aureus* Has a Unique Combination of Surface-Associated and Regulatory Genes. J. Bacteriol. *188*, 669–676.

Lister, J.A., Robertson, C.P., Lepage, T., Johnson, S.L., and Raible, D.W. (1999). *nacre* encodes a zebrafish microphthalmia-related protein that regulates neural-crest-derived pigment cell fate. Dev. *126*, 3757–3767.

Liu, C., and Chambers, H.F. (2003). *Staphylococcus aureus* with heterogeneous resistance to vancomycin: epidemiology, clinical significance, and critical assessment of diagnostic methods. Antimicrob. Agents Chemother. *47*, 3040–3045.

Liu, G.Y., Essex, A., Buchanan, J.T., Datta, V., Hoffman, H.M., Bastian, J.F., Fierer, J., and Nizet, V. (2005). *Staphylococcus aureus* golden pigment impairs neutrophil killing and promotes virulence through its antioxidant activity. J. Exp. Med. *202*, 209–215.

Liu, Z.Q., Deng, G.M., Foster, S., and Tarkowski, A. (2001). Staphylococcal peptidoglycans induce arthritis. Arthritis Res. *3*, 375–380.

Lo, C.-W., Lai, Y.-K., Liu, Y.-T., Gallo, R.L., and Huang, C.-M. (2011). *Staphylococcus aureus* Hijacks a Skin Commensal to Intensify Its Virulence: Immunization Targeting β-Hemolysin and CAMP Factor. J. Invest. Dermatol. *131*, 401–409.

Loffler, B., Hussain, M., Grundmeier, M., Bruck, M., Holzinger, D., Varga, G., Roth, J., Kahl, B.C., Proctor, R.A., and Peters, G. (2010). *Staphylococcus aureus* Panton-

Valentine Leukocidin Is a Very Potent Cytotoxic Factor for Human Neutrophils. PLoS Pathog. *6,* e1000715.

Lorenz, U., Ohlsen, K., Karch, H., Hecker, M., Thiede, A., and Hacker, J. (2000). Human antibody response during sepsis against targets expressed by methicillin resistant *Staphylococcus aureus*. FEMS Immunol. Med. Microbiol. *29*, 145–153.

Lowy, F.D. (1998). *Staphylococcus aureus* infections. N. Engl. J. Med. *339*, 520–532.

Lugo-Villarino, G., Balla, K.M., Stachura, D.L., Bañuelos, K., Werneck, M.B.F., and Traver, D. (2010). Identification of dendritic antigen-presenting cells in the zebrafish. Proc. Natl. Acad. Sci. *107*, 15850–15855.

Lysenko, E.S., Ratner, A.J., Nelson, A.L., and Weiser, J.N. (2005). The role of innate immune responses in the outcome of interspecies competition for colonization of mucosal surfaces. PLoS Pathog. *1*, e1.

Mackey-Lawrence, N.M., and Jefferson, K.K. (2013). Regulation of *Staphylococcus aureus* immunodominant antigen B (IsaB). Microbiol. Res. *168*, 113–118.

Mackey-Lawrence, N.M., Potter, D.E., Cerca, N., and Jefferson, K.K. (2009). *Staphylococcus aureus* immunodominant surface antigen B is a cell-surface associated nucleic acid binding protein. BMC Microbiol. *9*, 61.

MacLeod, M.K., Kappler, J.W., and Marrack, P. (2010). Memory CD4 T cells: generation, reactivation and re-assignment. Immunology *130*, 10–15.

Maddatu, T.P., Grubb, S.C., Bult, C.J., and Bogue, M.A. (2012). Mouse Phenome Database (MPD). Nucleic Acids Res. *40*, D887–D894.

Maguin, E., Duwat, P., Hege, T., Ehrlich, D., and Gruss, A. (1992). New thermosensitive plasmid for Gram-positive bacteria. J. Bacteriol. *174*, 5633–5638.

Mahan, M.J., Slauch, J.M., and Mekalanos, J.J. (1993). Selection of bacterial virulence genes that are specifically induced in host tissues. Science *259*, 686–688.

Maier, L., Diard, M., Sellin, M.E., Chouffane, E.-S., Trautwein-Weidner, K., Periaswamy, B., Slack, E., Dolowschiak, T., Stecher, B., Loverdo, C., et al. (2014). Granulocytes impose a tight bottleneck upon the gut luminal pathogen population during *Salmonella Typhimurium* colitis. PLoS Pathog. *10*, e1004557.

Mainiero, M., Goerke, C., Geiger, T., Gonser, C., Herbert, S., and Wolz, C. (2010). Differential Target Gene Activation by the *Staphylococcus aureus* Two-Component System *saeRS*. J. Bacteriol. *192*, 613–623.

Malachowa, N., Whitney, A.R., Kobayashi, S.D., Sturdevant, D.E., Kennedy, A.D., Braughton, K.R., Shabb, D.W., Diep, B.A., Chambers, H.F., Otto, M., et al. (2011). Global Changes in *Staphylococcus aureus* Gene Expression in Human Blood. PLoS ONE *6*, e18617.

Malone, C.L., Boles, B.R., Lauderdale, K.J., Thoendel, M., Kavanaugh, J.S., and Horswill, A.R. (2009). Fluorescent Reporters for *Staphylococcus aureus*. J. Microbiol. Methods *77*, 251–260.

Mantena, R.K.R., Wijburg, O.L.C., Vindurampulle, C., Bennett-Wood, V.R., Walduck, A., Drummond, G.R., Davies, J.K., Robins-Browne, R.M., and Strugnell, R.A. (2008). Reactive oxygen species are the major antibacterials against *Salmonella Typhimurium* purine auxotrophs in the phagosome of RAW 264.7 cells. Cell. Microbiol. *10*, 1058–1073.

Mantovani, B. (1975). Different roles of IgG and complement receptors in phagocytosis by polymorphonuclear leukocytes. J. Immunol. *115*, 15–17.

Martinon, F., Agostini, L., Meylan, E., and Tschopp, J. (2004). Identification of Bacterial Muramyl Dipeptide as Activator of the NALP3/Cryopyrin Inflammasome. Curr. Biol. *14*, 1929–1934.

Mashburn, L.M., Jett, A.M., Akins, D.R., and Whiteley, M. (2005). *Staphylococcus aureus* Serves as an Iron Source for *Pseudomonas aeruginosa* during *In vivo* Coculture. J. Bacteriol. *187*, 554–566.

Massaro, E.J., and Rogers, J.M. (2002). Folate and Human Development (Springer Science & Business Media).

Massey, R.C., Kantzanou, M.N., Fowler, T., Day, N.P., Schofield, K., Wann, E.R., Berendt, A.R., Höök, M., and Peacock, S.J. (2001). Fibronectin-binding protein A of *Staphylococcus aureus* has multiple, substituting, binding regions that mediate adherence to fibronectin and invasion of endothelial cells. Cell. Microbiol. *3*, 839–851.

Matalon, A. (2012). Efficacy profile of a bivalent *Staphylococcus aureus* glycoconjugate investigational vaccine in adults on haemodialysis: phase III randomized study. Int. Symp. Staphylococci Staphylococcal Infect. Lyon.

Mathieu, L.G., de Repentigny, J., Turgeon, S., and Sonea, S. (1968). Thymineless death of *Staphylococcus aureus* and formation of its alpha toxin. Can. J. Microbiol. *14*, 983–987.

Matsuura, K., Asano, Y., Yamada, A., and Naruse, K. (2013). Detection of *Micrococcus luteus* Biofilm Formation in Microfluidic Environments by pH Measurement Using an Ion-Sensitive Field-Effect Transistor. Sensors *13*, 2484–2493.

May, R.C., and Machesky, L.M. (2001). Phagocytosis and the actin cytoskeleton. J. Cell Sci. *114*, 1061–1077.

McCarthy, A.J., and Lindsay, J.A. (2010). Genetic variation in *Staphylococcus aureus* surface and immune evasion genes is lineage associated: implications for vaccine design and host-pathogen interactions. BMC Microbiol. *10*, 173.

McCarthy, A.J., Loeffler, A., Witney, A.A., Gould, K.A., Lloyd, D.H., and Lindsay, J.A. (2014). Extensive horizontal gene transfer during *Staphylococcus aureus* co-colonization *in vivo*. Genome Biol. Evol. *6*, 2697–2708.

McDevitt, D., Francois, P., Vaudaux, P., and Foster, T.J. (1994). Molecular characterization of the clumping factor (fibrinogen receptor) of *Staphylococcus aureus*. Mol. Microbiol. *11*, 237–248.

McDonald, C., Inohara, N., and Nuñez, G. (2005). Peptidoglycan Signaling in Innate Immunity and Inflammatory Disease. J. Biol. Chem. *280*, 20177–20180.

McFarland, W.C., and Stocker, B.A. (1987). Effect of different purine auxotrophic mutations on mouse-virulence of a Vi-positive strain of *Salmonella dublin* and of two strains of *Salmonella Typhimurium*. Microb. Pathog. *3*, 129–141.

McKercher, S.R., Torbett, B.E., Anderson, K.L., Henkel, G.W., Vestal, D.J., Baribault, H., Klemsz, M., Feeney, A.J., Wu, G.E., Paige, C.J., et al. (1996). Targeted disruption of the PU.1 gene results in multiple hematopoietic abnormalities. EMBO J. *15*, 5647–5658.

McVicker, G., Prajsnar, T.K., Williams, A., Wagner, N.L., Boots, M., Renshaw, S.A., and Foster, S.J. (2014). Clonal Expansion during *Staphylococcus aureus* Infection Dynamics Reveals the Effect of Antibiotic Intervention. PLoS Pathog. *10*, e1003959.

Mei, J.M., Nourbakhsh, F., Ford, C.W., and Holden, D.W. (1997). Identification of *Staphylococcus aureus* virulence genes in a murine model of bacteraemia using signature-tagged mutagenesis. Mol. Microbiol. *26*, 399–407.

Menzies, B.E., Kourteva, Y., Kaiser, A.B., and Kernodle, D.S. (2002). Inhibition of staphylococcal wound infection and potentiation of antibiotic prophylaxis by a recombinant fragment of the fibronectin-binding protein of *Staphylococcus aureus*. J. Infect. Dis. *185*, 937–943.

Mesnage, S., Dellarole, M., Baxter, N.J., Rouget, J.-B., Dimitrov, J.D., Wang, N., Fujimoto, Y., Hounslow, A.M., Lacroix-Desmazes, S., Fukase, K., et al. (2014). Molecular basis for bacterial peptidoglycan recognition by LysM domains. Nat. Commun. *5*, 4269.

Metzker, M.L. (2010). Sequencing technologies — the next generation. Nat. Rev. Genet. *11*, 31–46.

Meynell, G.G., and Stocker, B.A. (1957). Some hypotheses on the aetiology of fatal infections in partially resistant hosts and their application to mice challenged with *Salmonella paratyphi-B* or *Salmonella Typhimurium* by intraperitoneal injection. J. Gen. Microbiol. *16*, 38–58.

Michael, J.G., and Massell, B.F. (1962). Factors involved in the induction of non-specific resistance to streptococcal infection in mice by endotoxin. J. Exp. Med. *116*, 101–107.

Michelsen, C., Hossein Khademi, S.M., Krogh Johansen, H., Ingmer, H., Dorrestein, P.C., and Jelsbak, L. (2016). Evolution of metabolic divergence in *Pseudomonas aeruginosa* during long-term infection facilitates a proto-cooperative interspecies interaction. ISME J. *10***,** 1323–1336.

Miller, L.S., and Cho, J.S. (2011). Immunity against *Staphylococcus aureus* cutaneous infections. Nat. Rev. Immunol. *11*, 505–518.

Miller, R.R., Walker, A.S., Godwin, H., Fung, R., Votintseva, A., Bowden, R., Mant, D., Peto, T.E.A., Crook, D.W., and Knox, K. (2014). Dynamics of acquisition and loss of carriage of *Staphylococcus aureus* strains in the community: The effect of clonal complex. J. Infect. *68*, 426-439.

Mitragotri, S., and Lahann, J. (2009). Physical approaches to biomaterial design. Nat. Mater. *8*, 15–23.

Modun, B.J., Cockayne, A., Finch, R., and Williams, P. (1998). The *Staphylococcus aureus* and *Staphylococcus epidermidis* transferrin-binding proteins are expressed *in vivo* during infection. Microbiol. Read. Engl. *144*, 1005–1012.

Mody, L., Kauffman, C.A., McNeil, S.A., Galecki, A.T., and Bradley, S.F. (2003). Mupirocin-Based Decolonization of *Staphylococcus aureus* Carriers in Residents of 2 Long-Term Care Facilities: A Randomized, Double-Blind, Placebo-Controlled Trial. Clin. Infect. Dis. Off. Publ. Infect. Dis. Soc. Am. *37*, 1467–1474.

Mogensen, T.H. (2009). Pathogen Recognition and Inflammatory Signaling in Innate Immune Defenses. Clin. Microbiol. Rev. *22*, 240–273.

Monecke, S., Coombs, G., Shore, A.C., Coleman, D.C., Akpaka, P., Borg, M., Chow, H., Ip, M., Jatzwauk, L., Jonas, D., et al. (2011). A Field Guide to Pandemic, Epidemic and Sporadic Clones of Methicillin-Resistant *Staphylococcus aureus*. PLoS ONE *6*, e17936.

Monk, I.R. (2012). Genetic manipulation of Staphylococci—breaking through the barrier. Front. Cell. Infect. Microbiol. *2*, 49.

Monk, I.R., Shah, I.M., Xu, M., Tan, M.-W., and Foster, T.J. (2012). Transforming the Untransformable: Application of Direct Transformation To Manipulate Genetically *Staphylococcus aureus* and *Staphylococcus epidermidis*. mBio *3*, e00277.

Monk, I.R., Tree, J.J., Howden, B.P., Stinear, T.P., and Foster, T.J. (2015). Complete Bypass of Restriction Systems for Major *Staphylococcus aureus* Lineages. mBio *6*, e00308–e00315.

Monodane, T., Kawabata, Y., and Takada, H. (1997). *Micrococcus luteus* cells and cell walls induce anaphylactoid reactions accompanied by early death and serum cytokines in mice primed with muramyl dipeptide. FEMS Immunol. Med. Microbiol. *17*, 49–55.

Montgomery, C.P., Daniels, M., Zhao, F., Alegre, M.-L., Chong, A.S., and Daum, R.S. (2014). Protective immunity against recurrent *Staphylococcus aureus* skin infection requires antibody and interleukin-17A. Infect. Immun. *82*, 2125–2134.

Morrison, J.M., Anderson, K.L., Beenken, K.E., Smeltzer, M.S., and Dunman, P.M. (2012). The staphylococcal accessory regulator, SarA, is an RNA-binding protein that modulates the mRNA turnover properties of late-exponential and stationary phase *Staphylococcus aureus* cells. Front. Cell. Infect. Microbiol. *2*, 26.

Mouse Genome Sequencing Consortium, Waterston, R.H., Lindblad-Toh, K., Birney, E., Rogers, J., Abril, J.F., Agarwal, P., Agarwala, R., Ainscough, R., Alexandersson, M., et al. (2002). Initial sequencing and comparative analysis of the mouse genome. Nature *420*, 520–562.

Movita, D., Kreefft, K., Biesta, P., van Oudenaren, A., Leenen, P.J.M., Janssen, H.L.A., and Boonstra, A. (2012). Kupffer cells express a unique combination of phenotypic and functional characteristics compared with splenic and peritoneal macrophages. J. Leukoc. Biol. *92*, 723–733.

Moxon, E.R., and Murphy, P.A. (1978). *Haemophilus influenzae* bacteremia and meningitis resulting from survival of a single organism. Proc. Natl. Acad. Sci. *75*, 1534–1536.

Mulcahy, L.R., Burns, J.L., Lory, S., and Lewis, K. (2010). Emergence of *Pseudomonas aeruginosa* strains producing high levels of persister cells in patients with cystic fibrosis. J. Bacteriol. *192*, 6191–6199.

Murphy, A.G., O'Keeffe, K.M., Lalor, S.J., Maher, B.M., Mills, K.H.G., and McLoughlin, R.M. (2014). *Staphylococcus aureus* Infection of Mice Expands a Population of Memory γδ T Cells That Are Protective against Subsequent Infection. J. Immunol. *192*, 3697–3708.

Murray, N.E. (2000). Type I restriction systems: sophisticated molecular machines (a legacy of Bertani and Weigle). Microbiol. Mol. Biol. Rev. *64*, 412–434.

Myhre, A.E., Stuestøl, J.F., Dahle, M.K., Øverland, G., Thiemermann, C., Foster, S.J., Lilleaasen, P., Aasen, A.O., and Wang, J.E. (2004a). Organ Injury and Cytokine Release Caused by Peptidoglycan Are Dependent on the Structural Integrity of the Glycan Chain. Infect. Immun. *72*, 1311–1317.

Naber, C.K. (2009). *Staphylococcus aureus* Bacteremia: Epidemiology, Pathophysiology, and Management Strategies. Clin. Infect. Dis. *48*, S231–S237.

Naik, S., Bouladoux, N., Linehan, J.L., Han, S.-J., Harrison, O.J., Wilhelm, C., Conlan, S., Himmelfarb, S., Byrd, A.L., Deming, C., et al. (2015). Commensal-dendritic-cell interaction specifies a unique protective skin immune signature. Nature *520*, 104–108.

Nair, D., Memmi, G., Hernandez, D., Bard, J., Beaume, M., Gill, S., Francois, P., and Cheung, A.L. (2011). Whole-genome sequencing of *Staphylococcus aureus* strain RN4220, a key laboratory strain used in virulence research, identifies mutations that affect not only virulence factors but also the fitness of the strain. J. Bacteriol. *193*, 2332–2335.

Nakane, A., Okamoto, M., Asano, M., Kohanawa, M., and Minagawa, T. (1995). Endogenous gamma interferon, tumor necrosis factor, and interleukin-6 in *Staphylococcus aureus* infection in mice. Infect. Immun. *63*, 1165–1172.

Needham, A.J., Kibart, M., Crossley, H., Ingham, P.W., and Foster, S.J. (2004). *Drosophila melanogaster* as a model host for *Staphylococcus aureus* infection. Microbiol. *150*, 2347–2355.

Nelson, C.L., Pelak, K., Podgoreanu, M.V., Ahn, S.H., Scott, W.K., Allen, A.S., Cowell, L.G., Rude, T.H., Zhang, Y., Tong, A., et al. (2014). A genome-wide association study of variants associated with acquisition of *Staphylococcus aureus* bacteremia in a healthcare setting. BMC Infect. Dis. *14*, 83.

Nelson, J.A., Carpenter, J.W., Rose, L.M., and Adamson, D.J. (1975). Mechanisms of action of 6-thioguanine, 6-mercaptopurine, and 8-azaguanine. Cancer Res. *35*, 2872–2878.

Neth, O., Jack, D.L., Johnson, M., Klein, N.J., and Turner, M.W. (2002). Enhancement of Complement Activation and Opsonophagocytosis by Complexes of Mannose-Binding Lectin with Mannose-Binding Lectin-Associated Serine Protease After Binding to *Staphylococcus aureus*. J. Immunol. *169*, 4430–4436.

Neu, H.C., and Gootz, T.D. (1996). Antimicrobial Chemotherapy. In Medical Microbiology, S. Baron, ed. University of Texas Medical Branch at Galveston).

Ng, Y.H., Rome, S., Jalabert, A., Forterre, A., Singh, H., Hincks, C.L., and Salamonsen, L.A. (2013). Endometrial Exosomes/Microvesicles in the Uterine Microenvironment: A New Paradigm for Embryo-Endometrial Cross Talk at Implantation. PLoS ONE *8*, e58502.

Nielsen, A., Månsson, M., Bojer, M.S., Gram, L., Larsen, T.O., Novick, R.P., Frees, D., Frøkiær, H., and Ingmer, H. (2014). Solonamide B inhibits quorum sensing and reduces *Staphylococcus aureus* mediated killing of human neutrophils. PloS One *9*, e84992.

Nilsson, I.M., Bremell, T., Rydén, C., Cheung, A.L., and Tarkowski, A. (1996). Role of the staphylococcal accessory gene regulator (*sar*) in septic arthritis. Infect. Immun. *64*, 4438–4443.

Nippe, N., Varga, G., Holzinger, D., Löffler, B., Medina, E., Becker, K., Roth, J., Ehrchen, J.M., and Sunderkötter, C. (2011). Subcutaneous Infection with *S. aureus* in Mice Reveals Association of Resistance with Influx of Neutrophils and Th2 Response. J. Invest. Dermatol. *131*, 125–132.

Noble, W.C., and Pitcher, D.G. (1978). Microbial Ecology of the Human Skin. Adv Microb Ecol. 245–289.

Nordenfelt, P., and Tapper, H. (2011). Phagosome dynamics during phagocytosis by neutrophils. J. Leukoc. Biol. *90*, 271–284.

Nottebrock, H., and Then, R. (1977). Thymidine concentrations in serum and urine of different animal species and man. Biochem. Pharmacol. *26*, 2175–2179.

Nouwen, J., Boelens, H., Belkum, A. van, and Verbrugh, H. (2004a). Human Factor in *Staphylococcus aureus* Nasal Carriage. Infect. Immun. *72*, 6685–6688.

Nouwen, J., Ott, A., Kluytmans-Vandenbergh, M.F.Q., Boelens, H.A.M., Hofman, A., van Belkum, A., and Verbrugh, H.A. (2004b). Predicting the *Staphylococcus aureus* nasal carrier state: derivation and validation of a “culture rule.” Clin. Infect. Dis. Off. Publ. Infect. Dis. Soc. Am. *39*, 806–811.

Novick, R. (1967). Properties of a cryptic high-frequency transducing phage in *Staphylococcus aureus*. Virology *33*, 155–166.

Novick, R.P. (1991). Genetic systems in staphylococci. Methods Enzymol. *204*, 587–636.

Novick, R.P., Ross, H.F., Projan, S.J., Kornblum, J., Kreiswirth, B., and Moghazeh, S. (1993). Synthesis of staphylococcal virulence factors is controlled by a regulatory RNA molecule. EMBO J. *12*, 3967–3975.

Nunoshiba, T., DeRojas-Walker, T., Tannenbaum, S.R., and Demple, B. (1995). Roles of nitric oxide in inducible resistance of *Escherichia coli* to activated murine macrophages. Infect. Immun. *63*, 794–798.

Nusslein-Volhard, C., and Dahm, R. (2002). Zebrafish. A Practical Approach (New York: Oxford University Press).

Nüsslein-Volhard, C., and Wieschaus, E. (1980). Mutations affecting segment number and polarity in Drosophila. Nature *287*, 795–801.

O'Callaghan, D., Maskell, D., Liew, F.Y., Easmon, C.S., and Dougan, G. (1988). Characterization of aromatic- and purine-dependent *Salmonella Typhimurium*: attention, persistence, and ability to induce protective immunity in BALB/c mice. Infect. Immun. *56*, 419–423.

Oehlers, S.H., Flores, M.V., Hall, C.J., Swift, S., Crosier, K.E., and Crosier, P.S. (2011). The inflammatory bowel disease (IBD) susceptibility genes NOD1 and NOD2 have conserved anti-bacterial roles in zebrafish. Dis. Model. Mech. *4*, 832–841.

Ohno, N., Yadomae, T., and Miyazaki, T. (1982). Identification of 2-amino-2-deoxyglucose residues in the peptidoglucan of *Streptococcus pneumoniae*. Carbohydr. Res. *107*, 152–155.

Olitzki, L. (1948). Mucin as a resistance-lowering substance. Bacteriol. Rev. *12*, 149–172.

Olsen, R.J., Sitkiewicz, I., Ayeras, A.A., Gonulal, V.E., Cantu, C., Beres, S.B., Green, N.M., Lei, B., Humbird, T., Greaver, J., et al. (2010). Decreased necrotizing fasciitis capacity caused by a single nucleotide mutation that alters a multiple gene virulence axis. Proc. Natl. Acad. Sci. *107*, 888–893.

O'Neill, A.J. (2010). *Staphylococcus aureus* SH1000 and 8325-4: comparative genome sequences of key laboratory strains in staphylococcal research. Lett. Appl. Microbiol. *51*, 358–361.

O'Neill, L.A.J., Golenbock, D., and Bowie, A.G. (2013). The history of Toll-like receptors — redefining innate immunity. Nat. Rev. Immunol. *13*, 453–460.

Ostaff, M.J., Stange, E.F., and Wehkamp, J. (2013). Antimicrobial peptides and gut microbiota in homeostasis and pathology. EMBO Mol. Med. *5*, 1465–1483.

Ostrer, L., Hamann, B.L., and Khodursky, A. (2015). Perturbed states of the bacterial chromosome: a thymineless death case study. Front. Microbiol. *6*, 363.

Otto, M. (2009). *Staphylococcus epidermidis* – the "accidental" pathogen. Nat. Rev. Microbiol. *7*, 555–567.

Otto, M. (2012). Molecular basis of *Staphylococcus epidermidis* infections. Semin. Immunopathol. *34*, 201–214.

Palić, D., Andreasen, C.B., Ostojić, J., Tell, R.M., and Roth, J.A. (2007). Zebrafish (*Danio rerio*) whole kidney assays to measure neutrophil extracellular trap release and degranulation of primary granules. J. Immunol. Methods *319*, 87–97.

Parfentjev, I.A., and Catelli, A.R. (1964). Tolerance of *Staphylococcus aureus* to sodium chloride. J. Bacteriol. *88*, 1–3.

Peacock, S.J., Moore, C.E., Justice, A., Kantzanou, M., Story, L., Mackie, K., O'Neill, G., and Day, N.P.J. (2002). Virulent Combinations of Adhesin and Toxin Genes in Natural Populations of *Staphylococcus aureus*. Infect. Immun. *70*, 4987–4996.

Pearson, A., Chronias, A., and Murray, M. (2009). Voluntary and mandatory surveillance for methicillin-resistant *Staphylococcus aureus* (MRSA) and methicillin-susceptible *S. aureus* (MSSA) bacteraemia in England. J. Antimicrob. Chemother. *64*, i11–i17.

Périchon, B., and Courvalin, P. (2009). VanA-Type Vancomycin-Resistant *Staphylococcus aureus*. Antimicrob. Agents Chemother. *53*, 4580–4587.

Peterson, C.T., Sharma, V., Elmén, L., and Peterson, S.N. (2015). Immune homeostasis, dysbiosis and therapeutic modulation of the gut microbiota. Clin. Exp. Immunol. *179*, 363–377.

Phetsang, W., Chaturongakul, S., and Jiarpinitnun, C. (2013). Electron-withdrawing substituted benzenesulfonamides against the predominant community-associated methicillin-resistant *Staphylococcus aureus* strain USA300. Monatshefte Für Chem. *144*, 461–471.

Phillipson, M., Heit, B., Colarusso, P., Liu, L., Ballantyne, C.M., and Kubes, P. (2006). Intraluminal crawling of neutrophils to emigration sites: a molecularly distinct process from adhesion in the recruitment cascade. J. Exp. Med. *203*, 2569–2575.

Pilatz, S., Breitbach, K., Hein, N., Fehlhaber, B., Schulze, J., Brenneke, B., Eberl, L., and Steinmetz, I. (2006). Identification of *Burkholderia pseudomallei* Genes Required for the Intracellular Life Cycle and *In vivo* Virulence. Infect. Immun. *74*, 3576–3586.

Pindak, F.F. (1970). Protection of mice against bacterial infection by interferon inducers. Infect. Immun. *1*, 271–273.

Pishchany, G., Haley, K.P., and Skaar, E.P. (2013). *Staphylococcus aureus* growth using human hemoglobin as an iron source. J. Vis. Exp. *72*, pii: 50072.

Piters, W.A.A. de S., and Bogaert, D. (2016). Unraveling the Molecular Mechanisms Underlying the Nasopharyngeal Bacterial Community Structure. mBio *7*, e00009–e00016.

Pohlmann-Dietze, P., Ulrich, M., Kiser, K.B., Doring, G., Lee, J.C., Fournier, J.-M., Botzenhart, K., and Wolz, C. (2000). Adherence of *Staphylococcus aureus* to Endothelial Cells: Influence of Capsular Polysaccharide, Global Regulator *agr*, and Bacterial Growth Phase. Infect. Immun. *68*, 4865–4871.

Polissi, A., Pontiggia, A., Feger, G., Altieri, M., Mottl, H., Ferrari, L., and Simon, D. (1998). Large-scale identification of virulence genes from *Streptococcus pneumoniae*. Infect. Immun. *66*, 5620–5629.

Postma, B., Poppelier, M.J., van Galen, J.C., Prossnitz, E.R., van Strijp, J.A.G., de Haas, C.J.C., and van Kessel, K.P.M. (2004). Chemotaxis inhibitory protein of *Staphylococcus aureus* binds specifically to the C5a and formylated peptide receptor. J. Immunol. *172*, 6994–7001.

Powers, J.H. (2004). Antimicrobial drug development--the past, the present, and the future. Clin. Microbiol. Infect. *10*, 23–31.

Powers, M.E., and Wardenburg, J.B. (2014). Igniting the Fire: *Staphylococcus aureus* Virulence Factors in the Pathogenesis of Sepsis. PLoS Pathog *10*, e1003871.

Pragman, A.A., and Schlievert, P.M. (2004). Virulence regulation in *Staphylococcus aureus*: the need for *in vivo* analysis of virulence factor regulation. FEMS Immunol. Med. Microbiol. *42*, 147–154.

Prajsnar, T.K., Cunliffe, V.T., Foster, S.J., and Renshaw, S.A. (2008). A novel vertebrate model of *Staphylococcus aureus* infection reveals phagocyte-dependent resistance of zebrafish to non-host specialized pathogens. Cell. Microbiol. *10*, 2312–2325.

Prajsnar, T.K. (2009). Development, characterisation and validation of a novel model of *Staphylococcus aureus* infection in zebrafish embryos. PhD thesis. University of Sheffield.

Prajsnar, T.K., Hamilton, R., Garcia-Lara, J., McVicker, G., Williams, A., Boots, M., Foster, S.J., and Renshaw, S.A. (2012). A privileged intraphagocyte niche is responsible for disseminated infection of *Staphylococcus aureus* in a zebrafish model. Cell. Microbiol. *14*, 1600–1619.

Priest, N.K., Rudkin, J.K., Feil, E.J., Van Den Elsen, J.M., Cheung, A., Peacock, S.J., Laabei, M., Lucks, D.A., Recker, M., and Massey, R.C. (2012). From genotype to phenotype: can systems biology be used to predict *Staphylococcus aureus* virulence? Nat. Rev. Microbiol. *10*, 791–797.

Proctor, R.A. (2008). Role of folate antagonists in the treatment of methicillin-resistant *Staphylococcus aureus* infection. Clin. Infect. Dis. *46*, 584–593.

Proctor, R.A., Kahl, B., Eiff, C. von, Vaudaux, P.E., Lew, D.P., and Peters, G. (1998). Staphylococcal Small Colony Variants Have Novel Mechanisms for Antibiotic Resistance. Clin. Infect. Dis. *27*, S68–S74.

Proctor, R.A., von Eiff, C., Kahl, B.C., Becker, K., McNamara, P., Herrmann, M., and Peters, G. (2006). Small colony variants: a pathogenic form of bacteria that facilitates persistent and recurrent infections. Nat. Rev. Microbiol. *4*, 295–305.

Proctor, R.A., Kriegeskorte, A., Kahl, B.C., Becker, K., Loffler, B., and Peters, G. (2014). *Staphylococcus aureus* Small Colony Variants (SCVs): a road map for the metabolic pathways involved in persistent infections. Front. Cell. Infect. Microbiol. *4*, 99.

Public Health England (2015). Mandatory Surveillance of *Staphylococcus aureus* bacteraemia. https://www.gov.uk/government/organisations/public-health-england

Rajamuthiah, R., Fuchs, B.B., Jayamani, E., Kim, Y., Larkins-Ford, J., Conery, A., Ausubel, F.M., and Mylonakis, E. (2014). Whole Animal Automated Platform for Drug Discovery against Multi-Drug Resistant *Staphylococcus aureus*. PLoS ONE *9*, e89189.

Ratner, A.J., Aguilar, J.L., Shchepetov, M., Lysenko, E.S., and Weiser, J.N. (2007). Nod1 mediates cytoplasmic sensing of combinations of extracellular bacteria. Cell. Microbiol. *9*, 1343–1351.

Rauch, S., DeDent, A.C., Kim, H.K., Bubeck Wardenburg, J., Missiakas, D.M., and Schneewind, O. (2012). Abscess Formation and Alpha-Hemolysin Induced Toxicity in a Mouse Model of *Staphylococcus aureus* Peritoneal Infection. Infect. Immun. *80*, 3721–3732.

Read, T.D., and Massey, R.C. (2014). Characterizing the genetic basis of bacterial phenotypes using genome-wide association studies: a new direction for bacteriology. Genome Med. *6*, 109-120.

Regev-Yochay, G., Dagan, R., Raz, M., Carmeli, Y., Shainberg, B., Derazne, E., Rahav, G., and Rubinstein, E. (2004). Association between carriage of *Streptococcus pneumoniae* and *Staphylococcus aureus* in Children. JAMA *292*, 716–720.

Rego, R.O.M., Bestor, A., Stefka, J., and Rosa, P.A. (2014). Population bottlenecks during the infectious cycle of the Lyme disease spirochete *Borrelia burgdorferi*. PloS One *9*, e101009.

Reid, D.M., Montoya, M., Taylor, P.R., Borrow, P., Gordon, S., Brown, G.D., and Wong, S.Y.C. (2004). Expression of the beta-glucan receptor, Dectin-1, on murine leukocytes in situ correlates with its function in pathogen recognition and reveals potential roles in leukocyte interactions. J. Leukoc. Biol. *76*, 86–94.

Reizner, W., Hunter, J.G., O'Malley, N.T., Southgate, R.D., Schwarz, E.M., and Kates, S.L. (2014). A systematic review of animal models for *Staphylococcus aureus* osteomyelitis. Eur. Cell. Mater. *27*, 196–212.

Rejman, J., Oberle, V., Zuhorn, I.S., and Hoekstra, D. (2004). Size-dependent internalization of particles via the pathways of clathrin- and caveolae-mediated endocytosis. Biochem. J. *377*, 159–169.

Renshaw, S.A., and Trede, N.S. (2012). A model 450 million years in the making: zebrafish and vertebrate immunity. Dis. Model. Mech. *5*, 38–47.

Renshaw, S.A., Loynes, C.A., Trushell, D.M.I., Elworthy, S., Ingham, P.W., and Whyte, M.K.B. (2006). A transgenic zebrafish model of neutrophilic inflammation. Blood *108*, 3976–3978.

Reynolds, P.E. (1989). Structure, biochemistry and mechanism of action of glycopeptide antibiotics. Eur. J. Clin. Microbiol. Infect. Dis. *8*, 943–950.

Rhodes, J., Hagen, A., Hsu, K., Deng, M., Liu, T.X., Look, A.T., and Kanki, J.P. (2005). Interplay of *pu.1* and *gata1* determines myelo-erythroid progenitor cell fate in zebrafish. Dev. Cell *8*, 97–108.

Rigby, K.M., and DeLeo, F.R. (2012). Neutrophils in innate host defense against *Staphylococcus aureus* infections. Semin. Immunopathol. *34*, 237–259.

Rigoulay, C., Entenza, J.M., Halpern, D., Widmer, E., Moreillon, P., Poquet, I., and Gruss, A. (2005). Comparative Analysis of the Roles of HtrA-Like Surface Proteases in Two Virulent *Staphylococcus aureus* Strains. Infect. Immun. *73*, 563–572.

Rogers, D.E. (1959). Observations on the nature of staphylococcal infections. Bull. N. Y. Acad. Med. *35*, 25–38.

Rogers, K.L., Fey, P.D., and Rupp, M.E. (2009). Coagulase-negative staphylococcal infections. Infect. Dis. Clin. North Am. *23*, 73–98.

Rooijakkers, S.H.M., and van Strijp, J.A.G. (2007). Bacterial complement evasion. Mol. Immunol. *44*, 23–32.

Rooijakkers, S.H.M., van Kessel, K.P.M., and van Strijp, J.A.G. (2005). Staphylococcal innate immune evasion. Trends Microbiol. *13*, 596–601.

Rowley, D. (1956). Rapidly Induced Changes in the Level of Non-specific Immunity in Laboratory Animals. Br. J. Exp. Pathol. *37*, 223–234.

Rudkin, J.K., Edwards, A.M., Bowden, M.G., Brown, E.L., Pozzi, C., Waters, E.M., Chan, W.C., Williams, P., O'Gara, J.P., and Massey, R.C. (2012). Methicillin Resistance Reduces the Virulence of Healthcare-Associated Methicillin-Resistant *Staphylococcus aureus* by Interfering With the *agr* Quorum Sensing System. J. Infect. Dis. *205*, 798–806.

Rutherford, K., Parkhill, J., Crook, J., Horsnell, T., Rice, P., Rajandream, M.-A., and Barrell, B. (2000). Artemis: sequence visualization and annotation. Bioinformatics *16*, 944–945.

Saha, B., Singh, A.K., Ghosh, A., and Bal, M. (2008). Identification and characterization of a vancomycin-resistant *Staphylococcus aureus* isolated from Kolkata (South Asia). J. Med. Microbiol. *57*, 72–79.

Saha, S., Qi, J., Wang, S., Wang, M., Li, X., Kim, Y.-G., Núñez, G., Gupta, D., and Dziarski, R. (2009). PGLYRP-2 and Nod2 Are Both Required for Peptidoglycan-Induced Arthritis and Local Inflammation. Cell Host Microbe *5*, 137–150.

Sakiniene, E., Bremell, T., and Tarkowski, A. (1999). Complement depletion aggravates *Staphylococcus aureus* septicaemia and septic arthritis. Clin. Exp. Immunol. *115*, 95–102.

Samant, S., Lee, H., Ghassemi, M., Chen, J., Cook, J.L., Mankin, A.S., and Neyfakh, A.A. (2008). Nucleotide Biosynthesis Is Critical for Growth of Bacteria in Human Blood. PLoS Pathog. *4*, e37.

Sánchez García, M., De la Torre, M.A., Morales, G., Peláez, B., Tolón, M.J., Domingo, S., Candel, F.J., Andrade, R., Arribi, A., García, N., et al. (2010). Clinical outbreak of linezolid-resistant *Staphylococcus aureus* in an intensive care unit. JAMA. *303*, 2260–2264.

Sandrini, M.P.B., Clausen, A.R., Munch-Petersen, B., and Piskur, J. (2006). Thymidine kinase diversity in bacteria. Nucleosides Nucleotides Nucleic Acids *25*, 1153–1158.

Sanghvi, J.C., Regot, S., Carrasco, S., Karr, J.R., Gutschow, M.V., Bolival, B., and Covert, M.W. (2013). Accelerated discovery via a whole-cell model. Nat. Methods *10*, 1192-1195.

Saralahti, A., Piippo, H., Parikka, M., Henriques-Normark, B., Rämet, M., and Rounioja, S. (2013). Adult zebrafish model for pneumococcal pathogenesis. Dev. Comp. Immunol. *42*, 345-353.

Sauvage, E., Kerff, F., Terrak, M., Ayala, J.A., and Charlier, P. (2008). The penicillin-binding proteins: structure and role in peptidoglycan biosynthesis. FEMS Microbiol. Rev. *32*, 234–258.

Schaedler, R.W., and Dubos, R.J. (1957). Effects of cellular constituents of mycobacteria on the resistance of mice to heterologous infections. II. Enhancement of infection. J. Exp. Med. *106*, 719–726.

Schafer, D., Lam, T.-T., Geiger, T., Mainiero, M., Engelmann, S., Hussain, M., Bosserhoff, A., Frosch, M., Bischoff, M., Wolz, C., et al. (2009). A Point Mutation in the Sensor Histidine Kinase SaeS of *Staphylococcus aureus* Strain Newman Alters the Response to Biocide Exposure. J. Bacteriol. *191*, 7306–7314.

Schäffler, H., Demircioglu, D.D., Kühner, D., Menz, S., Bender, A., Autenrieth, I.B., Bodammer, P., Lamprecht, G., Götz, F., and Frick, J.-S. (2014). NOD2 stimulation by *Staphylococcus aureus*-derived peptidoglycan is boosted by Toll-like receptor 2 costimulation with lipoproteins in dendritic cells. Infect. Immun. *82*, 4681–4688.

Scharschmidt, T.C., Vasquez, K.S., Truong, H.-A., Gearty, S.V., Pauli, M.L., Nosbaum, A., Gratz, I.K., Otto, M., Moon, J.J., Liese, J., et al. (2015). A Wave of Regulatory T

Cells into Neonatal Skin Mediates Tolerance to Commensal Microbes. Immunity *43*, 1011–1021.

Schauber, J., and Gallo, R.L. (2008). Antimicrobial peptides and the skin immune defense system. J. Allergy Clin. Immunol. *122*, 261–266.

Schindler, C.A., and Schuhardt, V.T. (1964). Lysostaphin: a new bacteriolytic agent for the *Staphylococcus*. Proc. Natl. Acad. Sci. *51*, 414–421.

Schlecht, L.M., Peters, B.M., Krom, B.P., Freiberg, J.A., Hänsch, G.M., Filler, S.G., Jabra-Rizk, M.A., and Shirtliff, M.E. (2015). Systemic *Staphylococcus aureus* infection mediated by *Candida albicans* hyphal invasion of mucosal tissue. Microbiol. *161*, 168–181.

Schleifer, K.H., and Kandler, O. (1972). Peptidoglycan types of bacterial cell walls and their taxonomic implications. Bacteriol. Rev. *36*, 407–477.

Schmitt, M., Schuler-Schmid, U., and Schmidt-Lorenz, W. (1990). Temperature limits of growth, TNase and enterotoxin production of *Staphylococcus aureus* strains isolated from foods. Int. J. Food Microbiol. *11*, 1–19.

Schneider, T., and Sahl, H.-G. (2010). An oldie but a goodie - cell wall biosynthesis as antibiotic target pathway. Int. J. Med. Microbiol. *300*, 161–169.

Schneider, W., Doenecke, C., and Scheurlen, P.G. (1973). Detection of thymidine-phosphorylase in human blood platelets. Klin. Wochenschr. *51*, 287–288.

Scott, J.R., and Barnett, T.C. (2006). Surface proteins of Gram-positive bacteria and how they get there. Annu. Rev. Microbiol. *60*, 397–423.

Scully, I.L., Liberator, P.A., Jansen, K.U., and Anderson, A.S. (2014). Covering all the Bases: Preclinical Development of an Effective *Staphylococcus aureus* Vaccine. Front. Immunol. *5*, 109.

Seo, H.S., and Nahm, M.H. (2009). Lipoprotein Lipase and Hydrofluoric Acid Deactivate Both Bacterial Lipoproteins and Lipoteichoic Acids, but Platelet-Activating Factor-Acetylhydrolase Degrades Only Lipoteichoic Acids. Clin. Vaccine Immunol. *16*, 1187–1195.

Seok, J., Warren, H.S., Cuenca, A.G., Mindrinos, M.N., Baker, H.V., Xu, W., Richards, D.R., McDonald-Smith, G.P., Gao, H., Hennessy, L., et al. (2013). Genomic responses in mouse models poorly mimic human inflammatory diseases. Proc. Natl. Acad. Sci. *110*, 3507–3512.

Sepulcre, M.P., Alcaraz-Pérez, F., López-Muñoz, A., Roca, F.J., Meseguer, J., Cayuela, M.L., and Mulero, V. (2009). Evolution of lipopolysaccharide (LPS) recognition and signaling: fish TLR4 does not recognize LPS and negatively regulates NF-kappaB activation. J. Immunol. 1950 *182*, 1836–1845.

Serba, J.J.S. (2015). *In vivo* imaging of host – pathogen interactions in *Staphylococcus aureus* infection. PhD thesis. University of Sheffield.

Serbina, N.V., Jia, T., Hohl, T.M., and Pamer, E.G. (2008). Monocyte-mediated defense against microbial pathogens. Annu. Rev. Immunol. *26*, 421–452.

Shafer, W.M., and Iandolo, J.J. (1979). Genetics of staphylococcal enterotoxin B in methicillin-resistant isolates of *Staphylococcus aureus*. Infect. Immun. *25*, 902–911.

Shah, P.H., MacFarlane, R.C., Bhattacharya, D., Matese, J.C., Demeter, J., Stroup, S.E., and Singh, U. (2005). Comparative Genomic Hybridizations of *Entamoeba* Strains Reveal Unique Genetic Fingerprints That Correlate with Virulence. Eukaryot. Cell *4*, 504–515.

Shallcross, L.J., Fragaszy, E., Johnson, A.M., and Hayward, A.C. (2013). The role of the Panton-Valentine leucocidin toxin in staphylococcal disease: a systematic review and meta-analysis. Lancet Infect. Dis. *13*, 43–54.

Shankar-Hari M, Phillips GS, Levy ML, and et al (2016). Developing a new definition and assessing new clinical criteria for septic shock: For the third international consensus definitions for sepsis and septic shock (sepsis-3). JAMA *315*, 775–787.

Sharma, R., and Rao, D.N. (2012). Functional characterization of UvrD helicases from *Haemophilus influenzae* and *Helicobacter pylori*. FEBS J. *279*, 2134–2155.

Shen, Z., Zhang, X., Chai, Y., Zhu, Z., Yi, P., Feng, G., Li, W., and Ou, G. (2014). Conditional knockouts generated by engineered CRISPR-Cas9 endonuclease reveal the roles of coronin in *C. elegans* neural development. Dev. Cell *30*, 625–636.

Sher, N.A., Chaparas, S.D., Greenberg, L.E., and Bernard, S. (1975). Effects of BCG, *Corynebacterium parvum*, and methanol-extration residue in the reduction of mortality from *Staphylococcus aureus* and *Candida albicans* infections in immunosuppressed mice. Infect. Immun. *12*, 1325–1330.

Shimada, T., Park, B.G., Wolf, A.J., Brikos, C., Goodridge, H.S., Becker, C.A., Reyes, C.N., Miao, E.A., Aderem, A., Götz, F., et al. (2010). *Staphylococcus aureus* evades lysozyme-based peptidoglycan digestion that links phagocytosis, inflammasome activation, and IL-1beta secretion. Cell Host Microbe *7*, 38–49.

Shin, S.J., Wu, C., Steinberg, H., and Talaat, A.M. (2006). Identification of Novel Virulence Determinants in *Mycobacterium paratuberculosis* by Screening a Library of Insertional Mutants. Infect. Immun. *74*, 3825–3833.

Shukla, S.K., Rose, W., and Schrodi, S.J. (2015). Complex host genetic susceptibility to *Staphylococcus aureus* infections. Trends Microbiol. *23*, 529–536.

Sievert, D.M., Rudrik, J.T., Patel, J.B., McDonald, L.C., Wilkins, M.J., and Hageman, J.C. (2008). Vancomycin-resistant *Staphylococcus aureus* in the United States, 2002-2006. Clin. Infect. Dis. *46*, 668–674.

Sifri, C.D., Begun, J., Ausubel, F.M., and Calderwood, S.B. (2003). *Caenorhabditis elegans* as a model host for *Staphylococcus aureus* pathogenesis. Infect. Immun. *71*, 2208–2217.

Silhavy, T.J., Kahne, D., and Walker, S. (2010). The Bacterial Cell Envelope. Cold Spring Harb. Perspect. Biol. *2*.

Simor, A.E. (2011). Staphylococcal decolonisation: an effective strategy for prevention of infection? Lancet Infect. Dis. *11*, 952–962.

Skorko-Glonek, J., Sobiecka-Szkatula, A., Narkiewicz, J., and Lipinska, B. (2008). The proteolytic activity of the HtrA (DegP) protein from *Escherichia coli* at low temperatures. Microbiol. *154*, 3649–3658.

Smith, H. (1950). Virulence-enhancing Factor of Hog Gastric Mucin. Nature *165*, 77–77.

Sommerhäuser, J., Kloppert, B., Wolter, W., Zschöck, M., Sobiraj, A., and Failing, K. (2003). The epidemiology of *Staphylococcus aureus* infections from subclinical mastitis in dairy cows during a control programme. Vet. Microbiol. *96*, 91–102.

Sonenshein, A.L., Hoch, J.A., and Losick, R.M. (1993). *Bacillus subtilis* and Other Gram-Positive Bacteria: from Genes to Cells (Washington, D.C: ASM Press).

Soriano, A., Martínez, J.A., Mensa, J., Marco, F., Almela, M., Moreno-Martínez, A., Sánchez, F., Muñoz, I., Anta, M.T.J. de, and Soriano, E. (2000). Pathogenic Significance of Methicillin Resistance for Patients with *Staphylococcus aureus* Bacteremia. Clin. Infect. Dis. *30*, 368–373.

Spaan, A.N., Henry, T., van Rooijen, W.J.M., Perret, M., Badiou, C., Aerts, P.C., Kemmink, J., de Haas, C.J.C., van Kessel, K.P.M., Vandenesch, F., et al. (2013). The staphylococcal toxin Panton-Valentine Leukocidin targets human C5a receptors. Cell Host Microbe *13*, 584–594.

Spaulding, A.R., Salgado-Pabón, W., Merriman, J.A., Stach, C.S., Ji, Y., Gillman, A.N., Peterson, M.L., and Schlievert, P.M. (2013). Vaccination Against *Staphylococcus aureus* Pneumonia. J. Infect. Dis. *209*, 1955-1962.

Spinazzola, A., Marti, R., Nishino, I., Andreu, A.L., Naini, A., Tadesse, S., Pela, I., Zammarchi, E., Donati, M.A., Oliver, J.A., et al. (2002). Altered Thymidine Metabolism Due to Defects of Thymidine Phosphorylase. J. Biol. Chem. *277*, 4128–4133.

Stein, C., Caccamo, M., Laird, G., and Leptin, M. (2007). Conservation and divergence of gene families encoding components of innate immune response systems in zebrafish. Genome Biol. *8*, R251.

Stevens, N.T., Sadovskaya, I., Jabbouri, S., Sattar, T., O'Gara, J.P., Humphreys, H., and Greene, C.M. (2009). *Staphylococcus epidermidis* polysaccharide intercellular adhesin induces IL-8 expression in human astrocytes via a mechanism involving TLR2. Cell. Microbiol. *11*, 421–432.

Stojanov, M., Sakwinska, O., and Moreillon, P. (2012). Expression of SCCmec cassette chromosome recombinases in methicillin-resistant *Staphylococcus aureus* and *Staphylococcus epidermidis*. J. Antimicrob. Chemother. *68*, 749-57.

Stoll, H., Dengjel, J., Nerz, C., and Götz, F. (2005). *Staphylococcus aureus* Deficient in Lipidation of Prelipoproteins Is Attenuated in Growth and Immune Activation. Infect. Immun. *73*, 2411–2423.

Stuart, L.M., and Ezekowitz, R.A.B. (2005). Phagocytosis: elegant complexity. Immunity *22*, 539–550.

Sugai, M., Komatsuzawa, H., Akiyama, T., Hong, Y.M., Oshida, T., Miyake, Y., Yamaguchi, T., and Suginaka, H. (1995). Identification of endo-beta-N-acetylglucosaminidase and N-acetylmuramyl-L-alanine amidase as cluster-dispersing enzymes in *Staphylococcus aureus*. J. Bacteriol. *177*, 1491–1496.

Summerton, J., and Weller, D. (1997). Morpholino antisense oligomers: design, preparation, and properties. Antisense Nucleic Acid Drug Dev. *7*, 187–195.

Sun, F., Li, C., Jeong, D., Sohn, C., He, C., and Bae, T. (2010). In the *Staphylococcus aureus* Two-Component System *sae*, the Response Regulator SaeR Binds to a Direct Repeat Sequence and DNA Binding Requires Phosphorylation by the Sensor Kinase SaeS. J. Bacteriol. *192*, 2111–2127.

Surewaard, B.G.J., Deniset, J.F., Zemp, F.J., Amrein, M., Otto, M., Conly, J., Omri, A., Yates, R.M., and Kubes, P. (2016). Identification and treatment of the *Staphylococcus aureus* reservoir in vivo. J. Exp. Med.

Surewaard, B.G.J., Nijland, R., Spaan, A.N., Kruijtzer, J.A.W., Haas, C.J.C. de, and Strijp, J.A.G. van (2012). Inactivation of Staphylococcal Phenol Soluble Modulins by Serum Lipoprotein Particles. PLOS Pathog *8*, e1002606.

Swaim, L.E., Connolly, L.E., Volkman, H.E., Humbert, O., Born, D.E., and Ramakrishnan, L. (2006). *Mycobacterium marinum* Infection of Adult Zebrafish Causes Caseating Granulomatous Tuberculosis and Is Moderated by Adaptive Immunity. Infect. Immun. *74*, 6108–6117.

Sylvester, I., Suffredini, A.F., Boujoukos, A.J., Martich, G.D., Danner, R.L., Yoshimura, T., and Leonard, E.J. (1993). Neutrophil attractant protein-1 and monocyte chemoattractant protein-1 in human serum. Effects of intravenous lipopolysaccharide on free attractants, specific IgG autoantibodies and immune complexes. J. Immunol. 1950 *151*, 3292–3298.

Tabata, Y., and Ikada, Y. (1988). Effect of the size and surface charge of polymer microspheres on their phagocytosis by macrophage. Biomaterials *9*, 356–362.

Takeda, K., and Akira, S. (2003). Toll receptors and pathogen resistance. Cell. Microbiol. *5*, 143–153.

Takeuchi, O., Hoshino, K., and Akira, S. (2000). Cutting Edge: TLR2-Deficient and MyD88-Deficient Mice Are Highly Susceptible to *Staphylococcus aureus* Infection. J. Immunol. *165*, 5392–5396.

ten Broeke-Smits, N.J.P., Pronk, T.E., Jongerius, I., Bruning, O., Wittink, F.R., Breit, T.M., van Strijp, J.A.G., Fluit, A.C., and Boel, C.H.E. (2010). Operon structure of *Staphylococcus aureus*. Nucleic Acids Res. *38*, 3263–3274.

Thammavongsa, V., Kern, J.W., Missiakas, D.M., and Schneewind, O. (2009). *Staphylococcus aureus* synthesizes adenosine to escape host immune responses. J. Exp. Med. *206*, 2417–2427.

Then, R., and Angehrn, P. (1973). Sulphonamide-induced "Thymineless Death" in *Escherichia coli*. J. Gen. Microbiol. *76*, 255–263.

Theurl, I., Fritsche, G., Ludwiczek, S., Garimorth, K., Bellmann-Weiler, R., and Weiss, G. (2005). The macrophage: a cellular factory at the interphase between iron and immunity for the control of infections. Biometals Int. J. *18*, 359–367.

Thwaites, G.E., and Gant, V. (2011). Are bloodstream leukocytes Trojan Horses for the metastasis of *Staphylococcus aureus*? Nat. Rev. Microbiol. *9*, 215–222.

Thwaites, G.E., Edgeworth, J.D., Gkrania-Klotsas, E., Kirby, A., Tilley, R., Török, M.E., Walker, S., Wertheim, H.F., Wilson, P., and Llewelyn, M.J. (2011). Clinical management of *Staphylococcus aureus* bacteraemia. Lancet Infect. Dis. *11*, 208–222.

Timmerman, C.P., Mattsson, E., Martinez-Martinez, L., De Graaf, L., Van Strijp, J.A., Verbrugh, H.A., Verhoef, J., and Fleer, A. (1993). Induction of release of tumor necrosis factor from human monocytes by staphylococci and staphylococcal peptidoglycans. Infect. Immun. *61*, 4167–4172.

Tipper, D.J., and Berman, M.F. (1969). Structures of the cell wall peptidoglycans of *Staphylococcus epidermidis* Texas 26 and *Staphylococcus aureus* Copenhagen. I. Chain length and average sequence of cross-bridge peptides. Biochemistry. *8*, 2183–2192.

Todar, K. (2006). Online Textbook of Bacteriology (University of Wisconsin-Madison Department of Bacteriology).

Tokunaga, T., Oka, K., Takemoto, A., Ohtsubo, Y., Gotoh, N., and Nishino, T. (1997). Efficacy of trimethoprim in murine experimental infection with a thymidine kinase-deficient mutant of *Escherichia coli*. Antimicrob. Agents Chemother. *41*, 1042–1045.

Townsend, D.E., Kaenjak, A., Jayaswal, R.K., and Wilkinson, B.J. (1996). Proline is biosynthesized from arginine in *Staphylococcus aureus*. Microbiol. *142*, 1491–1497.

Tran, P.V., and Nichols, B.P. (1991). Expression of *Escherichia coli pabA*. J. Bacteriol. *173*, 3680–3687.

Travassos, L.H., Girardin, S.E., Philpott, D.J., Blanot, D., Nahori, M.-A., Werts, C., and Boneca, I.G. (2004). Toll-like receptor 2-dependent bacterial sensing does not occur via peptidoglycan recognition. EMBO Rep. *5*, 1000–1006.

Trede, N.S., Zapata, A., and Zon, L.I. (2001). Fishing for lymphoid genes. Trends Immunol. *22*, 302–307.

Trede, N.S., Langenau, D.M., Traver, D., Look, A.T., and Zon, L.I. (2004). The use of zebrafish to understand immunity. Immunity *20*, 367–379.

Trivier, D., and Courcol, R. J. (1996). Iron depletion and virulence in *Staphylococcus aureus*. FEMS Microbiol. Lett. *141*, 117–127.

Tsuda, Y., Takahashi, H., Kobayashi, M., Hanafusa, T., Herndon, D.N., and Suzuki, F. (2004). CCL2, a product of mice early after systemic inflammatory response syndrome (SIRS), induces alternatively activated macrophages capable of impairing antibacterial resistance of SIRS mice. J. Leukoc. Biol. *76*, 368–373.

Tuazon, C.U., Sheagren, J.N., and Quie, P.G. (1981). Variability in the degree of opsonization and phagocytosis of strains of *Staphylococcus aureus* isolated from patients with disseminated intravascular coagulation. J. Lab. Clin. Med. *98*, 949–955.

Turnidge, J.D., Kotsanas, D., Munckhof, W., Roberts, S., Bennett, C.M., Nimmo, G.R., Coombs, G.W., Murray, R.J., Howden, B., Johnson, P.D.R., et al. (2009). *Staphylococcus aureus* bacteraemia: a major cause of mortality in Australia and New Zealand. Med. J. Aust. *191*, 368–373.

Tzagoloff, H., and Novick, R. (1977). Geometry of cell division in *Staphylococcus aureus*. J. Bacteriol. *129*, 343–350.

Tzou, P., De Gregorio, E., and Lemaitre, B. (2002). How Drosophila combats microbial infection: a model to study innate immunity and host–pathogen interactions. Curr. Opin. Microbiol. *5*, 102–110.

Ueda, A., Ishigatsubo, Y., Okubo, T., and Yoshimura, T. (1997). Transcriptional regulation of the human monocyte chemoattractant protein-1 gene. Cooperation of two NF-kappaB sites and NF-kappaB/Rel subunit specificity. J. Biol. Chem. *272*, 31092–31099.

Ueta, M., Iida, T., Sakamoto, M., Sotozono, C., Takahashi, J., Kojima, K., Okada, K., Chen, X., Kinoshita, S., and Honda, T. (2007). Polyclonality of *Staphylococcus epidermidis* residing on the healthy ocular surface. J. Med. Microbiol. *56*, 77–82.

Uhlén, M., Guss, B., Nilsson, B., Gatenbeck, S., Philipson, L., and Lindberg, M. (1984). Complete sequence of the staphylococcal gene encoding protein A. A gene evolved through multiple duplications. J. Biol. Chem. *259*, 1695–1702.

Ulland, T.K., Janowski, A.M., Buchan, B.W., Faron, M., Cassel, S.L., Jones, B.D., and Sutterwala, F.S. (2013). *Francisella tularensis* live vaccine strain folate metabolism and pseudouridine synthase gene mutants modulate macrophage caspase-1 activation. Infect. Immun. *81*, 201–208.

Underhill, D.M., Ozinsky, A., Hajjar, A.M., Stevens, A., Wilson, C.B., Bassetti, M., and Aderem, A. (1999). The Toll-like receptor 2 is recruited to macrophage phagosomes and discriminates between pathogens. Nature *401*, 811–815.

Valentino, M.D., Foulston, L., Sadaka, A., Kos, V.N., Villet, R.A., Santa Maria, J., Lazinski, D.W., Camilli, A., Walker, S., Hooper, D.C., et al. (2014). Genes contributing

to *Staphylococcus aureus* fitness in abscess- and infection-related ecologies. mBio *5*, e01729–01714.

Valero, A., Pérez-Rodríguez, F., Carrasco, E., Fuentes-Alventosa, J.M., García-Gimeno, R.M., and Zurera, G. (2009). Modelling the growth boundaries of *Staphylococcus aureus*: Effect of temperature, pH and water activity. Int. J. Food Microbiol. *133*, 186–194.

Van Buren, C.T., and Rudolph, F. (1997). Dietary nucleotides: a conditional requirement. Nutr. *13*, 470–472.

van der Sar, A.M., Spaink, H.P., Zakrzewska, A., Bitter, W., and Meijer, A.H. (2009). Specificity of the zebrafish host transcriptome response to acute and chronic mycobacterial infection and the role of innate and adaptive immune components. Mol. Immunol. *46*, 2317–2332.

van der Vaart, M., Spaink, H.P., and Meijer, A.H. (2012). Pathogen Recognition and Activation of the Innate Immune Response in Zebrafish. Adv. Hematol. *2012*, e159807.

van Kessel, K.P.M., Bestebroer, J., and van Strijp, J.A.G. (2014). Neutrophil-Mediated Phagocytosis of *Staphylococcus aureus*. Front. Immunol. *5*, 467.

van Kuilenburg, A.B.P., and Zoetekouw, L. (2006). Determination of thymidine phosphorylase activity in human blood cells and fibroblasts by a nonradiochemical assay using reversed-phase high-performance liquid chromatography. Nucleosides Nucleotides Nucleic Acids *25*, 1261–1264.

van Opijnen, T., and Camilli, A. (2012). A fine scale phenotype-genotype virulence map of a bacterial pathogen. Genome Res. *22*, 2541–2551.

van Opijnen, T., and Camilli, A. (2013). Transposon insertion sequencing: a new tool for systems-level analysis of microorganisms. Nat. Rev. Microbiol. *11*, 435–442.

Vandecandelaere, I., Depuydt, P., Nelis, H.J., and Coenye, T. (2014). Protease production by *Staphylococcus epidermidis* and its effect on *Staphylococcus aureus* biofilms. Pathog. Dis. 70, 321–331.

Varshney, G.K., Pei, W., LaFave, M.C., Idol, J., Xu, L., Gallardo, V., Carrington, B., Bishop, K., Jones, M., Li, M., et al. (2015). High-throughput gene targeting and phenotyping in zebrafish using CRISPR/Cas9. Genome Res. *25*, 1030–1042.

Veiga, P., Bulbarela-Sampieri, C., Furlan, S., Maisons, A., Chapot-Chartier, M.-P., Erkelenz, M., Mervelet, P., Noirot, P., Frees, D., Kuipers, O.P., et al. (2007). SpxB regulates O-acetylation-dependent resistance of *Lactococcus lactis* peptidoglycan to hydrolysis. J. Biol. Chem. *282*, 19342–19354.

Verbrugh, H.A., Van Dijk, W.C., Peters, R., Van Der Tol, M.E., and Verhoef, J. (1979). The role of *Staphylococcus aureus* cell-wall peptidoglycan, teichoic acid and protein A in the processes of complement activation and opsonization. Immunology *37*, 615–621.

Verhoeven, P.O., Grattard, F., Carricajo, A., Lucht, F., Cazorla, C., Garraud, O., Pozzetto, B., and Berthelot, P. (2012). Quantification by real-time PCR assay of

Staphylococcus aureus load: a useful tool for rapidly identifying persistent nasal carriers. J. Clin. Microbiol. *50*, 2063–2065.

Verkaik, N.J., Lebon, A., de Vogel, C.P., Hooijkaas, H., Verbrugh, H.A., Jaddoe, V.W.V., Hofman, A., Moll, H.A., van Belkum, A., and van Wamel, W.J.B. (2010a). Induction of antibodies by *Staphylococcus aureus* nasal colonization in young children. Clin. Microbiol. Infect. *16*, 1312–1317.

Verkaik, N.J., Boelens, H.A., de Vogel, C.P., Tavakol, M., Bode, L.G.M., Verbrugh, H.A., van Belkum, A., and van Wamel, W.J.B. (2010b). Heterogeneity of the humoral immune response following *Staphylococcus aureus* bacteremia. Eur. J. Clin. Microbiol. Infect. Dis. *29*, 509–518.

Vickers, A.A., Potter, N.J., Fishwick, C.W.G., Chopra, I., and O'Neill, A.J. (2009). Analysis of mutational resistance to trimethoprim in *Staphylococcus aureus* by genetic and structural modelling techniques. J. Antimicrob. Chemother. *63*, 1112–1117.

Visvanathan, K., Skinner, N.A., Thompson, A.J.V., Riordan, S.M., Sozzi, V., Edwards, R., Rodgers, S., Kurtovic, J., Chang, J., Lewin, S., et al. (2007). Regulation of Toll-like receptor-2 expression in chronic hepatitis B by the precore protein. Hepatol. *45*, 102–110.

Volkman, H.E., Pozos, T.C., Zheng, J., Davis, J.M., Rawls, J.F., and Ramakrishnan, L. (2010). Tuberculous granuloma induction via interaction of a bacterial secreted protein with host epithelium. Science *327*, 466–469.

Vollmer, W., Blanot, D., and de Pedro, M.A. (2008a). Peptidoglycan structure and architecture. FEMS Microbiol. Rev. *32*, 149–167.

Vollmer, W., Joris, B., Charlier, P., and Foster, S. (2008b). Bacterial peptidoglycan (murein) hydrolases. FEMS Microbiol. Rev. *32*, 259–286.

Volz, T., Nega, M., Buschmann, J., Kaesler, S., Guenova, E., Peschel, A., Röcken, M., Götz, F., and Biedermann, T. (2010). Natural *Staphylococcus aureus*-derived peptidoglycan fragments activate NOD2 and act as potent costimulators of the innate immune system exclusively in the presence of TLR signals. FASEB J. *24*, 4089–4102.

von Eiff, C., Becker, K., Machka, K., Stammer, H., and Peters, G. (2001). Nasal carriage as a source of *Staphylococcus aureus* bacteremia. N. Engl. J. Med. *344*, 11–16.

von Köckritz-Blickwede, M., and Nizet, V. (2009). Innate immunity turned inside-out: antimicrobial defense by phagocyte extracellular traps. J. Mol. Med. *87*, 775–783.

von Kockritz-Blickwede, M., Rohde, M., Oehmcke, S., Miller, L.S., Cheung, A.L., Herwald, H., Foster, S., and Medina, E. (2008). Immunological Mechanisms Underlying the Genetic Predisposition to Severe *Staphylococcus aureus* Infection in the Mouse Model. Am. J. Pathol. *173*, 1657–1668.

Voynow, J.A., and Rubin, B.K. (2009). Mucins, mucus, and sputum. Chest *135*, 505–512.

Wakabayashi, G., Gelfand, J.A., Jung, W.K., Connolly, R.J., Burke, J.F., and Dinarello, C.A. (1991). *Staphylococcus epidermidis* induces complement activation, tumor necrosis factor and interleukin-1, a shock-like state and tissue injury in rabbits without endotoxemia. Comparison to *Escherichia coli*. J. Clin. Invest. *87*, 1925–1935.

Waldron, D.E., and Lindsay, J.A. (2006). Sau1: a novel lineage-specific type I restriction-modification system that blocks horizontal gene transfer into *Staphylococcus aureus* and between *S. aureus* isolates of different lineages. J. Bacteriol. *188*, 5578–5585.

Walev, I., Weller, U., Strauch, S., Foster, T., and Bhakdi, S. (1996). Selective killing of human monocytes and cytokine release provoked by sphingomyelinase (beta-toxin) of *Staphylococcus aureus*. Infect. Immun. *64*, 2974–2979.

Wang, J.E., Dahle, M.K., Yndestad, A., Bauer, I., McDonald, M.C., Aukrust, P., Foster, S.J., Bauer, M., Aasen, A.O., and Thiemermann, C. (2004). Peptidoglycan of *Staphylococcus aureus* causes inflammation and organ injury in the rat. Crit. Care Med. *32*, 546–552.

Wang, L., Bi, C., Wang, T., Xiang, H., Chen, F., Hu, J., Liu, B., Cai, H., Zhong, X., Deng, X., et al. (2015). A coagulase-negative and non-haemolytic strain of *Staphylococcus aureus* for investigating the roles of SrtA in a murine model of bloodstream infection. Pathog. Dis. *73*, ftv042.

Wang, R., Braughton, K.R., Kretschmer, D., Bach, T.-H.L., Queck, S.Y., Li, M., Kennedy, A.D., Dorward, D.W., Klebanoff, S.J., Peschel, A., et al. (2007). Identification of novel cytolytic peptides as key virulence determinants for community-associated MRSA. Nat. Med. *13*, 1510–1514.

Wardenburg, J.B., and Schneewind, O. (2008). Vaccine protection against *Staphylococcus aureus* pneumonia. J. Exp. Med. *205*, 287–294.

Watanabe, T., Asano, N., Murray, P.J., Ozato, K., Tailor, P., Fuss, I.J., Kitani, A., and Strober, W. (2008). Muramyl dipeptide activation of nucleotide-binding oligomerization domain 2 protects mice from experimental colitis. J. Clin. Invest. *118*, 545-59.

Waterfield, N.R., Sanchez-Contreras, M., Eleftherianos, I., Dowling, A., Yang, G., Wilkinson, P., Parkhill, J., Thomson, N., Reynolds, S.E., Bode, H.B., et al. (2008). Rapid Virulence Annotation (RVA): Identification of virulence factors using a bacterial genome library and multiple invertebrate hosts. Proc. Natl. Acad. Sci. *105*, 15967–15972.

Weber, J.T. (2005). Community-Associated Methicillin-Resistant *Staphylococcus aureus*. Clin. Infect. Dis. *41*, 269–272.

Weber, M., Mickoleit, M., and Huisken, J. (2014). Multilayer Mounting for Long-term Light Sheet Microscopy of Zebrafish. J. Vis. Exp. *84*.

Wegkamp, van Oorschot, W., de Vos, W.M., and Smid, E.J. (2007). Characterization of the role of para-aminobenzoic acid biosynthesis in folate production by *Lactococcus lactis*. Appl. Environ. Microbiol. *73*, 2673–2681.

Weiss, G., and Schaible, U.E. (2015). Macrophage defense mechanisms against intracellular bacteria. Immunol. Rev. *264*, 182–203.

Wertheim, H.F.L., Vos, M.C., Ott, A., van Belkum, A., Voss, A., Kluytmans, J.A.J.W., van Keulen, P.H.J., Vandenbroucke-Grauls, C.M.J.E., Meester, M.H.M., and Verbrugh, H.A. (2004). Risk and outcome of nosocomial *Staphylococcus aureus* bacteraemia in nasal carriers versus non-carriers. Lancet *364*, 703–705.

Wertheim, H.F.L., Walsh, E., Choudhurry, R., Melles, D.C., Boelens, H.A.M., Miajlovic, H., Verbrugh, H.A., Foster, T., and van Belkum, A. (2008). Key Role for Clumping Factor B in *Staphylococcus aureus* Nasal Colonization of Humans. PLoS Med *5*, e17.

Wheeler, R., Turner, R.D., Bailey, R.G., Salamaga, B., Mesnage, S., Mohamad, S.A.S., Hayhurst, E.J., Horsburgh, M., Hobbs, J.K., and Foster, S.J. (2015). Bacterial Cell Enlargement Requires Control of Cell Wall Stiffness Mediated by Peptidoglycan Hydrolases. mBio *6*, e00660–15.

Wicken, A.J., and Knox, K.W. (1975). Lipoteichoic acids: a new class of bacterial antigen. Science *187*, 1161–1167.

Wiles, T.J., Norton, J.P., Russell, C.W., Dalley, B.K., Fischer, K.F., and Mulvey, M.A. (2013). Combining Quantitative Genetic Footprinting and Trait Enrichment Analysis to Identify Fitness Determinants of a Bacterial Pathogen. PLoS Genet *9*, e1003716.

Williams, R.E. (1963). Healthy carriage of *Staphylococcus aureus*: its prevalence and importance. Bacteriol. Rev. *27*, 56–71.

Wilson, R., and Cockcroft, W.H. (1952). Penicillin Resistant Staphylococcal Infection. Can. Med. Assoc. J. *66*, 548–551.

Winstel, V., Kühner, P., Salomon, F., Larsen, J., Skov, R., Hoffmann, W., Peschel, A., and Weidenmaier, C. (2015). Wall Teichoic Acid Glycosylation Governs *Staphylococcus aureus* Nasal Colonization. mBio *6*, e00632–15.

Wolf, A.J., Arruda, A., Reyes, C.N., Kaplan, A.T., Shimada, T., Shimada, K., Arditi, M., Liu, G., and Underhill, D.M. (2011). Phagosomal Degradation Increases TLR Access to Bacterial Ligands and Enhances Macrophage Sensitivity to Bacteria. J. Immunol. *187*, 6002–6010.

Wood (1988). The Nematode *Caenorhabditis elegans* (Cold Spring Harbor Laboratory Press).

Woods, I.G., Kelly, P.D., Chu, F., Ngo-Hazelett, P., Yan, Y.-L., Huang, H., Postlethwait, J.H., and Talbot, W.S. (2000). A Comparative Map of the Zebrafish Genome. Genome Res. *10*, 1903–1914.

Wright, J.A., and Nair, S.P. (2012). The lipoprotein components of the Isd and Hts transport systems are dispensable for acquisition of heme by *Staphylococcus aureus*. FEMS Microbiol. Lett. *329*, 177–185.

Wyllie, D.H., Walker, A.S., Miller, R., Moore, C., Williamson, S.R., Schlackow, I.,

Finney, J.M., O'Connor, L., Peto, T.E., and Crook, D.W. (2011). Decline of meticillin-resistant *Staphylococcus aureus* in Oxfordshire hospitals is strain-specific and preceded infection-control intensification. BMJ Open *1*, e000160.

Xia, G., and Wolz, C. (2014). Phages of *Staphylococcus aureus* and their impact on host evolution. Infect. Genet. Evol. *21*, 593–601.

Xia, W., Hilgenbrink, A.R., Matteson, E.L., Lockwood, M.B., Cheng, J.-X., and Low, P.S. (2009). A functional folate receptor is induced during macrophage activation and can be used to target drugs to activated macrophages. Blood *113*, 438–446.

Xiong, Y.Q., Willard, J., Yeaman, M.R., Cheung, A.L., and Bayer, A.S. (2006). Regulation of *Staphylococcus aureus* α-Toxin Gene (hla) Expression by *agr*, *sarA* and *sae In vitro* and in Experimental Infective Endocarditis. J. Infect. Dis. *194*, 1267–1275.

Xu, S.-Y., Corvaglia, A.R., Chan, S.-H., Zheng, Y., and Linder, P. (2011). A type IV modification-dependent restriction enzyme SauUSI from *Staphylococcus aureus* subsp. aureus USA300. Nucleic Acids Res. *39*, 5597–5610.

Yamamoto, M., Yamaguchi, R., Munakata, K., Takashima, K., Nishiyama, M., Hioki, K., Ohnishi, Y., Nagasaki, M., Imoto, S., Miyano, S., et al. (2012). A microarray analysis of gnotobiotic mice indicating that microbial exposure during the neonatal period plays an essential role in immune system development. BMC Genomics *13*, 335-350.

Yang, S., Sugawara, S., Monodane, T., Nishijima, M., Adachi, Y., Akashi, S., Miyake, K., Hase, S., and Takada, H. (2001). *Micrococcus luteus* Teichuronic Acids Activate Human and Murine Monocytic Cells in a CD14- and Toll-Like Receptor 4-Dependent Manner. Infect. Immun. *69*, 2025–2030.

Yee, Peng Cui, Wanliang Shi, and Jie Feng (2015). Genetic Screen Reveals the Role of Purine Metabolism in *Staphylococcus aureus* Persistence to Rifampicin. Antibiotics *4*, 627–642.

Yoo, S.K., and Huttenlocher, A. (2011). Spatiotemporal photolabeling of neutrophil trafficking during inflammation in live zebrafish. J. Leukoc. Biol. *89*, 661–667.

Yoong, P., and Torres, V.J. (2015). Counter inhibition between leukotoxins attenuates *Staphylococcus aureus* virulence. Nat. Commun. *6*, 8125.

Zander, J., Besier, S., Saum, S.H., Dehghani, F., Loitsch, S., Brade, V., and Wichelhaus, T.A. (2008). Influence of dTMP on the Phenotypic Appearance and Intracellular Persistence of *Staphylococcus aureus*. Infect. Immun. *76*, 1333–1339.

Zander, J., Besier, S., Ackermann, H., and Wichelhaus, T.A. (2010a). Synergistic antimicrobial activities of folic acid antagonists and nucleoside analogs. Antimicrob. Agents Chemother. *54*, 1226–1231.

Zander, J., Hartenfeller, M., Hähnke, V., Proschak, E., Besier, S., Wichelhaus, T.A., and Schneider, G. (2010b). Multistep virtual screening for rapid and efficient identification of non-nucleoside bacterial thymidine kinase inhibitors. Chem. *16*, 9630–9637.

Zaworski, P.G., and Gill, G.S. (1988). Precipitation and recovery of proteins from culture supernatants using zinc. Anal. Biochem. *173*, 440–444.

Zecconi, A., and Scali, F. (2013). *Staphylococcus aureus* virulence factors in evasion from innate immune defenses in human and animal diseases. Immunol. Lett. *150*, 12–22.

Zhang, B.Z., Hua, Y.H., Yu, B., Lau, C.C.Y., Cai, J.P., Zheng, S.Y., Yam, W.C., Kao, R.Y.T., Sze, K.H., Zheng, B.J., et al. (2015). Recombinant ESAT-6-like proteins provoke protective immune responses against invasive *Staphylococcus aureus* disease in a murine model. Infect. Immun. *83*, 339–345.

Zhang, D., de Souza, R.F., Anantharaman, V., Iyer, L.M., and Aravind, L. (2012). Polymorphic toxin systems: Comprehensive characterization of trafficking modes, processing, mechanisms of action, immunity and ecology using comparative genomics. Biol. Direct *7*, 18.

Zhu, F., Zhou, Y., Jiang, C., and Zhang, X. (2015). Role of JAK-STAT signaling in maturation of phagosomes containing *Staphylococcus aureus*. Sci. Rep. *5*, 14854.